Advances in Solid State Photo-Detectors
and comparison with vacuum devices developments

G.Collazuol
Dipartimento di Fisica ed Astronomia
Universita` di Padova

Overview
- Physical principles, characteristics and developments of
→ vacuum based photo-detectors (focusing on PM Tubes)
→ solid state photo-detectors (focusing on Silicon PM)
- Associated electronics
- Applications

Photo-detection steps

1. Photo-electric conversion with or without emission in vacuum

"external" photo-emission

"internal" photo-emission

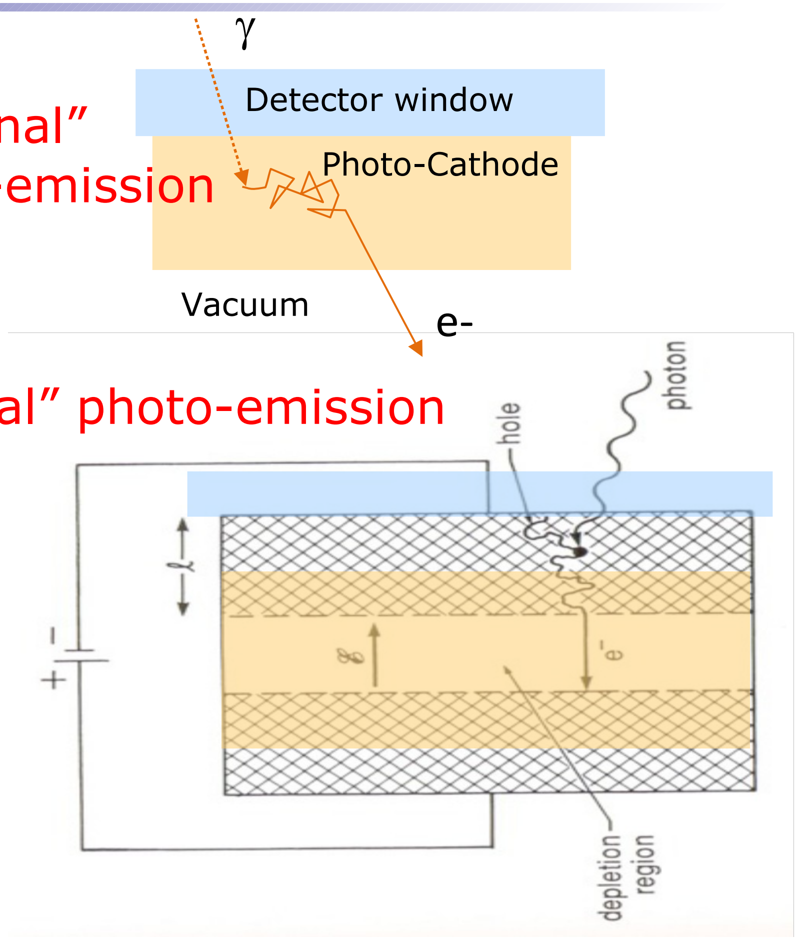

Emission in vacuum implies

→ low detection efficiency

→ low dark count rate

...source of differences between vacuum and solid state devices including multiplication mechanisms...

2. Internal charge multiplication

Charge multiplication within the device implies

→ better Signal/Noise ratio (wrt external amplification)

→ intrinsic fluctuations in amplitude and timing (depending on the multiplication mechanism)

Photo-detector family tree

Gas
External photoemission

gas photoionization
(TMAE, TEA, …)

and/or

multiplication in gas
by avalanche
(MWPC, GEM, …)

Vacuum devices
External photoemission

secondary electron multiplication

Dynodes:
- discrete (PMT)
- continuous dynode (channeltron, MCP)

Anode:
- multi-anode
- strip lines RF

hybrid
photocathode +

- multiplication by **ionization in Si** (HPD, HAPD, …)

or

- multiplication by **luminescent anodes** (light amplifiers: SMART/Quasar, X-HPD, …)

Solid state
Internal photoemission

- PIN-Photo-diode
- APD, GM-APD (SiPM)
- Imaging CMOS, CCD

- Quantum well detectors
- Supercond. Tunnel Junc.

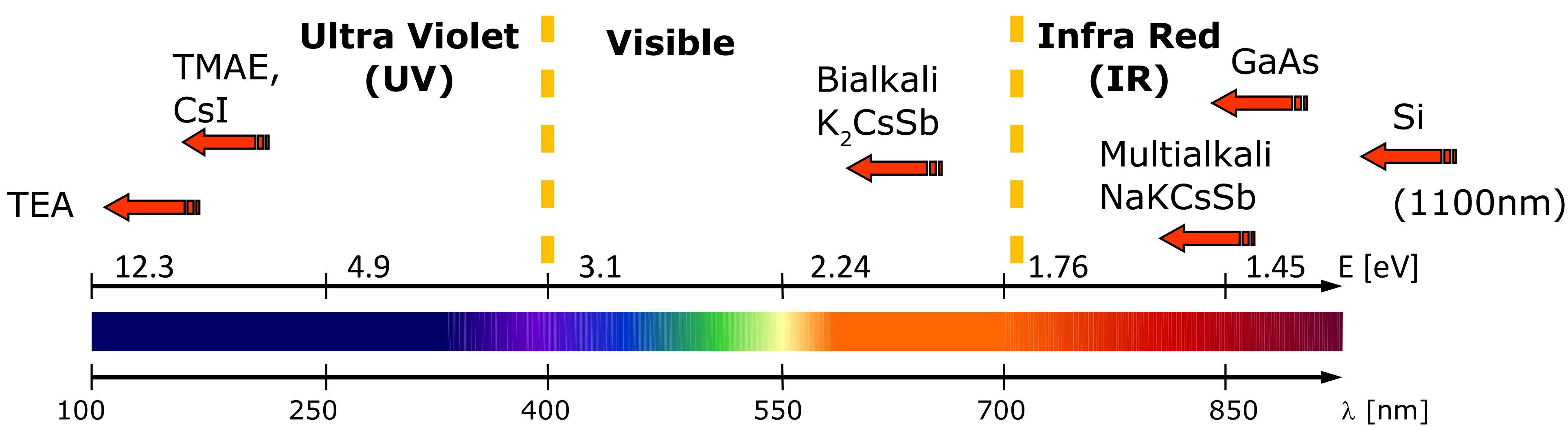

Single photon sensitive detectors

PMT (Hamamatsu R5600)

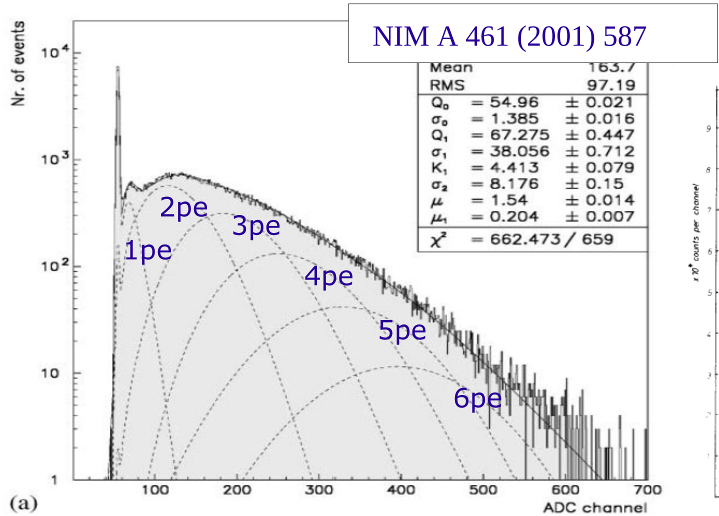

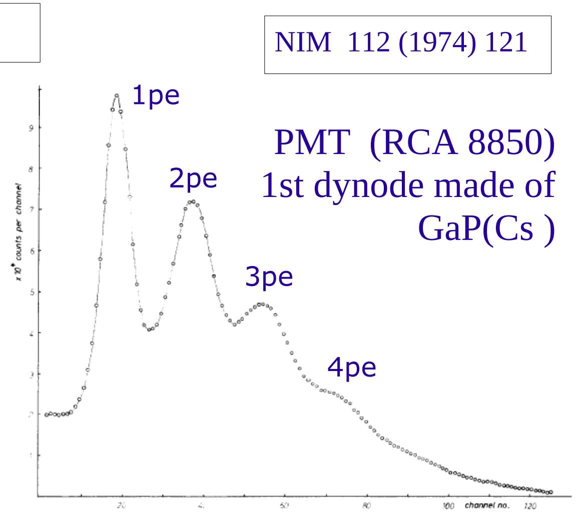

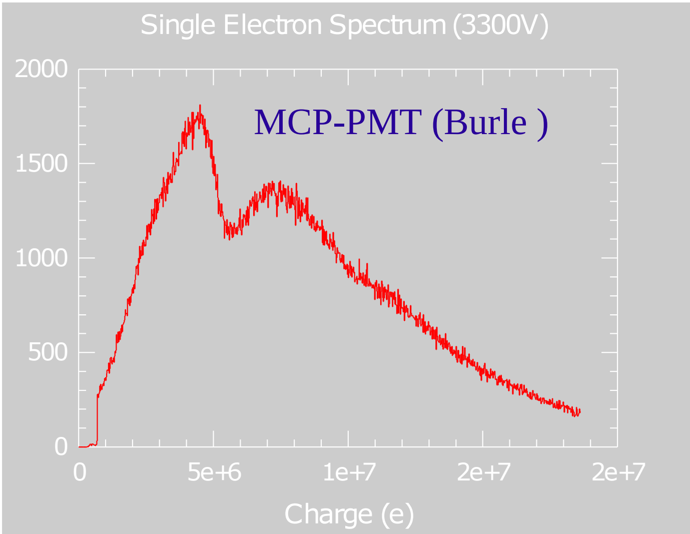

SiPM

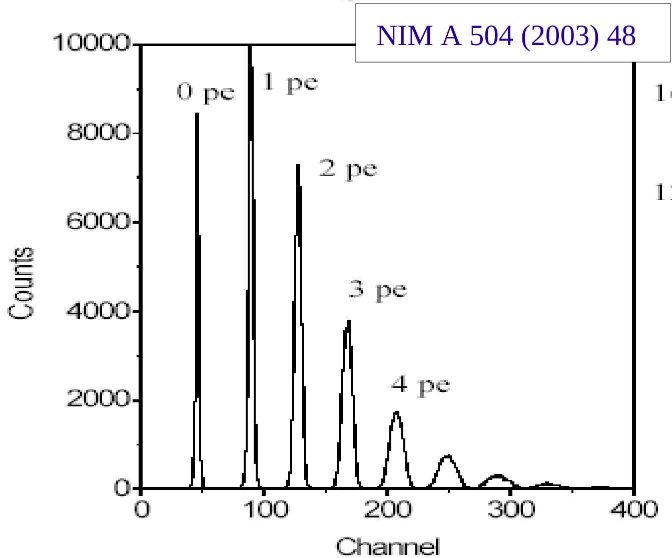

VLPC

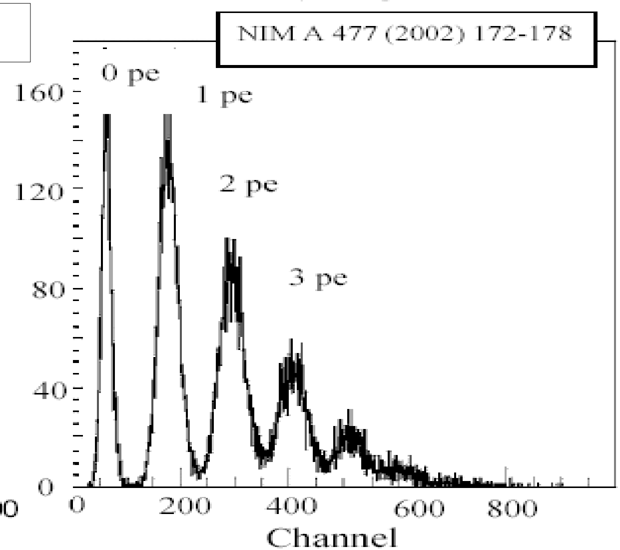

HPD

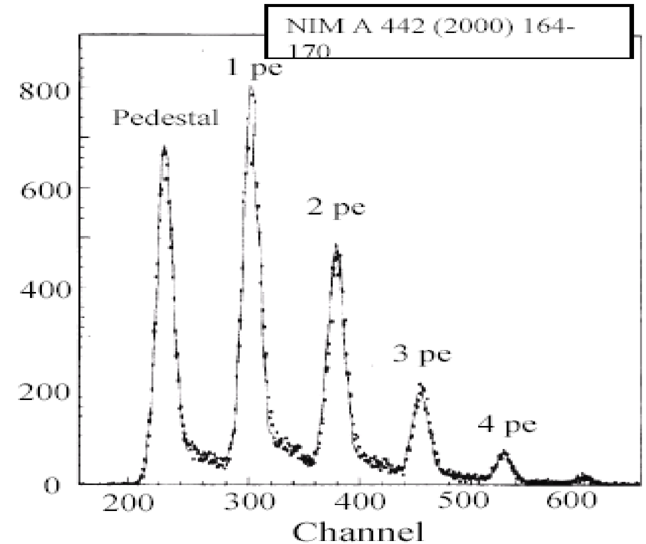

Silicon Photo-Multiplier
- room T
- V~50V

Visible Light Photon Counter
- T=6.5K
- V~5V

Hybrid PhotoDiode
- room T
- V~20000V

Vacuum based Photo-Detectors

Based on two phenomena:

1) photo-emission

2) secondary emission

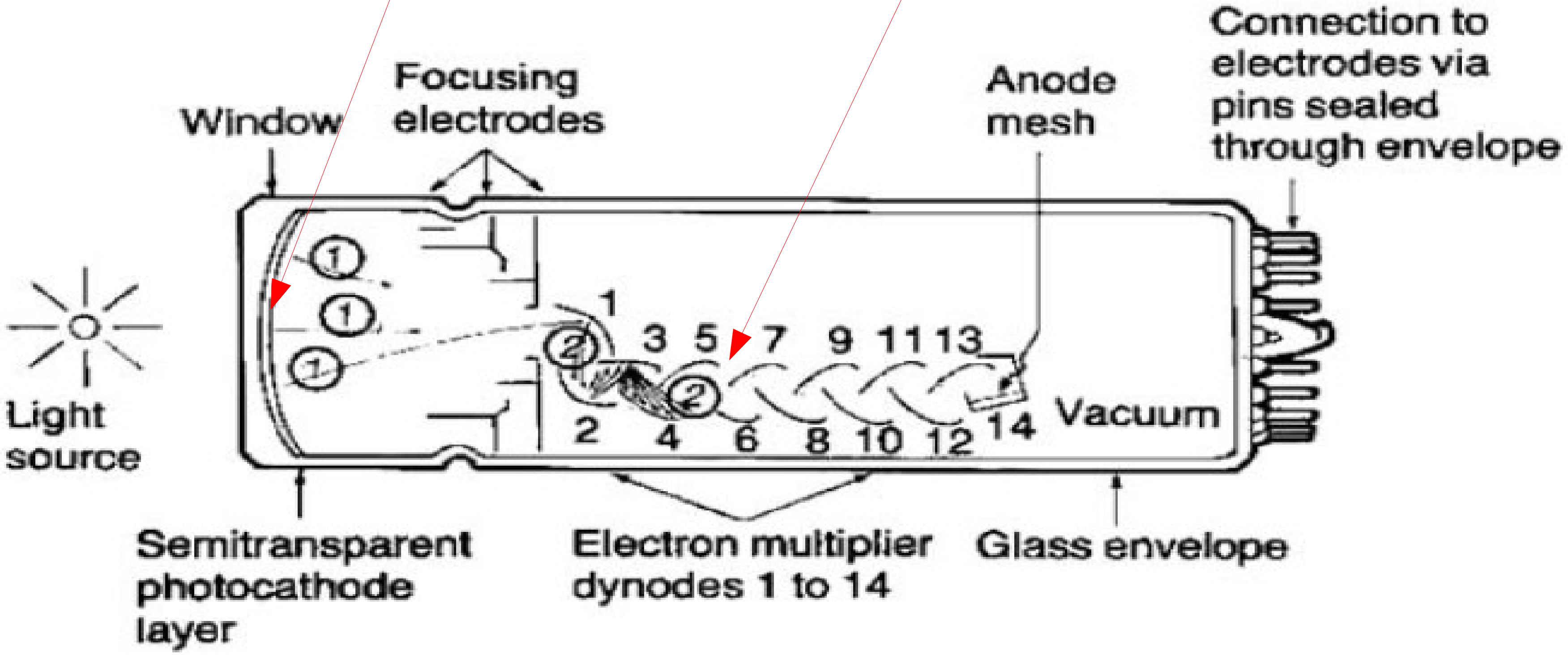

Solid state physics implied

Vacuum PD fundamental parameters

Photo-Detection Efficiency

→ **PDE = QE * CE**
QE = quantum efficiency
CE = collection efficiency

Gain and Signal formation

→ **$G = g_1 g_2 \dots g_n$**
g_n = single stage gain

Noise sources

→ **Dark count**
→ **After-Pulsing**

fluctuations in measurement of

- **Amplitude** (number of photons)
- **Position** (photon impact position)
- **Timing** (photon arrival time)

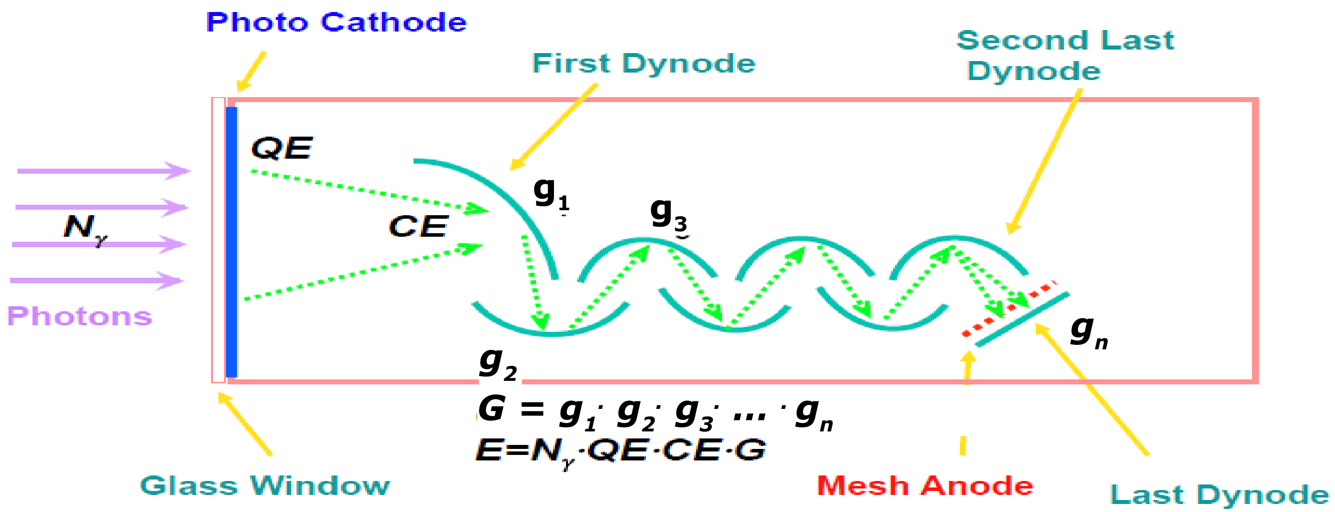

Photo Detection Efficiency (PDE)

$$\frac{\#\text{emitted photo-electrons}}{\#\text{incident photons}} \qquad \frac{\#\text{ph.e captured by } 1^{st} \text{ dynode}}{\#\text{emitted ph.e}}$$

$$PDE = QE \times CE$$

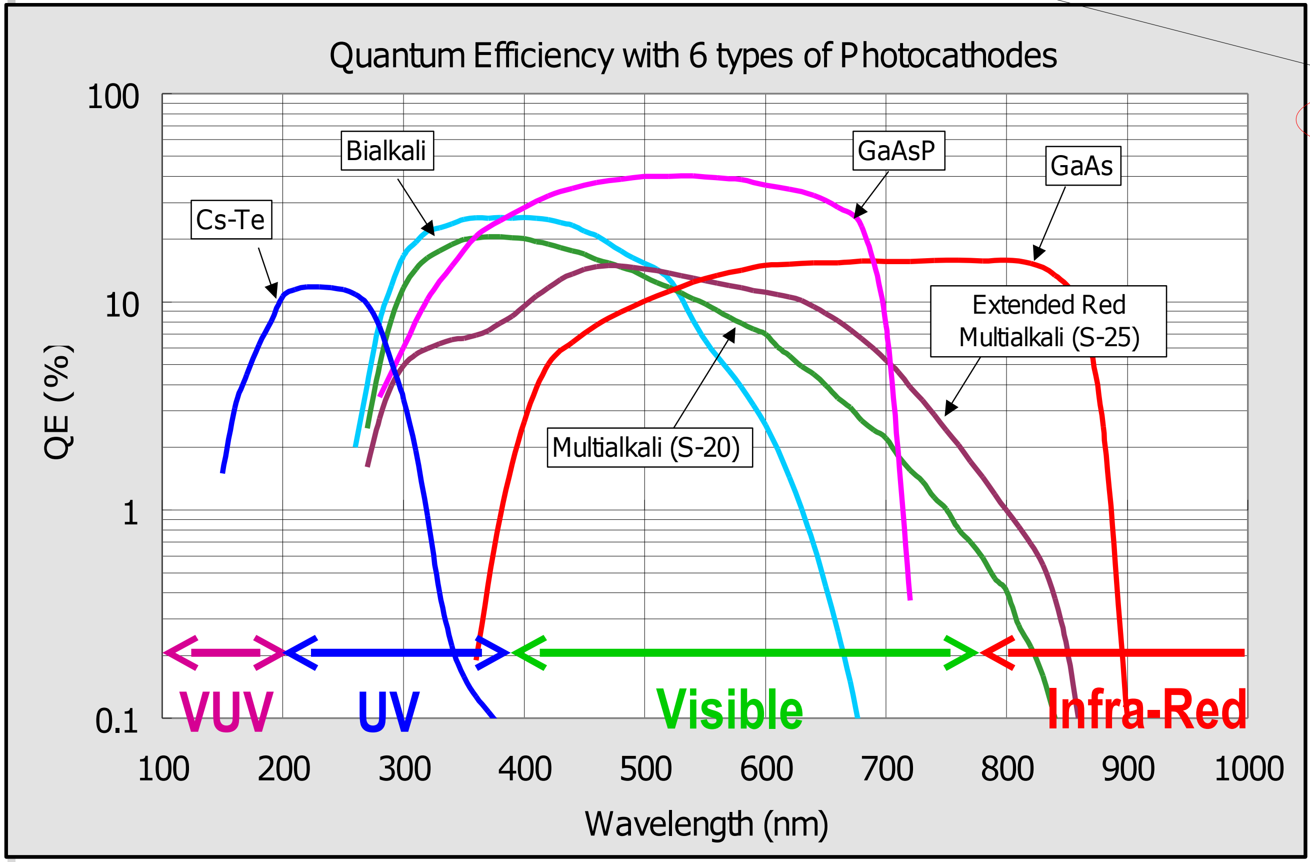

Photo-cathode determines

- quantum efficiency QE(λ)
- angular and energy distribution of 1st photo-electron
- noise behavior
- timing fluctuations (contrib.)

Photo-cathode: most crucial element in any PMT type
→ relatively complex working principles
→ complex construction → still **room for improvement** !
→ since last 10 years revived interest in R&D for new photo-cathodes

Photo-emission: a bulk process in 3 steps

W.E.Spicer, Phys. Rev.112 (1958) 114

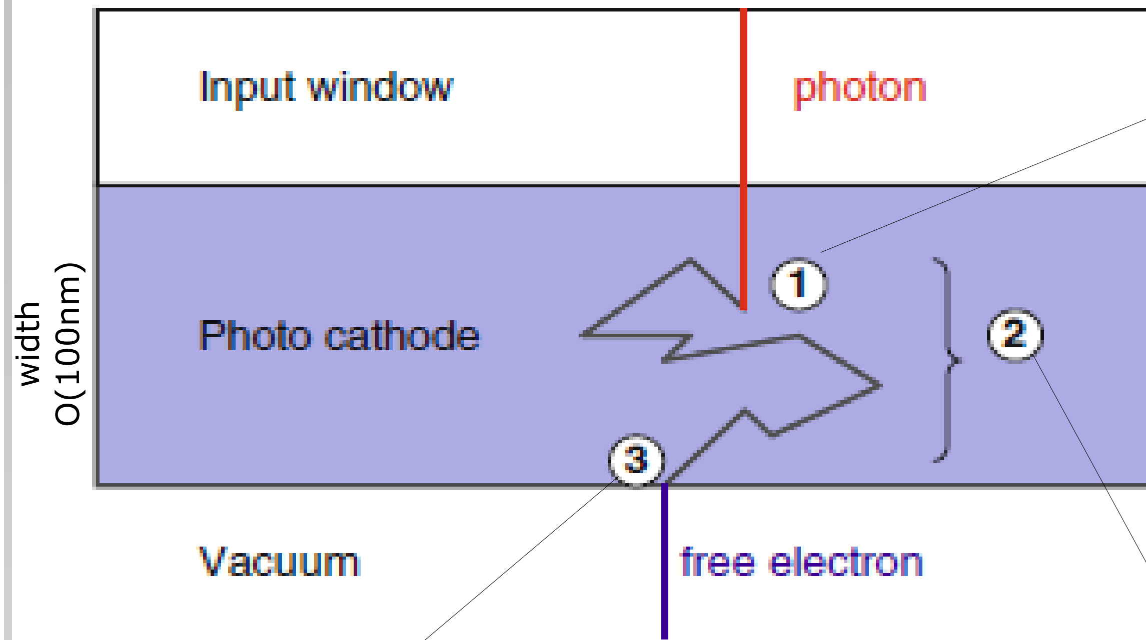

Absorption and Excitation

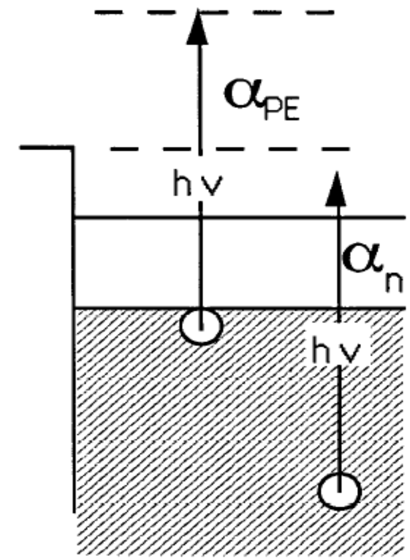

Escape to vacuum

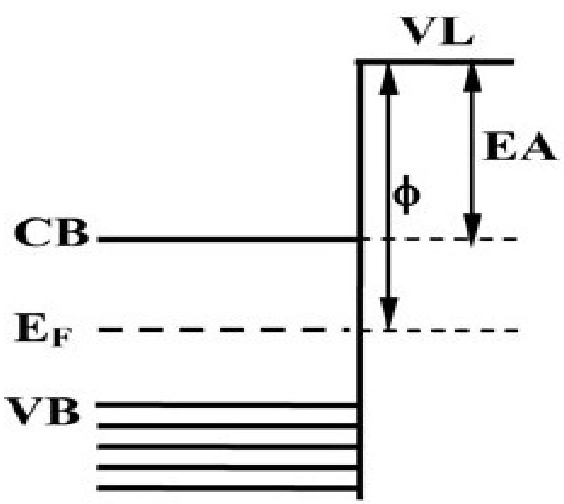

Transport

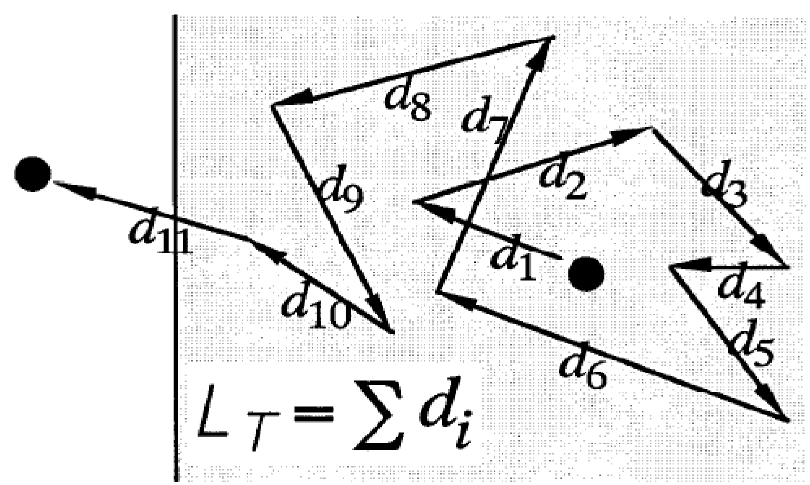

Photo-emission: a bulk process in 3 steps

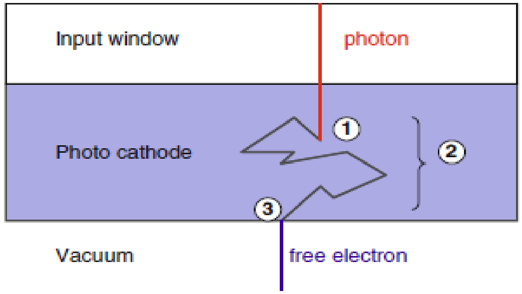

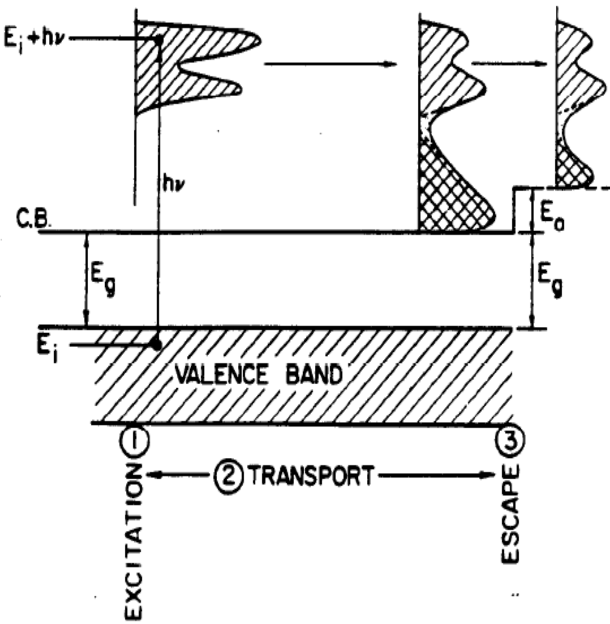

W.E.Spicer, Phys. Rev.112 (1958) 114

$$QE = (1-R)\frac{\alpha_{PE} P_E}{\alpha}\frac{1}{1+{l_a}/{L}}$$

(1)

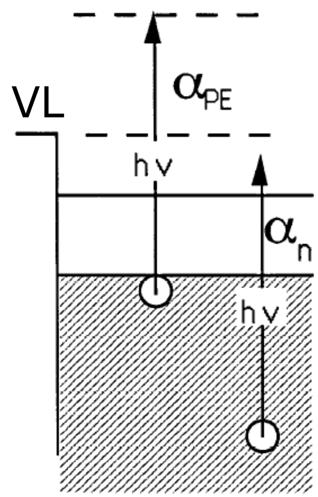

Absorption and Excitation

R = reflection coeff. is a function of angle of incidence and polarization

α_{PE}/α = fraction of the electrons that are **excited above the vacuum level** (VL)

(2)

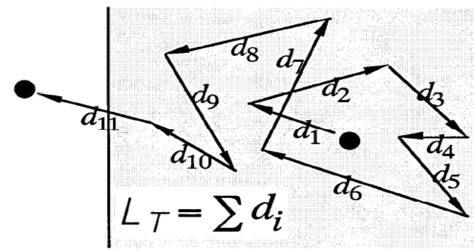

Transport

from conversion location to vacuum interface by **diffusion.** In presence of band bending (BB) near interface then also **drift** (outward BB help escape)

During transport :
1) E loss (**thermalization**) down towards bottom CB by scattering (hundreds of collisions)

2) Electron **losses** due to:
• trapping due to inward BB at vacuum interface or outward BB at window itface
• **recombination** due to impurities (cristallinity is a crucial factor)

l_a/L = photon absorption length over electron scattering length (wide range 1-10⁴) The lower l_a/L the less recombination

(3)

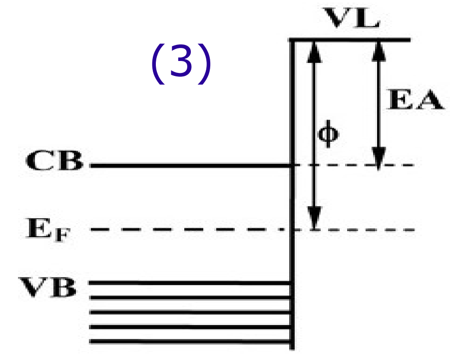

Escape to vacuum

P_E = fraction of electrons that reach the surface keeping sufficient energy E to escape (usually P_E <0.5)

E > electron affinity (E_A)

EA = E vacuum – E CB bulk (work function for metals)

Longest wavelength cutoff in QE due to Ebandgap + EA

Special semiconductor threatment → negative EA

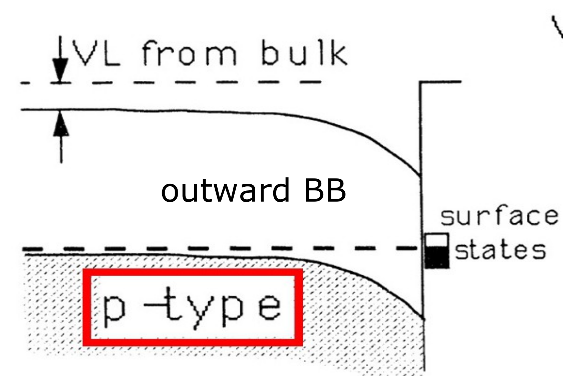

Photo-cathodes

Most efficient bulk material for **photo-cathode are semiconductors**

Metal photo-cathodes show much lower QE than Semiconductor due to:

- energy-momentum conservation forbid absorption on free e^- in CB
  → high reflectivity

- electrons suffer e-e scattering → escape depth L very short (large l_a/L)
  NOTE: in semiconductors e-e is not allowed for optical excitations due to band-gap → only energy loss via electron-phonon → small l_a/L

- work function ϕ > 2eV (metals) compares with smaller affinity
  E_A (few 0.1eV) or (even better) negative in semiconductors (NEA)

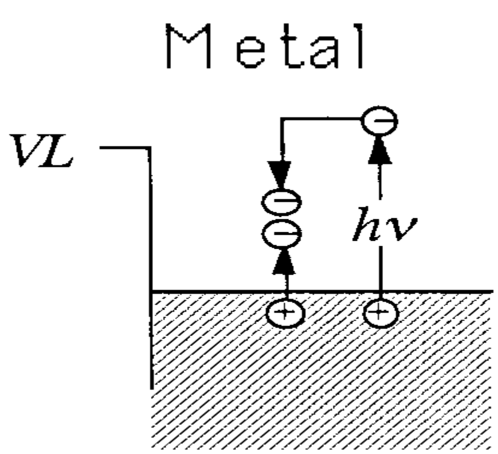

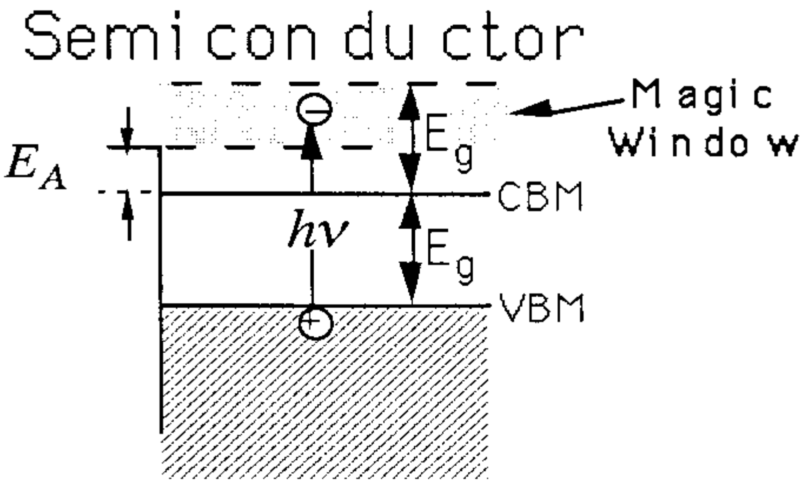

W.E.Spicer, A.Herrera-Gomez SLAC-PUB-6306 (1993)

Photo-cathodes – Negative Electron Affinity

Cesium (Cs) plays a large role for NEA:

1) band bending (BB) through donor surface states → vacuum level shifted down
- Cs-induced donor-like surface states contribute their electrons to the bulk
- Hole depleted region (negatively charged acceptors) lead to BB region
  → internal built-in electric field (acceletation in BB region)

2) dipole surface layer from polarized Cs atoms
- Majority of Cs atoms become only polarized forming a dipole layer (e- Cs+)
  → external electric field (cusp barrier → tunneling)

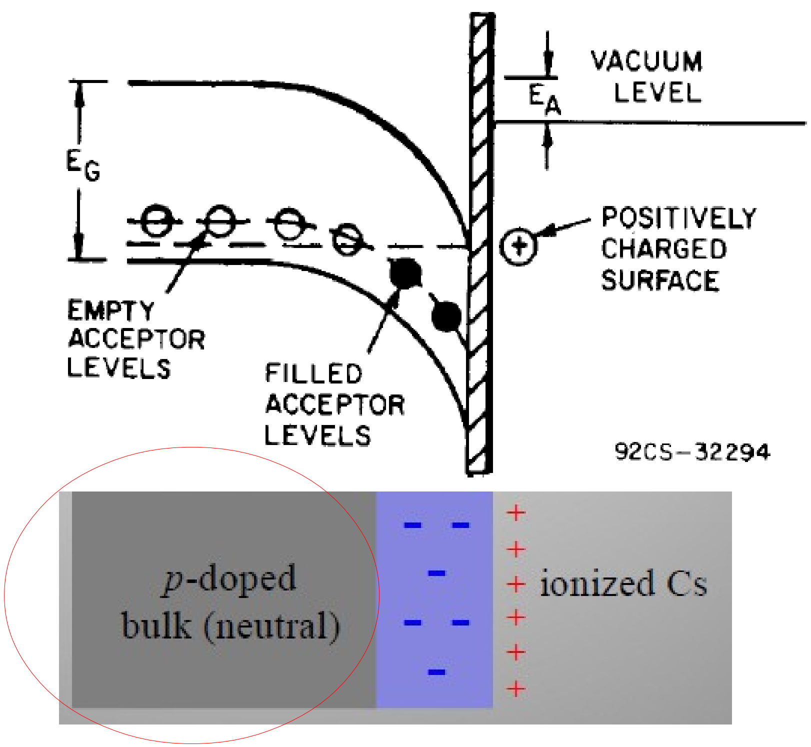

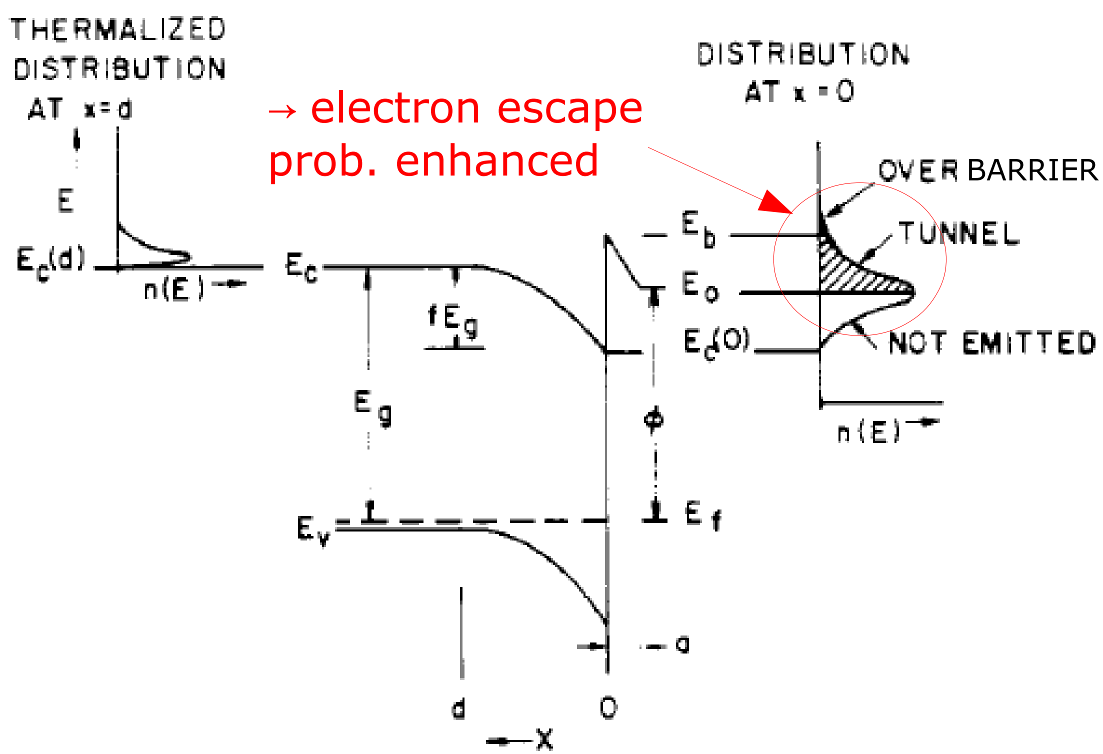

R.Martinelli, D.G.Fisher IEEE Procs 62 (1974)

Most common photo-cathodes

1) Bi/Multi-alkali-antimonides
→ K/Na + Sb in bulk + Cs/Rb at surface
→ poly-crystalline layers w/ high carrier lifetime
→ very good absorbers for photons 200-850nm
eg. Na_3Sb, K_3Sb (Bialkali), Na_2KSb (S20, S25)

Weak points:
- recombination centers in poly-crystalline struct.
- active layer directly deposited on window
  → electron sink due to outward band bending

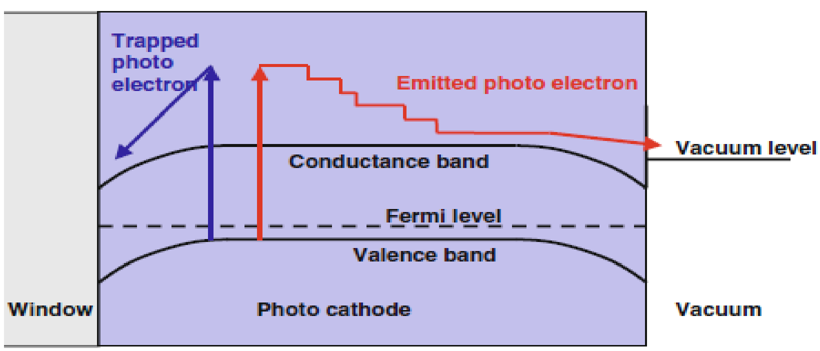

Examples:
- S20 has PEA (cutoff at 820nm)
  only hot e- escape → thin layer (60nm)
  low dark rate (<Khz/cm^2)
- S25 has NEA (cutoff at bandgap, 890nm)
  → thick layer (170nm)
  higher dark rate (10KHz/cm^2)

2) III-V semiconductors
→ GaAs, GaAsP bulk + Cs for NEA
→ very pure mono-crystalline layers
→ easy doping and hetero-junctions

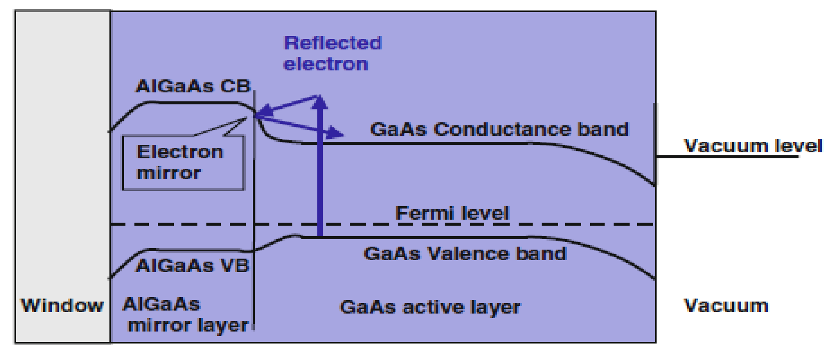

Weak points:
- extreme sensitivity to over-exposure and ion feed-back
- high dark rate (10KHz/cm^2)

Note: alkali metals are very strong oxidizers
→ the smallest amount of O_2 or H_2O totally burn any cathode
→ ultra high vacuum (10^{-9} mbar) needed

Future photo-cathodes

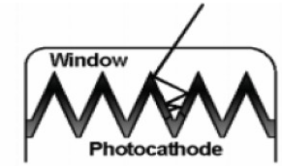

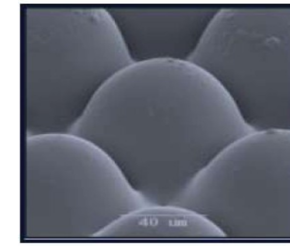

1) Search for new photo-cathode (PC) materials
- bi- and multi-alkali revisited (eg. Li_2CsSb)
- III-Nitrides (eg. GaN, $Al_xGa_{1-x}N$)
- II-VI (eg. ZnO, $Zn_{1-x}Mg_xO$)

2) Electron emission enhancement
- Piezo-electrically enhanced photo-cathodes (no Cs;in air)
- Electric field assisted emission
- anti-reflecting structures (nano-wires)

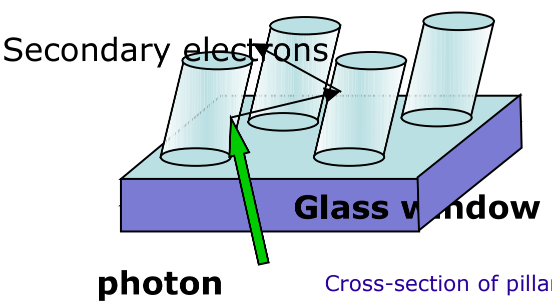

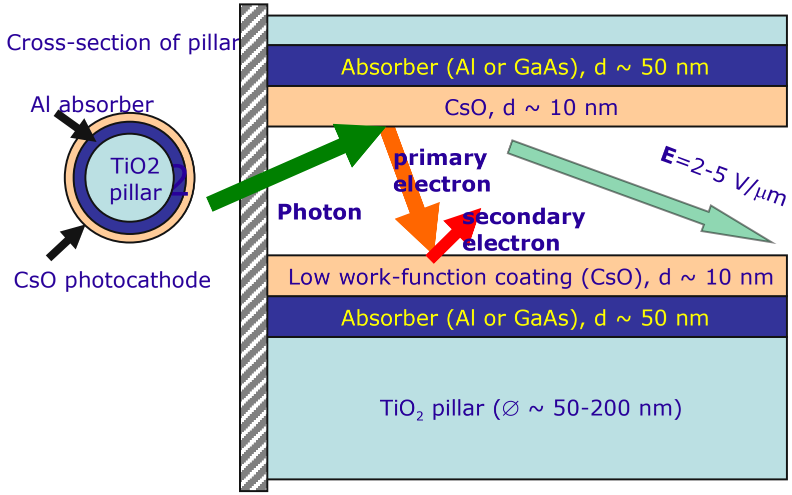

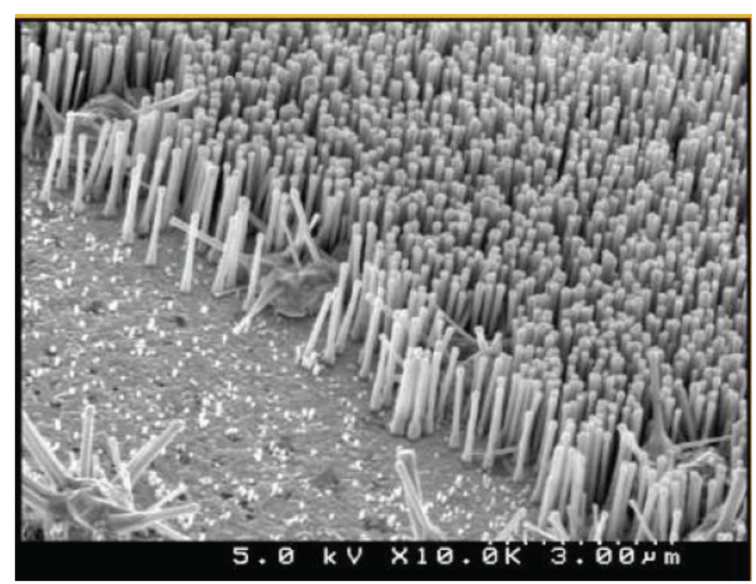

Photocathode Workshop
University of Chicago July 2009
http://psec.uchicago.edu/photocathodeConference/

Spectral Sensitivity - Quantum Efficiency

long wavelength limit caused by
the photoemission threshold of the material
(shape fits the Spicer model, see spares)

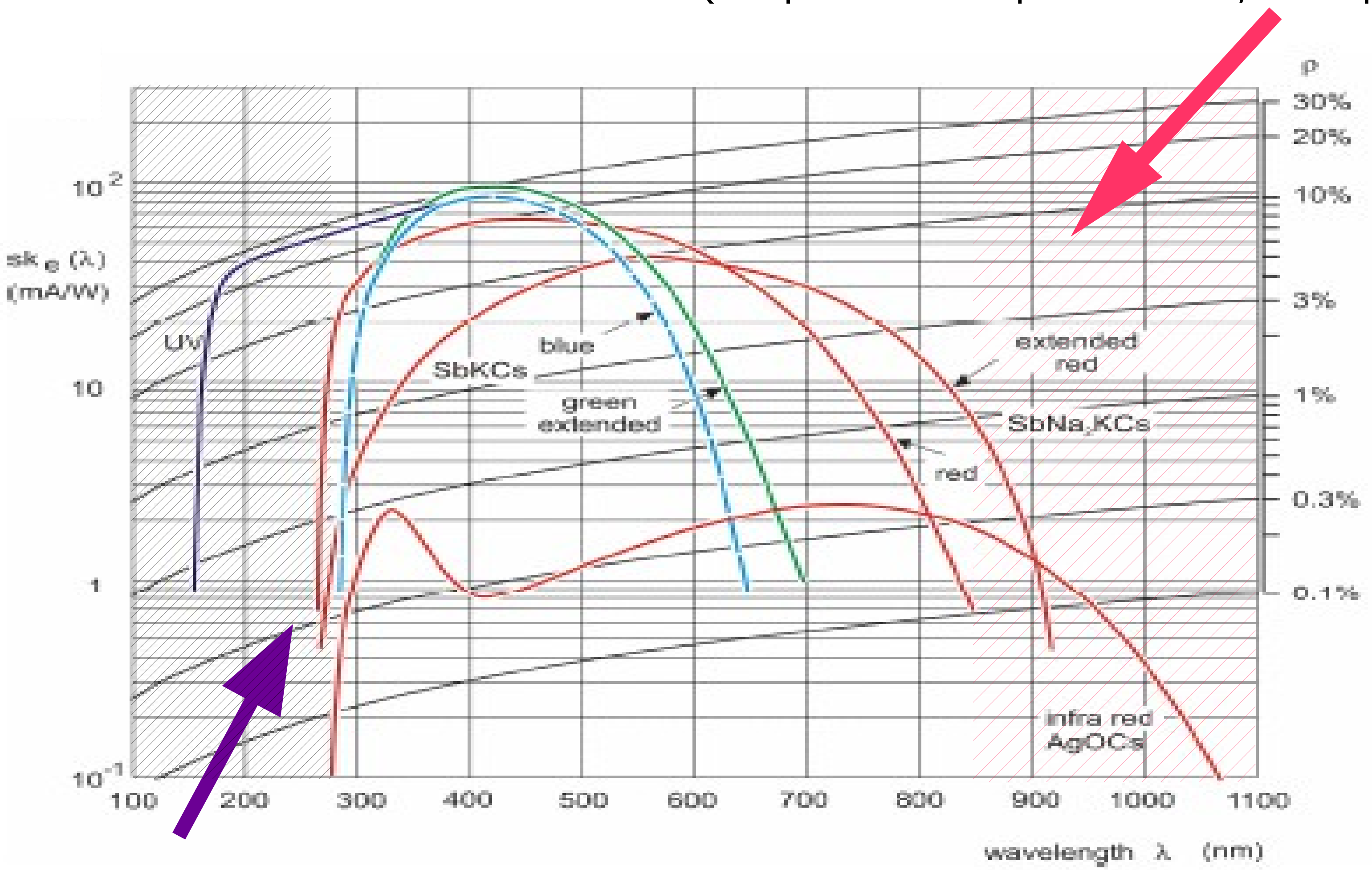

short wavelength limited by
the input window material of the photomultiplier

Transmission of optical windows

2 types of losses:

• Fresnel reflection at interface air/window and window/photocathode
$R_{Fresnel} = (n-1)^2 / (n+1)^2$ n = refractive index (wavelength dependent!)
$n_{glass} \sim 1.5$ $R_{Fresnel} = 0.04$ (per interface)

• Bulk absorption due to impurities or intrinsic cut-off limit. Absorption is proportional to proportional to window thickness

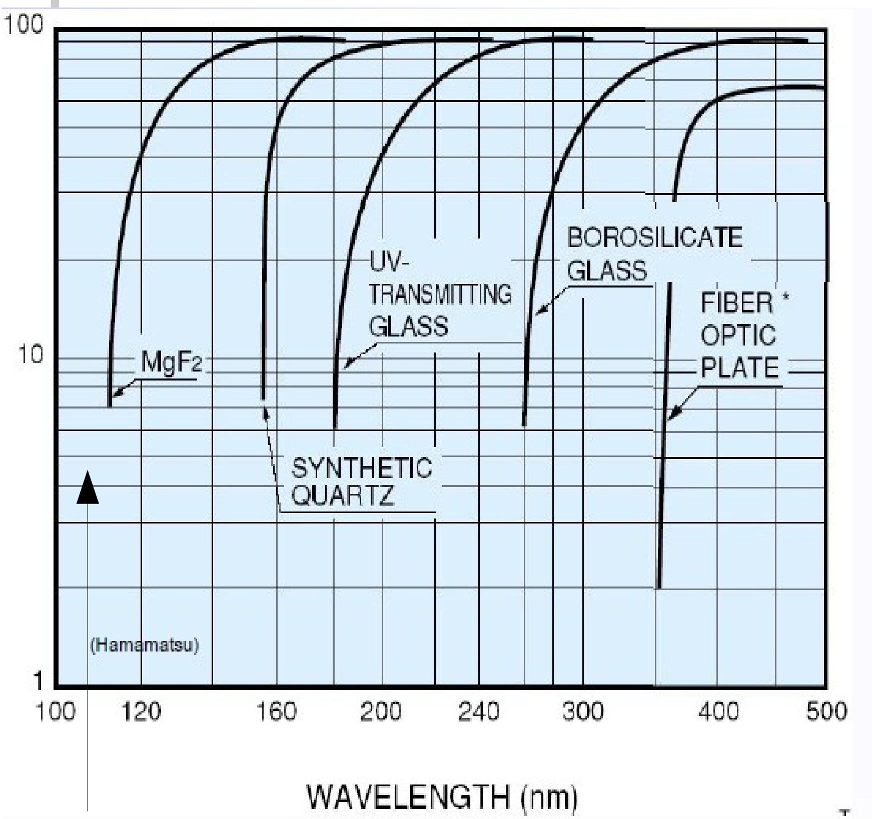

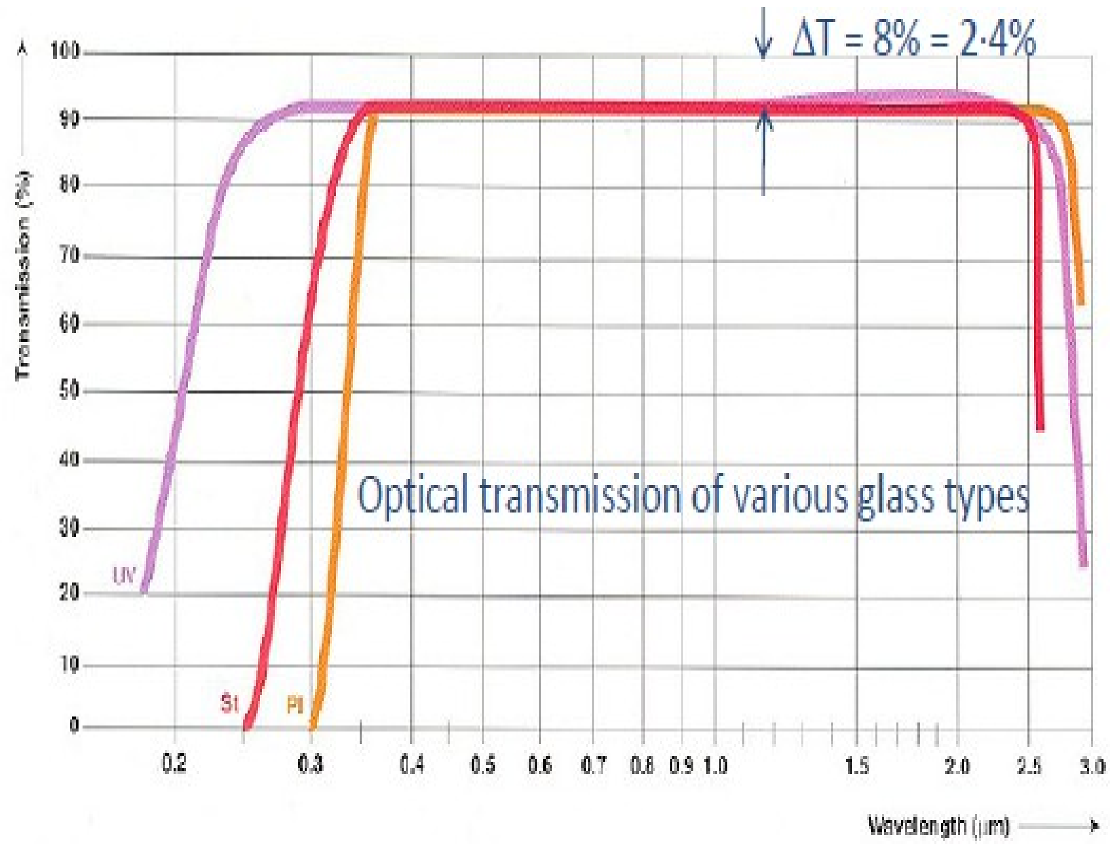

G.C.

transparency below 100nm...

Windows / Substrates

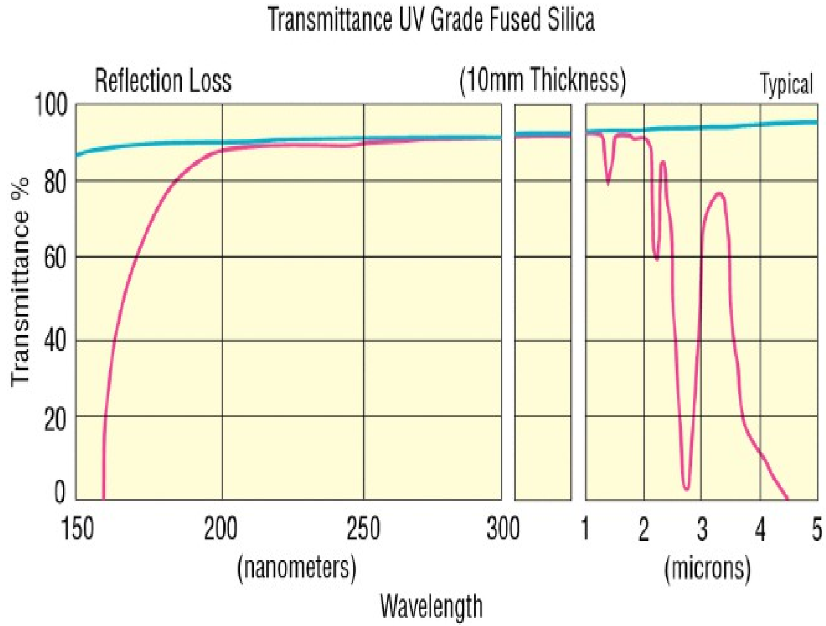

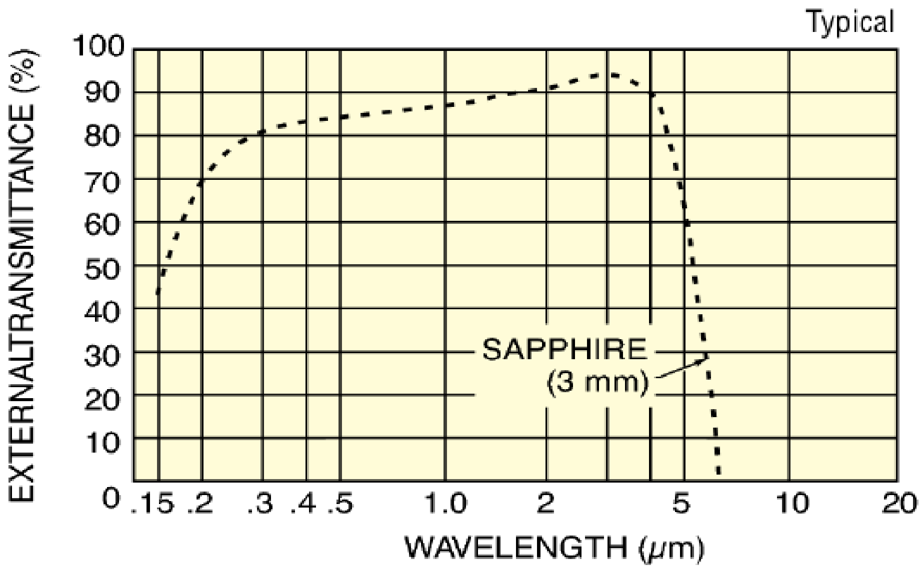

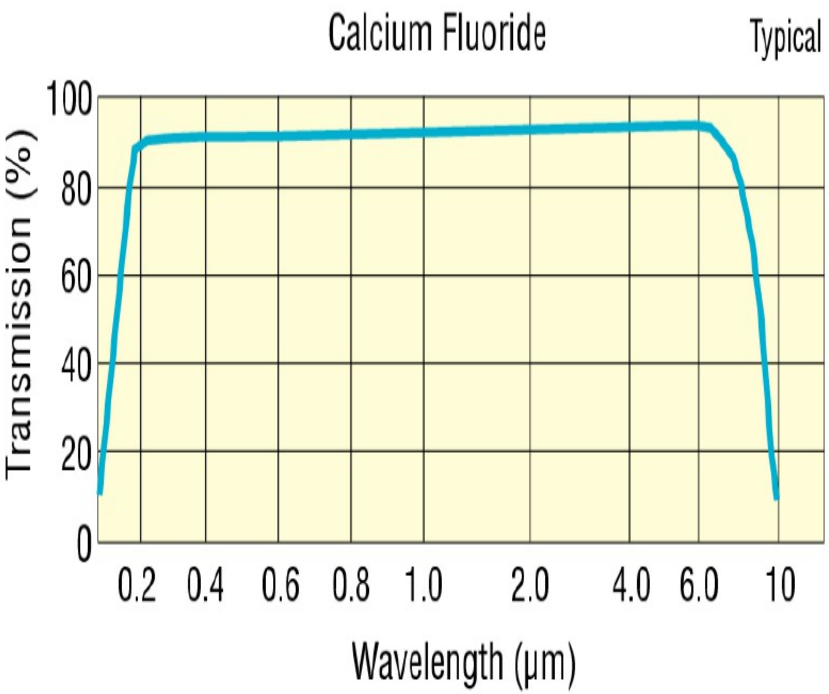

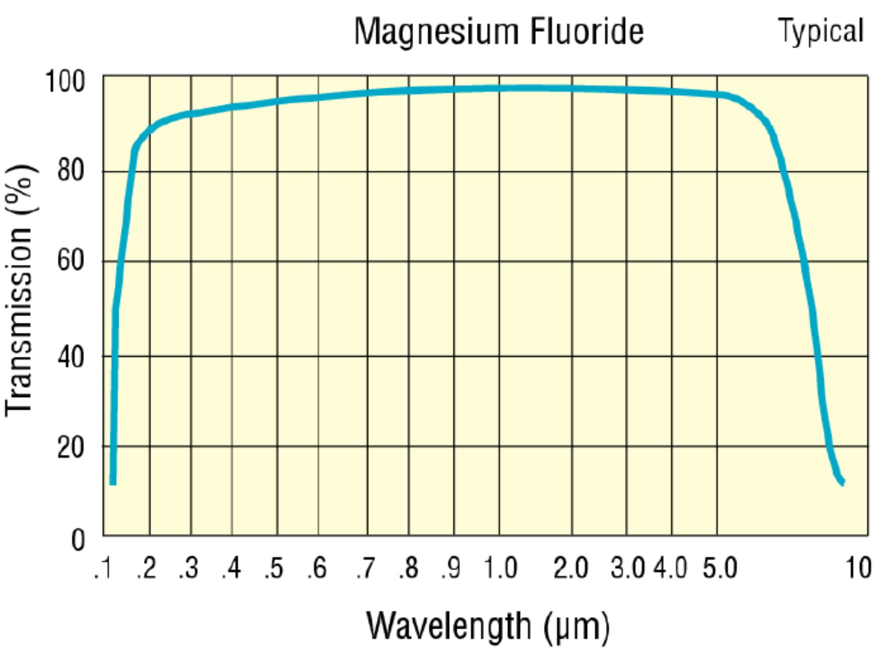

Most recent high QE photo-cathodes

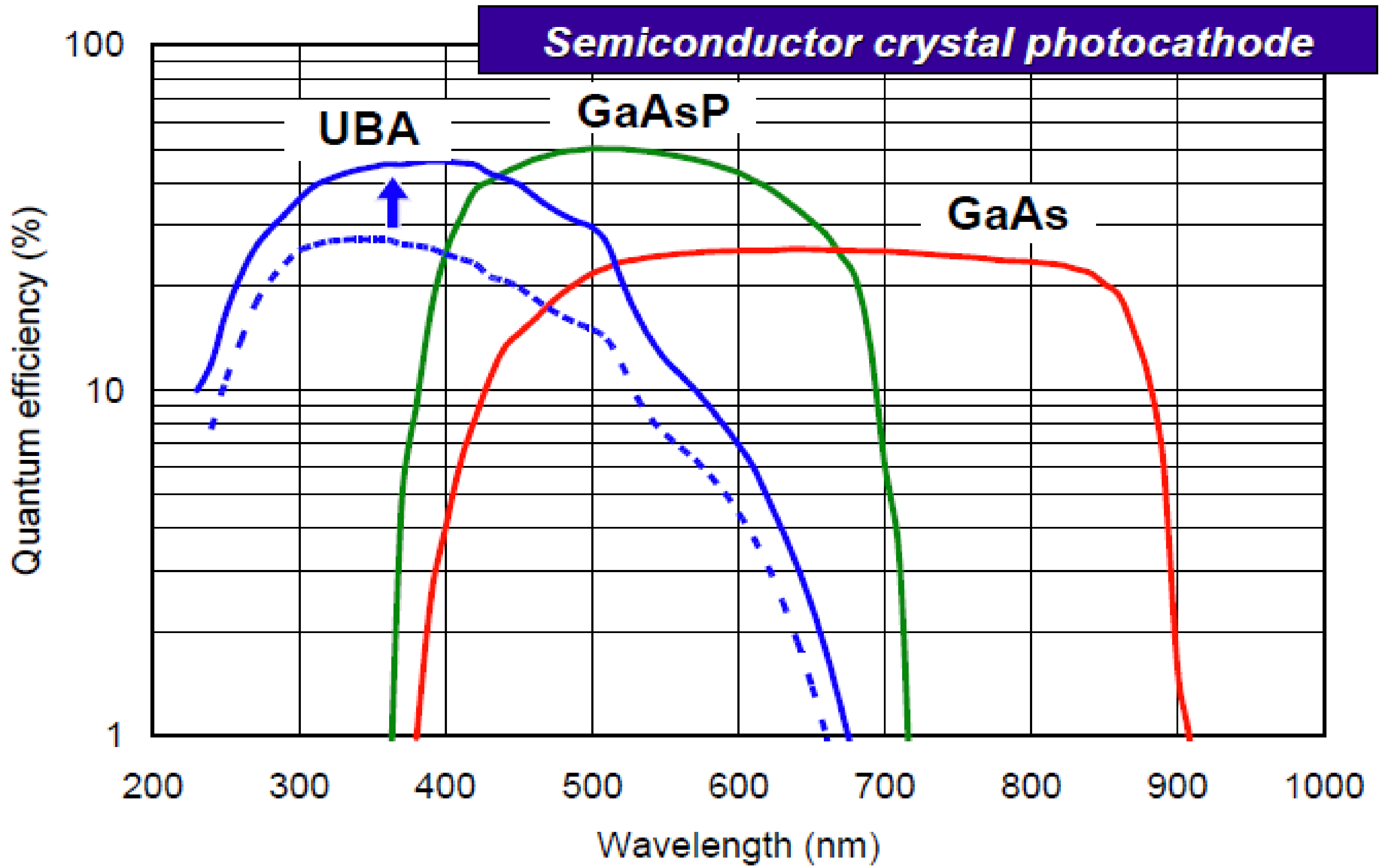

Hamamatsu just says:
"recent improvements in QE due to better crystallinity" ...

Question: how to measure PDE ?
Answer: PDE = QE x CE → measure QE,CE

1) **measure QE** from the ratio of cathode currents I_C for PMT and calibrated detector (known QE)

→ $QE = QE_{cal}\ I_C / I_{C\ cal}$ (All dynodes connected to anode at +100V wrt cathode)

2) **measure CE** from the ratio between single ph.e counting rate $R_{ph.e}$ and cathode current I_C

→ $CE = q_e R_{ph.e} / T / I_C$ (using a calibrated neutral filter when counting single ph.e with known transmission coefficient T)

Example of setup for measuring PDE

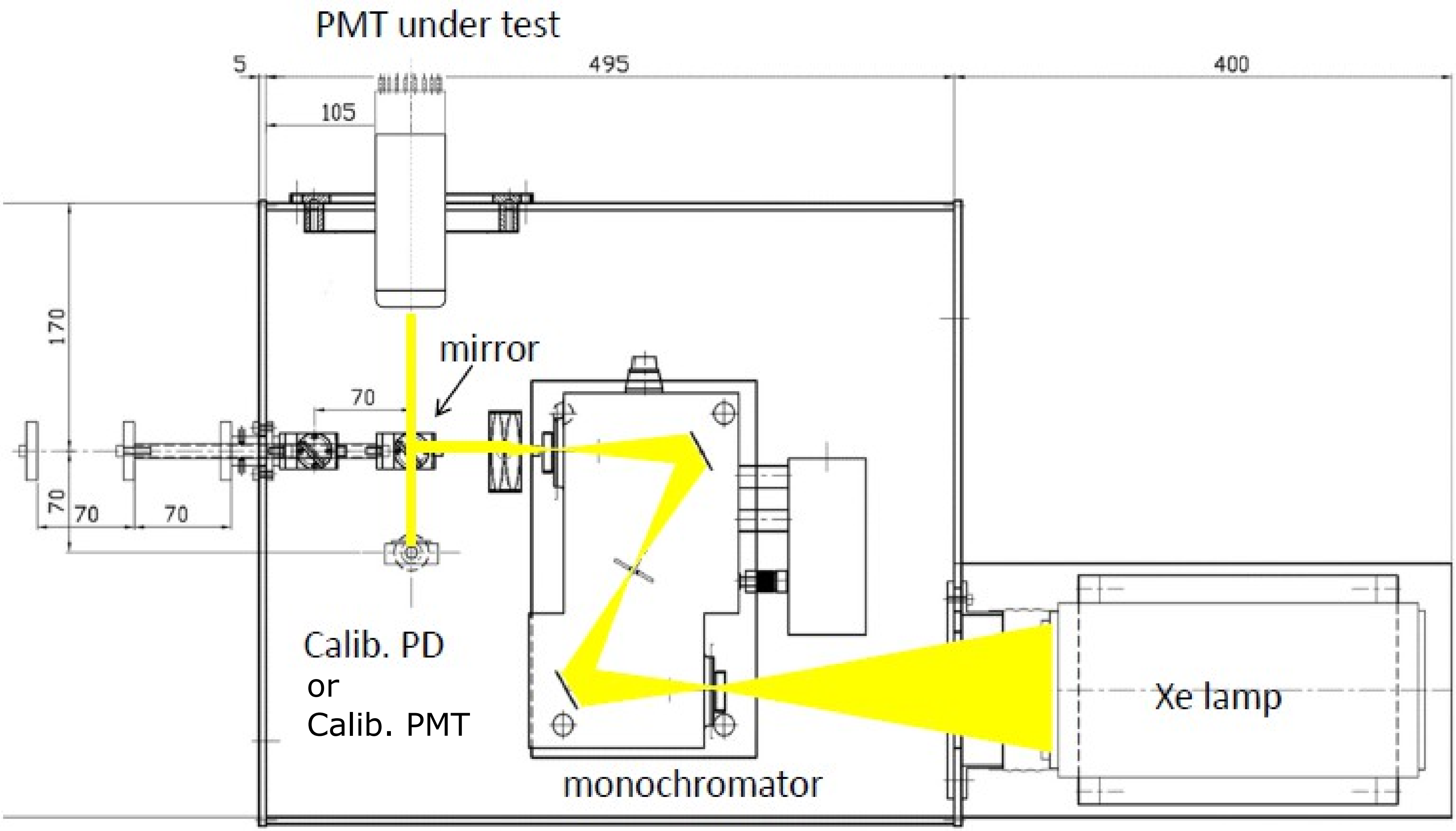

Vacuum PD fundamental parameters

Photo-Detection Efficiency

→ **PDE = QE * CE**
QE = quantum efficiency
CE = collection efficiency

Gain and
Signal formation

→ **$G = g_1 g_2 \dots g_n$**
g_n = single stage gain

Noise sources

→ **Dark count**
→ **After-Pulsing**

fluctuations in measurement of

- **Amplitude** (number of photons)
- **Position** (photon impact position)
- **Timing** (photon arrival time)

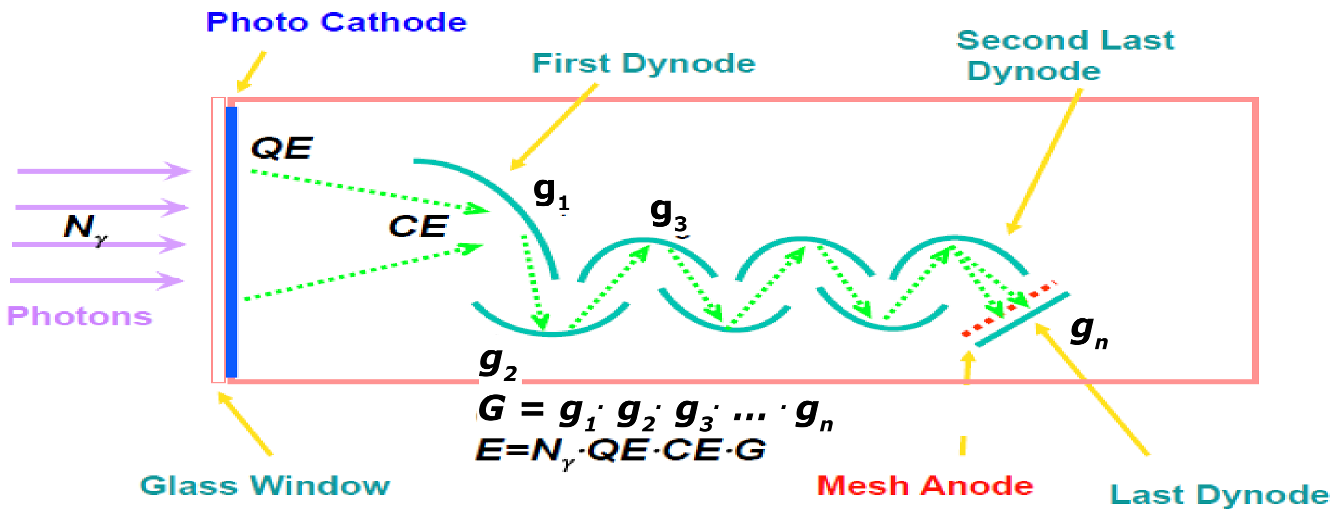

Gain mechanisms: electron multiplication

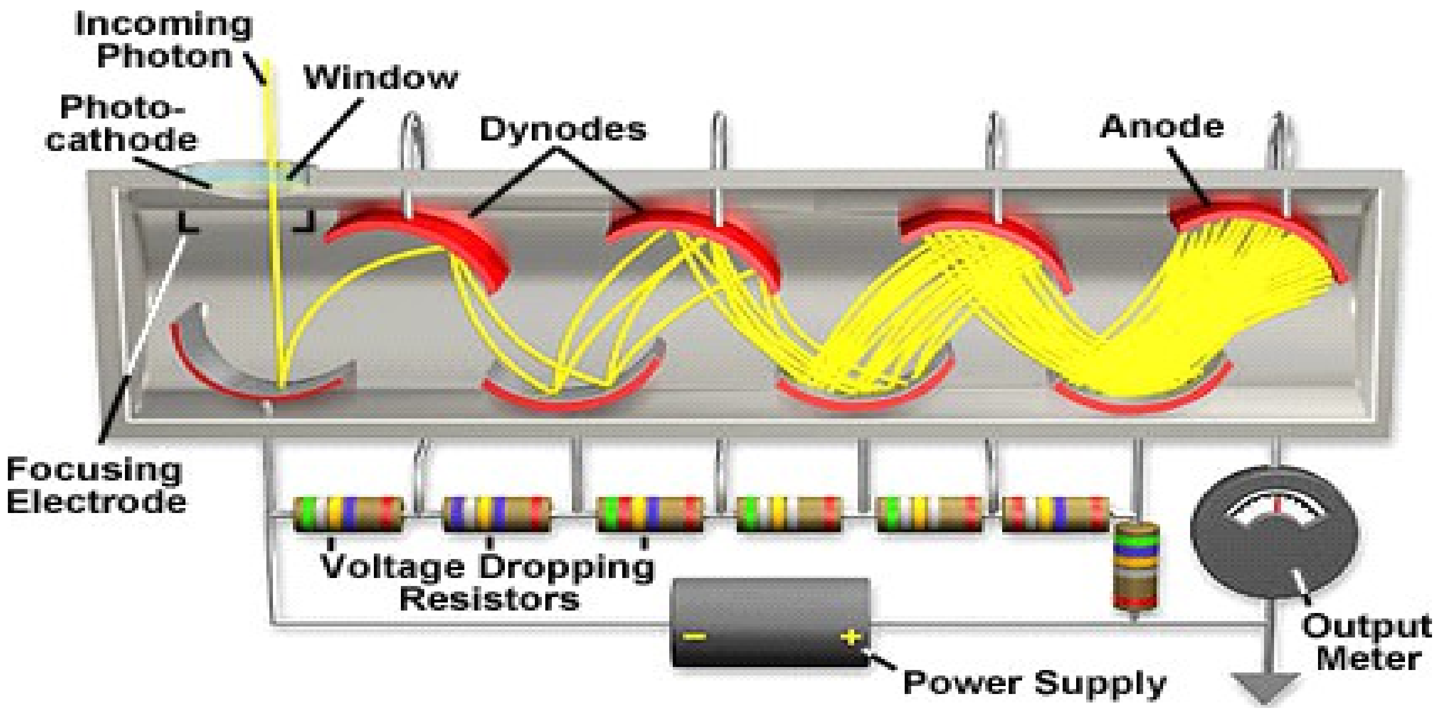

Potential difference between adjacent dynodes typically
→ΔV ~ 100V

Secondary emission from n dynodes → photo-electron multiplication

$$\text{Gain} = \frac{\#\text{electrons delivered to the anode}}{\#\text{ph.e captured by } 1^{st} \text{ dynode}}$$

dynode gain g~3-50 (function of incoming electron energy)
→ total gain $\mathbf{G = g_1 g_2 \ldots g_n \sim g^n}$

Example: 10 dynodes with g=4 → $g = 4^{10} \sim 10^6$

Secondary electron multiplication

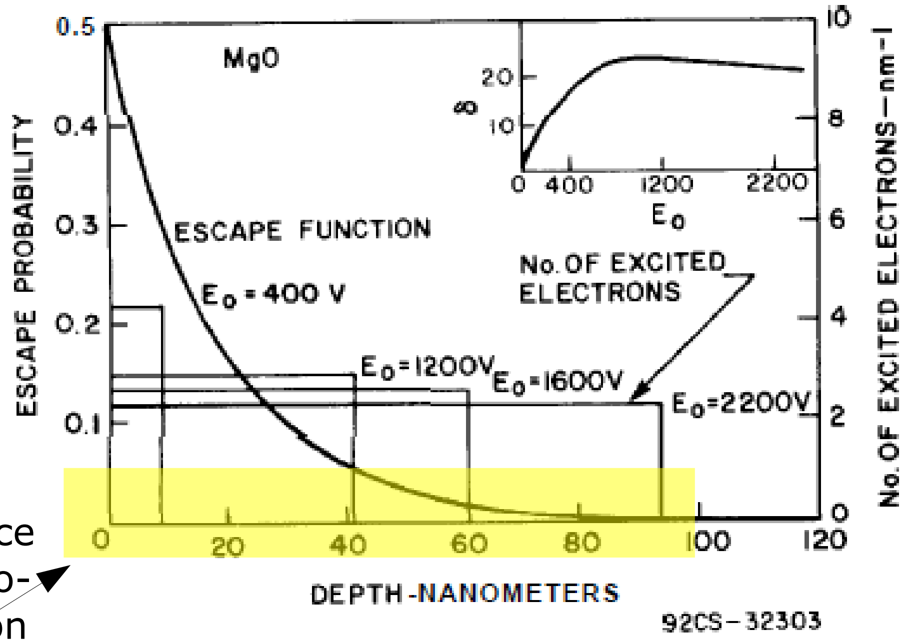

surface pheno-menon

Process in 3 steps (again):

1) absorbed primary electrons impart energy to electrons in the material (depending on their energy, primary electrons may back-scatter)
2) energized electrons diffuse through the material
3) electrons reaching the surface with sufficient excess energy escape into the vacuum

Steps 2 and 3 are similar to photoemission:
→ **best materials are semiconductors (activated by Cs)**
→ **NEA improves secondary production**

$g \sim HV^{\alpha} \rightarrow G \sim HV^{\alpha n}$ g = dynode gain
α = 0.65-0.75

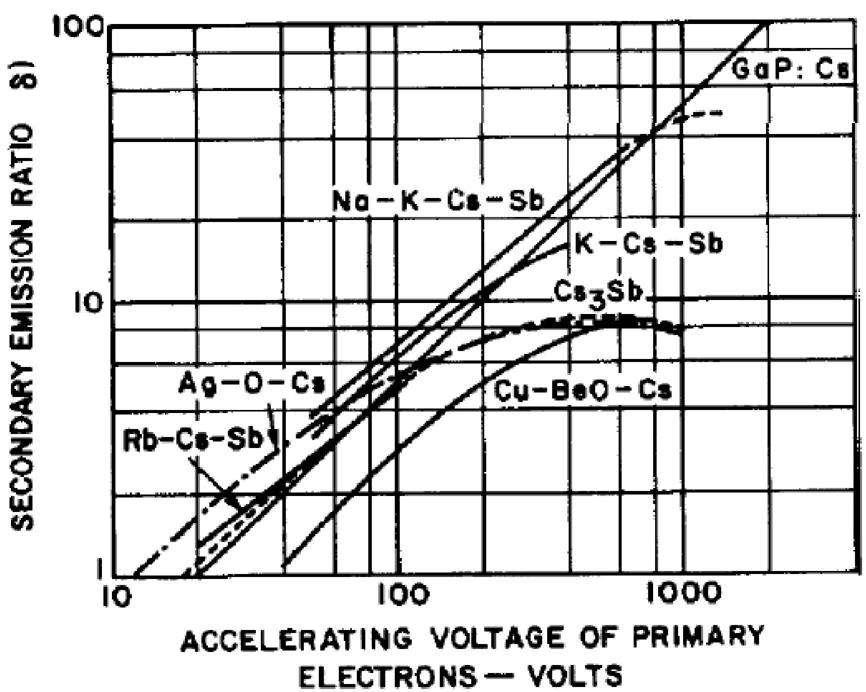

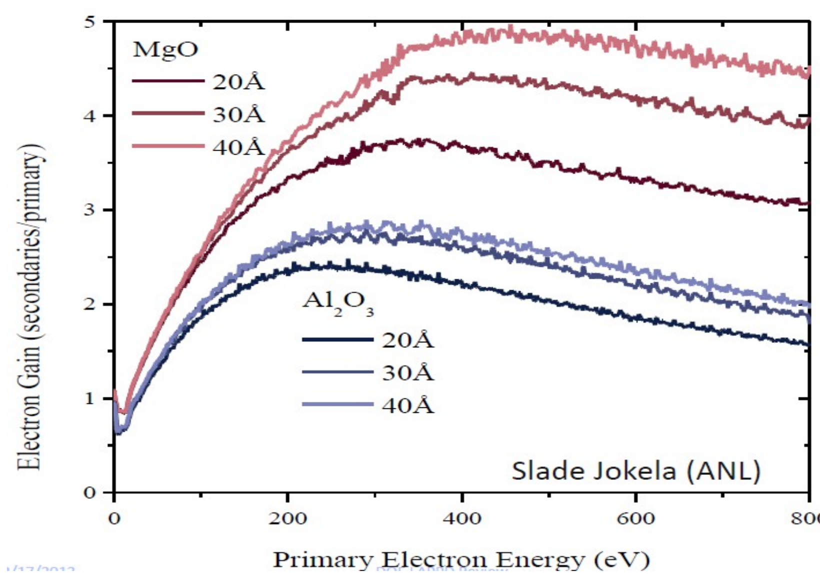

Electron multiplier types

discrete multiplication

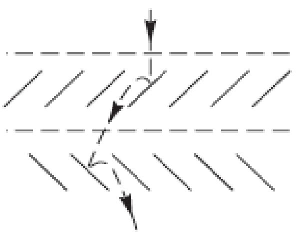

venetian blind

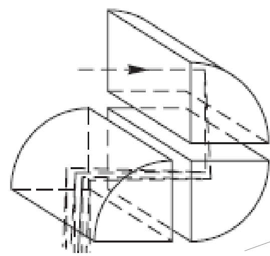

box & grid

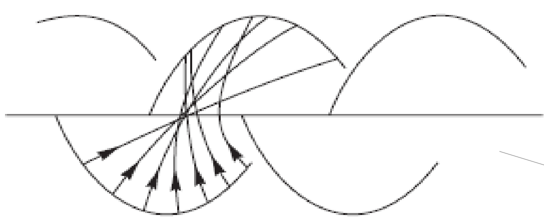

linear focus

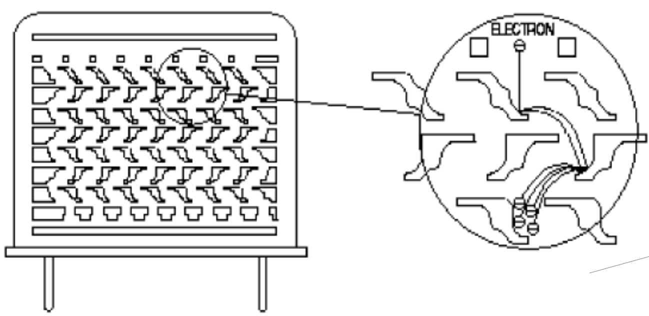

metal channel

PDE (CE)	Gain stability	Timing	B field immun.

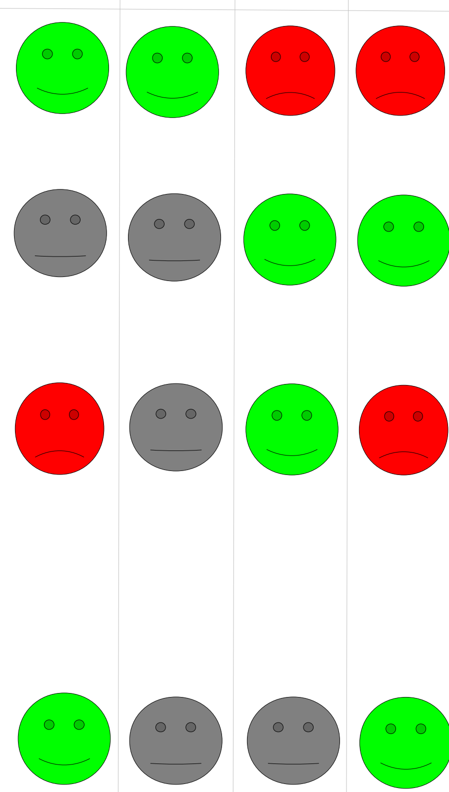

continuous multiplication

micro-channel plate (MCP)

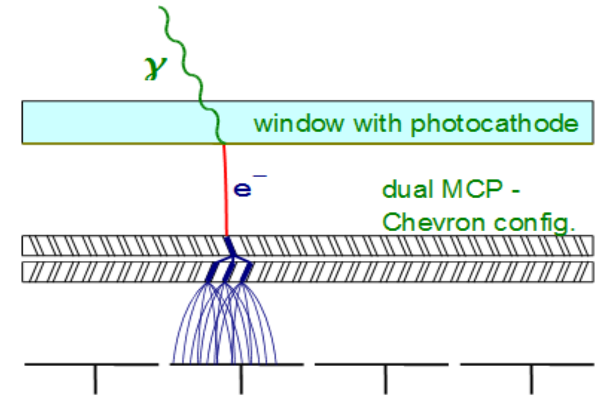

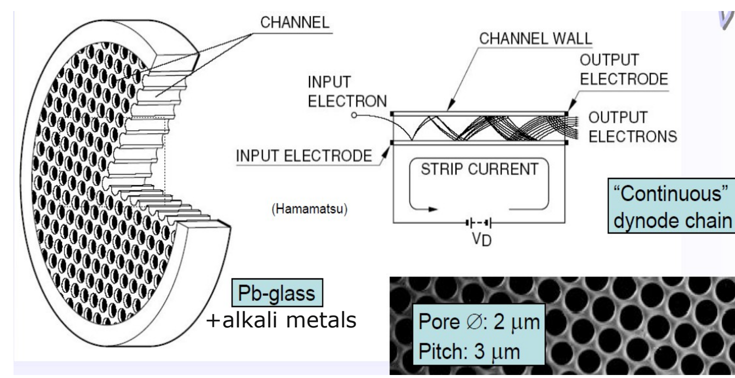

Pore length: 400µm

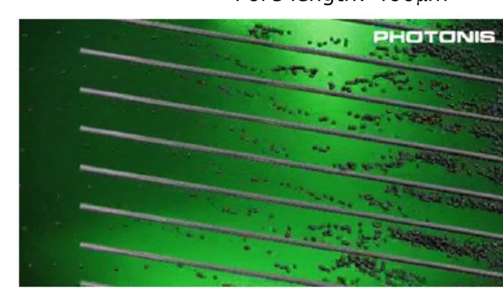

...plus a number of variants...

Electron multiplier: discrete type

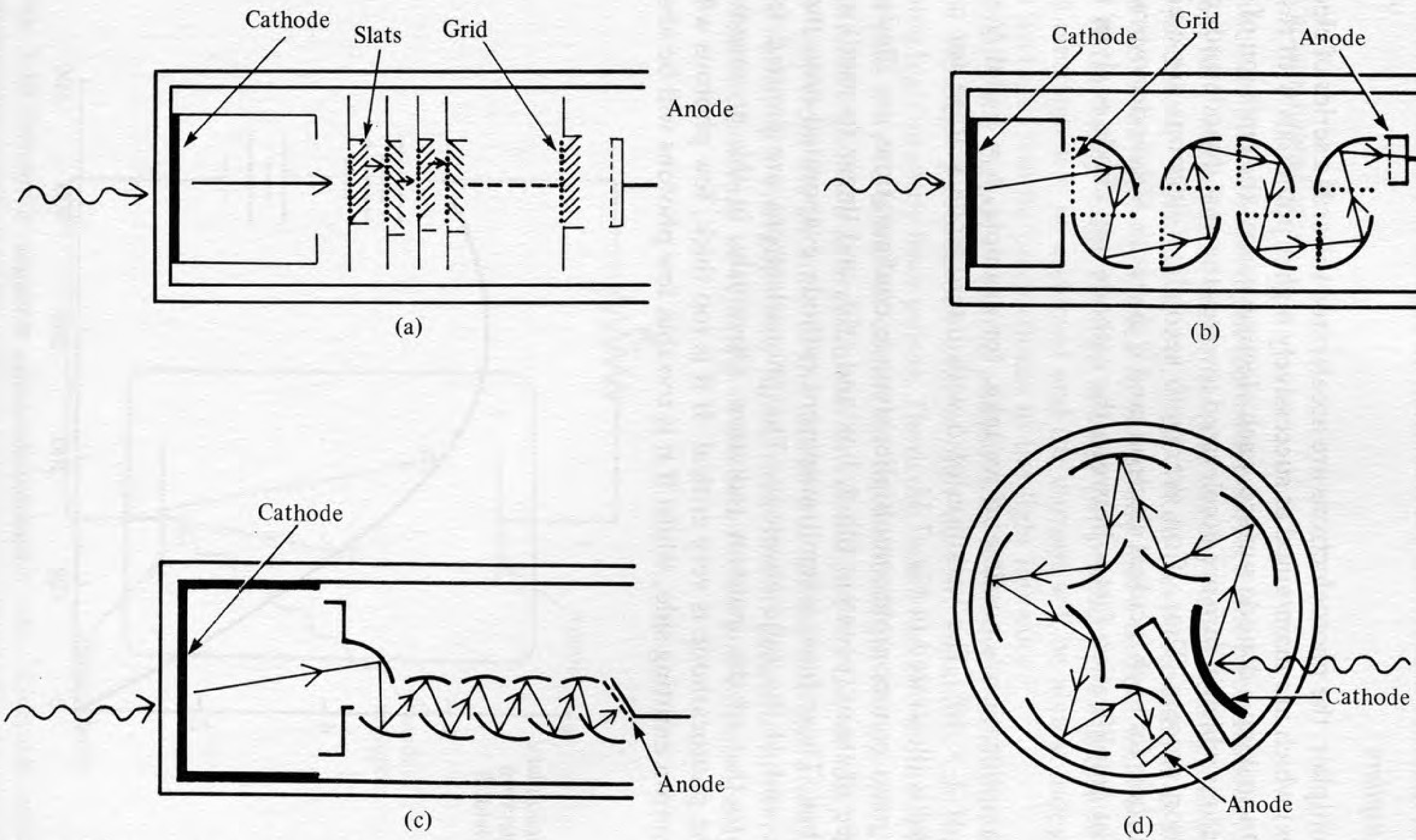

Fig. 7.12 Dynode structures of four common types of photomultiplier: (a) venetian blind, (b) box and grid, (c) linear focused and (d) circular cage focused. Typical trajectories of an electron through the systems are also shown.

Electron multiplier: continuous type

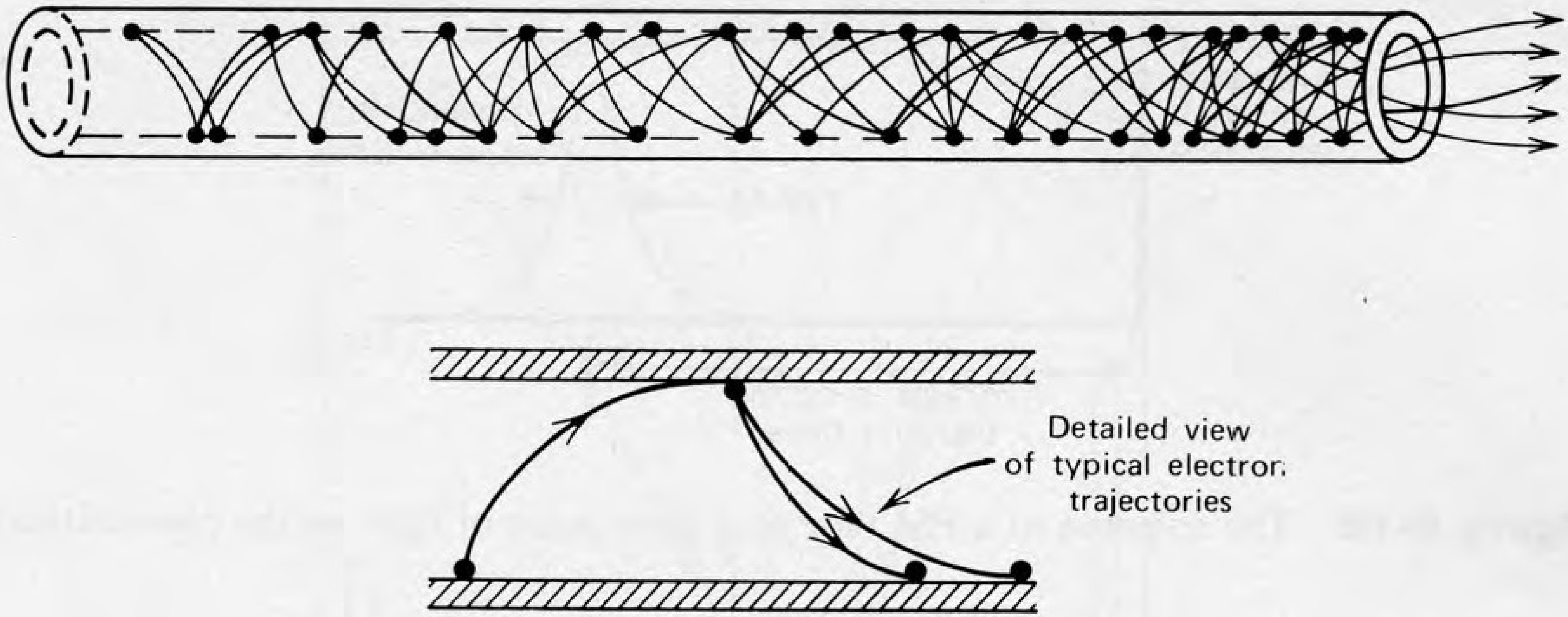

Figure 9-8 Continuous channel electron multiplier.

- Potential difference along length of tube
- Often curved to prevent positive feedback

Pulse formation

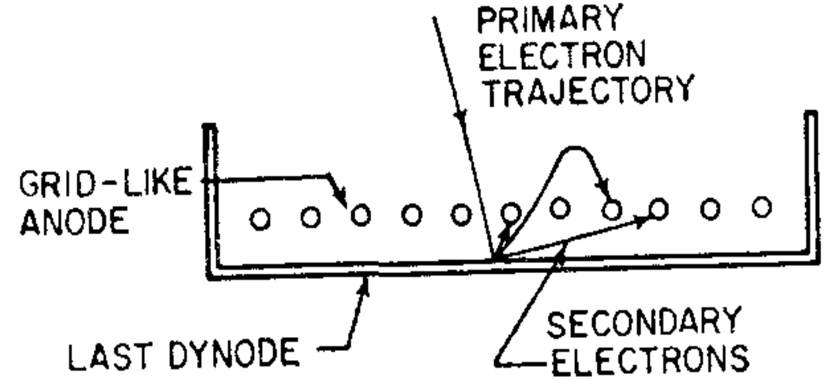

Fig. 21 — The simplest anode structure, a grid-like collector.

Pulse due to current induced by the electron cloud approaching anode

→ use Shockley-Ramo theorem to calculate the pulse shape for each electron: $i = q\,v\,E_w$

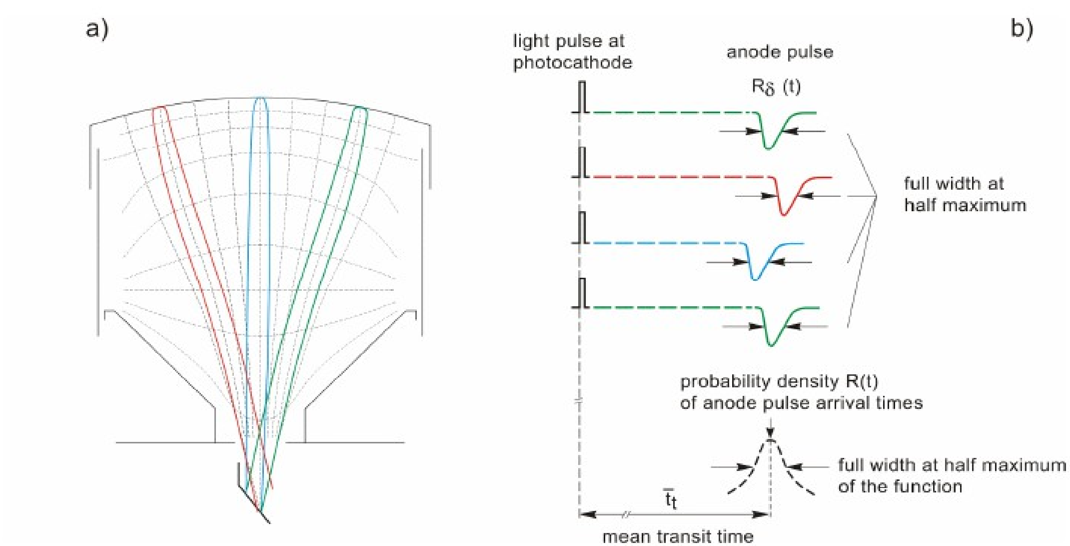

Fig. 4. Photoelectron trajectories and equipotential lines of the electric field in a fast photomultiplier (a). Diagram of an anode pulse transit time spread (b).

Note: timing fluctuations

1) of first photo-electron
→ most relevant

2) of electrons in the cloud
→ less relevant

(see later)

Pulse shape - Basic electrical model

PMT is basically a current source
+ arrangement of inductors, capacitors and transmission lines.

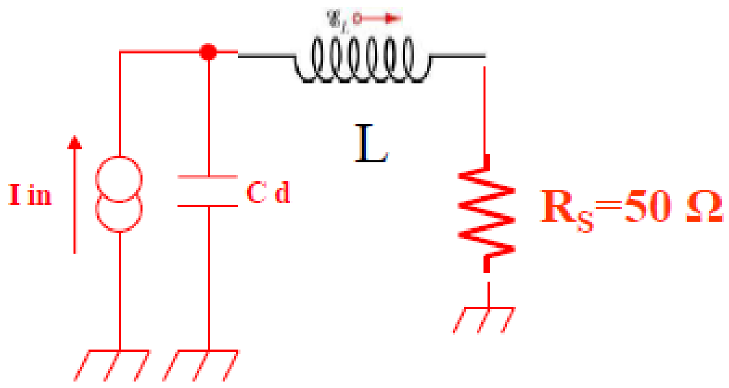

G = 10^5 – 10^7
Cd ~ 10 pF
L ~ 10 nH

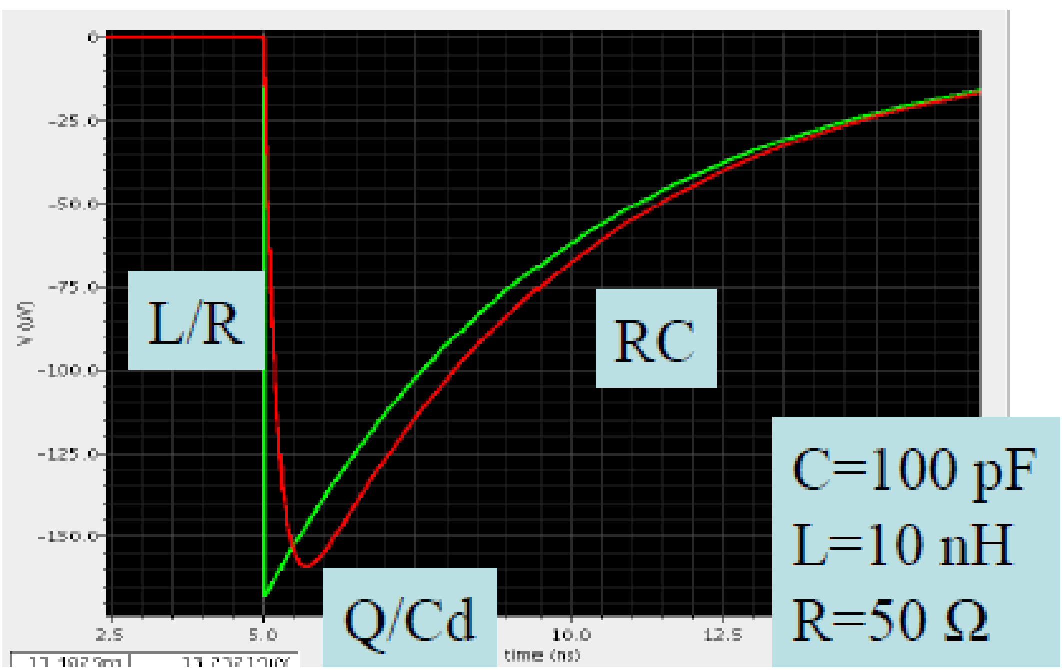

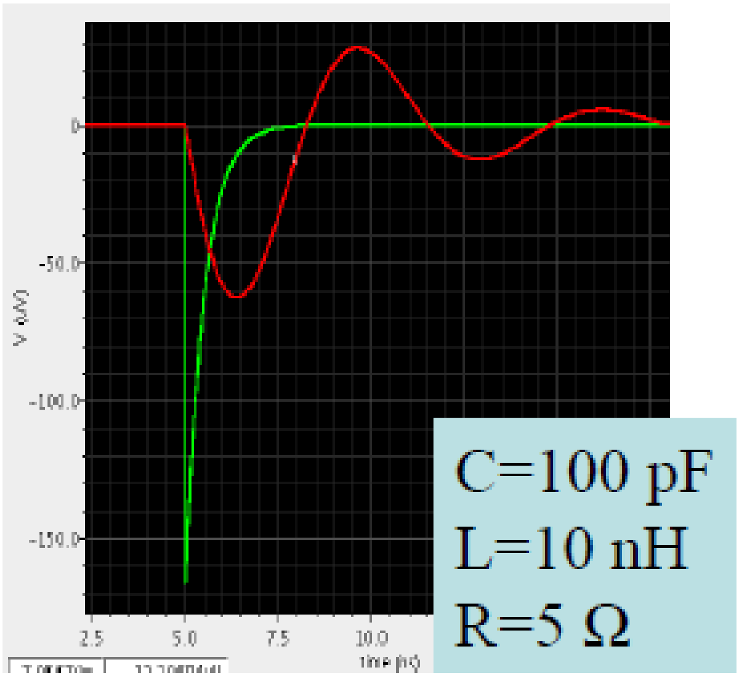

C. De la Taille "Short course on preamplifiers" Porquerolles 2013

Pulse shape - Basic electrical model

PMT is basically a current source
+ arrangement of inductors, capacitors and transmission lines.

Often desire voltage output for use in signal processing circuit
→ can use load resistor or op-amps to convert current to voltage

Load resistance limited by:
- desired frequency response $\nu_c = 1/(2\pi\ C_s\ R_L)$
- output linearity
- RL choice → stability
- heating → gain stability

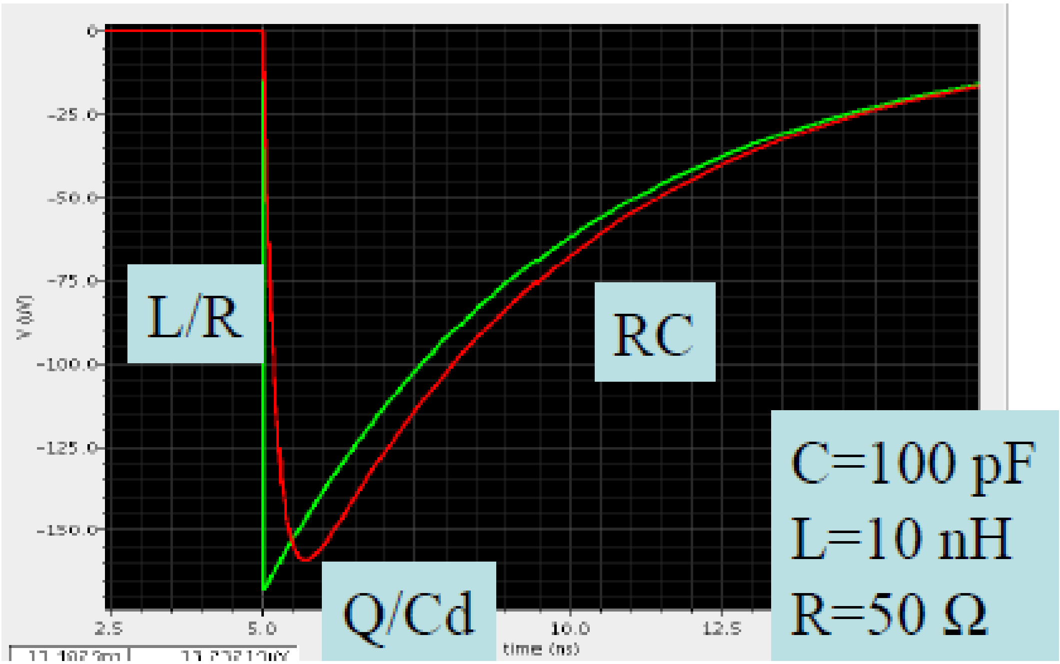

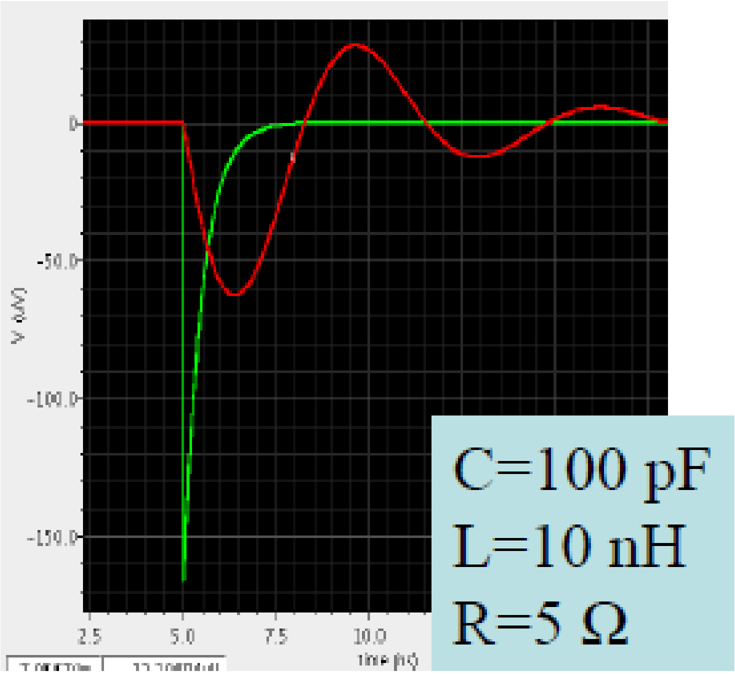

Response linearity - pulse mode

Deviation from linear response due to
1) **space charge** between last and 2nd to last dynode ← anode current saturation
2) multiplication current ~ divider current → gain unstable
3) slow photo-cathode recharge (eg at low T) ← cathode current saturation

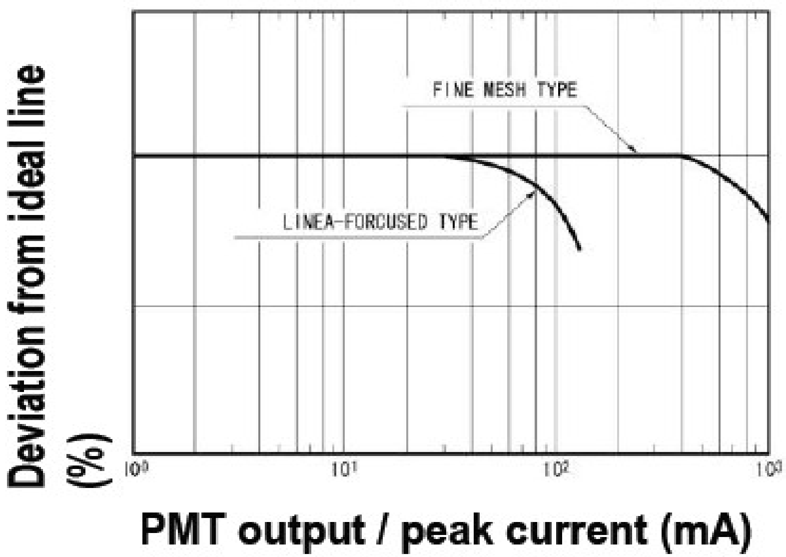

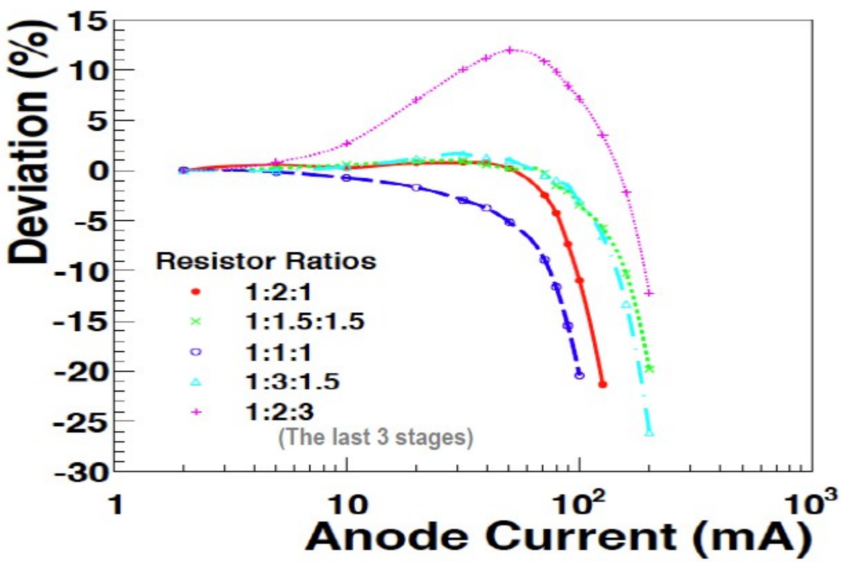

Tapered voltage divider

K.Arisaka – PMT lecture at IEEE NSS 2012 (Anaheim)

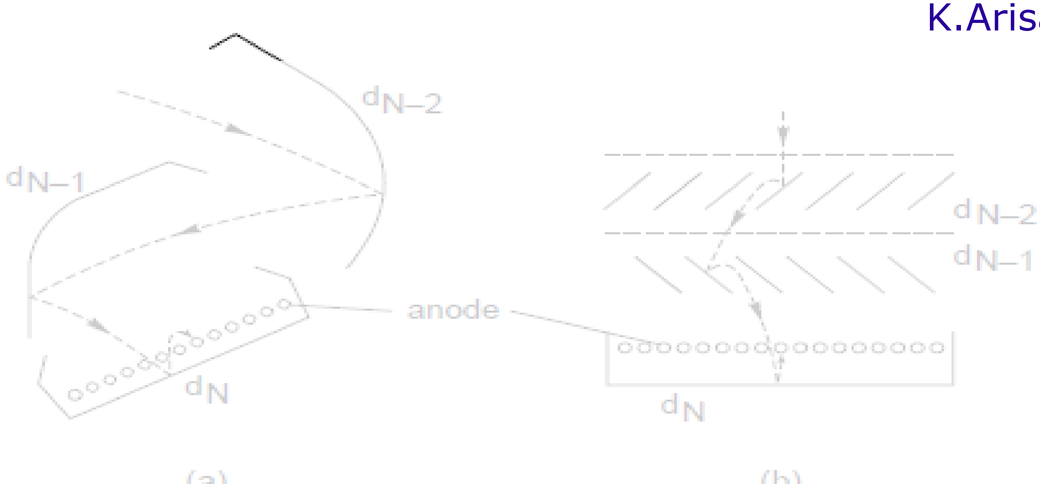

Anode shape: grid positioned close to the last dynode → allow **high electric field** between the last dynode and anode → reduce the space charge effect in the last stage

Flyckt and Marmorier – "PMT principles and applications"

Question: how to measure

pulse linearity ?

Double Pulse linearity measurement

K.Arisaka – PMT lecture at IEEE NSS 2012 (Anaheim)

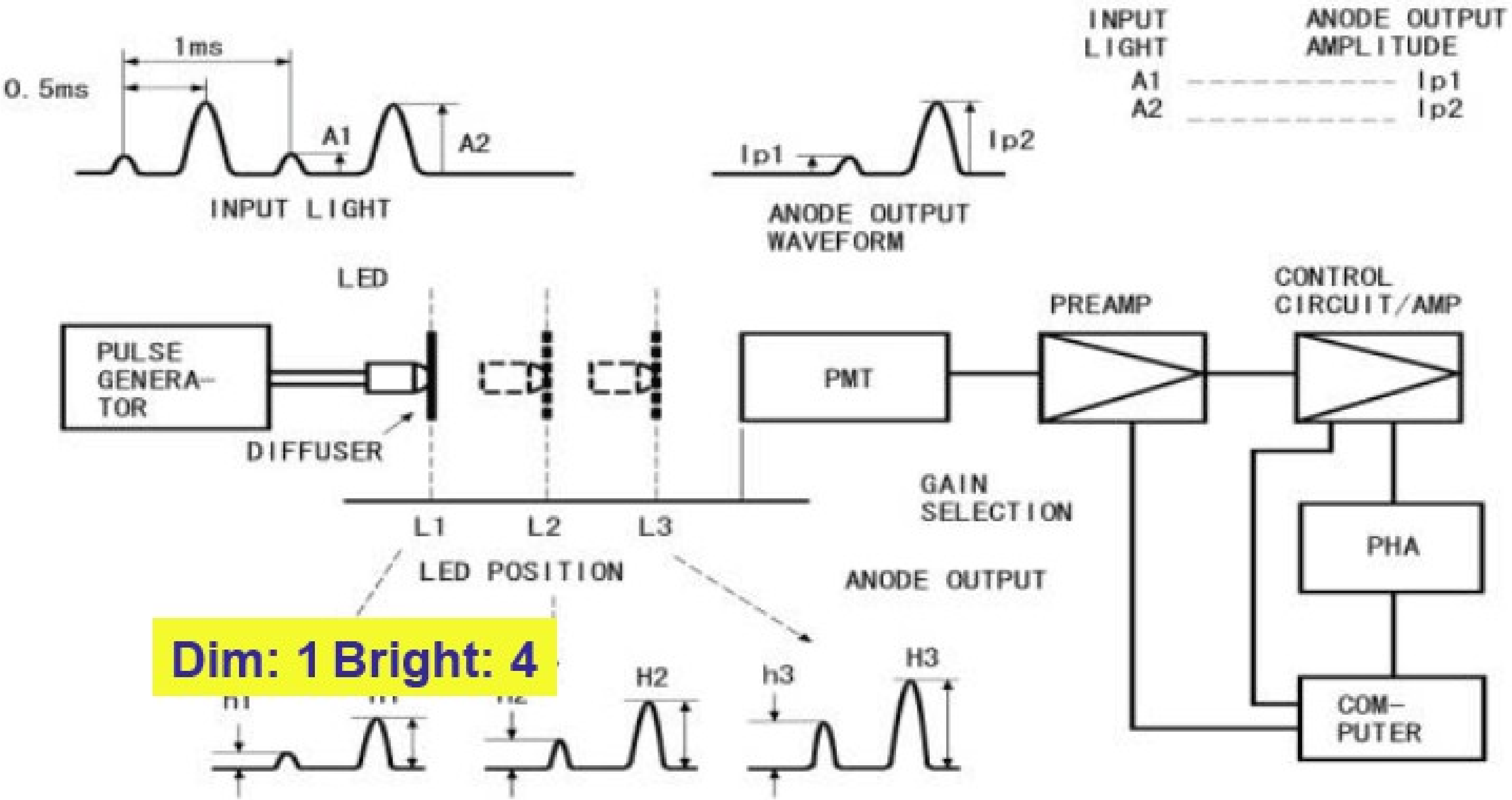

Block Diagram for Double-Pulsed Mode

Response linearity – current mode

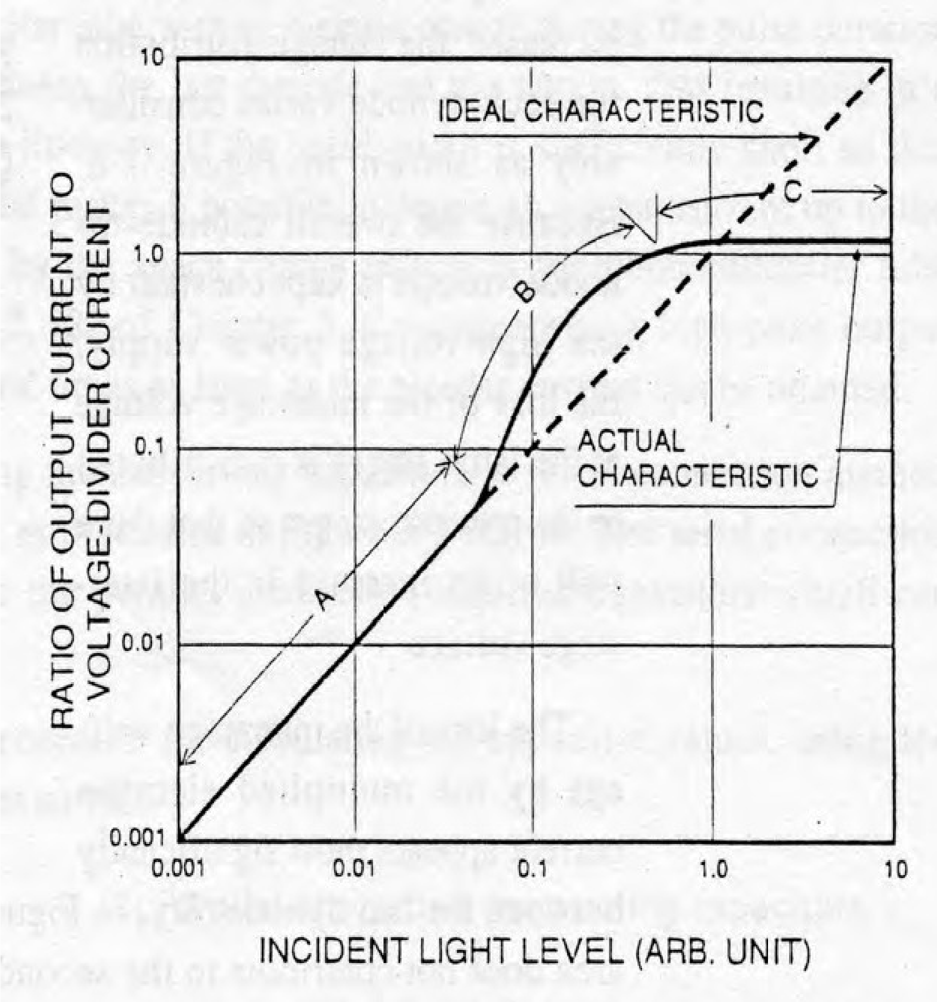

Figure 7-4: Output linearity of a photomultiplier tube

Region A: linear region for low output current (low incident light)

As light intensity increases, dynode voltages begin to vary from ideal (shift to earlier stages)

Region B: shift results in increased current amplification

Region C: saturation occurs as voltage between last dynode and anode goes to zero

If large linear region is desired – could use individual power supplies for each dynode

Improving response linearity

Deviation from linear response due to
1) **space charge** between last and 2nd to last dynode ← anode current saturation
2) multiplication current ~ divider current → gain unstable
3) slow photo-cathode recharge (eg at low T) ← cathode current saturation

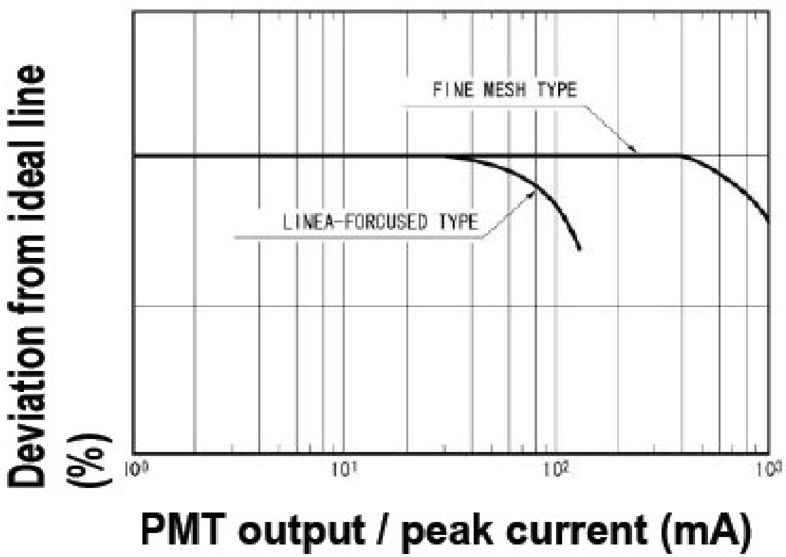

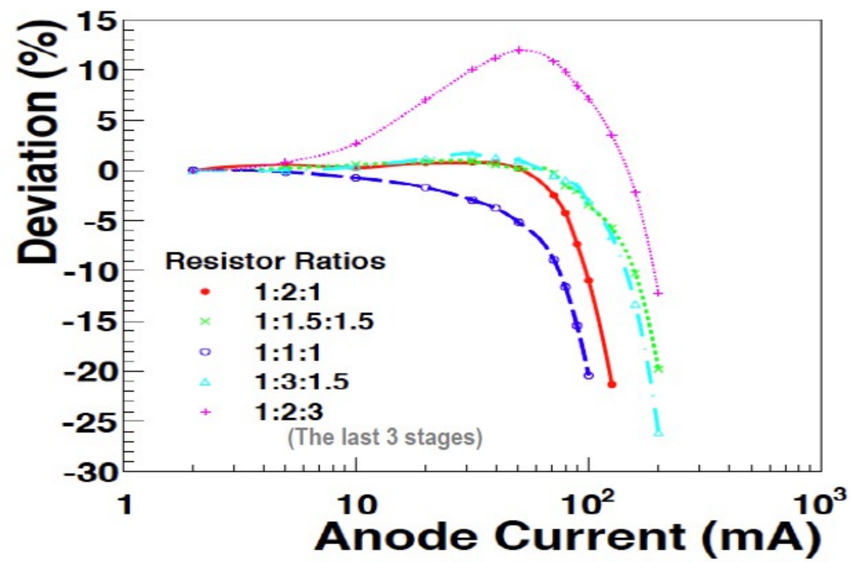

Tapered voltage divider

K.Arisaka – PMT lecture at IEEE NSS 2012 (Anaheim)

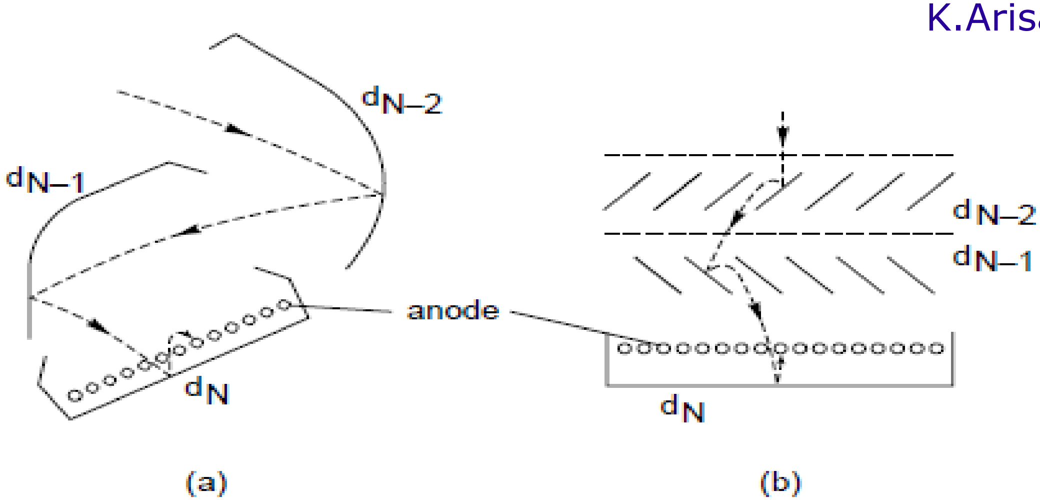

Anode shape: grid positioned close to the last dynode → allow **high electric field** between the last dynode and anode → reduce the space charge effect in the last stage

Flyckt and Marmorier – "PMT principles and applications"

Response linearity – improved bleeder

Passive Voltage Divider

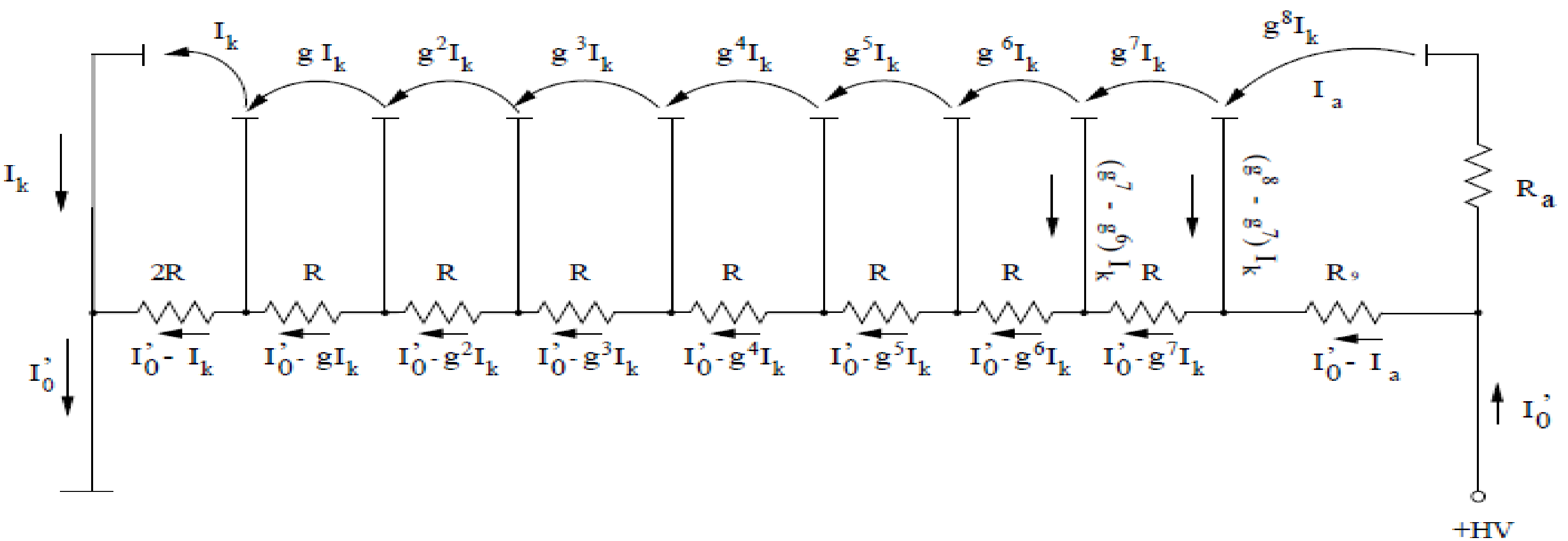

1) Tapered voltage divider reduces effects due to space-charge (progressive voltage distribution)

2) Charge storage capacitors give prompt charge

Active Voltage Divider

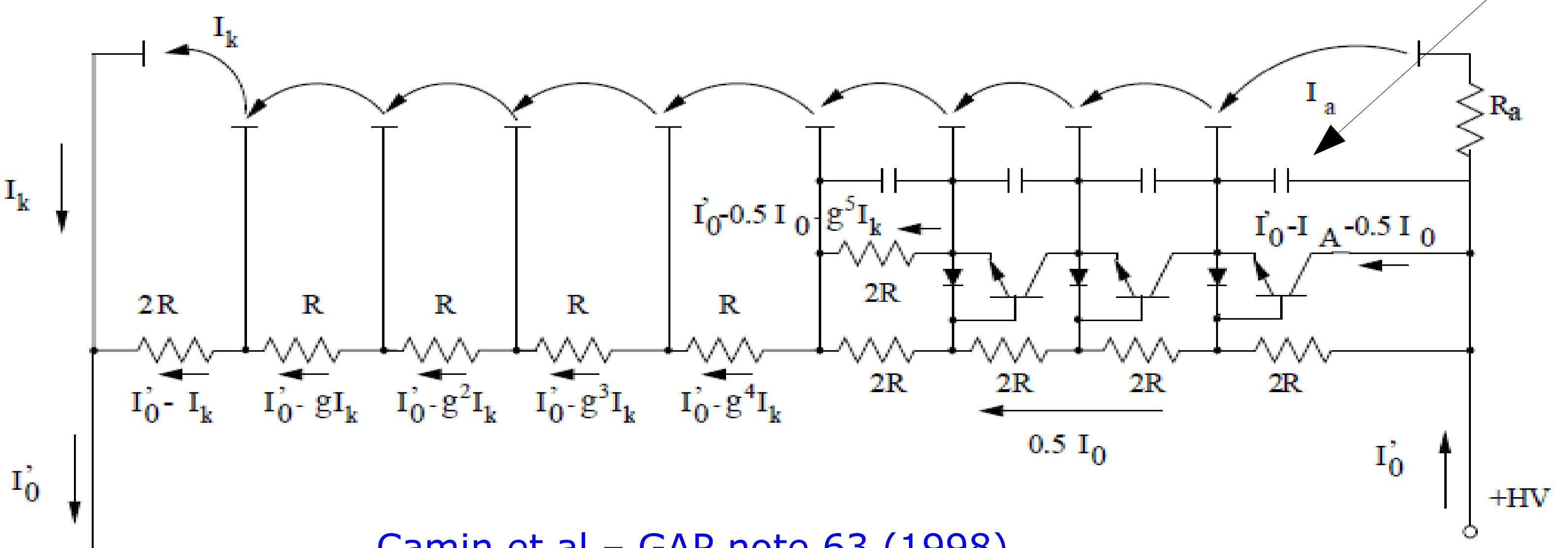

3) Transistors keep constant collector-emitter voltage (ie fix dynode potential) independent of the divider current

Camin et al – GAP note 63 (1998)

Response linearity – stray oscillations

→ Damping resistors might reduce ringing in output signal

J.P.Boutot, J.Nussli, D.Vallat "Recent trends in PMTs for Nuclear Physics" Advances in Electronics and Electron Physics Vol.60

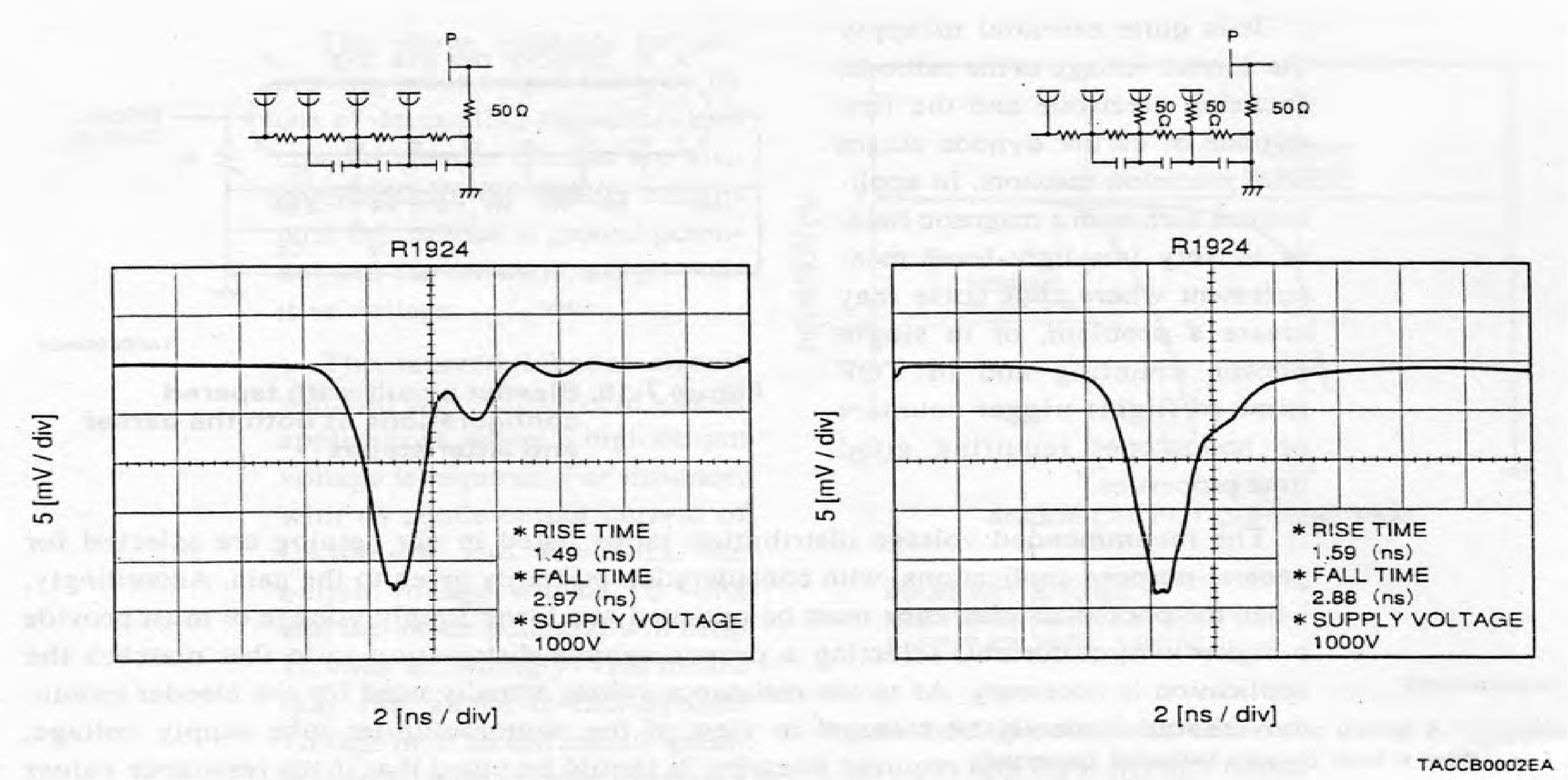

Figure 7-12: Effect of damping resistors on ringing

→ but... oscillations of the electron cloud back and fourth through the relatively transparent anode in the space between the last and second to last dynode also results in anode pulse ringing

B.H.Candy "Photomultiplier characteristics and practice relevant to photon counting" Rev. Sci. Instrum. 56, 183 (1985)

Effects of magnetic fields on response

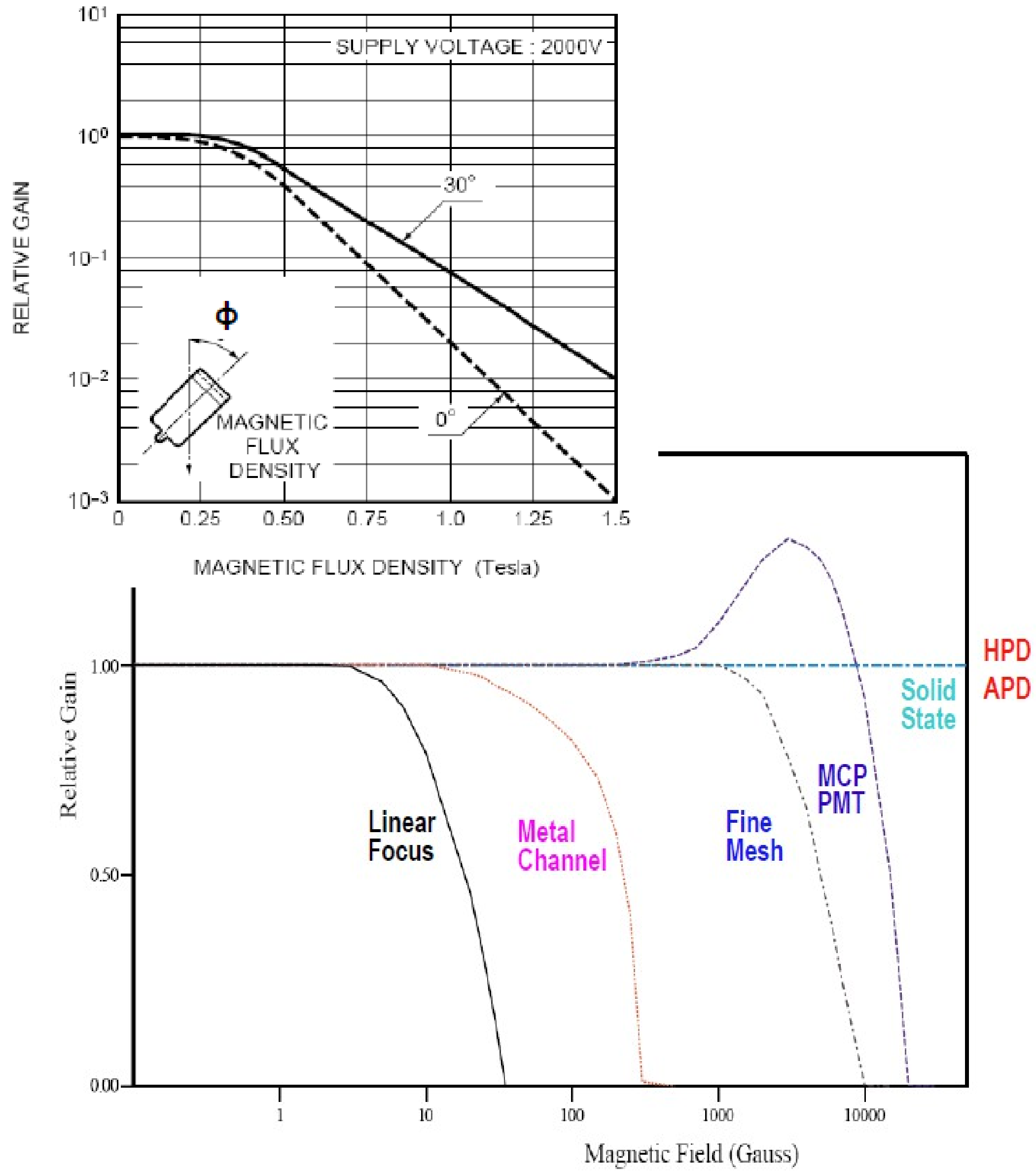

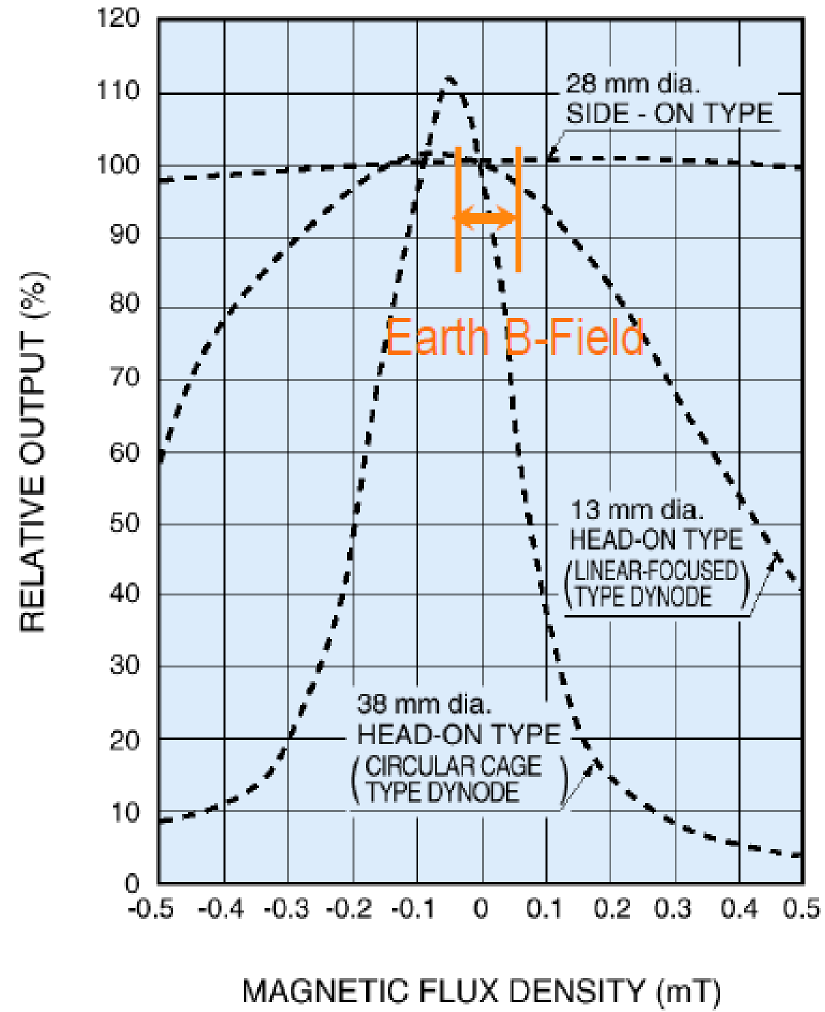

PMT is very sensitive to B fields → need shield (μ metal)

Vacuum PD fundamental parameters

Photo-Detection Efficiency

→ **PDE = QE * CE**
QE = quantum efficiency
CE = collection efficiency

Gain and
Signal formation

→ **$G = g_1 g_2 \ldots g_n$**
g_n = single stage gain

Noise sources

→ **Dark count**
→ **After-Pulsing**

fluctuations in measurement of

- **Amplitude** (number of photons)
- **Position** (photon impact position)
- **Timing** (photon arrival time)

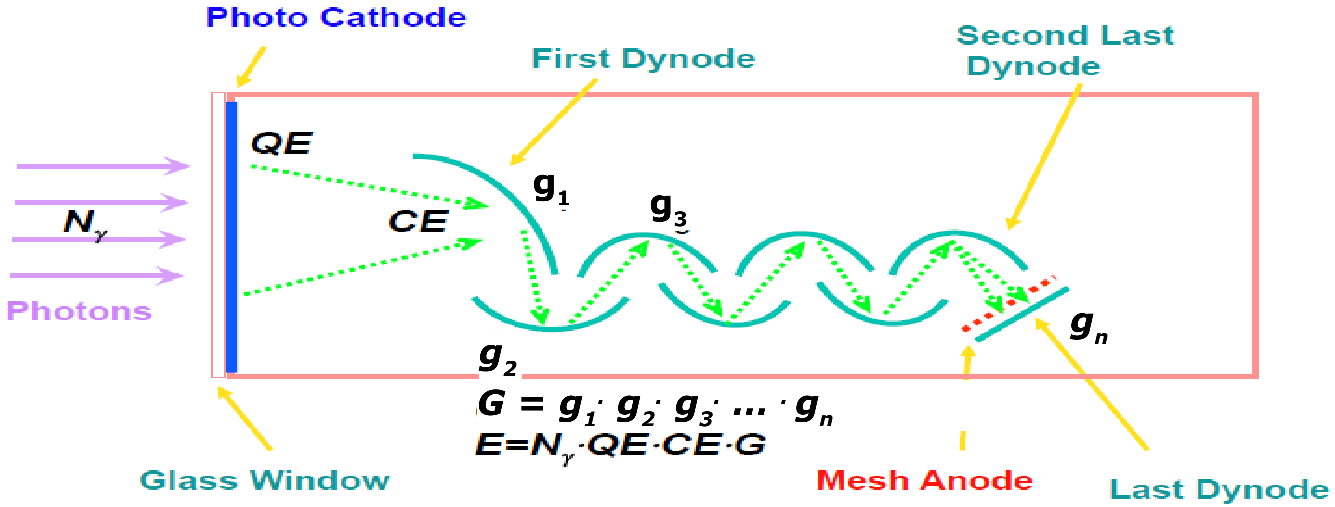

Gain fluctuations: single electron spectrum

Secondary emission process → **large amplitude fluctuations**
→ measure **single electron response** (SER) in amplitude

SER relative variance

$$\frac{\sigma_G^2}{G^2} = \frac{1}{g_1} + \frac{1}{g_1 g_2} + \ldots + \frac{1}{g_1 g_2 \ldots g_n}$$

Note: dynode multiplication is assumed Poisson process (only a first approximation; consider for instance dynodes non-uniformity

Main contribution is from 1st dynode
→ improvement when higher $V_{K\text{-}Dy1}$

Note: small amplitudes due to photoelectrons back-scattered from 1st dynode ($g_1=1$)

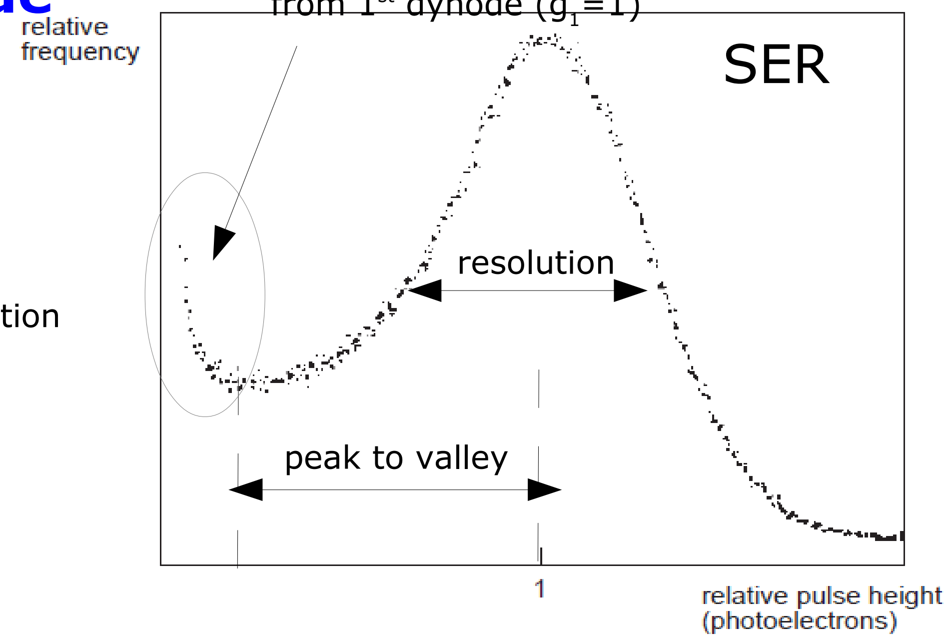

Fig.2.4 Typical single-electron spectrum. Resolution 67% FWHM. Peak-to-valley ratio 2.8:1

Excess Noise Factor (ENF)
for a multiplication process

$$ENF \equiv \frac{\sigma_{output}^2}{\sigma_{input}^2} = \frac{\langle G^2 \rangle}{\langle G \rangle^2} = 1 + \frac{\sigma_G^2}{G^2}$$

Multiplication noise

ENF in the case of PMT:

$$ENF = 1 + \frac{1}{g_1} + \frac{1}{g_1 g_2} + \ldots + \frac{1}{g_1 g_2 \ldots g_n}$$

SER variance is multiplication variance !
Typical ENF~1.2

Flyckt and Marmorier –
"PMT principles and applications"

Gain fluctuations: single photon resolution

Single photon resolution
only when **$g_1 \geq 12$**

either 1) **higher $V_{K\text{-}Dy1}$** (modify divider ratio)
or 2) use PMT with **NEA for 1st dynode**
… anyway the price is **higher dark noise**

PMT (Hamamatsu R5600)

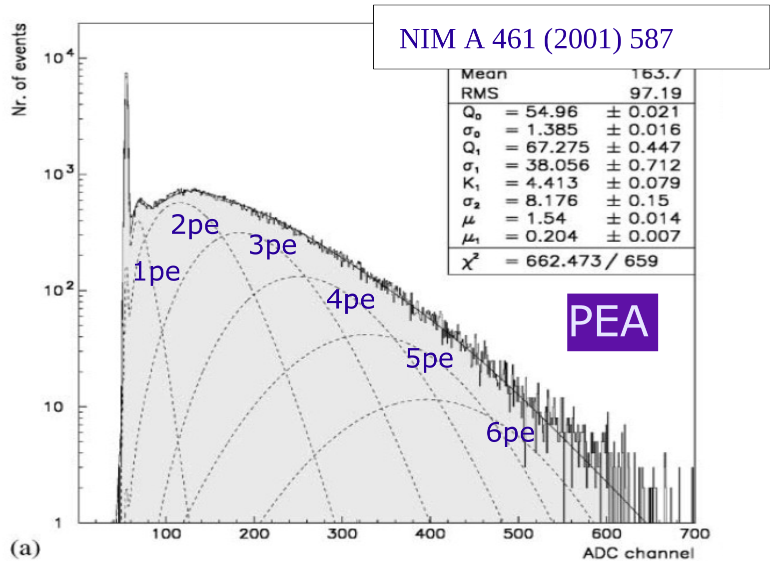

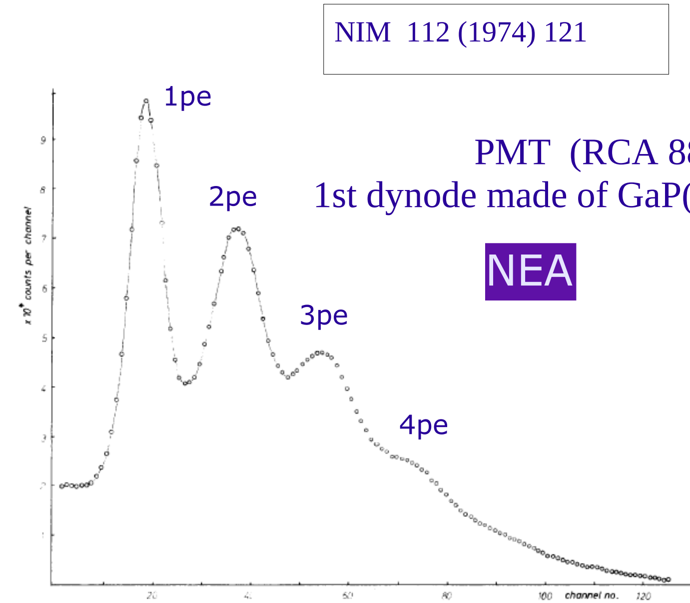

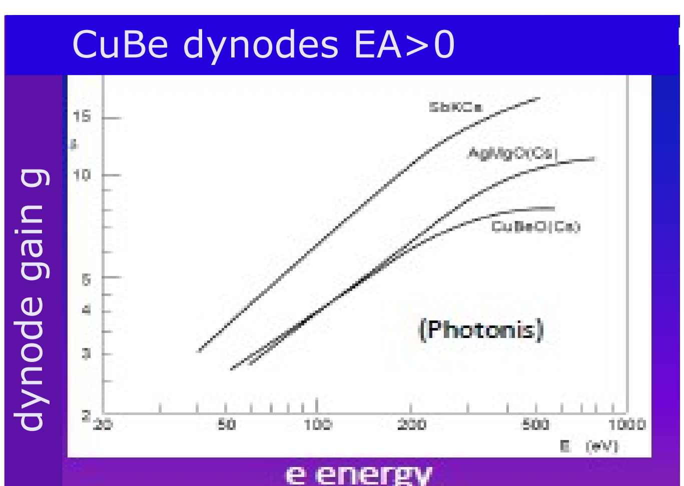

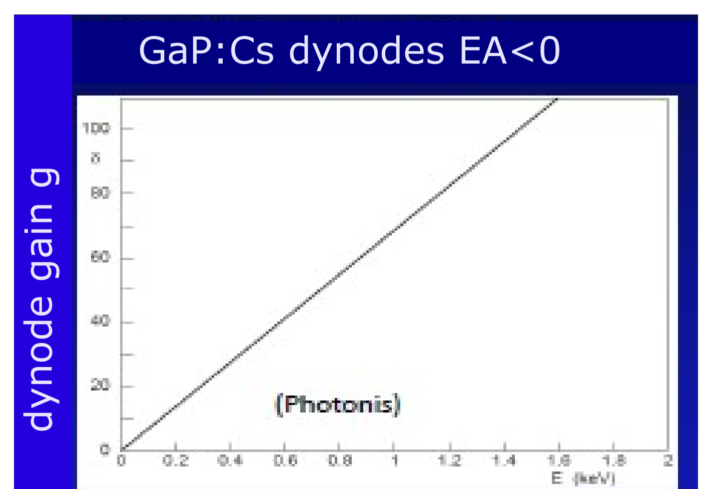

Amplitude fluctuations

→ Amplitude resolution → Energy resolution

Due to gain + photo-conversion fluctuations

Combining **Photo-conversion fluctuations** (binomial statistics) and **Gain fluctuations** (Poisson, in good approximation) → get PMT contribution to **amplitude resolution** ($E = N_\gamma$ PDE G)

$$\frac{\sigma_E}{E} = \frac{\sigma_{N_\gamma}}{N_\gamma} = \sqrt{\frac{ENF - PDE}{N_\gamma \; PDE}} = \sqrt{\frac{ENF - (QE \;\; CE)}{N_\gamma \; QE \;\; CE}}$$

(Multiplicative processes)

Combined fluctuations from a multiplicative process:
N → p N (Binomial) → M p N (Poisson cascade) [here M = G gain]

$$\frac{\sigma_N^2}{N^2} = \frac{\sigma_{pN}^2}{p^2 \; N^2} + \frac{1}{p \;\; N} \frac{\sigma_M^2}{M^2}$$

Cascade Variance theorem

$$\langle n \rangle = \langle \alpha \rangle \langle m \rangle$$

$$var(n) = \langle \alpha \rangle^2 var(m) + \langle m \rangle var(\alpha)$$

$$F_n = \frac{var(n)}{\langle n \rangle} = \langle \alpha \rangle F_m + F_\alpha$$

Binomial

$$\frac{\sigma_{pN}^2}{p^2 \; N^2} = \frac{1-p}{p\,N}$$

Poisson cascade

$$\frac{\sigma_M^2}{M^2} = \frac{1}{m_1} + \frac{1}{m_1 m_2} + \ldots + \frac{1}{m_1 \ldots m_n} \equiv ENF - 1$$

$$\longrightarrow \frac{\sigma_N^2}{N^2} = \frac{ENF - p}{p \;\; N}$$

G.Collazuol - Siena - IDPASC 2013

Question: how to measure $N\gamma$?
Answer: must measure PDE, G and ENF

1) **measure PDE** as discussed previously

2) **measure G** from SER → G = <A>

Alternative: measure G x CE from ratio
between anode and cathode currents → G x CE = I_A/I_C

3) **measure ENF** from SER relative variance $$\frac{\sigma_A}{A} = \sqrt{ENF-1}$$

Vacuum PD fundamental parameters

Photo-Detection Efficiency

→ **PDE = QE * CE**
QE = quantum efficiency
CE = collection efficiency

Gain and
Signal formation

→ $G = g_1 g_2 \dots g_n$
g_n = single stage gain

Noise sources

→ **Dark count**
→ **After-Pulsing**

fluctuations in measurement of

- **Amplitude** (number of photons)
- **Position** (photon impact position)
- **Timing** (photon arrival time)

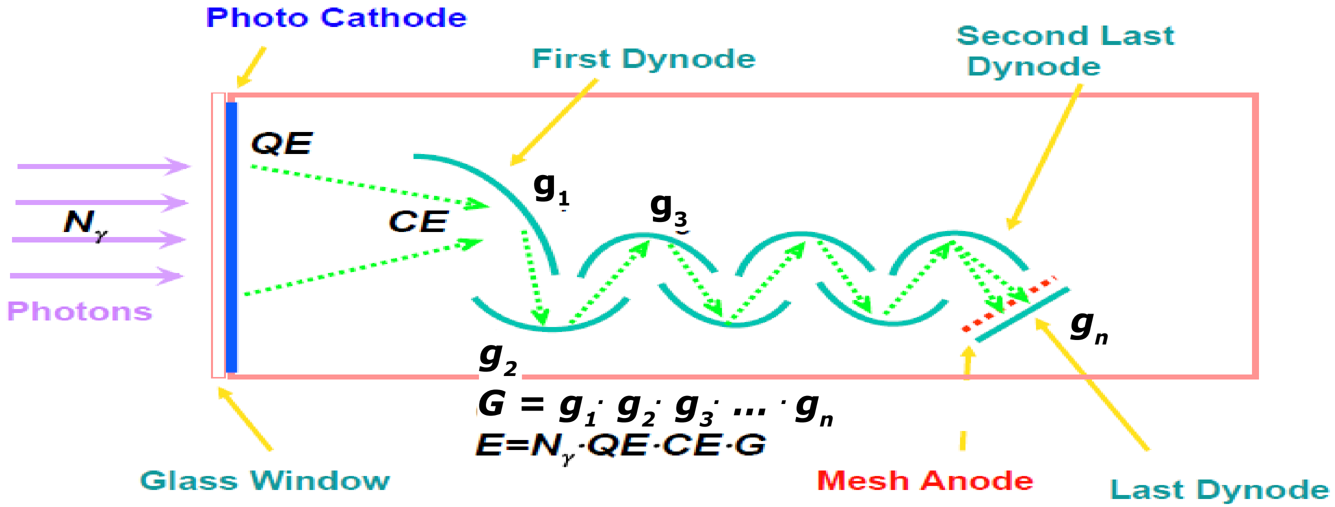

Dark Noise sources in PMT

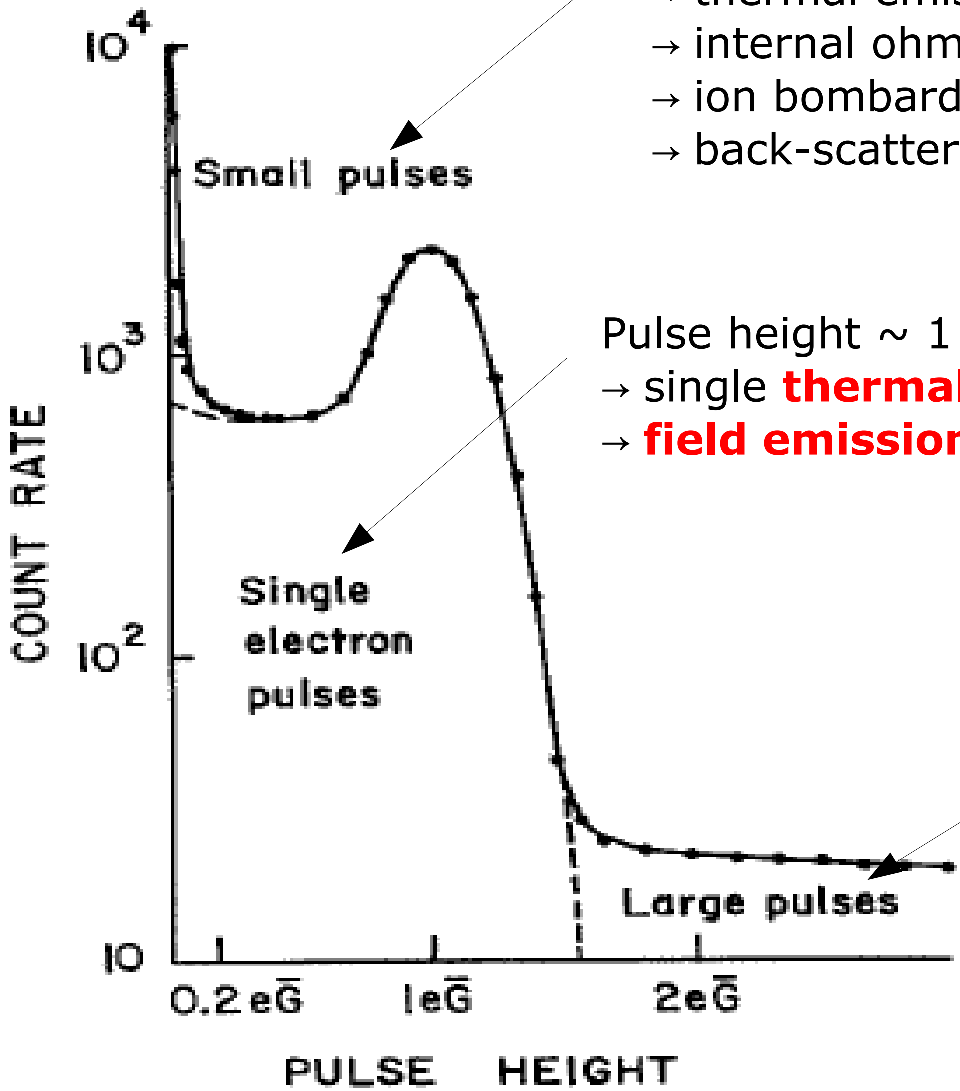

Dark amplitude spectrum
for high gain PMT (10^7) - K_2CsSb cathode - GaP 1st dynode

Pulse height < 0.2 ph.e
→ thermal emission from dynodes
→ internal ohmic **leakage current** between dynodes-anode
→ ion bombardment on dynodes (electron emission)
→ back-scattering 1st ph.e

Pulse height ~ 1 ph.e
→ single **thermal electrons** (**shot noise**) from photocathode
→ **field emission** (**1/f noise**) from photocathode

Pulse height > 2 ph.e
→ **ion** bombardment on photocathode
(see afterpulses, **correlated noise**)
→ light **glow** from anode
(see afterpulses, **correlated noise**)
→ **cherenkov** light from cosmic rays
on PMT window (ultrashort pulses)

Dark Noise (HV and T dependence)

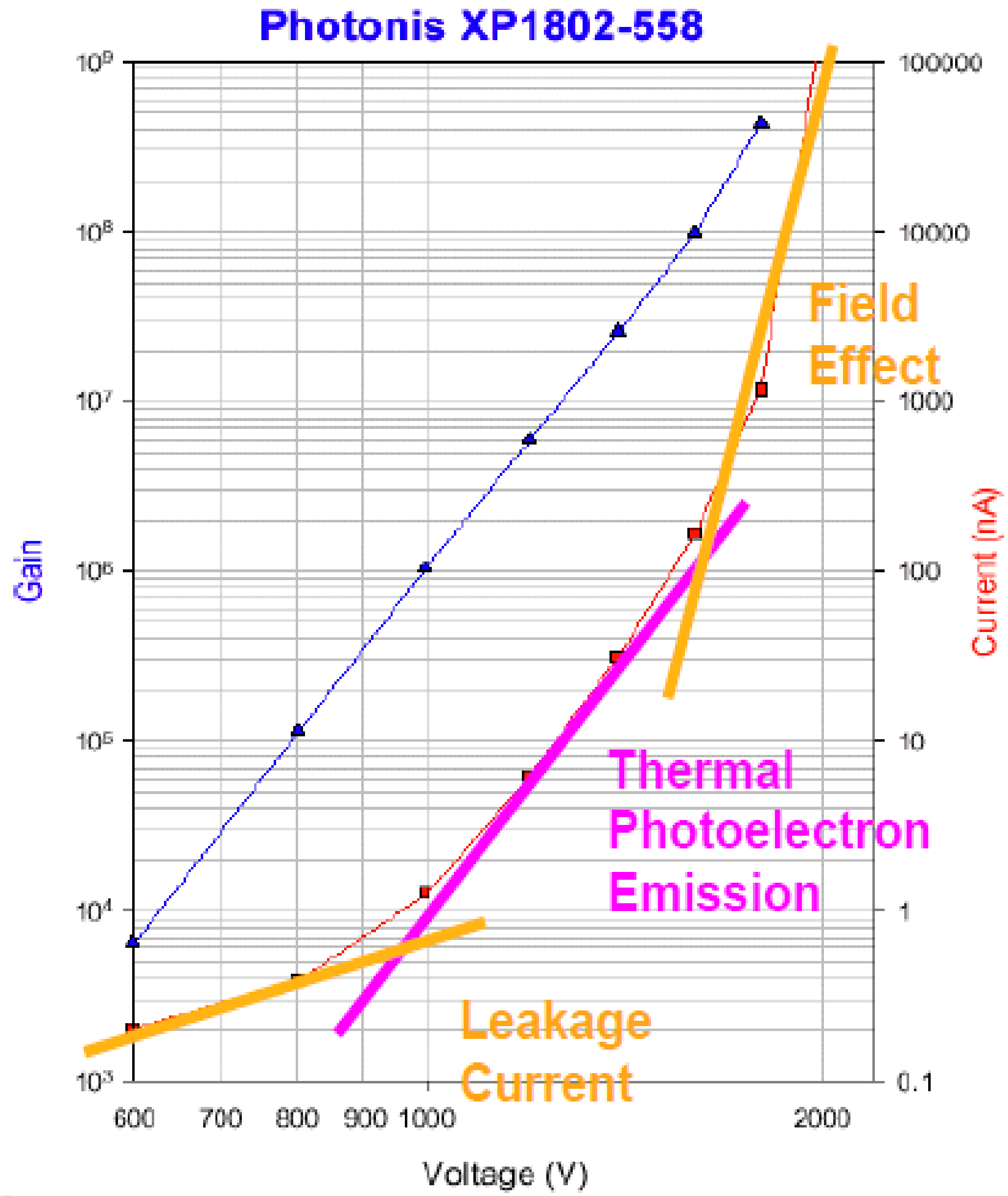

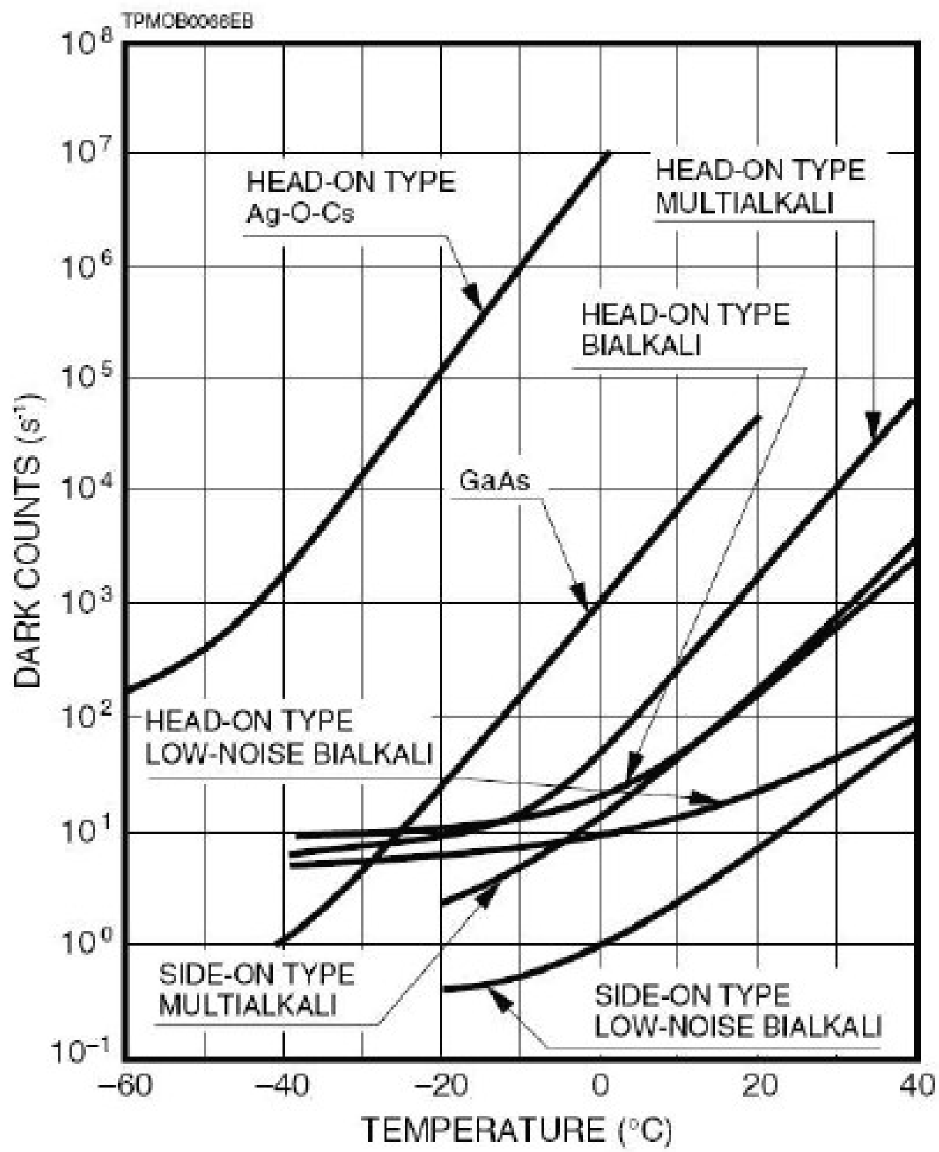

Dark Counts – typical rates

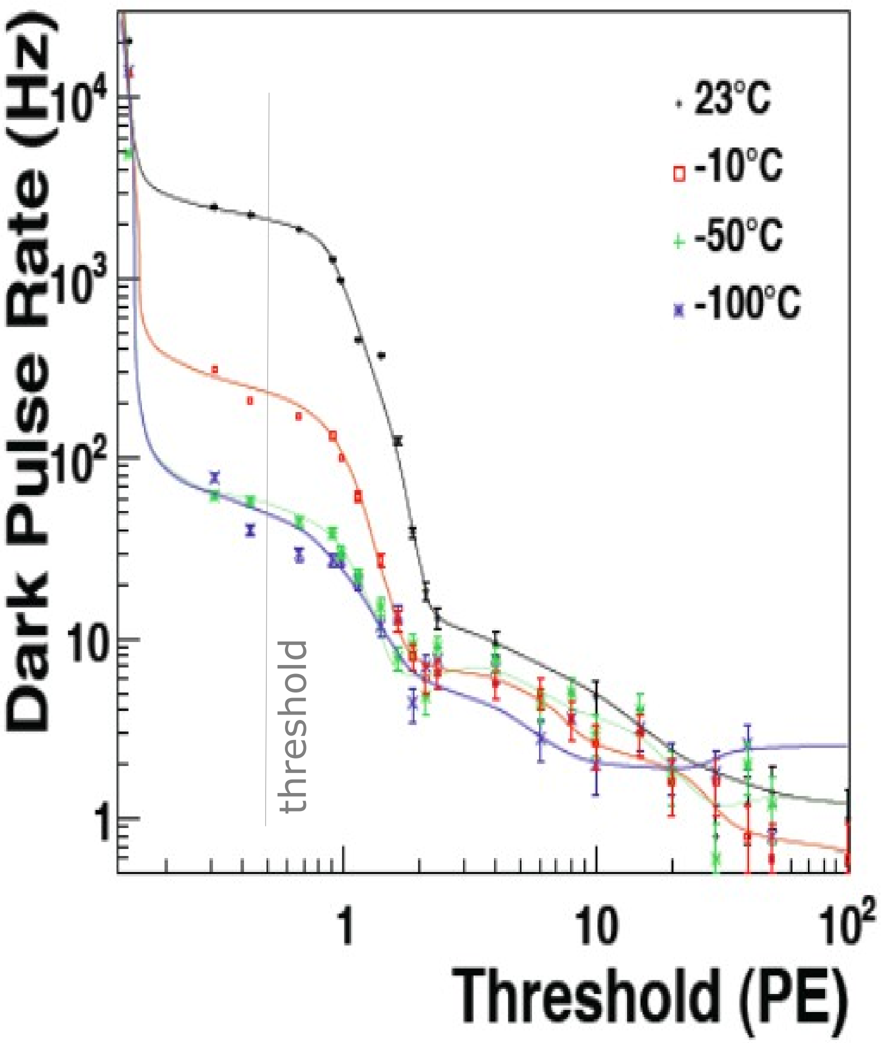

Typical D.C. rates
(T room, 1 ph.e. threshold)

→ PEA cathodes
- S20 < KHz/cm^2
- bialkali < 10Hz/cm^2

→ NEA cahtodes
- S25 ~ 10KHz/cm^2
- III-V < 30KHz/cm^2

Afterpulses – correlated noise

Spurious signals correlated with the photon arrival may appear:

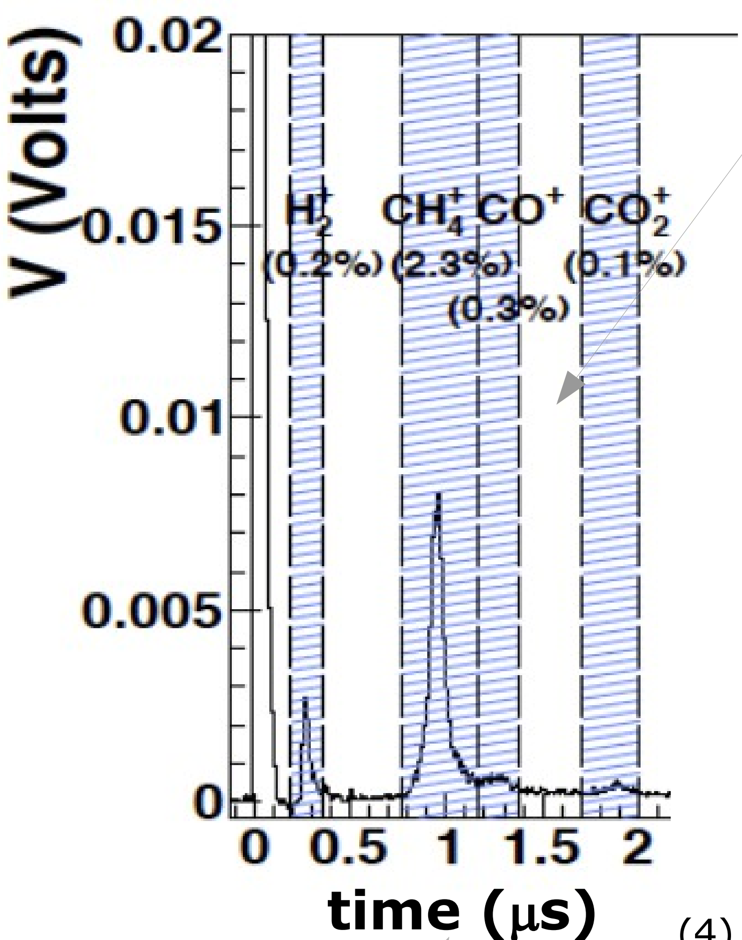

K.Arisaka – IEEE NSS 2012

(1) **Afterpulses** stem from ionisation of the residual gas atoms or those adsorbed by the 1st dynode surface
→ ion feedback delay 100ns – 10μs

Note: afterpulses and anode glow consist in additional delayed signal

(3) **"late pulses"** due to 1st photo-electron inelastic or elastic back-scattering on 1st dynode

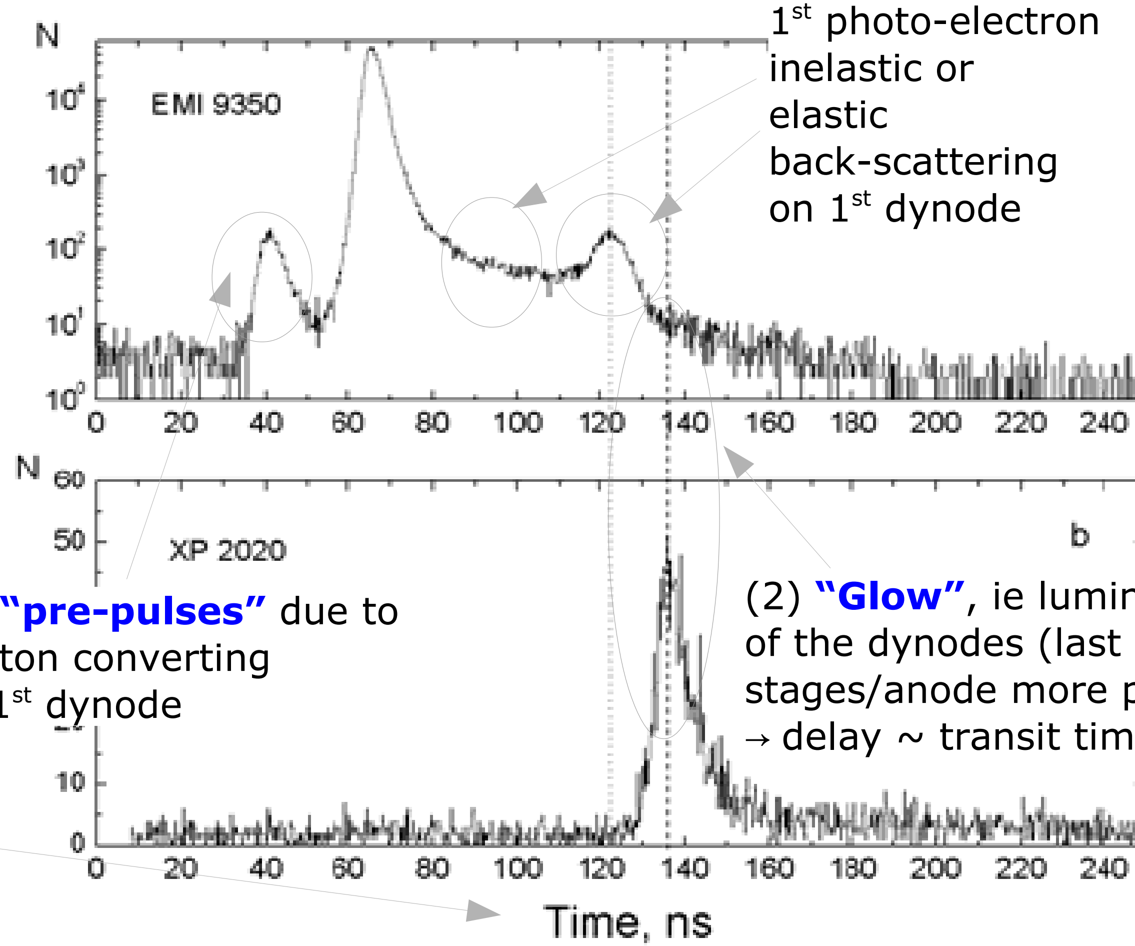

(4) **"pre-pulses"** due to photon converting on 1st dynode

(2) **"Glow"**, ie luminescence of the dynodes (last stages/anode more probable)
→ delay ~ transit time

note: different time scales

B.K.Lubsandorzhiev et al "Photoelectron backscattering in vacuum phototubes"

Vacuum PD fundamental parameters

Photo-Detection Efficiency

→ **PDE = QE * CE**
QE = quantum efficiency
CE = collection efficiency

Gain and
Signal formation

→ $G = g_1 g_2 \dots g_n$
g_n = single stage gain

Noise sources

→ **Dark count**
→ **After-Pulsing**

fluctuations in measurement of

- **Amplitude** (number of photons)
- **Position** (photon impact position)
- **Timing** (photon arrival time)

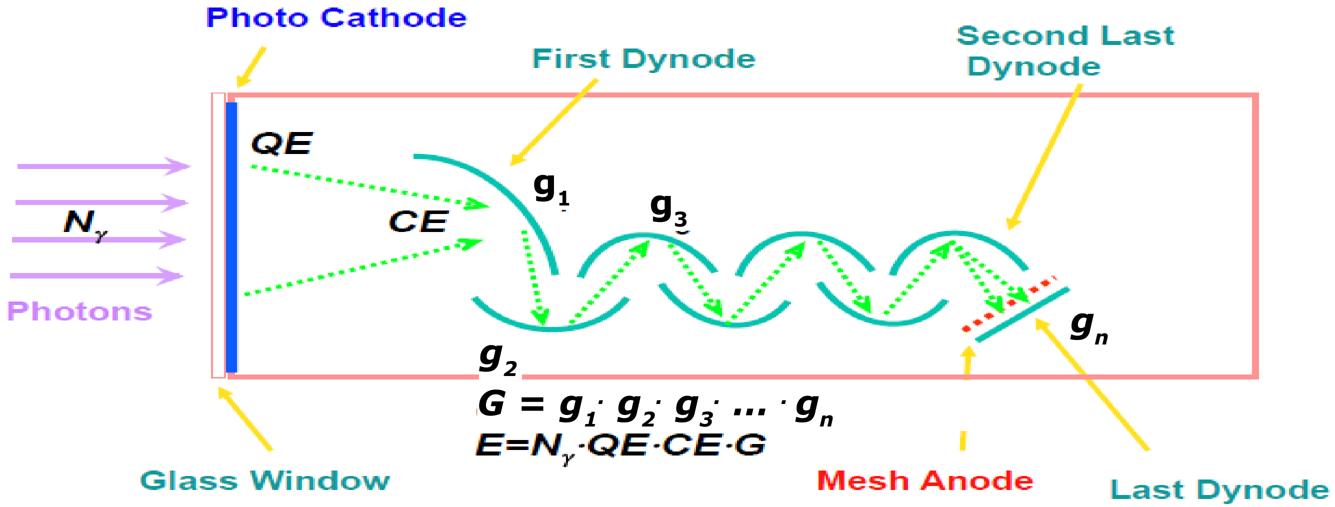

Timing resolution – Single electron response

<Transit Time> = sum of <time of flight> between stages $K \to Dy_1 \to \dots Dy_n \to A$

$TT = t_{K\text{-}Dy1} + t_{Dy1\text{-}Dy2} + \dots + t_{Dyn\text{-}A}$ (ignoring charge induction $Dy_n \to A$)

TT fluctuations → **timing jitter** $\sigma^2_{TT} \sim \sigma^2_{KDy1} + \dfrac{\sigma^2_{Dy1Dy2}}{g_1} + \dfrac{\sigma^2_{DyDy}}{g_1(g-1)}$

main contributions $\begin{cases} \text{cathode} \to 1^{st} \text{ dynode} \\ 1^{st} \to 2^{nd} \text{ dynode} \end{cases}$

Note: time of flight of the following stages are sampled many times (due to multiplication) → little contribution

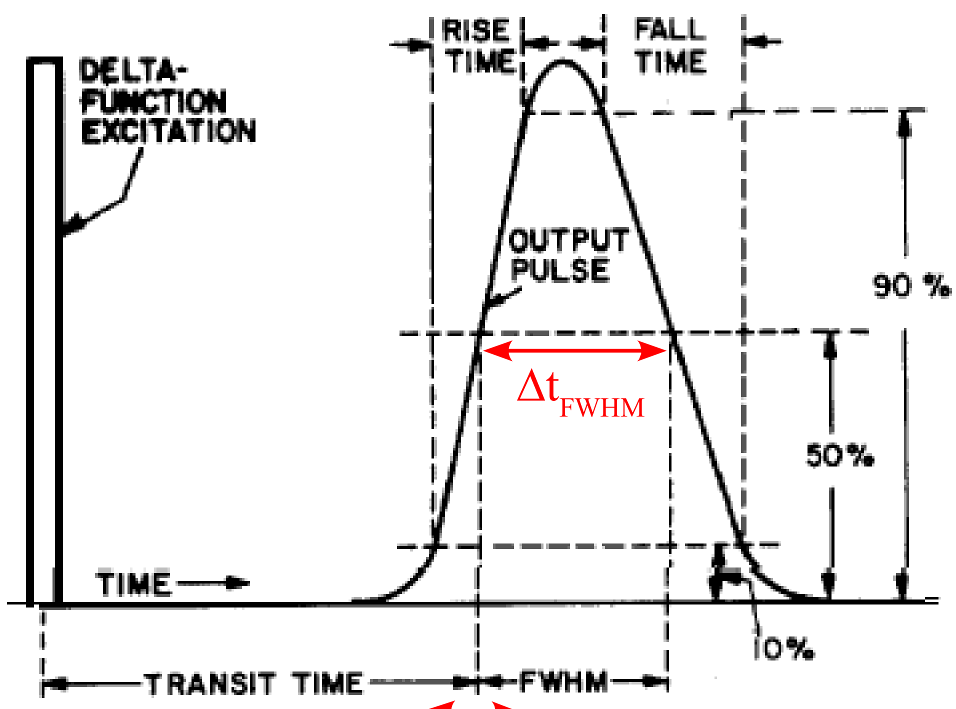

jitter σ_{TT}

Pulse width → **rate limit**

$$\Delta t_{FWHM} \sim \sqrt{n\,\sigma^2_{DyDy} + \sigma^2_{Dy_n A}}$$

Note: 1) the front stages give little contribution to pulse width
→ **time resolution is independent of frequency response of the PMT**

2) LC ringing and RC usually affect signal fall front

Single photon timing resolution

S.K.Poultney – "single photon detection and timing"

$$\sigma_{TT}^2 \sim \sigma_{KDy1}^2 + \frac{\sigma_{Dy1Dy2}^2}{g_1} + \frac{\sigma_{DyDy}^2}{g_1\left(g-1\right)}$$

1st high gain dynode
strongly reduce time jitter

main contribution
depends on
1) electrode geometry
2) ph.e- velocity || and ⊥
3) process of photo-emission

In PMT for fast timing:
dedicated dynode shapes
allow compensation of different
time of flight along different paths
between adjacent dynodes
(eg linear focus multiplier)

Despite time of flight
equalization, residual
time difference across
photocathode area O(100ps)

- Small contribution from fluctuations of time lag due to photocathode response (relevant only for NEA cathodes)
- Important contribution from the different velocities of emitted electrons

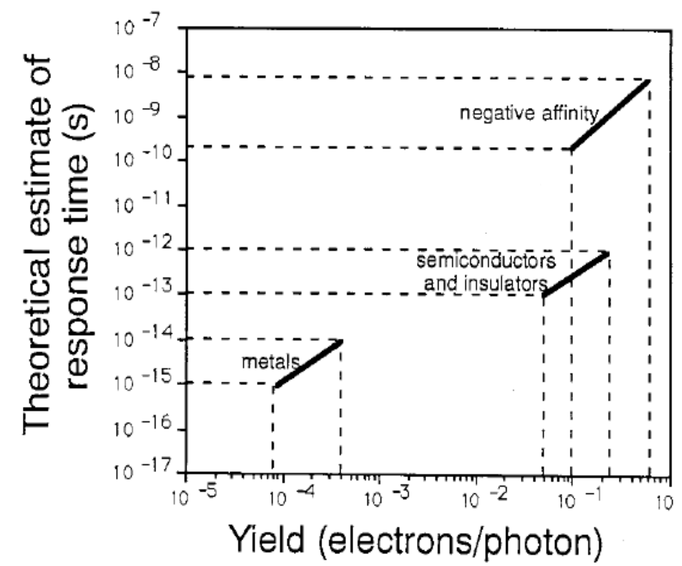

fluctuations of
distance K-Dy1

fluctuations of e- velocity
normal to emission surf

$$\sigma_{KDy1} \approx \sqrt{\frac{m}{q_e}}\frac{\sigma_L}{\sqrt{V}} \; (+) \; \frac{m}{q_e}\frac{\sigma_{v_n} L}{V}$$

distance K-Dy1

ddp K-Dy1

single photon time resolution σ_{TT}

1) **depends on wavelength** (improves at long wavelengths)

2) lower limit for $\sigma_{TT} \geq$ **150ps**

Photo-electron energy distribution

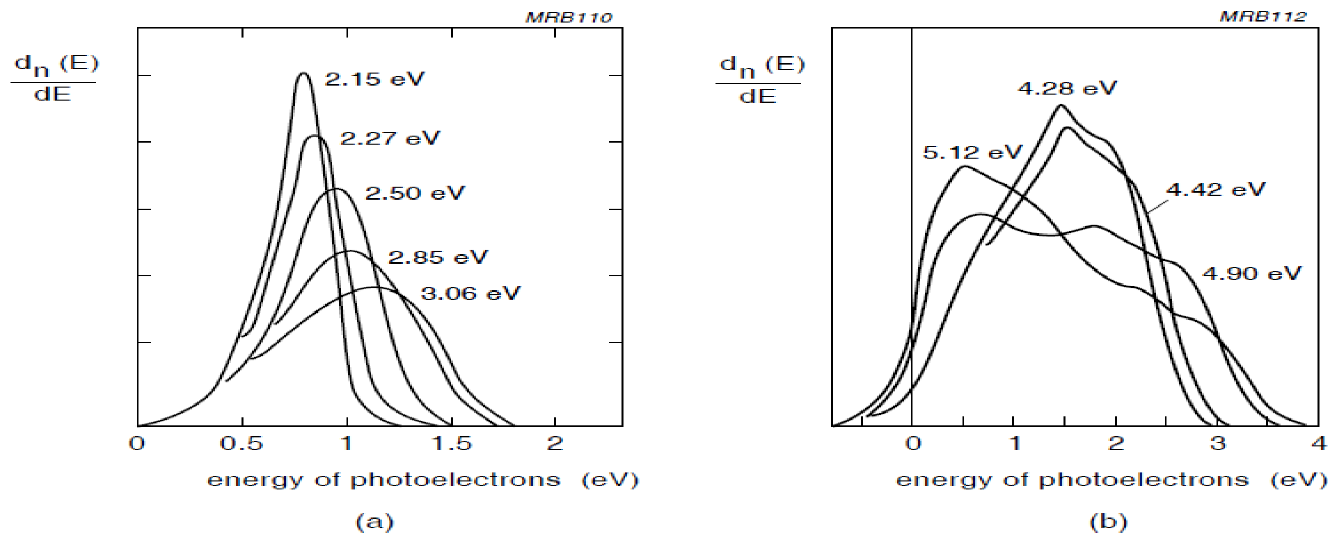

Fig.A1.8 Relative distribution of photoelectron energies, E_{ph}, from a layer of SbKCs at 290 K, for incident photon energies (a) from 2.15 eV to 3.06 eV, and (b) from 4.28 eV to 5.12 eV

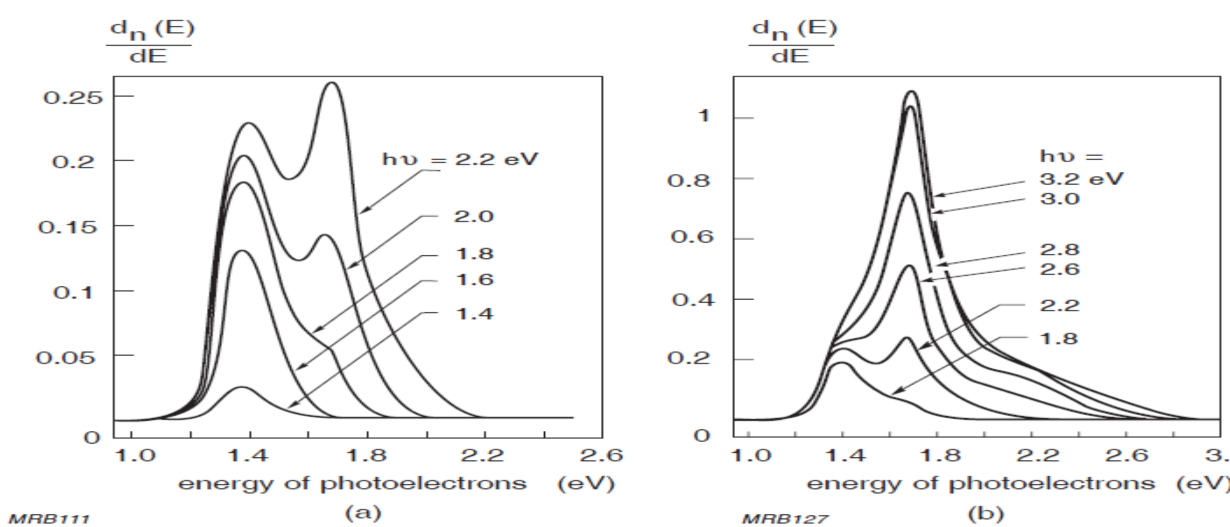

Fig.A1.9 Photoelectron energy distribution (in electrons per photon per eV) from a layer of GaAs(Cs) for incident-photon energies (a) from 1.4 eV to 2.2 eV, and (b) from 1.8 eV to 3.2 eV

Single photon timing resolution

Single ph.e
time spectra
for incident light
at different
wavelengths

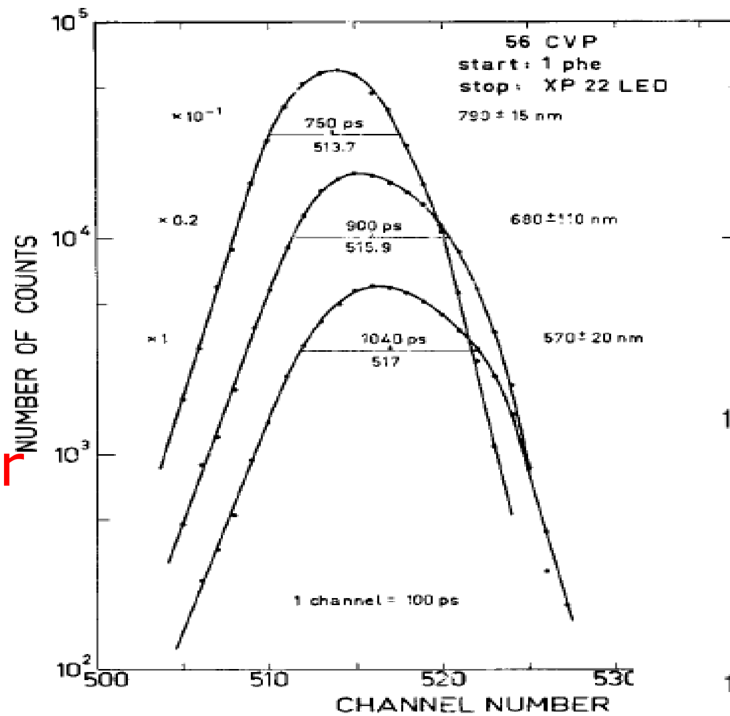

M.Moszynski NIM 141 (1977) 319

Dependence on V

TT ~ 1/V

σ_{TT} *~ 1/V*

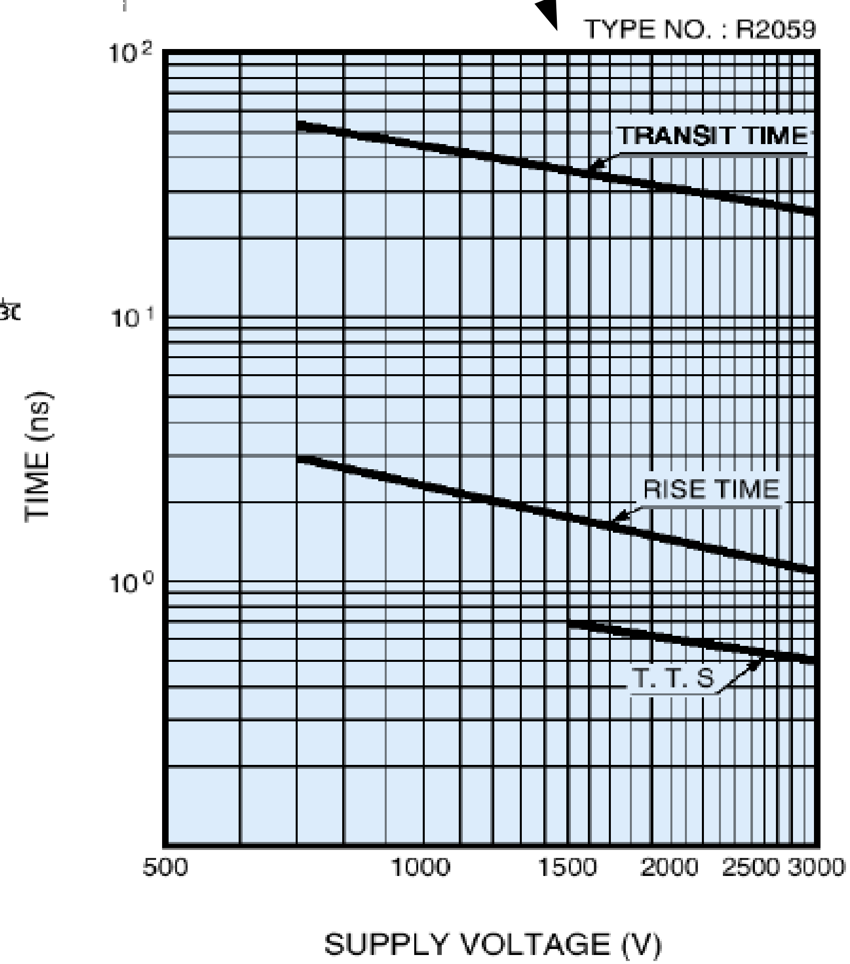

Dependence on λ

longer λ → less jitter

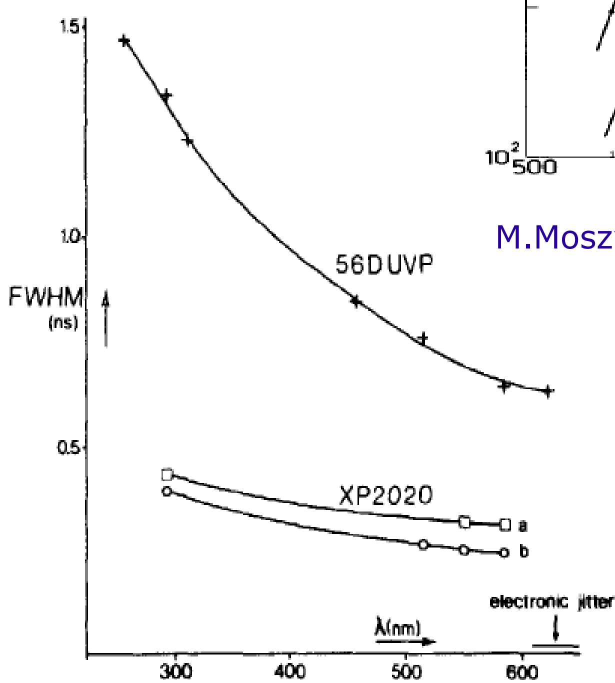

Bebelaar Rev Sci Instr 57 (1986)

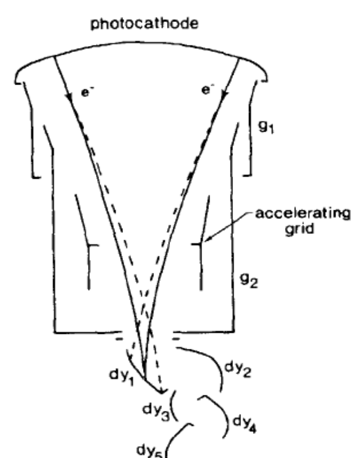

Single photon timing resolution

Contributions from pulse shape

Slower rise front
without screening
grid at anode

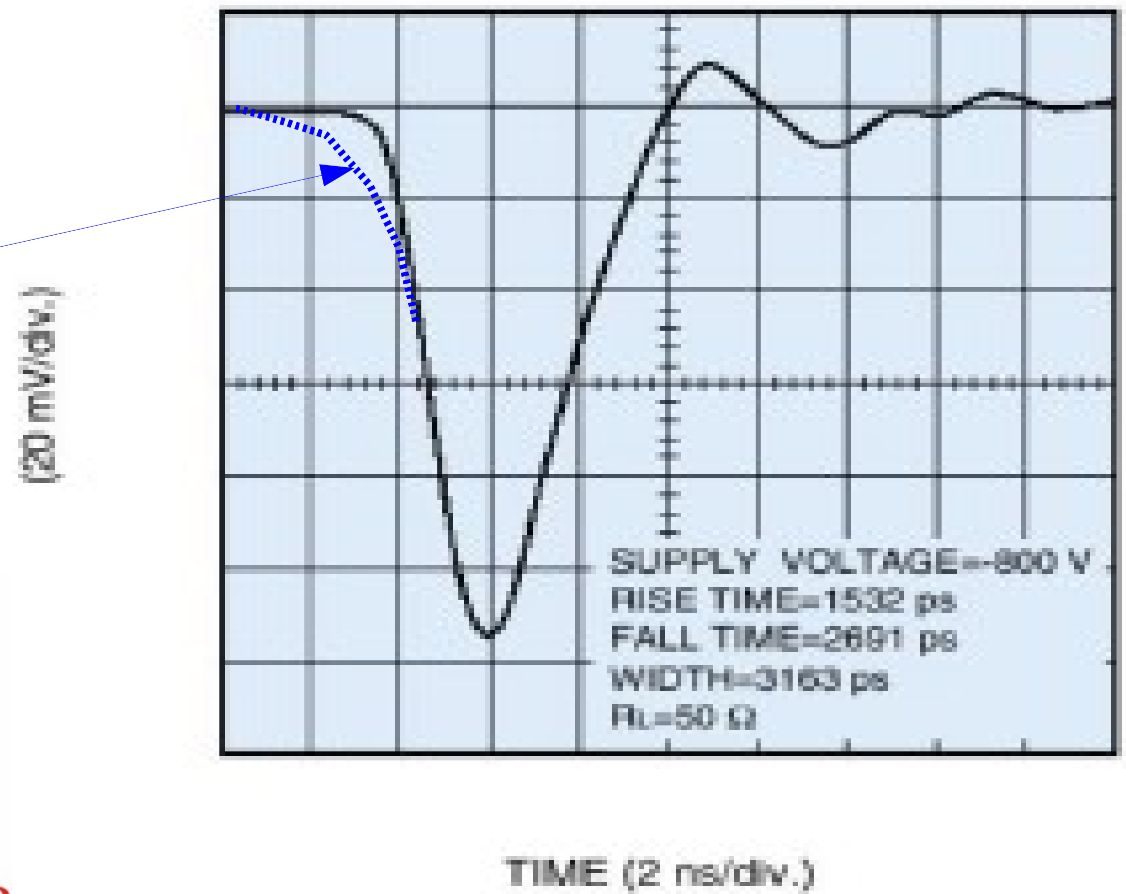

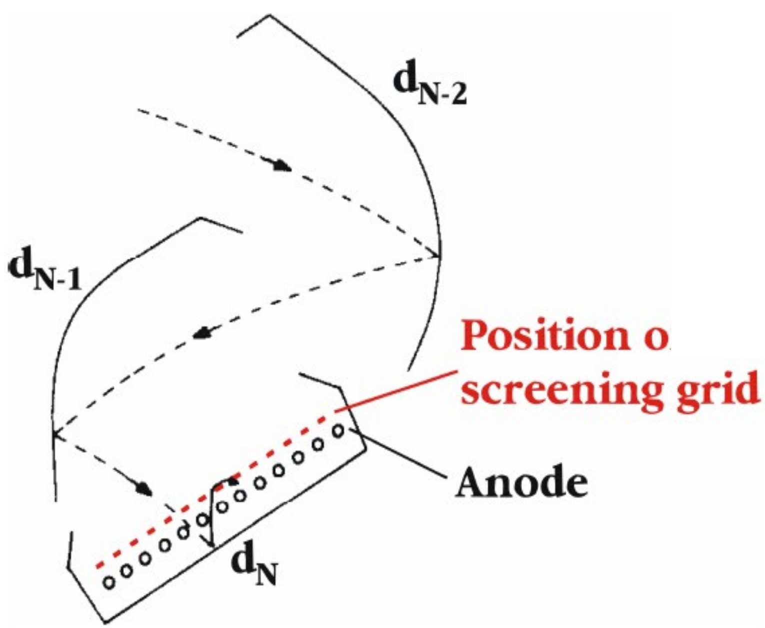

Single photon timing resolution

Contributions from pulse shape

back-scattering also plays a role in pulse rising front
→ affecting timing resolution

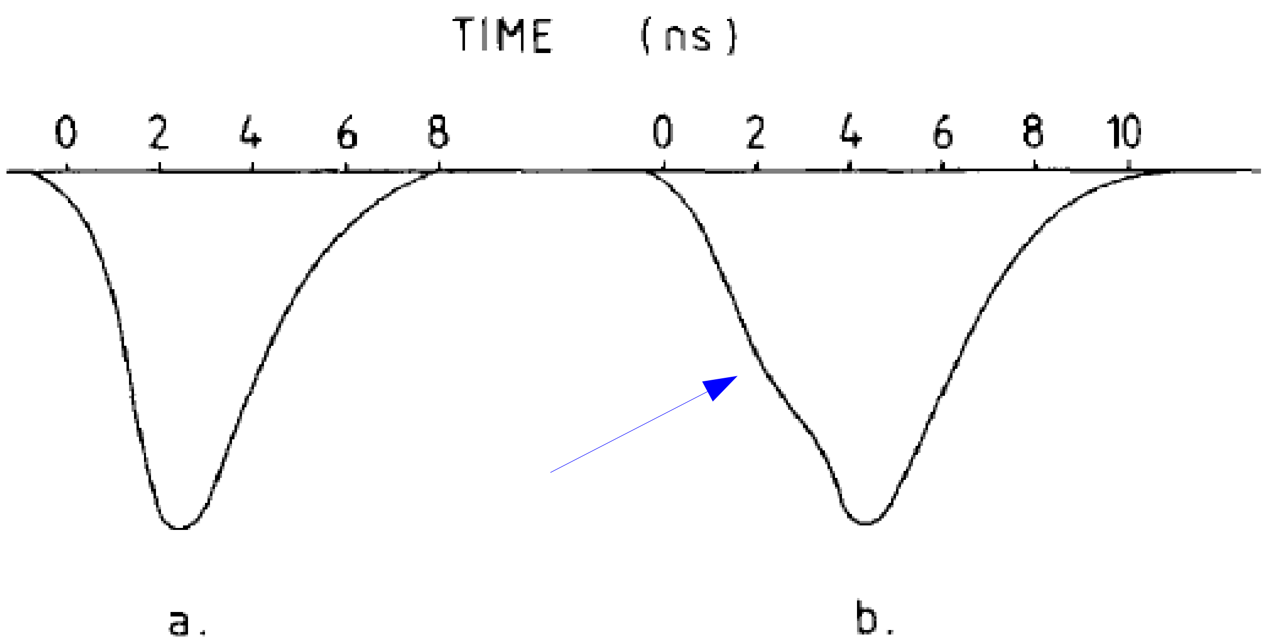

FIG. 7. (a) The most common pulse shape from an EMI 9814. (b) Uncommon pulse shapes possibly associated with backscattering effects. The count rate was set ~1 kHz and the frequency of occurrence of "nonstandard" pulses, of which (b) is an example, is about 1 in ten.

B.H.Candy "Photomultiplier characteristics and practice relevant to photon counting"
Rev. Sci. Instrum. 56, 183 (1985)

Micro Channel Plates - MCP-PMT

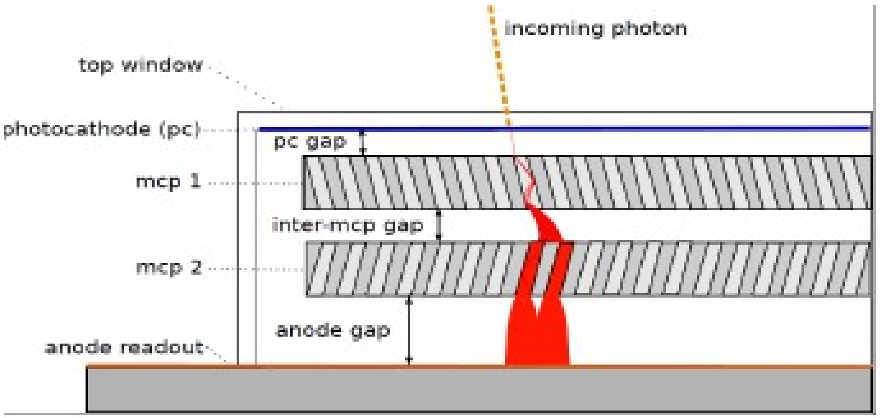

Can operate under **magnetic field**

Position measurement
- analog charge division
- Multi-anode readout
- Strip-lines readout
– σ_x ~ O(mm), not intrinsic

Noise
quite low noise ~ 0.1 Hz/cm^2
(Rb,K contamination)

Tiny electron multipliers
Diameter 20μm, 10μm, 6μm, 3μm
Length ~ O(500μm)

High Gain
G ~10^6 for two-stage type

Very Fast time Response
Rise time < 500ps
σ_{TT} < 50ps

Large Area
→ recent developments
cheap production: ALD on glass

Ageing
ion feed-back on cathode
→ recent improvements

MCP – single photon timing resolution

Short channel (500μm) and high E field in the channel (few 10kV/cm)
→ **ultra fast response** limited by
1) TTS in the gaps → short gaps
2) RC and parasitic LC filtering → **RF impedance matching**

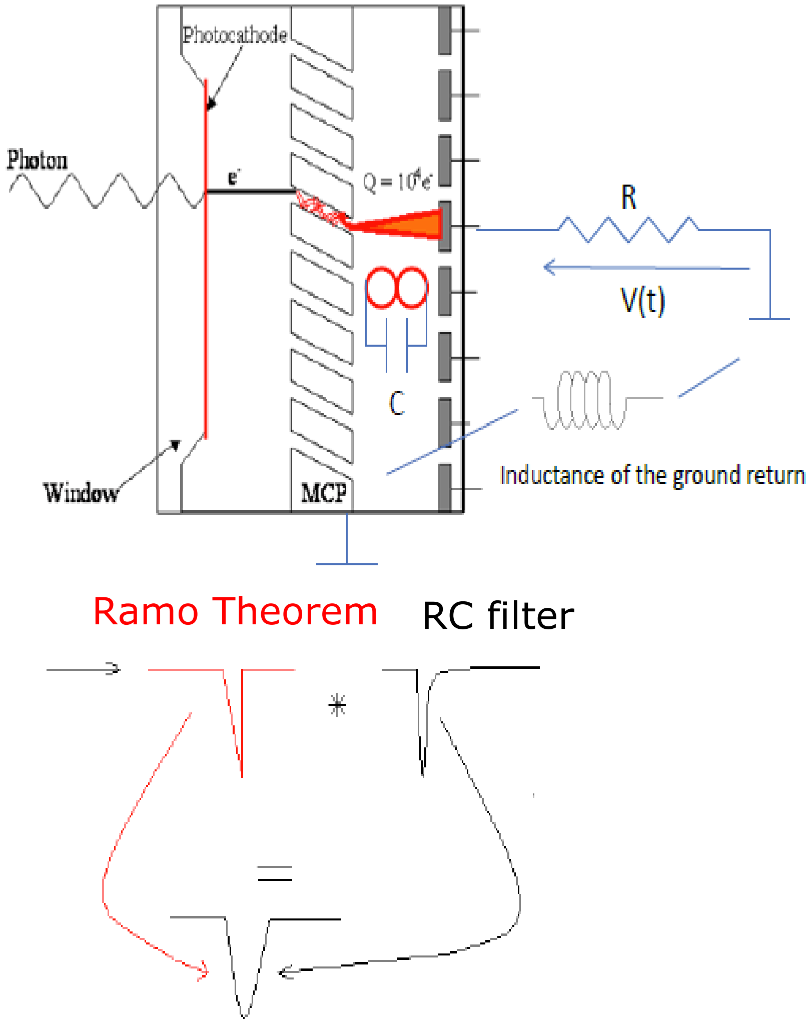

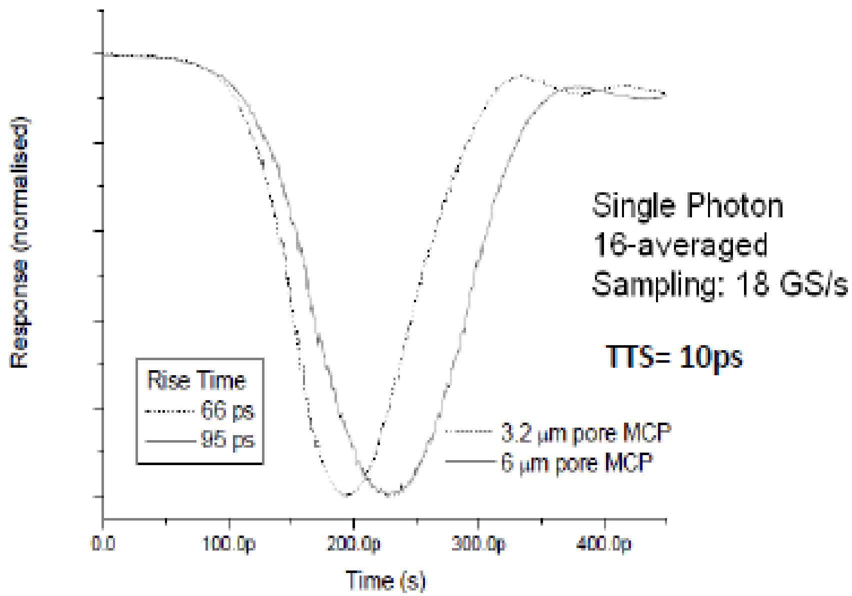

Time response curves for two models of PMT110 with different MCP pore diameters.

From Photek

11 mm diameter Micro-Channel Plate signal
Signal full bandwidth: 10 GHz

Typical Timing resolution:
Single Photoelectron Time Transit Spread: 10ps

MCP – single photon timing resolution

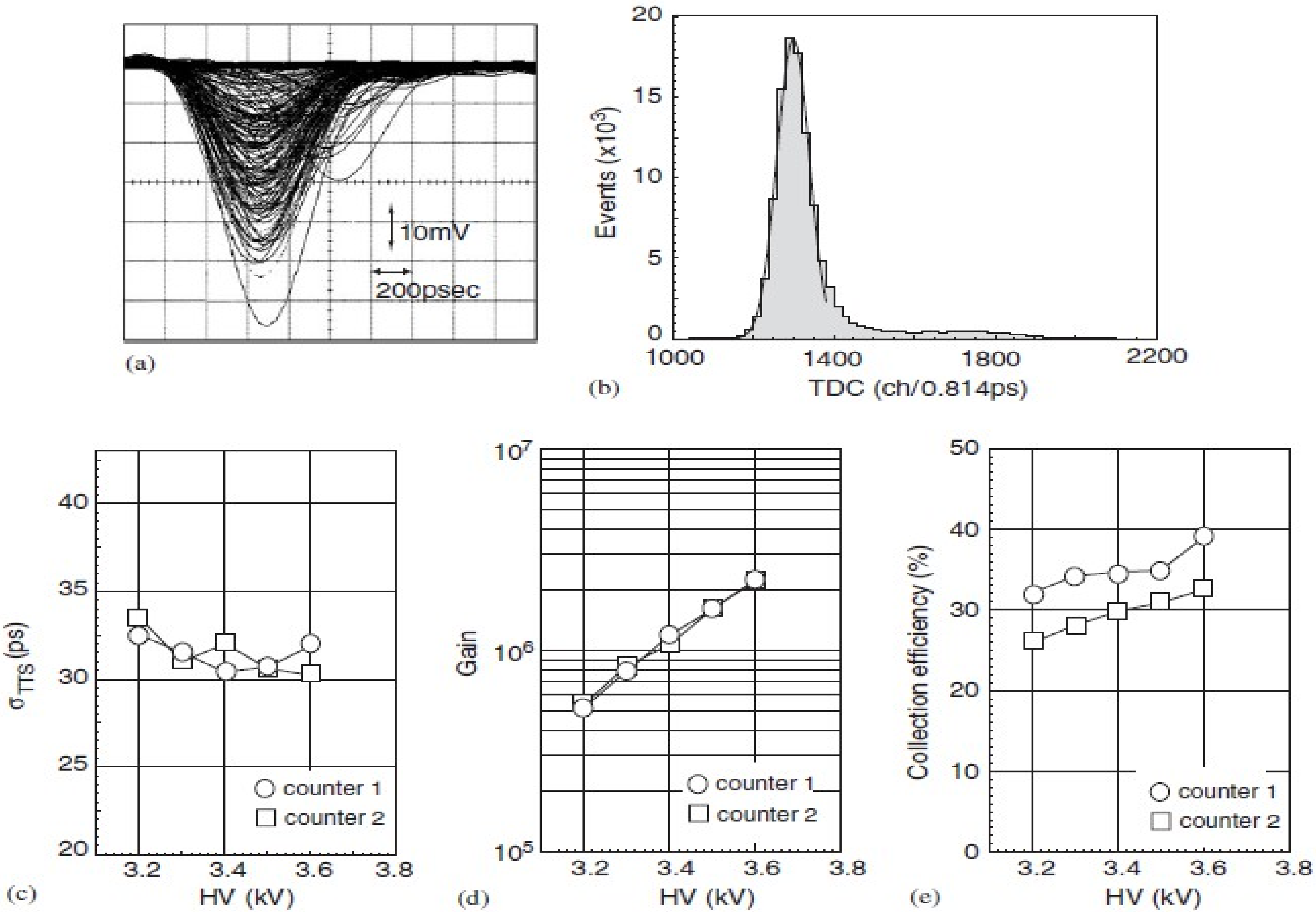

Fig. 3. Performance of the HPK6, measured using single-photons.

Inami et al NIM A 560 (2006) 303

Fast Timing & Imaging devices

	Multi-anodes PMTs Dynodes	matrices of Silicon-PMTs [10] Quenched Geiger in Silicon	Micro-Channel Plates [1] Micro-Pores
		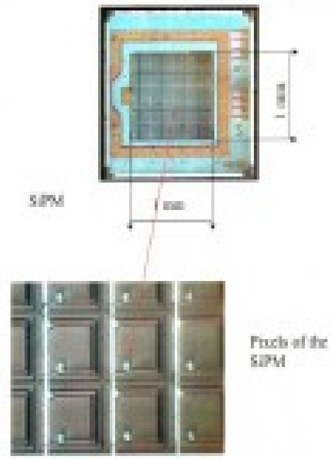	
Quantum Eff.	30%	90%	30%
Collection Eff.	90%	70%	70%
Rise-time	0.5-1ns	250ps	50-500ps
Timing resolution (1PE)	150ps	100ps	20-30ps
Pixel size	$2x2mm^2$	$50x50\mu m^2$	$1.5x1.5mm^2$
Dark counts	1-10Hz	$1-10MHz/mm^2$	$1Hz-1kHz/cm^2$
Dead time	5ns	100-500ns	$1\mu s$
Magnetic field	no	yes	15kG
Radiation hardness		1kRad=noisex10	good (a-Si, Al_2O_3)

Recovery Time

J.F.Genat, LAPPD Electronics Workshop (2012)

Large Area Pico-second Photo-detectors

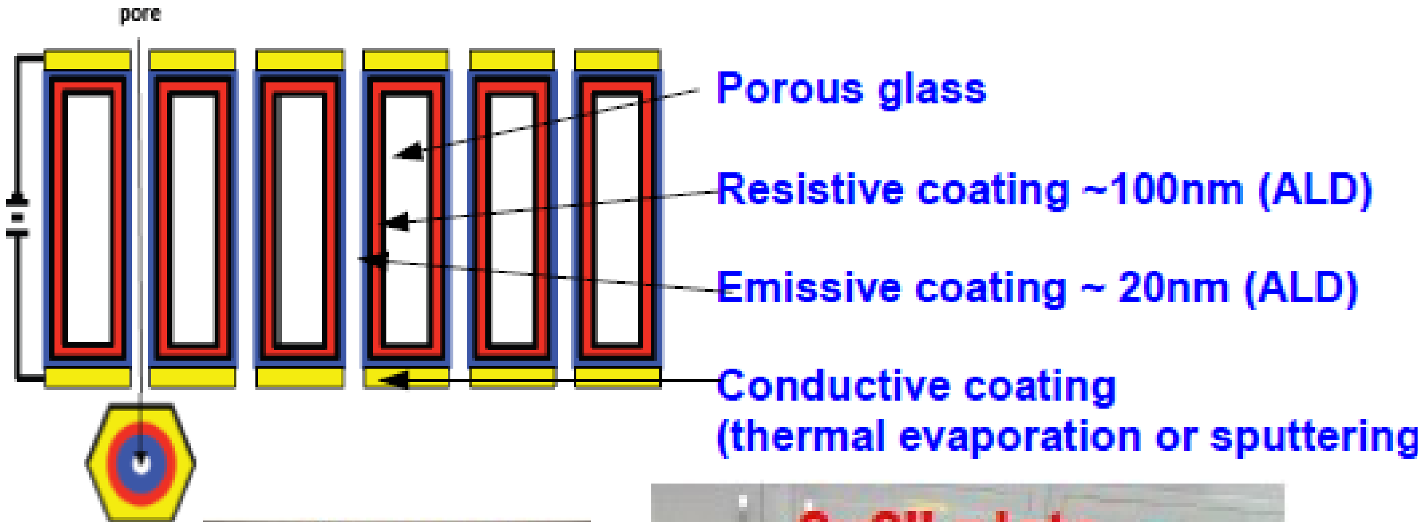

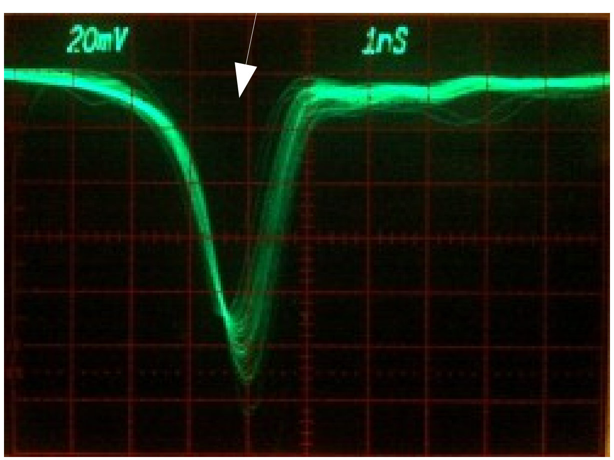

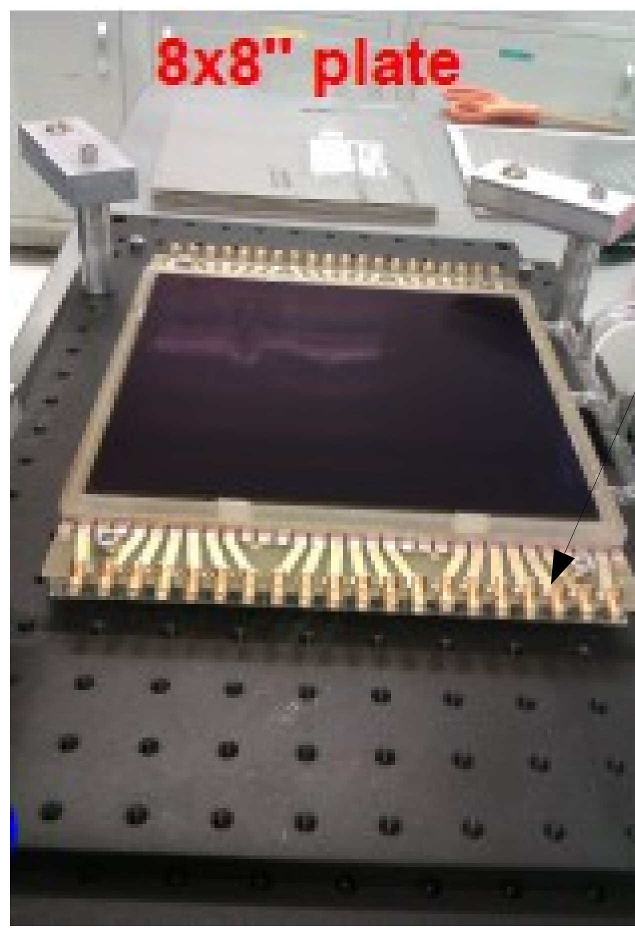

RF strip-line anodes

- 50 Ω impedance
- 1.6-0.4GHz bandwidth

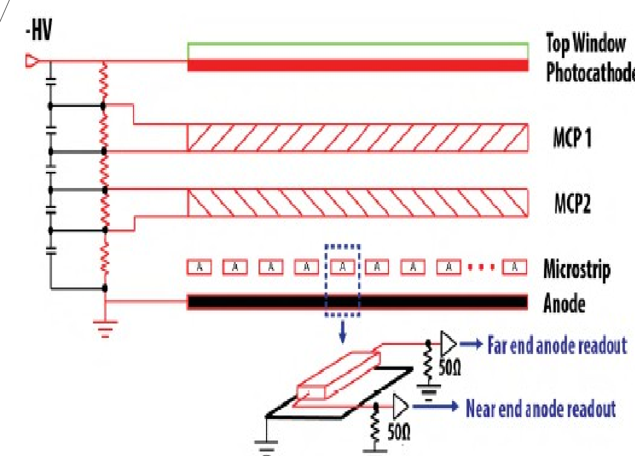

LAPPD
http://psec.uchicago.edu/

Solid state devices

Solid state devices with semiconductors

Basic working principles:

→ The two charge sheets on the n+ and p+ sides produce an **electric field**

→ separate e^--h^+ charges produced by (photo-)ionization in the **depleted region** (even without an external E field)

Charges surviving **recombination** are swept to terminals
→ can be detected as an **induced current**

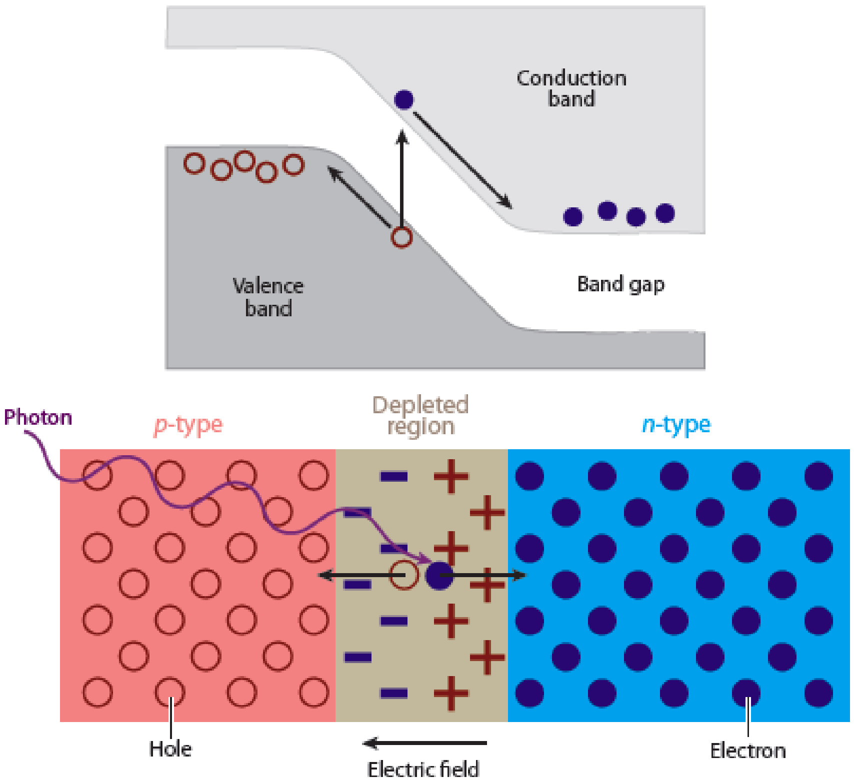

Picture from Krizan, Ann Rev Nucl Phys 2013

Note: Shockley-Ramo theorem → e- and h+ give "same sign" contribution to induced current; but integral of current induced on electrodes is Q and not 2Q

Solid state devices – a selection here

PN or PIN

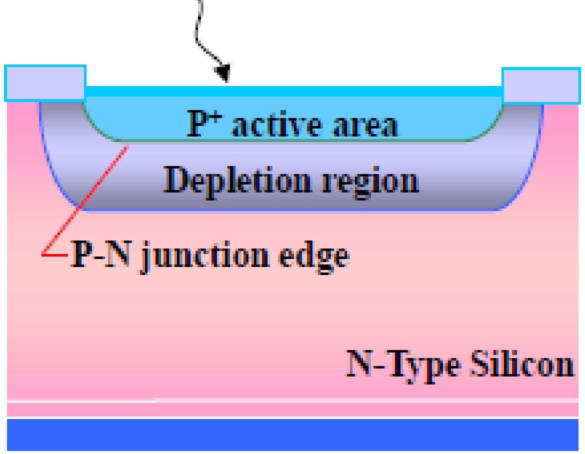

p-n junction,
reversed V_{bias} – 0-3 V

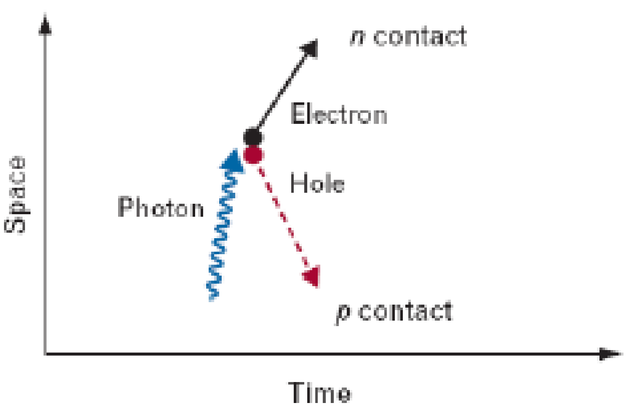

Gain = 1

APD

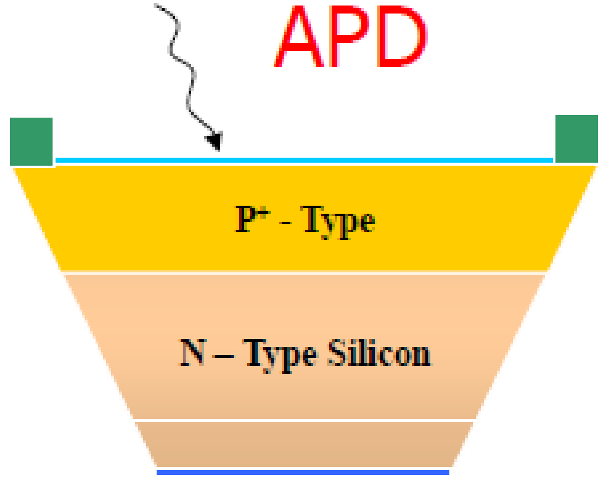

p-n junction,
reversed $V_{bias} < V_{BD}$

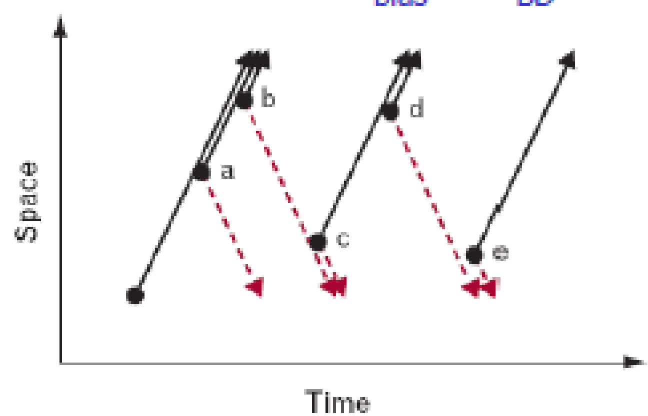

Gain = M (~ 50-500)

- linear mode operation-

GM-APD

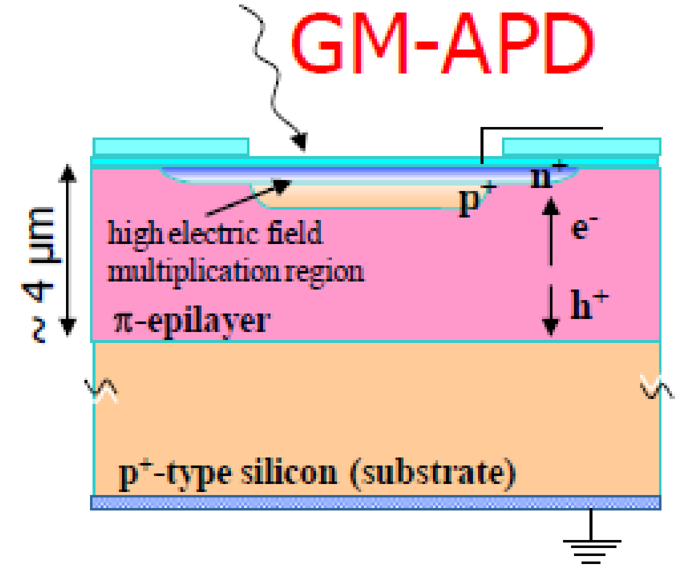

p-n junction,
reversed $V_{bias} > V_{BD}$

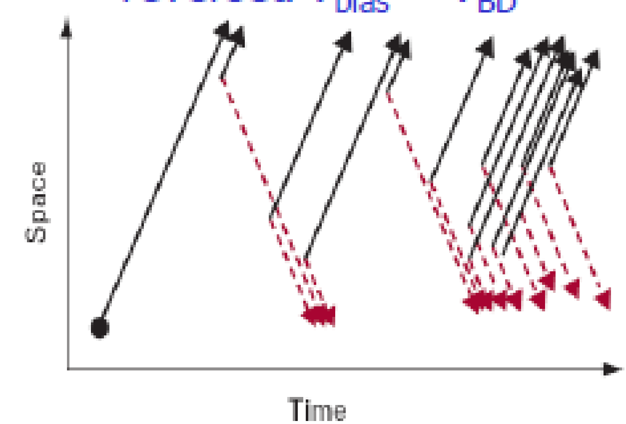

Gain → infinite

-Geiger-mode operation-

Solid state devices – PIN

One of the simplest kind of photo-diodes is the **p-i-n photodiode**
→ intrinsic piece of semiconductor sandwiched between two heavily (oppositely) doped regions

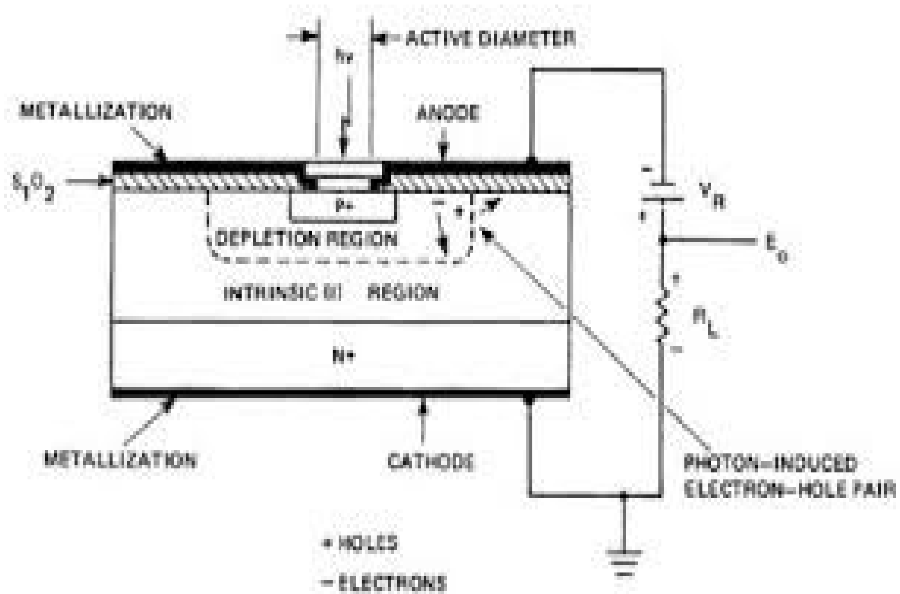

Intrinsic region for:
→ lower capacitance → faster/low noise
→ lower dark current
→ higher efficiency for NIR

Basic model: current generator
Electronics: either I → V conversion
→ w/ R → limited sensibility
→ Op. Amp. w/ R feedback better choice or charge amplifier

Anyway long integration time (low bandwidth) is needed for detecting low light level detection above noise due to leakage current and large capacitance
→ limit is O(100) photons with time filter O(μs) for O(cm^2) detector

see Akiba et al Optics Letters 28 (2003) 1010 for Ultralow noise detection system with a PIN diode

Groom's theorem on photo-det. resolution

About the #photon resolution of an assembly
scintillator + semiconductor photo-diode

Noise/Signal ratio (→ resolution) ~ scintillator area (A)
and
independent of the detector Area (a)

Indeed: amount of light collected is proportional to a/A (crude approx. due to internal reflections) and noise is proportional to the PD capacitance → to a (also crude approx. not valid for very small a)

… ok a should as large as possible but there is little sensitivity to a

D. Groom NIM A 219 (1984) 141

Solid state devices – APD a diode with gain

"Reach Through" "Beleved Edge" "Reverse"

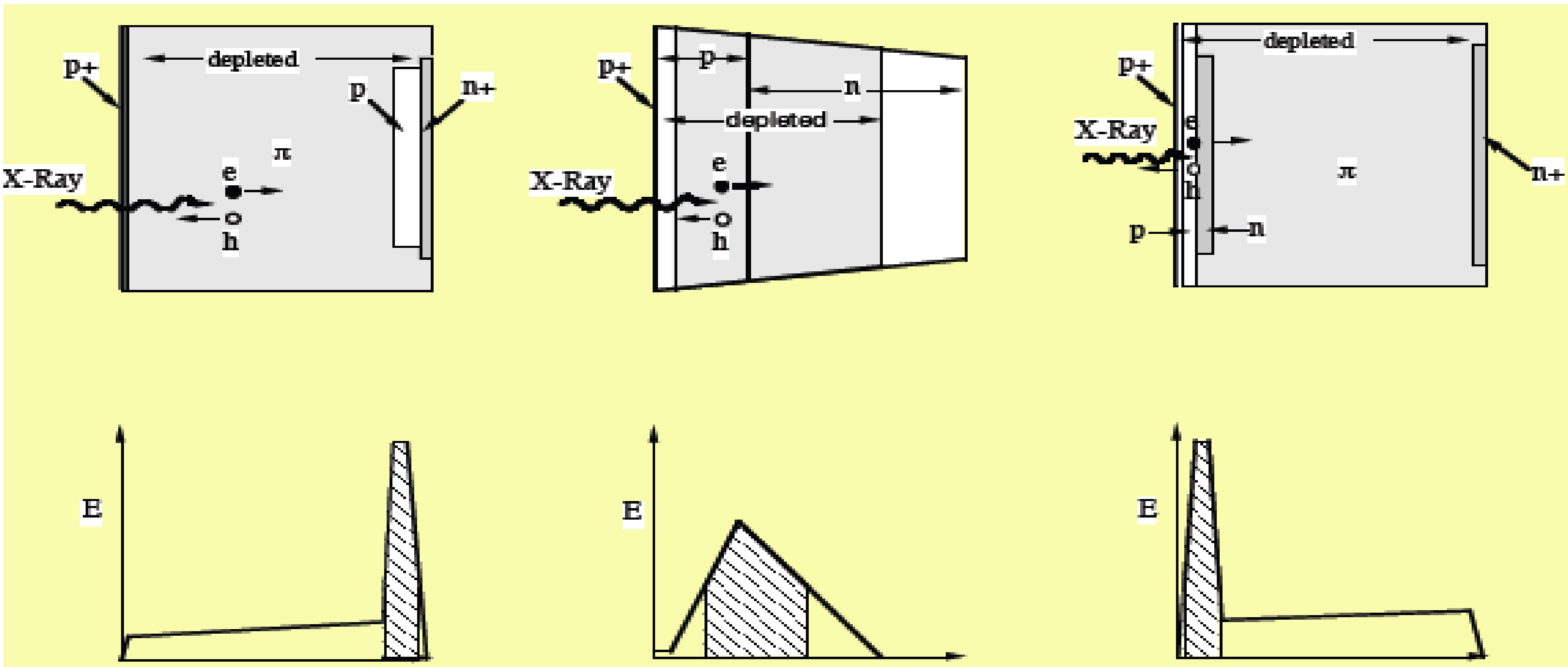

"Reach Through"	"Beleved Edge"	"Reverse"
Narrow Gain Region Medium Voltage 50-700V Large Drift Region Modest Gains (<200)	Wide Gain Region High Voltage (1-2 kV) High Gains Possible Larger Areas Possible	Narrow Gain Region Medium Voltage <500V Small Drift Region

Solid state devices – APD a diode with gain

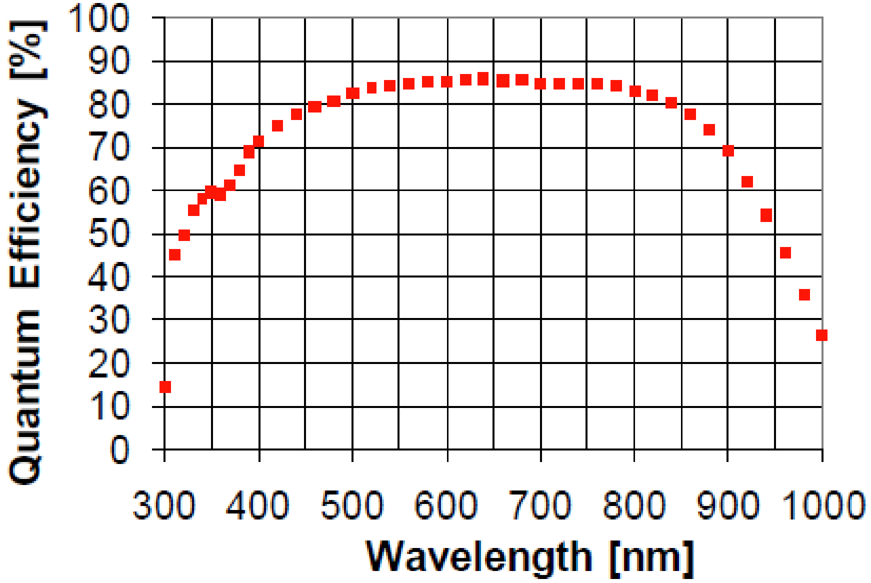

Example of modern APD characteristics
(CMS EM calorimeter massive use)

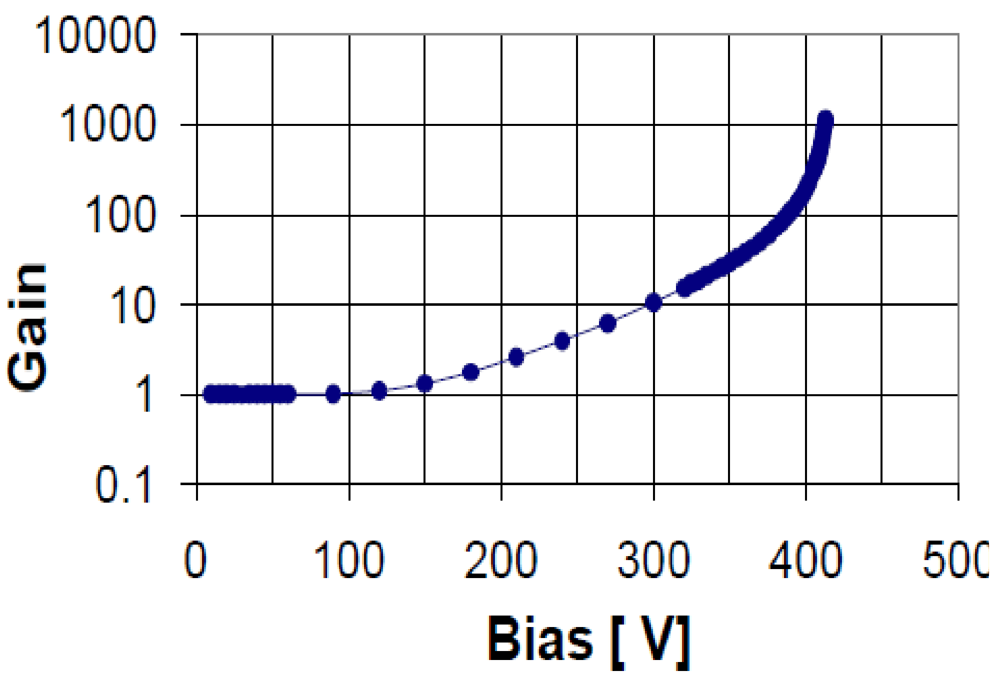

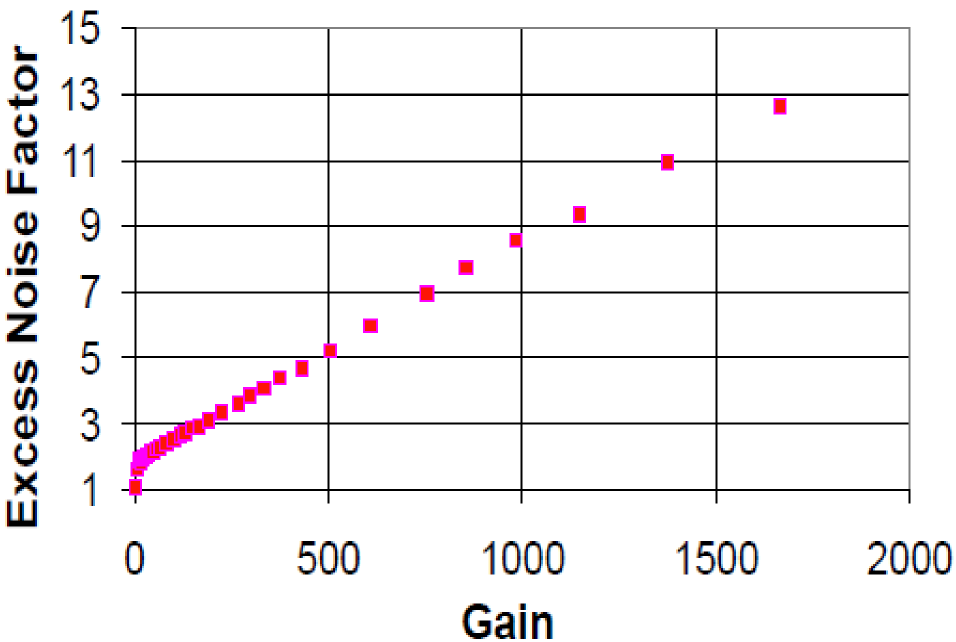

Y.Musienko – SiPM review – CERN feb 2011

APD – Multiplication illustrated

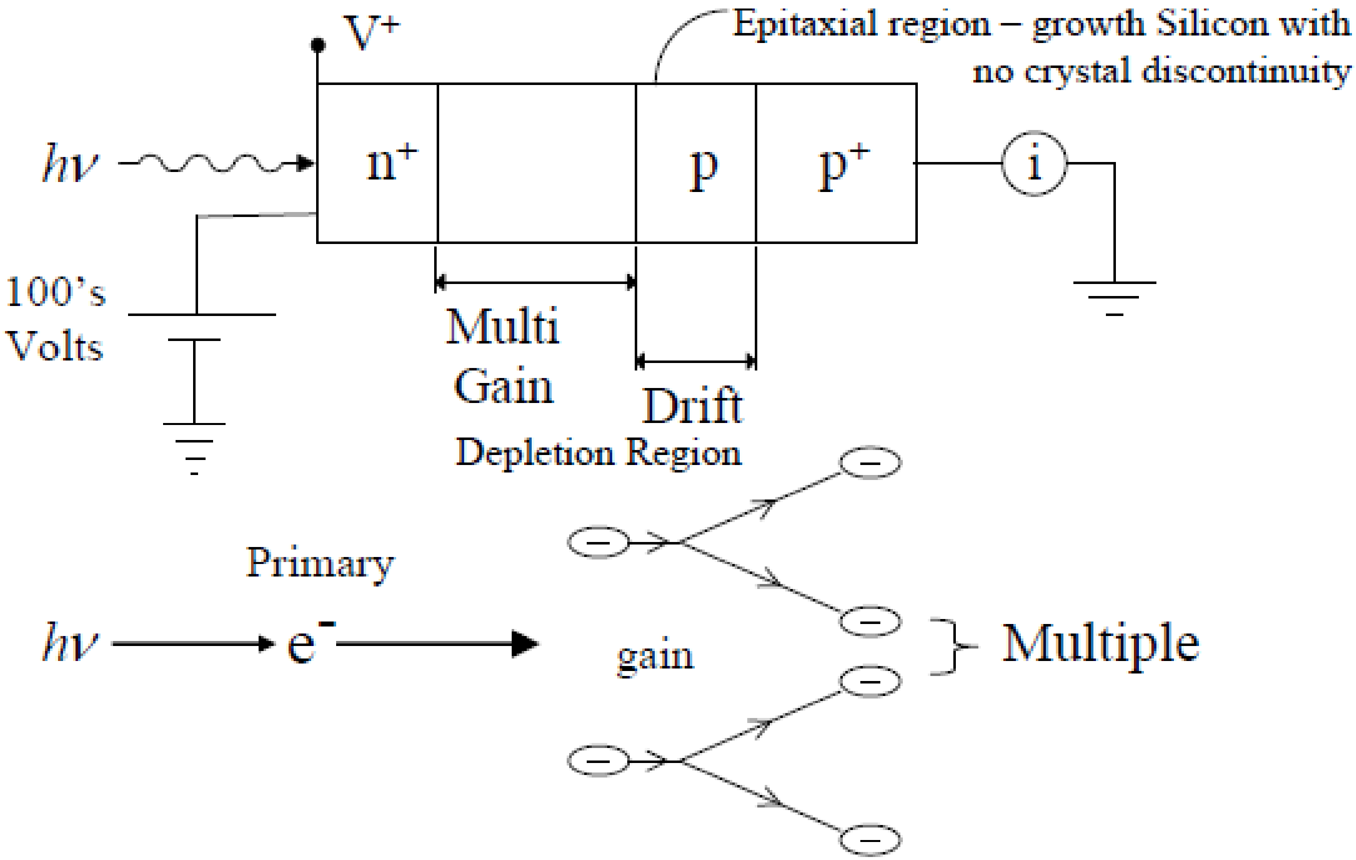

Electrons gain sufficient kinetic energy to cause another electron to conduction band

Hole multiplication is not as important, because mobility is less, but it causes slow feedback and process excess noise

APD – Multiplication factor

$$M_n = \frac{J}{J_n(0)} = \frac{1}{1 - \int_0^W dx' \alpha_n e^{-(\alpha_n - \beta_p)x'}}$$

$$M_n = \frac{1}{1 - \frac{\alpha_n}{\alpha_n - \beta_p}\left(1 - e^{-(\alpha_n - \beta_p)W}\right)}$$

$$= \frac{\alpha_n - \beta_p}{\alpha_n e^{-(\alpha_n - \beta_p)W} - \beta_p}$$

Define $k = \frac{\beta_p}{\alpha_n}$

$$\boxed{M_n = \frac{1-k}{e^{-(1-k)\alpha_n W} - k}}$$

Breakdown if $1 = \int_0^W dx' \alpha_n e^{-(\alpha_n - \beta_p)x'}$

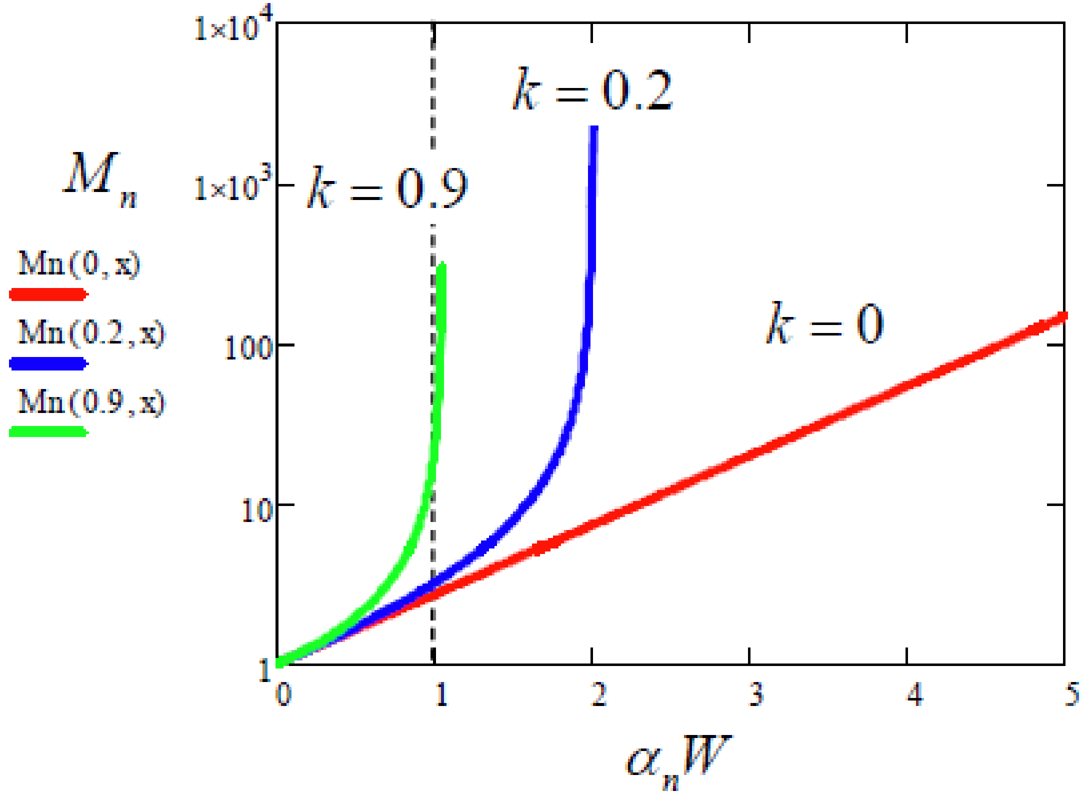

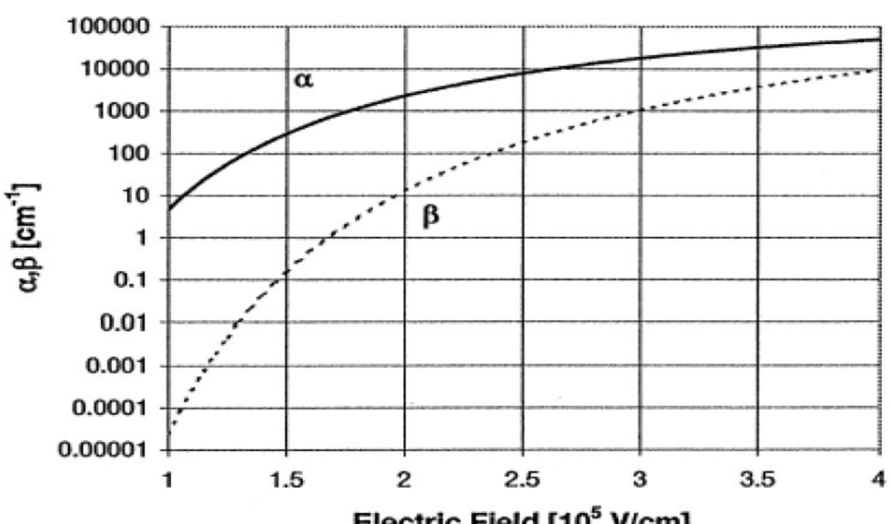

APD – Multiplication illustrated

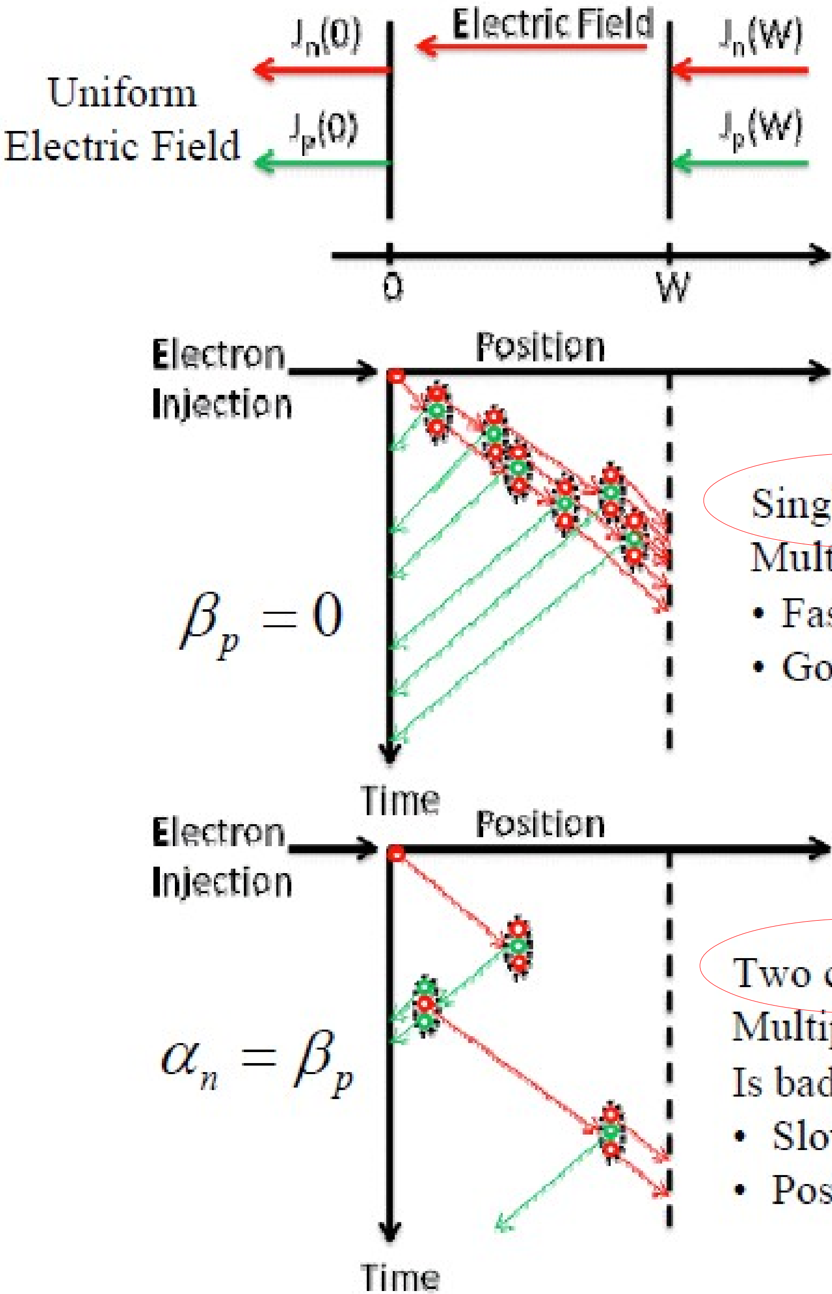

$e^- \rightarrow$

$h^+ \leftarrow$

Two ideal special cases

k = 0

Single Carrier Multiplication

- Fast
- Good

} PMT

For $\beta_p = 0$ and a uniform electric field

$$M_n = \exp\left(\int_0^W \alpha_n dx\right) = \exp(\alpha_n W)$$

No avalanche breakdown and M_n increases exponentially with bias

k = 1

Two carrier Multiplication Is bad

- Slow
- Positive feedback

For $\alpha_n = \beta_p$ and a uniform electric field

$$M_n = M_p = \frac{1}{1 - \int_0^W \alpha_n dx} = \frac{1}{1 - \alpha_n W}$$

True avalanche breakdown at the voltage where $\alpha_n W = 1$

G.E. Stillman and C.M. Wolfe, "Avalanche Photodiodes", in Semiconductors and Semimetals Vol. 12, ed. by R.K. Willardson and A.C. Beer (Academic, N.Y., 1977).

APD – Multiplication in practice

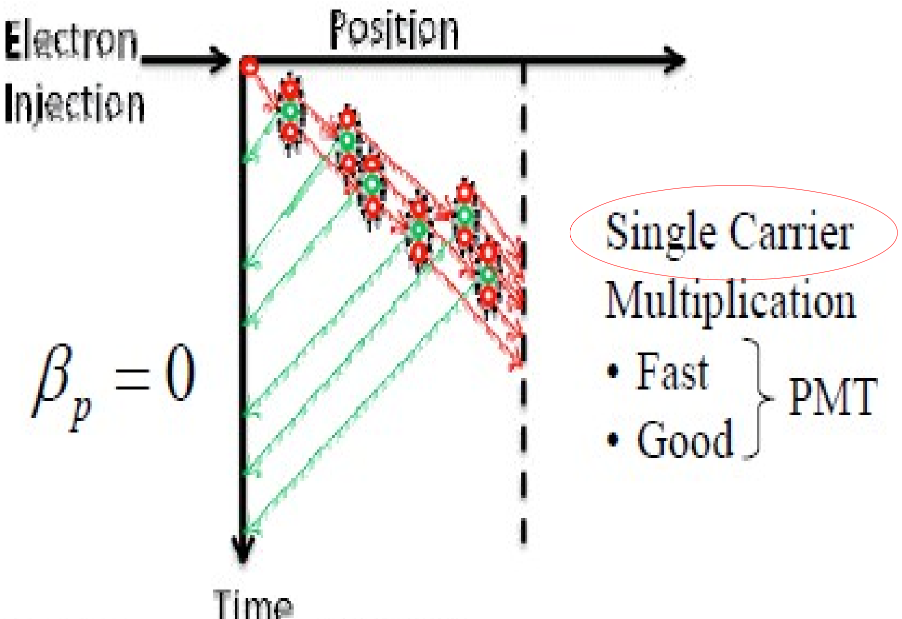

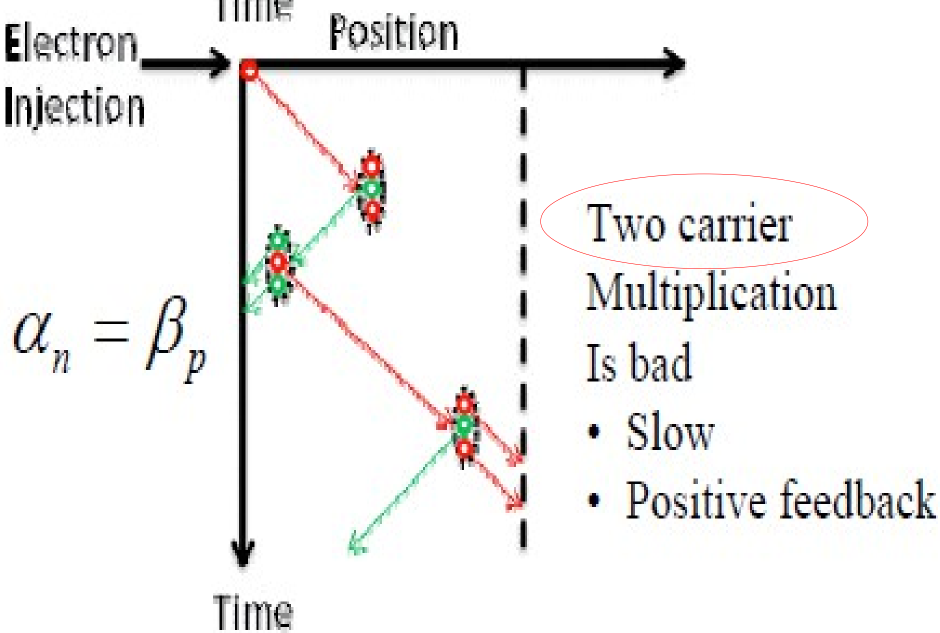

G.E. Stillman and C.M. Wolfe, “Avalanche Photodiodes”, in Semiconductors and Semimetals Vol. 12, ed. by R.K. Willardson and A.C. Beer (Academic, N.Y., 1977).

When APD biased for low gain **M < 1/k**

- fast “normal” exponential growing
  - current → 0 in $\sim\tau_h$ hole transit time
  - pulse duration ~ 2x w/o gain
  - no gain-BW limitation
- high number of carriers in high field region at given time: variations of impact ionization induce
  → small fluctuations

When APD biased for high gain **M > 1/k**

- significant prob. of hole ionization event within a given avalanche
- **slow buildup** and long pulse due to many carriers over long time
  - gain-BW limitation
- low number of carriers in high field region at given time
  → large fluctuations
- hole ionization near cathode result in larger pulses

APD – Fluctuations of Gain

Excess Noise Factor

$$ENF \equiv F \equiv \frac{\langle M^2 \rangle}{\langle M \rangle^2}$$

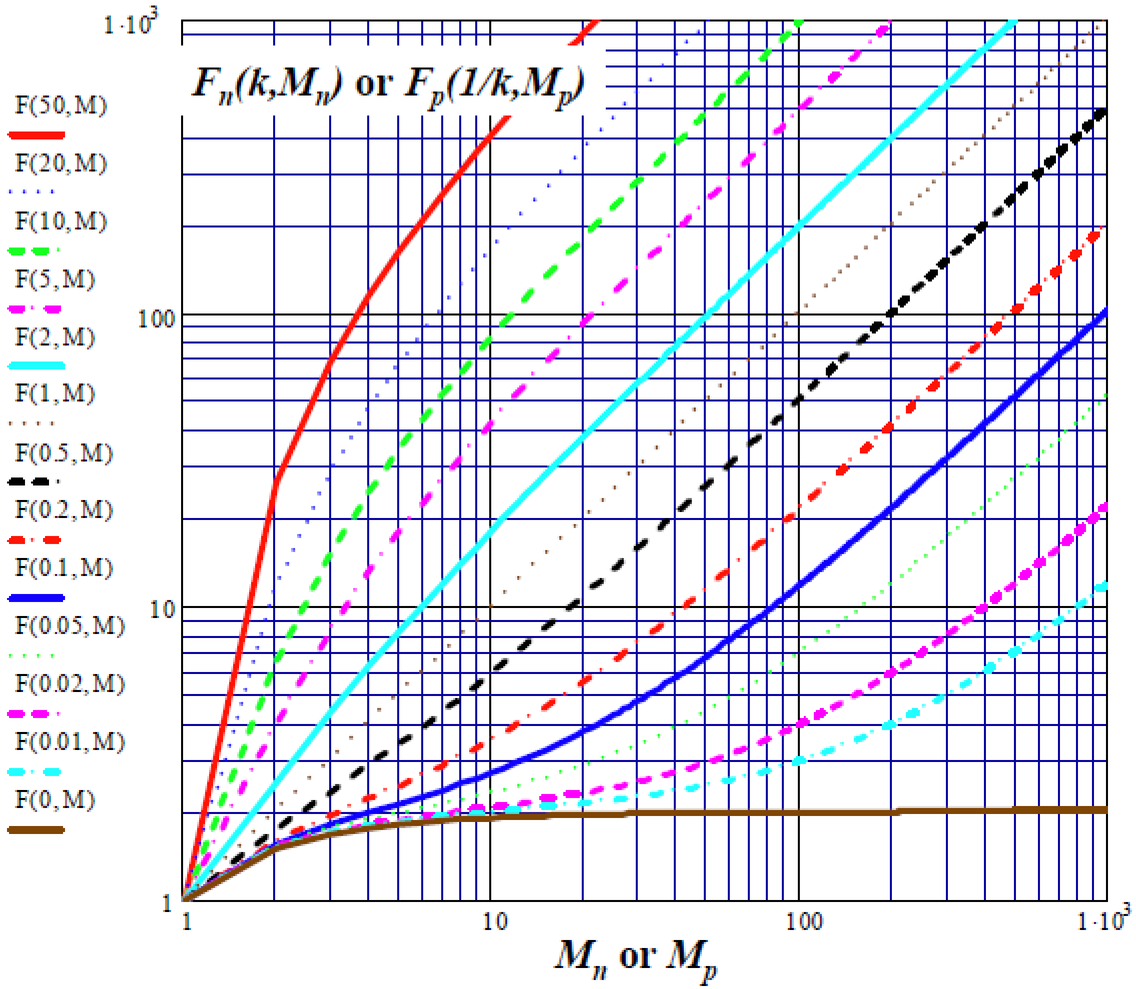

$$F_n = M_n\left\{1-(1-k)\left[\frac{M_n-1}{M_n}\right]^2\right\}$$

$$F_p = M_p\left\{1-\left(1-\frac{1}{k}\right)\left[\frac{M_p-1}{M_p}\right]^2\right\}$$

McIntyre 1966

APD – Fluctuations of Gain

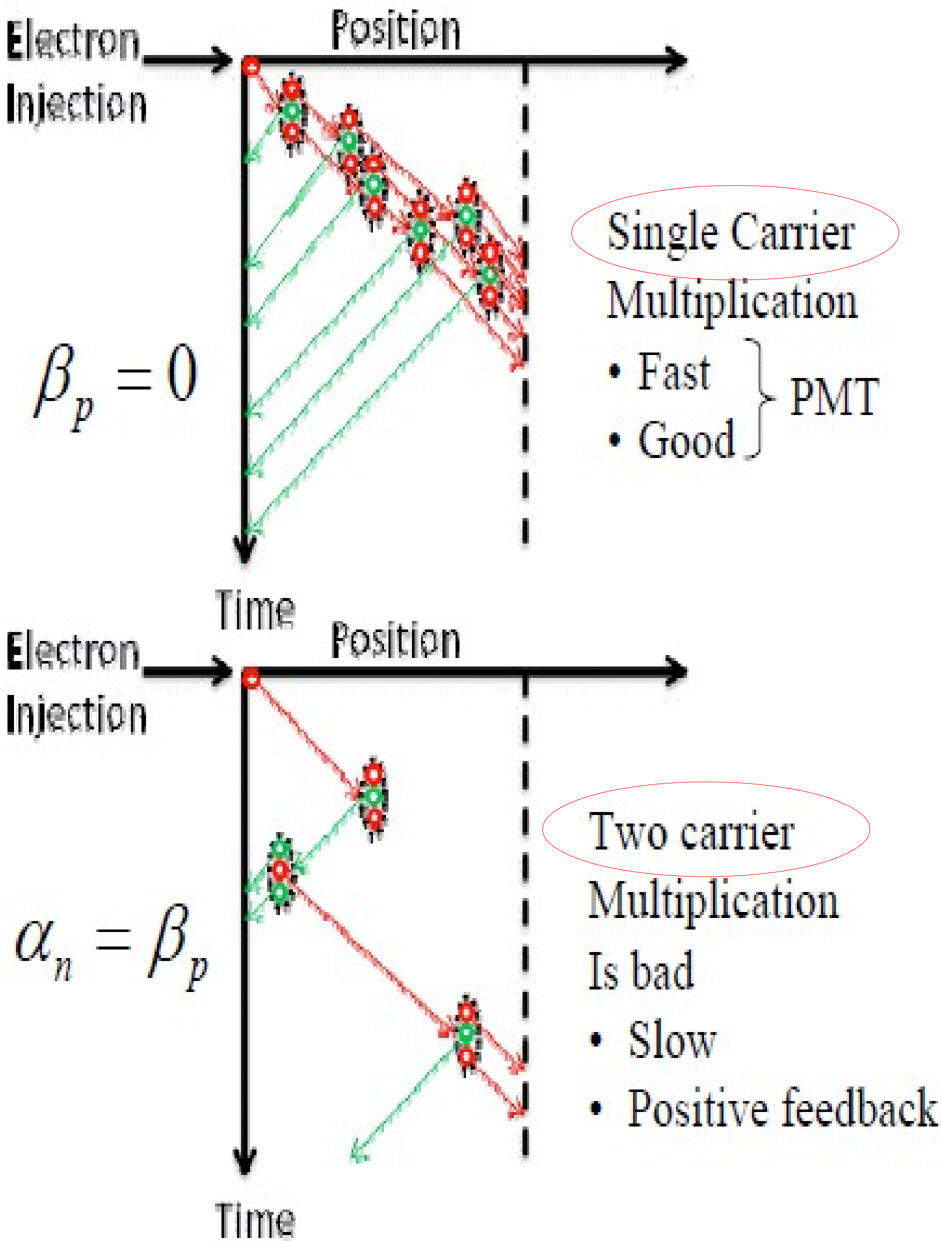

When APD biased for low gain **M < 1/k**

$$F \rightarrow 2$$

When APD biased for high gain **M > 1/k**

$$F \rightarrow 2 + kM$$

For device gains >> 1/k further increases of gain are the result of small numbers of relatively large pulses that are due to one or more hole ionization initiated secondary avalanches

Note: in PMT also avalanche is a Markov process but constrained to a fixed number of events (dynodes) → ENF limited to F~1.2

Interesting papers: Waks et al "High Photon Number detection for Quantum Information Processing" IEEE Sel. Topics Q. Ele. 9 (2003) 1502 and Fox et al "Characterization of cooled large-area silicon avalanche photodiodes" Rev. Sci. Instr. 70 (1999) 1951

APD – Fluctuations of Gain and Timing

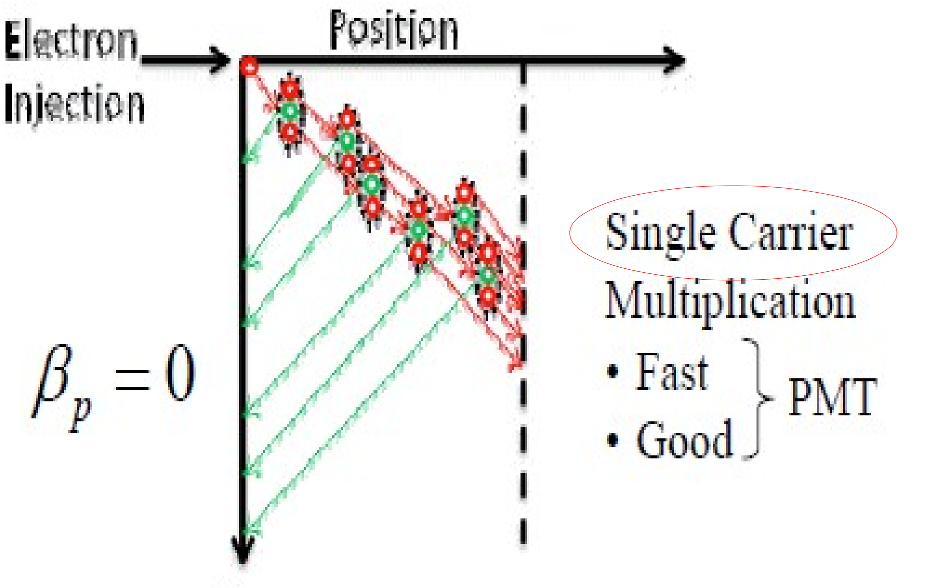

When APD biased for low gain **M < 1/k**

Timing fluctuations are small limited by the length of depletion region
→ time resolution limited by electronics
(high Amplification for low light signals)

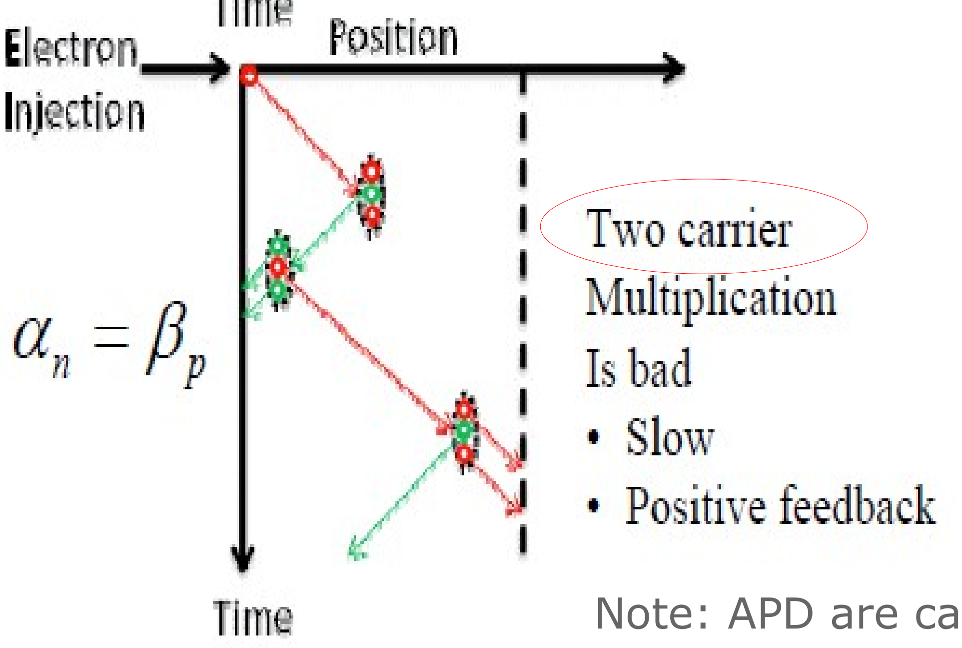

When APD biased for high gain **M > 1/k**

Timing fluctuations are large due to fluctuations in avalanche

see for instance Hayat et al J. Lightwave Tech. 24 (2006) 755

Note: APD are capable of Single Photon detection but quite low T cooling mandatory. See for instance

APD – Timing with x-rays

Timing

S5343
(1mm dia., 10µm)

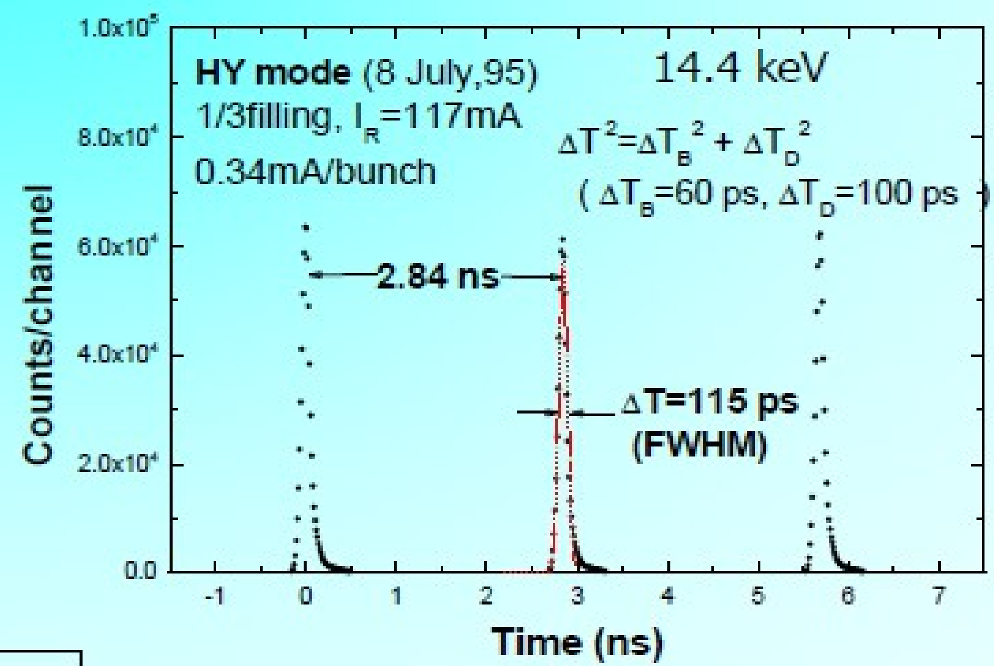

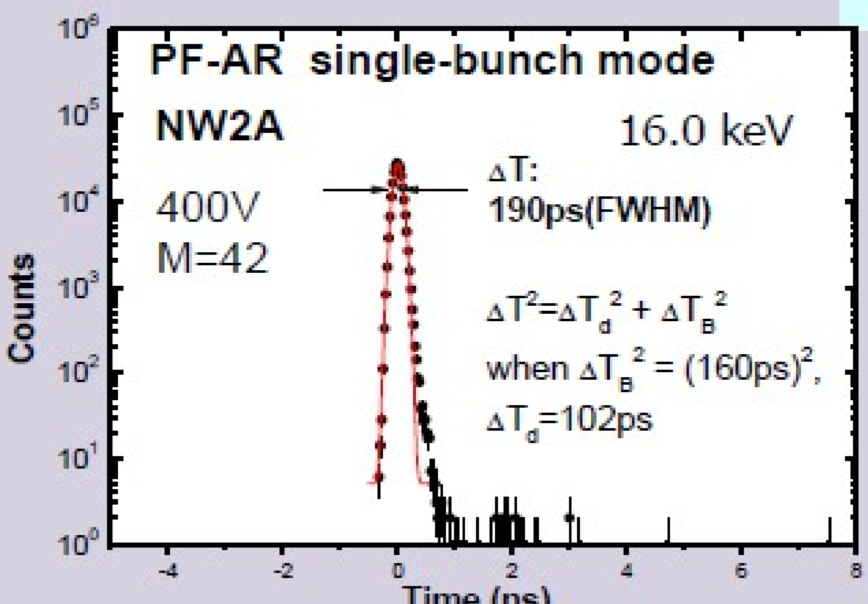

S8664-30
(3mm dia., 7-10 µm)

ΔT< 100ps is possible !

… with x-rays …

S.Kishimoto APD detector Workshop ESFR 2005

APD disadvantages

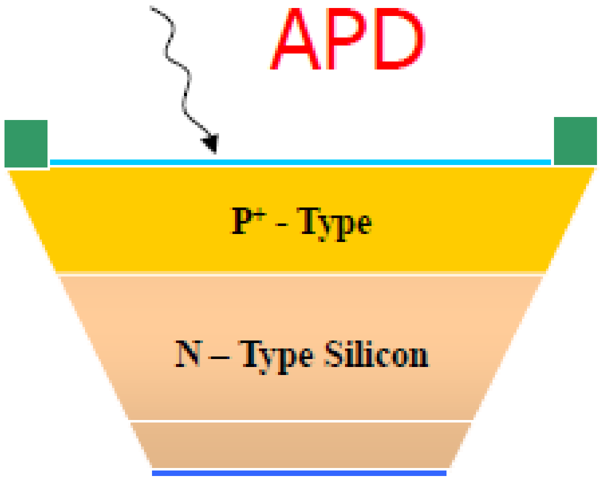

Main disadvantages:

→ ENF increases with increasing gain
→ Temperature coefficient also increases with gain
(… gain stability)

Devices with high multiplication noise are not good for single photon counting

Single photon counting is possible, but at low temperature (T~77K) and with slow electronics (PDE~20%)

A. Dorokhovet.al.,JournalMod.Opt. v51 2004 p.1351

Additional disadvantage:

→ sensitive to charged particles, neutrons, … (nuclear counter effect)

Solid state devices

Reverse biased junction: internal gain via impact ionization in high E field

APD: avalanche photo-diode

- Bias BELOW V_{bd} ($V_{APD} < V < V_{bd}$)
- Linear Mode/ AMPLIFIER device
- Multiplication < 10^3 (lim. by fluctuations)
- Sensitivity ~ 5 ph.e

  (1ph.e. at low T with slow electronics...)

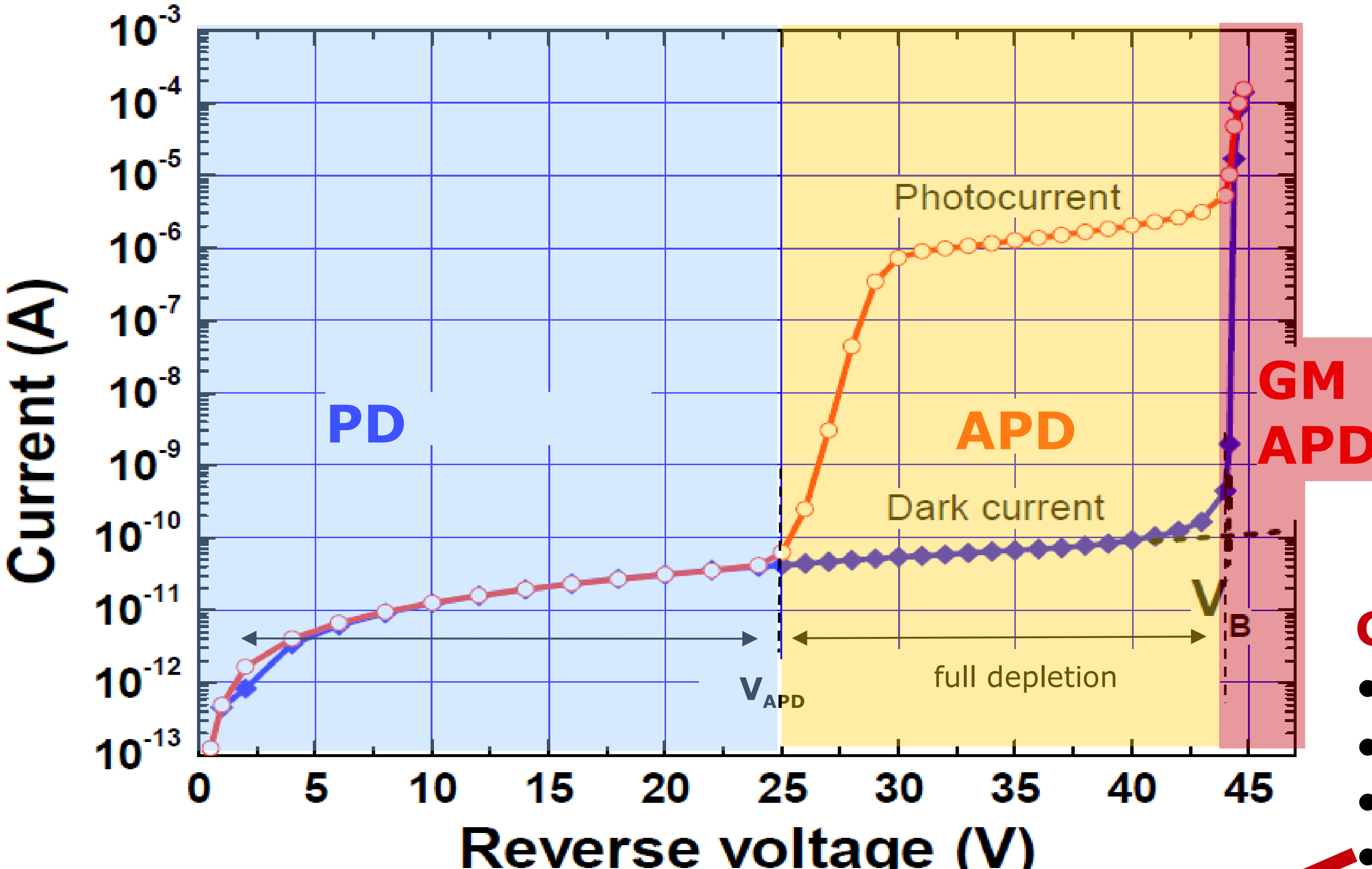

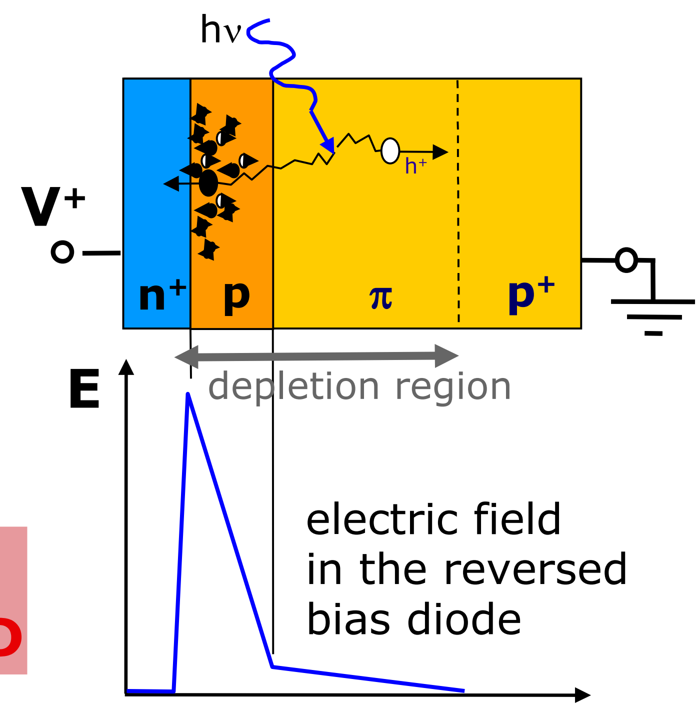

GM-APD: Geiger Mode

- Bias ABOVE V_{bd} (a few V)
- **BINARY** device
- Gain: ~10^6 (lim. by C)
- **Single ph.e. resolution**
- Limited by dark count rate
- **Need Quenching/Reset**

basis for building alternative to PMT

G.C

Geiger Mode APD → SPAD

- Two types of implementation (→ arrays)

planar - - reach through

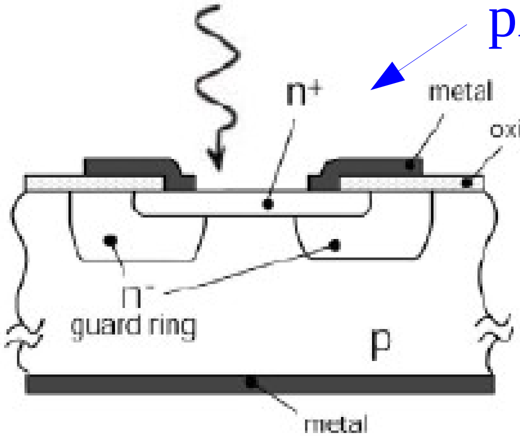

R.H. Haitz
J. Appl. Phys.,
Vol. 36, No. 10 (1965) 3123

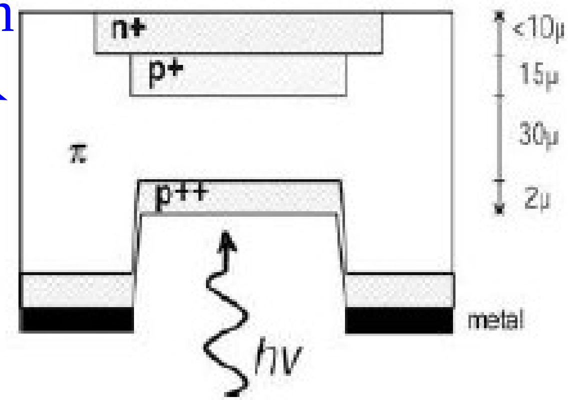

J.R. McIntire
IEEE Trans. Elec. Dev.
ED-13 (1966) 164

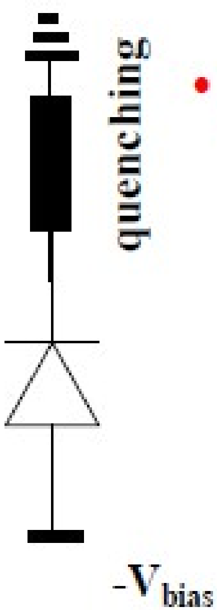

- Quenching mechanisms
  - Passive quenching: large resistance
  - Active quenching: analog circuits

S. Cova & al., App. Opt. 35 (1996) 1956-1976

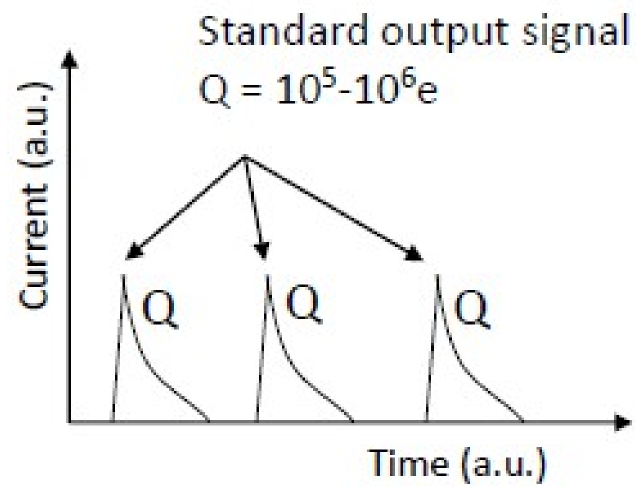

Binary device

- If one or more simultaneous photons fire the GM-APD, the output is anytime a standard signal: $Q \sim C(V_{bias} - V_{BD})$
- GM-APD does not give information on the light intensity

The Silicon PM: array of GM-APD

Single GM-APD gives **no information** on light intensity → use array of GM-APDs' first proposed in the late '80-ies by Golovin and Sadygov

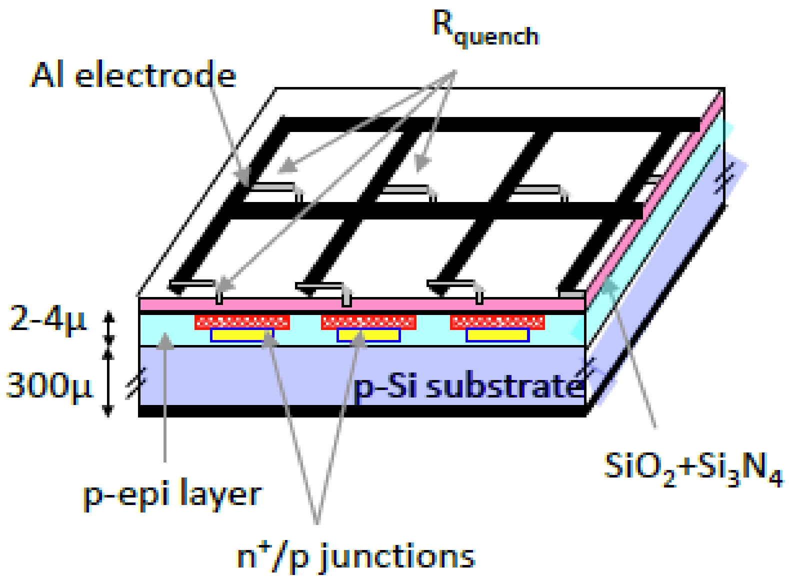

A SiPM is segmented in tiny GM-APD cells and connected in parallel trough a decoupling resistor, which is also used for quenching avalanches in the cells

Each element is independent and gives the same signal when fired by a photon

Σ of binary signals → analog signal

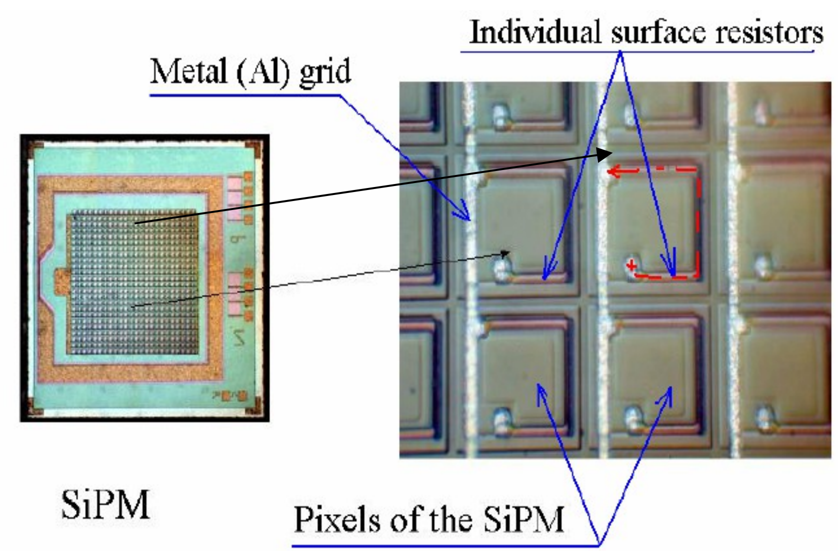

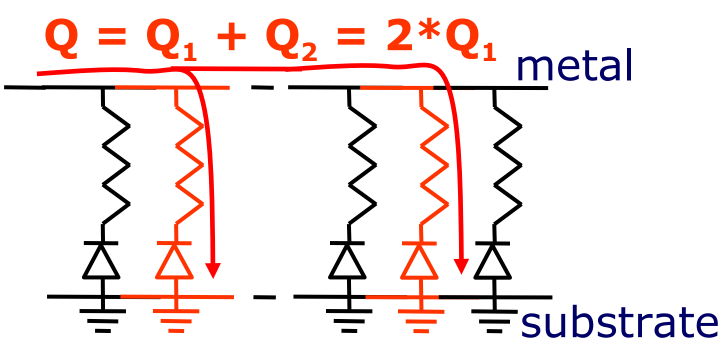

Output ∝ number incident photons

The Silicon PM: array of GM-APD

Single GM-APD gives **no information** on light intensity → use array of GM-APDs' first proposed in the late '80-ies by Golovin and Sadygov

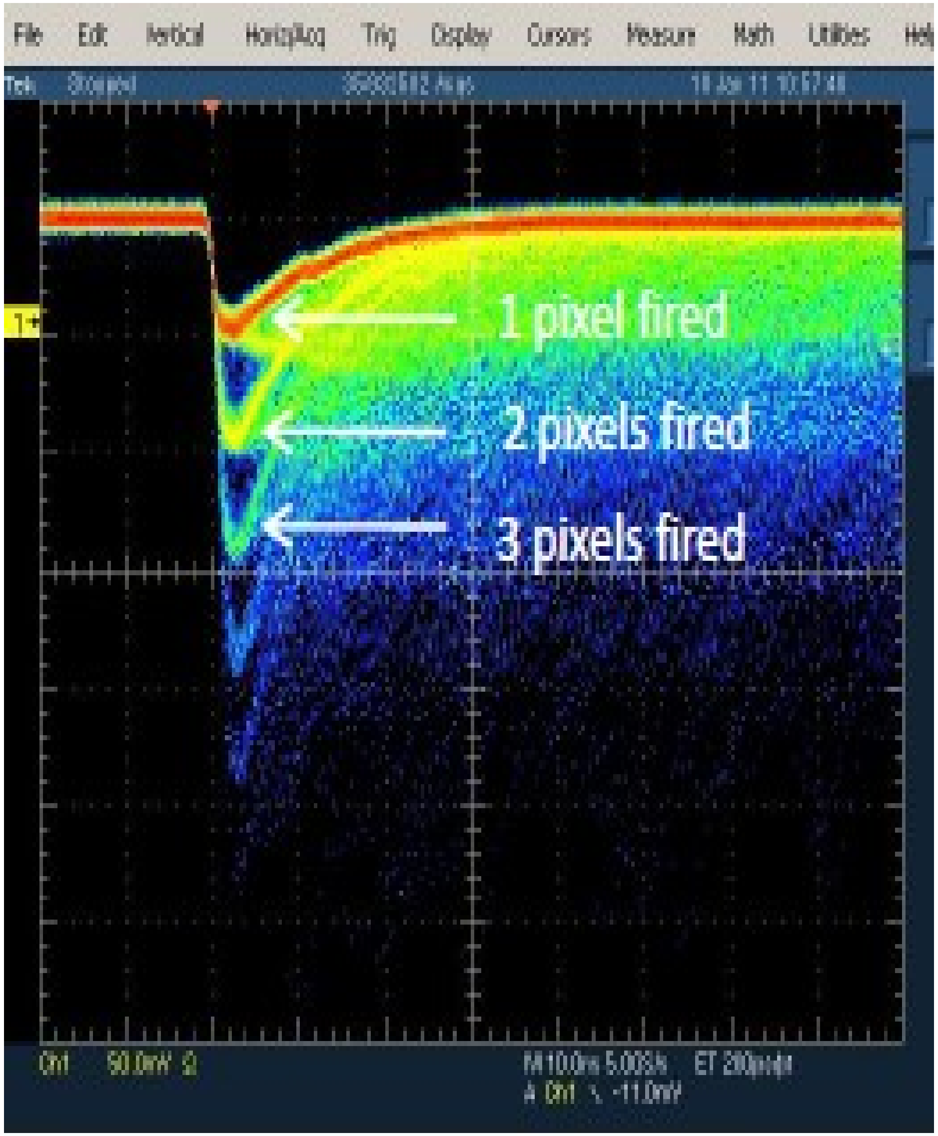

A SiPM is segmented in tiny GM-APD cells and connected in parallel trough a decoupling resistor, which is also used for quenching avalanches in the cells

Each element is independent and gives the same signal when fired by a photon

Σ of binary signals → analog signal

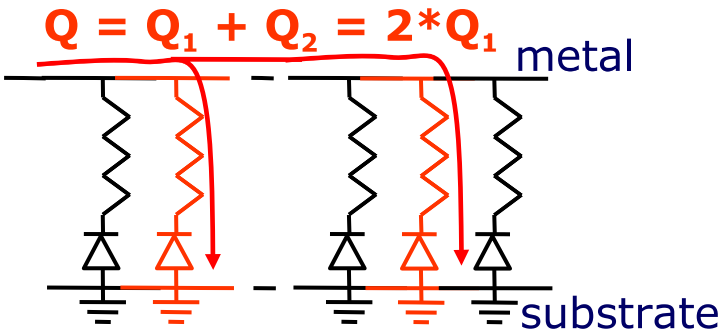

Output ∝ number incident photons

A bit of history

Pioneering work since late 80-ies at Russian institutes

Investigations of various multi-layer silicon structures with local micro-plasma suppression effect to develop low-cost GM-APD arrays

Early devices ageing quickly, unstable, noisy

Sadygov – JINR/Micron (Dubna)

Avalanche Micro-channel/pixel Photo Diodes (AMPD)

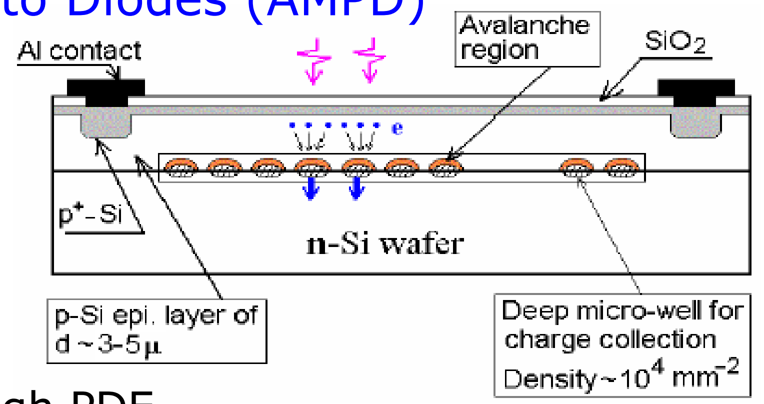

- high PDE
- very high density of micro-cells

eg Sadygov, NIMA 567 (2006)

Dolgoshein - MePhi/Pulsar (Moscow)

Poly-silicon resistor

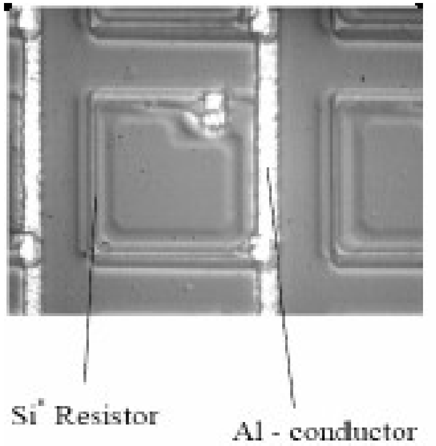

- Low fill-factor
- Simple fabrication technology

e.g., Dolgoshein, NIMA 563 (2006)

Golovin - Obninsk/CPTA (Moscow)

Metal-Resistive-Semiconductor (MRS)

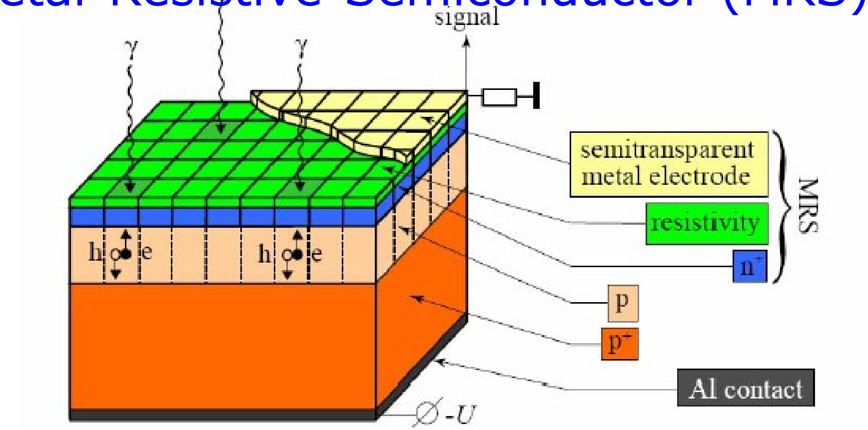

- High fill factor
- Good pixel to pixel uniformity

e.g., Golovin NIMA 539 (2005)

Today

Many institutes/companies are involved in SiPM development/production:

- **CPTA**, Moscow, Russia
- **MePhi/Pulsar** Enterprise, Moscow, Russia
- **Zecotek,** Vancouver, Canada
- **Hamamatsu HPK**, Hamamatsu, Japan
- **FBK-AdvanSiD**, Trento, Italy
- **ST Microelectronics**, Catania, Italy
- **Amplification Technologies** Orlando, USA
- **SensL**, Cork, Ireland
- **MPI-HLL**, Munich, Germany
- **RMD**, Boston, USA
- **Philips**, Aachen, Germany
- **Excelitas** tech. (formerly Perkin-Elmer)
- **KETEK**, Munich, Germany
- **National Nano Fab Center**, Korea
- **Novel Device Laboratory** (**NDL**), Bejing, China
- **E2V**
- **CSEM**

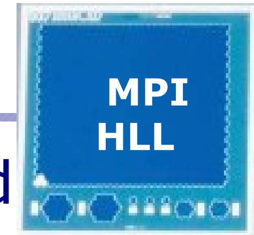

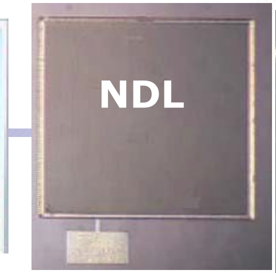

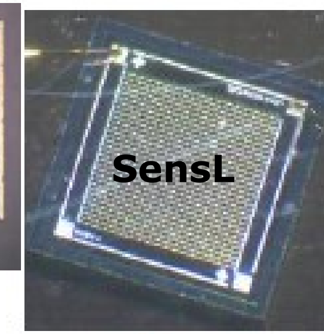

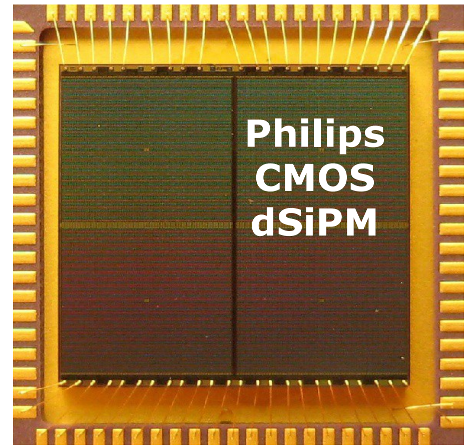

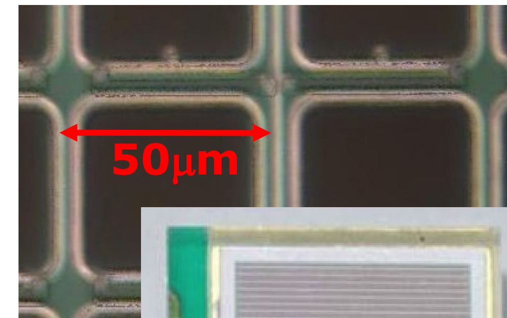

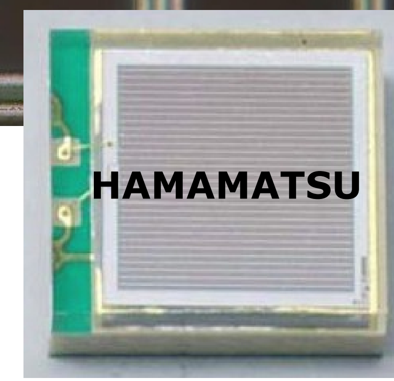

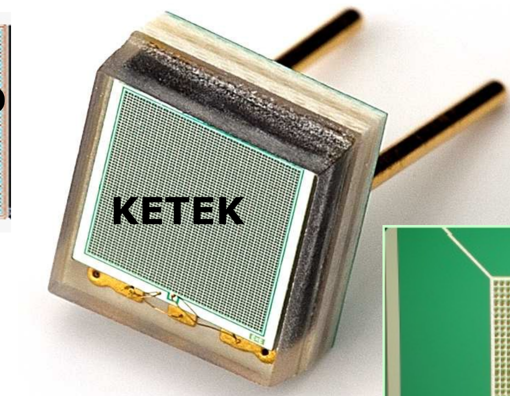

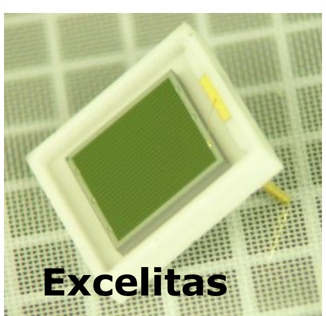

Amplification Technologies (DAPD)

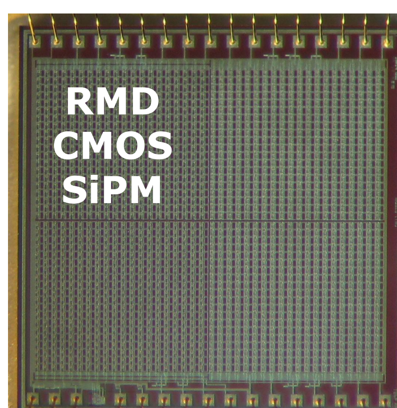

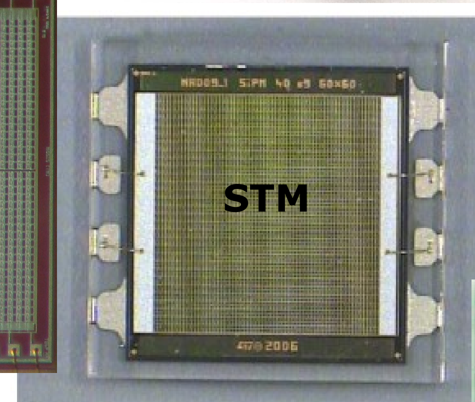

Few examples

SiPM's of small area



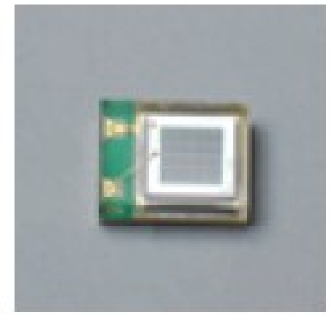

Hamamatsu HPK
S10362-11-025,050,100
1 X 1 mm^2

SiPM's of large area

ZEKOTEK
MAPD-3N
3 X 3 mm^2

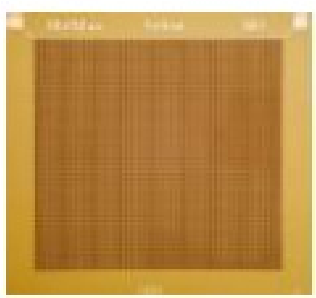

FBK - AdvanSiD
ASD-SiPM4s
4 X 4 mm^2

Hamamatsu HPK
S10985-50C
4 X 4 mm^2

KETEK
PM3350
3 X 3 mm^2

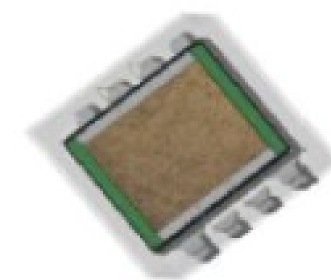

STMicroelectronics
SPM35AN
3,5 X 3,5 mm^2

ZECOTEK MAPD-3N

ASD-SiPM4S

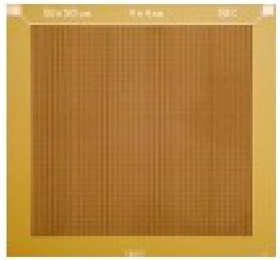

HAMAMATSU S10985

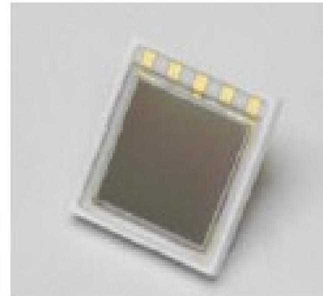

KETEK PM3350

STMicroelectronics

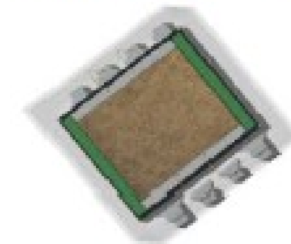

Producer	Reference	Area (mm^2)	PDE max @ 25 °C *	Dark Count Rate (Hz) @ 25°C *	Gain *
ZECOTEK	MAPD-3N	3 x 3	30% @ 480 nm	$9.10^5 – 9.10^6$	10^5
FBK - AdvanSiD	ASD-SiPM4S	4 x 4	30% @ 480 nm	$5.5\ 10^7$ - $9.5\ 10^7$	$4.8\ 10^6$
HAMAMATSU	S10985-50C	6 x 6	50% @ 440 nm (includes afterpulses & crosstalk)	$6.10^6– 10.10^6$	$7.5\ 10^5$
KETEK	PM3350	3 x 3	40% @ 420 nm	4.10^6	$2\ 10^6$
STMicrolectronics	SPM35AN	3,5 x 3,5	16% @ 420 nm	$7.5\ 10^6$	$3.2\ 10^6$

** datasheet data*

Ongoing R&D to increase the active area at KETEK, AdvanSiD, Excelitas (6 x 6 mm^2)
Other solution to get larger area : connection of several channels of a matrix

Discrete arrays

Producer	Device ID	Picture	Total area (mm^2)	SiPM area (mm^2/channel)	Nr. channels	µcell size
Hamamatsu	S11064-025P S11064-050P	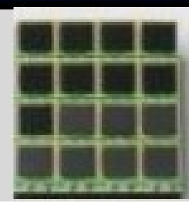	18 x 16.2	3x3	16(4x4) ch	25x25 µm 50x50 µm
Hamamatsu	C11206-0404DF	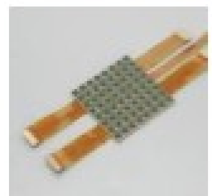		3x3	64(8x8) ch	
Hamamatsu	S11834-3388DF		72x64.8	3x3	256(16x16)ch	
FBK AdvanSiD	ASD-SiPM4s-P-4x4T-50 ASD-SiPM4s-P-4x4T-69	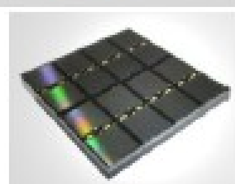	8.2 x 8.2	4x4	16(4x4) ch	50x50 µm 69x69 µm
FBK AdvanSiD	SiPM tile	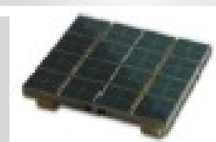	32.7x32.7	4x4	64(8x8) ch	
SensL	ArraySM-4P9 ArraySB-4P9 (blue sensitive)	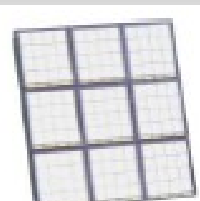	46.3 x 47.8	3x3	144(12x12) ch (based on monolithic Array SM4)	35x35 µm

Monolithic Arrays

Producer	Device ID	Picture	Effective area (mm^2)	SiPM area/channel (mm^2)	Nr. channels	µcell size
Hamamatsu	S10984-025P S10984-050P S10984-100P	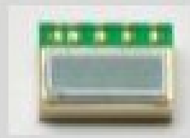	1 x 4	1x1	4(1x4) ch	25x25 µm 50x50 µm 100 x 100 µm
Hamamatsu	S10985-025C S10985-050C S10985-100C	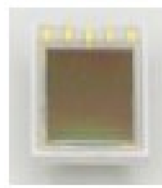	6 x 6	3x3	4(2x2) ch	25x25 µm 50x50 µm 100 x 100 µm
Hamamatsu	S11828-3344M	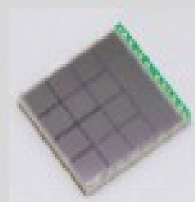	12 x 12	3x3	16(4x4) ch	50x50 µm
FBK AdvanSiD	ASD-SiPM1.5s-P-8X8A	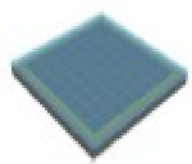	11.6 x 11.6	1.45x1.45	64(8x8) ch	50x50 µm
FBK AdvanSiD	ASD-SiPM3S-P-4X4A	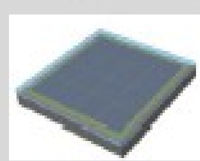	11.8 x 11.8	2.95x2.95	16(4x4) ch	50x50 µm
SensL	Array SM-4 Array SB-4 (blue sensitive)	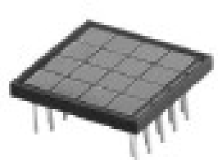	12 x 12	3x3	16(4x4) ch	35x35 µm

Technologies around the world

Pioneering work in '90s by Russian institutes

- **CPTA**, Moscow
- **JINR**, Dubna

Metal-Resistive-Semiconductor

- **MePhi/Pulsar** Enterprise, Moscow — **Poly-silicon resistor**

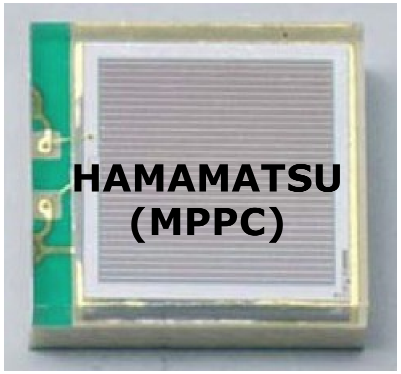

Recently more institutes/companies involved

- **Hamamatsu HPK**, Hamamatsu
- **FBK-AdvanSiD**, Trento
- **SensL**, Cork
- **ST Microelectronics**, Catania
- **Excelitas** techn. (formerly Perkin-Elmer)
- **National Nano Fab Center**, Korea
- **Novel Device Laboratory** (**NDL**), Bejing

SiPM Matrixes

vias to avoid bonding

Poly-silicon resistor

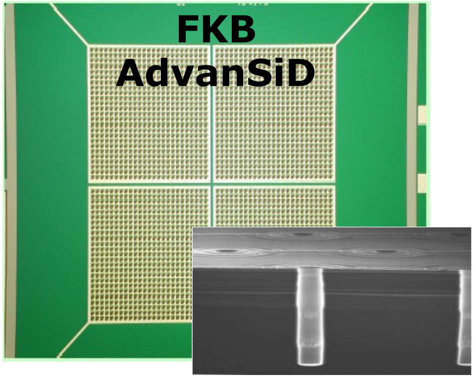

- **MPI-HLL**, Munich — **Resistor embedded in the bulk**
- **RMD**, Boston — **CMOS process**
- **Philips**, Aachen — **Digital SiPM (CMOS)**
- **Zecotek,** Vancouver — **Quenching with floating wells**
- **Amplification Technologies**, Orlando

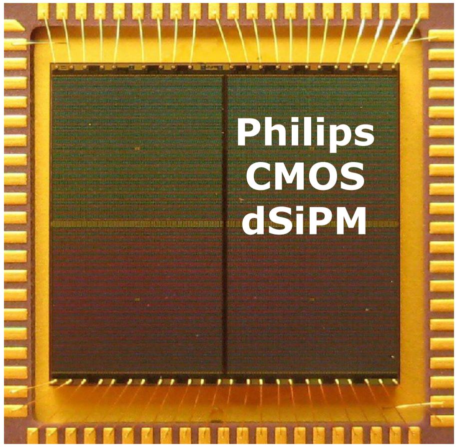

Some are commercially available, other are prototypes

Physics & Technology
Key features

- Closeup of a cell – Custom vs CMOS

- Guard Ring and Optical isolation

- Operation principles of GM-APD and quenching modes

Silicon technology

Two different approaches for SPAD or GM-APD arrays

Custom technology

- control/tune shape of E field
  → high PDE
  → optimized timing resolution
  → low Dark Count Rate
  → low After-pulsing

- possible both Planar and Reach Through
  → tune spectral sensitivity

- limited integrated electronics
  (no libraries for complex functionalities
  and for deep-submicron features)
  → simple integrated electronics
  (few large MOS)
  → it limits array dimensions and fill factor

  Ancillary electronics (quenching/readout):
  → completely external → **SiPM**
  → hybrid → **SPAD arrays** … complex fabrication

CMOS HV technology

- no optimization of shape of E field
  + high curvature sub-micron tech.
  → special care for guard ring
  (limited range of GR possible
  only STI demonstrated ok)

- only Planar structures
  → UV/Blue sensitivity

- fully supported sub-micron technology
  with models and libraries →complex electr.
  → processing of large amount of data
  → high density → imaging
  → ultra-fast timing

Ultrafast and/or **imaging**
monolithic SPAD arrays

Silicon technology – few examples

Custom technology

SiPM "RGB" FBK – no electronics

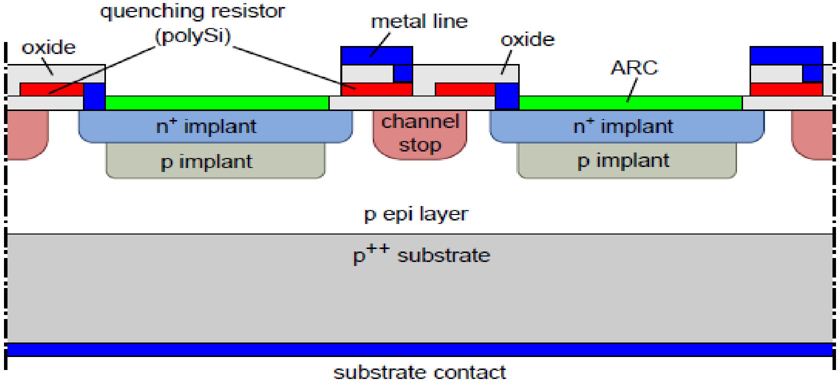

N.Serra et al JINST 8 (2013) P03019

CMOS HV technology

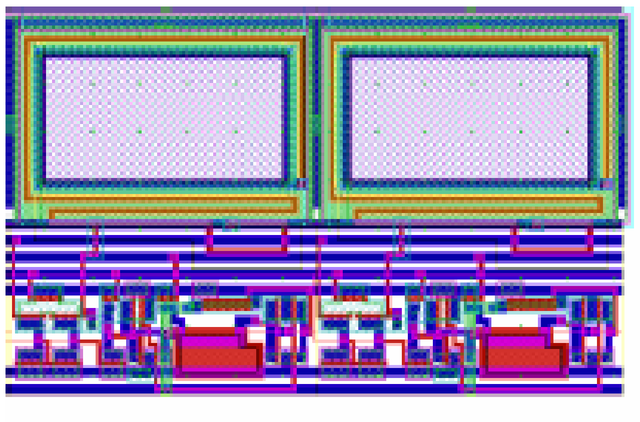

Stapels et al Procs. SPIE 7720 2009

SPAD custom CMOS – hybrid electronics

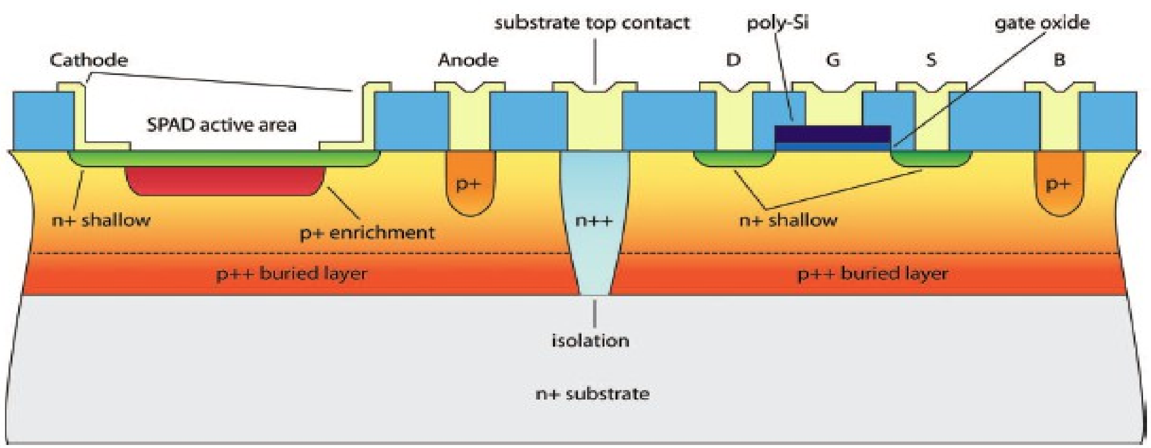

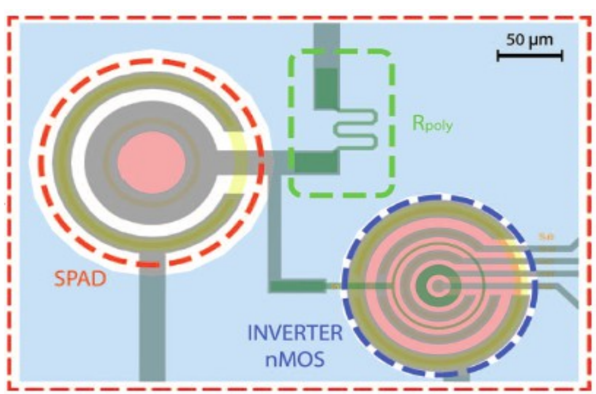

Cammi et al Rev Sci Instr 83 (2012) 033104

Close up of a cell – custom process

Shallow-Junction APD

Example of implementation

C.Piemonte NIM A 568 (2006) 224

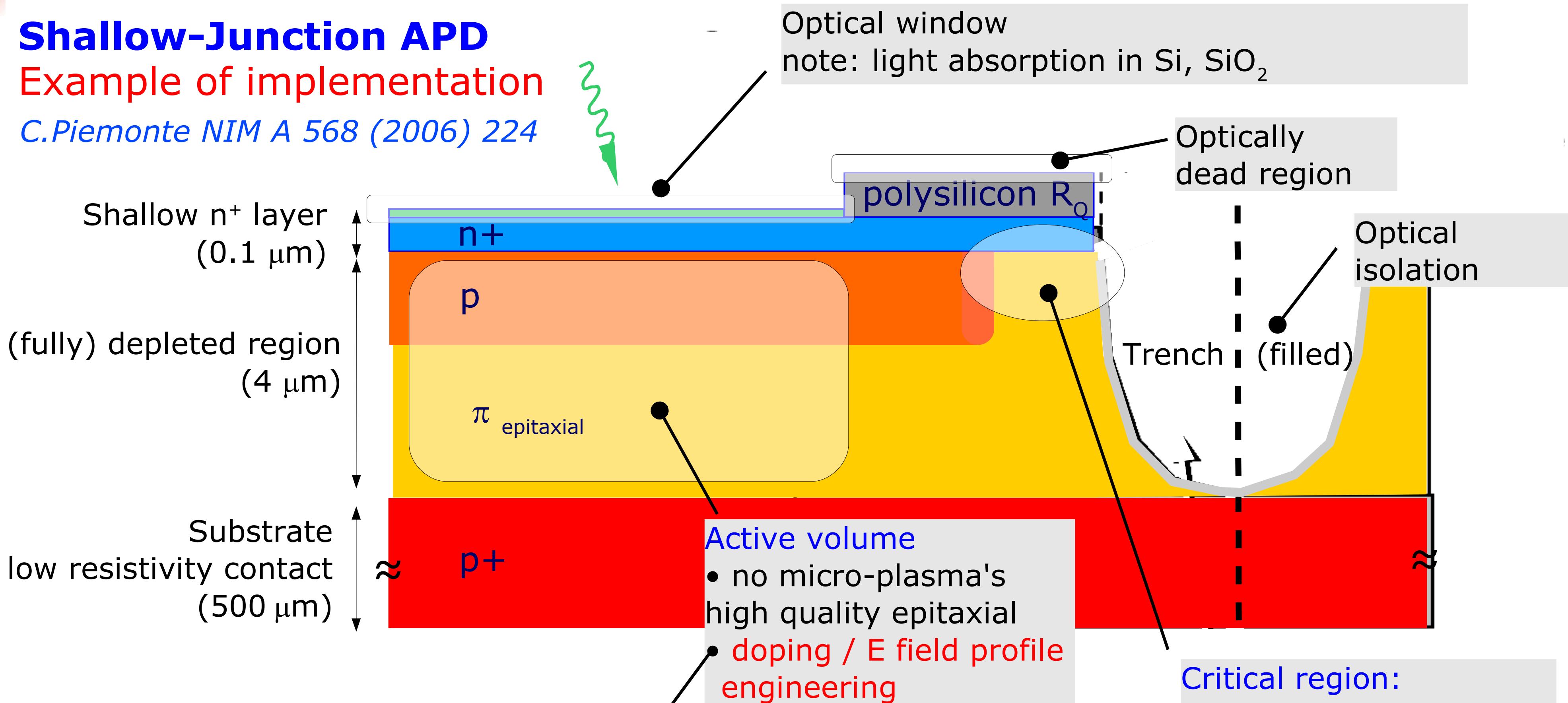

Critical region:
- Leakage current
- Surface charges
- Guard Ring for
  - preventing early edge-breakdown
  - isolating cells
  - tuning E field shape

→impact on Fill Factor

- n^+ on p abrupt junction structure
- Anti-reflective coating (ARC)
- Very thin (100nm) n^+ layer: “low” doping
  → minimize Auger and SHR recombination
- Thin high-field region: “high” doping p layer
  → limited by tunneling breakdown
  → fixes V_{BD} junction well below V_{BD} at edge

Optimization for blue light (420nm)

- R_Q by poly-silicon
- Trenches for optical insulation (cross-talk)
- Fill factor: 20% - 80%

Close up of a cell – custom process

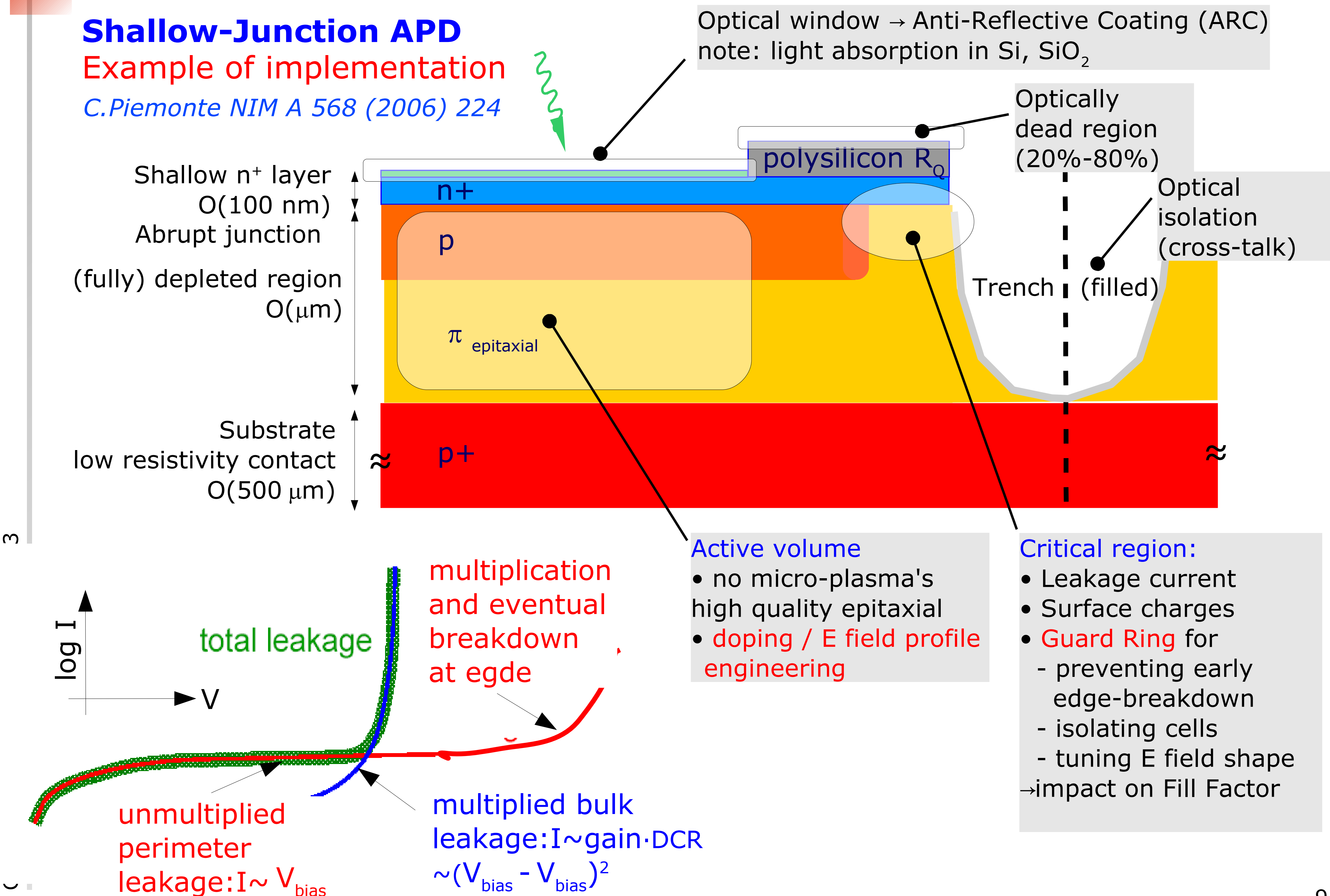

Close up of a CMOS cell

Key elements for CMOS SiPMs
- **APD cell isolation** from CMOS circuitry
- **guard ring**

APD integration into CMOS

Example of implementation *T.Frach in US patent 2010/0127314*

Note
- extended CMOS processes exploited
- careful design of cell isolation and guard ring

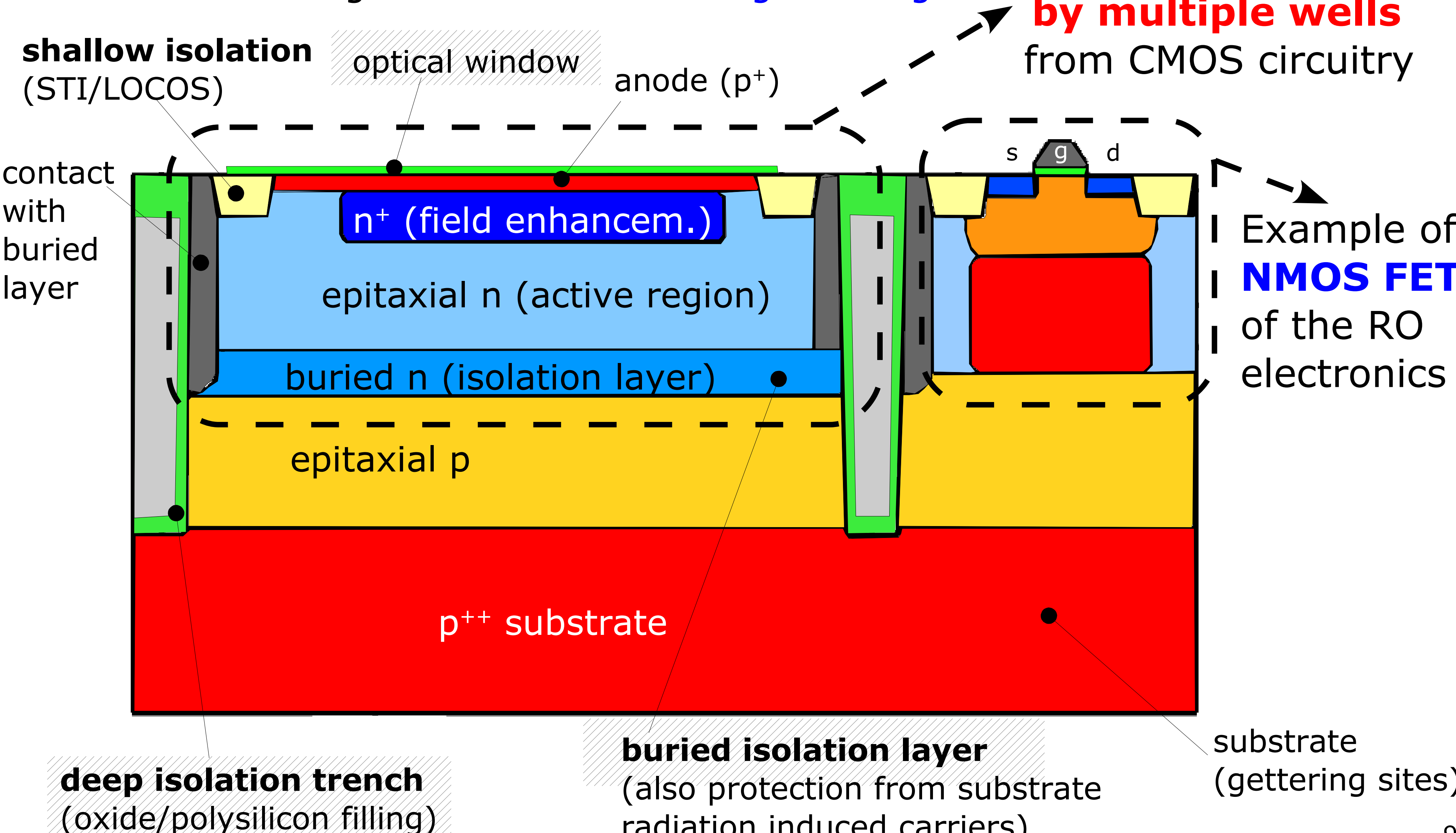

CMOS vs Custom processes

"Standard" CMOS processes

- shallow implant depths
- high doping concentrations
- shallow trench isolation (STI)
- deep well implants (flash extension)
- no extra gettering and high T annealing
- non optimized optical stacks
- design rule restrictions

high E field (low V_{bd}) → tunneling

lattice stress (defects/traps)

→ **high DCR**

→ **limited PDE** (often p-on-n)

→ **limited timing performances** (long diffusion tails)

Recent progresses in CMOS APDs due to:

1) **high voltage (flash) extension** often available in **standard** processes
   - deep wells (needed for the high voltages used in flash memories)

2) **Additional processes** (custom) available:
   - buried implants
   - deep trench isolation
   - optical stack optimization

Key elements for CMOS SiPMs
- **APD cell isolation** from CMOS circuitry
- **guard ring**

Physics & Technology
Key features

- Closeup of a cell – Custom vs CMOS

- Guard Ring and Optical isolation

- Operation principles of GM-APD and quenching modes

Guard Ring

Guard Ring is needed to:

- avoid premature edge breakdown (due to junction's high curvature)
  - → either reduce electric field at edge (floating GR)
  - → or by terminating electric field lines "within" the high field region
  - → or by exploiting special edge geometry (trenches)
- drain leakage currents (for avoiding its multiplication)
- electrical isolation of cell from electronics
- optical isolation of cell against cross-talk

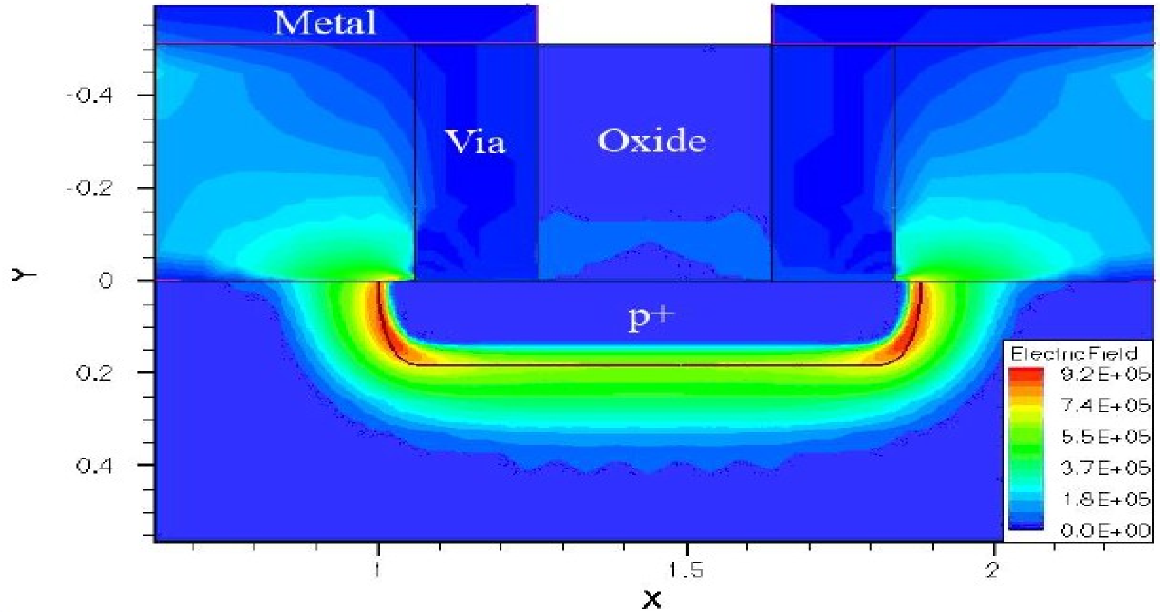

Fig. 1. ISE-TCAD simulation of electric field distribution across a pn junction formed by consecutive implantation and diffusion steps. A uniform field exists in the planar junction region but the field is significantly higher in the curved regions, resulting in premature breakdown and in a higher avalanche probability in these areas. Field strengths are in V/cm and coordinates are in microns.

Finkelstein et al. "An ultrafast Geiger-mode SPAD in 180nm CMS technology" Procs. SPIE 6372 2006

The Guard Ring structure

- high E field structure, not uniform
- neutral region (timing tails)
- limited fill factor

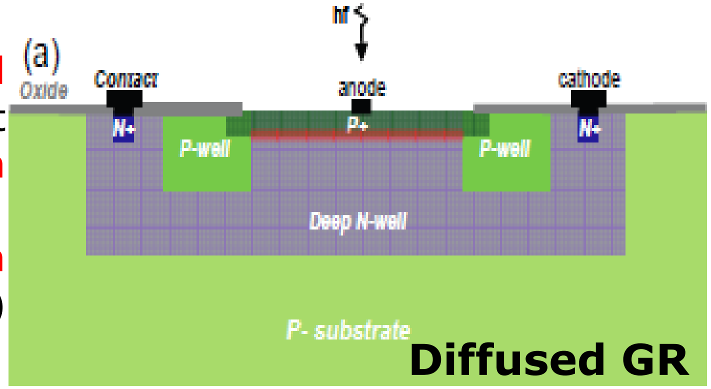

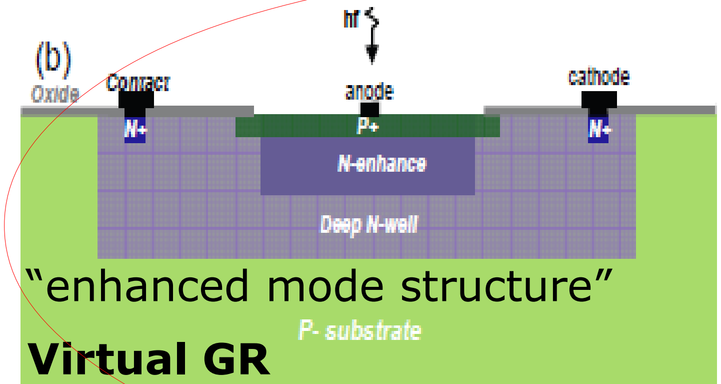

- well tuned high E field structure
- no additional neutral regions
- fill factor less limited

- alternative to Diffused GR
- difficult to implement

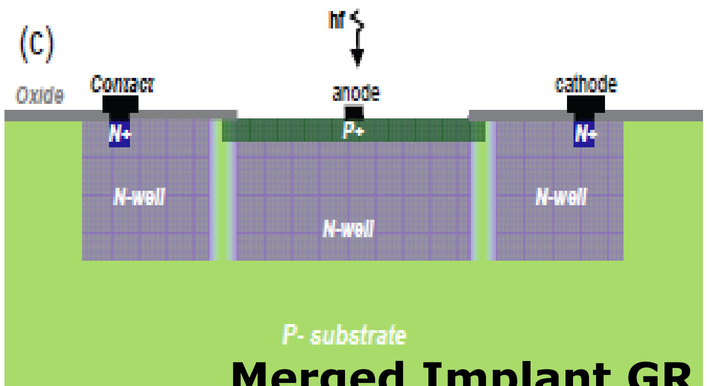

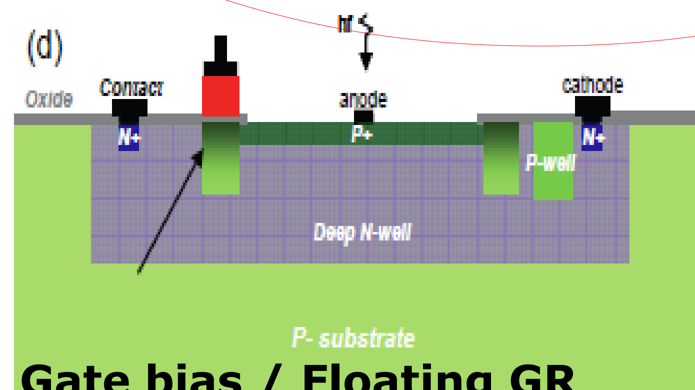

- less commonly exploited
- careful modeling required

- developed by S.Cova and coll. (fully custom)
- state of the art SPAD timing and PDE (red enhanced)

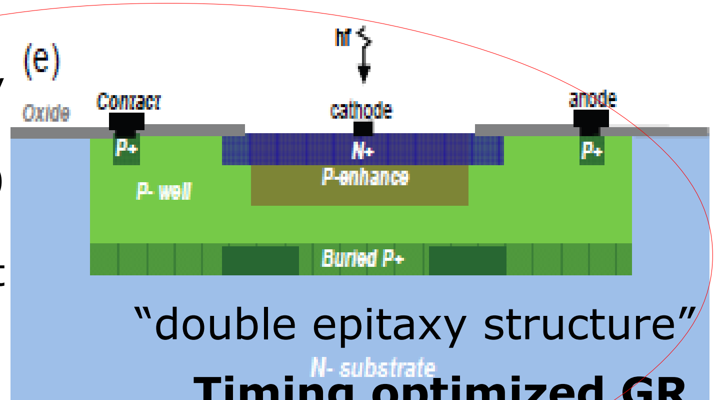

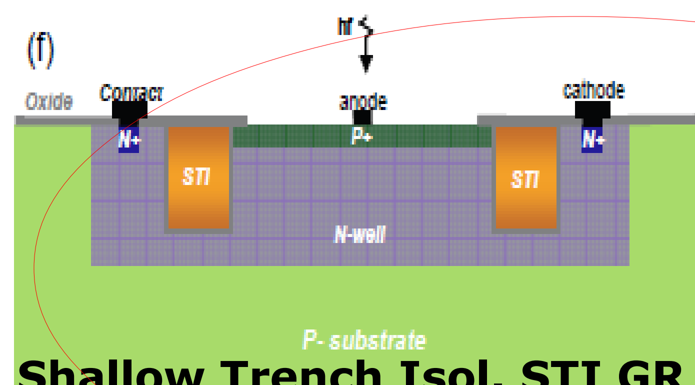

- physically blocks and confines the high E field in active region
- might cause high DCR due to
  - tunneling
  - etching induced defects/traps

from "Avalanches in Photodiodes" G.F.Dalla Betta Ed., InTech Pub. (2011)

Guard Ring structures in SiPM

Sul et al, IEEE EDL 31 2010 "G.R. Structures for SiPM"

Virtual guard ring
most often used

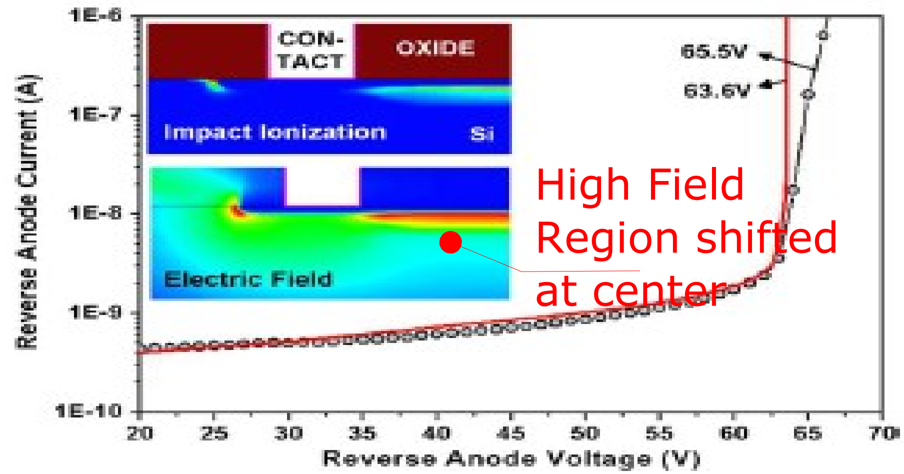

Implant / Gate bias

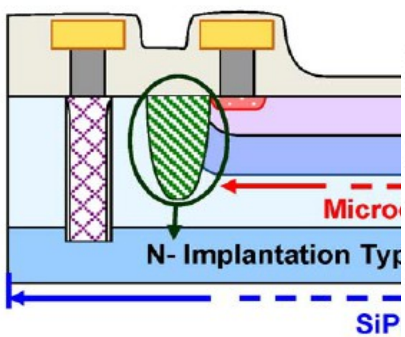

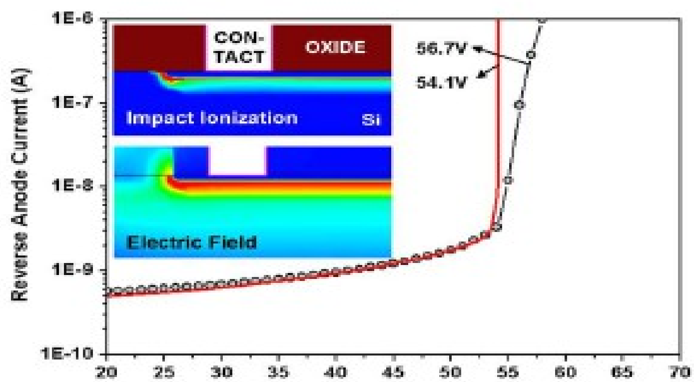

Trench type

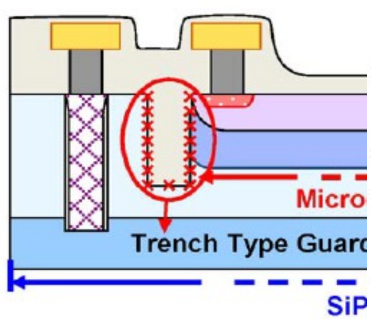

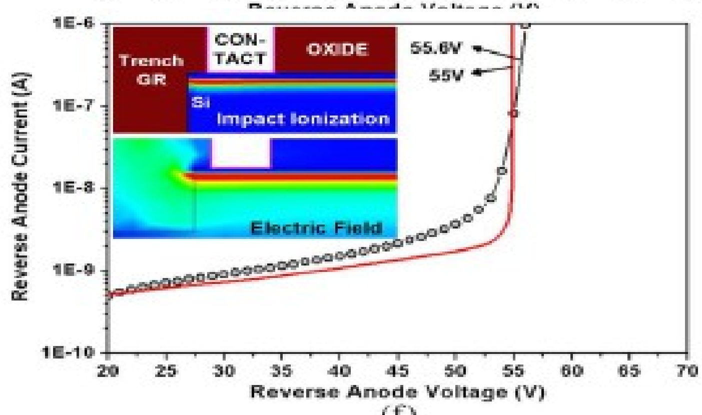

Maresca et al. Proc. of SPIE Vol. 8072
"Floating field ring ...
to enhance fill factor of SiPM"

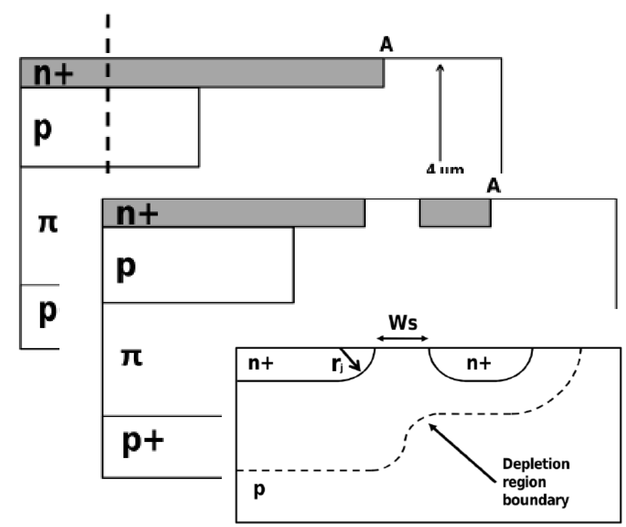

G.Collazuol - Siena - IDPASC 2013

Physics & Technology
Key features

- Closeup of a cell – Custom vs CMOS

- Guard Ring and Optical isolation

- Operation principles of GM-APD and quenching modes

Operation principle of a GM-APD

Avalanche processes in semiconductors are studied in detail since the '60 for modeling micro-plasma instabilities

McIntyre JAP 32 (1961), Haitz JAP 35 (1964) and Ruegg IEEE TED 14 (1967)

currents **internal** / **external**

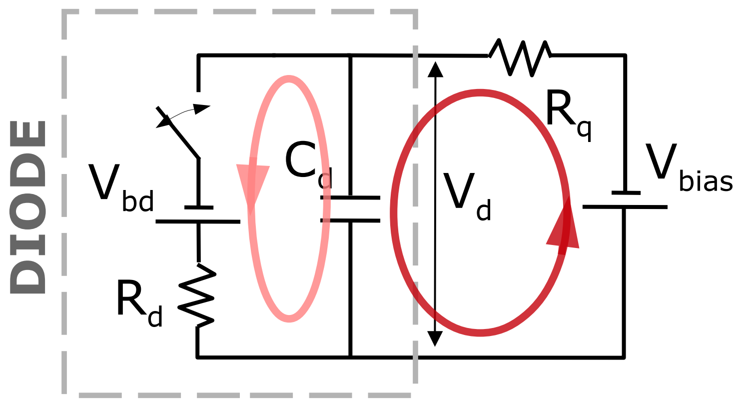

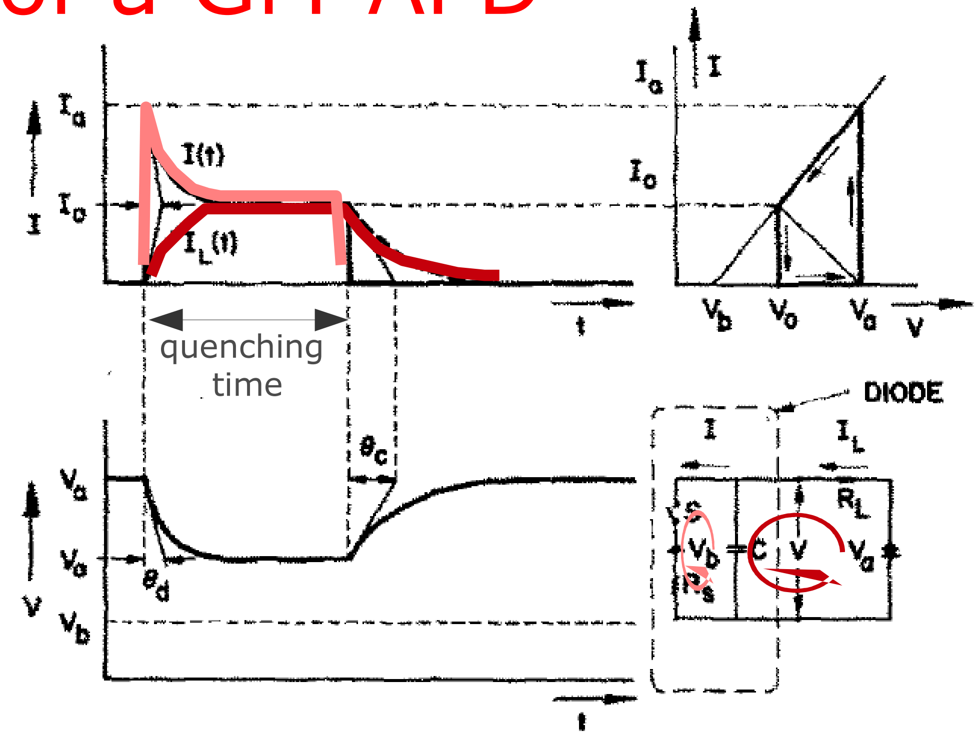

FIG. 3. Shape of current pulse for $\theta_d \ll \tau_1(I_0)$.

ON condition: avalanche triggered, switch closed C_d discharges to V_{bd} with a time constant $R_dC_d = \tau_{discharge}$ at the same time the external current asymptotic grows to $(V_{bias}-V_{bd})/(R_q+R_d)$

P_{10} = turn-off probability
probability that the number of carriers traversing the high-field region fluctuates to 0

P_{01} = turn-on probability
probability that a carrier traversing the high-field region triggers the avalanche

OFF condition: avalanche quenched, switch open, capacitance charged until no current flowing from V_{bd} to V_{BIAS} with time constant $R_qC_d = \tau_{recovery}$

Operation principle of a GM-APD

Avalanche processes in semiconductors are studied in detail since the '60 for modeling micro-plasma instabilities

McIntyre JAP 32 (1961), Haitz JAP 35 (1964) and Ruegg IEEE TED 14 (1967)

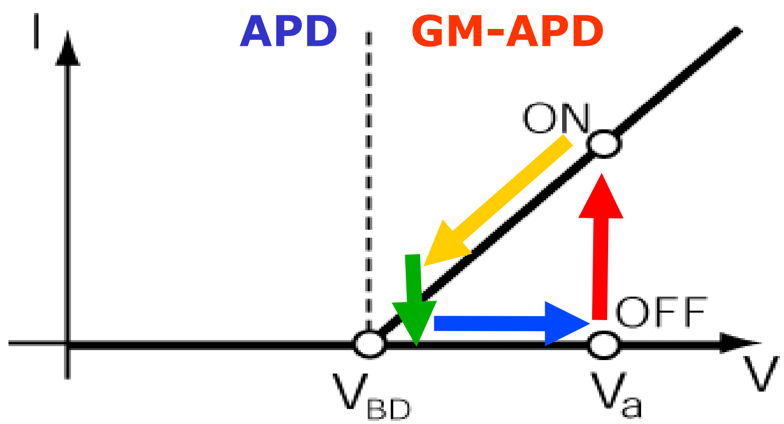

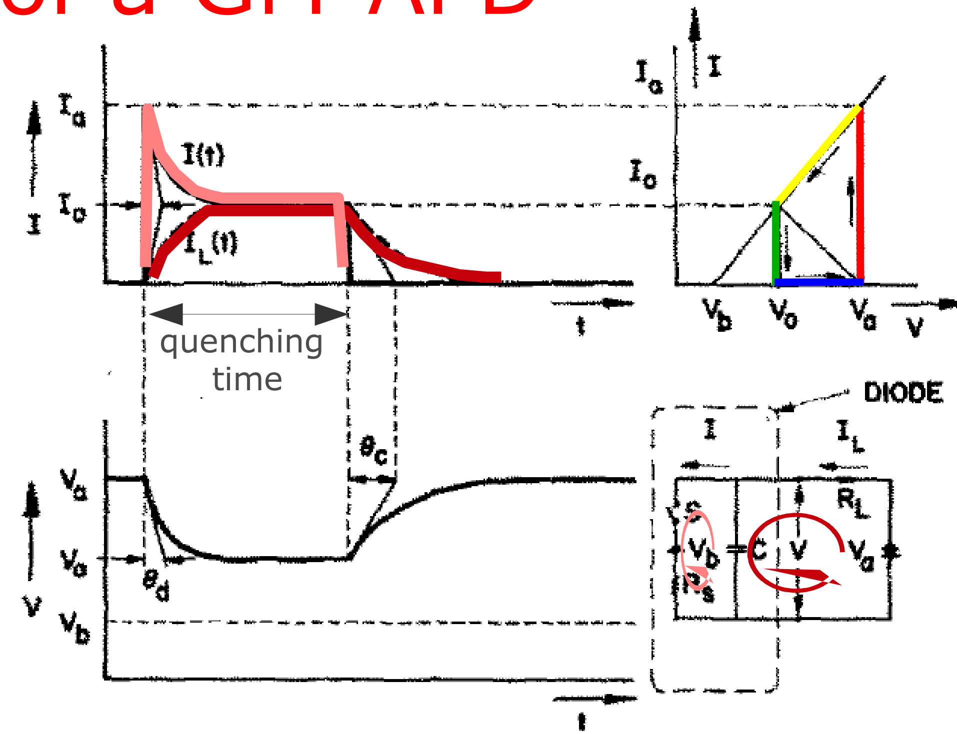

FIG. 3. Shape of current pulse for $\theta_d \ll \tau_1(I_0)$.

ON condition: avalanche triggered, switch closed C_d discharges to V_{bd} with a time constant $R_dC_d = \tau_{discharge}$ at the same time the external current asymptotic grows to $(V_{bias}-V_{bd})/(R_q+R_d)$

P_{10} = turn-off probability
probability that the number of carriers traversing the high-field region fluctuates to 0

P_{01} = turn-on probability
probability that a carrier traversing the high-field region triggers the avalanche

OFF condition: avalanche quenched, switch open, capacitance charged until no current flowing from V_{bd} to V_{BIAS} with time constant $R_qC_d = \tau_{recovery}$

Operation model and ideal pulse shape

Diode (capacitor) fast discharge
and slow recharge

charge stored defines Gain
→ Gain ~ $C\,\Delta V$
$\Delta V = V_{bias} - V_{bd}$ "Over-Voltage"

currents internal / external

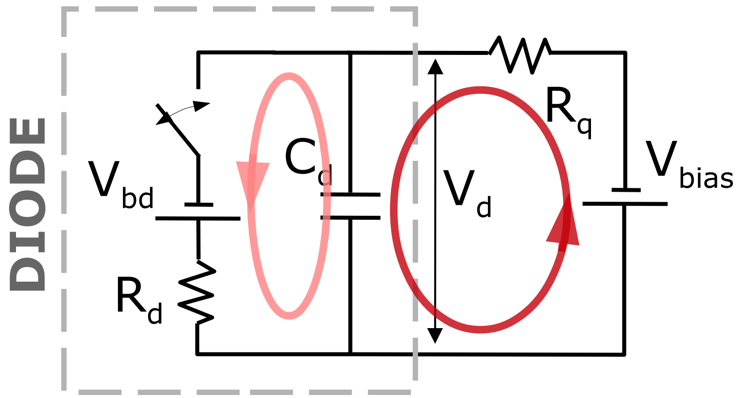

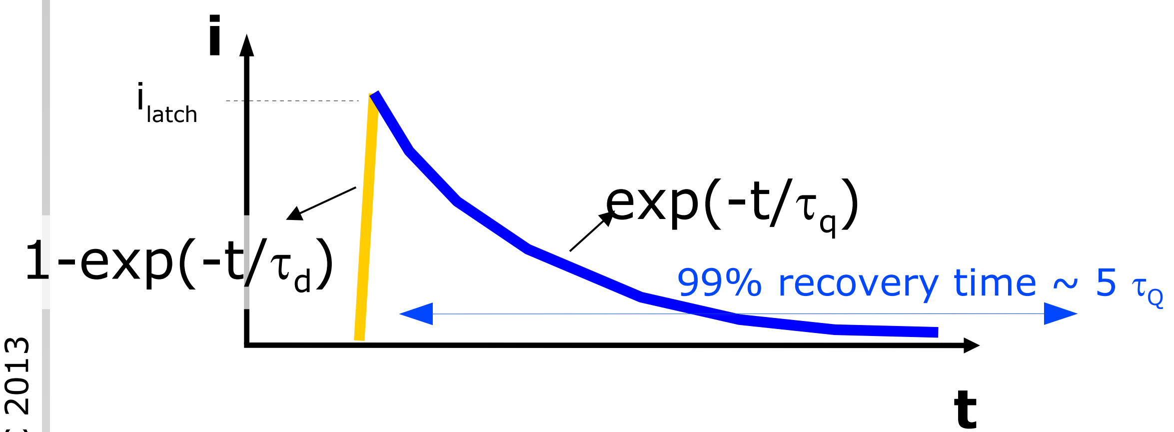

Rise time Fall time (recovery)

$\tau_d = R_d C_d \ll \tau_q = R_q C_d$

Gain → linear with ΔV (≠ APD)
→ no intrinsic fluctuations !!! (≠ APD)
→ independent of T at fixed ΔV (≠ APD)

Rise time T dependence (weak) due to R_d

Recovery time T dependence (strong) due to R_q
C_d is independent of T

Passive Quenching: tread-off τ_{quench} vs $\tau_{recovery}$

If R_Q is high enough the internal current is so low that statistical fluctuations may quench the avalanche

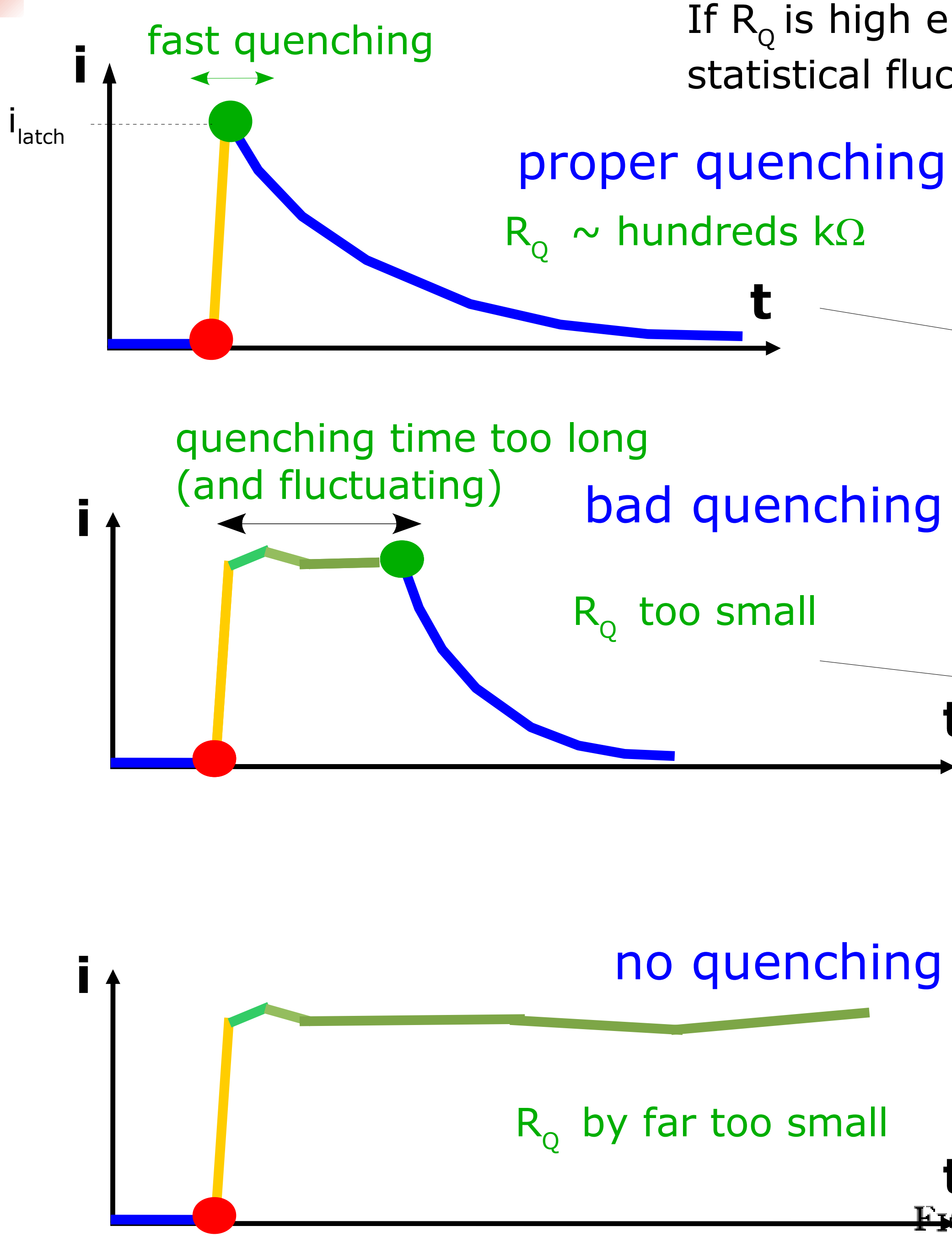

Haitz JAP 35 (1964)

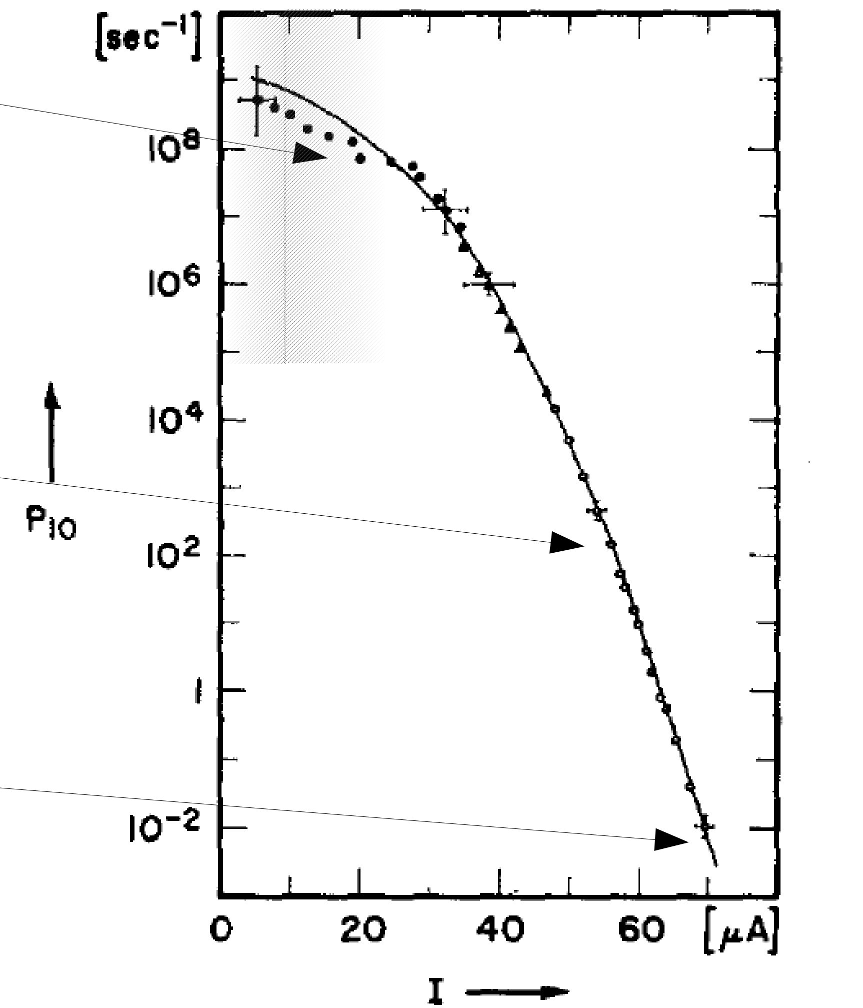

FIG. 2. Turnoff probability per second as function of pulse cu

Passive Quenching Regime

Proper value of quenching resistance Rq is crucial to let the internal current decrease to a level such that statistical fluctuations may quench the avalanche → sub-ns quenching time → crucial to have well defined gain

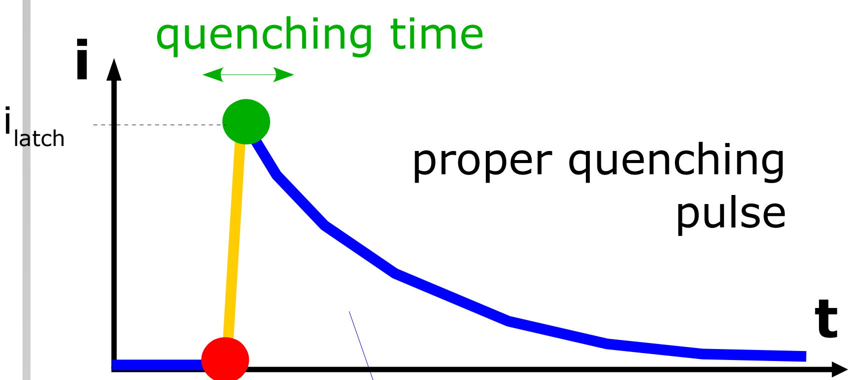

Given Rq the proper quenching regime is for ΔV in the range:

$$0 < \Delta V < R_q I_{latch}$$

where as a rule of thumb
$I_{latch} \sim 20\mu A \rightarrow \Delta V_{max}$ ~ a few Volts (typically)

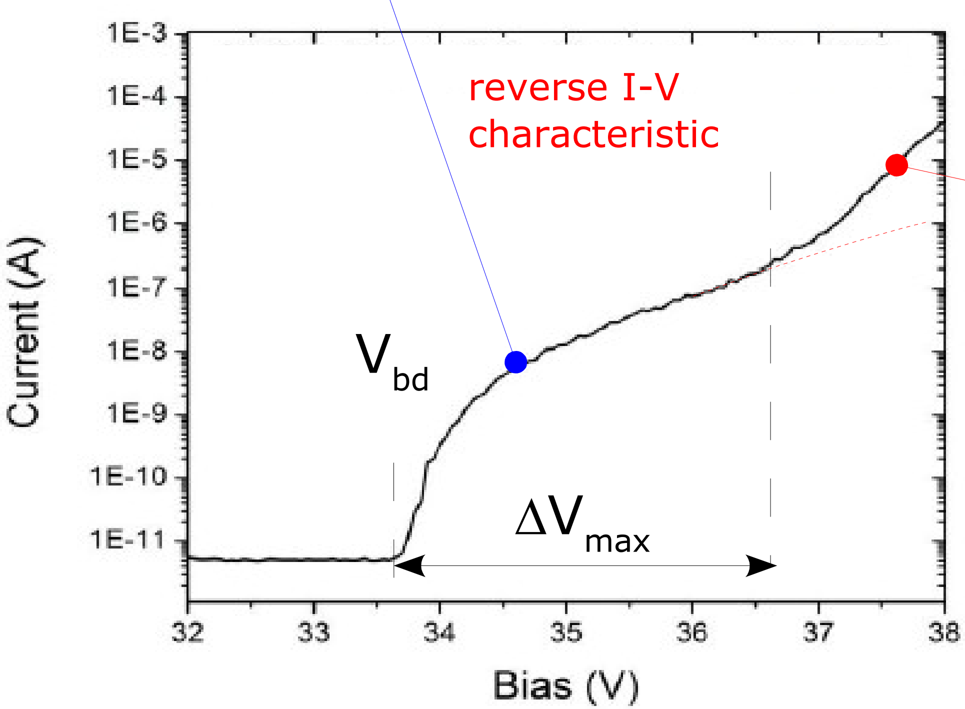

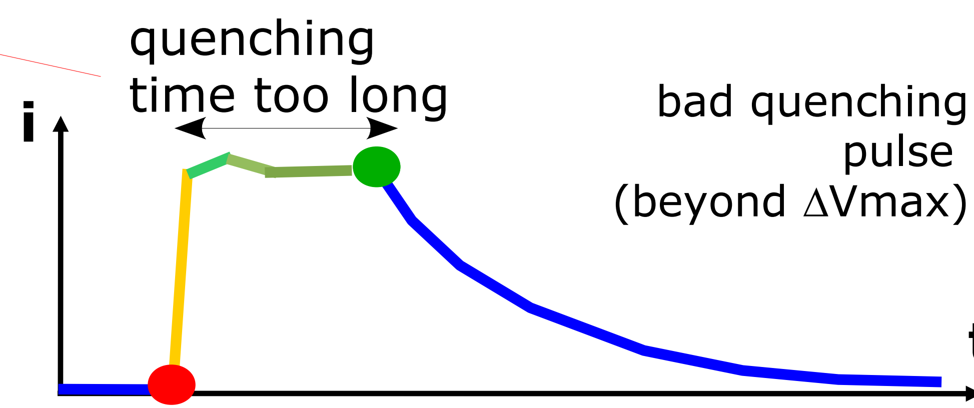

Operative ΔV Range – I_{dark}/DCR

Operative ΔV limited by:

1) I_{latch}~20μA → ΔV < I_{latch} R_q (non-quenching regime)
2) Dark Count Rate (DCR) acceptable level ← PDE vs ΔV ← E field shape
3) V_{bd}^{edge} edge breakdown (usually some 10V above V_{bd})

A practical method for estimating the operative range (limited by effect 1) is to measure the ratio R_I of the measured dark current I_D to the dark current I'_D calculated from the measured dark rate and pixel count spectra:

after Jendrysik et al NIM A 2011
doi:10.1016/j.nima.2011.10.007

$$\rho_I = \frac{I_D}{I'_D = DCR \cdot \bar{N} \cdot G \cdot q_e}$$

where $\bar{N}$ is the average N of fired cells

Non-quenching regime for values of ΔV when R_I deviates significantly from 1

Jendrysik et al suggest R_I=2 as reasonable threshold

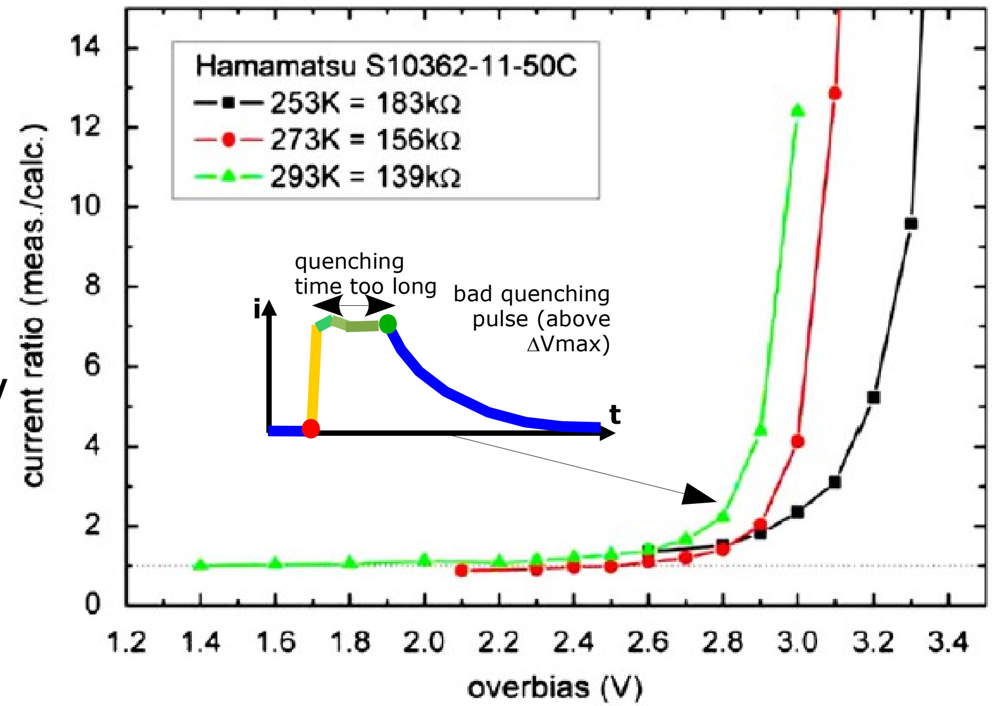

Excess Charge Factor (ECF)

The above mentioned current ratio is indeed a measure of total correlated noise ("Excess Charge Factor", after *N.Serra et al JINST 8 P03019*)

$$ECF \equiv \frac{I}{Counts\ Rate \cdot \bar{N} \cdot G \cdot q_e}$$

→ It accounts for any extra charge introduced by After-pulsing and Cross-Talk (see later)

→ it is not multiplication noise !

Passive Quenching (Resistive)

1) common solution: poly-silicon

2) alternative: metal thin film
→ higher fill factor
→ milder T dependence

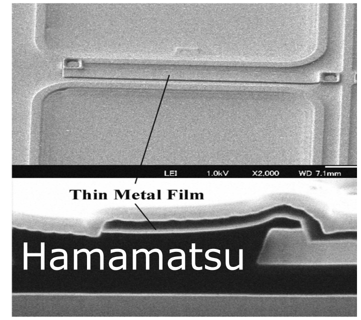

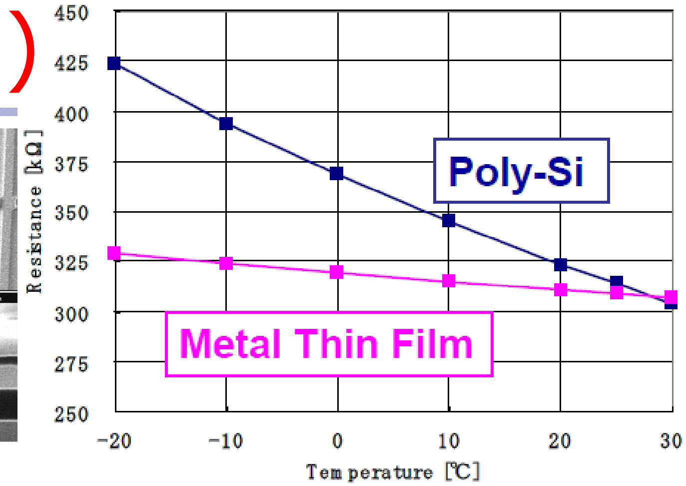

Nagano IEEE NSS-MIC 2011

3) alternative principle: bulk integrated resistor
→ flat optical window → simpler ARC
→ fully active entrance window
  → high fill factor (constraints only from guard ring and X-talk)
→ diffusion barrier against minorities
  → less X-talk
→ positive T coeff. (R~ $T^{+2.4}$)
→ production process simplified → cost

pros

contra

← Rq matching constraints
cells' pitch/wafer thickness

← vertical R is JFET
  → non-linear I-V
    → long recovery

Ninkovic et al NIM A610 (2009) 142
and NIM A628 (2011) 407
Richter et al US patent № 2011/0095388

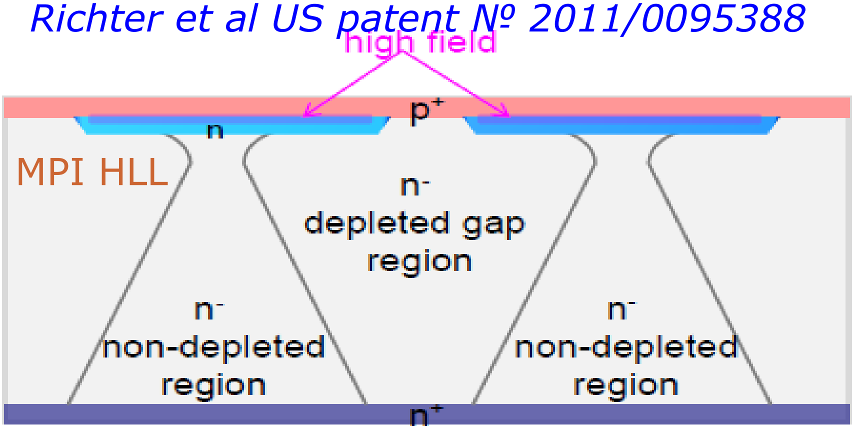

principle proved

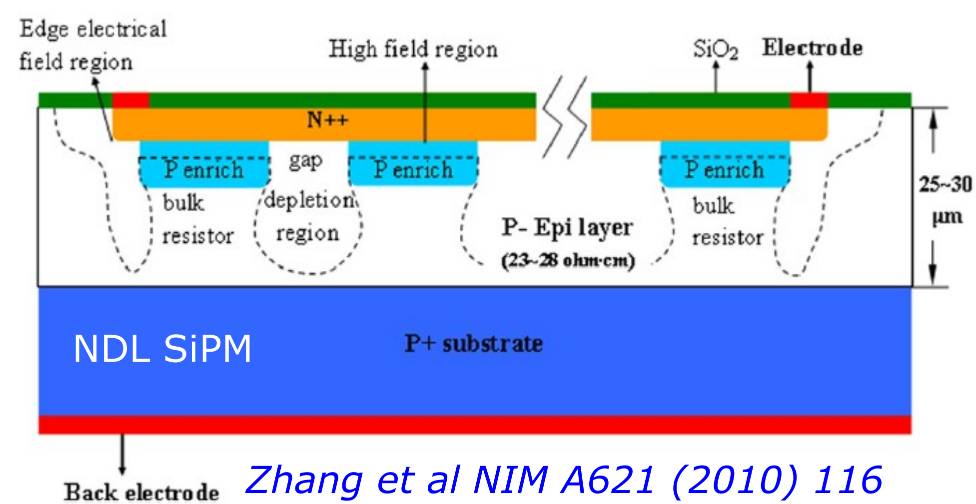

Zhang et al NIM A621 (2010) 116

Passive Quenching (Capacitive)

Quenching feedback due to charge accumulated by means by semiconductor barriers

AmplificationTechnologies
Shushakov et al US Patents № 2004/6885827 and № 2011/7899339

FIG. 3

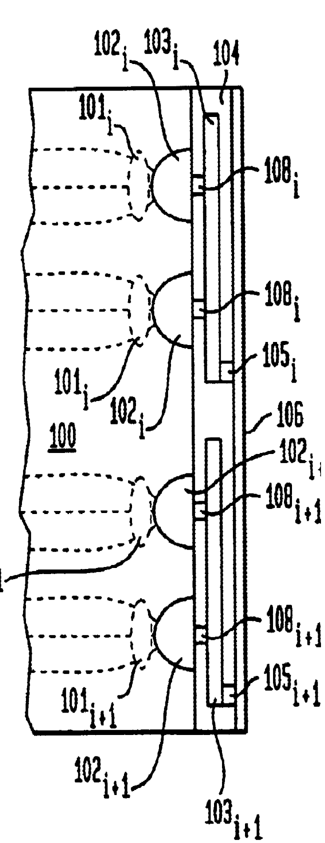

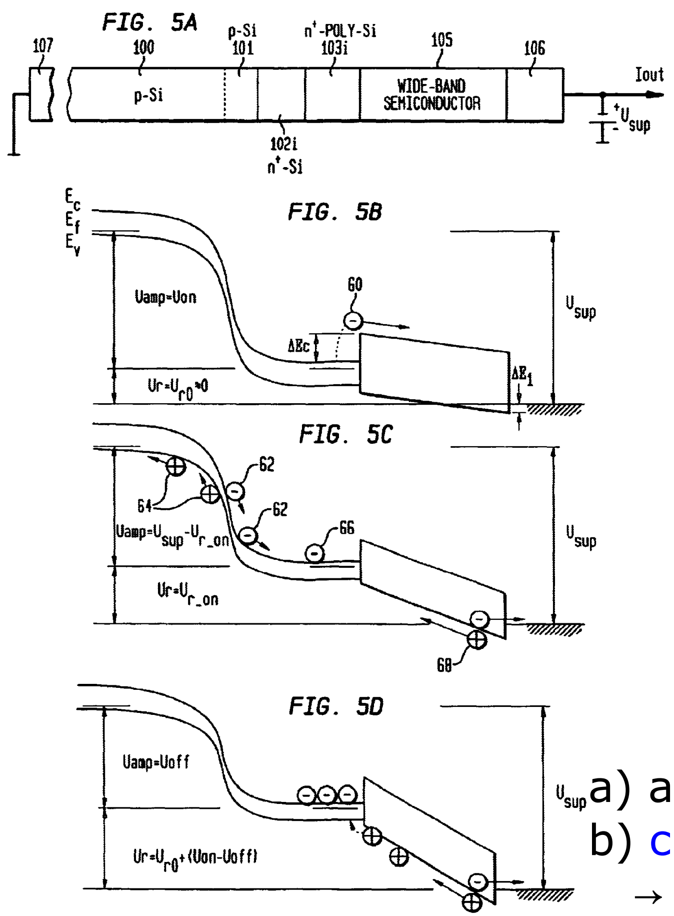

Zecotek
Sadygov et al arXiv 1001.3050
Sadygov RU Patents № 1996/2102820 and № 2006/2316848

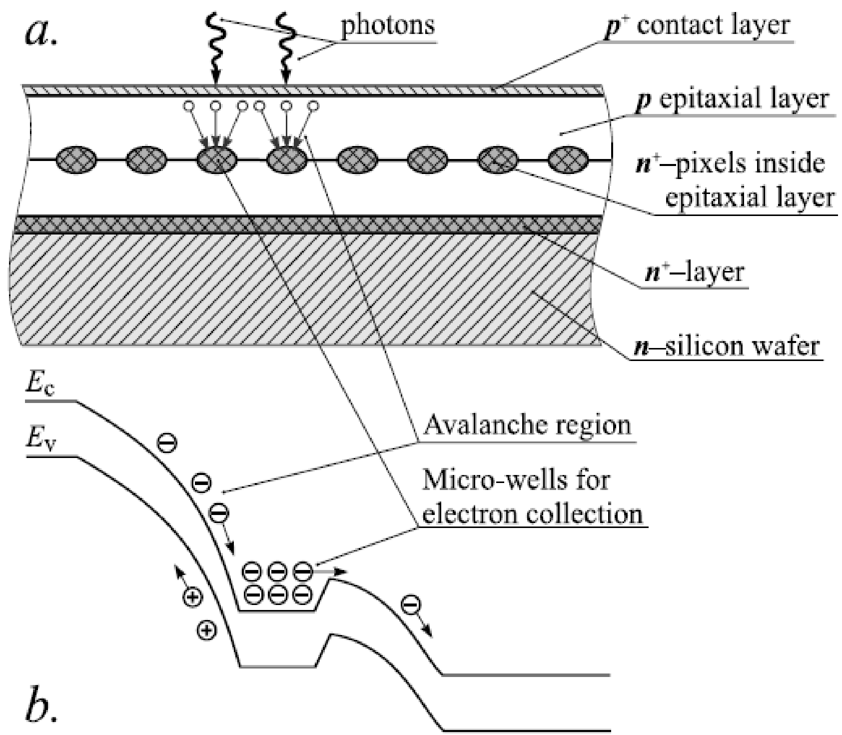

a) avalanche at internal high field regions
b) charges accumulated in isolated potential wells
→ E field reduced (locally) → avalanche quenched
→ Fast signal induced (capacitive) outside
c) potential wells discharge slowly by tunneling
(discharge must be delayed for good quenching)
→ high E field recovered

Note: induced signal is fast (ns) but recovery quite slow (ms) (non exponential)

Passive / Active quenching and recharge

Passive Quenching and Reset

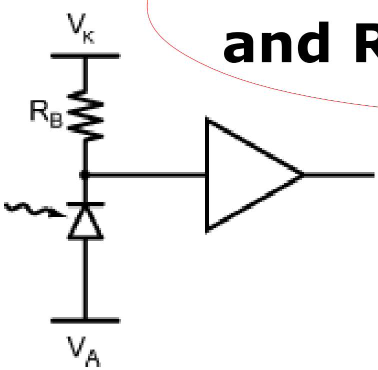

SiPM

Passive Quenching Active Reset

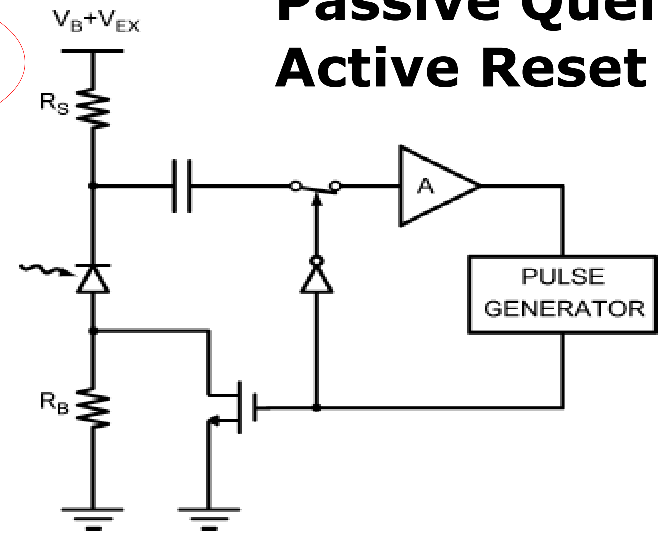

Active Quenching and Reset

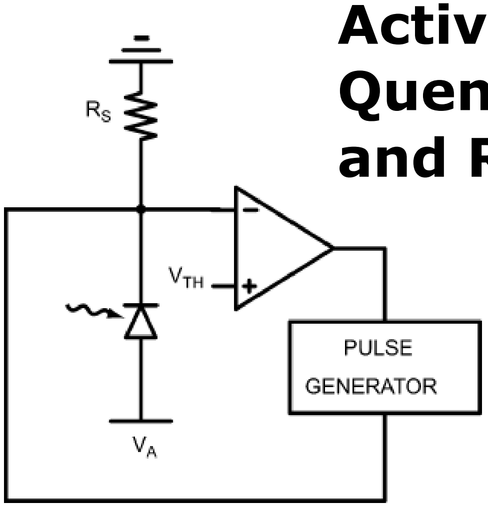

Mixed Active/Passive Quenching Active Reset

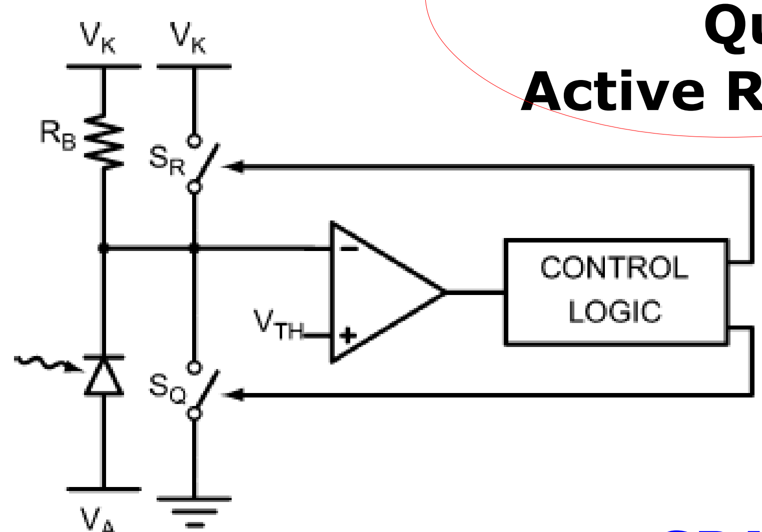

modern SPAD arrays

Gallivanoni et al IEEE TNS 57 (2010) 3815

Passive / Active quenching and recharge

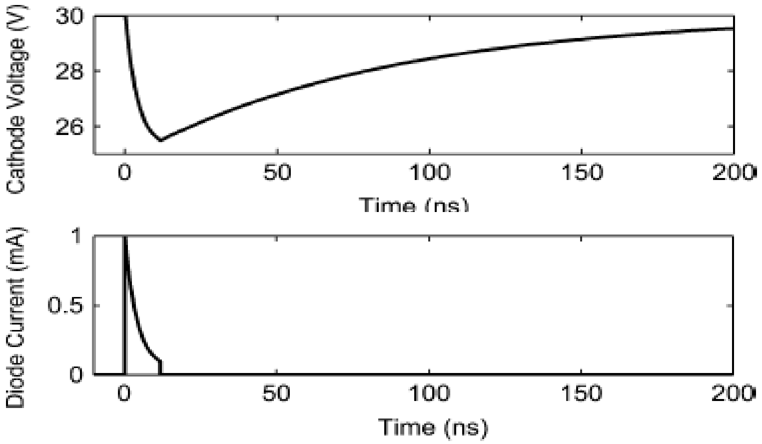

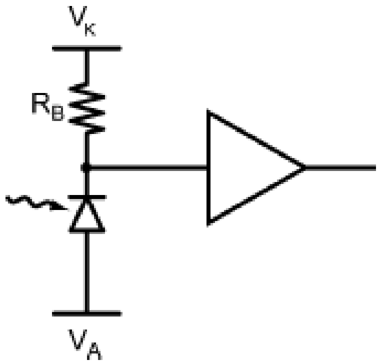

Passive Quenching

Need active elements for gaining control over:
→ quenching time against fluctuations (if Rq small)
→ avalanche charge (→ limiting AP and cross-talk)
→ recovery / reset time (→ limiting dead-time and
→ allowing gate or hold-off)

Passive Quenching
Active Reset

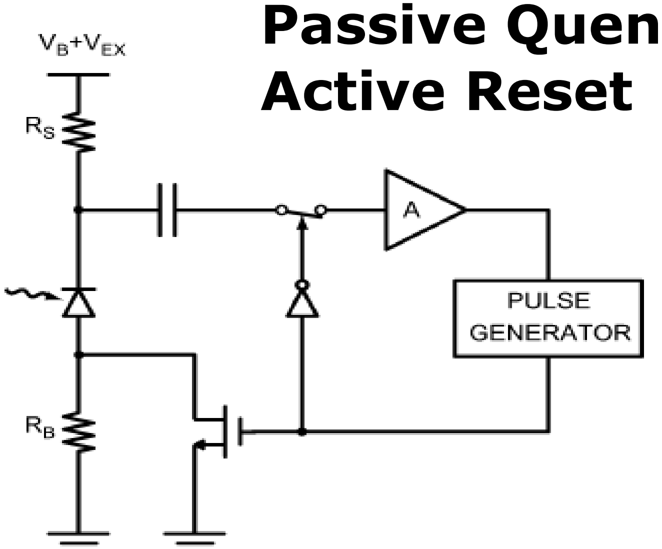

- reset ok
- hold-off (to exhaust trapped carriers) limited by passive reset

Passive / Active quenching and recharge

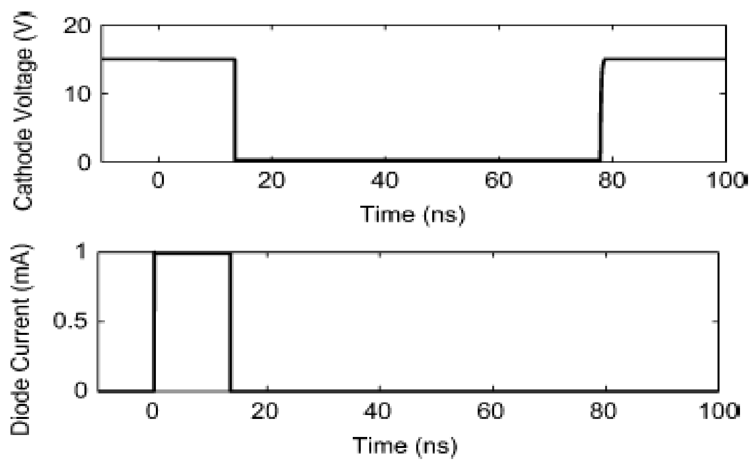

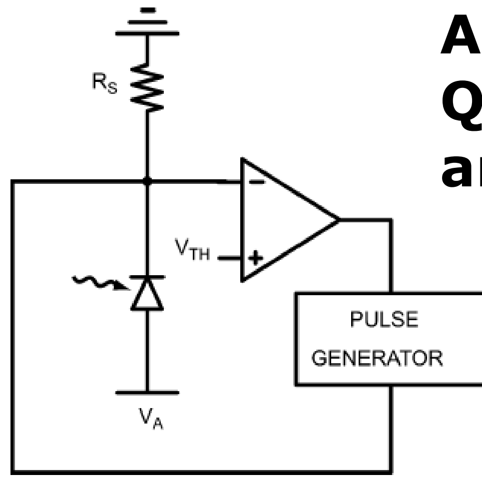

Active Quenching and Reset

- Quenching time: critical
- Reset: ok,
  well defined dead-time
- Hold-off: ok

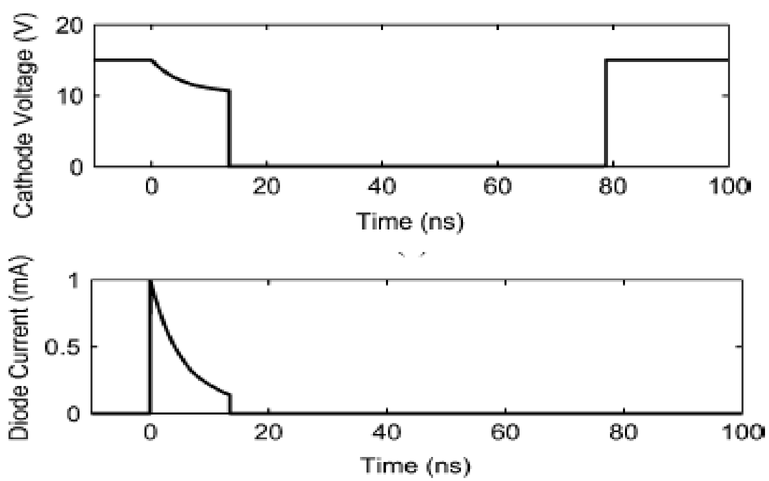

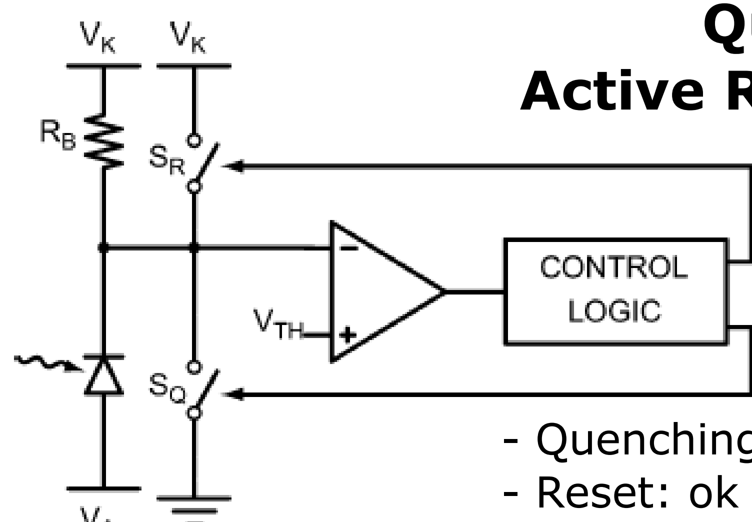

Mixed Active/Passive Quenching Active Reset

- Quenching time: ok
- Reset: ok
- Hold-off: ok

… integrated circuit is quite complex → arrays: hybrid or CMOS

Mixed Quenching/Recharge

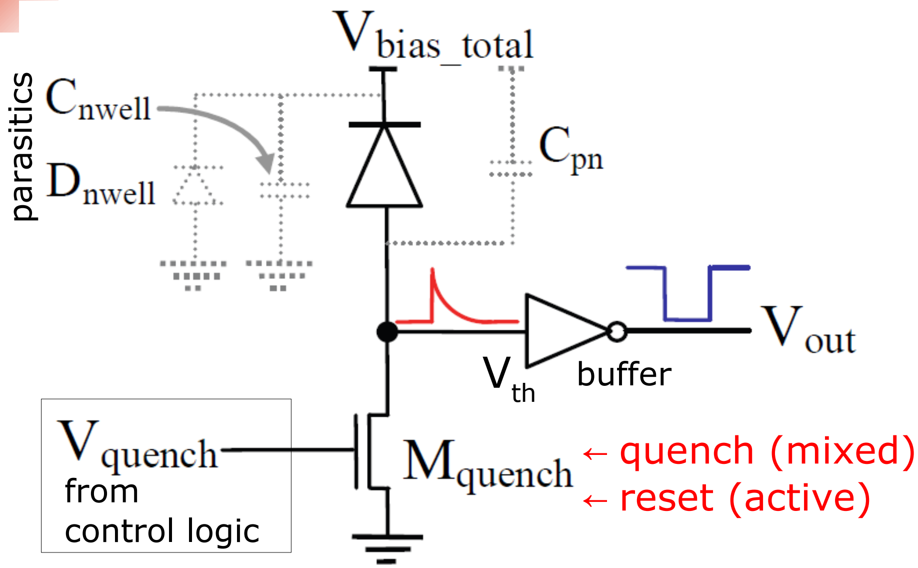

Basic circuit elements:
1) quench circuit to detect and stop the avalanche and restore bias conditions
2) buffer (low capacitive load) for isolating the APD from the external electronics capacitance
(pulse shaper and impedance adapter)
Configuration with anode to ground potential is best: only C_{det} is involved → minimum RC load
→ minimum quenching dead-time
→ minimum charge flow in APD (less after-pulses)
(in addition n-well regions (cathode) can be shared among many cells)

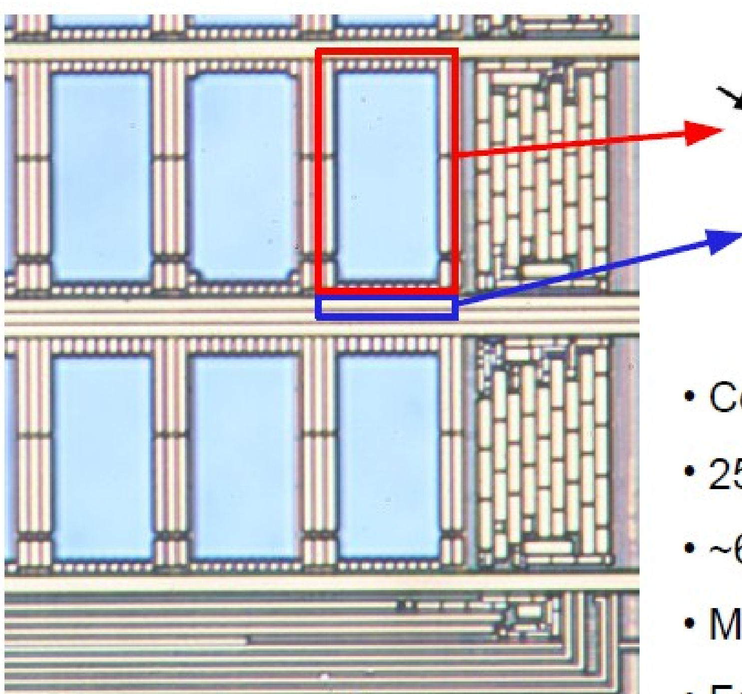

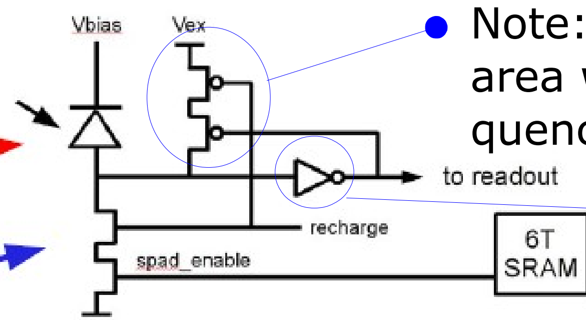

- Note: use of PMOS to minimize the area wrt NMOS for the same target quenching resistance
- buffer → simple inverter as input signal is already digital (avalanche saturated current)

dSiPM cell electronics

- Cell electronics area: 120μm²
- 25 transistors including 6T SRAM
- ~6% of total cell area
- Modified 0.18μm 5M CMOS
- Foundry: NXP Nijmegen

- Cell area ~ 30x50μm²
- Fill Factor ~ 50%

T.Frach at LIGHT 2011

Analog vs Digital SiPM

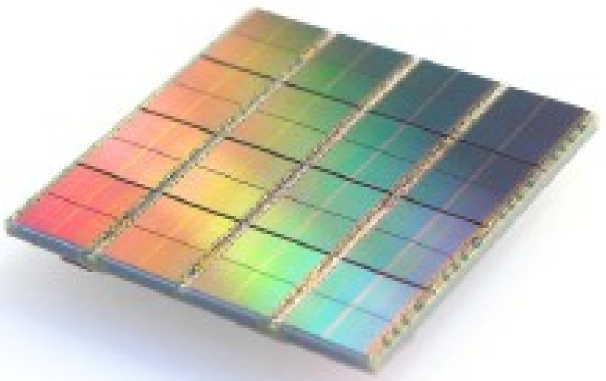

Analog Silicon Photomultiplier

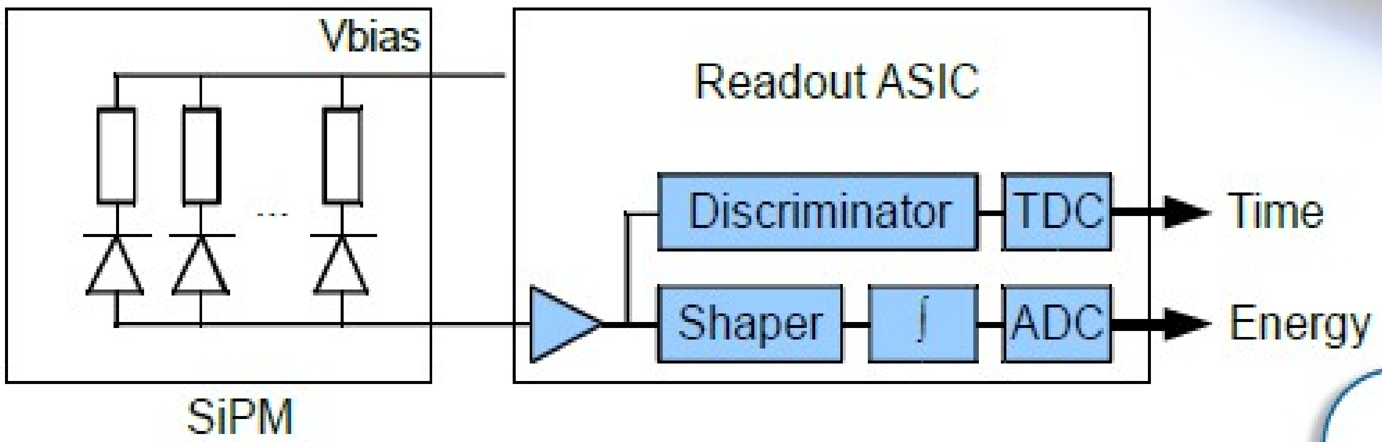

Digital Silicon Photomultiplier

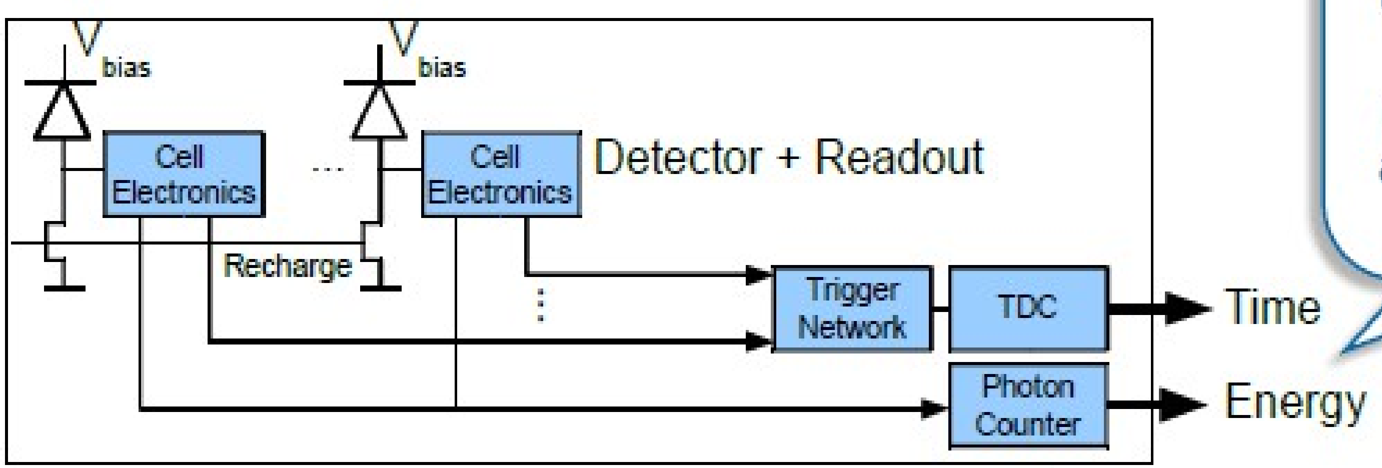

dSiPM provides a digital timestamp and the photon count for each light pulse, without the need of any analog front-end electronics

!!! control over individual SPADs

Fundamental SiPM parameters

related to the recharge of the diode capacitance from V_{bd} to V_{bias} during the avalanche quenching time after I_{latch} is reached

Gain, Signal formation and Dynamic Range - Linearity

pulses triggered by non-photo-generated carriers (thermal / tunneling generation in the bulk or in the surface depleted region around the junction)

carriers can be trapped during an avalanche and then released triggering another avalanche

Noise: dark count
afterpulses
optical cross-talk

photo-generation during the avalanche discharge. Some of the photons can be absorbed in the adjacent cell possibly triggering new discharges

PDE = QE * P_{01} * ε

QE = quantum efficiency
P_{01} = avalanche triggering prob.
ε = geometrical fill factor

Photo-detection efficiency

Related to the photo-generation and to the avalanche propagation

Time resolution

but… wait: how to measure

V_{bd}, R_q ,$T_{junction}$?

I-V characteristics

- Information from Forward current → - Rq
  - junction Temperature
  ...

- Information from Reverse current → - breakdown V_{bd}
  - T coefficient
  ...

I-V characterization: forward bias

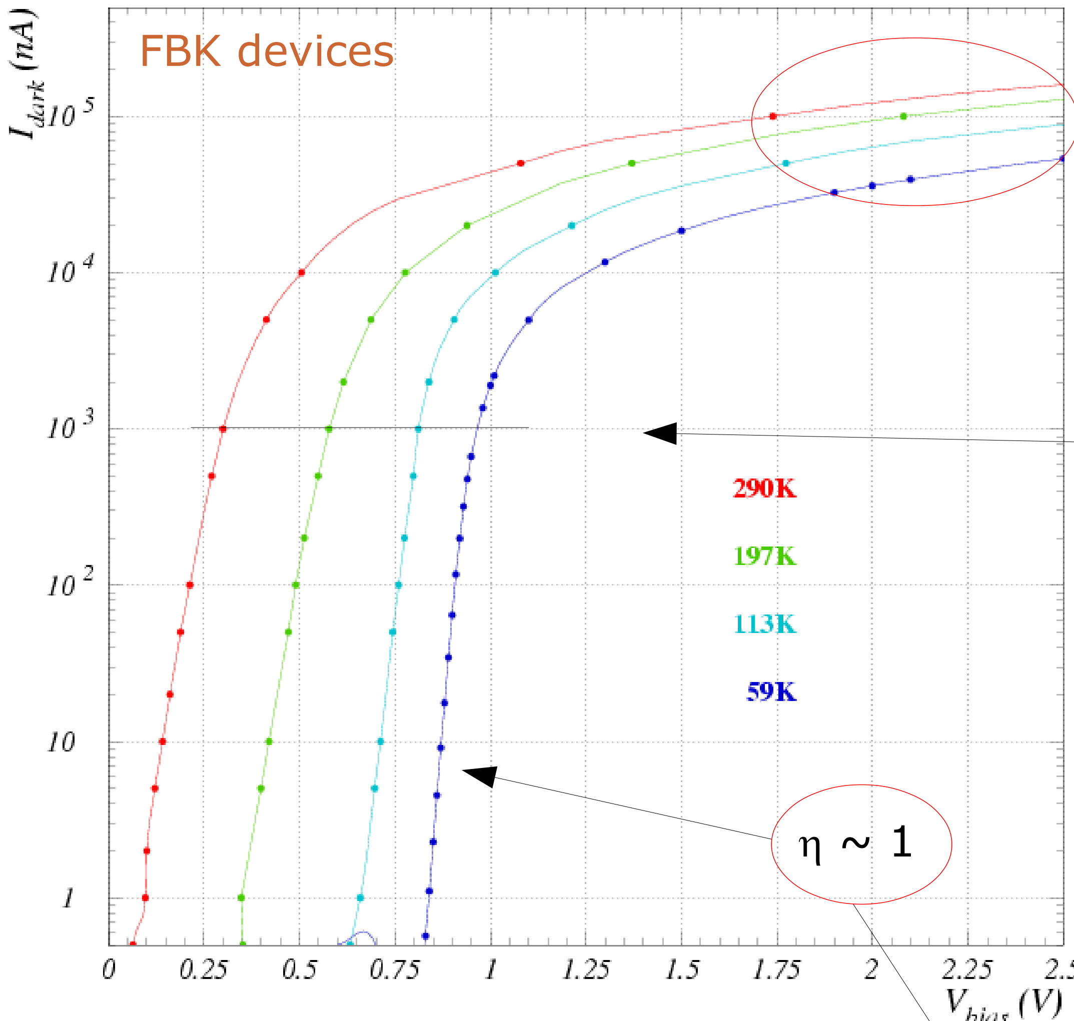

3 **Ohmic** behavior at high current

Linear fit → R_{series} ~ R_q / N_{cells}

2 **Voltage drop** (V_d) decreases linearly with T decreasing (e.g. at 1μA)

Strong variation with T
→ negative T coeff of V_d

1 **Forward current**

$$I_{forward} \sim C(\eta) A(T) \left[\exp\left(\frac{q V_d}{\eta k T} \right) - 1 \right]$$

Shockley et al. Proc. IRE 45 (1957)

η ideality factor

Diffusion current dominating: η → 1

Recombination current dominating: η → 2

Forward I-V → Junction Temperature probe

Voltage drop at fixed forward current → precise **measurement of junction T**…

for T→0 ideally V_d→ Eg
(freeze-out effects apart)

… otherwise not trivially measured !

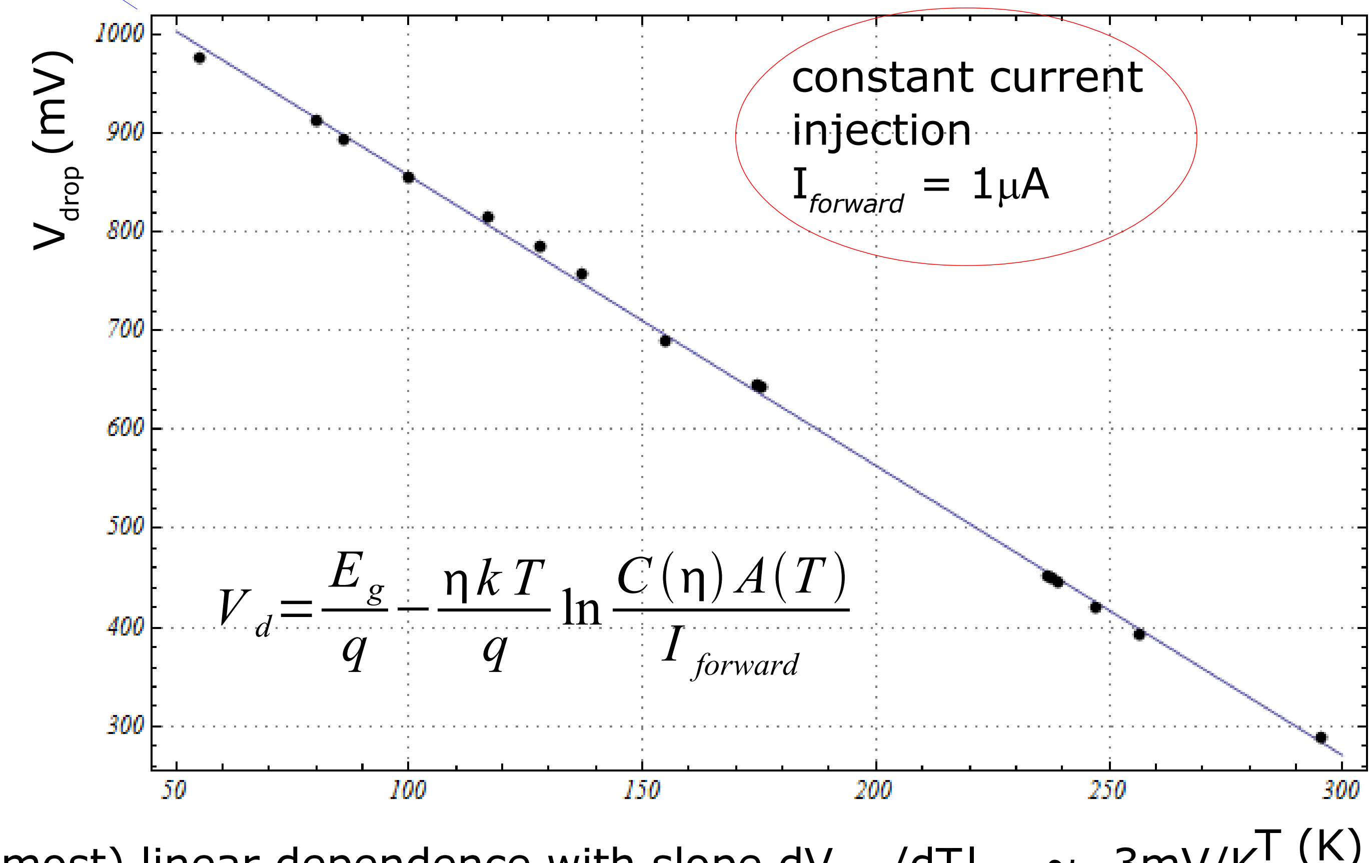

- (almost) linear dependence with slope $dV_{drop}/dT|_{1\mu A}$ ~ -3mV/K
  (we don't see freeze-out effects down to 50K)

- direct and precise **calibration/probe** of junction(s) Temperature

I-V characteristics

- Information from Forward current → - Rq
  - junction Temperature
  - ...

- Information from Reverse current → - breakdown V_{bd}
  - T coefficient
  - ...

Forward I-V → Series Resistance (vs T)

Two ways for measuring series resistance (R_s)

1) Fit at high V of forward characteristic
2) Exponential recovery time (afterpulses envelope)

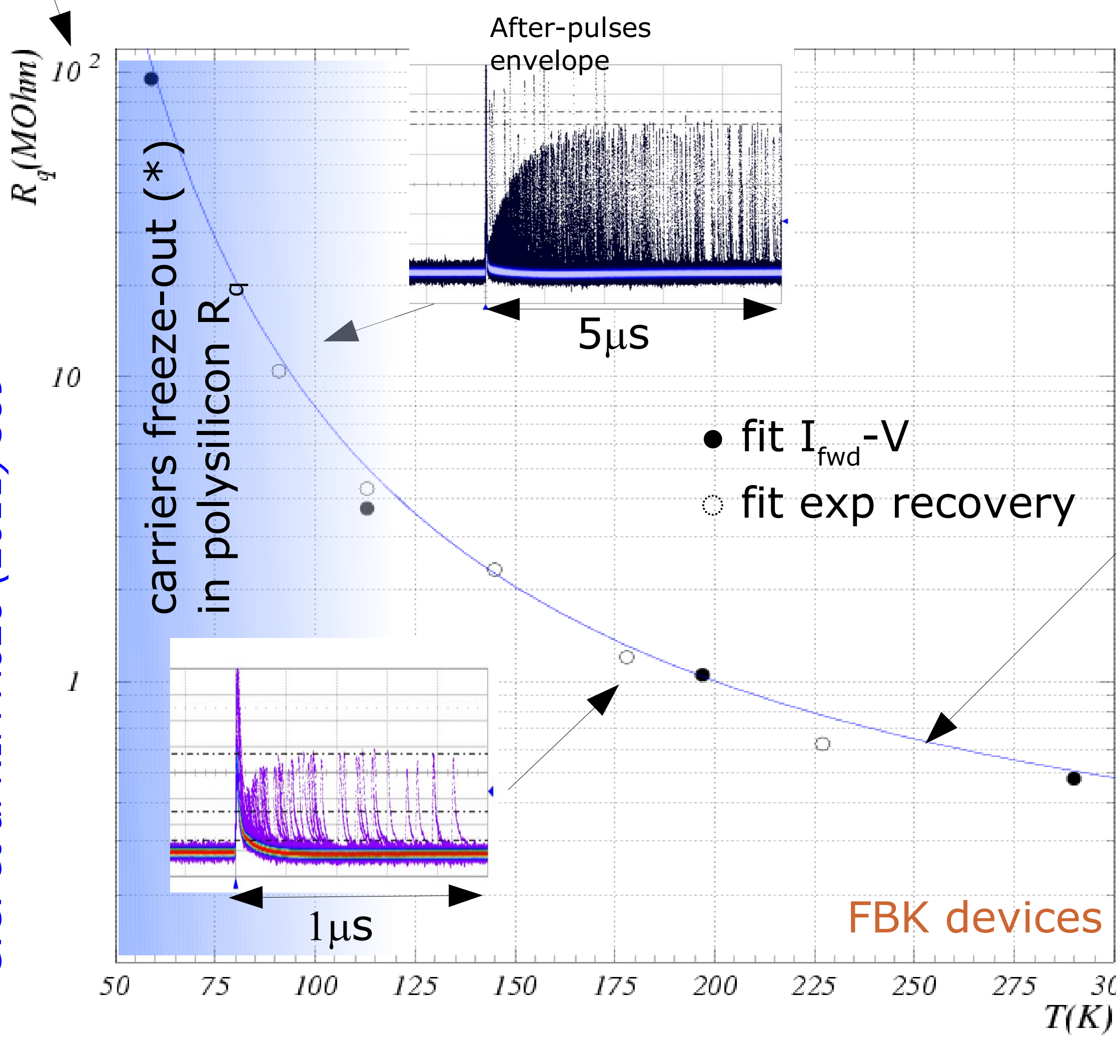

Measurements (1) and (2) consistent → **dominant effect from quenching resistor R_q**
(→ series R bulk gives smaller contribution)

Empirical fit:

$$R_q(T) \sim 0.13\,(1 + 300/T\, e^{300/T})\, M\Omega$$

Afterpulses envelope

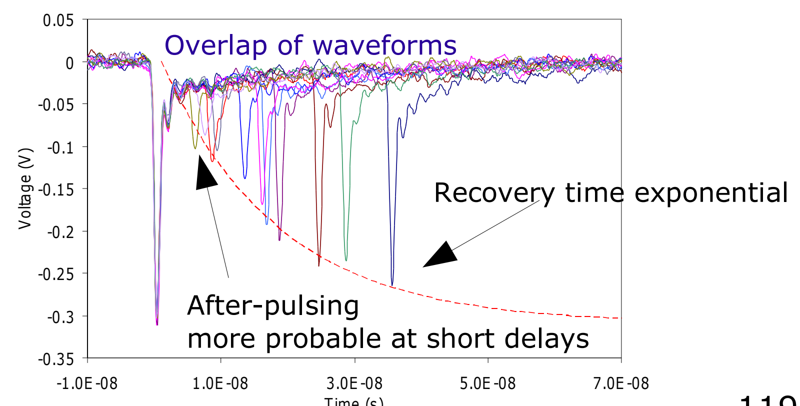

Note: SiPM for low T applications must have appropriate quenching R (not quenching at room T !)

G.C. et al NIM A628 (2011) 389

Quenching resistor

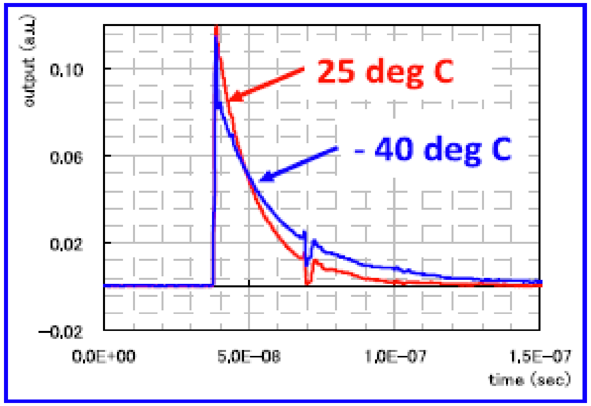

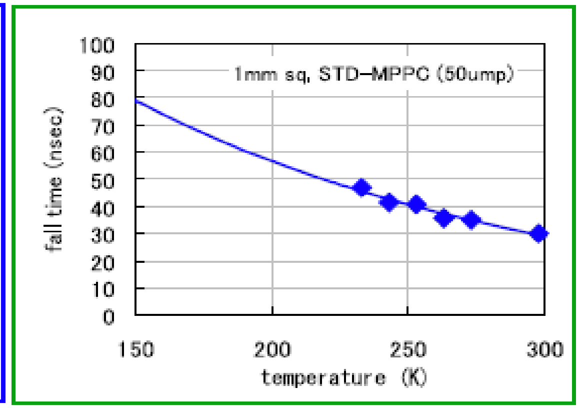

The quenching resistor value increases as environmental temperature decreases. The larger resistor makes the pulse amplitude lower and the tail longer.

Adopting metal quenching resistor

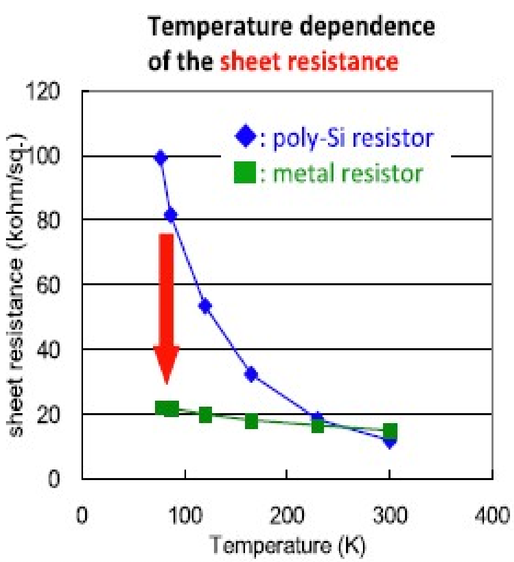

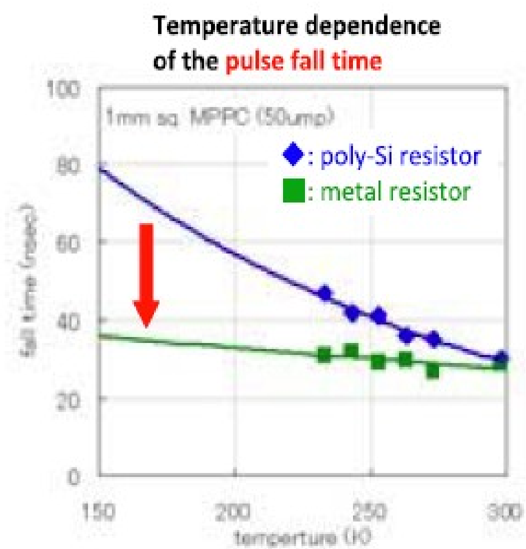

Improved temperature stability

Metal quenching resistor achieved 1/5 temperature dependence

Reverse I-V

→ Dark Current behavior and V_{bd} measurement

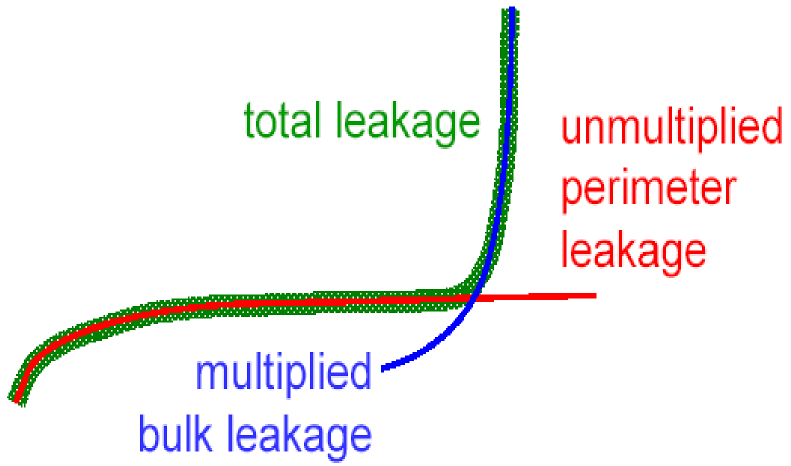

~ linear with Vbias → linear with ΔV (overvoltage)

~q · Gain (G) · Dark Count Rate (DCR)
~ q · ΔV · ΔV → quadratic with ΔV

Note:
- G is linear with ΔV
- Dark Count Rate is ~PDE which is linear with ΔV (at least for few volts)

Reverse I-V characteristics at fixed T

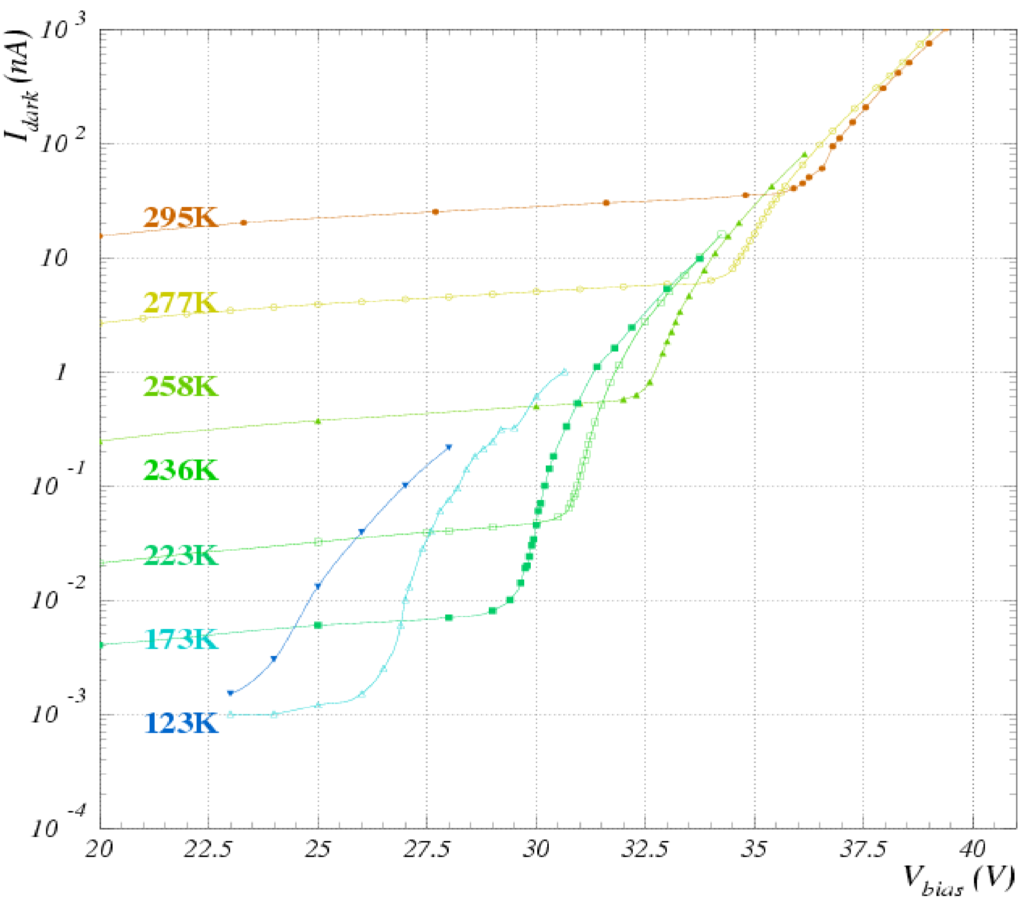

Reverse I-V → Dark Current and V_{bd}

Reverse I-V characteristics at fixed T

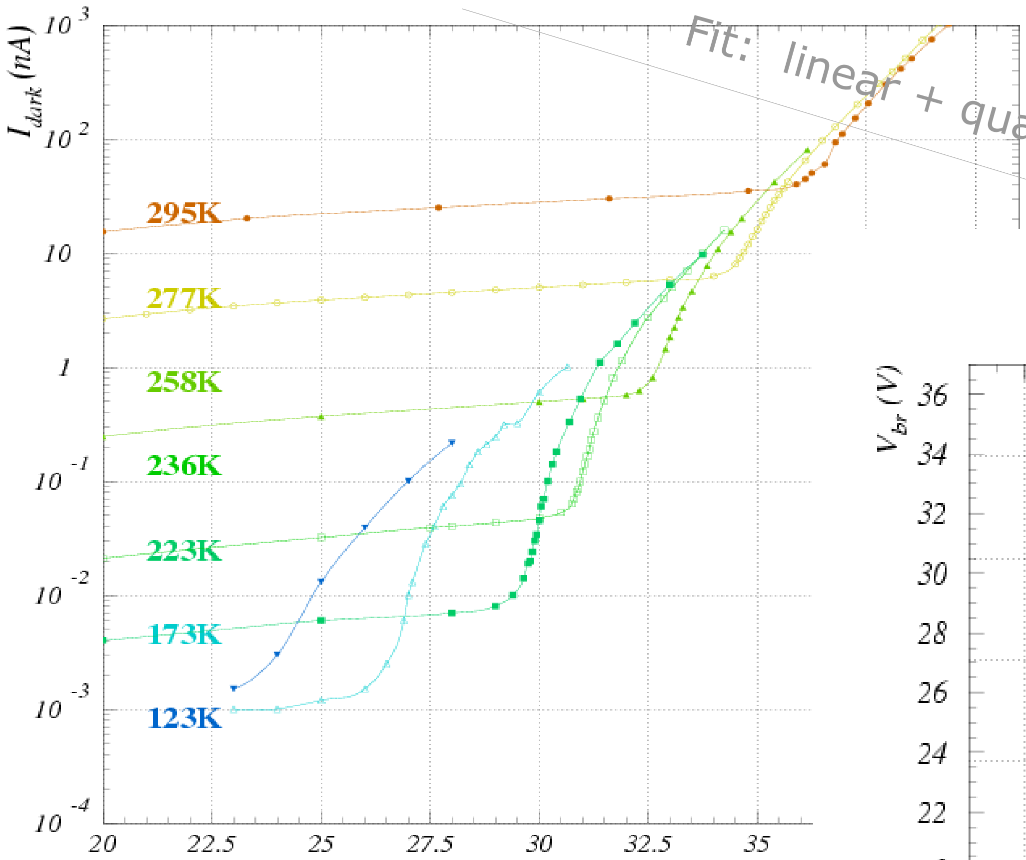

Dark current decreases rapidly with T at rate ~ x2 / 10K

Fit: linear + quadratic ($V > V_{breakdown}$)

Breakdown Voltage vs T

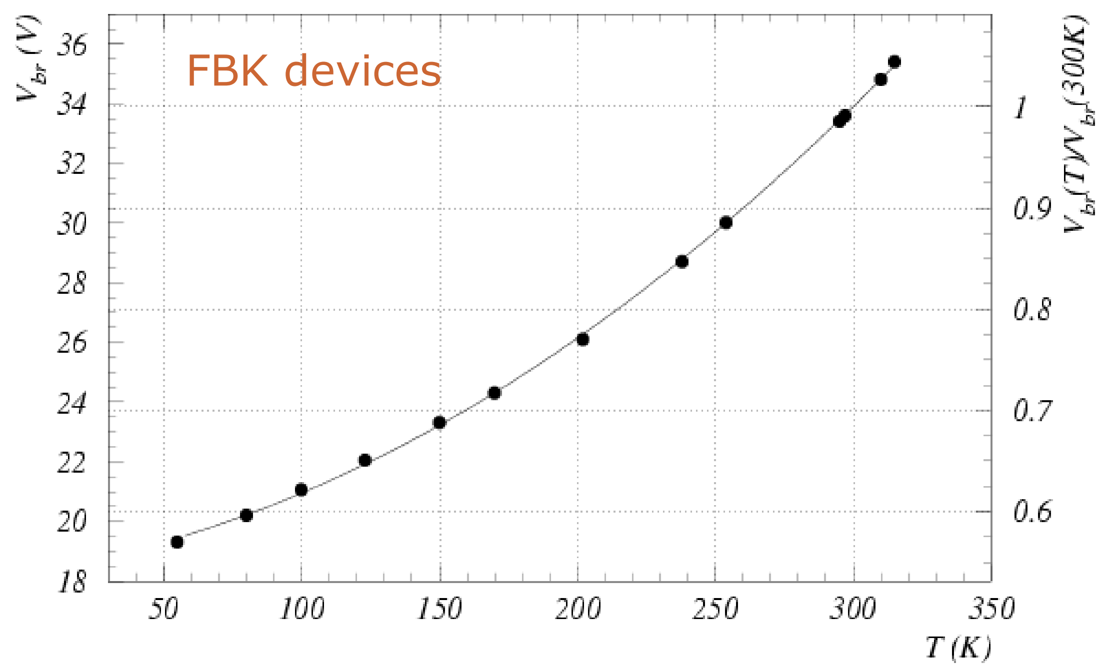

Breakdown voltage decreases
at low T due to larger carriers mobility
→ larger ionization rate (electric E field fixed)

G.C. et al NIM A628 (2011) 389

V_{bd} vs T → T coefficient (ΔV stability)

Breakdown Voltage

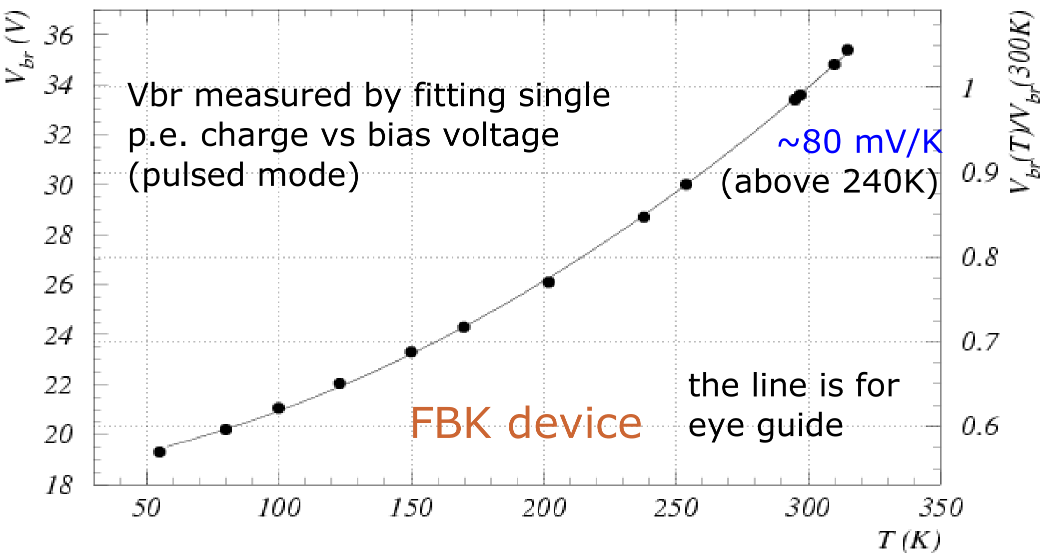

G.C. et al NIM A628 (2011) 389

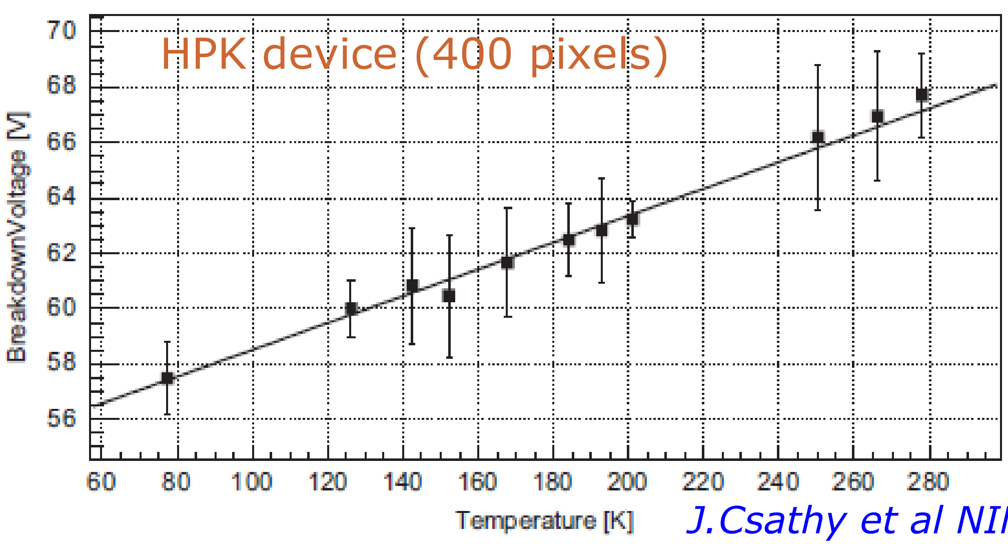

J.Csathy et al NIM A 654 (2011) 225

Fig. 6. Breakdown voltage as a function of temperature of the MPPC with 400 pixels.

Temperature coefficient

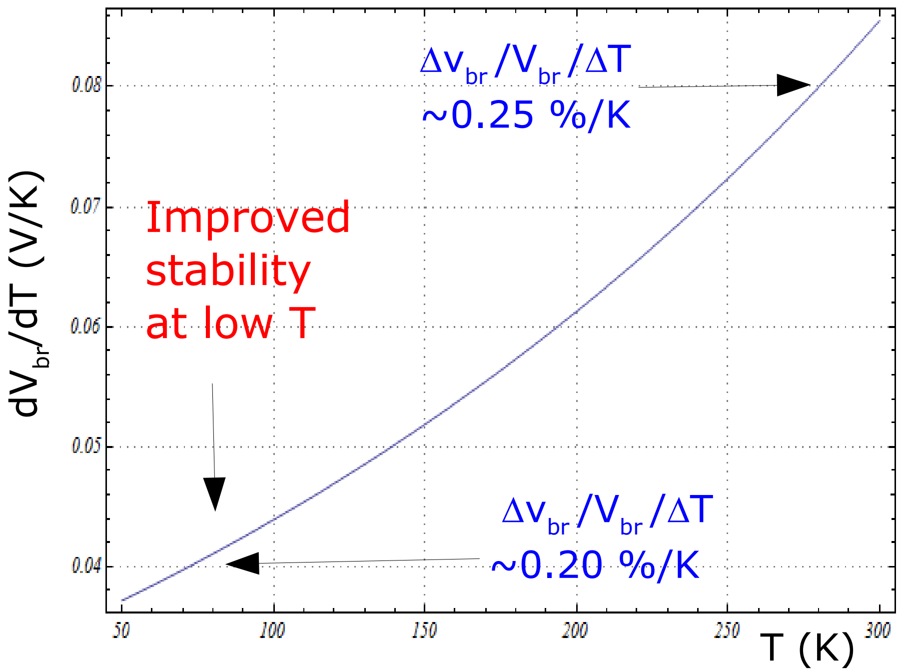

Depletion layer → V_{bd} dependence on T

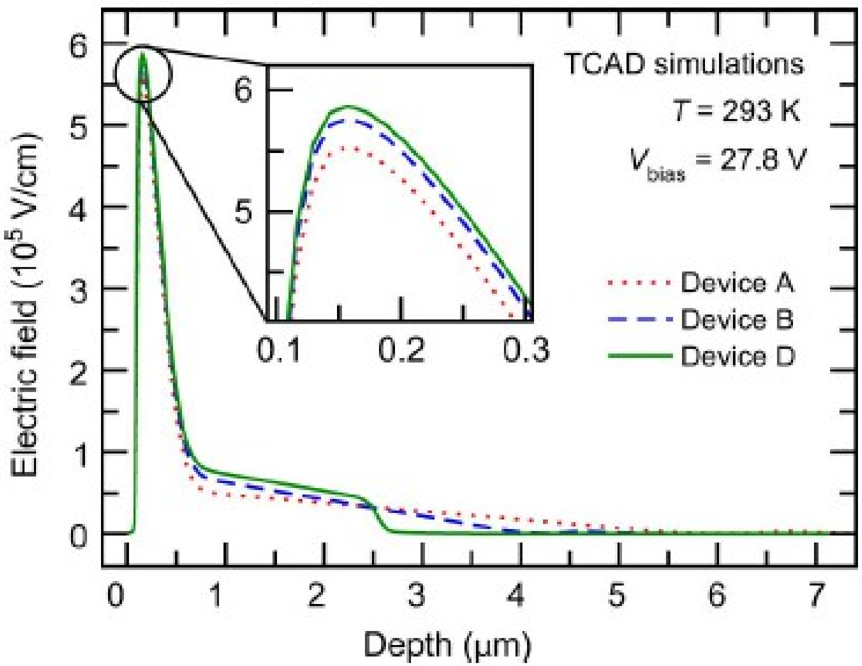

Serra et. al. (FBK) IEEE TNS 58 (2011) 1233
"Experimental and TCAD Study of Breakdown Voltage Temperature Behavior in n+/p SiPMs"

Note: precise agreement simulation/data is not trivial at all. Definition of ionization coefficients is device dependent...

Narrow depletion layer (high background doping(*) or thin epitaxial layer)
→ minimize V_{bd} dependence on T
→ gain stability $\frac{\delta V_{bd}/V_{bd}}{\delta T} = \frac{\delta G/G}{\delta T}$

(*) resulting in epitaxial layer not fully depleted at V_{bd}

Trade off:
→ PDE (thickness)
→ minimum gain (capacity) against after-pulses and cross-talk

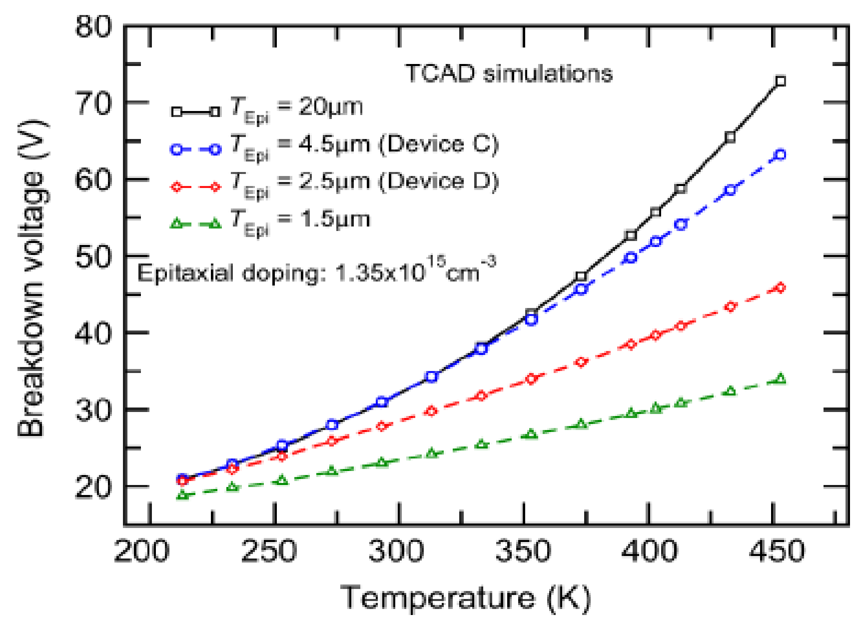

Fig. 9. TCAD simulated V_{BD} in the GM-APDs of this work (see Table I) in an extended temperature range. Two additional epitaxial layer thickness are considered (20 μm, 1.5 μm) to emphasize the impact of the depletion layer width on the V_{BD} vs. temperature characteristic.

Improved V_{bd} uniformity and T coefficient

Recent FBK-Advansid devices

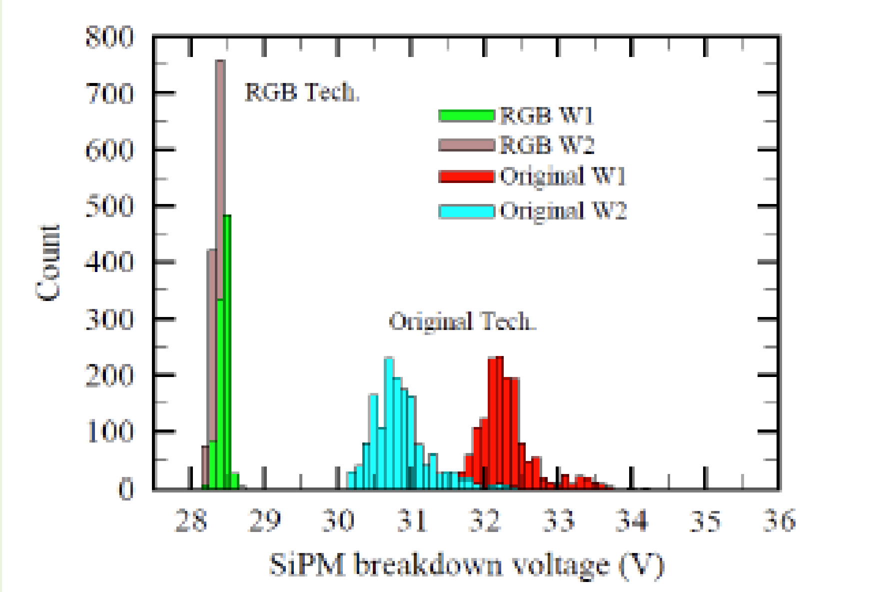

breakdown voltage non-uniformity strongly reduced both at wafer level and from wafer to wafer

breakdown voltage temperature dependence

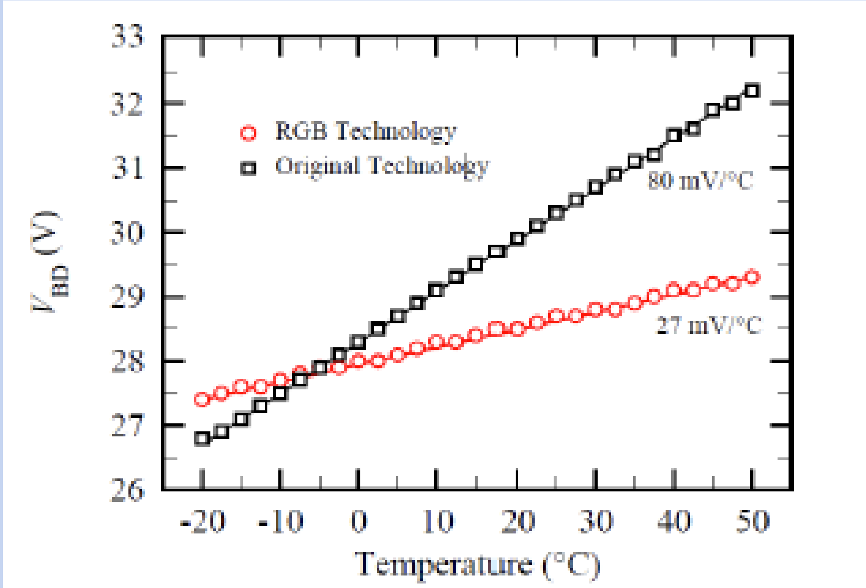

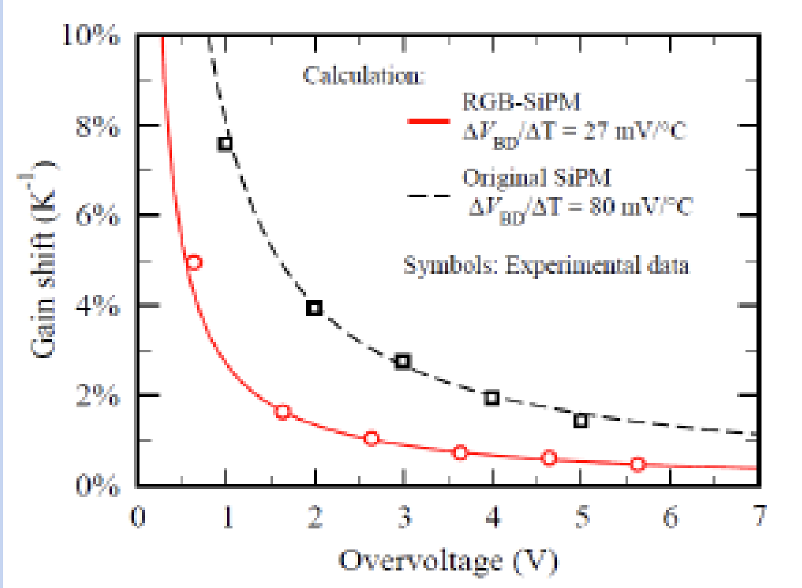

C.Piemonte, Scuola Nazionale Rivelatori Legnaro 2013

Pulse shape, Gain and Response

(mostly for passive mode)

- Detailed electrical model
- Pulse shape
- Gain and Gain fluctuation
- Response non-linearity

Simple electrical model – ideal signal shape

Diode (capacitor) fast discharge
and slow recharge

charge stored defines Gain
→ Gain ~ C ΔV
$\Delta V = V_{bias} - V_{bd}$ "Over-Voltage"

currents internal / external

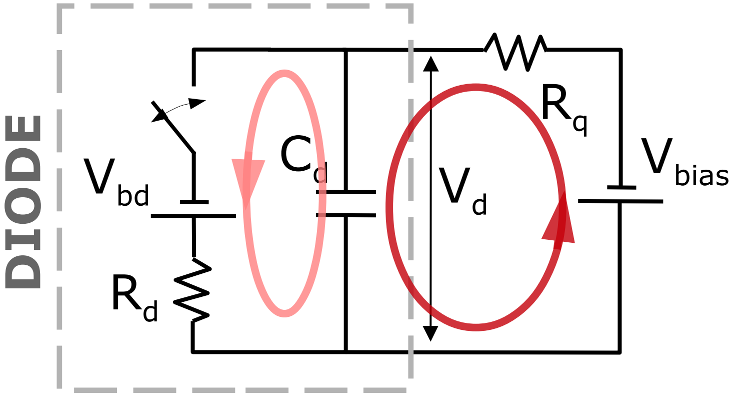

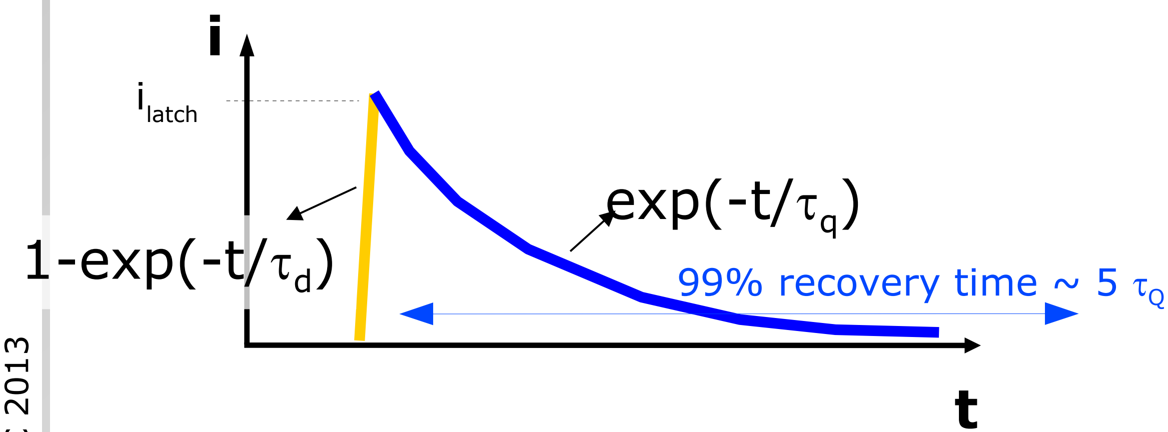

Rise time — Fall time (recovery)

$\tau_d = R_dC_d \ll \tau_q = R_qC_d$

Gain → linear with ΔV (≠ APD)
→ no intrinsic fluctuations !!! (≠ APD)
→ independent of T at fixed ΔV (≠ APD)

Rise time — T dependence (weak) due to R_d

Recovery time — T dependence (strong) due to R_q
C_d is independent of T

Actual pulse shape and Gain

Pulse shape

1. fast component
(parasitic transient)

2. slow component due to
(99% recovery time ~100ns)

Waveform (Dark noise)

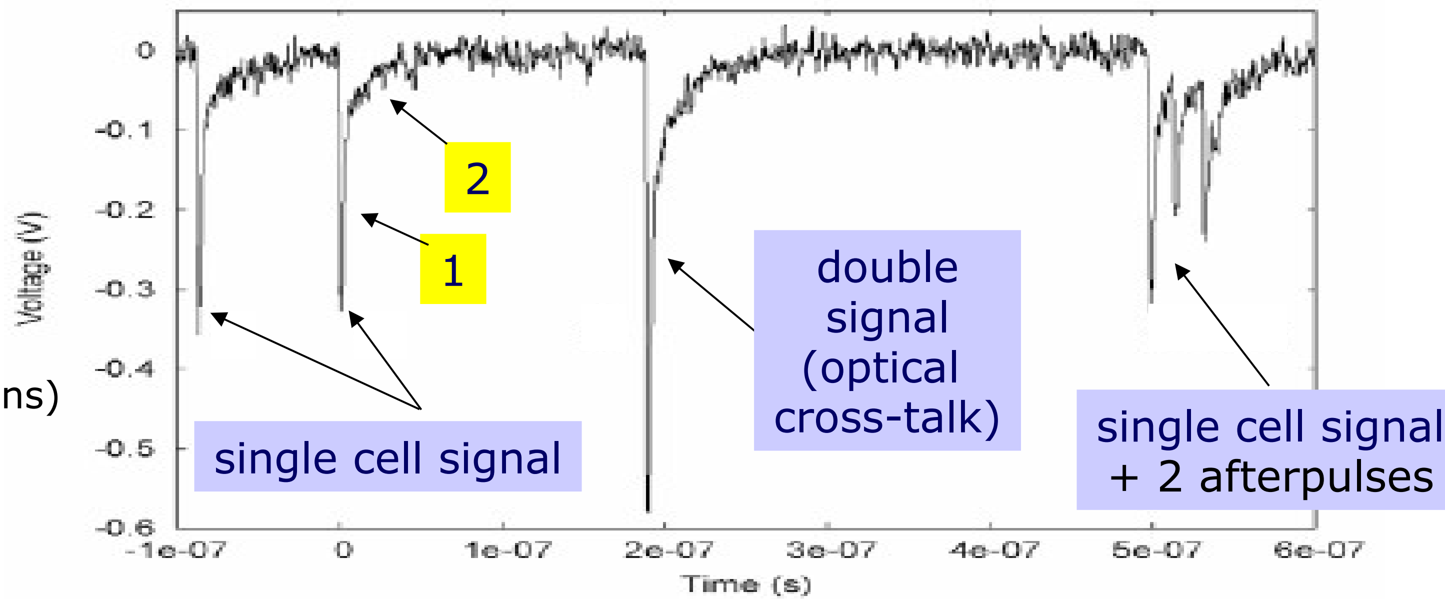

Charge spectrum

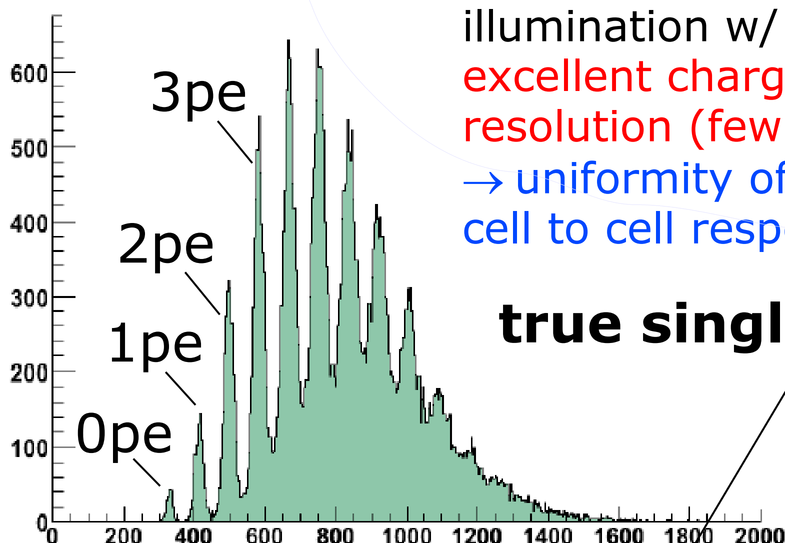

illumination w/ LED
excellent charge resolution (few%)
→ uniformity of cell to cell response

true single ph.e

NOTE: gain easily measured

Gain

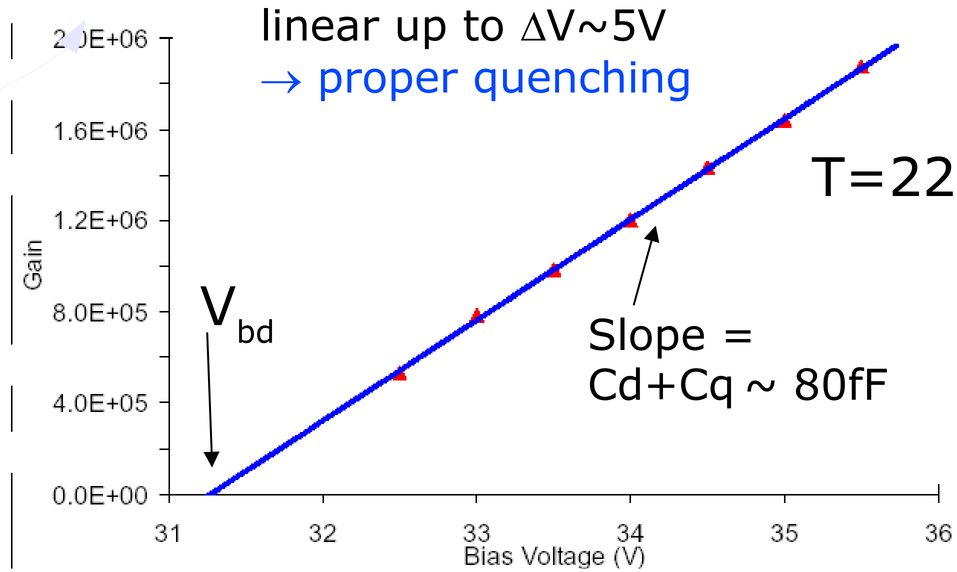

SiPM equivalent circuit and pulse shape

Single cell model → $(R_d||C_d)+(R_q||C_q)$

SiPM + load → $(||Z_{cell})||C_{grid} + Z_{load}$

Signal = slow pulse ($\tau_{d\ (rise)}, \tau_{slow\ (fall)}$) +
+ fast pulse ($\tau_{d\ (rise)}, \tau_{fast\ (fall)}$)

- $\tau_{d\ (rise)} \sim R_d(C_q+C_d)$
- $\tau_{fast\ (fall)} = R_{load}\ C_{tot}$ (fast; parasitic spike)
- $\tau_{slow\ (fall)} = R_q\ (C_q+C_d)$ (slow; cell recovery)

F.Corsi, et al. NIM A572 (2007) 416

S.Seifert et al. IEEE TNS 56 (2009) 3726

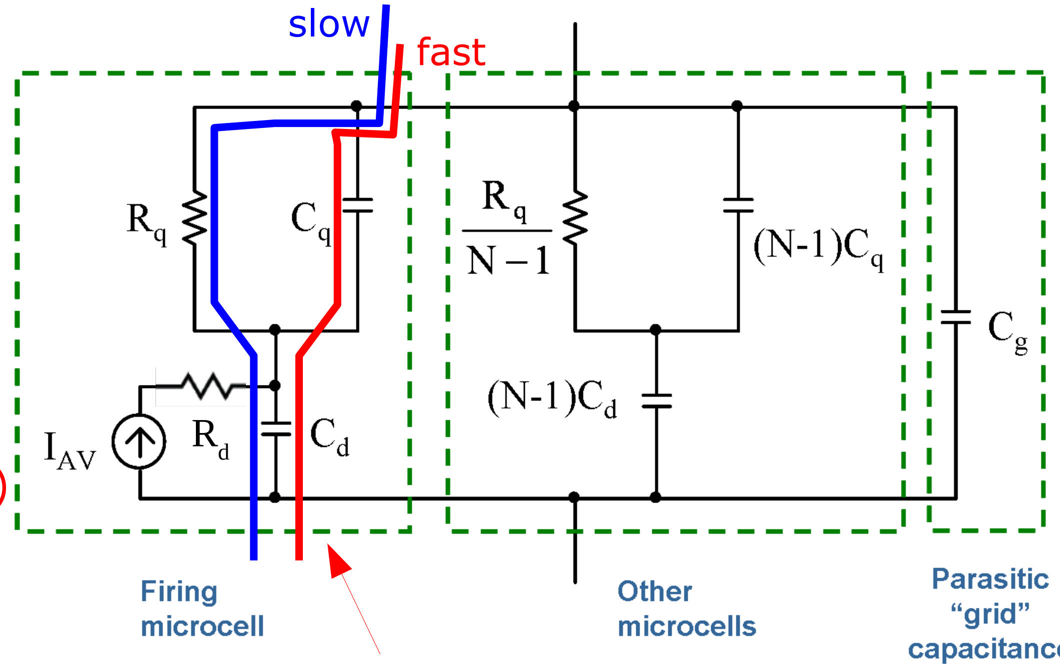

Cq → fast current supply path in the beginning of avalanche

Pulse shape

- Rise: Exponential → Sp.Charge Rd x Cd,q filtered by parasitic inductance, stray C, ... (Low Pass)
- Fall: Sum of 2 exponentials: transient + recovery

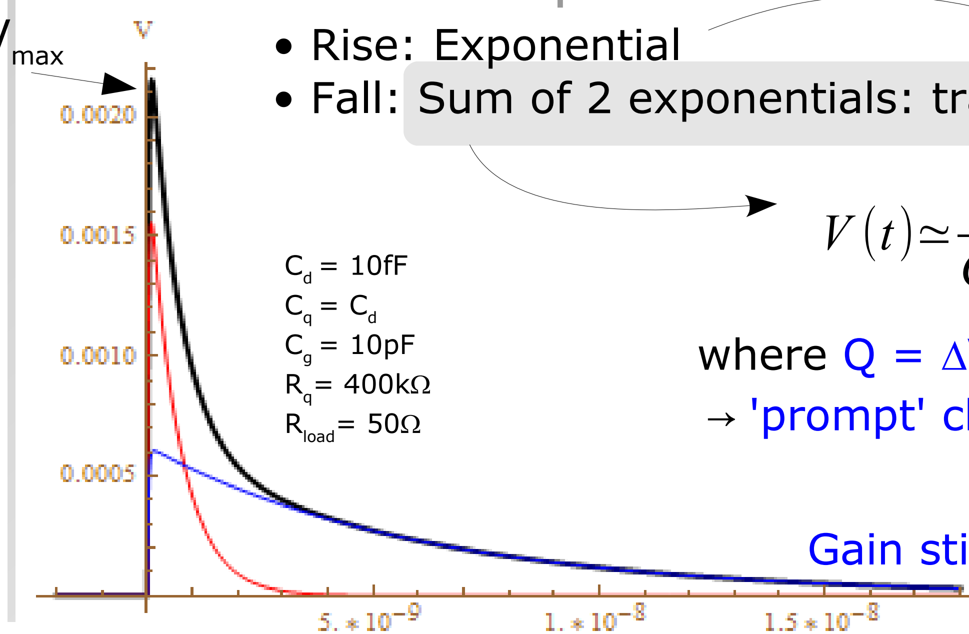

$$V(t) \simeq \frac{Q}{C_q+C_d}\left(\frac{C_q}{C_{tot}} e^{\frac{-t}{\tau_{FAST}}} + \frac{R_{load}}{R_q}\frac{C_d}{C_q+C_d} e^{\frac{-t}{\tau_{SLOW}}}\right) \text{ for } R_{load} << R_q$$

where $Q = \Delta V\ (C_q+C_d)$ is the total charge released by the cell
→ 'prompt' charge on C_{tot} is $Q_{fast} = Q\ C_q/(C_q+C_d)$

Gain still well defined:
$$G = \int dt \frac{V(t)}{q_e R_{load}} = Q/q_e = \boxed{\frac{\Delta V(C_d+C_q)}{q_e}}$$

Pulse shape

$$V(t) \simeq \frac{Q}{C_q + C_d}\left(\frac{C_q}{C_{tot}} e^{\frac{-t}{\tau_{fast}}} + \frac{R_{load}}{R_q}\frac{C_d}{C_q + C_d} e^{\frac{-t}{\tau_{slow}}}\right) = \frac{Q\,R_{load}}{C_q + C_d}\left(\frac{C_q}{\tau_{fast}} e^{\frac{-t}{\tau_{fast}}} + \frac{C_d}{\tau_{slow}} e^{\frac{-t}{\tau_{slow}}}\right)$$

Note: valid for low impedance load $R_{load} << Rq$

- $\tau_{fast} = R_{load}\ C_{tot}$
- $\tau_{slow} = R_q\,(C_q + C_d)$

→ gain $\quad G = \int dt \frac{V(t)}{q_e R_{load}} = Q/q_e = \frac{\Delta V (C_d + C_q)}{q_e}$ independent of R_q

→ charge ratio $\quad \frac{Q_{slow}}{Q_{fast}} \sim \frac{C_d}{C_q}$

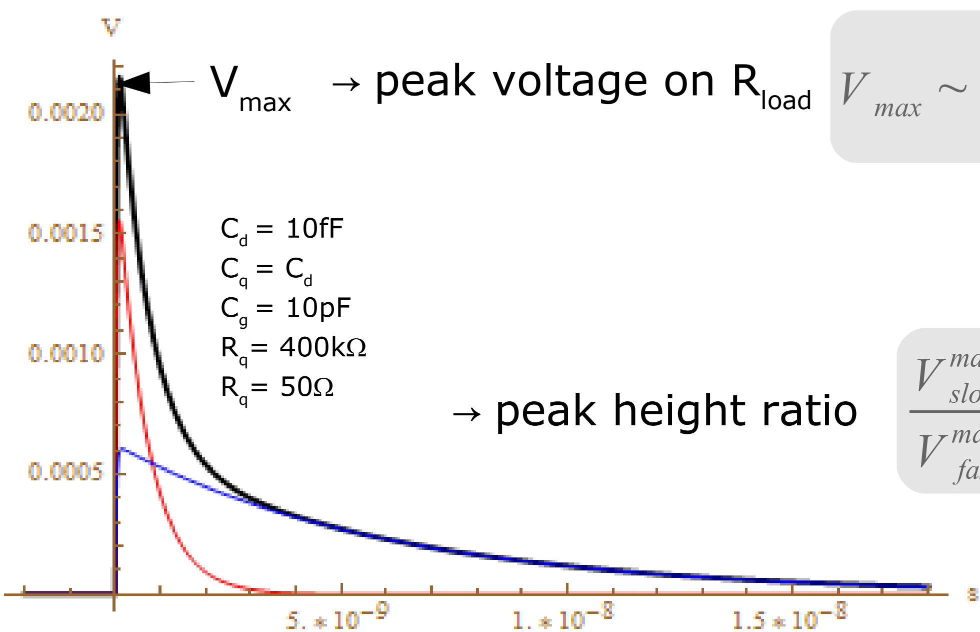

→ peak voltage on R_{load} $\quad V_{max} \sim R_{load}\left(\frac{Q_{fast}}{\tau_{fast}} + \frac{Q_{slow}}{\tau_{slow}}\right)$ dependent on R_q (increasing with $1/R_q$)

→ peak height ratio $\quad \frac{V^{max}_{slow}}{V^{max}_{fast}} \sim \frac{C_d\, C_{tot}\, R_{load}}{C_q^2\, R_q}$ increasing with C_d and $1/R_q$

Pulse shape: dependence on Temperature

The two current components behave differently with Temperature

→ fast component is independent of T because C_{tot} couples to external R_{load}

→ slow component is dependent on T because $C_{d,q}$ couple to $R_q(T)$

H.Otono, et al. PD07

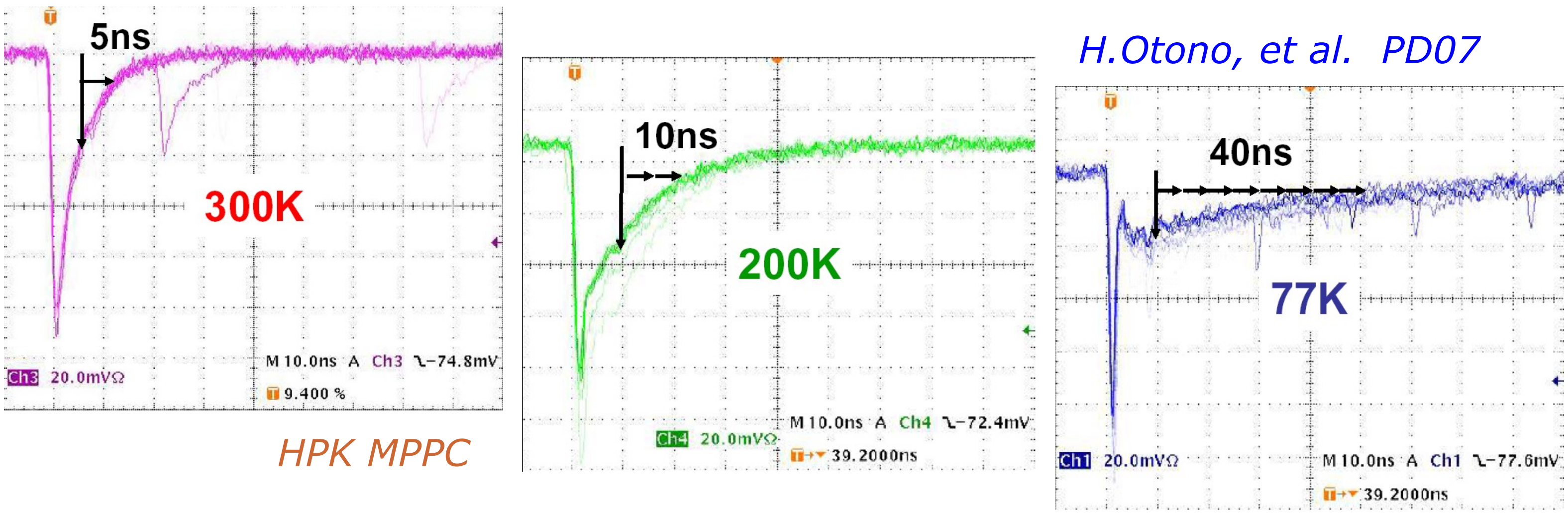

HPK MPPC

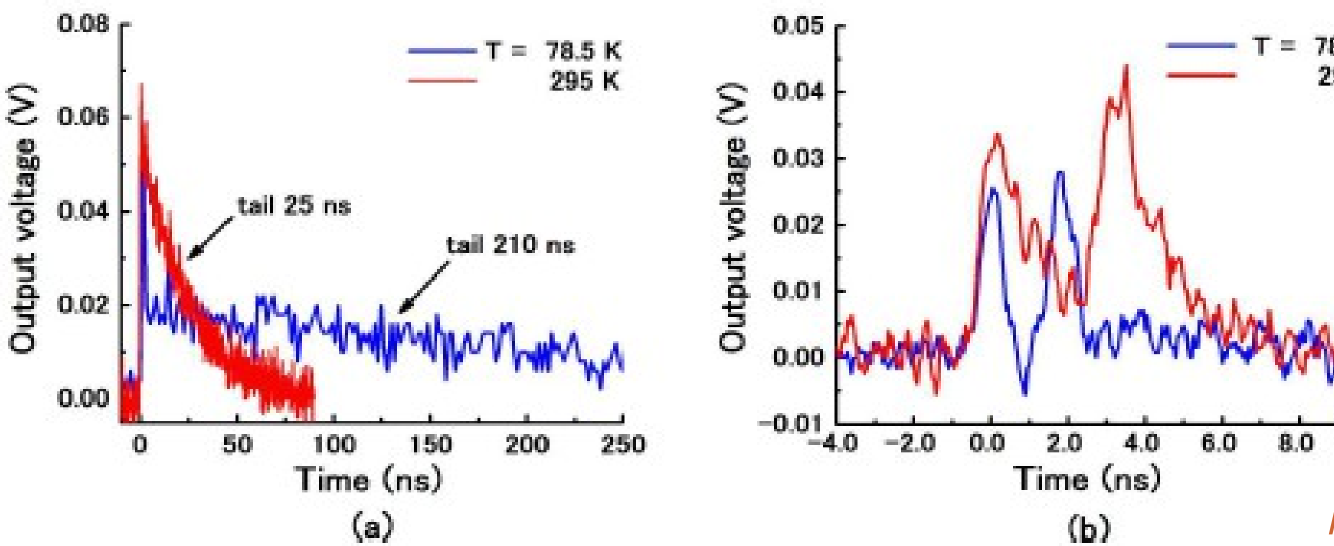

high pass filter / shaping
→ recover fast signals

HPK MPPC

Fig. 2. (a) Output signals from the MPPC when no high-pass filter is used, and (b) output signals from the high-pass filter when two pulses were generated successively.

Akiba et al Optics Express 17 (2009) 16885

Pulse shape vs T

HPK MPPC: 25μm, 50μm, 100μm

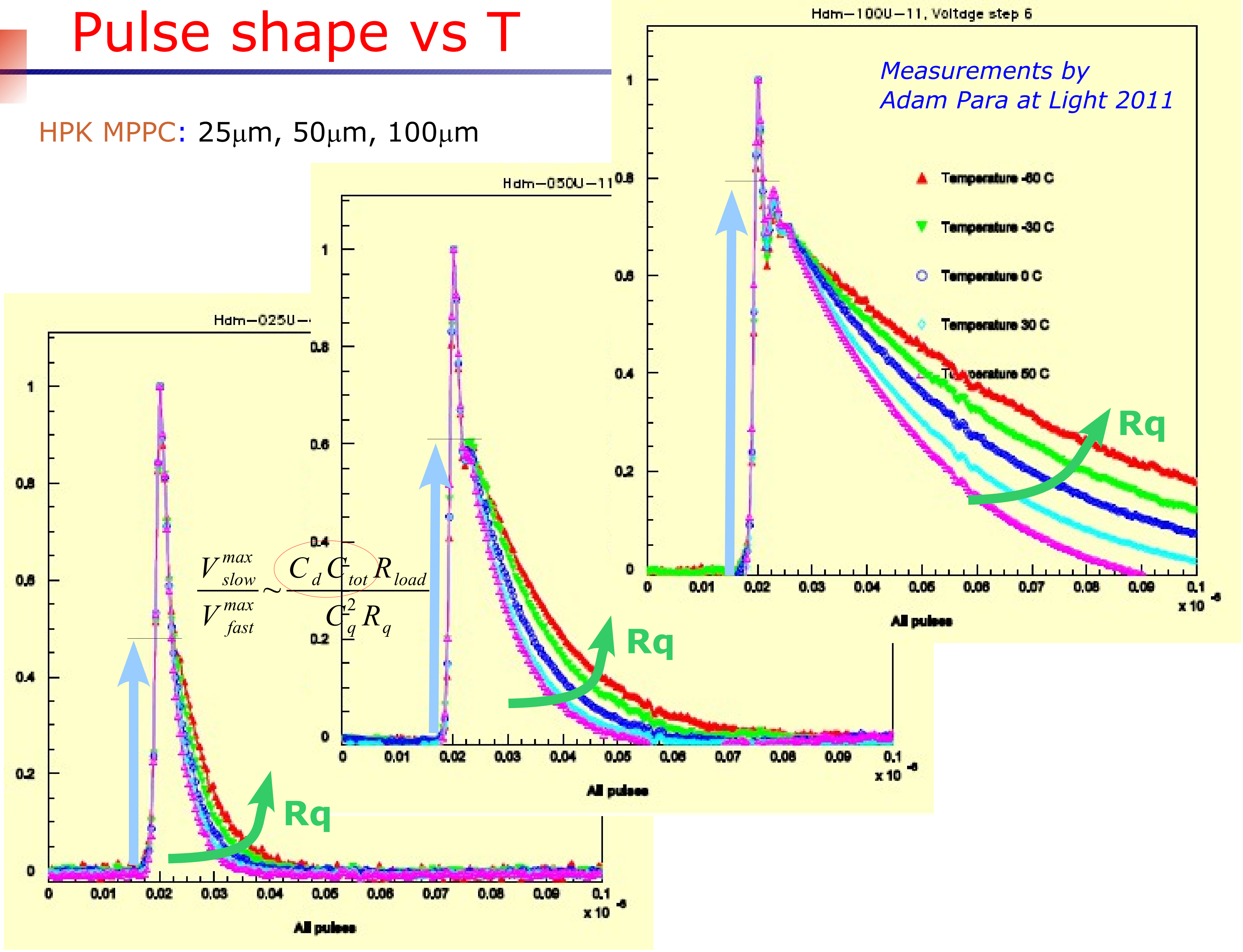

$$\frac{V_{slow}^{max}}{V_{fast}^{max}} \sim \frac{C_d C_{tot} R_{load}}{C_q^2 R_q}$$

Single cell charge resolution

Device illuminated with short weak light pulses from a blue LED.
Device biased at 3V over-voltage.

Effective quenching and cell-to-cell uniformity !

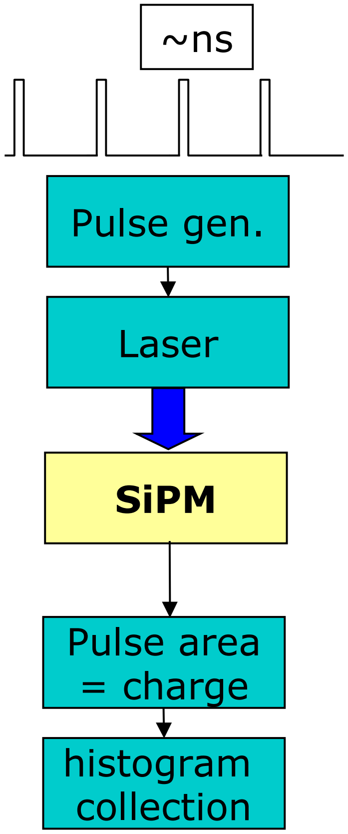

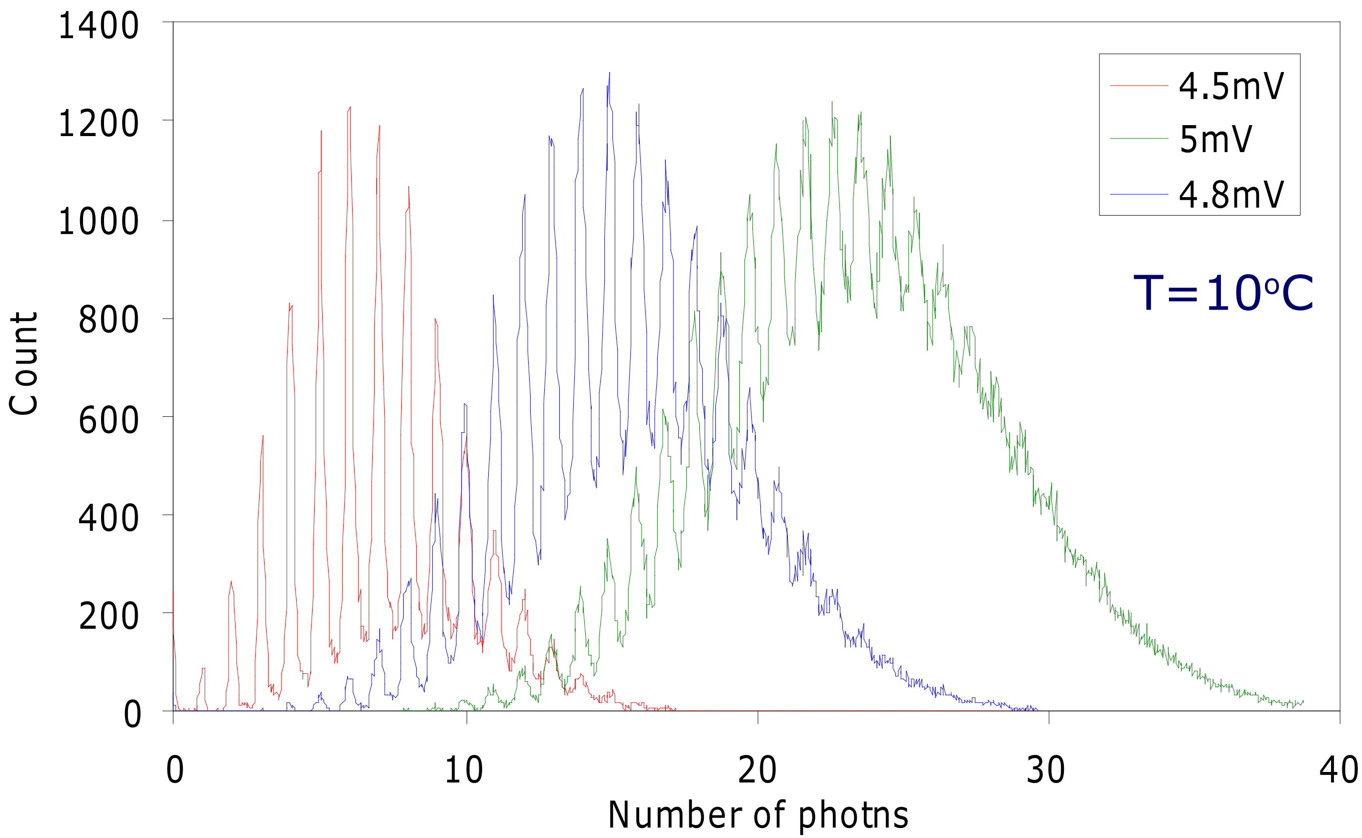

NOTE: resolution limited by electronic noise

C.Piemonte, Workshop on "Photon Detection" - Perugia 2007

Gain and its Fluctuations

$$G=\Delta V\left(C_q+C_d\right)/q_e$$

→ Gain is linear if ΔV in quenching regime

but

there are many sources for non-linearity of response (non proportionality)

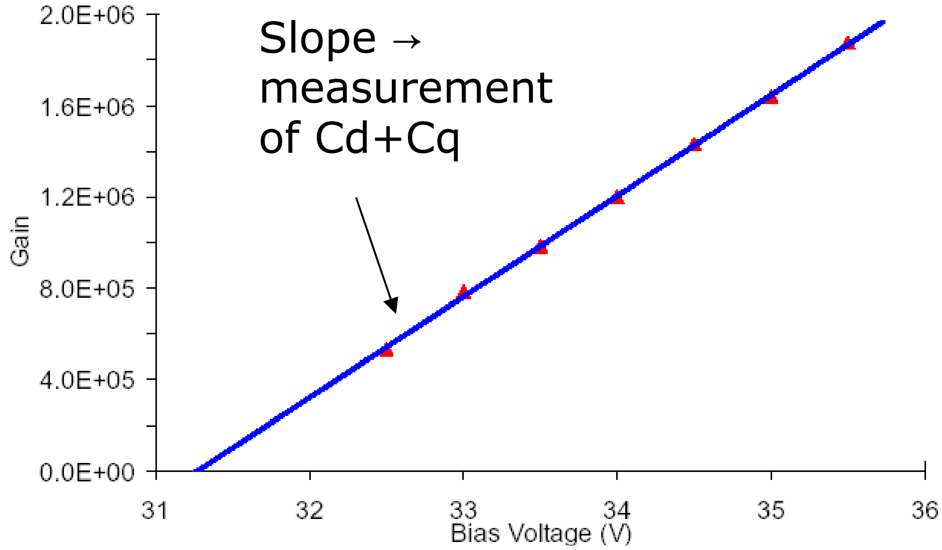

SiPM gain fluctuations (intrinsic) differ in nature compared to APD where the statistical process of internal amplification shows a characteristic fluctuations

$$\frac{\delta G}{G}=\frac{\delta V_{bd}}{V_{bd}}\oplus\frac{\delta C_{dq}}{C_{dq}}$$

cell to cell uniformity (active area and volume) control at % level

- doping densities (Poisson): $\delta V_{bd} \geq 0.3V$
  Shockley, Sol. State Ele. 2 (1961) 35
- doping, epitaxial, oxide (processing): $\delta V_{bd} \sim O(0.1V)$

SES MEPhI/PULSAR APD, U=57.5V, T=-28 C

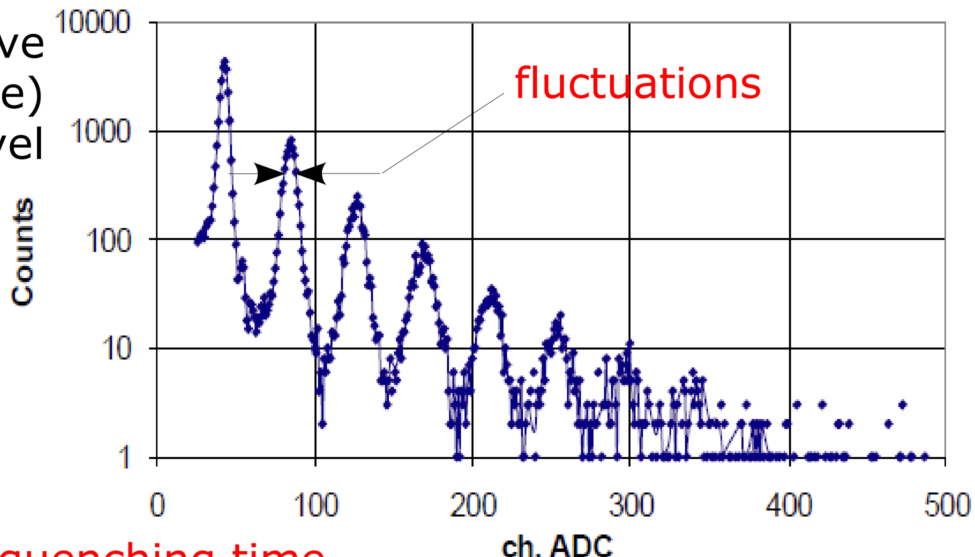

In addition δG might be due to fluctuations in quenching time
… and of course after-pulses contribute too (not intrinsic → might be corrected)

Improved V_{bd} uniformity and T coefficient

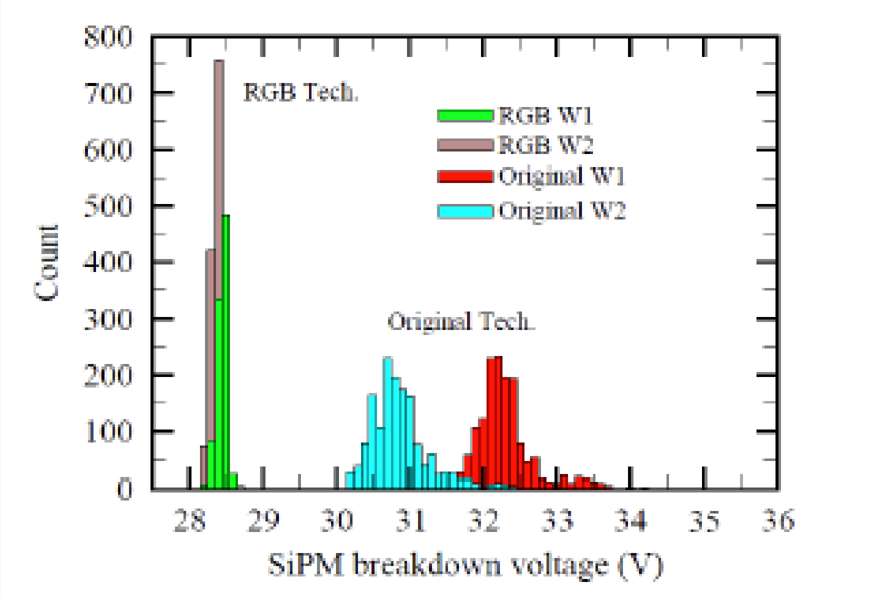

Recent FBK-Advansid devices

breakdown voltage non-uniformity strongly reduced both at wafer level and from wafer to wafer

breakdown voltage temperature dependence

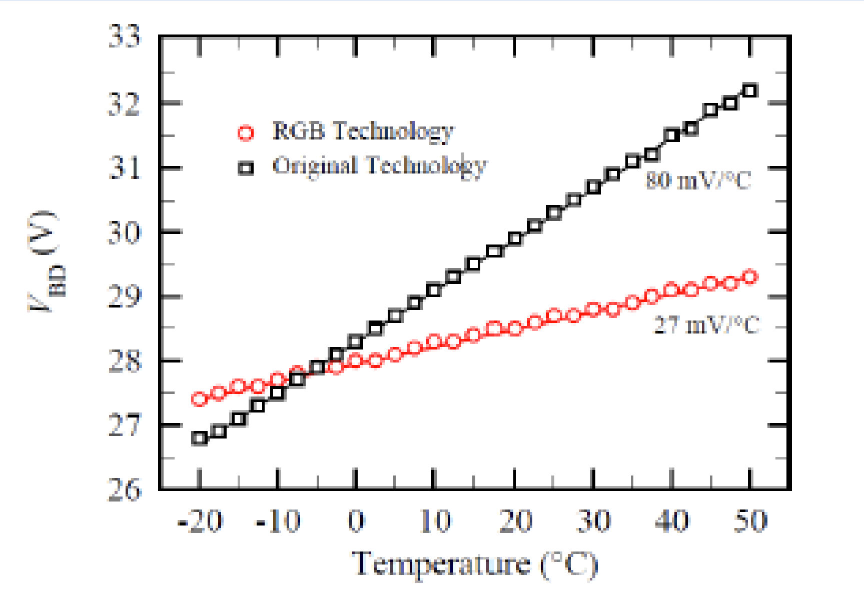

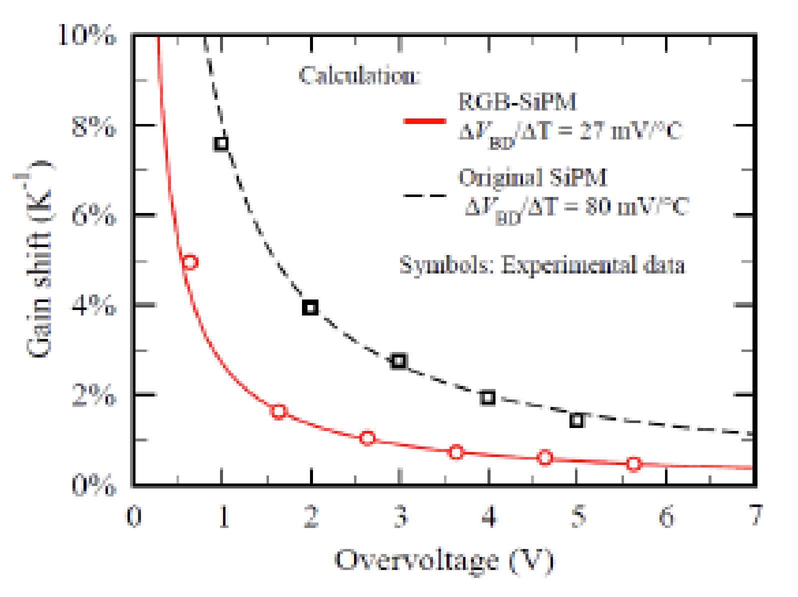

C.Piemonte, Scuola Nazionale Rivelatori Legnaro 2013

Note:

1) no multiplication (excess) noise in SER

2) SER width due to intrinsic fluctuations in doping densities and variations among cells

3) Correlated noise is there (AP, CT)
$\rightarrow$ excess charge factor (ECF)

Response Non-Linearity

Non-proportionality of charge output w.r.t. number of photons (i.e. response) at level of several % might show up even in quenching regime (negligible quenching time), depending on ΔV and on the intensity and duration of the light pulse.

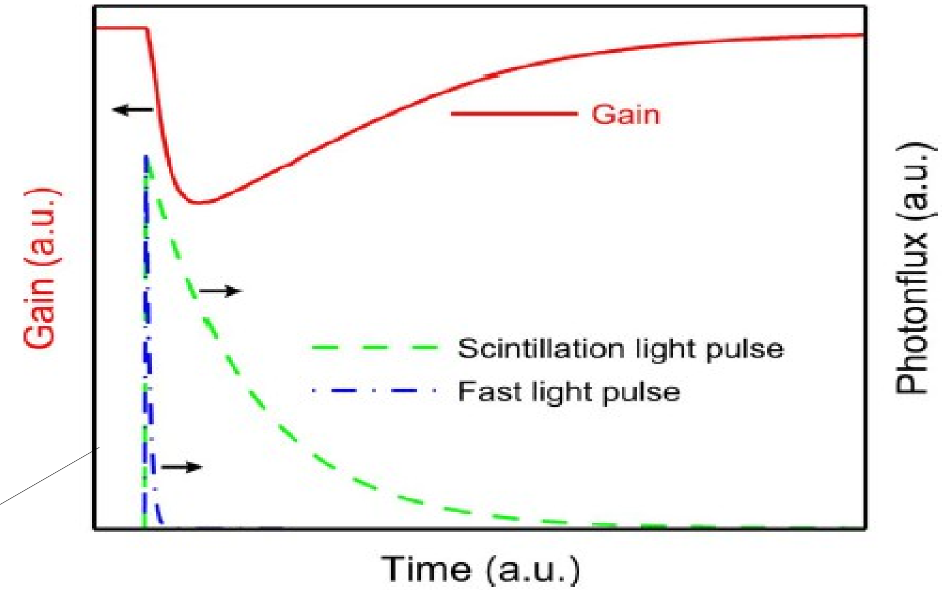

Main sources are:

- finite number of pixels
- finite recovery time w.r.t. pulse duration
- after-pulses, cross-talk
- drop of ΔV during the light pulse

due to relevant signal current on (large) series resistances (eg ballast)

T.van Dam IEEE TNS 57 (2010) 2254

Detailed model to estimate non-lin. corrections

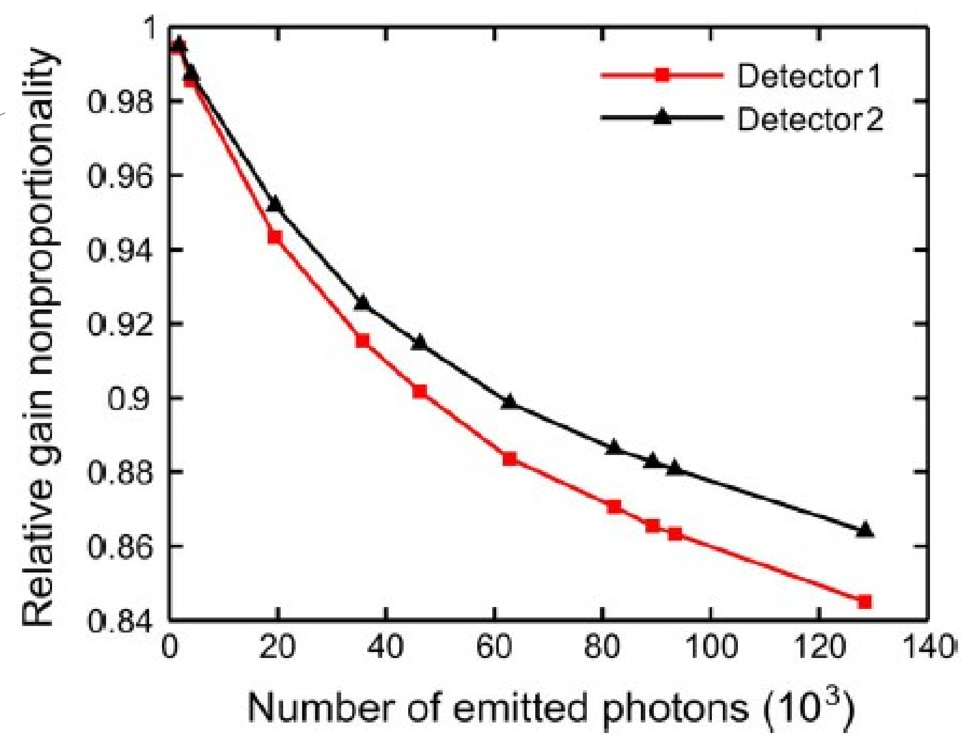

Finite number of cells is main contribution in case number of photons ~ O(number of cells) (dynamic range not adequate to application)

→ saturation $\quad n_{fired} = n_{all}\left(1 - e^{-\frac{n_{phot.} PDE}{n_{all}}}\right)$

→ loss of energy resolution

see Stoykov et al JINST 2 P06500 and Vinogradov et al IEEE NSS 2009 N28-3

Dynamic range and non-linearity

analog SiPM output =
sum of binary cell's output

• Due to **finite number of cells** → signal **saturation**

• Correction possible BUT
→ **degraded resolution**

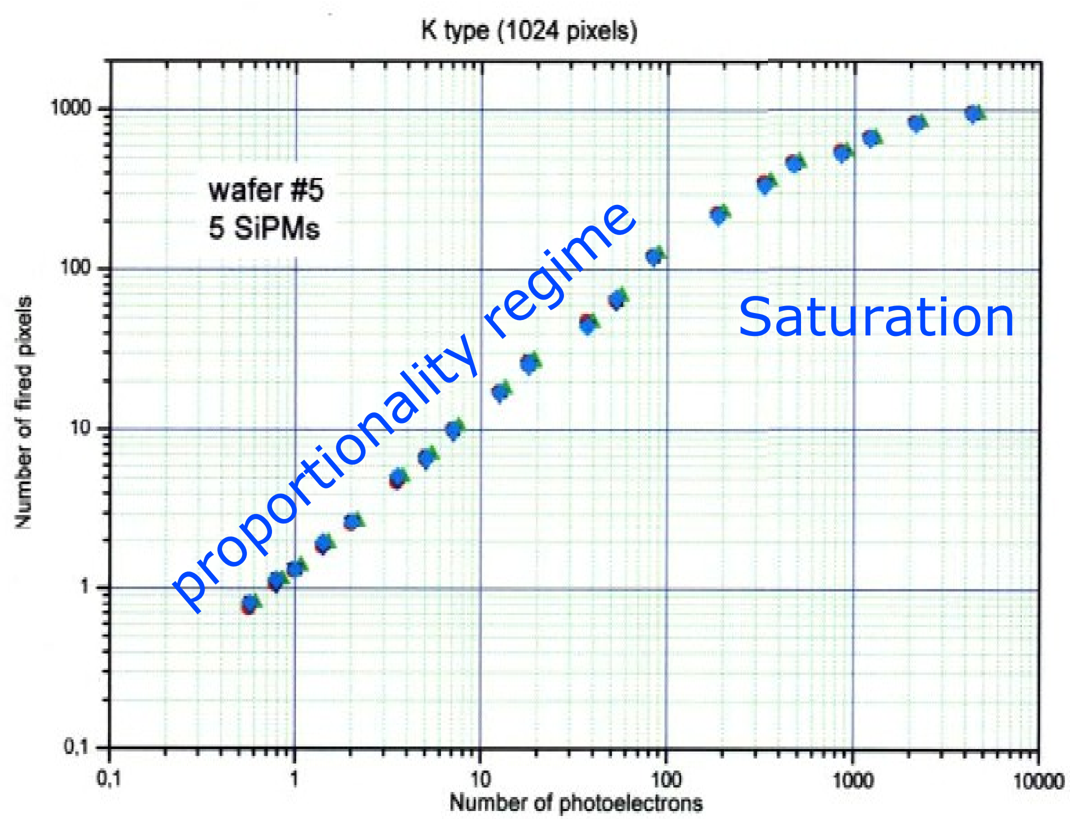

$$A \approx N_{firedcells} = N_{total} \cdot (1 - e^{-\frac{N_{photon} \cdot PDE}{N_{total}}})$$

eg: 20% deviation from linearity
if 50% of cells respond

Best working conditions: $N_{\text{photo-electrons}} < N_{\text{SiPM cells}}$

Additional complications:
1) need correction to $N_{\text{fired-cells}}$ due to cross-talk and after-pulse
2) effective dynamic range depends on recovery time and time scale of signal burst

Amplitude fluctuations

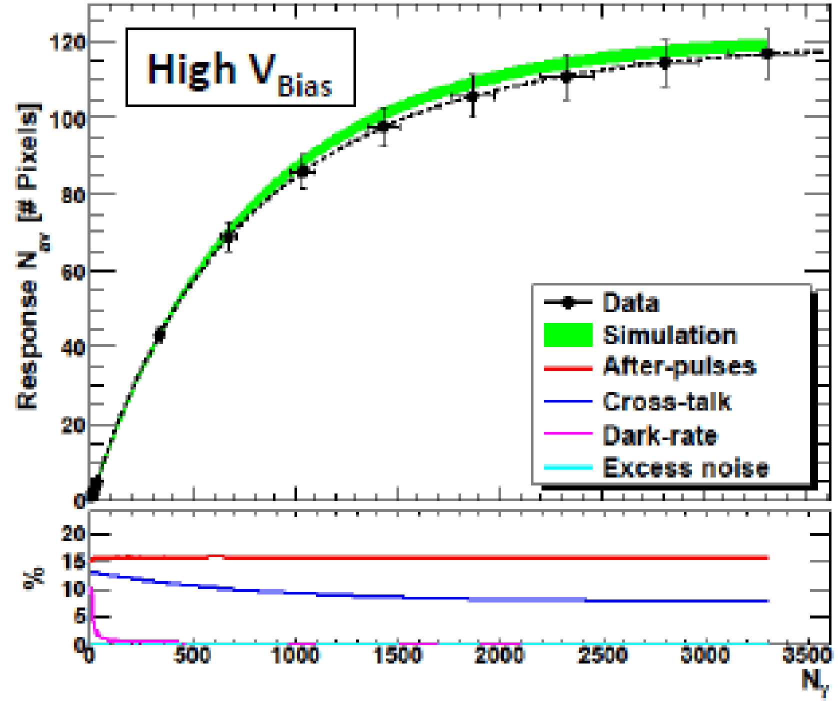

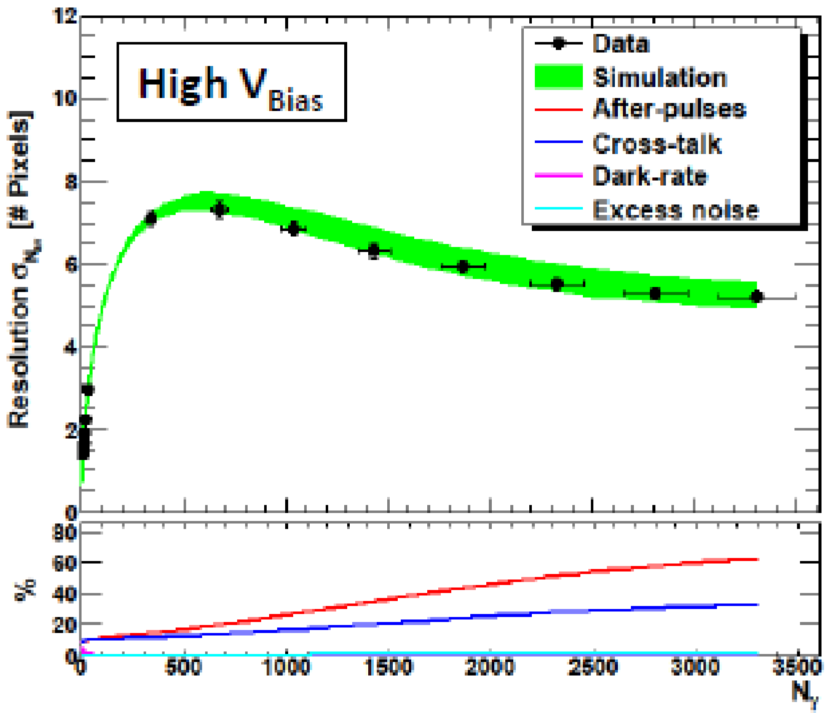

finite number of pixels: constraint
→ limit in resolving the number of photons

Eckert et al, Procs. of PhotoDet 2012

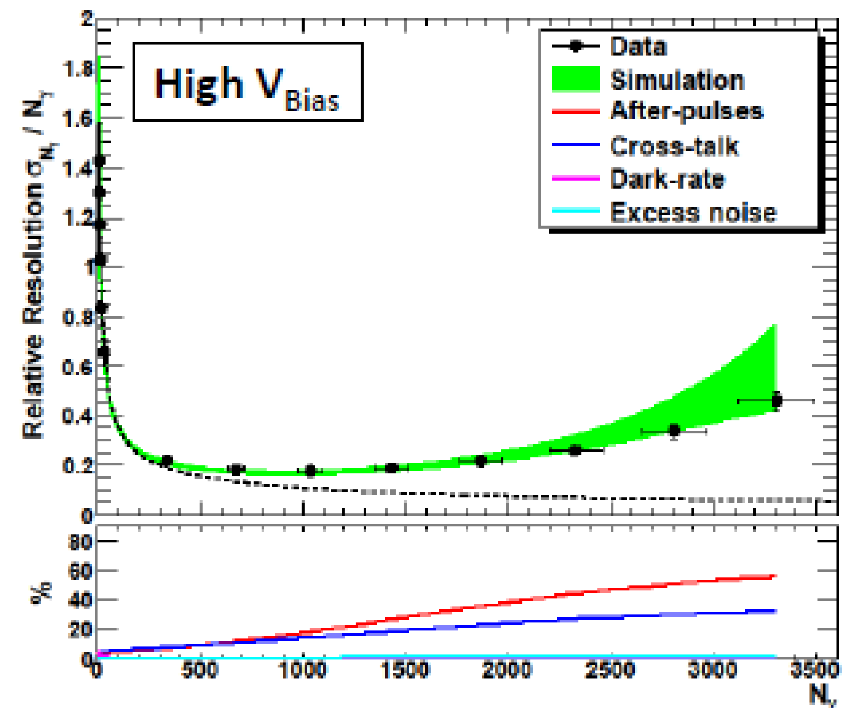

DR PDE, CT, AP

$$\frac{\Delta N_\gamma}{N_\gamma} \approx \frac{a}{N_\gamma} \oplus \frac{b}{\sqrt{N_\gamma}}$$

see also Musienko et al JINST 2 2007 P0600

Calibration caveat

S.Uozumi – PD07
Kobe - 27 June 2007

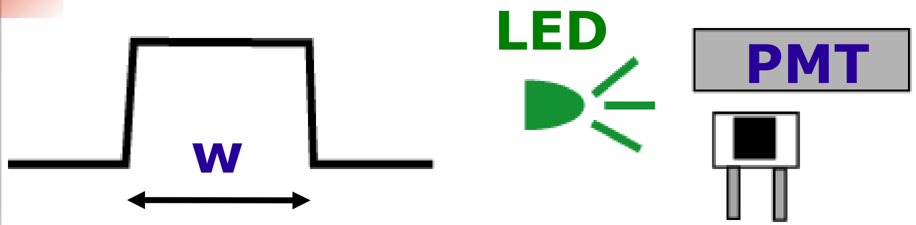

Response curves taken with various width of LED light pulses. (gate width = 100 ns)

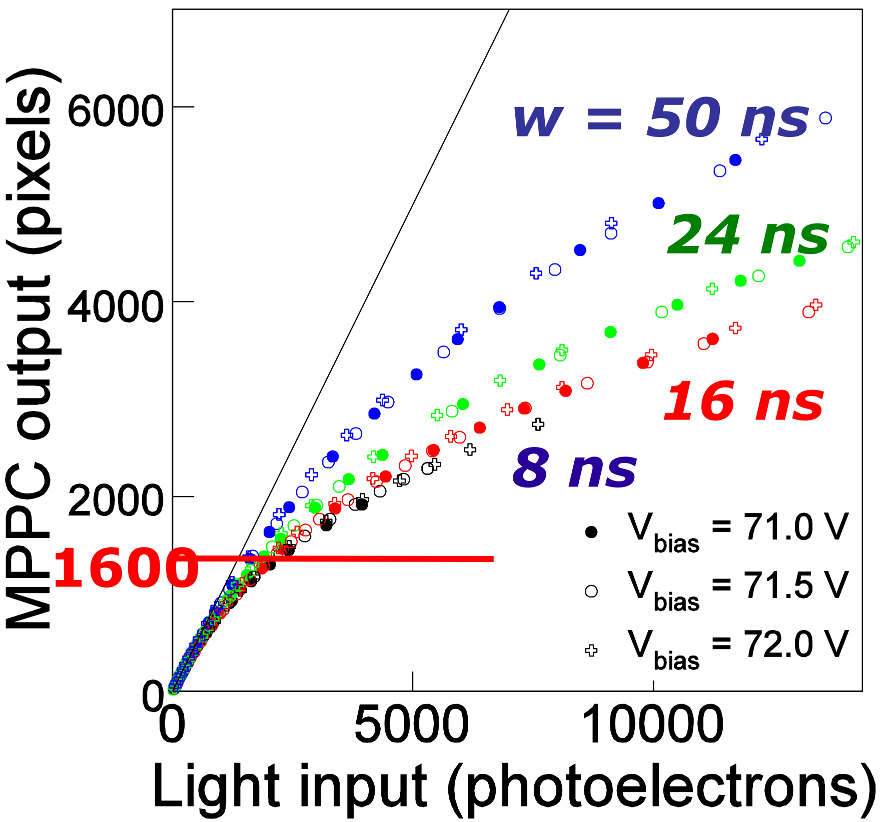

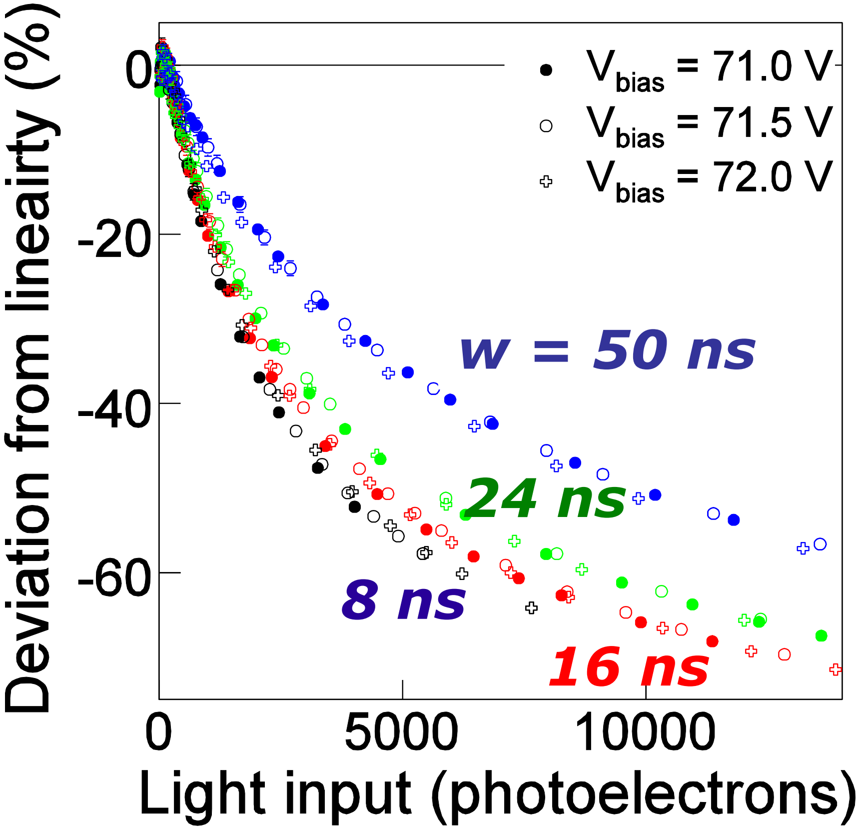

- Dynamic range is enhanced with longer light pulse
- Time structure of the light pulse gives large effects in non-linear region.
- No significant influence with changing bias voltage.
- Knowing time structure of scintillator/WLS light signal is crucial

High dynamic range new SiPMs

Latest MPPC tiny cell by Hamamatsu

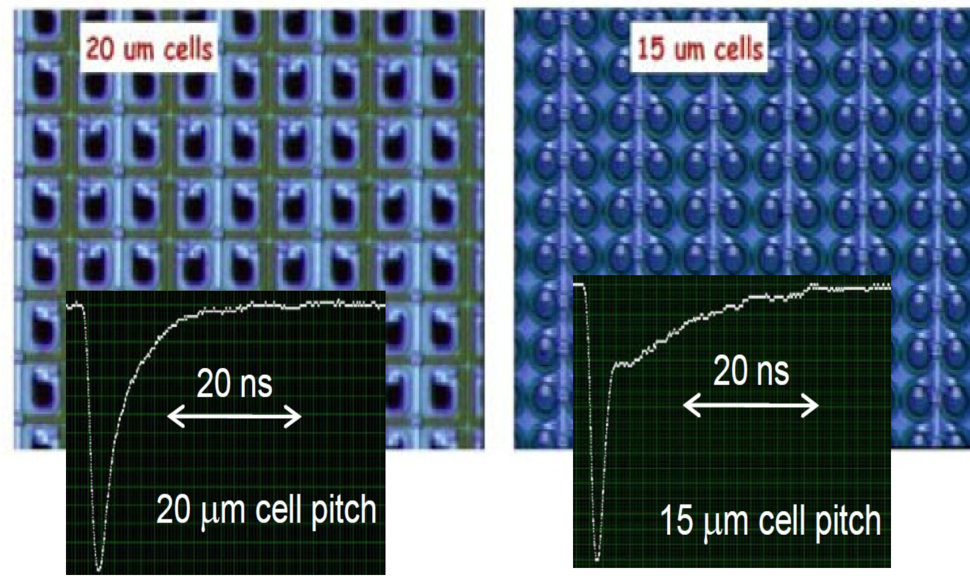

Different types available or in preparation:

- tiny cells (→ 15μm)
  → HPK, FBK-Advansid(*), NDL, MPI-LL

  (*) fill factor → 50% !!!

- micro cells (→ μm)
  → Zecotek, AmplititicationTechn.

SiPMs NDL (Bejiing)

Zhang et al NIM A621 (2010) 116
Han at NDIP 2011

- type: n-on-p, Bulk Rq
- high cell density (10000/mm²)
- fast recovery (5ns)
- low gain
- **better timing**

→ dynamic range

→ less after-pulsing
→ less cross-talk
→ radiation hardness

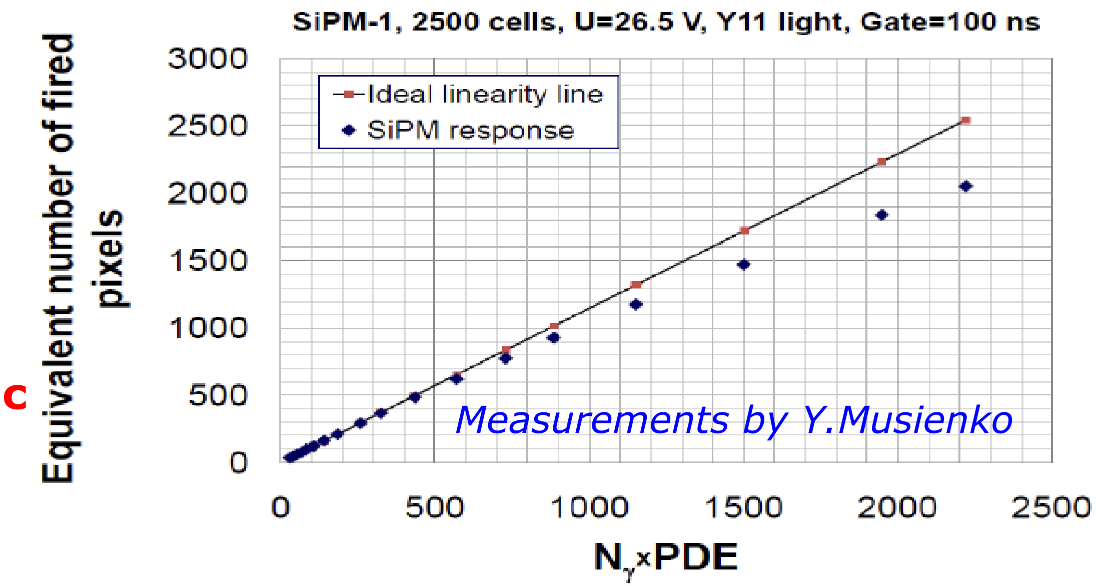

Noise sources:

Dark counts

After-pulsing

Cross-Talk

"optical"

pulses triggered by non-photo-generated carriers (thermal / tunneling generation in the bulk or in the surface depleted region around the junction)

carriers can be trapped during an avalanche and then released triggering another avalanche

photo-generation during the avalanche discharge. Some of the photons can be absorbed in the adjacent cell possibly triggering new discharges

Dark Count Rate

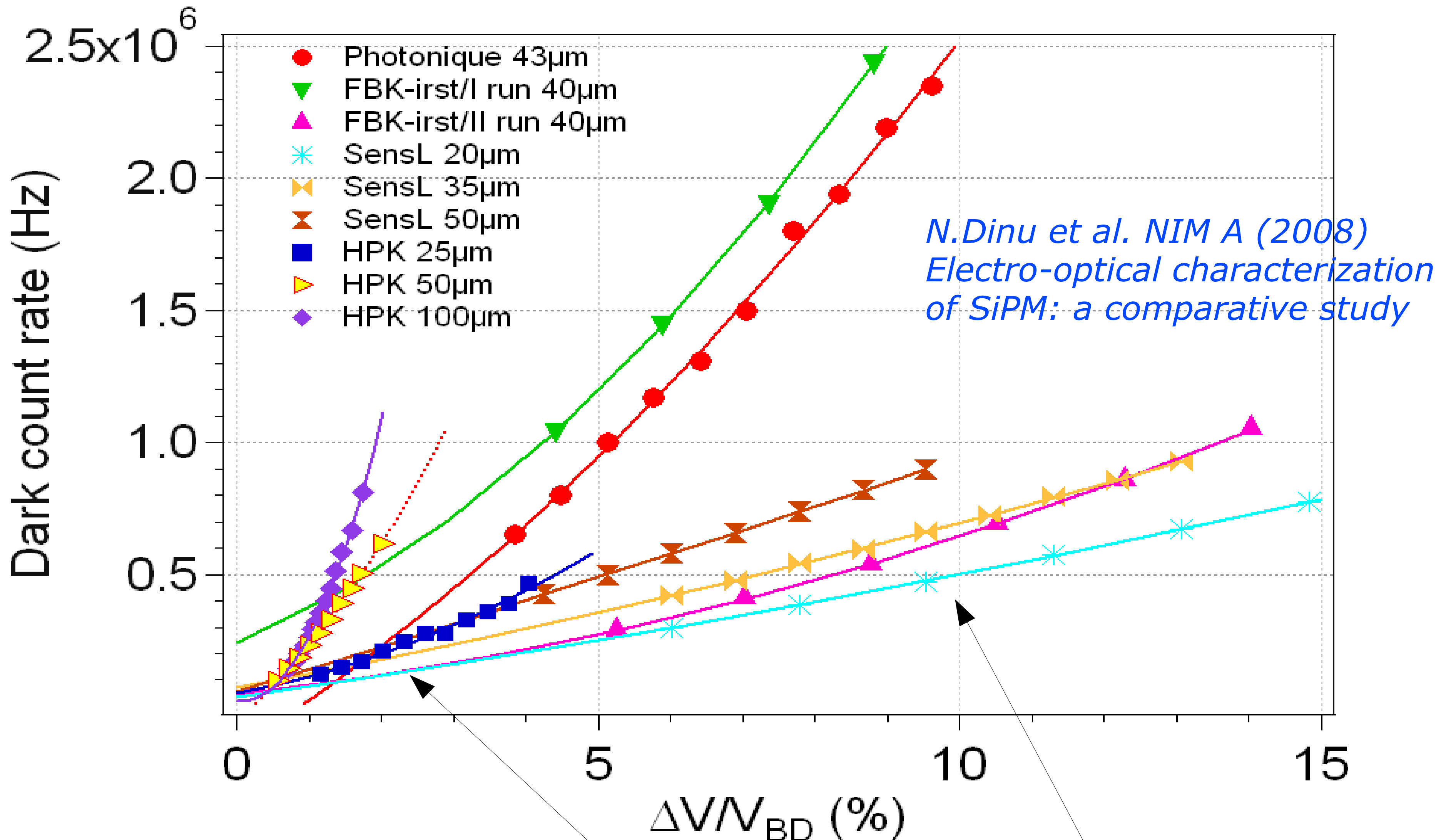

- DCR → linear dependence due to $P_{01} \propto \Delta V$ (→ same as PDE vs ΔV)
  → non-linear at high ΔV due to cross-talk and after-pulsing → $\propto \Delta V^2$
- DCR scales with active surface (not with volume: high field region dominating)

Dark Count Rate

- DCR → linear dependence due to $P_{01} \propto \Delta V$ (→ same as PDE vs ΔV)
  → non-linear at high ΔV due to cross-talk and after-pulsing → $\propto \Delta V^2$
- DCR scales with active surface (not with volume: high field region)

KETEK PM 3350 (p^+-on-n, shallow junction)
3x3mm² active area pixel size 50x50 μm²

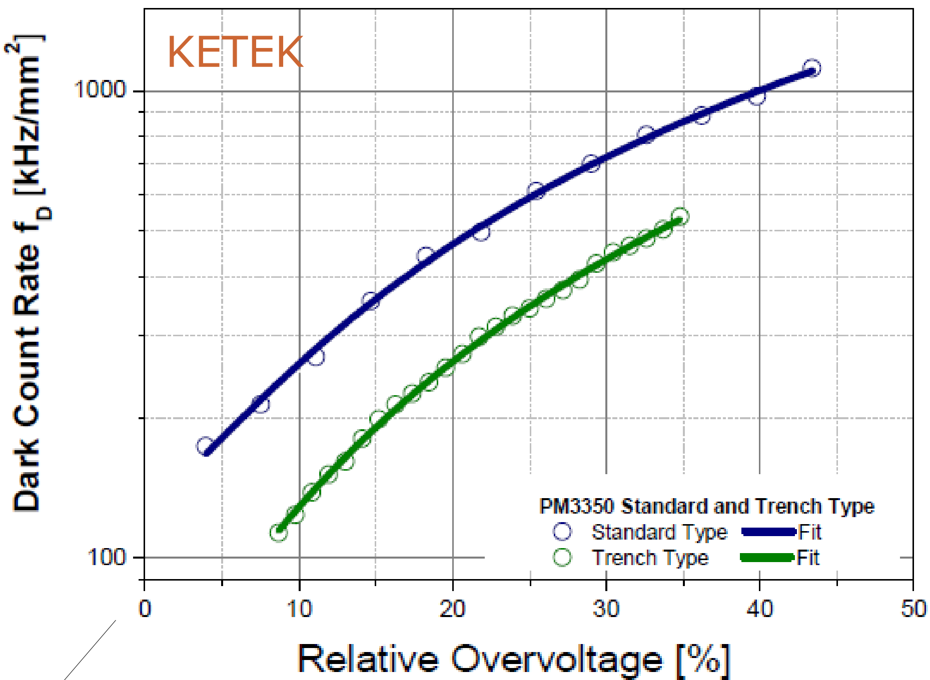

V_{bd} ~ 25V

F.Wiest – AIDA 2012 at DESY

Critical issues:
- quality of epitaxial layer
- gettering techniques
- Electric field engineering

Exelitas 1st generation SiPM 2011
(p^+-on-n) 1x1mm²

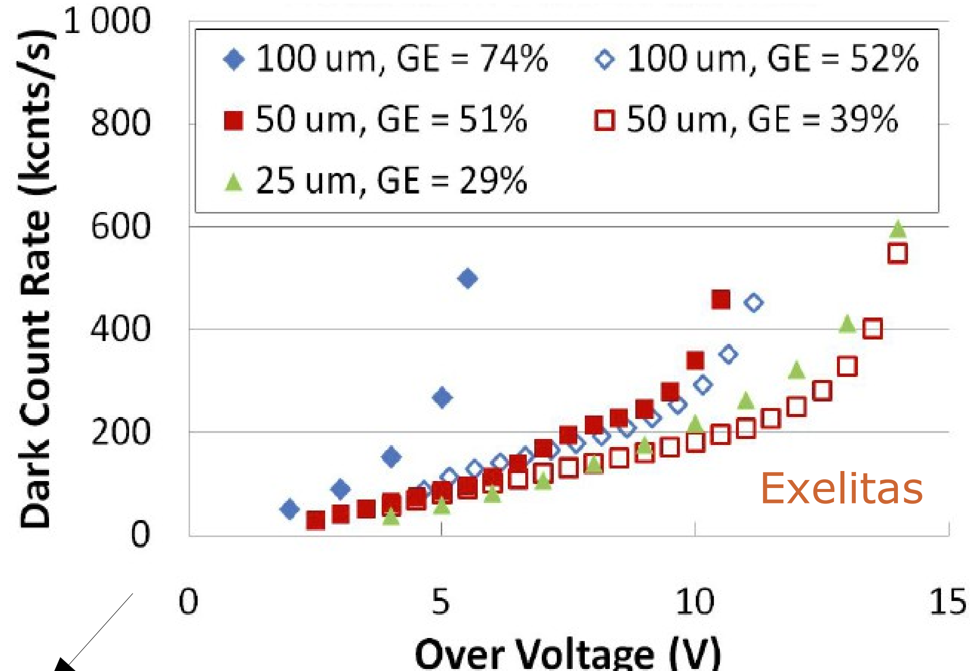

V_{bd} ~ 140V

P.Berard – NDIP 2011

Latest Hamamatsu devices reached ~80kHz/mm²

HPK claiming for additional improvements coming (*HPK at LIGHT 2011*)

Dark Count Rate

dSiPM

Control over individual SPADs enables detailed device characterization

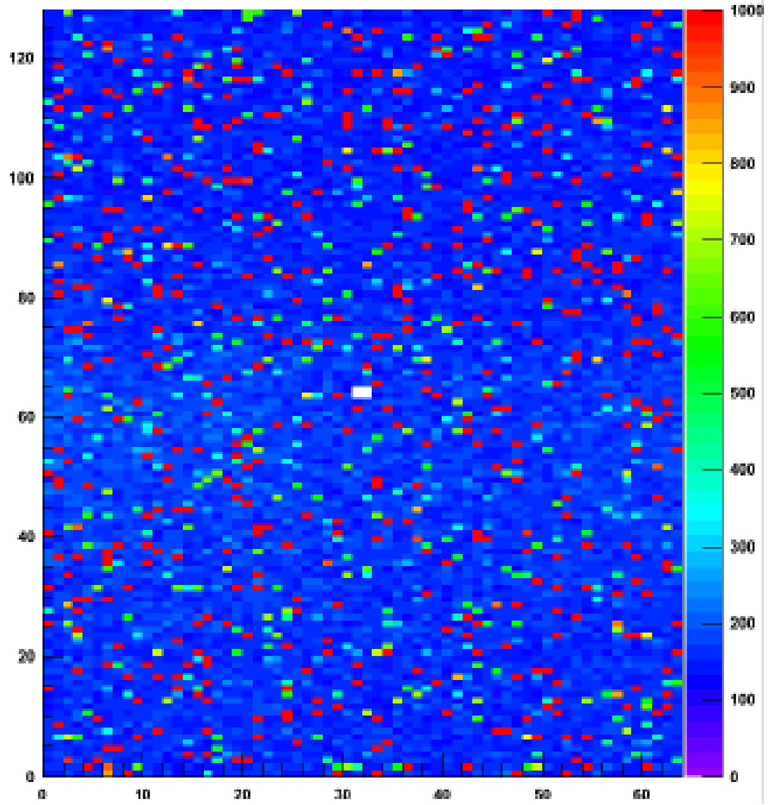

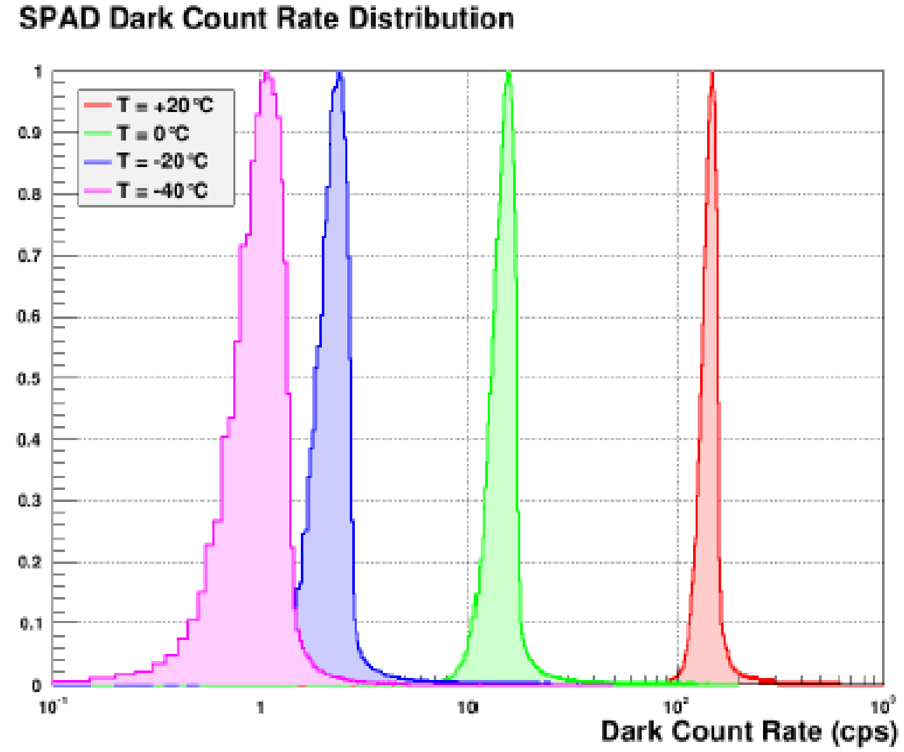

- Over 90% good diodes (dark count rate close to average)
- Typical dark count rate at 20°C and 3.3V excess voltage: ~150cps / diode
- Low dark counts (~1-2cps) per diode at -40°C

T.Frach at NDIP 2011

Dark current vs T sources of DCR

contribution to DCR from diffusion of minority carriers negligible below 350K

Noise mainly comes from the high E Field region (no whole depletion region)

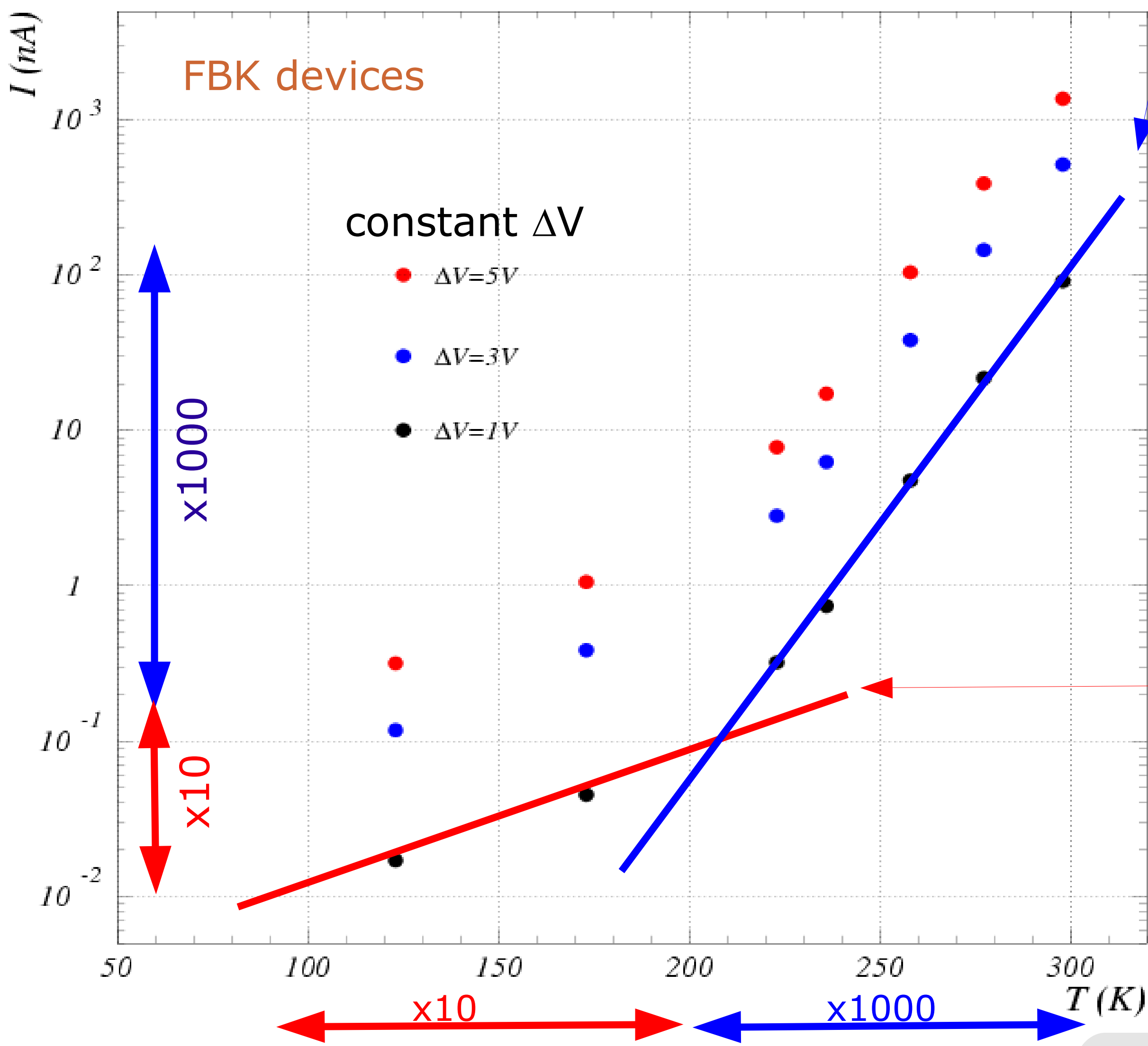

1) Generation/Recombination SRH noise (enhanced by trap assisted tunneling)

$$I_{reverse} \sim T^{1.5} \exp\frac{-E_{act}}{K_B T}$$

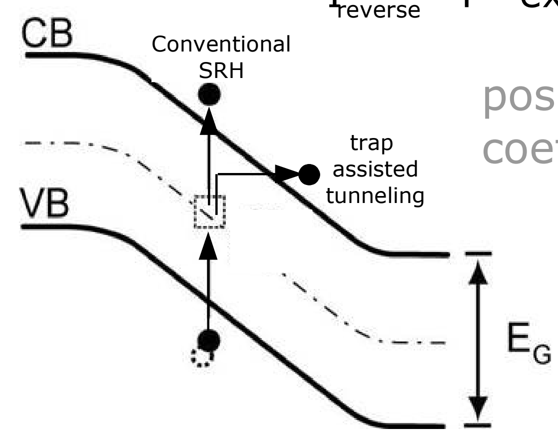

positive T coefficient

2) Band-to-band Tunneling noise (strong dependence on the Electric field profile)

negative T coefficient

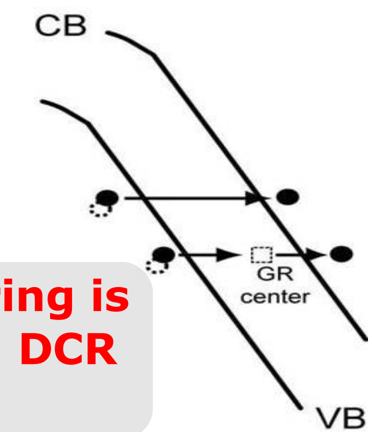

Tunneling noise dominating for T<200K (sharp high E field region → higher noise)

Efield engineering is crucial for min. DCR (esp. at low T)

Dark Count Rate vs T (constant ΔV)

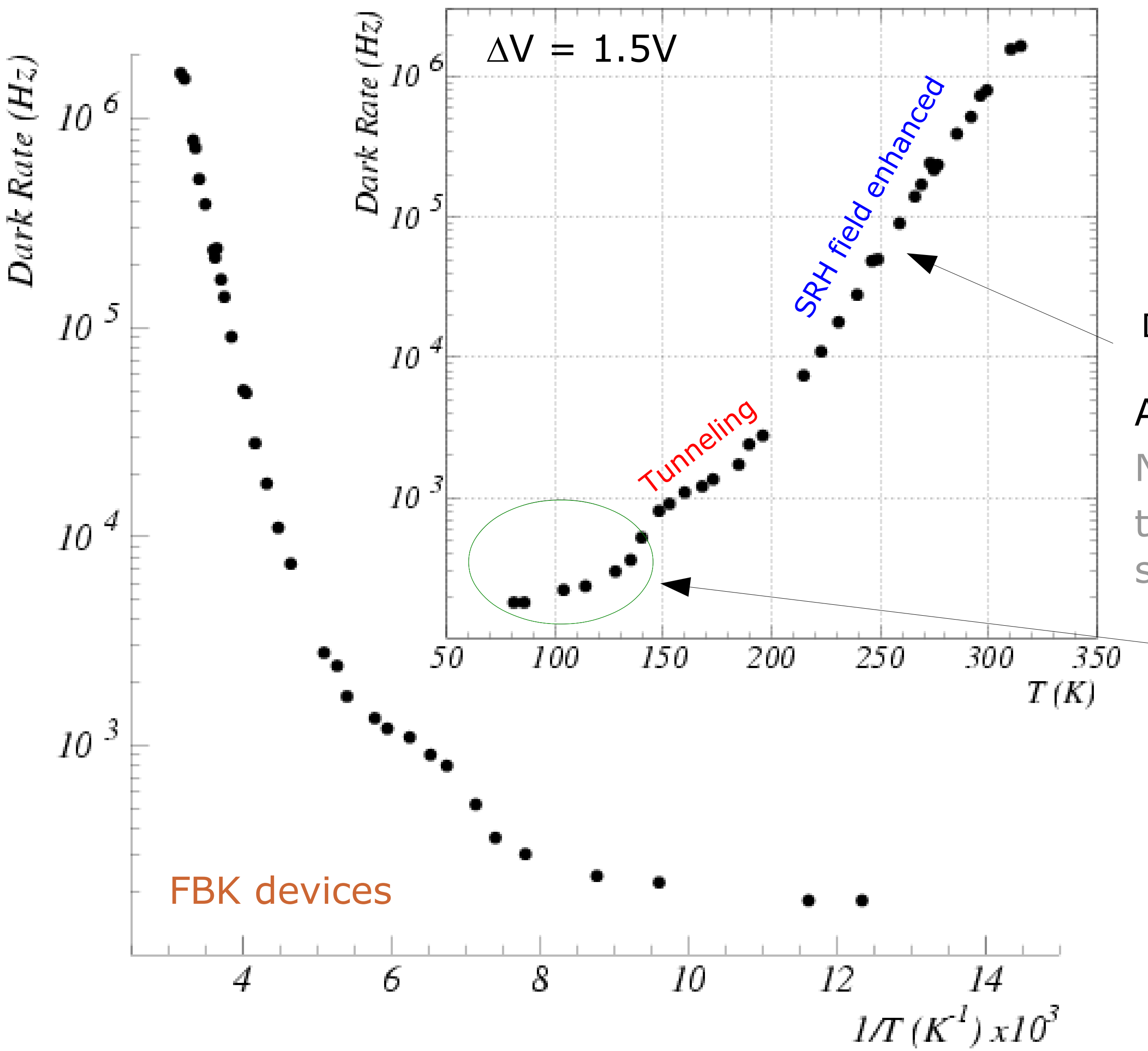

Measurement of **counting rate of ≥1p.e.** at fixed ΔV=1.5V (→ constant gain)

$$DCR \sim T^{1.5} \exp \frac{-E_{act}}{2K_B T}$$

Activation energy E_{act}~0.72eV

Note: E_{act} should be ~ E_g but tunneling makes effective gap smaller

Additional structure carriers freeze-out (?)

(carrier collection losses at very low T due to ionized impurities acting as shallow traps → drop in PDE)

G.C. et al NIM A628 (2011) 389

Dark Count Rate vs T

Hamamatsu
(100μm pixels)

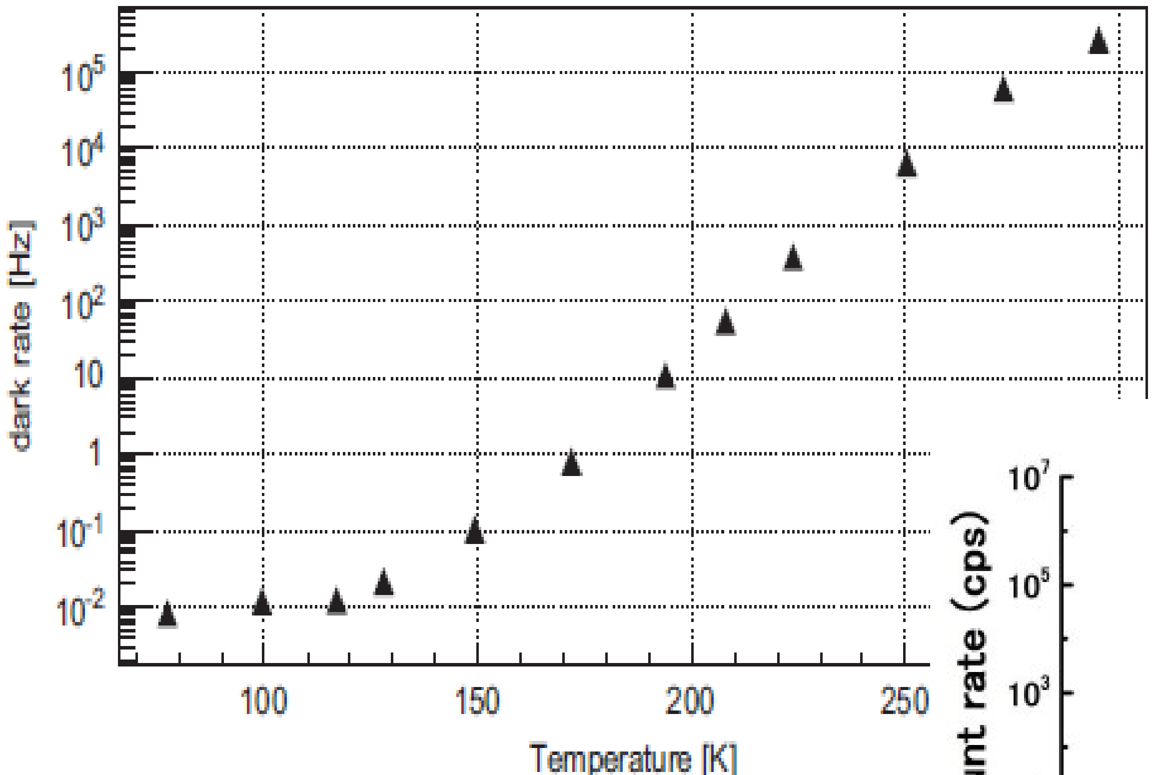

J.Csathy et al NIM A 654 (2011) 225

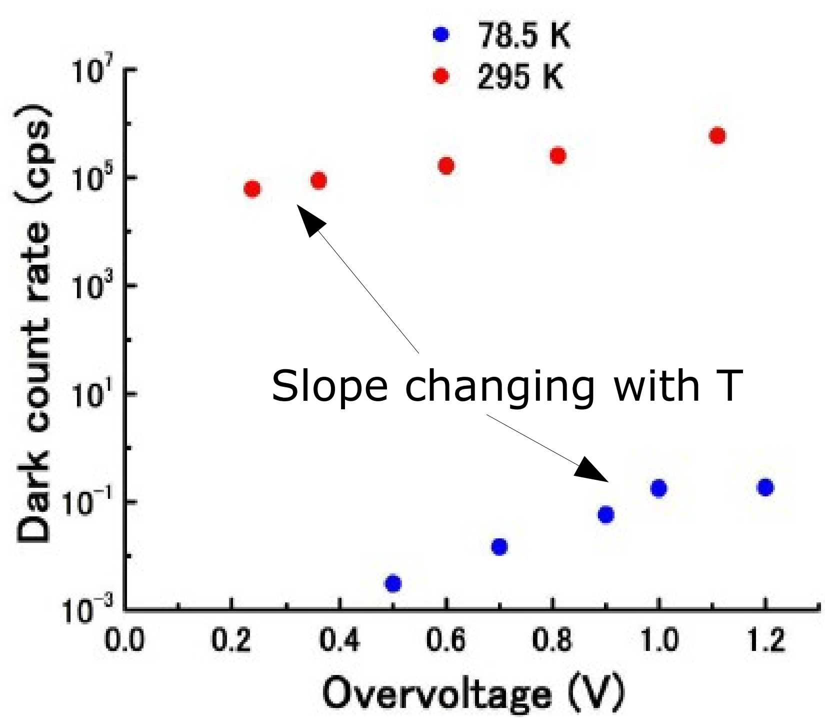

Slope changing with T

Comprehensive MPPC characterization at low T → *Akiba et al Optics Express 17 (2009) 16885*

After-Pulsing Carrier trapping and delayed release

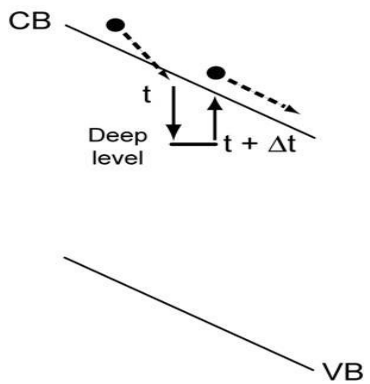

$$P_{afterpulsing}(t) = P_c \cdot \frac{\exp(-t/\tau)}{\tau} \cdot P_{01} \quad \propto \Delta V^2$$

~Few % level at 300K

avalanche triggering probability
$\propto \Delta V(t)$

τ : trap lifetime
depends on trap level position

quadratic dependence on ΔV

P_c : trap capture probability
$\propto$ carrier flux (current) during avalanche $\propto \Delta V$
$\propto$ N traps

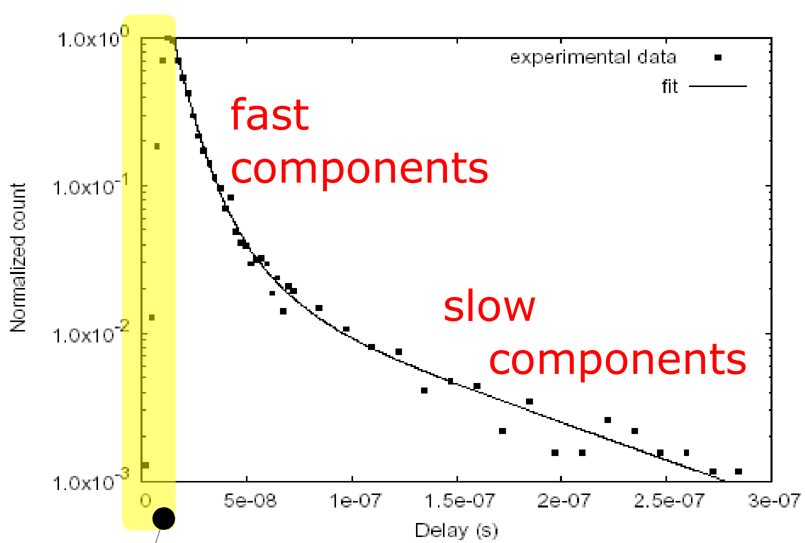

Fig. 10. Spectrum of the delay time from the primary pulse to the after-pulse.

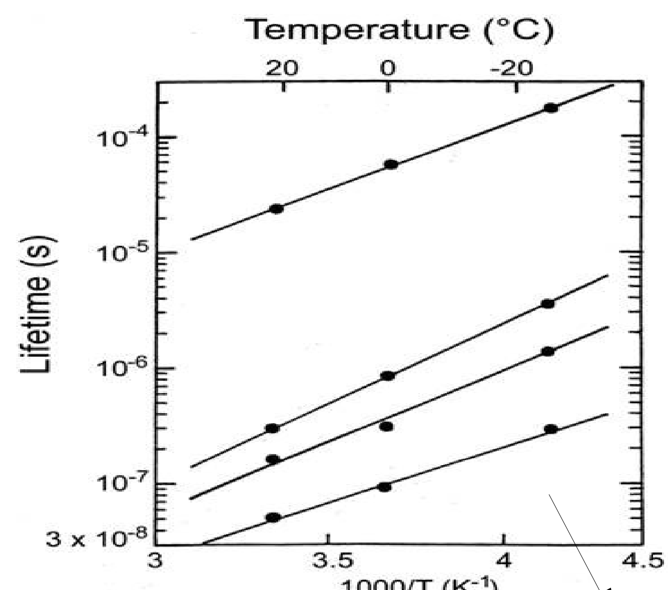

S.Cova, A.Lacaita, G.Ripamonti, IEEE EDL (1991)

not trivial dependence on T

Only partially sensitive to after-pulsing during recovery
ie recovery hides After-pulses (does not cancel them)

After-Pulses vs T (constant ΔV)

Measurement by waveform analysis:
- trigger on single carrier pulses (with no preceding pulses within $\Delta t=5\mu s$), **count subsequent pulses** within $\Delta t=5\mu s$ (find the after-pulsing rate r_{AP})
- **Subtract dark count** contribution
- extract **after-pulsing probability P_{AP}**

corrected for after-pulsing cascade

$$P_{AP}=\frac{r_{AP}}{1+r_{AP}}$$

ΔV = 1.5V

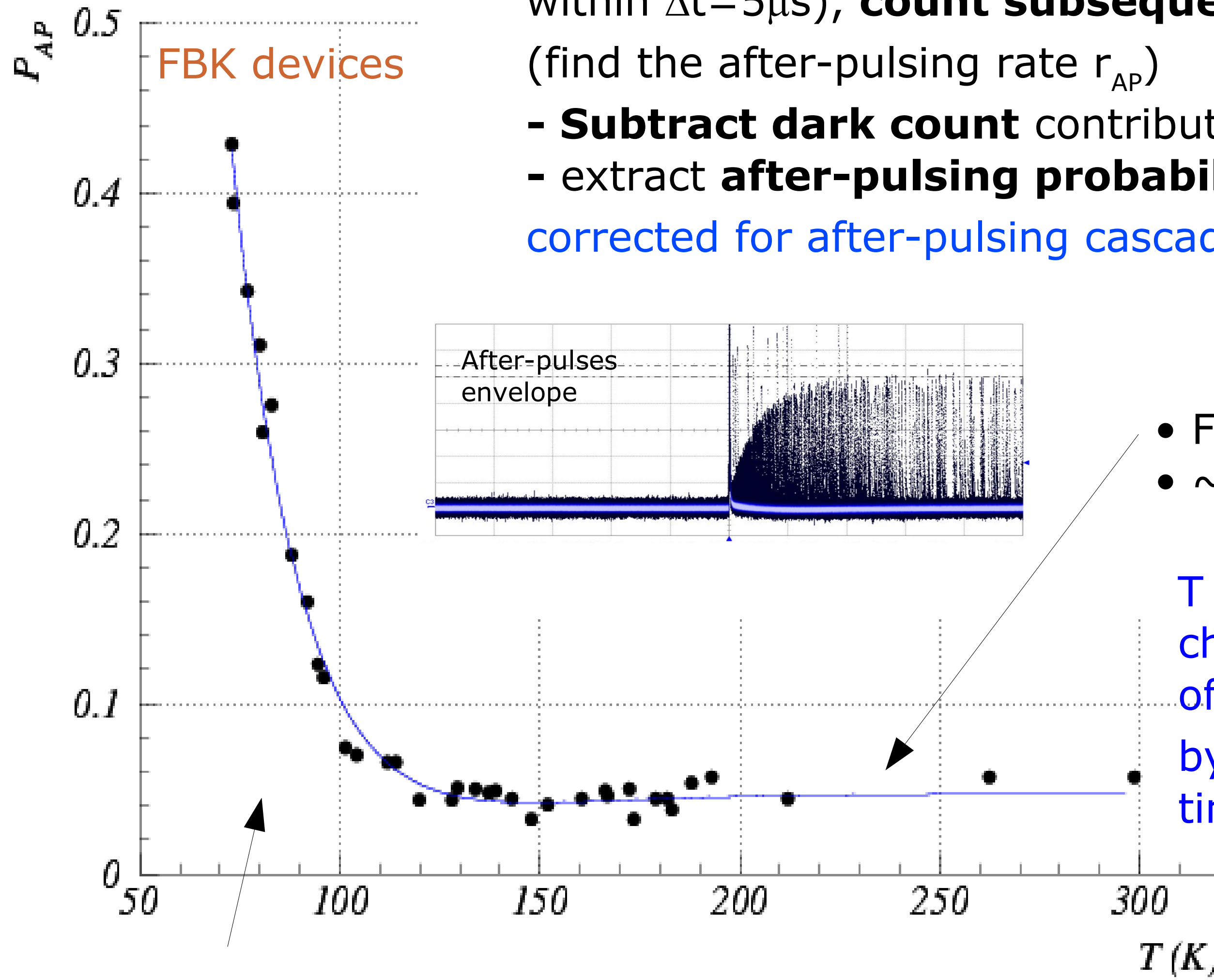

- Few % at room T
- ~constant down to ~120K

T decreasing: increase of characteristic time constants of traps (τ_{traps}) compensated by increasing cell recovery time (R_q)

- several % below 100K

T<100K: additional trapping centers activated possibly (?) related to onset of carriers freeze-out

→ Analysis of life-time evolution vs T of the various traps (at least 3 types at T_{room})

G.C. et al NIM A628 (2011) 389

Optical cross-talk

Avalanche luminescence (NIR)

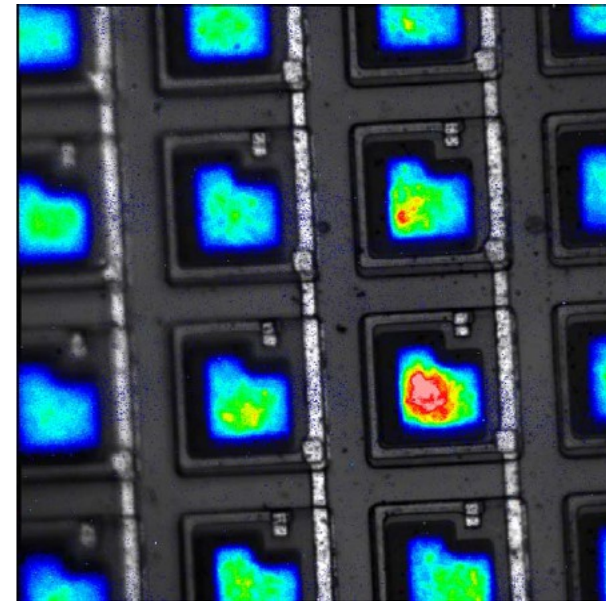

N.Otte, SNIC 2006

Carriers' luminescence (spontaneous direct relaxation in the conduction band) during the avalanche: probability 3.10^{-5} per carrier to emit photons with E> 1.14 eV

A.Lacaita et al. IEEE TED (1993)

Photons can induce avalanches in neighboring cells. Depends on distance between high-field regions

ΔV^2 dependence on over-voltage:

- carrier flux (current) during avalanche $\propto \Delta V$
- gain $\propto \Delta V$

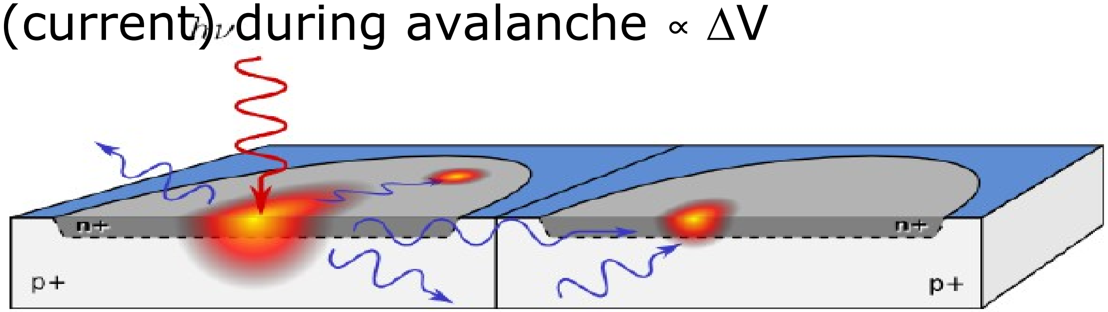

Counteract:

- optical isolation between cells by trenches filled with opaque material
- low over-voltage operation helps

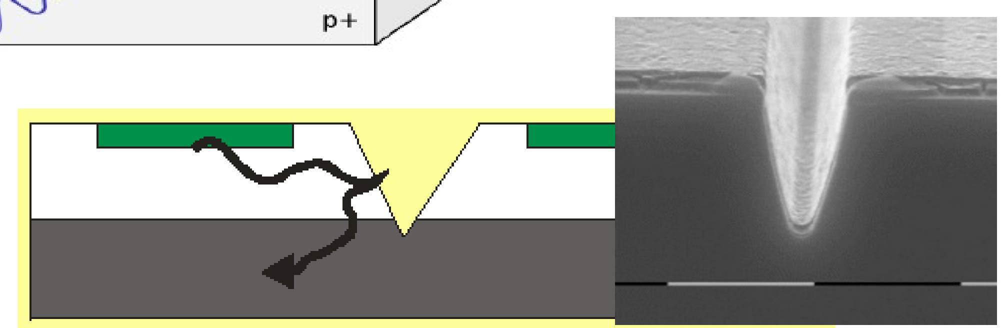

It can be reduced to a level below % in a wide ΔV range

Optical cross-talk:reflections from the bottom

Measured Emission spectrum

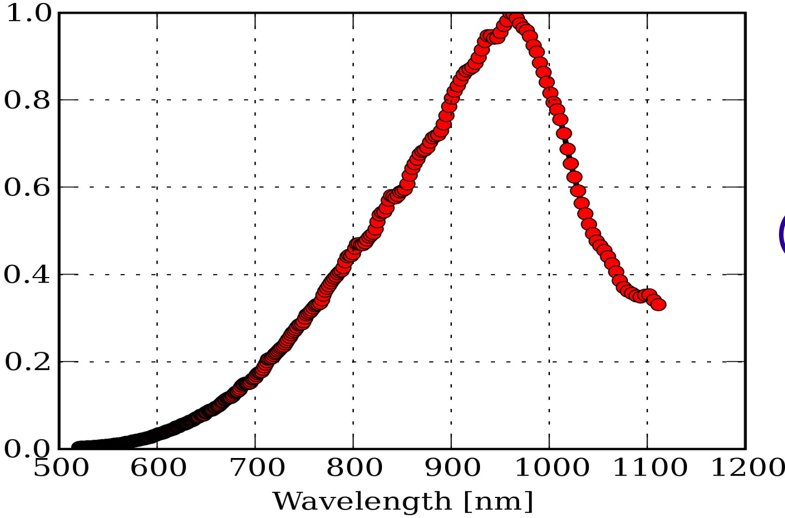

⊗

PDE

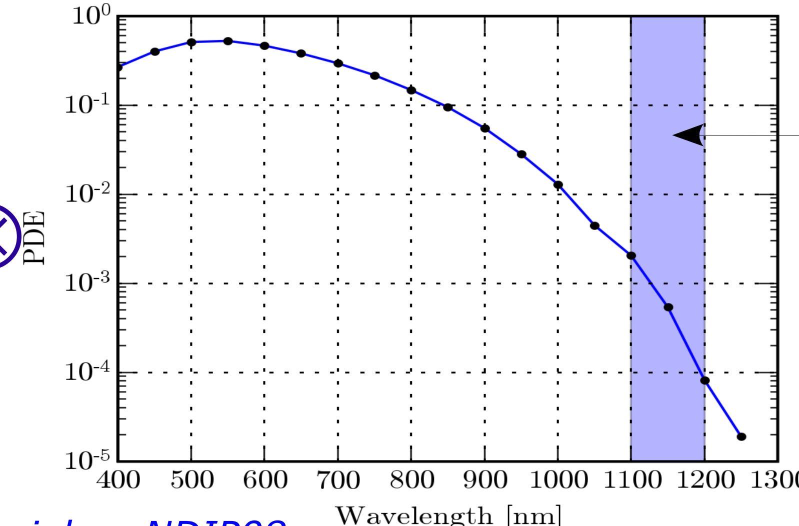

(1) Cross-talk due to narrow λ range (<100nm)

A.Ingargiola – NDIP08
Rech et al Proc. of SPIE Vol. 6771 677111-1

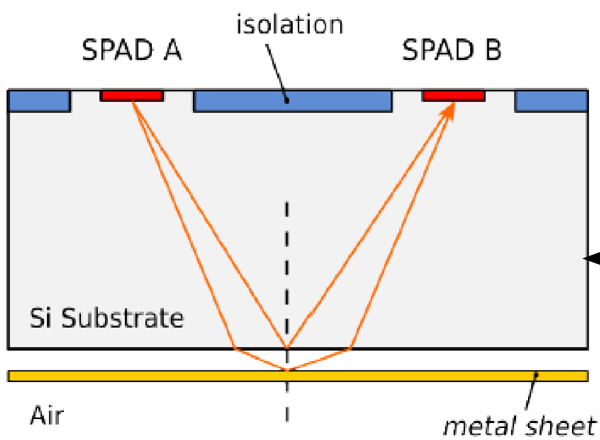

(2) Main component due to total reflection internal from the bottom (substrate)

(3) Isolation implants are sufficient to stop direct component

Silicon absorption coefficients:

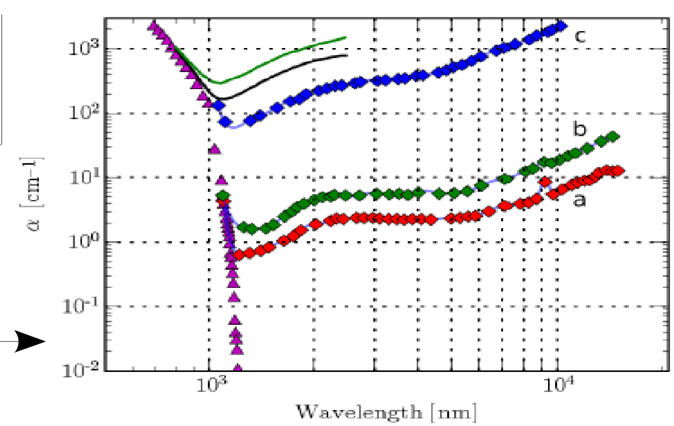

→ Crosstalk can't be eliminated simply by means of trenches
→ Main contribution to crosstalk comes from bottom reflections (using trenches)

Reflections and "external" cross-talk

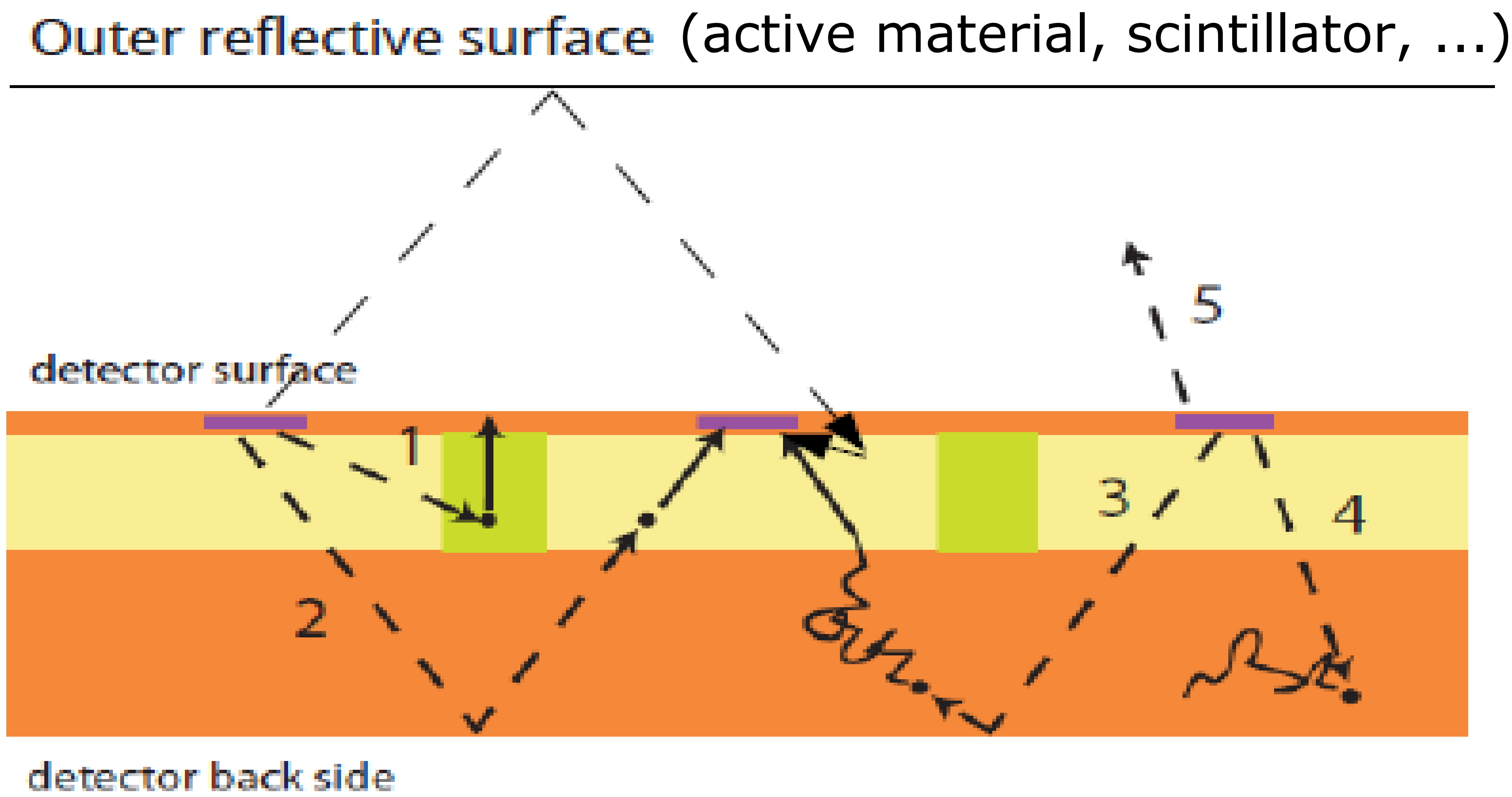

Additional components:

- reflections of avalanche photons on external surfaces
- delayed avalanches (see also F.Retiere Procs. of PhotoDet 2012)

Questions: - how to measure SiPM noise ?
- how to disentagle its components ?

How to measure SiPM noise components

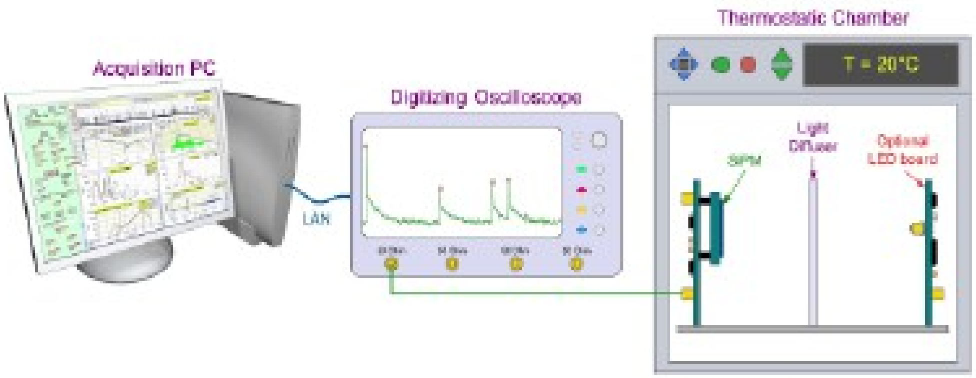

We acquire ms-long waveforms

Signal filtered to reduce pulse length

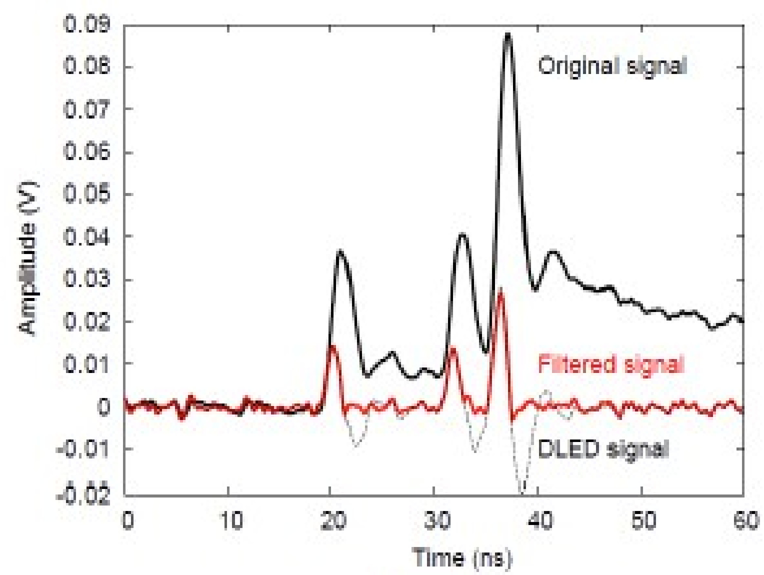

→ time delay array
→ amplitude array

How to measure SiPM noise components

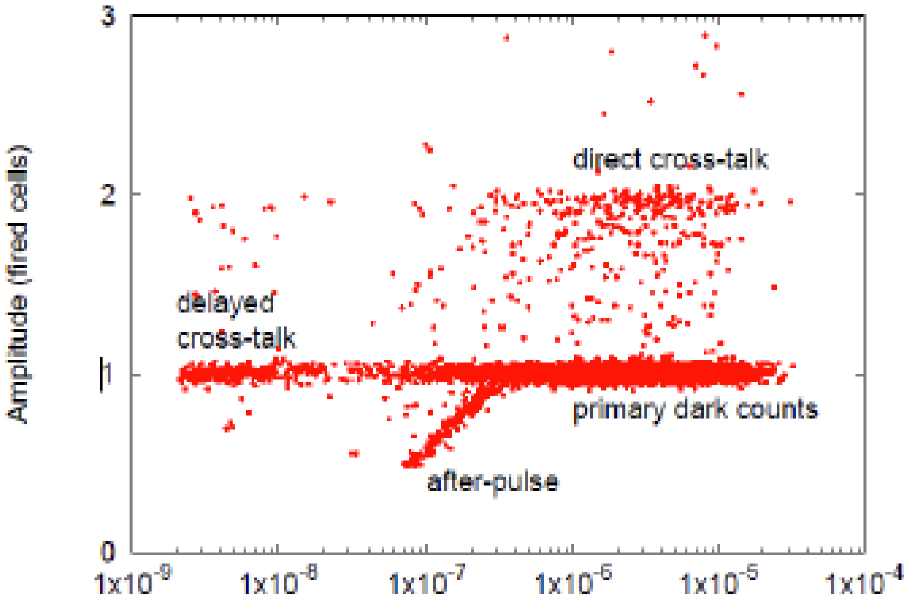

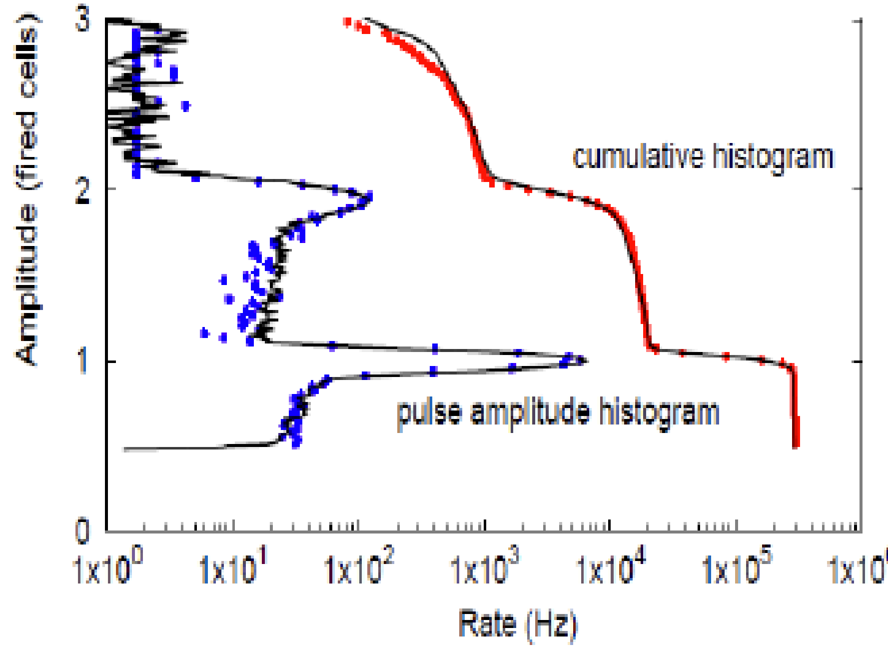

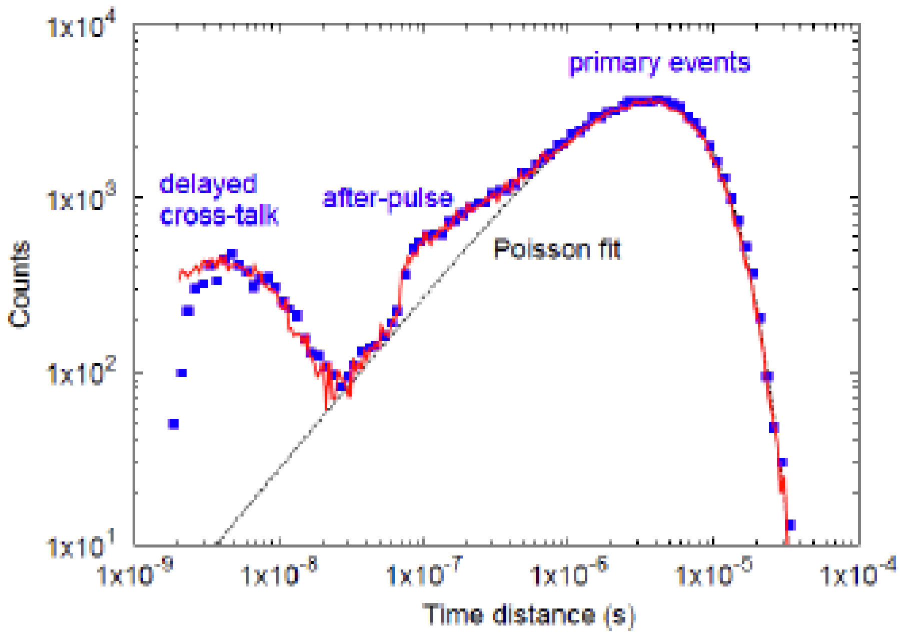

→ primary dark rate (DCR)
→ direct cross-talk
→ delayed correlated components

Photo-Detection Efficiency - PDE

$PDE = QE \cdot P_{01} \cdot FF$

QE: carrier Photo-generation

probability for a photon to generate a carrier that reaches the high field region

→ λ and T dependent

→ ΔV independent if full depletion at V_{bd}

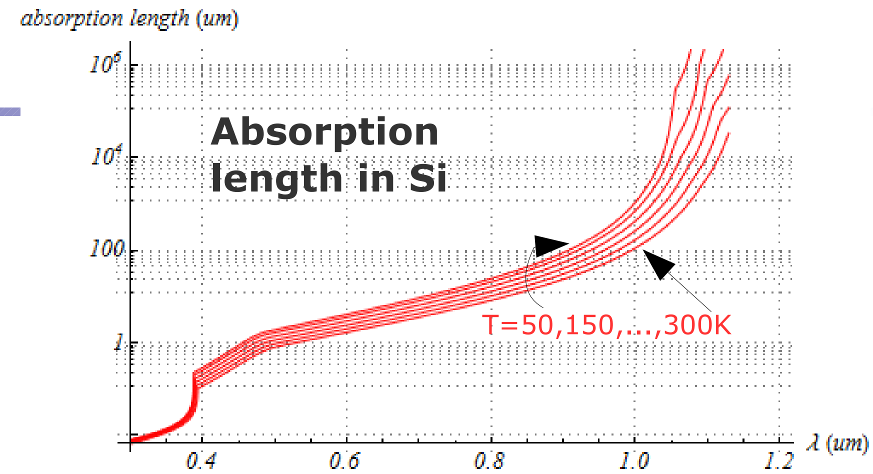

P_{01} : avalanche triggering probability

probability for a carrier traversing the high-field to generate the avalanche

→ λ, T and ΔV dependent

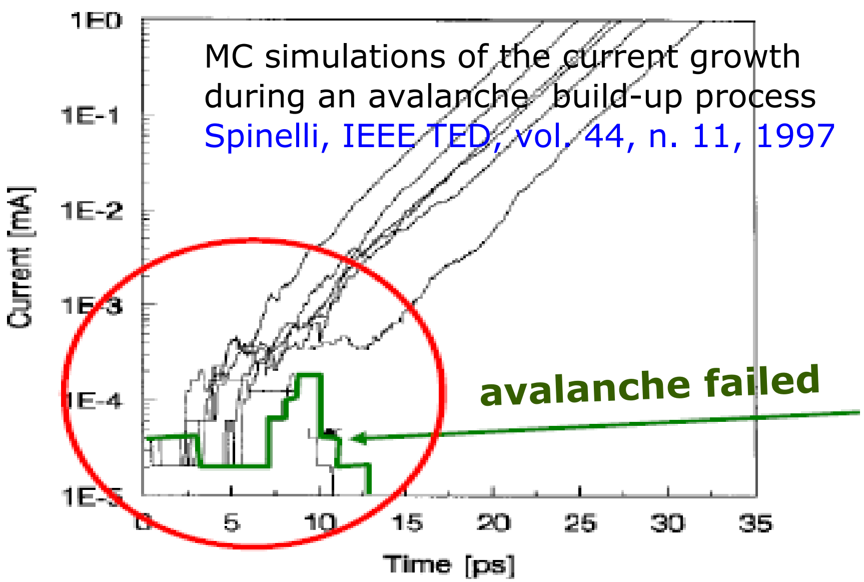

FF: geometrical Fill Factor

fraction of dead area due to structures between the cells, eg. guard rings, trenches

→ moderate ΔV dependence (cell edges)

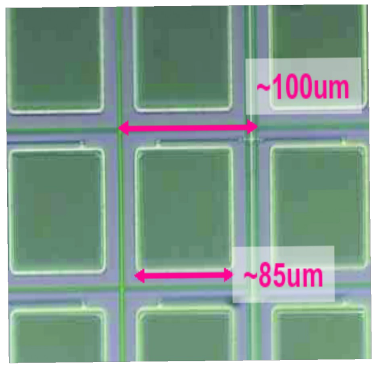

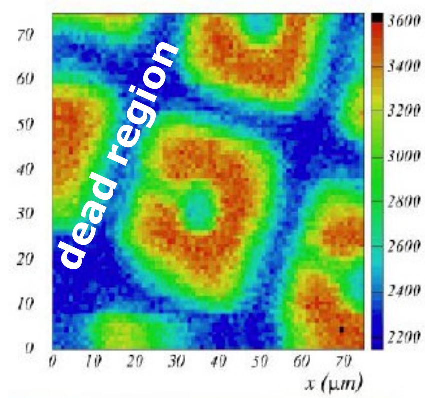

QE factors

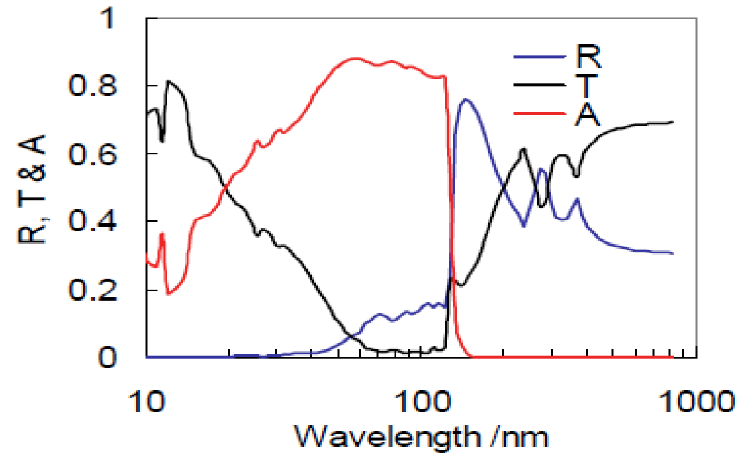

R,T,A coeff. in SiO_2 (example: 30nm SiO_2 on Si layer)

optical T,A,R of the entrance window (SiO_2 /Si_3N_4 dielectric on top of Si)

→ angular and polarization dependence

carrier recombination loss: collection efficiency (CE) front, depl. region, back

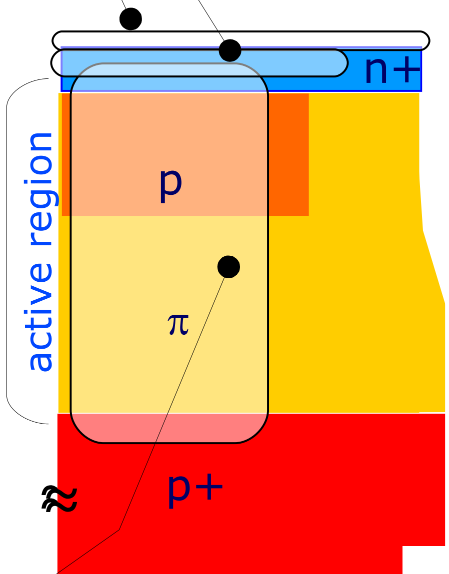

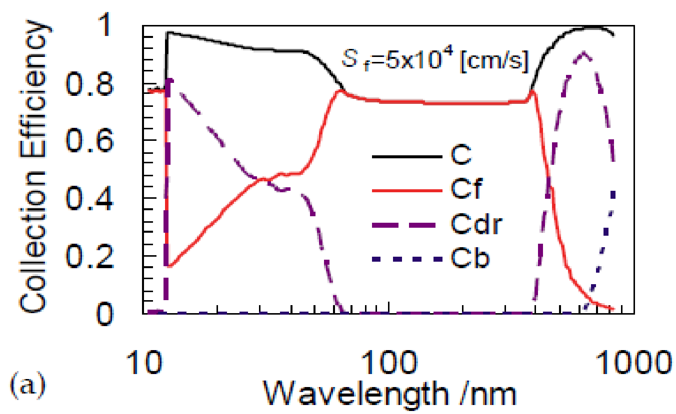

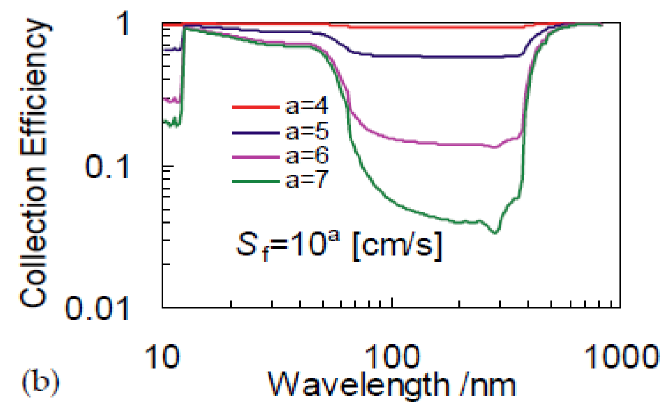

→ front region critical for 60nm < λ < 400nm

→ CE depends on surface recombination velocity S_f

→ freeze-out at low T

internal quantum efficiency: prob. to photo-generate an e-h pair ~ E_{photon} (above threshold)

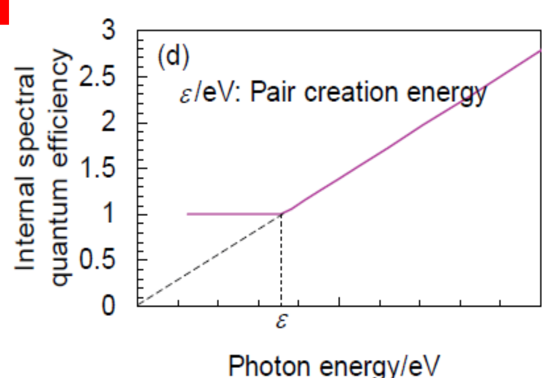

Commercial devices PDE → 0 in VUV due to:

1) protection coating (epoxy resin/silicon rubber)
2) reflectivity of Oxide/Nitride layers
3) insensitive top layer (p+ layer with E_{field} ~0)
4) high reflectivity for VUV on Si surface
5) absorption length in Si VUV photon: a few nm
6) superficial recombination

QE → PDE dependence on wavelength λ

FBK single diode (2006) photo-voltaic regime (V_{bias} ~ 0 V)

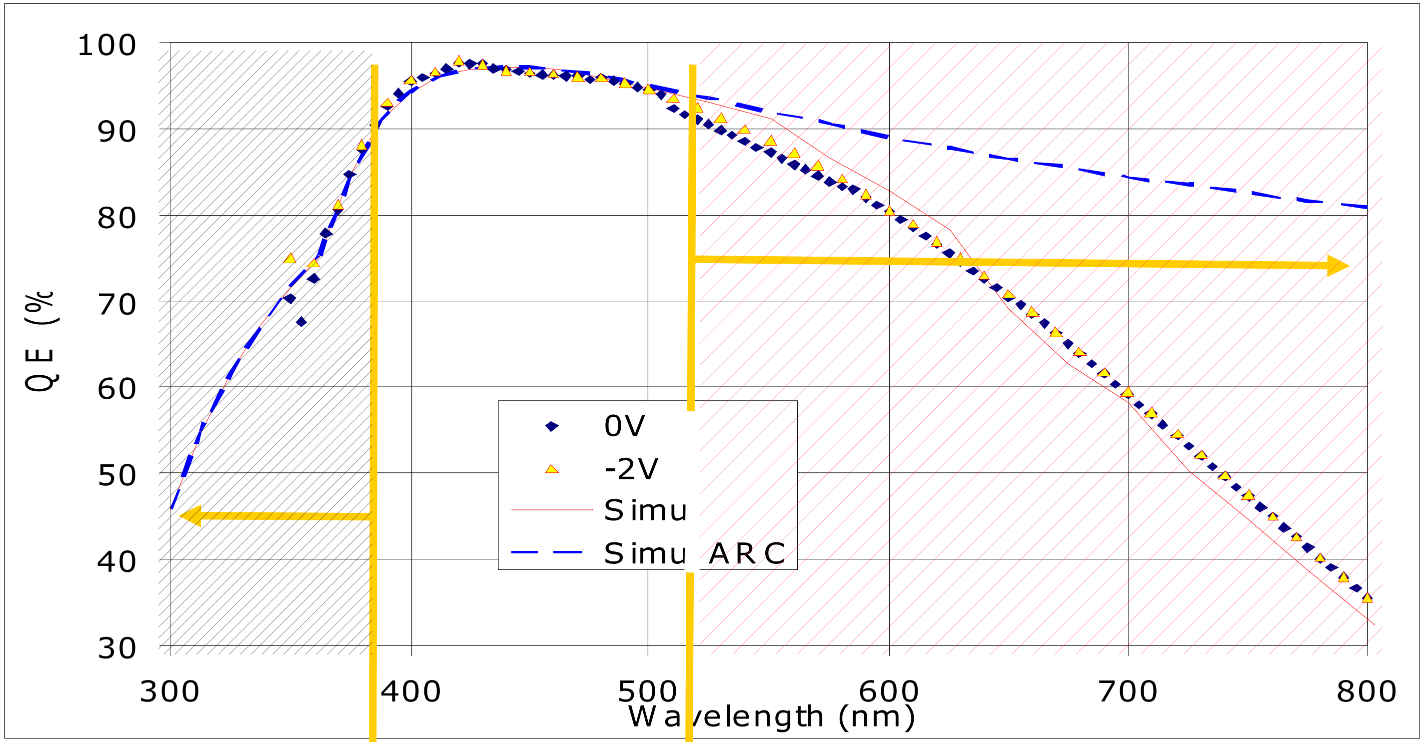

limited by ARC Transmittance & Superficial Recombination

limited by the small π layer thickness

Most critical issue for **Deep UV SiPM**
note: reduced superficial recombination in n-on-p wrt p-on-n

Trigger prob. P_{01} → PDE depends on λ and ΔV

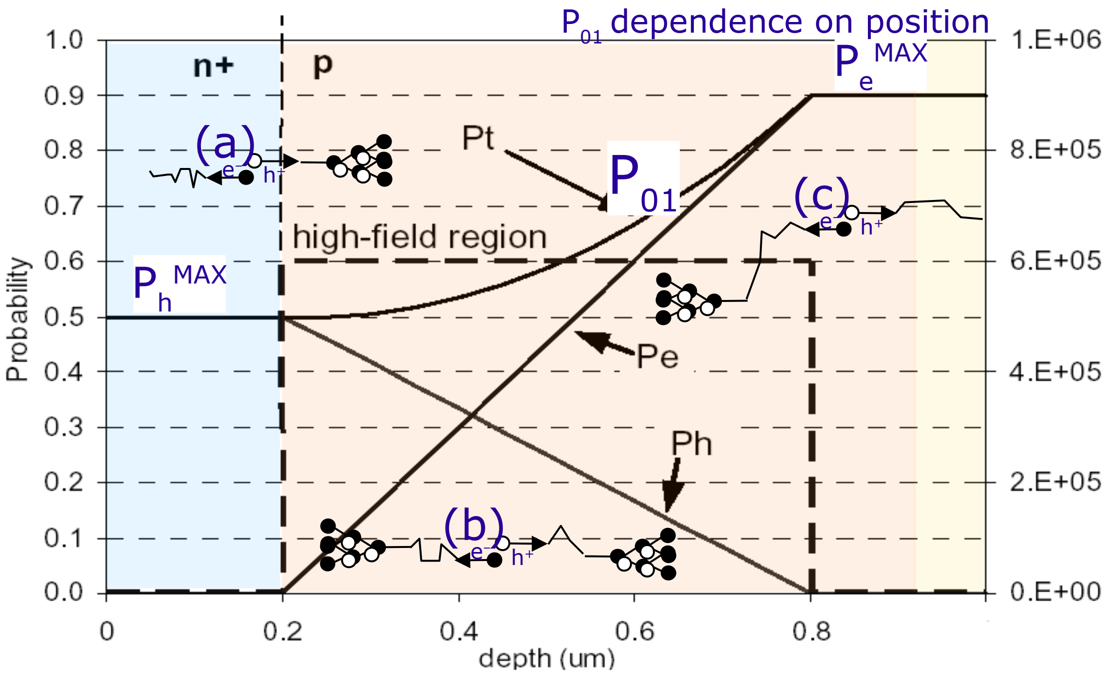

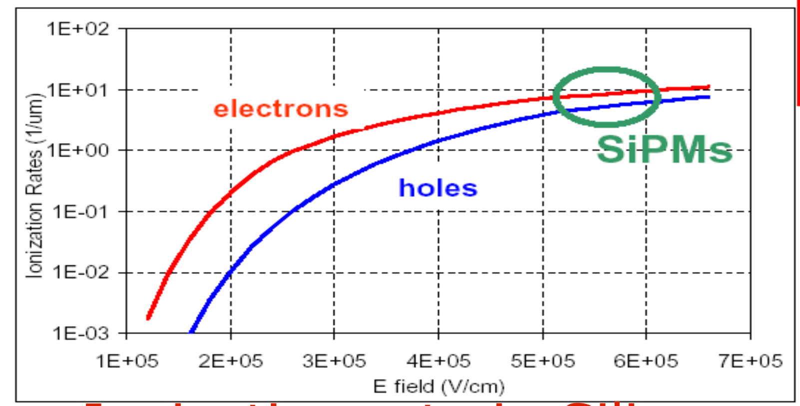

Ionization rate in Silicon

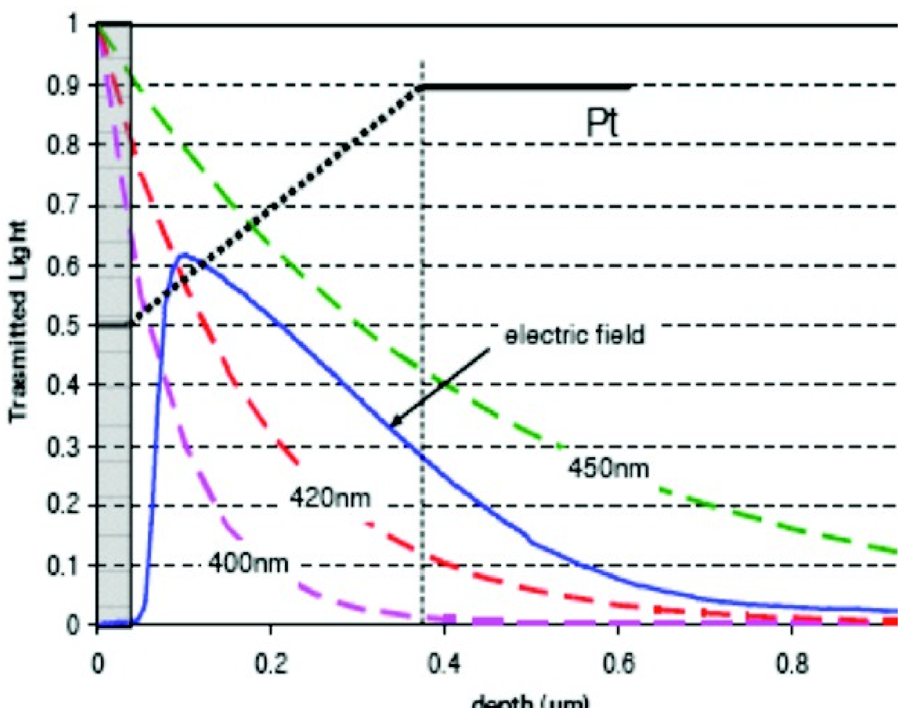

Example with constant high-field:
(a) only holes trigger the avalanche
(b) both electrons and holes trigger
(c) only electrons trigger

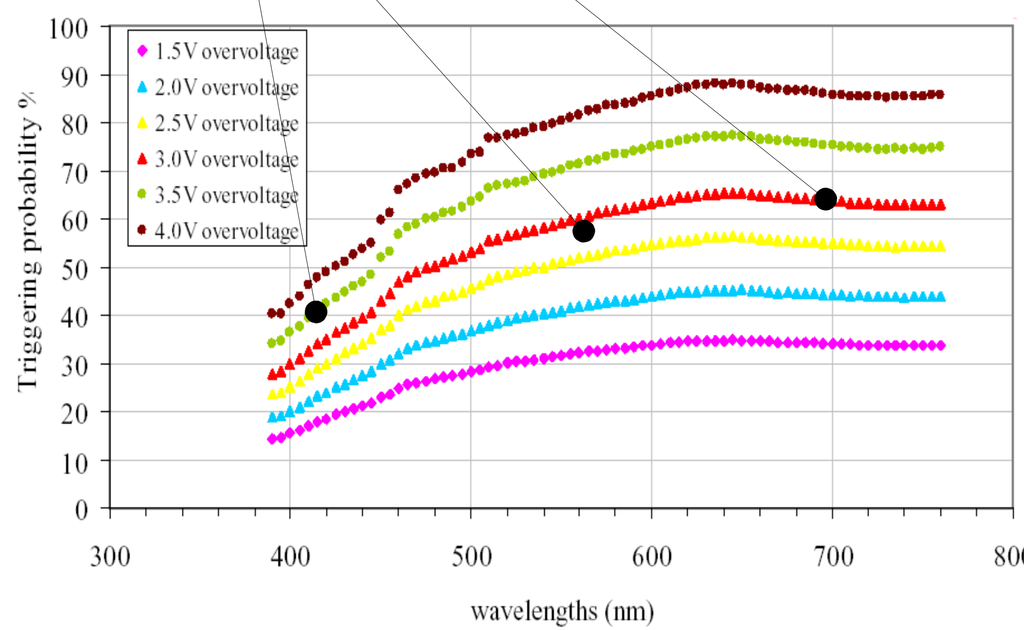

G.Collazuol - Siena - IDPASC 2013

PDE vs ΔV

Ionization rate in Silicon → P_{01} optimization (n-on-p)

- high over-voltage
- photo-generation in the p-side of the junction

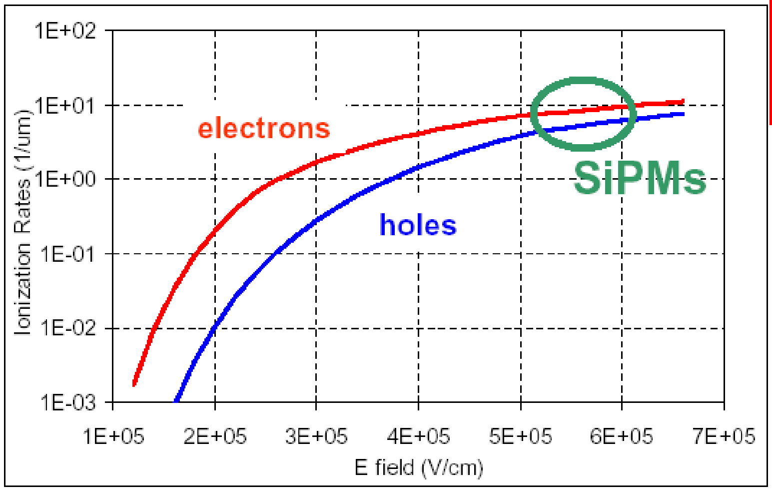

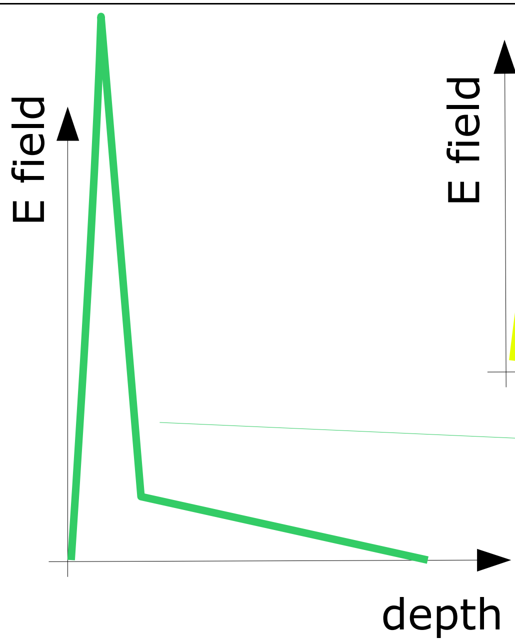

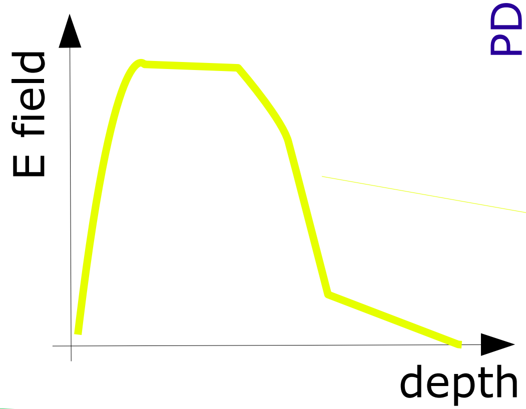

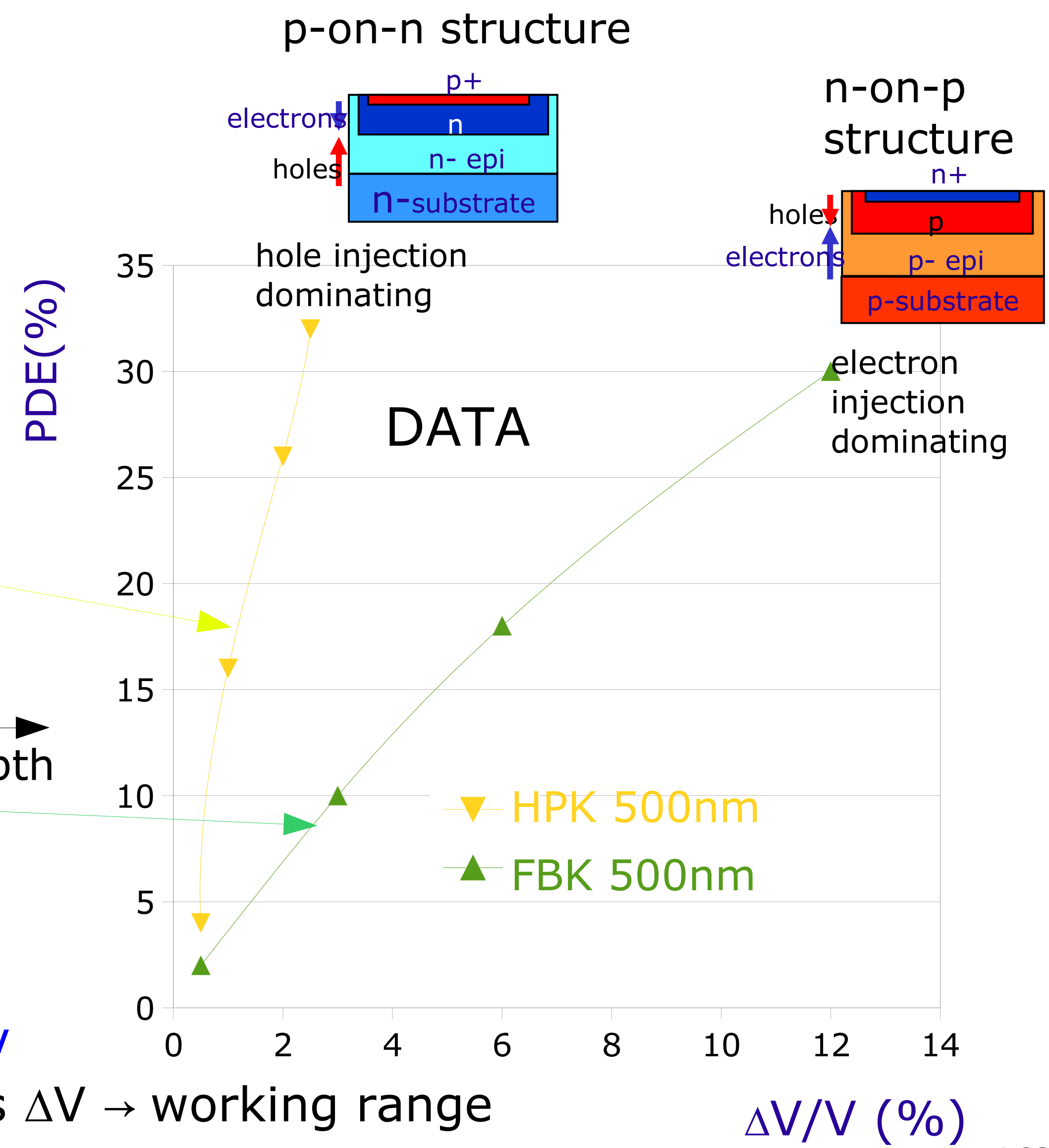

E field profile → the slope of PDE vs ΔV

note: P_{01} fixes also the slope of DCR vs ΔV → working range

G.Collazuol - Siena - IDPASC 2013

Improving PDE by E field engineering

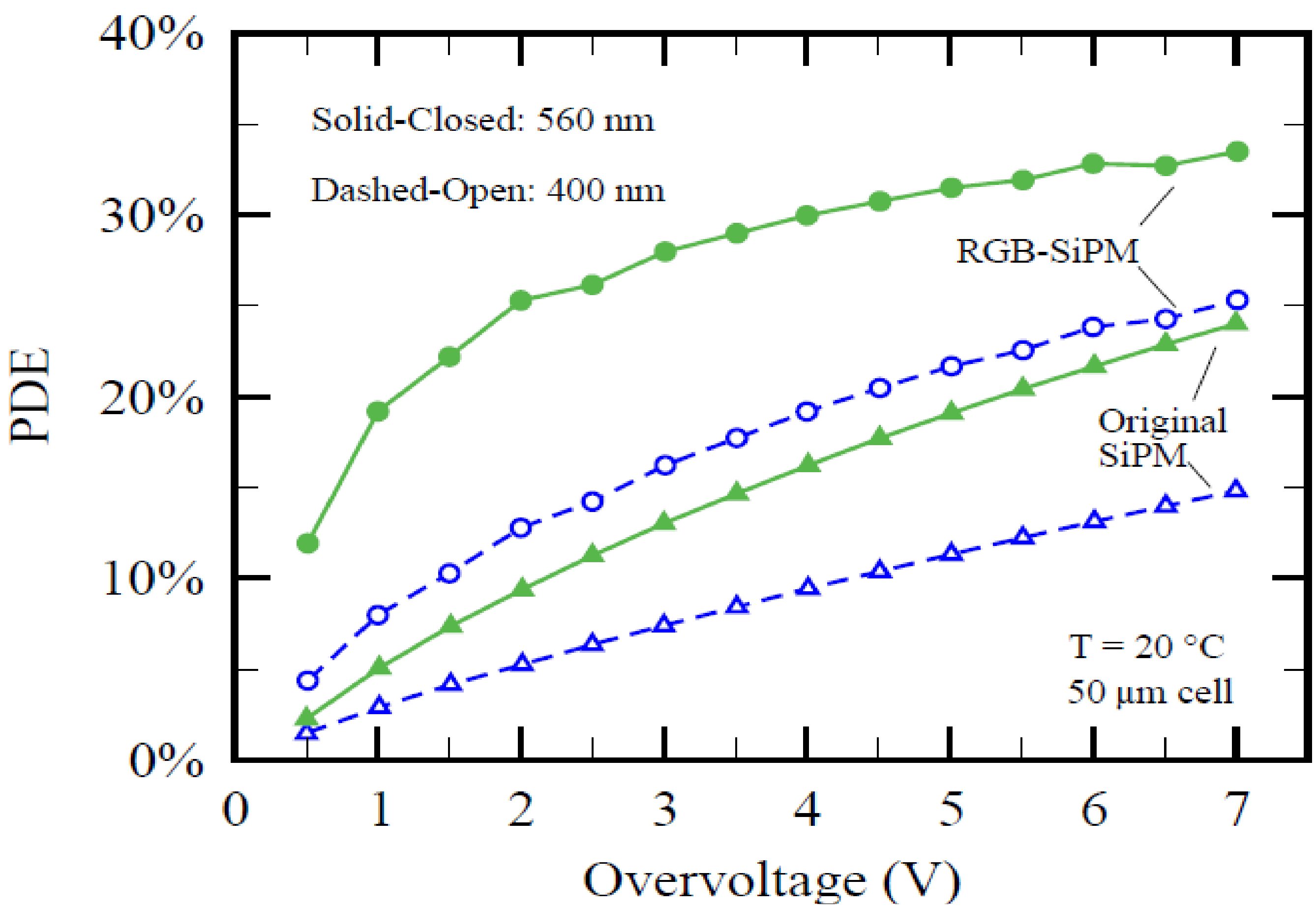

Latest "RGB" FBK devices vs older devices

N.Serra et al
JINST 8 (2013) P03019

Table 1. Main properties of the fabricated RGB-SiPMs.

FBK n-on-p RGB-SiPMs.			
SiPM size (mm^2)	1×1, 3×3, 4×4	Gain (1)	$4\cdot10^6$
Cell pitch (μm)	25-50-70-100	R quenching (at 20°C)	500 kΩ
Fill-factor (%)	21-45-58-72	Cell capacitance (1)	170 fF
V_{BD} (at 20°C)	28.5 V	Rise time (1)(2)	5.6 ns
Dark count rate (1)	480 kHz	Recovery time (1)(2)	350 ns

(1) 1×1 mm^2 SiPM, 50 μm cell at 20°C, OV=4 V; (2) Single-cell pulse, see figure 2.

Question: how to measure PDE

Example of experimental setup

Measuring PDE – pulsed/continuous light

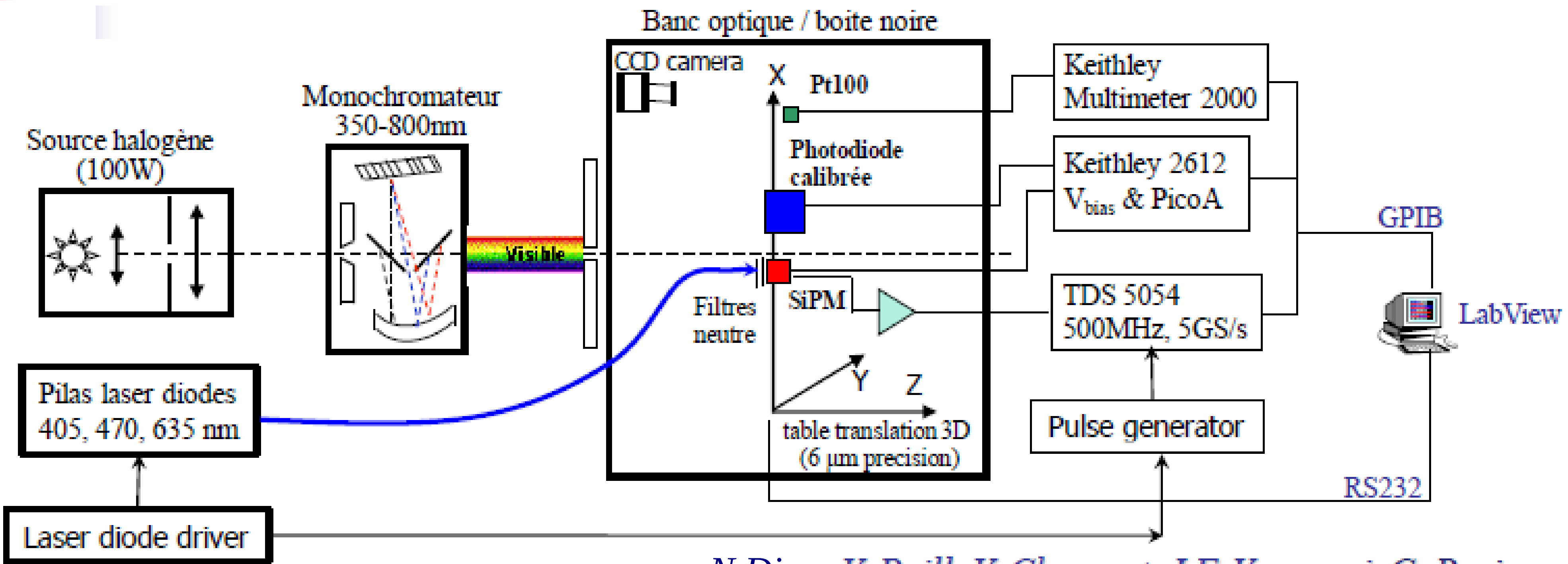

N.Dinu V. Puill, V. Chaumat, J.F. Vagnucci, C. Bazin

- Continuous light: PDE vs λ (350-800nm):
  - low incident flux (~ 10^7 incident photons /s/mm^2) – to avoid the SiPM saturation
  - calibrated photodiodes (HPK S3590-18, UDT Instrument 221)
  - the number of the photons recorded by the SiPM – evaluated by two methods:
    - DC method & AC counting methods
- Pulsed light: PDE, timing resolution, non-linearity
  - the number of the incident photons – evaluated with a PMT (HPK R614-00U)

PDE VS λ (shape)

N.Dinu et al. NIM A (2008)

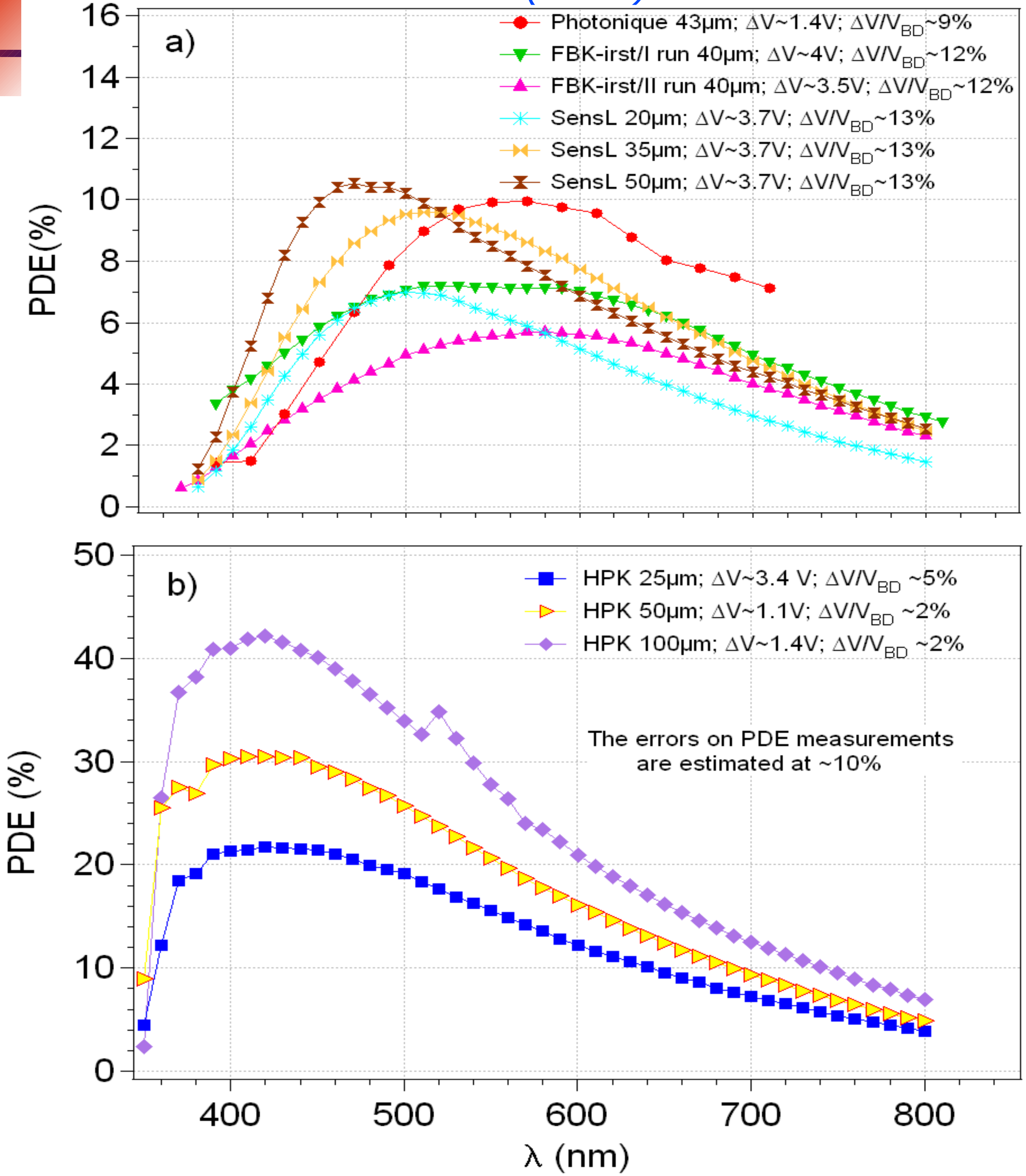

Fig. 5a) The PDE vs. λ of the Photonique, FBK-irst and SensL devices and b) HPK

n-on-p structures

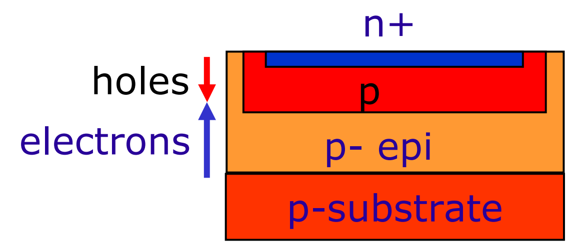

p-on-n structure

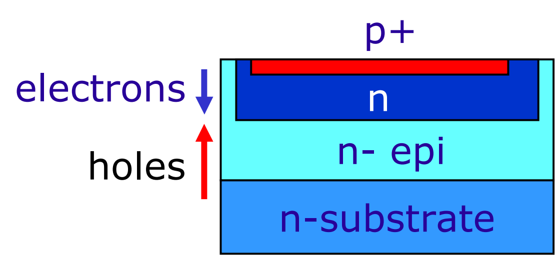

Note: geometrical fill factor included

Improving PDE

Barlow – LIGHT 2011

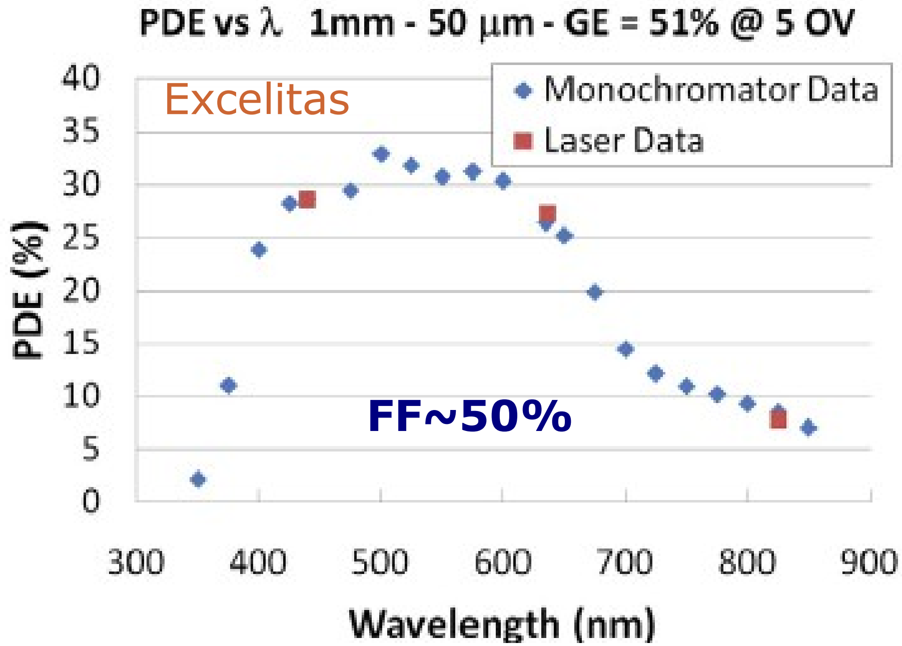

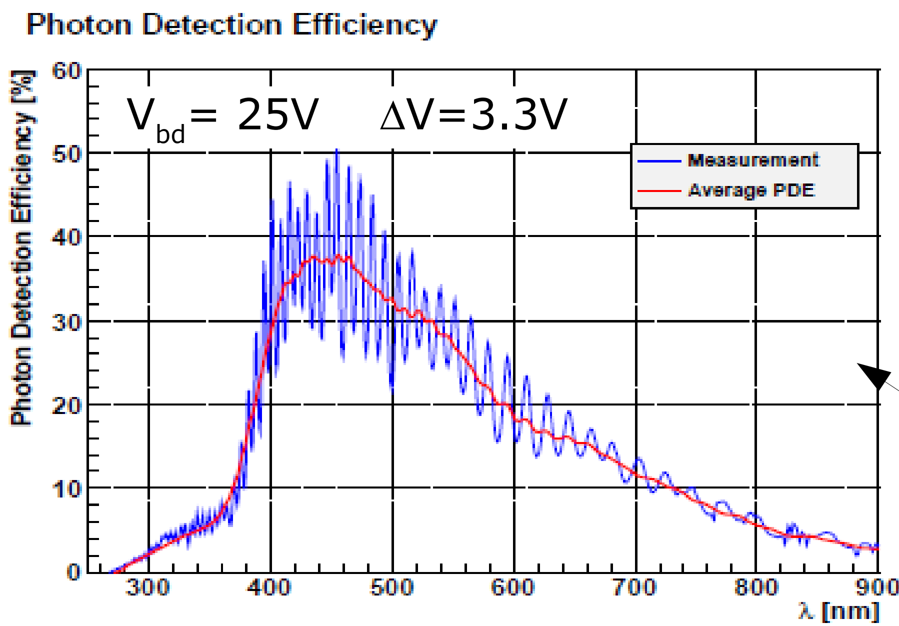

T.Frach 2012 JINST 7 C01112

→ PDE peak constantly improving for many devices
→ every manufacturer shape PDE for matching target applications
→ UV SiPM eg from MePhi/Excelitas (see *E.Popova at NDIP 2011*)
→ VUV SiPMs in development too

F.Wiest – AIDA 2012 at DESY

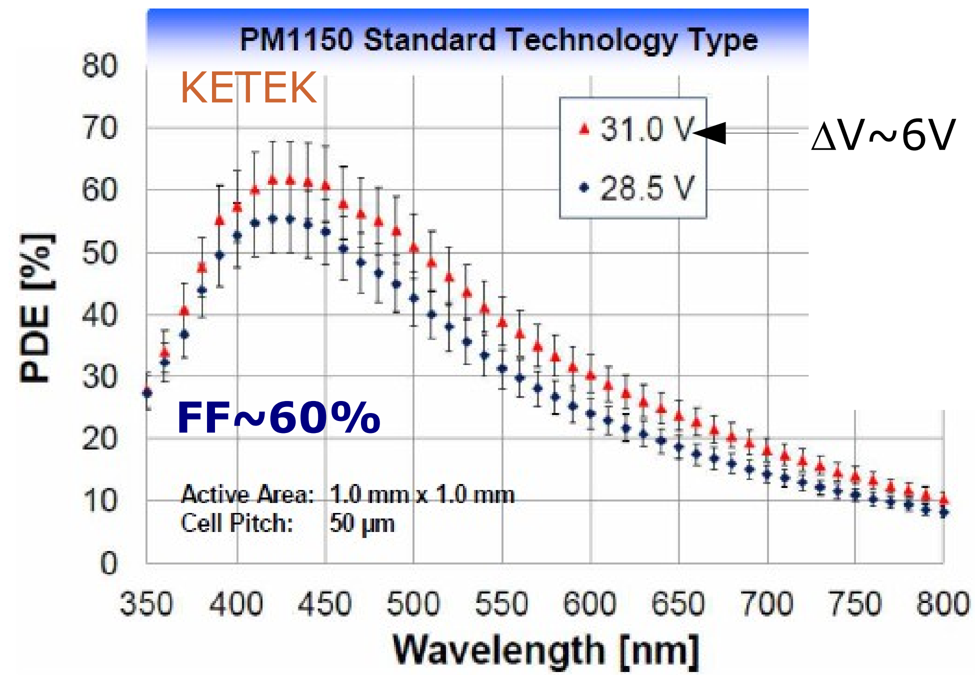

dSiPM (latest sensor 2011)
→ up to now no optical stack optimization
→ no anti-reflecting coating
→ potential improvement up to 60% peak PDE (*Y.Haemish at AIDA 2012*)

Higher PDE and lower noise

D.Renker JINST 5 2010 P01001

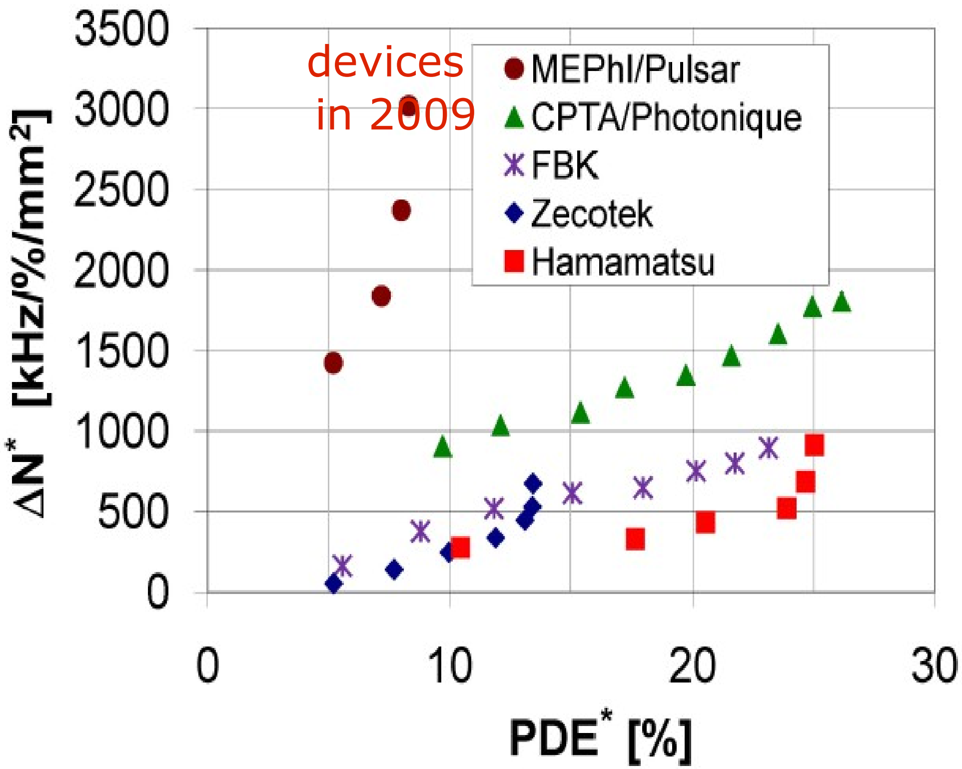

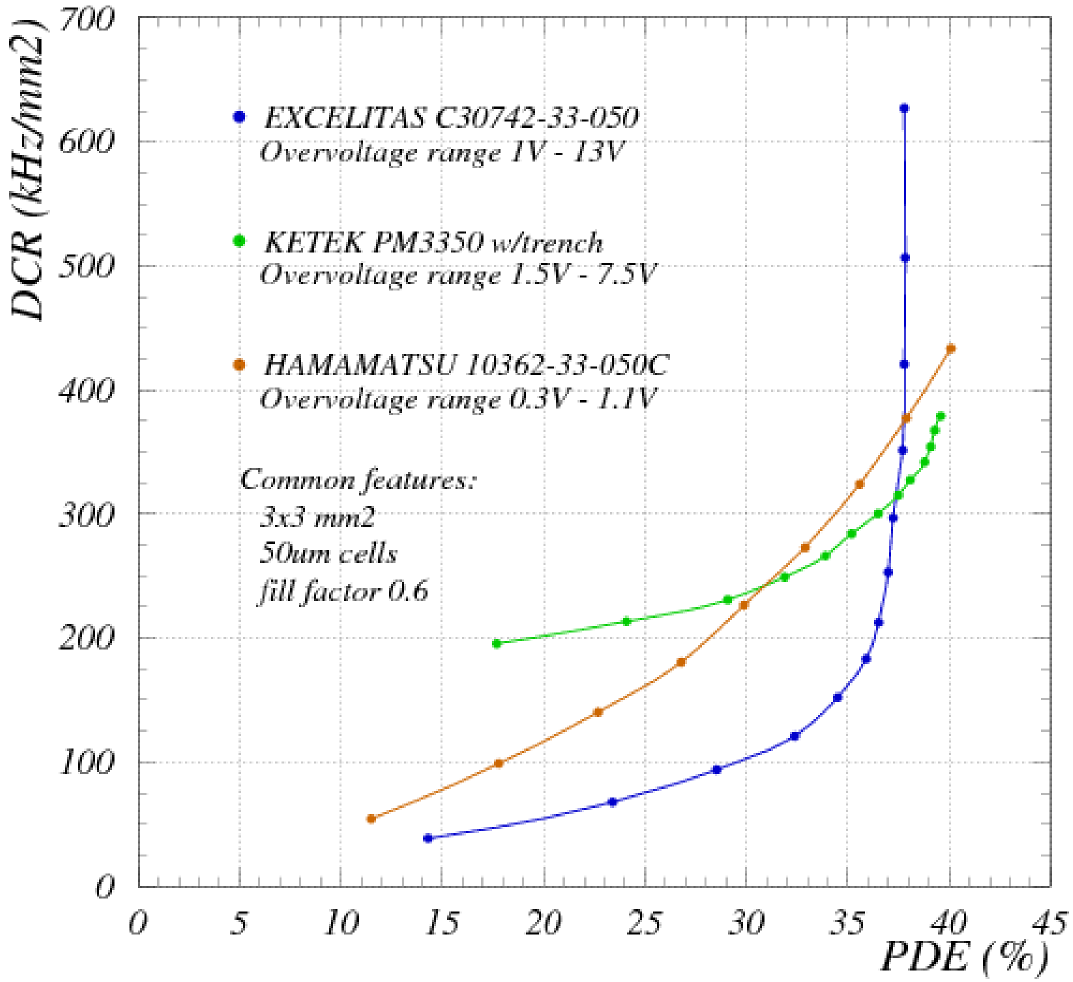

G.Collazuol from published data

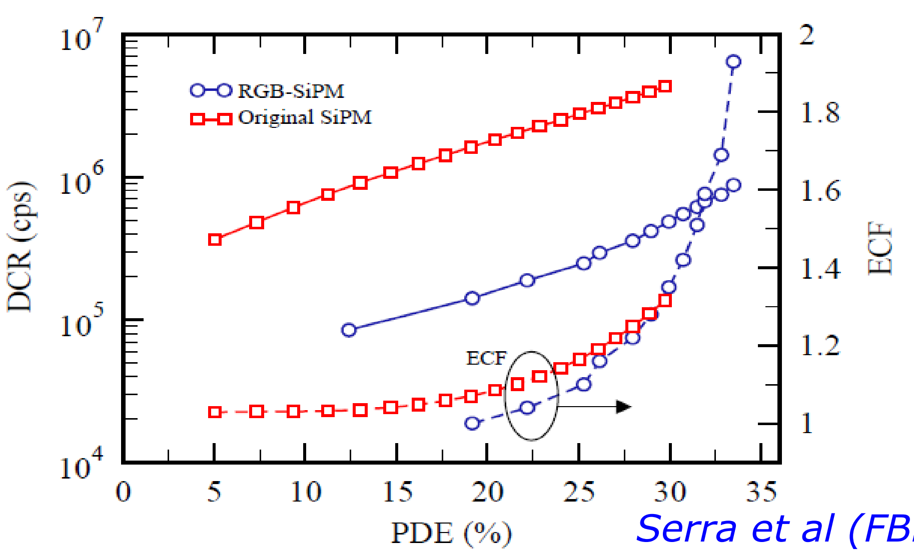

Serra et al (FBK) JINST 8 2013 P03019

VUV SiPM - development

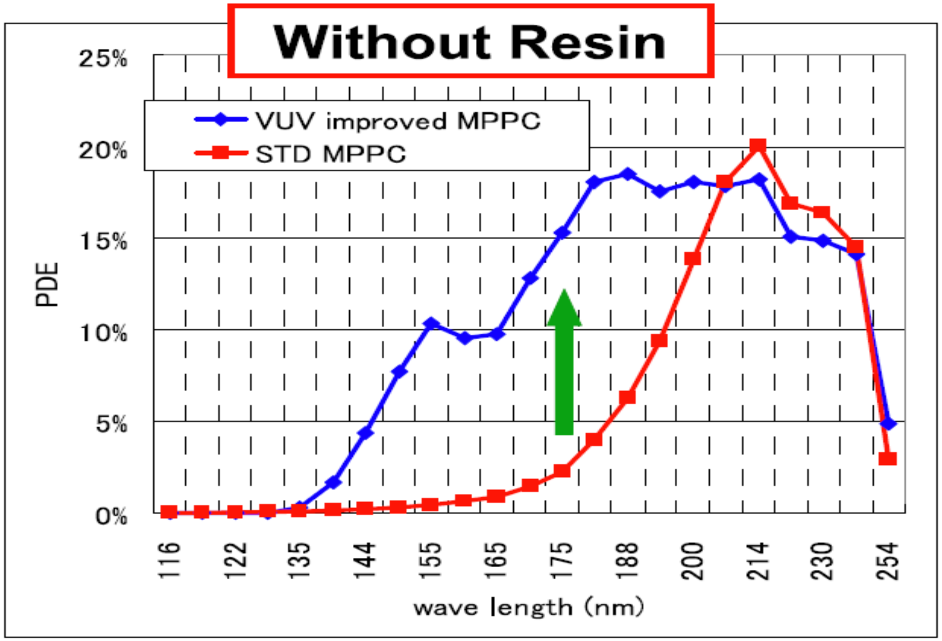

Sato et al (**Hamamatsu**) - Vienna Conf. on Instr. 2013

VUV-enhanced SiPM
→ removal of protection coating
→ optimization of the parameters
- thinner junction
- optimized superficial layer optics

…

New windows for applications in fundamental Physics experiments

- **Dark matter detection**
  ZEPLIN, LUX, DARWIN, XENON100
- **Double beta decay measurement**
  EXO
- **Search for rare decay mode**
  MEG

FBK - Advansid

NUV-SiPM (Near-UV SiPM)

- PDE (350nm) ~ 27 % (FF = 45 %)
- DCR = 200 kHz @ 20°C (ΔV = 5V)

1x1mm^2 50x50 µm^2 cell

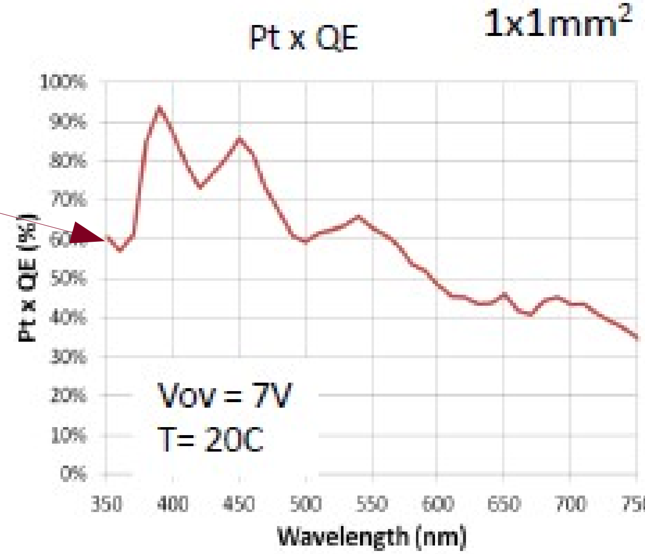

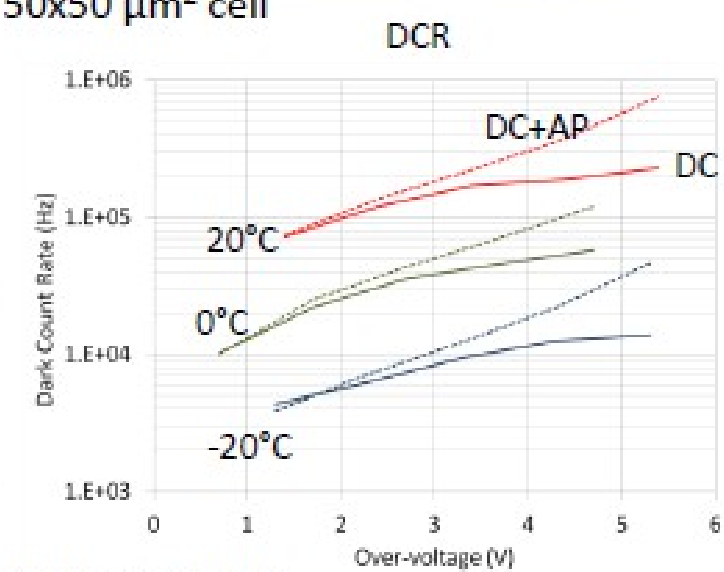

See lecture by A.Ferri at IDPASC 2013

C. Piemonte, private communication

PDE vs Temperature (ΔV constant)

When T decreases:

1) silicon E_{gap} increasing
→ larger attenuation length
→ lower QE (for larger λ)

2) mobility increasing
→ larger impact ionization
→ larger trigg. avalanche P_{01}

3) carriers freeze-out
onset below 120K
→ loss of carriers

G.C. et al NIM A628 (2011) 389

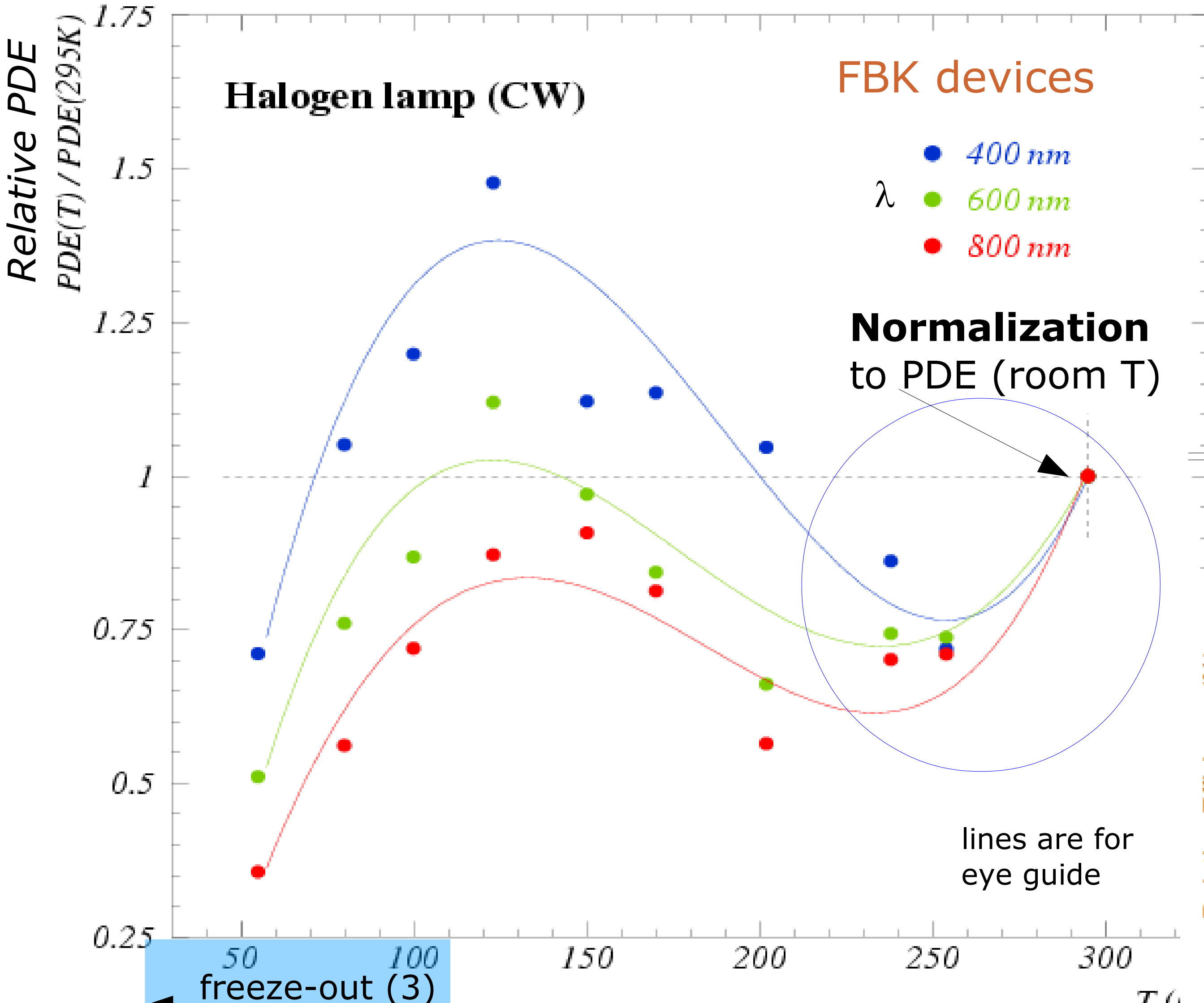

??? interplay between (1) and (2): modulation
… drop in 250<T<300 not well understood
(common feature with APDs')

RMD APD at 400nm < λ < 700nm
Johnson et al, IEEE NSS 2009

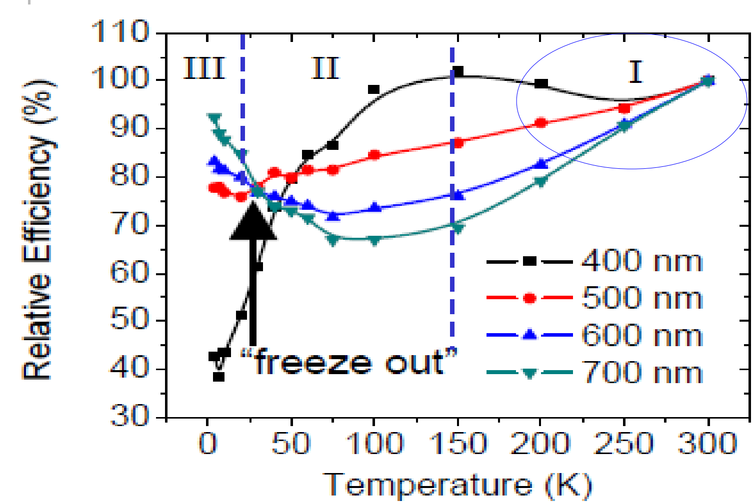

Additional effects in APD
(depletion region depends on T, ...)

PDE vs Temperature (ΔV=2V) – LED and Laser

PDE dependence on T at constant gain:
similar results with LED (cont. light - 380nm)
and Laser (pulsed light – 405nm)

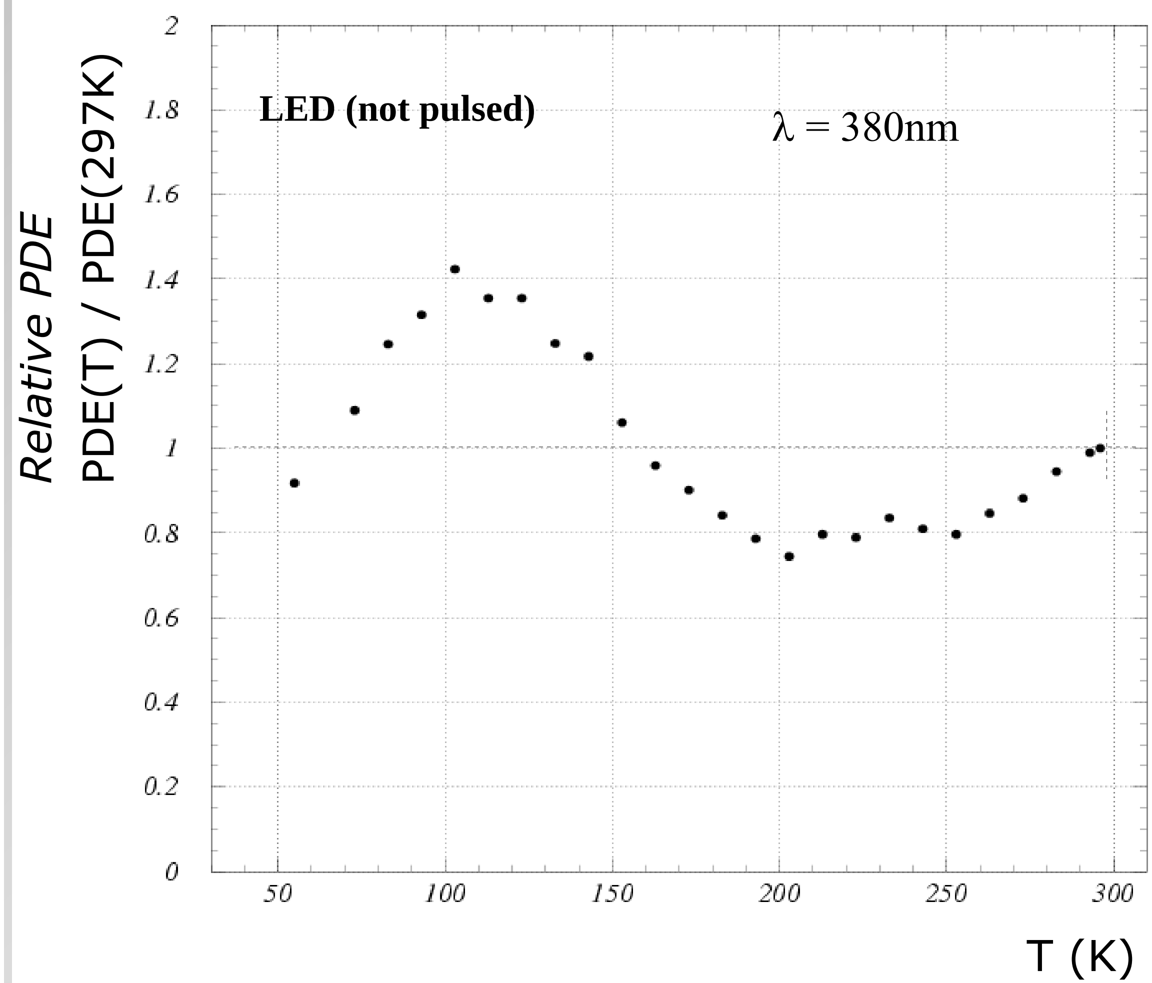

$PDE\ (T) \equiv I_{SiPM}\ (T) \,/\, I_{LED}$

Normalization with PDE at T=297K

Some common features
with APDs (proportional mode)

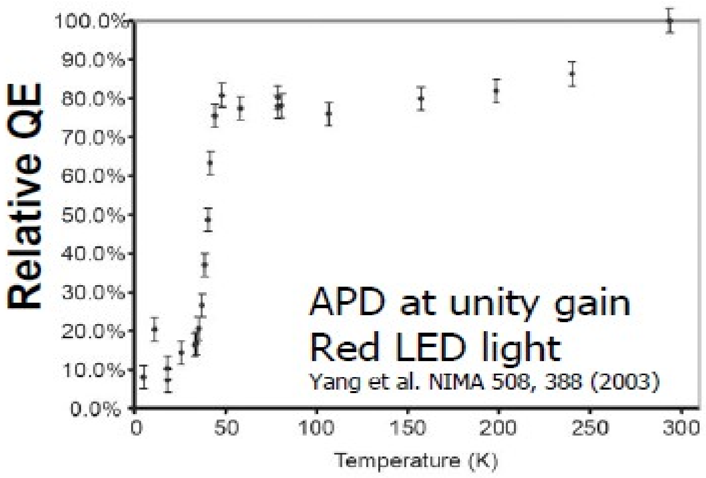

APD at 400nm < λ < 700nm
Johnson et al, IEEE NSS 2009

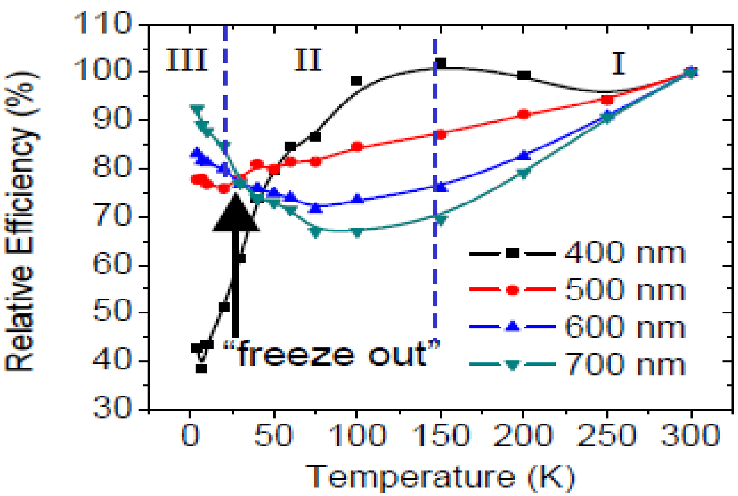

Additional effects in APD
(depletion region depends on T, ...)

PDE dependences, changing with Temperature

PDE vs λ (ΔV constant)

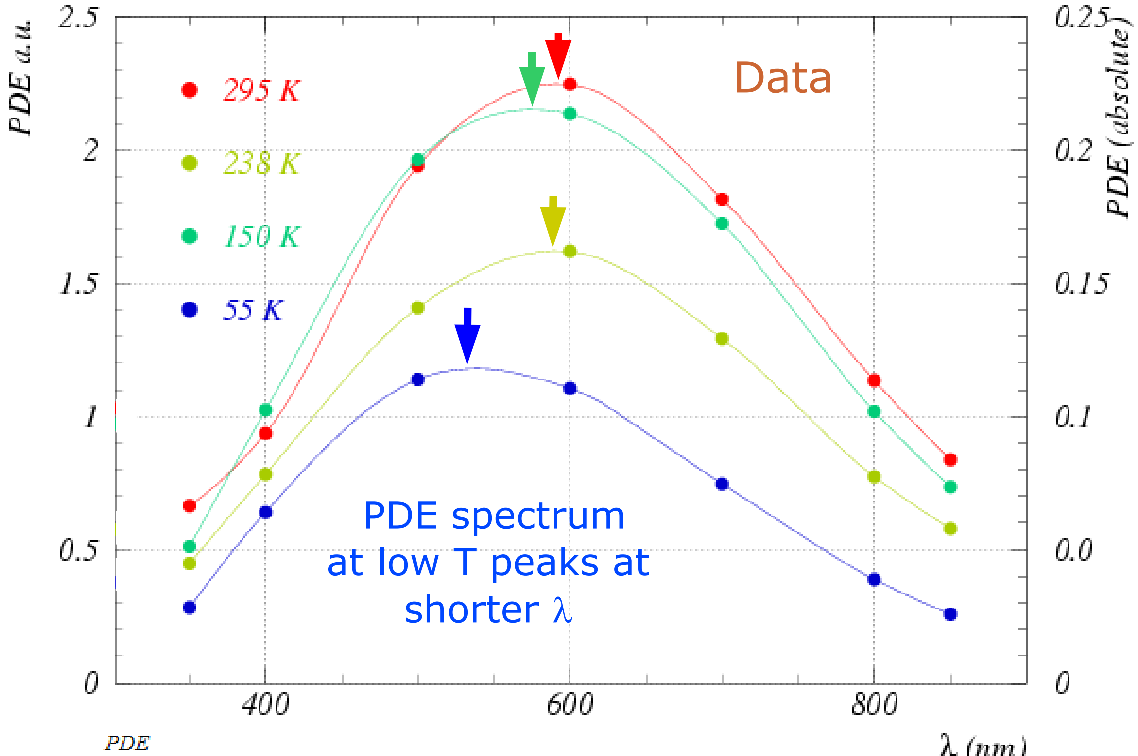

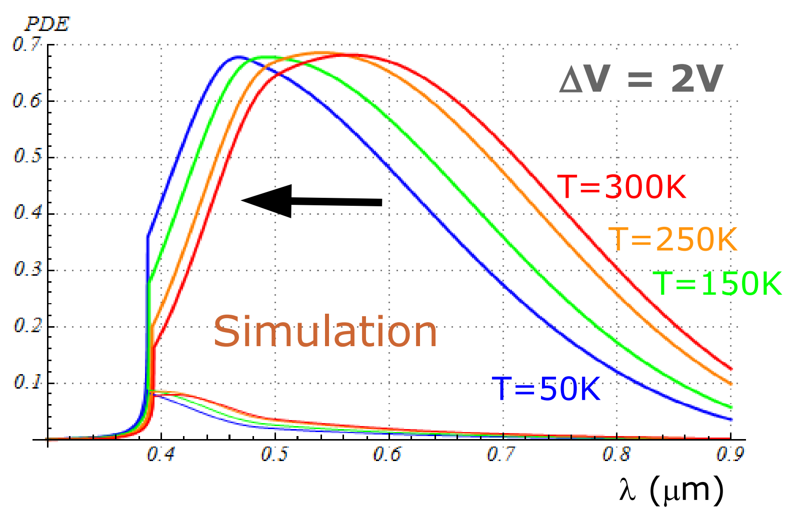

PDE ΔV vs (λ constant)

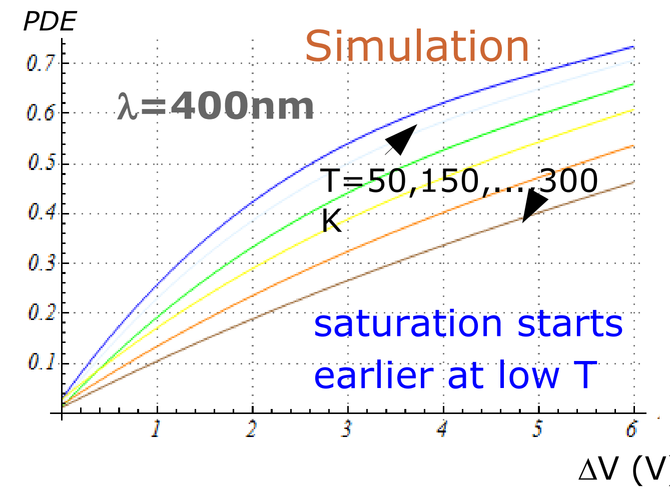

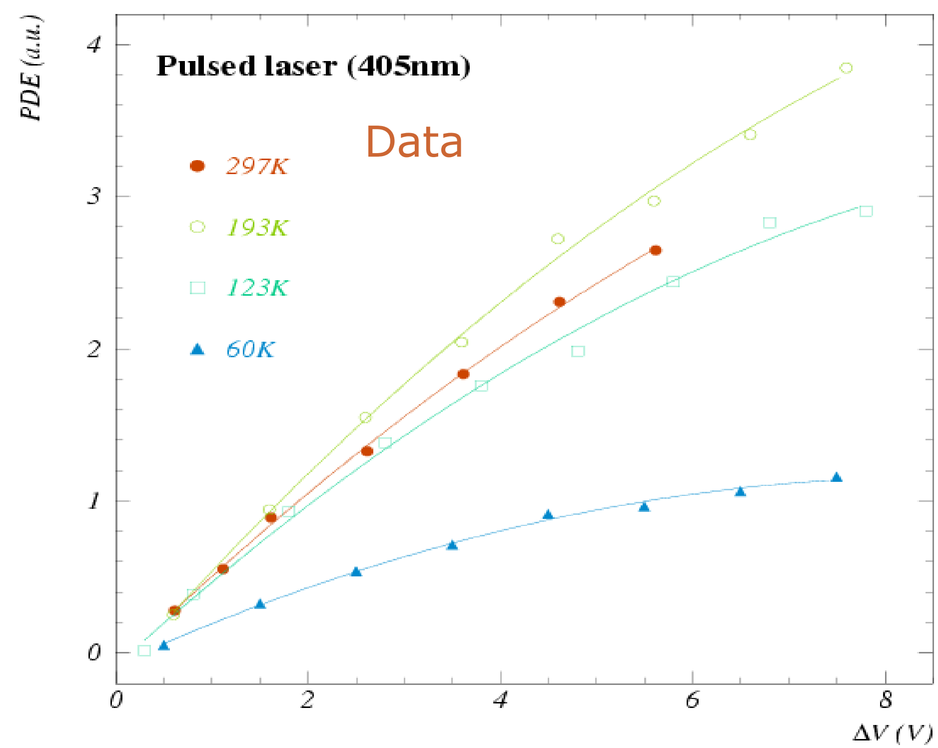

Understanding PDE vs T: 1D model

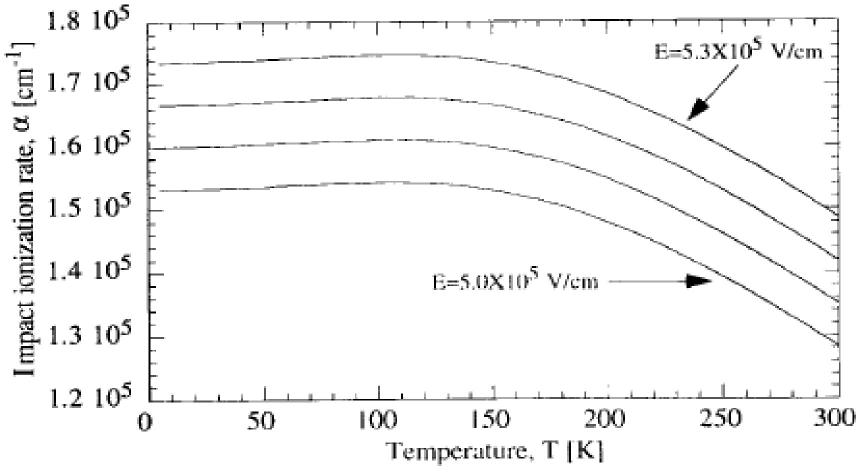

FIGURE 1.43. The impact ionization rate α as a function of temperature T_A with the electric field E as a parameter calculated from Okuto and Crowell's (85) model.

E field profile +

+ impact ionization

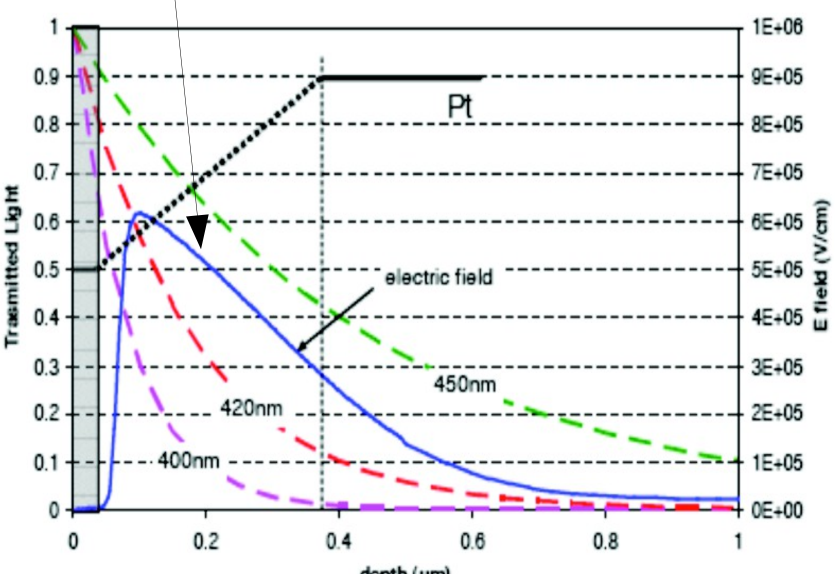

Breakdown voltage

Avalanche triggering probability
for electrons and holes ($P_{trigger}e$, $P_{trigger}h$)
(using differential equations method after Oldham et al, IEEE TNS 19 (1972) 1056)

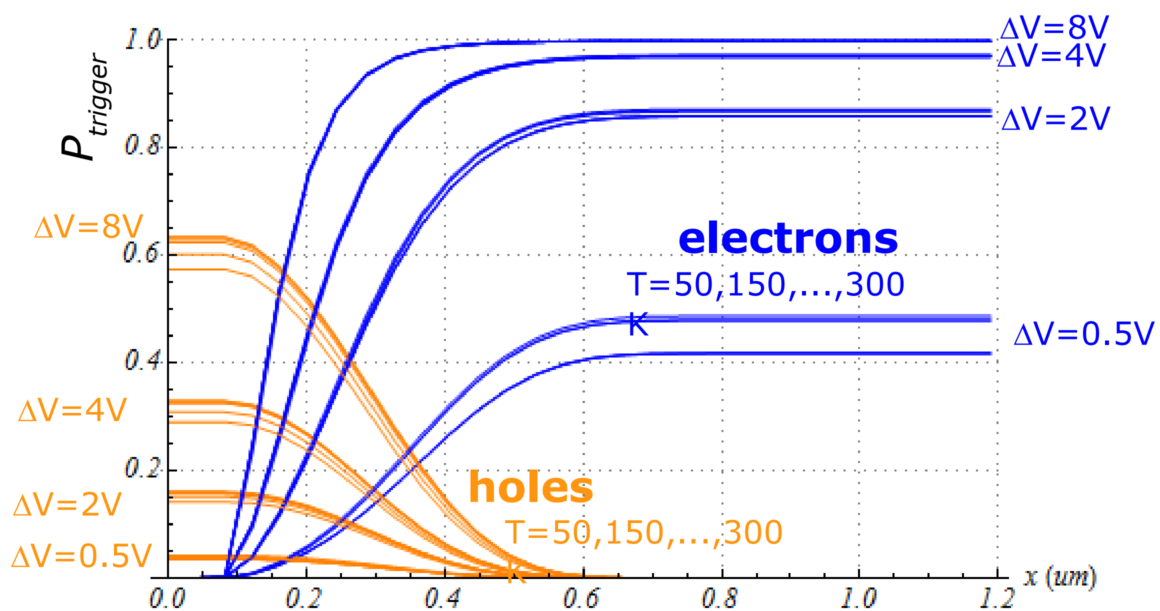

Understanding PDE vs T: 1D model

avalanche triggering probability +

+ light **absorption length in Si (1/α)**

PDE as a function of (λ ,T,ΔV) obtained by the convolution of $P_{trigg}(x)$ and $\alpha\exp(-\alpha x)$ (integrated over the depletion layer)

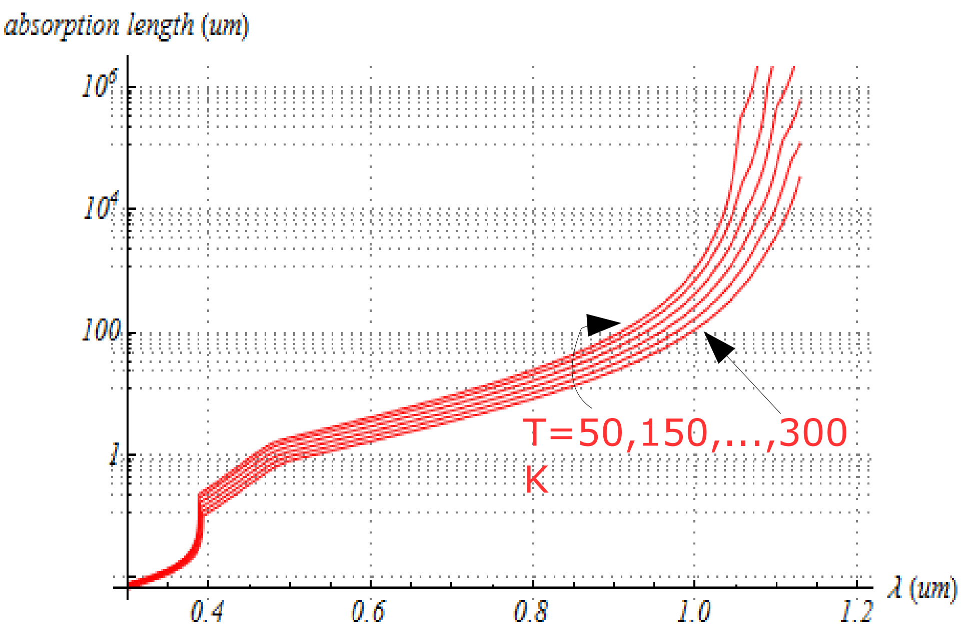

Rajkanan et al, Solid State Ele 22 (1979) 793

Accounting E_{gap} variations with T, etc...

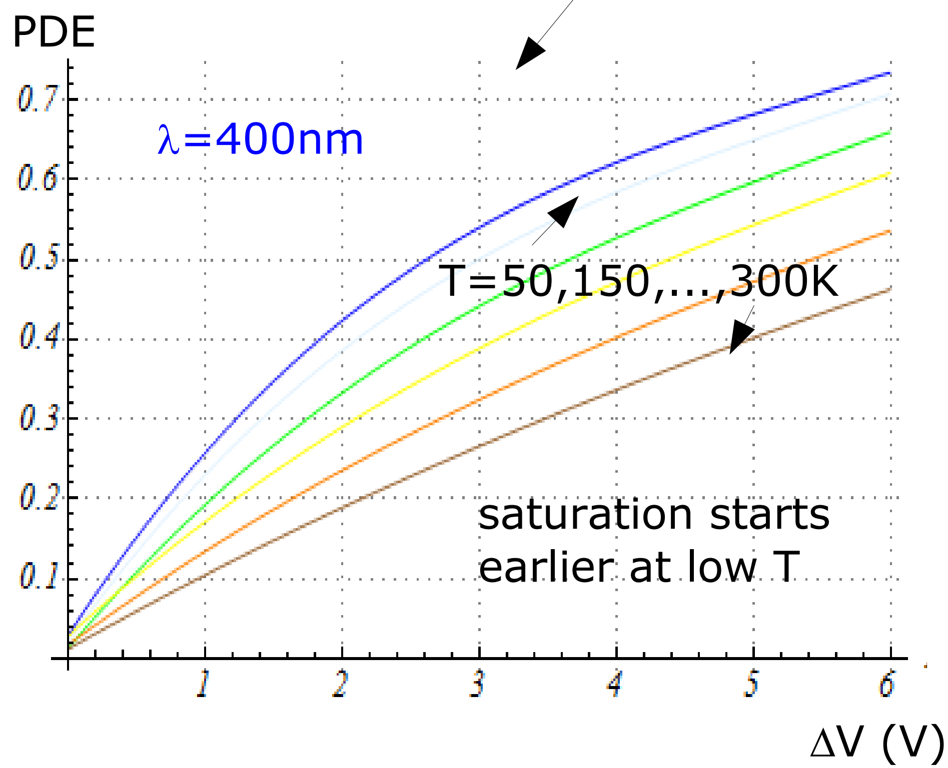

Understanding PDE vs T: 1D model

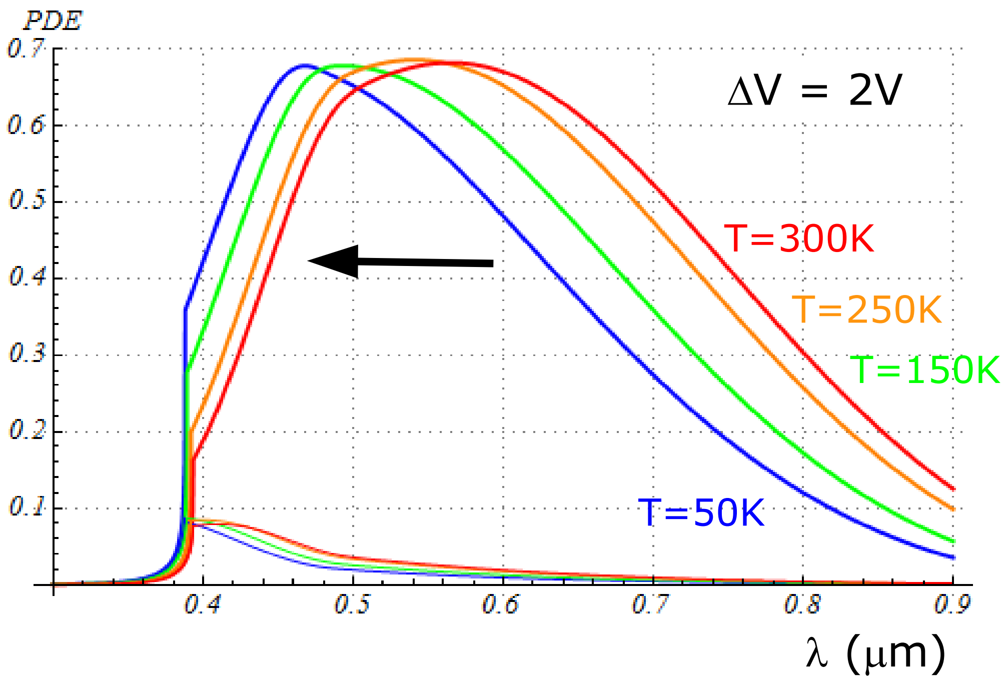

1) main contribution to PDE from electrons → PDE distribution shifted toward short λ at low T because of larger absorption length (photo-generation deeper into depletion layer → gain for shorter λ, loss for longer λ)

(see also PDE vs T)

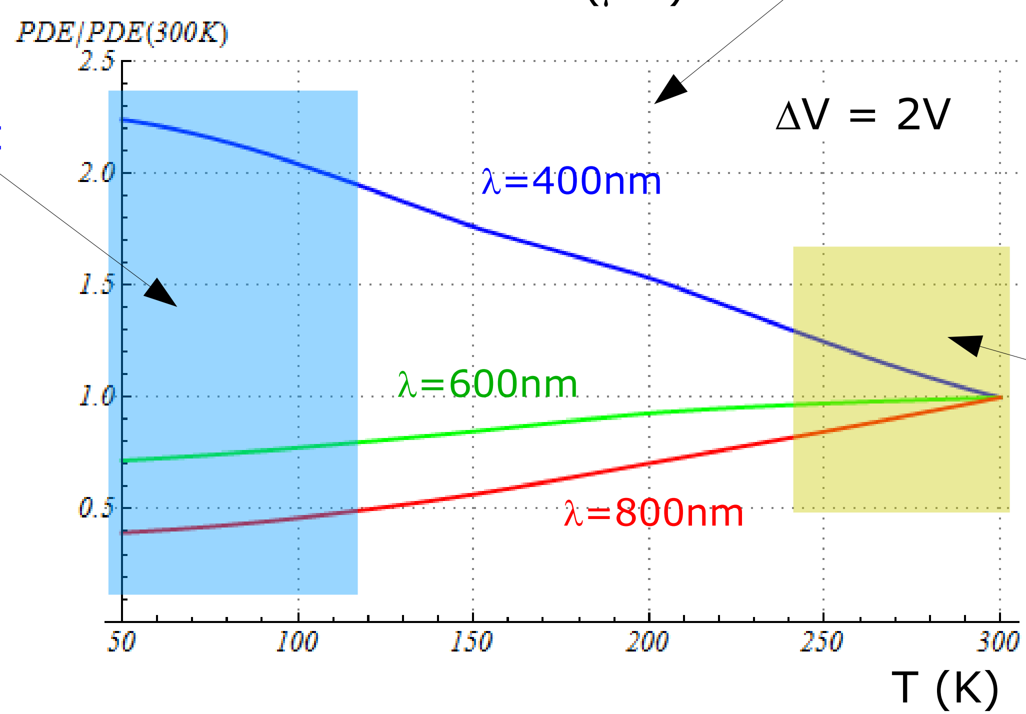

2) tunneling effects not (yet) included in the model (enhancement of PDE, interplay with band gap variations with T)

3) freeze-out not (yet) included in the model

4) something else is missing: need to explain PDE decreasing with T for 250K<t<300K

...to be understood

Question: how to perform low T characterization

Example of low T experimental setup

Experimental Setup

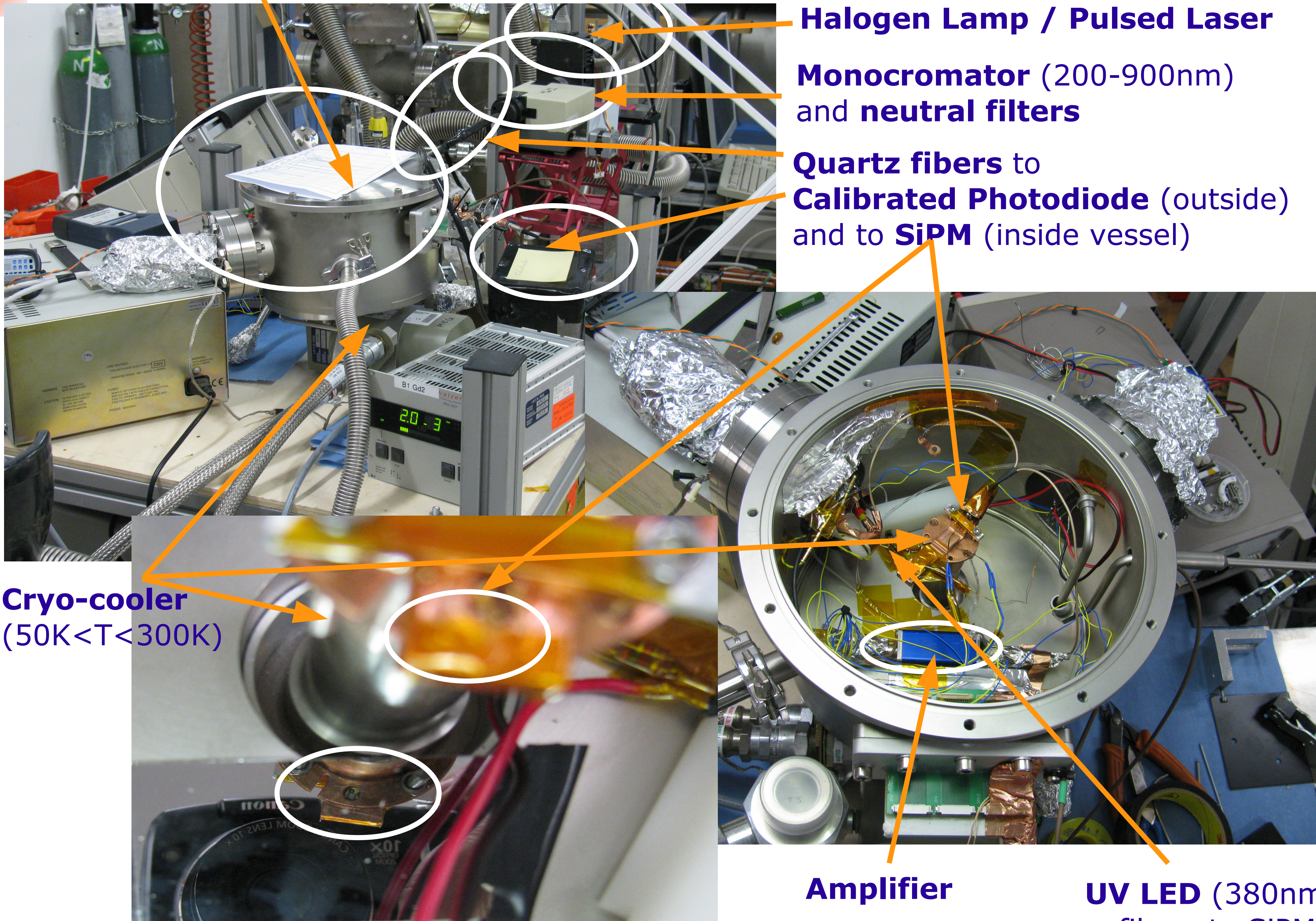

Experimental setup

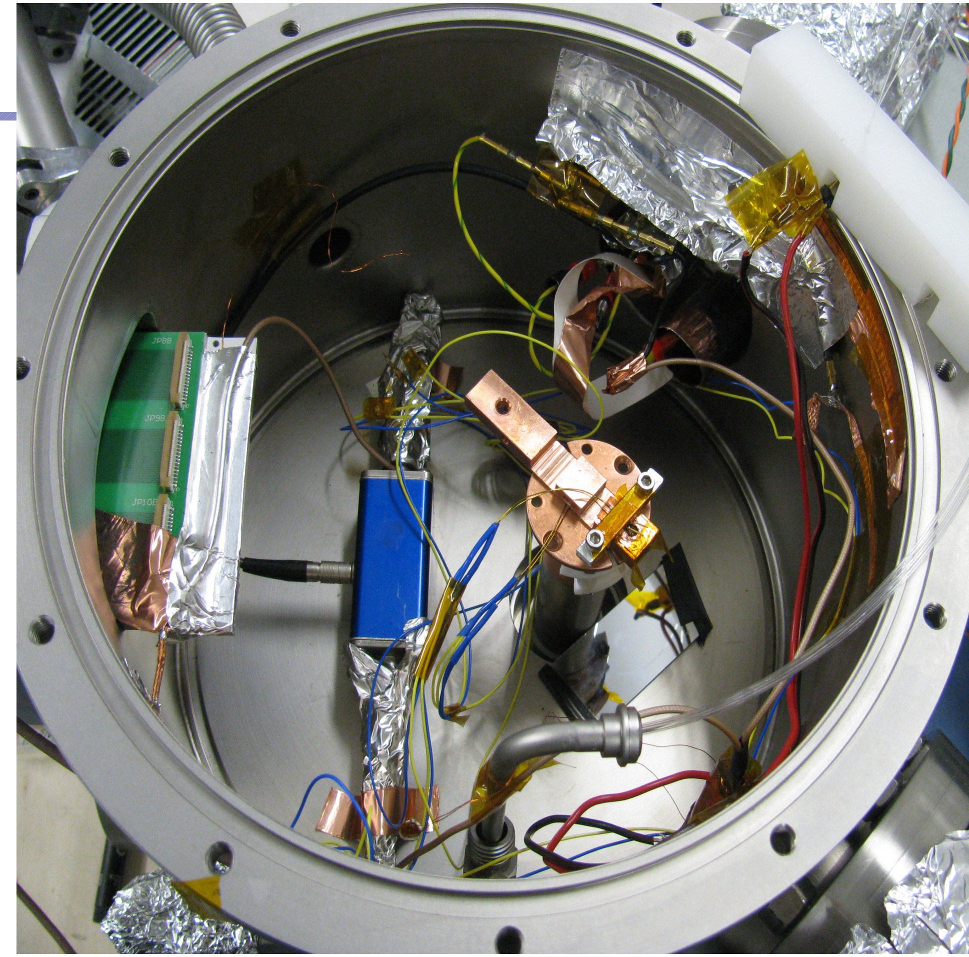

Temperature control/measurement

- Close cycle, two stages, He cryo-cooler and heating with low R resistor
- Vacuum with P< 10^{-3} mbar
- thermal contact (critical) with cryo-cooler head: SIPM within a copper rod + kapton (electrical insulation)
- T measurement with 3 pt100 probes
- Measurements on SiPM carried after thermalization, ie all probes at the same T
- check junction T with forward characteristic

Light sources

- CW: halogen lamp and UV LED (λ~380nm)
- Pulsed: laser (30ps rms, λ~405nm)

V_{bias} and current measurements

- Keytley 2148
  Voltage/Current source/meter

Pulse/Wavef. measurements

- Care against HF noise
  → feedthroughs !!!
- Amplifier Photonique/CPTA (gain~30, BW~300MHz)
- Lecroy o.scope, 1GHz, 20GS/s

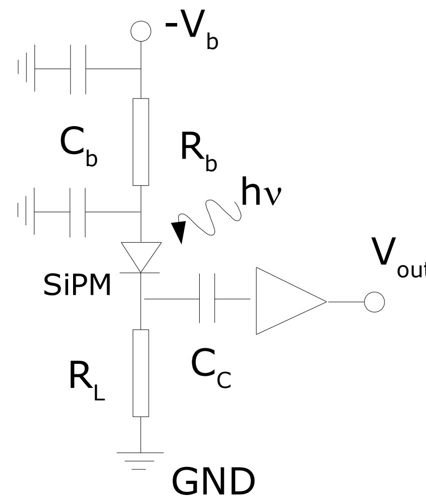

SiPM samples

FBK SiPM runII – 1mm²
(Vbr~33V, fill factor~20%)

- n-on-p shallow junction
- 4μm fully depleted region (active volume)
- no protective epoxy

DCR, AP, Gain, X-talk vs ΔV (various T)

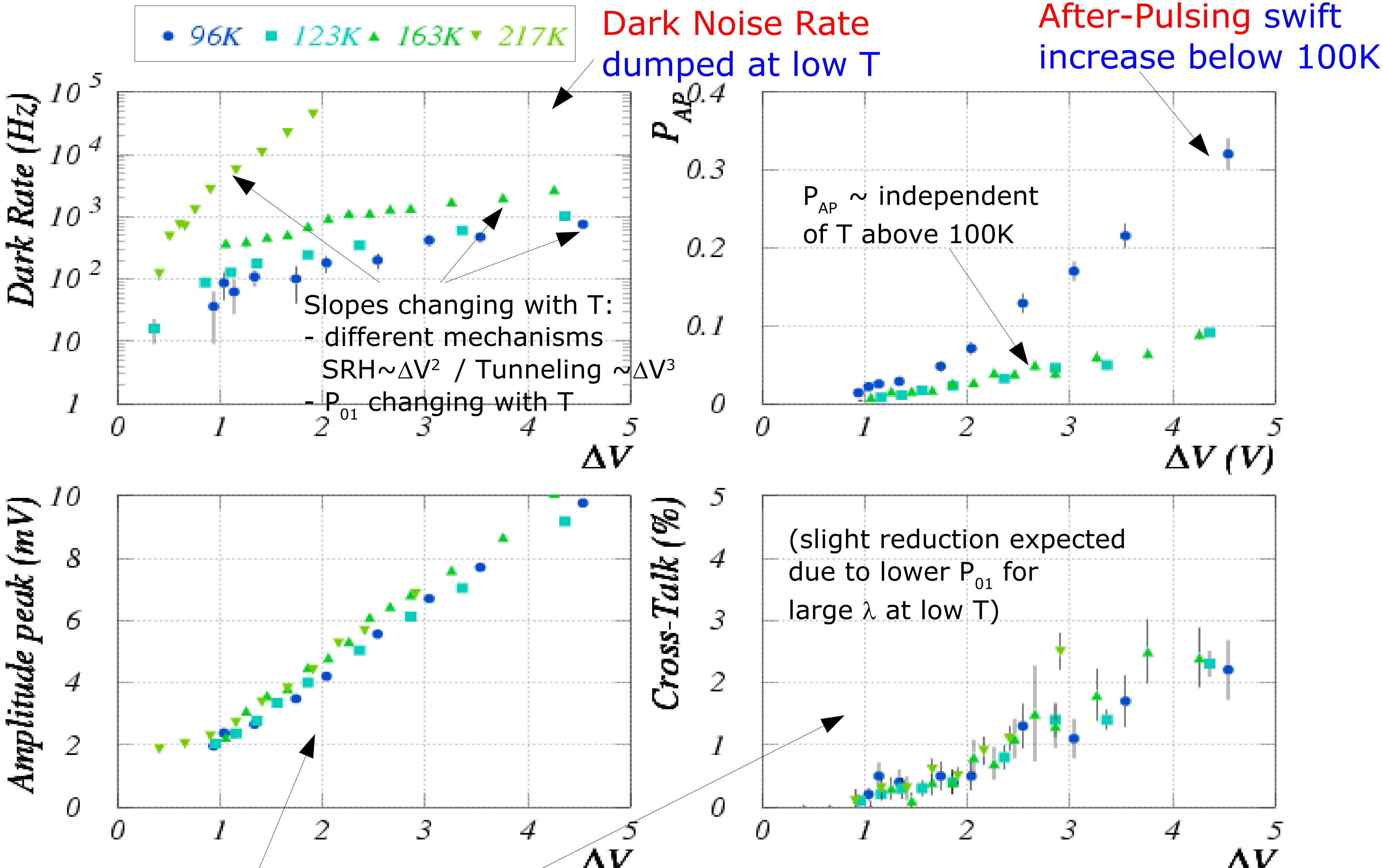

Gain and Cross-Talk are independent of T

FBK devices
G.C. et al NIM A628 (2011) 389

Timing fluctuations

- **SiPM are intrinsically very fast**

Two timing components (related to avalanche developement)
1) prompt → gaussian time jitter well below **100ps** (depending on ΔV, and λ)
2) delayed → non-gaussian tails up to **few ns** (depending on λ)

- **Models and Simulations**

- **Measurements**

- **Optimization of devices for timing**
  - → use of fast signal shape component
  - → use waveform, it's better than CFD and ... don't use ToT

- **Timing with scintillators**

GM-APD avalanche development

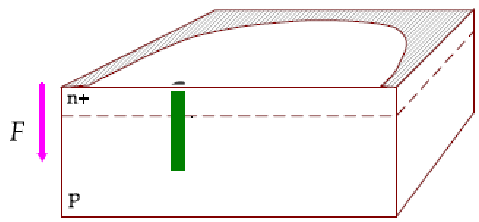

Longitudinal multiplication

Duration ~ few **ps**

Internal current up to ~ few **µA**

(1) Avalanche "seed": free-carrier concentration rises exponentially by **"longitudinal" multiplication**

(1') Electric field locally lowered (by **space charge R effect**) towards breakdown level

Multiplication is self-sustaining
Avalanche current steady until new multiplication triggered in near regions

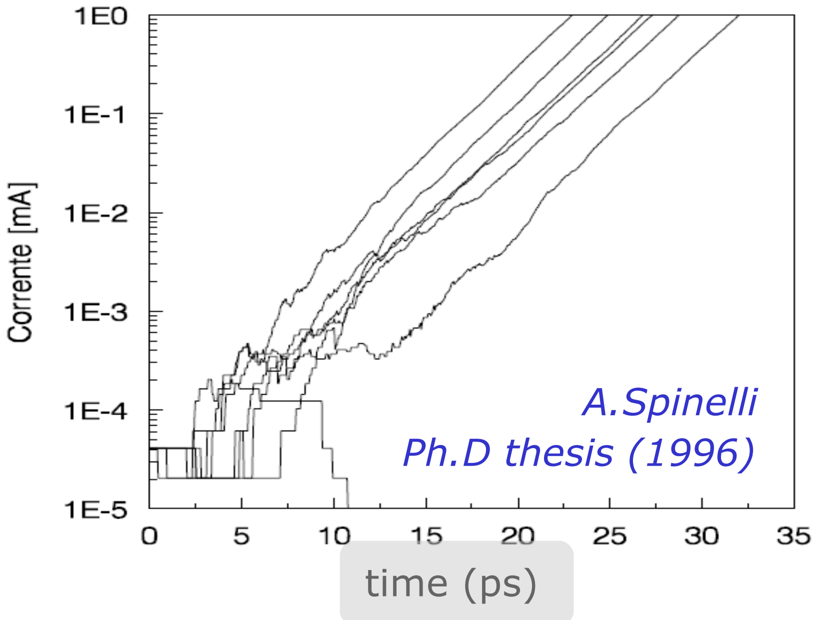

x100

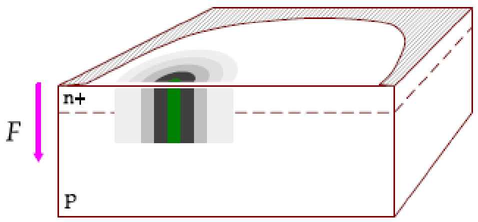

Transverse multiplication

Duration ~ few **100ps**

Internal current up to ~ several **10µA**

(2) Avalanche spreads "transversally" across the junction

(**diffusion speed ~up to 50µm/ns** enhanced by multiplication)

(2') Passive quenching mechanism effective after transverse **avalanche size ~10µm**

(if no quench, avalanche spreads over the whole active depletion volume → avalanche current reaches a final saturation steady state value)

Simulation w/o quenching:
→ steady current reached

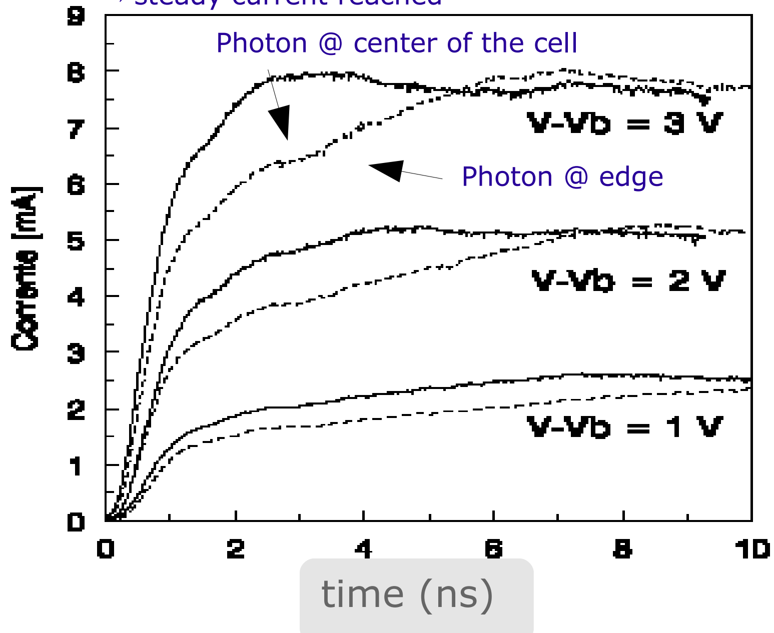

GM-APD avalanche transverse propagation

Avalanche transverse propagation by a kind of shock wave: the wavefront carries a high density of carriers and high E field gradients (inside: carriers' density lower and E field decreasing toward breakdown level)

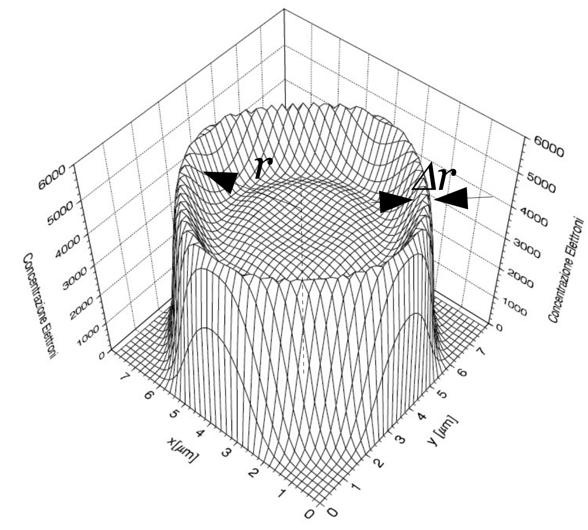

$$\frac{dS}{dt}=\frac{d}{dt}2\pi r(t)\Delta r=2\pi v_{diff}\Delta r=4\pi\Delta r\sqrt{\frac{D}{\tau}}$$

Rate of current production: $$\frac{dI}{dt}=\frac{dI}{dS}\frac{dS}{dt}\sim\frac{\sqrt{D}}{R_{sp}\sqrt{\tau}}$$

$$\frac{dI}{dS}=J=\frac{V_{bias}}{R_{sp}(S)}$$

S = surface of wavefront (ring of area $2\pi\, r\Delta r$)
$R_{sp}(S)$ = space charge resistance $\sim w^2/2\varepsilon v \sim O(50\ k\Omega\ \mu m^2)$
$v_{diff} \sim$ O(some 10 μm/ns)
D = transverse diffusion coefficient ~ O(μm^2/ns)
τ = longitudinal (exponential) buildup time ~ O(few ps)

Internal current rising front:
the faster it grows, the lower the jitter
dI/dt → understand/engineer timing features of SiPM cells

$$\tau\sim\frac{1}{1-(E_{max}/E_{breakdown})^n}$$

→ timing resolution improves at high V_{bias}
→ E field profile affects τ and R_{sp} (wider E field profile → smaller R) (should be engineered when aiming at ultra-fast timing)
→ T dependence of timing through τ and D
→ slower growth at GAPD cell edges → higher jitter at edges reduced length of the propagation front

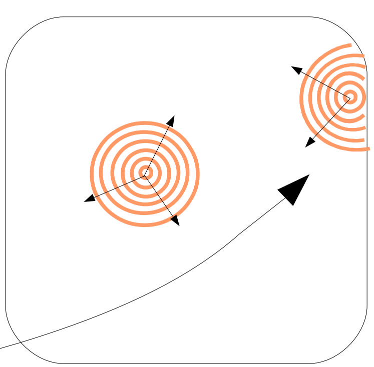

SiPM cell

Avalanche transverse propagation (simul.)

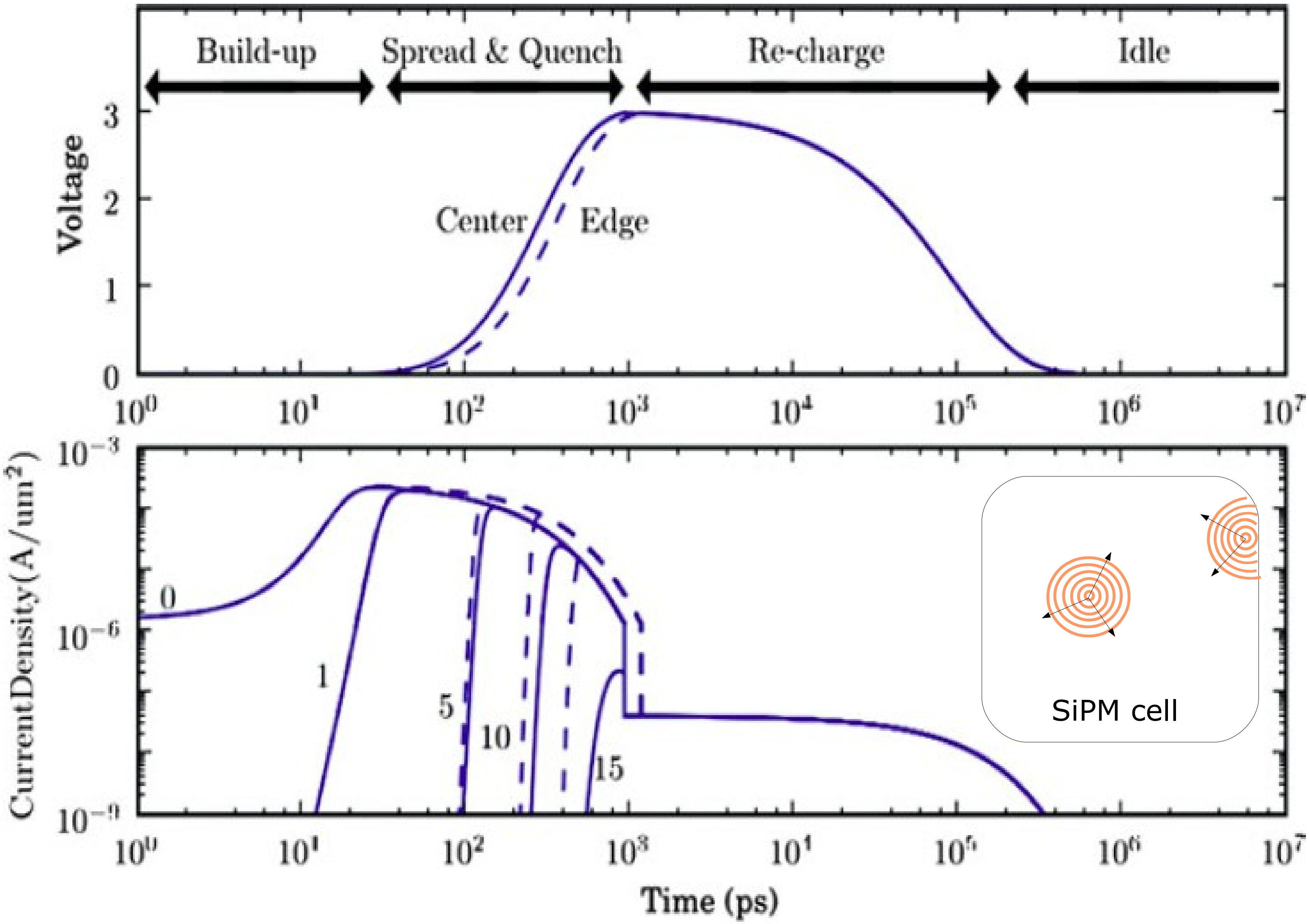

Slower growth at GAPD cell edges → larger cells ↔ larger jitter

Timing jitter: prompt and delayed components

1) Prompt component: gaussian with time scale O(100ps)

Statistical fluctuations in the avalanche:

- **Longitudinal** build-up (minor contribution)
- **Transversal** propagation (main contribution)

  - via multiplication assisted diffusion (dominating in few μm thin devices)
    A.Lacaita et al. APL and El.Lett. 1990

  - via photon assisted propagation (dominating in thick devices – O(100μm))
    PP.Webb, R.J. McIntyre RCA Eng. 1982
    A.Lacaita et al. APL 1992

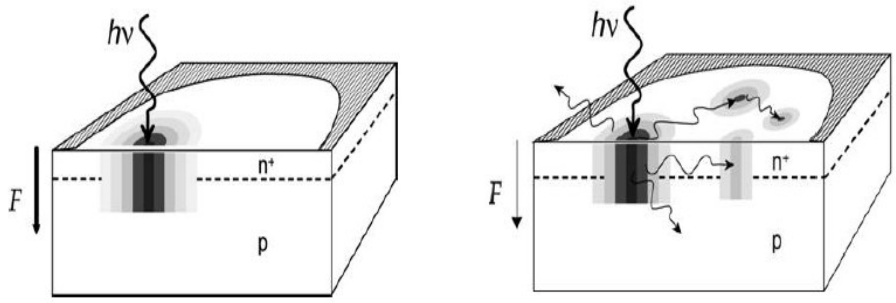

Multiplication assisted diffusion

Photon assisted propagation

Fluctuations due to
a) impact ionization statistics

b) variance of longitudinal position of photo-generation: finite drift time even at saturated velocity
note: saturated ve ~ 3 vh
(n-on-p are faster in general)

→ Jitter at minimum → **O(10ps)**
(very low threshold → not easy)

Fluctuations in shock-wave due to
c) variance of the transverse diffusion speed v_{diff}

d) variance of transverse position of photo-generation: slope of current rising front depends on transverse position

→ Jitter → **O(100ps)**
(usually threshold set high)

Timing jitter: prompt and delayed components

2) delayed component: non-gaussian tails with time scale O(ns)

Carriers photo-generated in the neutral regions above/beneath the junction and reaching the electric field region by diffusion

G.Ripamonti, S.Cova Sol.State Electronics (1985)

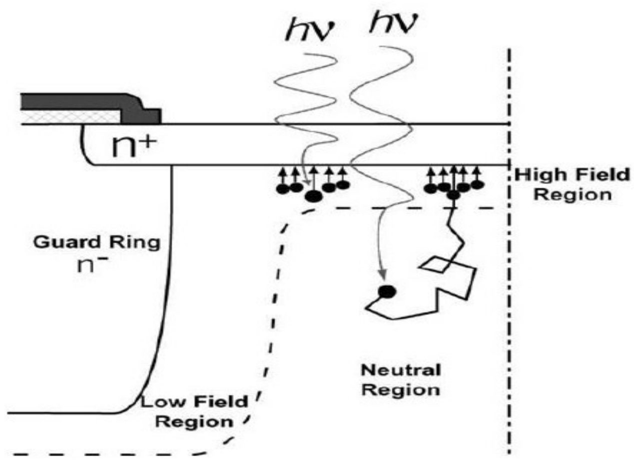

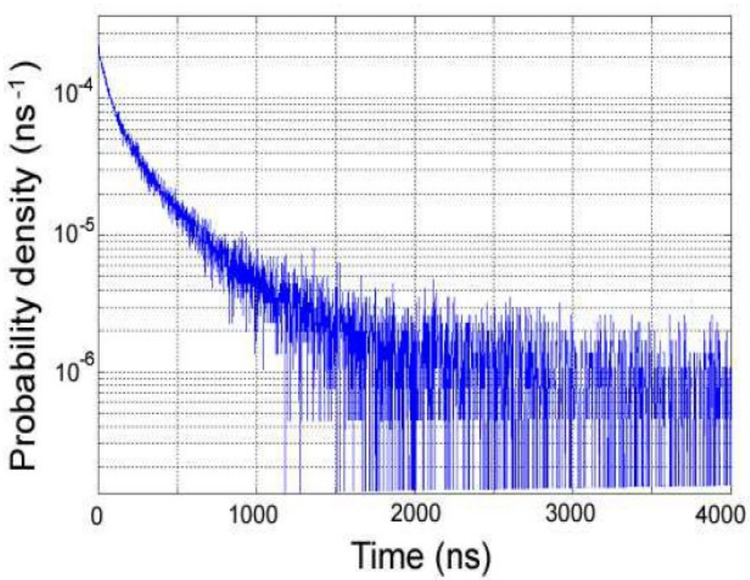

tail lifetime: $\tau \sim L^2 / \pi^2 D$ ~ up to some ns
L = effective neutral layer thickness
D = diffusion coefficient

S.Cova et al. NIST Workshop on SPD (2003)

→ **Neutral regions** underneath the junction : timing tails for long wavelengths
→ **Neutral regions** in APD entrance: timing tails for short wavelengths

Question: how to perform timing characterization

Example of experimental setup

Measurements - experimental setup

Pump Laser
Millenia V (Spectra-physics)
solid state CW visible laser

Crystal for Second Harmonic Generation (SHG)
conversion 800 nm → 400 nm
efficiency at % level

Low noise LV suppliers

Dark box

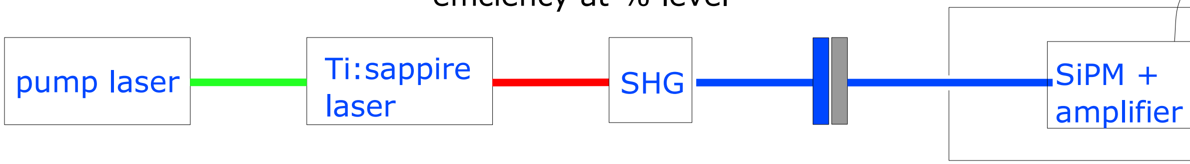

LeCroy SDA 6020

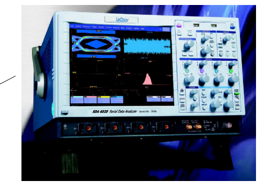

Analog bandwidth: 6GHz
Sampling rate: 20GS/s
Vertical resolution: 8 bits

External trigger from Ti:sapphire laser signal

Filters
blue + neutral
for rejecting IR light and tune intensity

Mode-locked Ti:sapphire Laser
Tsunami (Spectra-physics)
femtosecond pulsed laser

wavelength: tuned at 800±15 nm
pulse width: ~ 60 fs FWHM
pulse period: ~ 12 ns
pulse timing jitter < 100 fs

Electronics
I → V conversion via R_L (500Ω)
Two stage voltage amplification (= x50) based on high-bandwidth low-noise RF amplifier: gali-5 (MiniCircuits)
Z_{in} = 50Ω

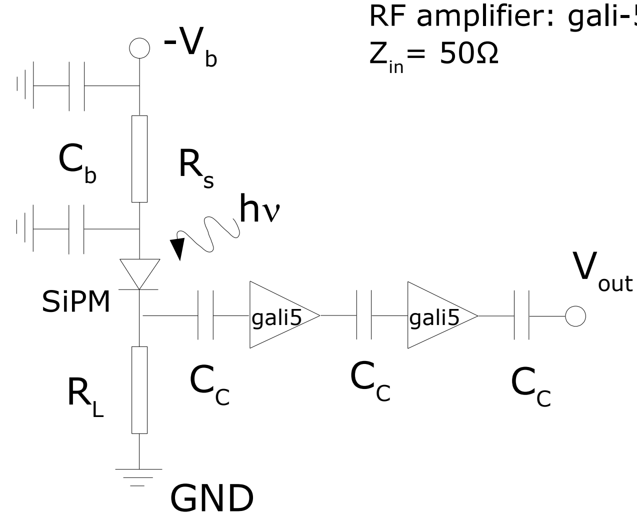

Data taking conditions:
- different V_{bias}
- both at 800 nm and 400 nm
- with different light intensities (counting rates in the range 10÷20 Mhz ie 15÷30 KHz per single cell)

Waveform analysis: optimum timing filter

Example of intrinsic SPTR measurement from Δt of consecutive pulses by laser shots

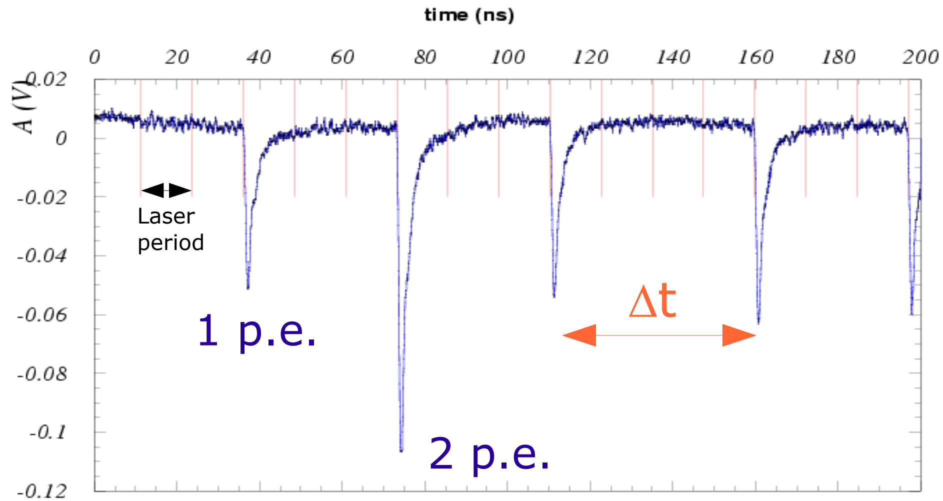

Different algorithms to reconstruct the time of the pulses:

✗ parabolic fit to find the peak maximum
✗ CFD (digital)
✗ average of time samples weighted by the waveform derivative
✔ digital filter: weighting by the derivative of a reference signal
→ optimum against (white) noise (if signal shape fixed)

G.C. et al NIMA 581 (2007) 461

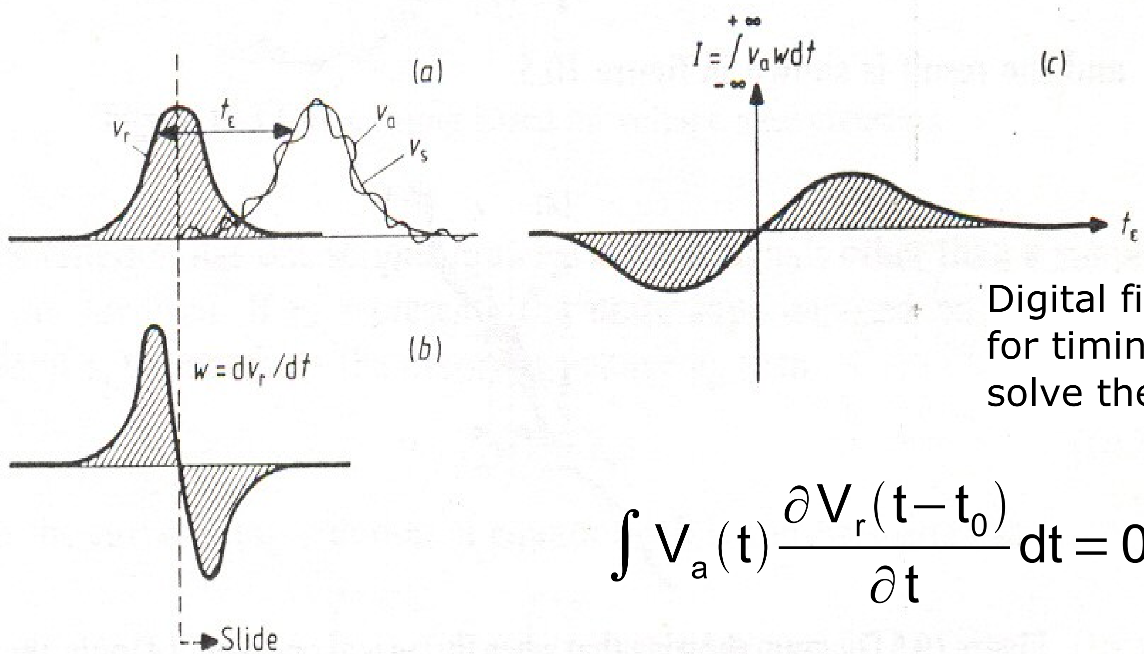

Digital filter to minimize N/S for timing measurements: solve the following equation on t_0 :

$$\int V_a(t) \frac{\partial V_r(t - t_0)}{\partial t} dt = 0$$

Va = measured signal (includes noise)
Vr = reference signal
t_0 = reference time

see e.g. Wilmshurst "Signal recovery from noise in electronic instrumentation"

Timing fluctuations

- **SiPM are intrinsically very fast**

Two timing components (related to avalanche developement)
1) prompt → gaussian time jitter well below **100ps** (depending on ΔV, and λ)
2) delayed → non-gaussian tails up to **few ns** (depending on λ)

- **Models and Simulations**

- **Measurements**

- **Optimization of devices for timing**

  → use of fast signal shape component
  → use waveform, it's better than CFD and … don't use ToT

- **Timing with scintillators**

Single photon pulse shape (Rising and falling edges)

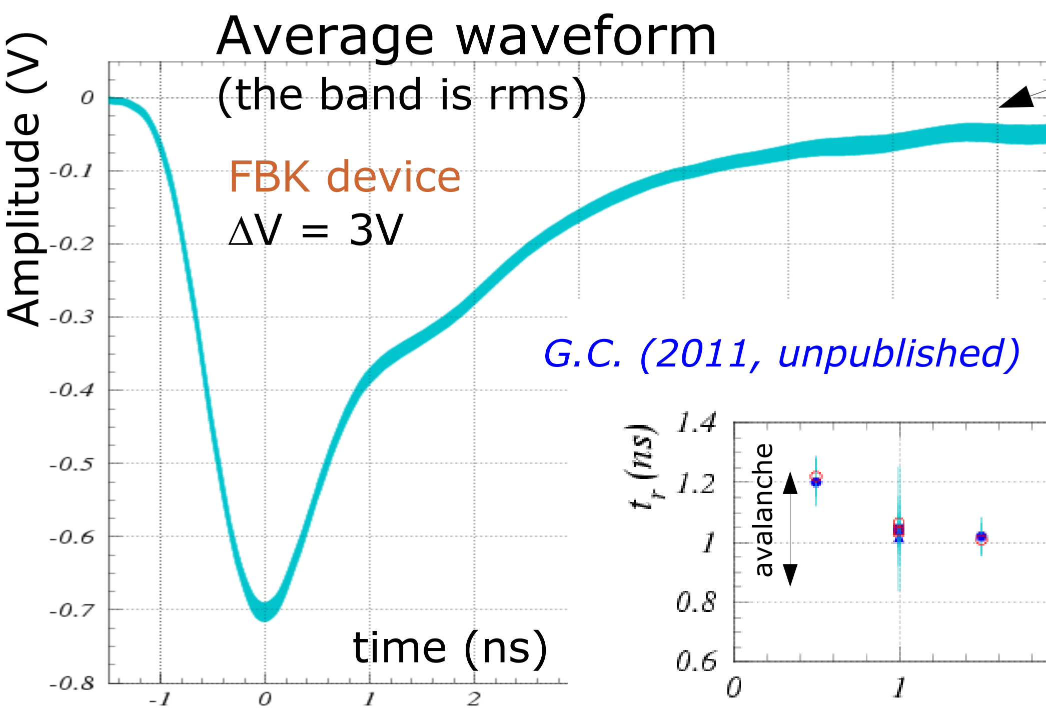

Additional contribution to rms (after-pulses)

Rise time (10%-90%)
(dominated by electronics contribution)

G.C. (2011, unpublished)

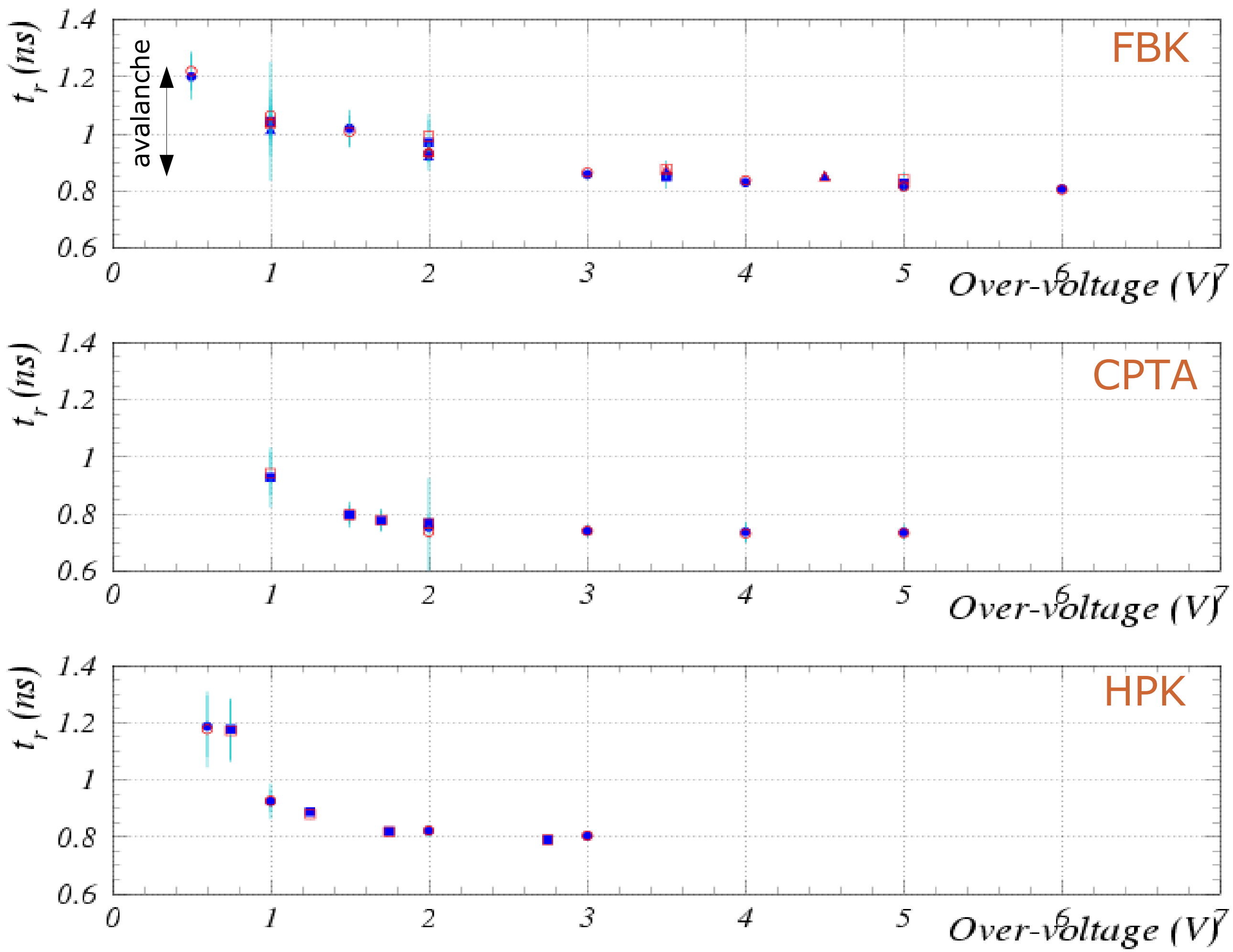

Reminder:

$$\frac{dI}{dt} \sim \frac{\sqrt{D}}{R_{sp}\sqrt{\tau}}$$

$$\tau \sim \frac{1}{1-(E_{max}/E_{breakdown})^n}$$

For comparison about rise-time of HKP devices see P.Avella et al doi:10.1016/j.nima.2011.11.049

Single photon pulse shape (Rising and falling edges)

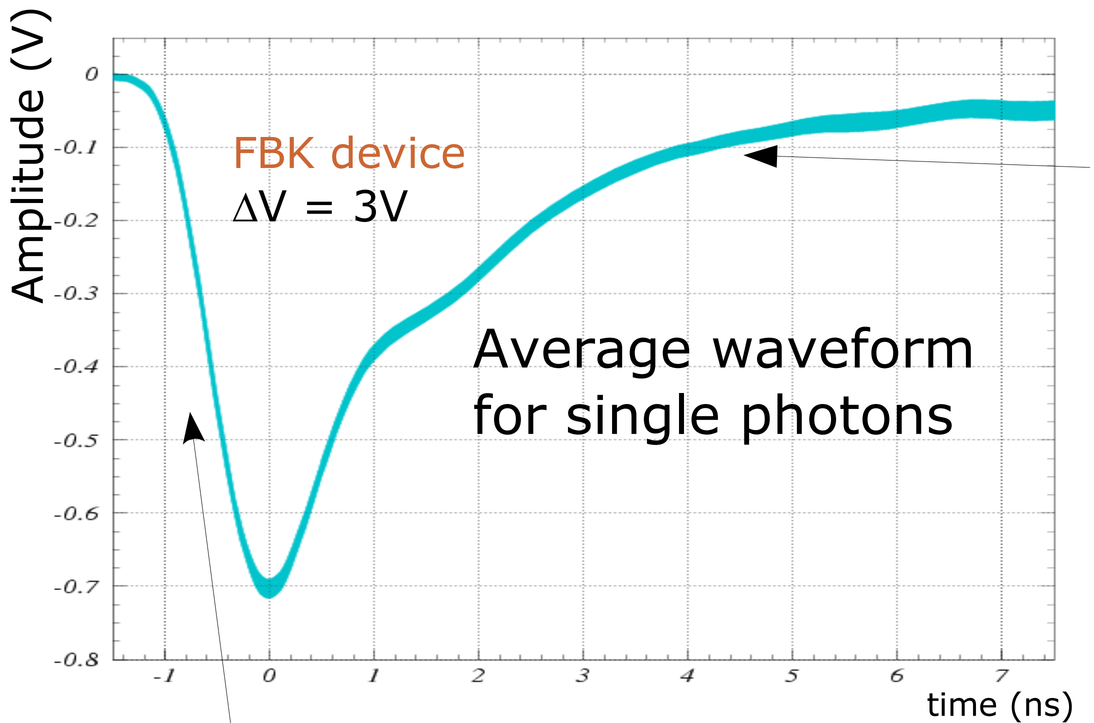

Falling signal shape fluctuates considerably (due eg to after-pulses) → signal tail is non useful for timing, if not detrimental

note: using Time-over-Threshold method for slew correction might lead to worse resolution

Reminder:

$$\begin{cases} \frac{dI}{dt} \sim \frac{\sqrt{D}}{R_{sp}\sqrt{\tau}} \\ \tau \sim \frac{1}{1-(E_{max}/E_{breakdown})^n} \end{cases}$$

Rise-time depends on **ΔV**, **T** and **impact position**
ie **signal shape is not constant**, then:
1) CFD method only partially effective in canceling time walk effects
2) any digital timing filter should account for shape variations (ΔV, T)

For comparison about waveform method and various digital algorithms
see Ronzhin et al NIM A 668 (2012) 94

Single Photon Time Resolution = gaussian + tails

Time resolution of SiPM is not just a gaussian, but gaussian + tails
(in particular at long wavelengths)

G.C. et al NIMA 581 (2007) 461

Gaussian + Tails (long λ)

rms ~ 50-100 ps ~ exp (-t / O(ns))

contrib. several % for long wavelengths

Data at **λ=400nm**

A simple **gaussian component** fits fairly

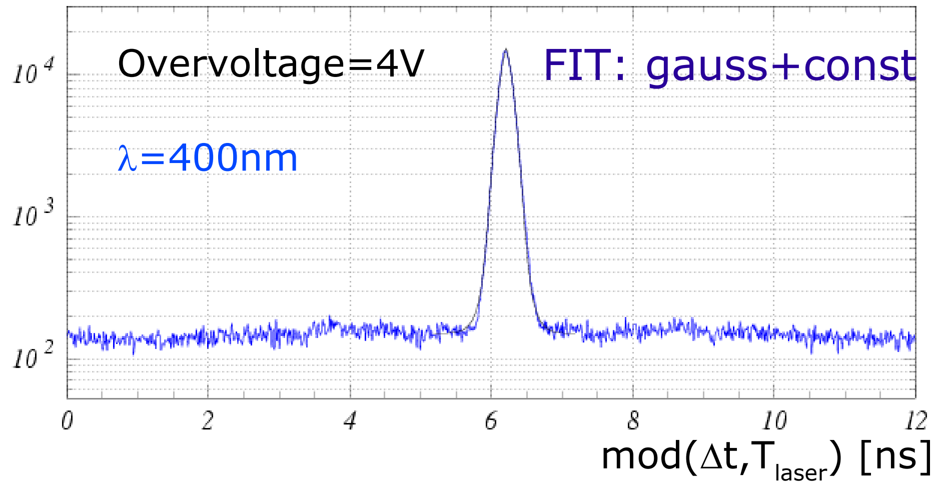

Data at **λ=800nm**

fit gives reasonable χ^2 in case of an **additional exponential term** exp(-|Δt|/τ) summed with a weight

- **τ ~ 0.2÷0.8ns** (depending on device) in rough agreement with diffusion tail lifetime: $\tau \sim L^2 / \pi^2 D$ where L is the diffusion length
- Weight of the **exp. tail ~ 10%÷30%** (depending on device)

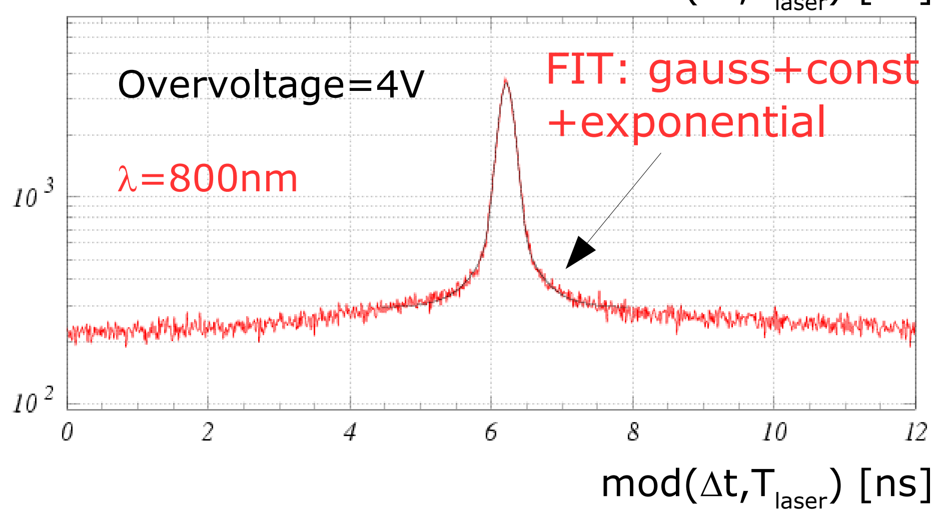

Distributions of the difference in time between successive peaks

SPTR: FBK devices – shallow junction

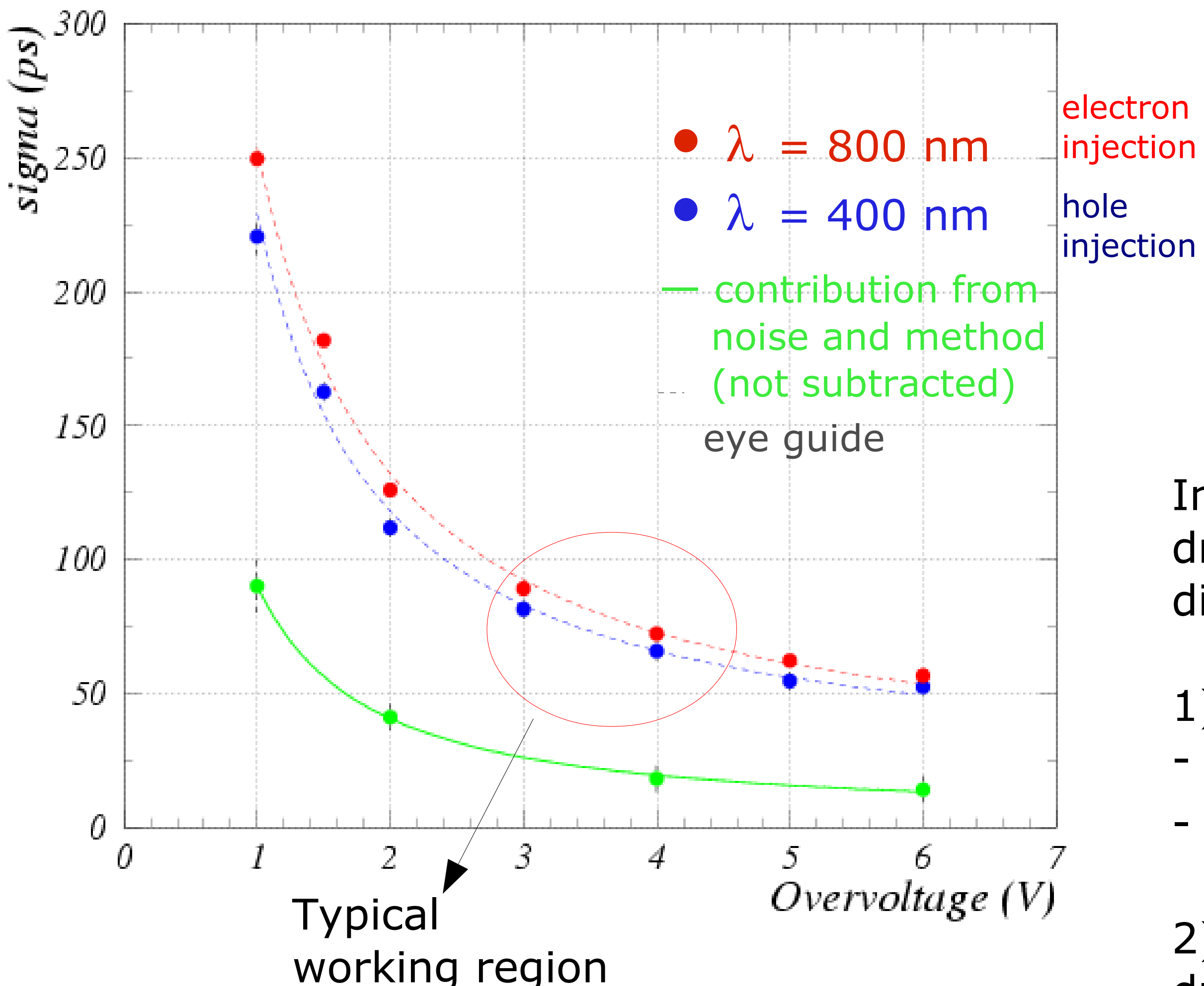

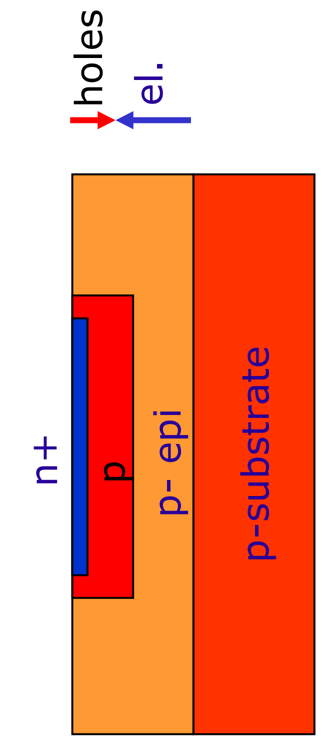

G.C. et al NIMA 581 (2007) 461

In general due to drift, resolution differences

1) high field junction position
- shallow junction: $\sigma_t^{red} > \sigma_t^{blue}$
- buried junction: $\sigma_t^{red} < \sigma_t^{blue}$

2) n^+-on-p smaller jitter than p^+-on-n due to electrons drifting faster in depletion region (but λ dependence)

3) above differences more relevant in thick devices than thin

NOTE: good timing performances kept up to 10MHz/mm² photon rates

SPTR: Hamamatsu

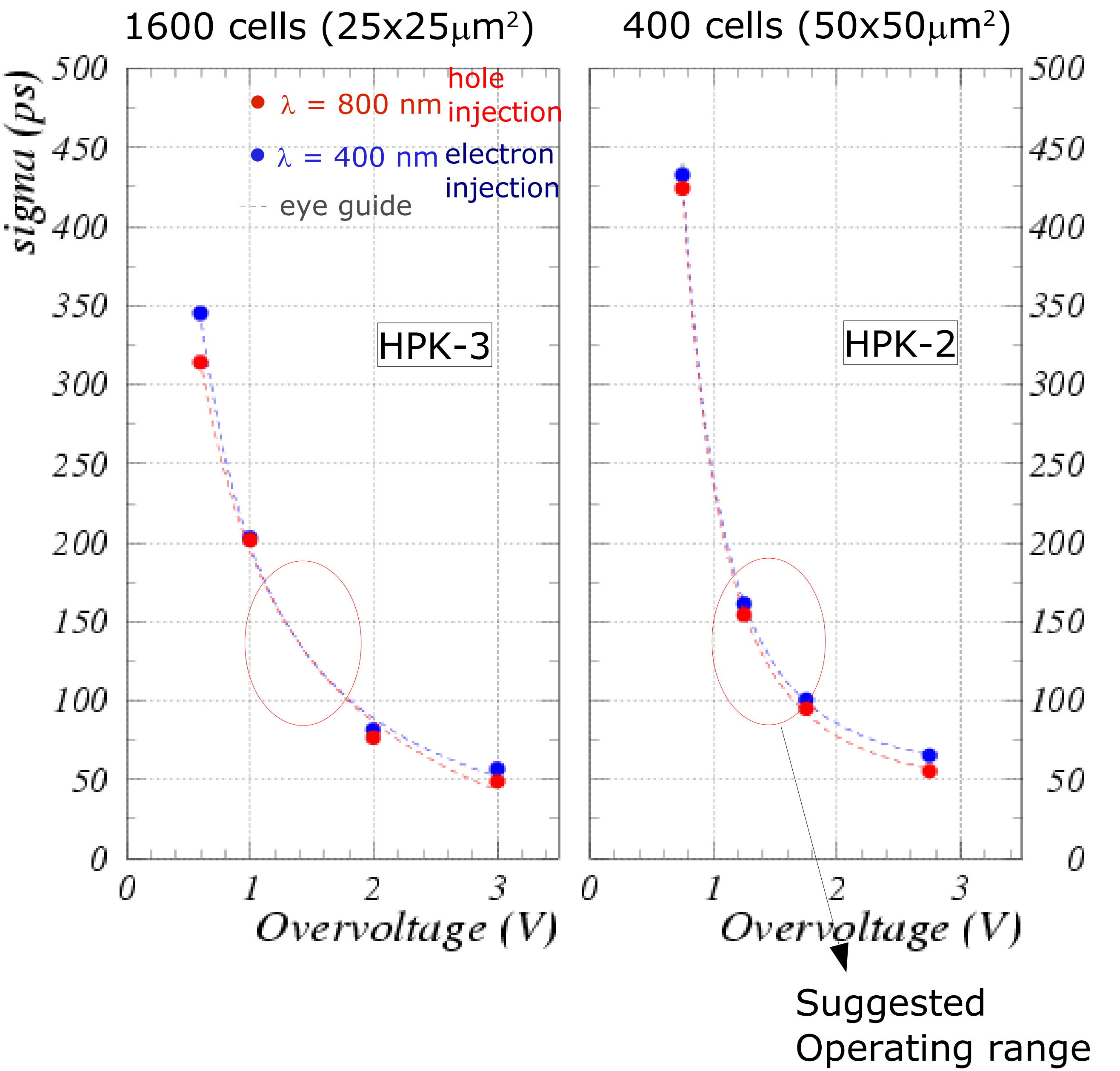

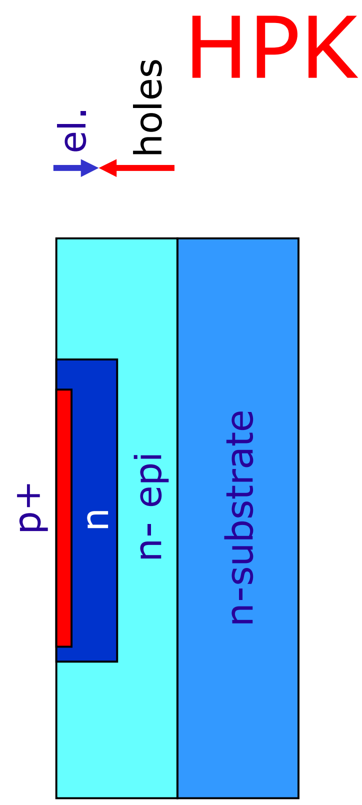

SPTR: CPTA/Photonique – thick structures

a) Green-Red sensitive
SSPM 050701GR_TO18

b) Blue sensitive
SSPM 050901B_TO18

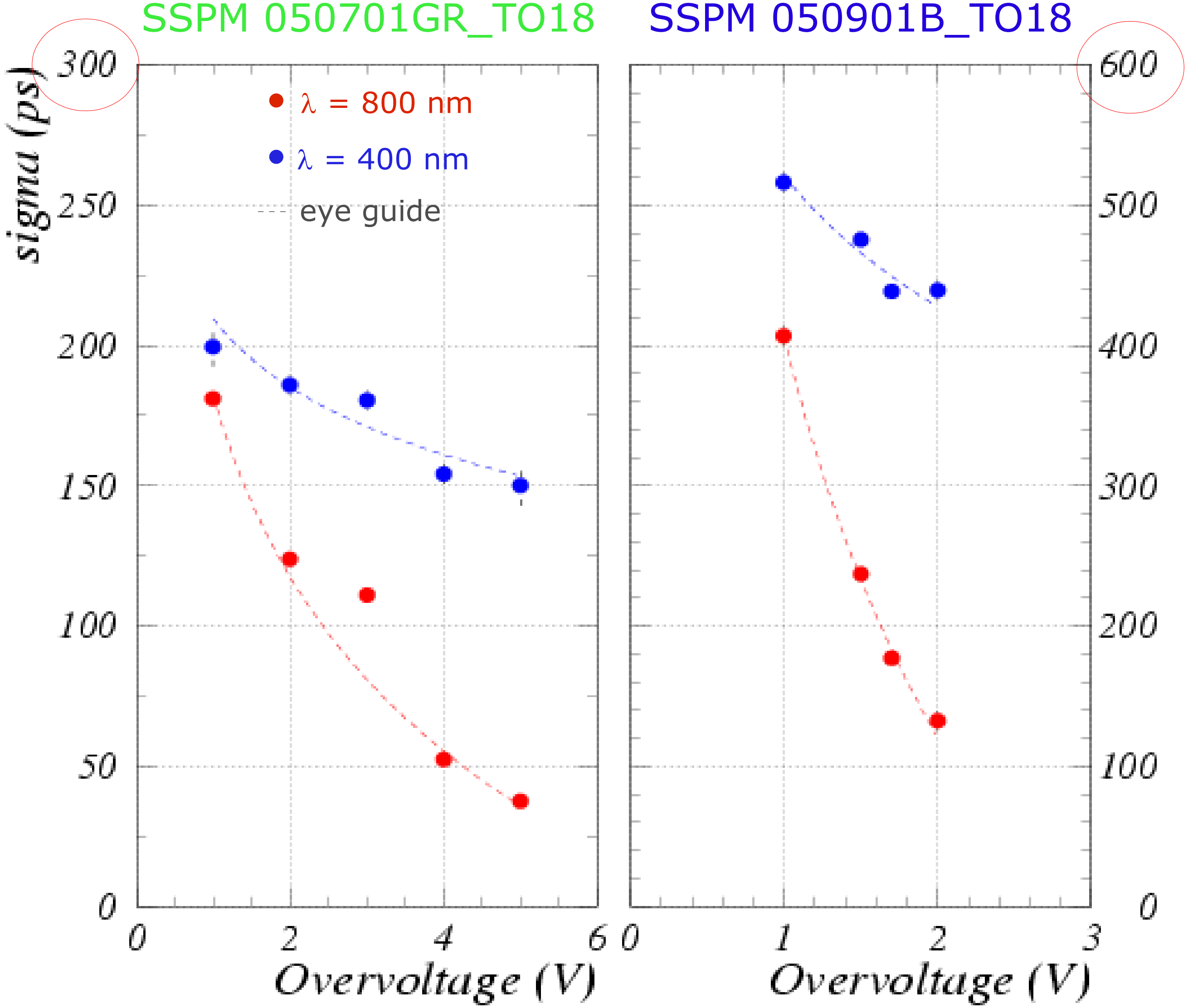

- thick structures
- deep junctions

a) n^+-on-p
→ electrons drift

b) p^+-on-n
→ holes drift ($v_e/3$)

Many photons (simultaneous)

Dependence of SiPM timing on the number of simultaneous photons

Poisson statistics: $\sigma_t \propto 1/\sqrt{N_{pe}}$

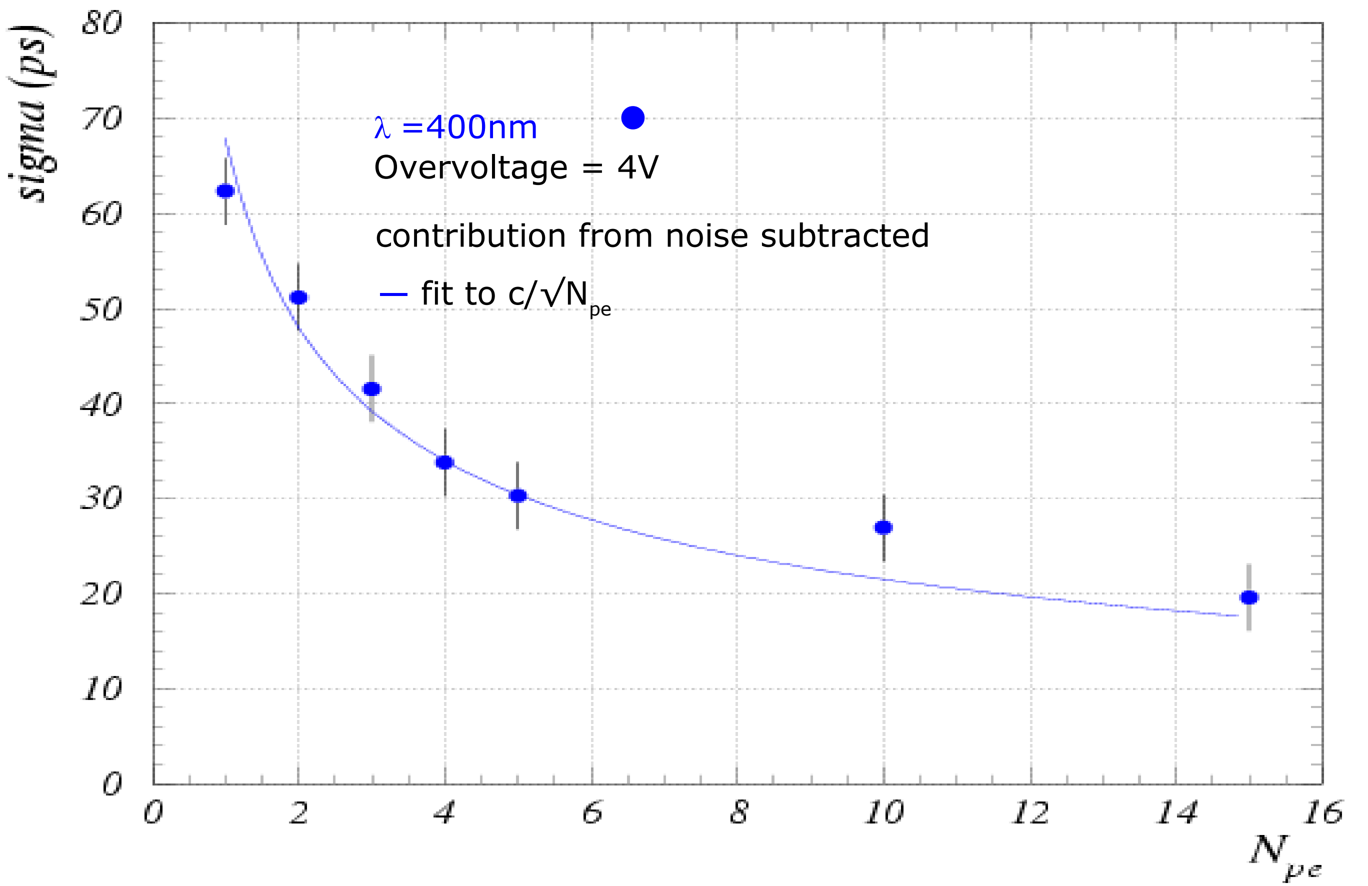

N of simultaneous photo-electrons

dSiPM timing resolution

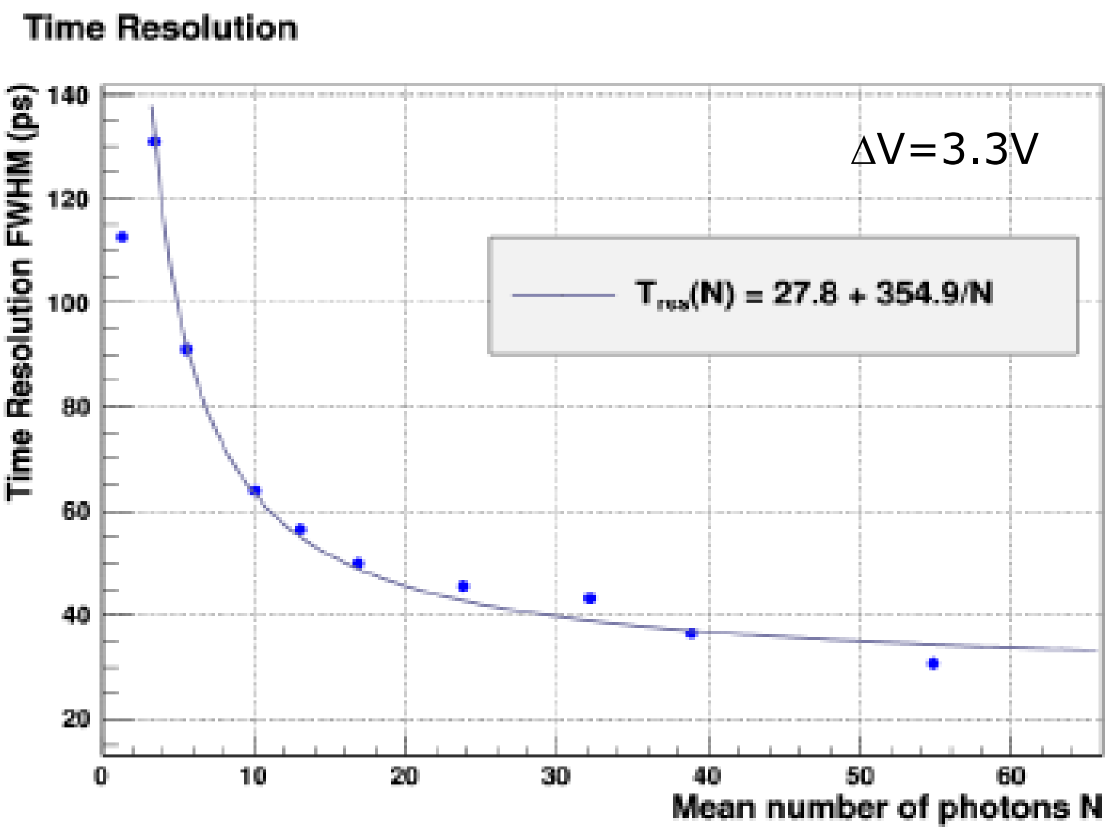

T.Frach at LIGHT 2011

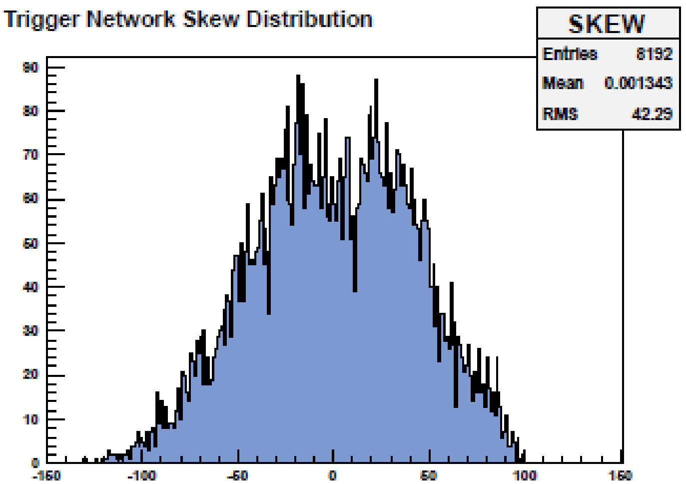

- Sensor triggered by attenuated laser pulses at first photon level
- Laser pulse width: 36ps FWHM, λ = 410nm
- Contribution to time resolution (FWHM):

SPAD: 54ps, trigger network: 110ps, TDC: 20ps

- Trigger network skew currently limits the timing resolution

SPTR: position dependence → cell size

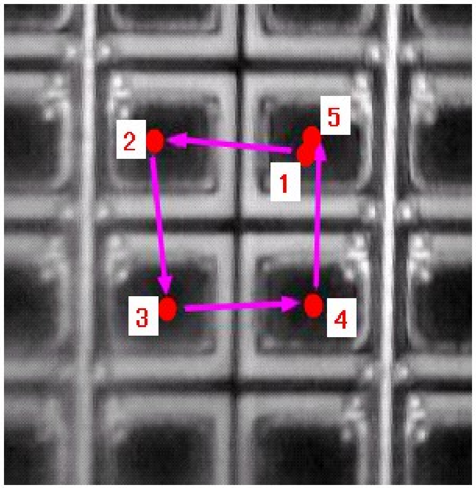

	FWHM (ps)	FWTM (ps)
1	199	393
2	197	389
3	209	409
4	201	393
5	195	383

K.Yamamoto PD07

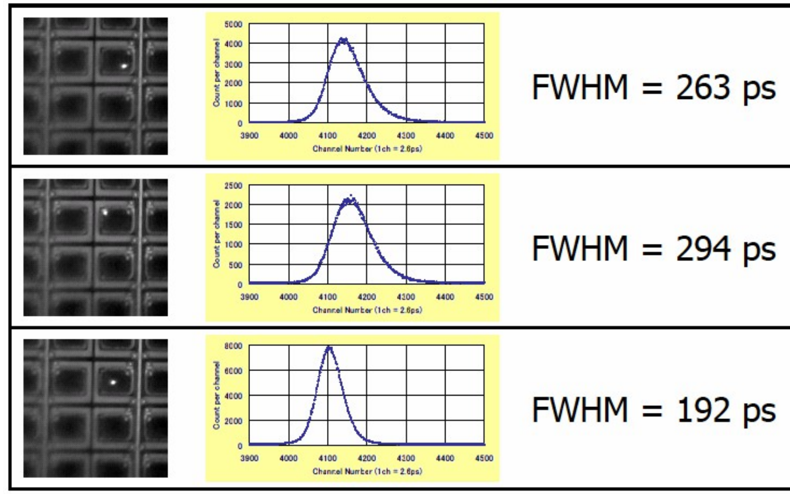

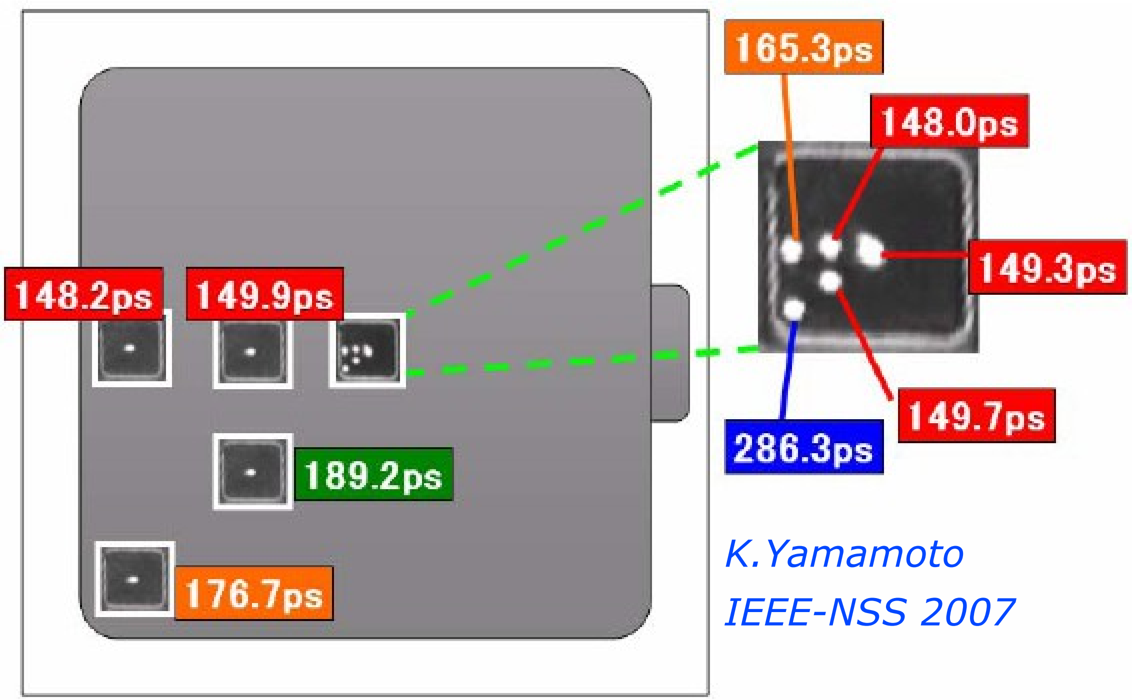

K.Yamamoto
IEEE-NSS 2007

Larger jitter if photo-conversion at the border of the cell

Due to:
1) slower avalanche front propagation

2) lower E field at edges

→ cfr PDE vs position

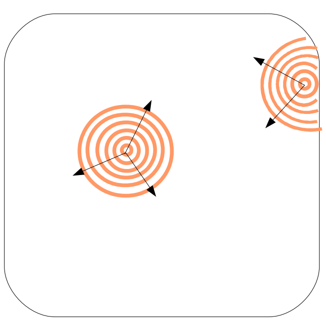

Data include the system jitter (common offset, not subtracted)

SPTR: timing at low T

Timing: improves at low T

Lower jitter at low T due to **higher mobility**: → a) avalanche process is faster
b) reduced fluctuations

(Over-voltage fixed)

Note:

$$\frac{dI}{dt} \sim \frac{\sqrt{D}}{R_{sp}\sqrt{\tau}}$$

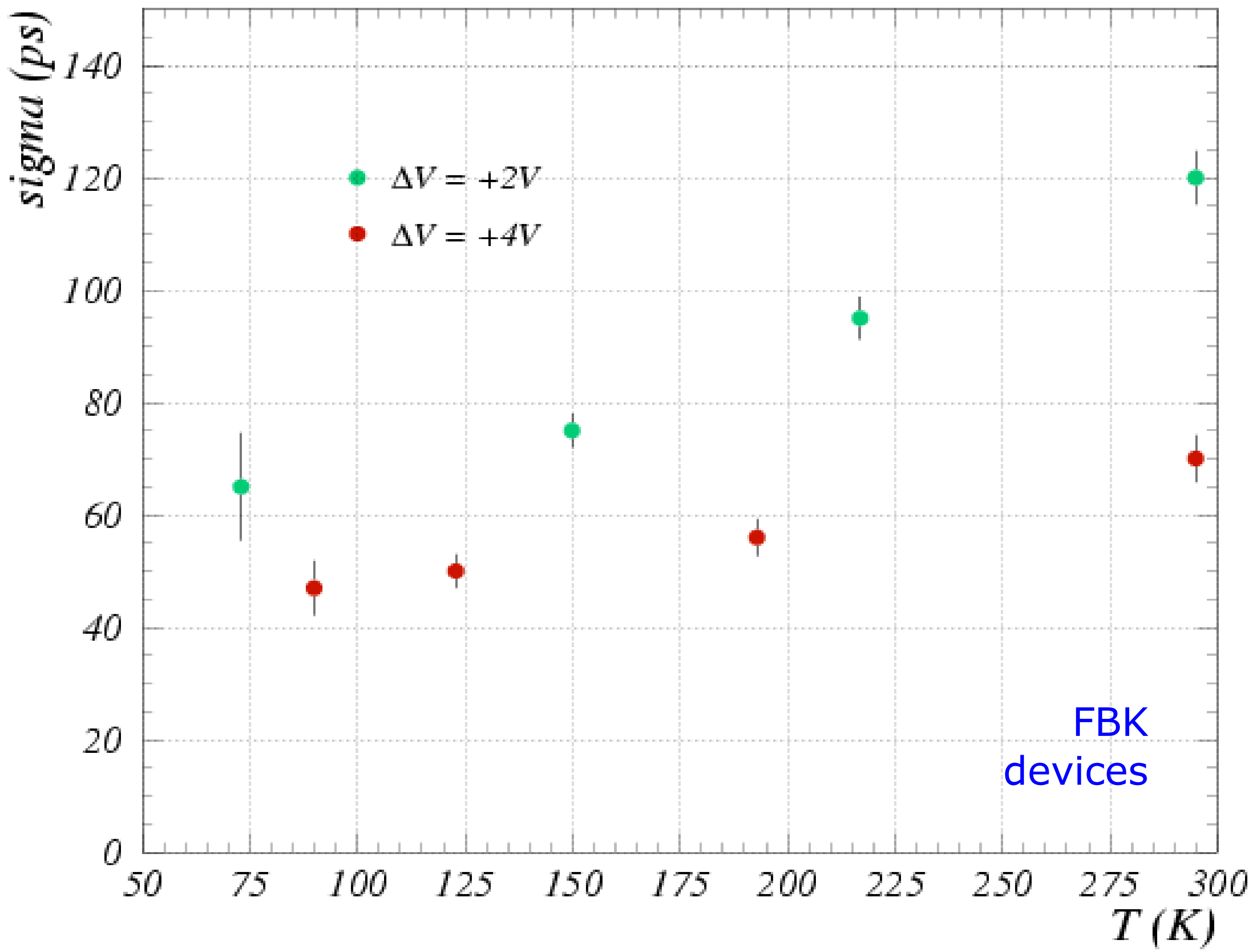

G.C. (2011, unpublished)

Timing fluctuations

- **SiPM are intrinsically very fast**

Two timing components (related to avalanche developement)
1) prompt → gaussian time jitter well below **100ps** (depending on ΔV, and λ)
2) delayed → non-gaussian tails up to **few ns** (depending on λ)

- **Models and Simulations**

- **Measurements**

- **Optimization of devices for timing**
  → PDE vs TIMING trade off
  → use of fast signal shape component
  → use waveform, it's better than CFD and … don't use ToT

- **Timing with scintillators**

PDE vs timing trade off / optimization

C.H.Tan et al IEEE J.Quantum Electronics 13 (4) (2007) 906

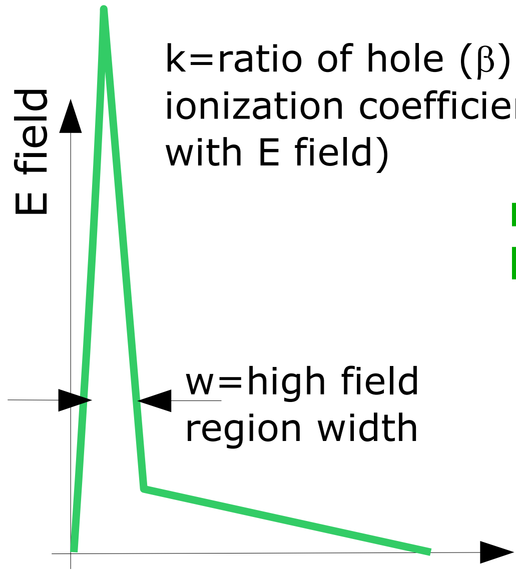

k=ratio of hole (β) to electron (α) ionization coefficient (increasing with E field)

narrow avalanche region, high E:
- **small w**
- **high k = β / α**

better for **TIMING**

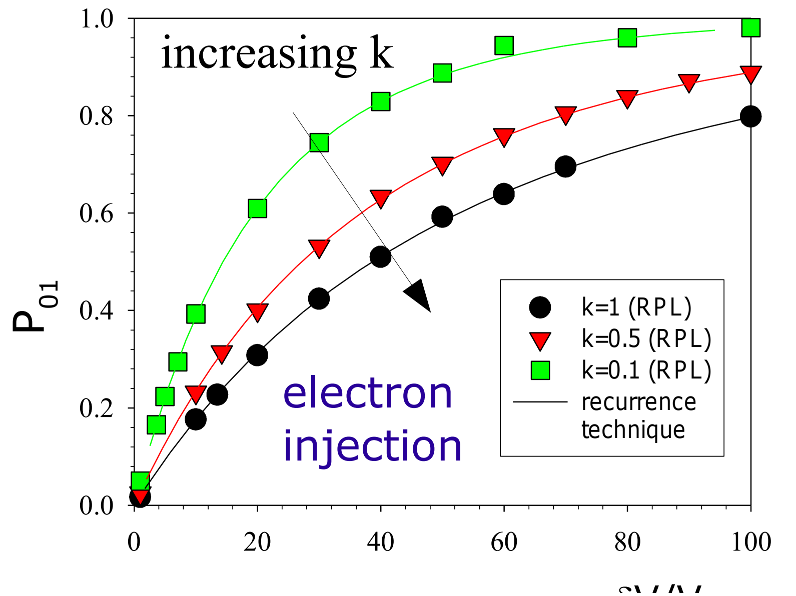

better for **PDE**

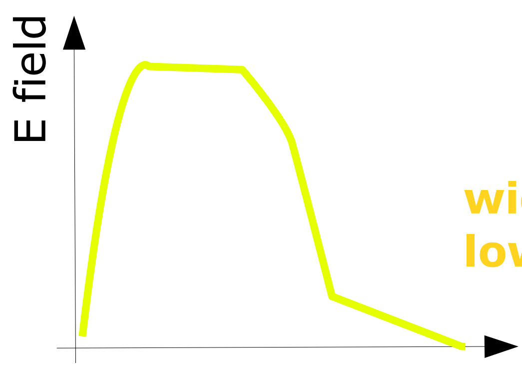

wide avalanche region, low E:
- **wide w**
- **small k = β / α**

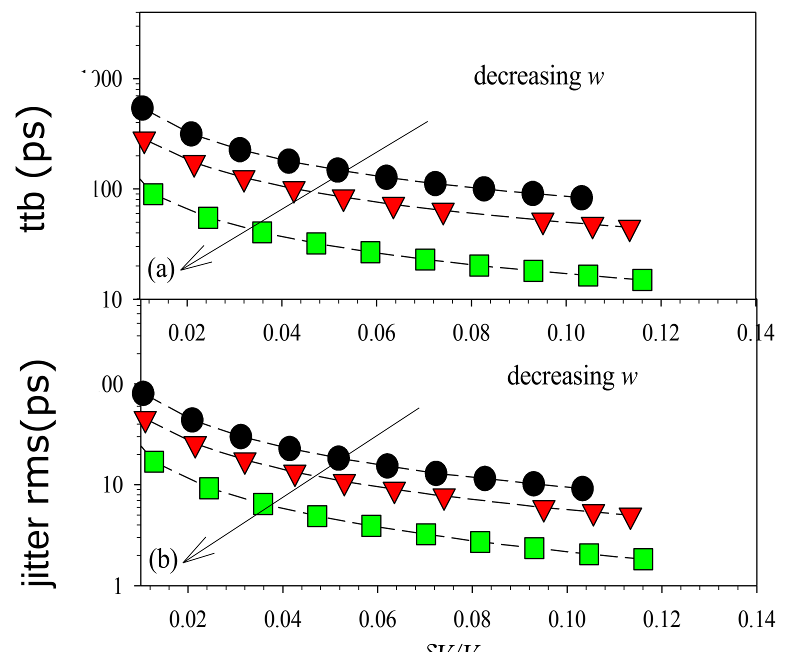

plots: courtesy of C.H.Tan

PDE vs timing trade off / optimization

C.H.Tan et al IEEE J.Quantum Electronics 13 (4) (2007) 906

k=ratio of hole (β) to electron (α) ionization coefficient (increasing with E field)

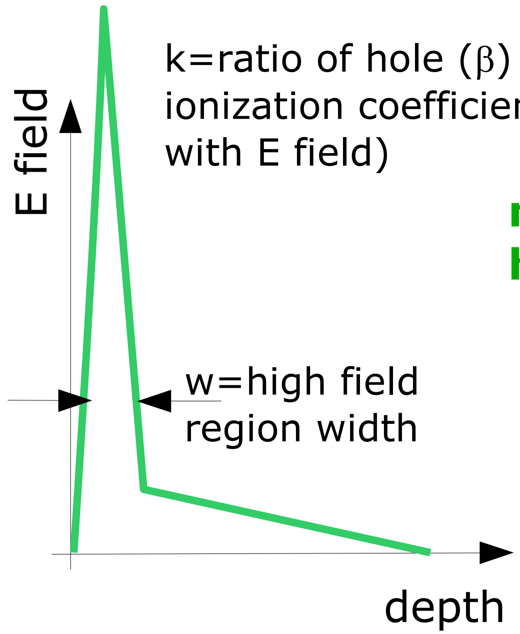

narrow avalanche region, high E:
- **small w**
- **high k = β / α**

better for **TIMING**

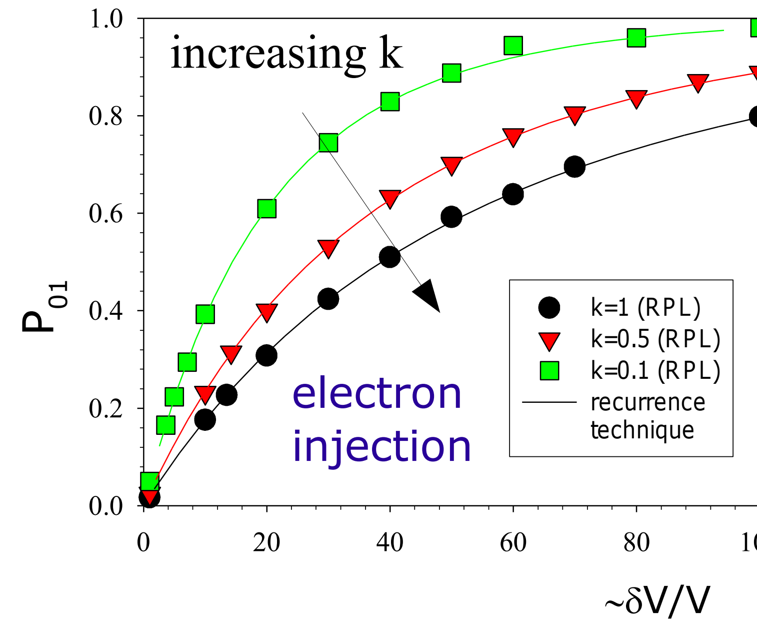

better for **PDE**

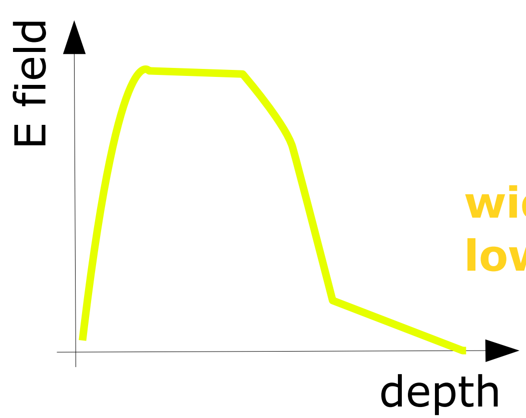

wide avalanche region, low E:
- **wide w**
- **small k = β / α**

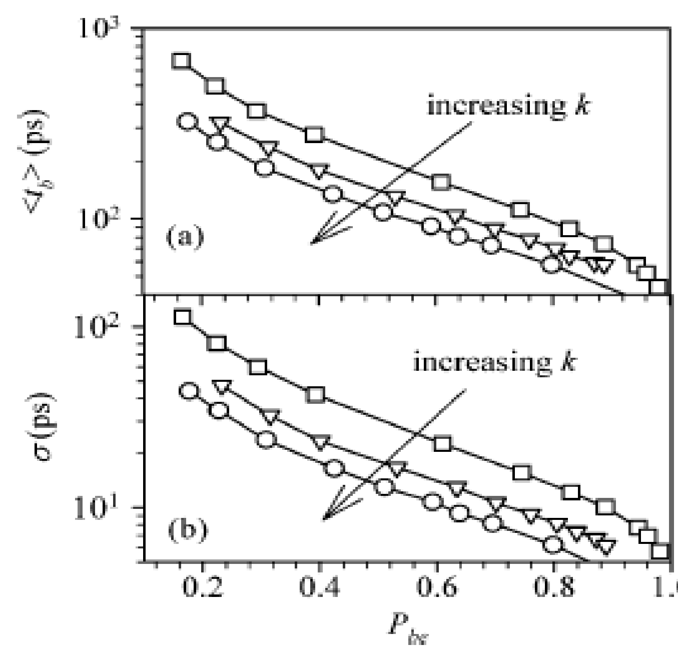

RPL model: example of fast simulation

"Statistics of Avalanche Current Buildup Time in Single-Photon Avalanche diodes"
C.H.Tan, J.S.Ng, G.J.Rees, J.P.R.David (Sheffield U.)
IEEE J.Quantum Electronics 13 (4) (2007) 906

Numerical model (MC): Random distribution of impact ionization Path Length (RPL)

Analysis of breakdown probability, breakdown time and timing jitter as functions of avalanche region width (w), ionization coefficient ratio ($k=\beta_{hole}/\alpha_{electron}$) and dead space parameter (d) (uniform E field, constant carrier velocity)

1) increasing k:
- improves timing performances
- but breakdown probability P_{br} increases slowly with overvoltage

1a) hole injection results in better timing than electron injection (in Si devices)

2) dead space effects worsen timing performances (the more at small k)
Important for devices with small w

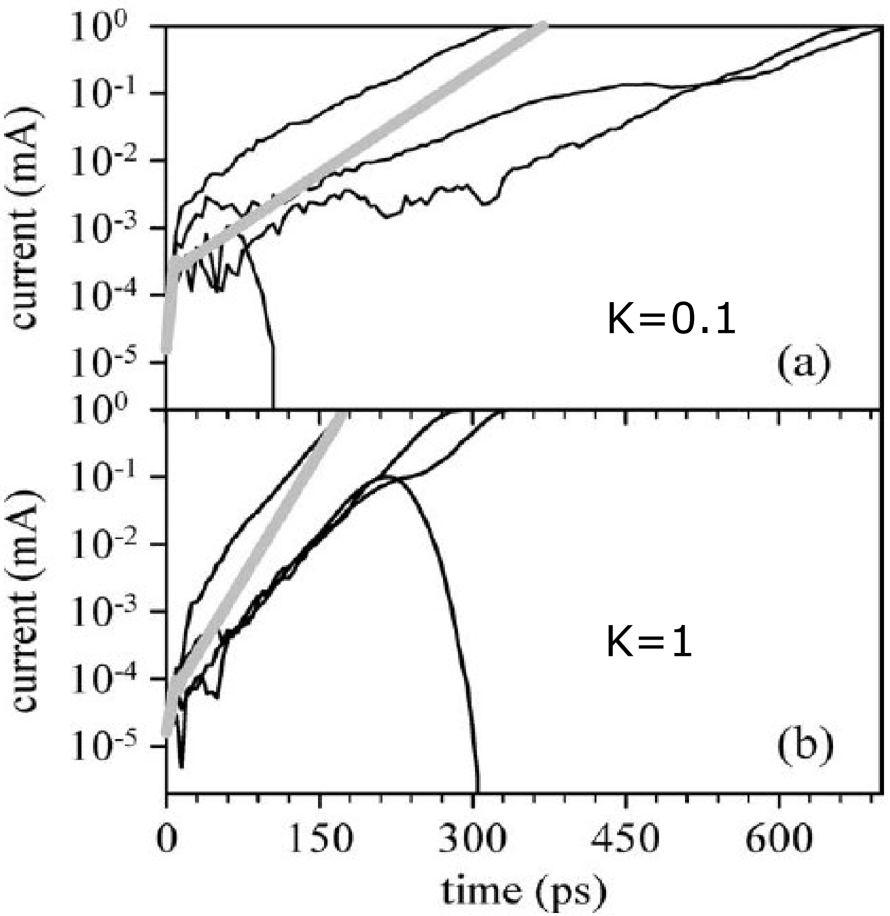

Geiger Mode Avalanche (crude picture)

APD below breakdown (already discussed)
Total avalanche duration depends on the carrier group
If k large: feedback effect is strong → long multiplication chain

...You need to "wait" to collect all the new carriers created in order to achieve the high avalanche gain...

APD Geiger Mode
We are only interested in those events that reach a certain current threshold (breakdown definition). Such interesting multiplication events have current growing after a few transit times
If k large: the rate that this current grows is faster → short mean time to breakdown and smaller timing jitter

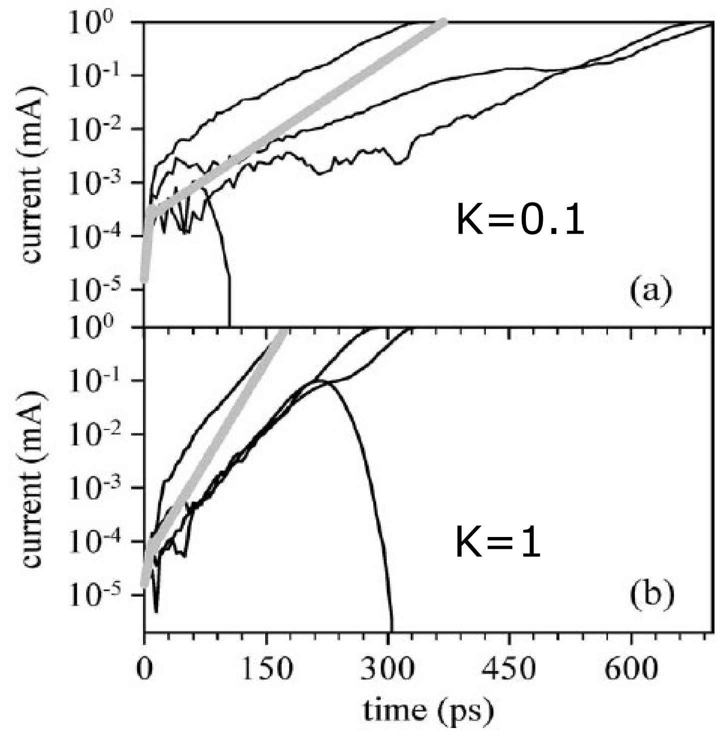

Large variability in mean current evolution (corresponding to large multiplication fluct.): the mean current:

- either decay to zero
- stay at close to a constant value
- rapidly reach breakdown

→ number of events that reach breakdown is smaller → need to increase V_{bias}

Optimizing signal shape for timing

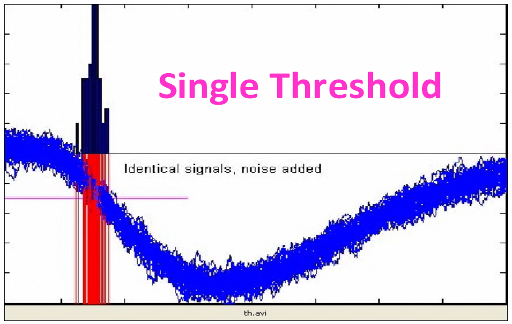

Timing by (single) threshold:

→ time spread proportional to 1/rise-time and noise

$$\sigma_{time} = \frac{\sigma_{amplitude}}{\frac{df(t)}{dt}}$$

Timing with optimum filtering:

→ best resolution with f'(t) weighting function

$$\sigma^2_{time} = \frac{\sigma^2_{amplitude}}{\int dt \left[\frac{df(t)}{dt}\right]^2}$$

Pulse sampling and Waveform analysis:

Sample, digitize, fit the (known) waveform
→ get time and amplitude

$$\sigma^2_{time} = \frac{\sigma^2_{amplitude}}{N_{samples} \int dt \left[\frac{df(t)}{dt}\right]^2}$$

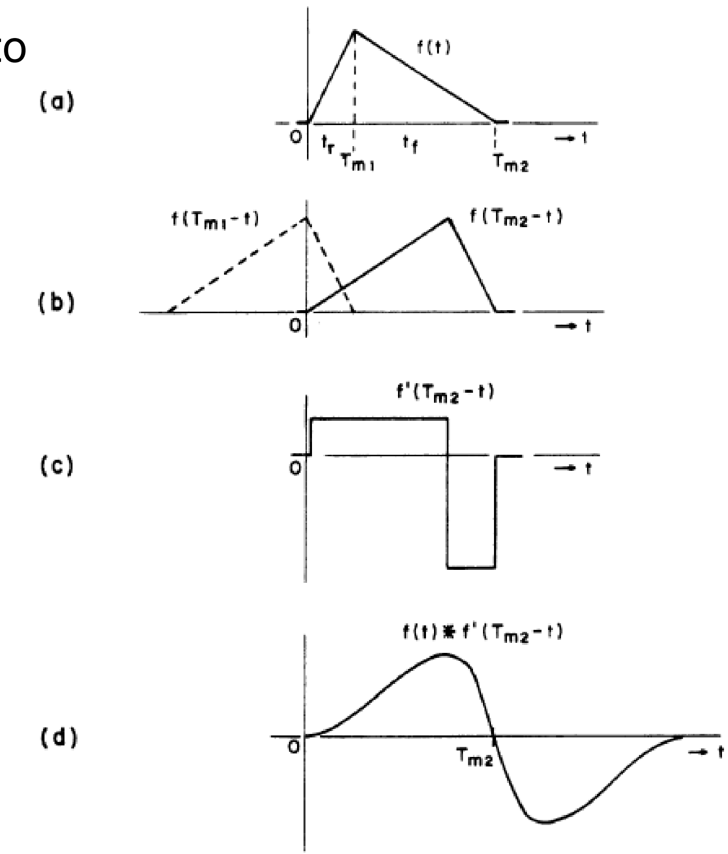

Fig. 7. Optimum filter for timing in presence of white noise (method of derivation).
(a) signal waveform
(b) optimum filter for amplitude measurements.
(c) optimum filter for timing - derivative of (b).
(d) output waveform.

V.Radeka IEEE TNS 21 (1974)...

Optimizing signal shape for timing

Single cell model → $(R_d||C_d)+(R_q||C_q)$

SiPM + load → $(||Z_{cell})||C_{grid} + Z_{load}$

Signal = slow pulse $(\tau_{d\ (rise)}, \tau_{q\text{-slow}\ (fall)})$ +

+ fast pulse $(\tau_{d\ (rise)}, \tau_{q\text{-fast}\ (fall)})$

- $\tau_{d\ (rise)} \sim R_d(C_q+C_d)$
- $\tau_{q\text{-fast}\ (fall)} = R_{load}\ C_{tot}$ (fast; parasitic spike)
- $\tau_{q\text{-slow}\ (fall)} = R_q\ (C_q+C_d)$ (slow; cell recovery)

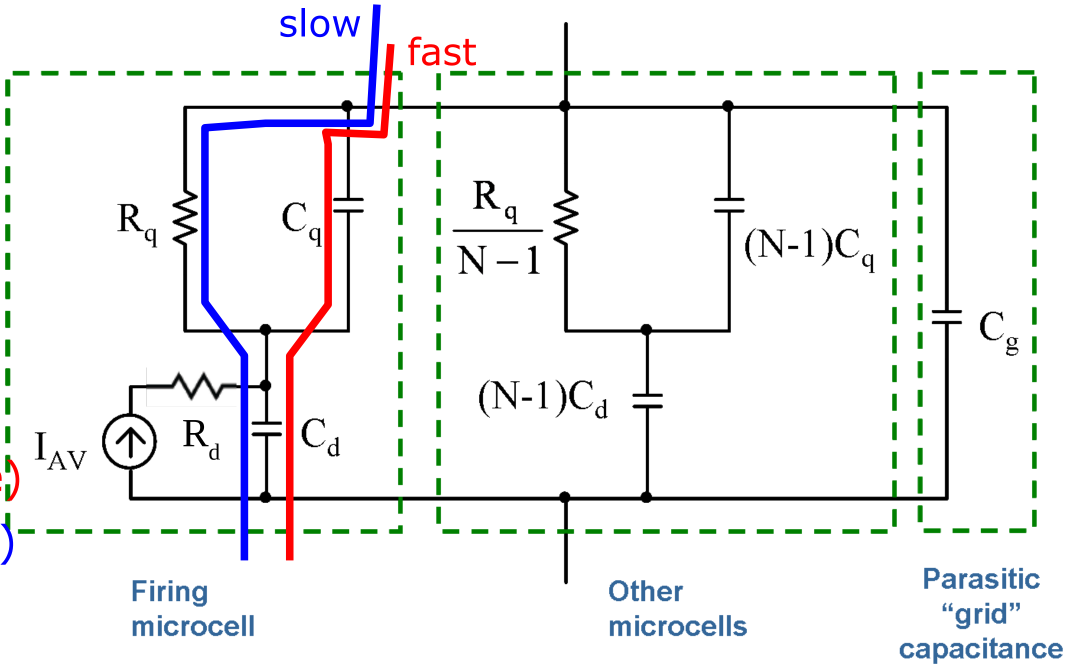

Pulse shape

$$V(t) \simeq \frac{Q}{C_q+C_d}\left(\frac{C_q}{C_{tot}} e^{\frac{-t}{\tau_{FAST}}} + \frac{R_{load}}{R_q}\frac{C_d}{C_q+C_d} e^{\frac{-t}{\tau_{SLOW}}}\right)$$

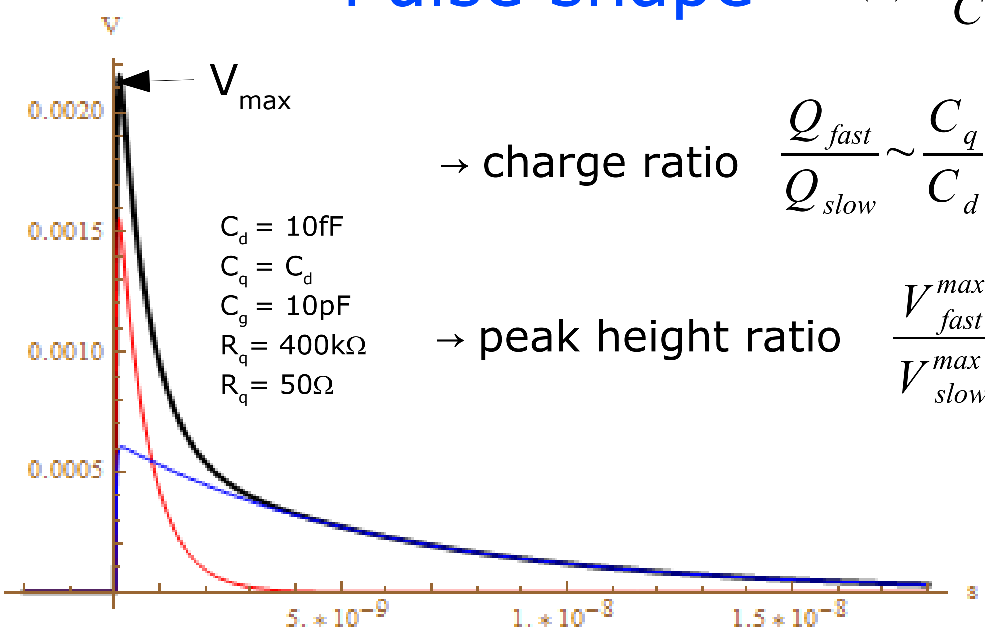

→ charge ratio $\frac{Q_{fast}}{Q_{slow}} \sim \frac{C_q}{C_d}$

→ peak height ratio $\frac{V_{fast}^{max}}{V_{slow}^{max}} \sim \frac{C_q^2 R_q}{C_d C_{tot} R_{load}}$

increasing with Rq and $1/R_{load}$ (and Cq of course)

Increasing C_q/C_d or/and R_q/R_{load}
→ spike enhancement
→ better timing

Pulse shape (reminder)

$$V(t) \simeq \frac{Q}{C_q+C_d}\left(\frac{C_q}{C_{tot}}\, e^{\frac{-t}{\tau_{fast}}} + \frac{R_{load}}{R_q}\frac{C_d}{C_q+C_d}\, e^{\frac{-t}{\tau_{slow}}}\right) = \frac{Q\,R_{load}}{C_q+C_d}\left(\frac{C_q}{\tau_{fast}}\, e^{\frac{-t}{\tau_{fast}}} + \frac{C_d}{\tau_{slow}}\, e^{\frac{-t}{\tau_{slow}}}\right)$$

Note: valid for low impedance load $R_{load} << Rq$

- $\tau_{fast} = R_{load}\ C_{tot}$
- $\tau_{slow} = R_q\,(C_q+C_d)$

→ gain $\quad G = \int dt \frac{V(t)}{q_e R_{load}} = Q/q_e = \frac{\Delta V\,(C_d+C_q)}{q_e}$ independent of R_q

→ charge ratio $\quad \frac{Q_{slow}}{Q_{fast}} \sim \frac{C_d}{C_q}$

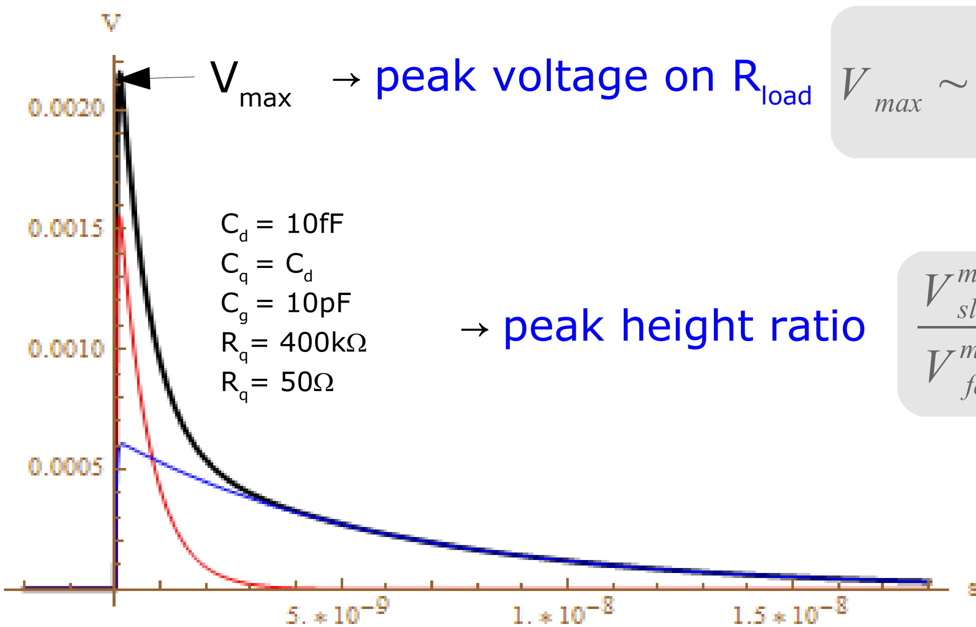

V_{max} → peak voltage on R_{load} $\quad V_{max} \sim R_{load}\left(\frac{Q_{fast}}{\tau_{fast}} + \frac{Q_{slow}}{\tau_{slow}}\right)$ dependent on R_q (increasing with $1/R_q$)

C_d = 10fF
$C_q = C_d$
C_g = 10pF
R_q = 400kΩ
R_q = 50Ω

→ peak height ratio $\quad \frac{V^{max}_{slow}}{V^{max}_{fast}} \sim \frac{C_d\,C_{tot}\,R_{load}}{C_q^2\,R_q}$ increasing with C_d and $1/R_q$

Increasing C_q/C_d or/and R_q/R_{load}
→ spike enhancement
→ better timing

SPTR: cell and sipm size dependence

B.Dolgoshein – LIGHT07

SiPM – MePhI/Pulsar:
576 cells (25x25μm^2)
Area = 1x1 mm^2

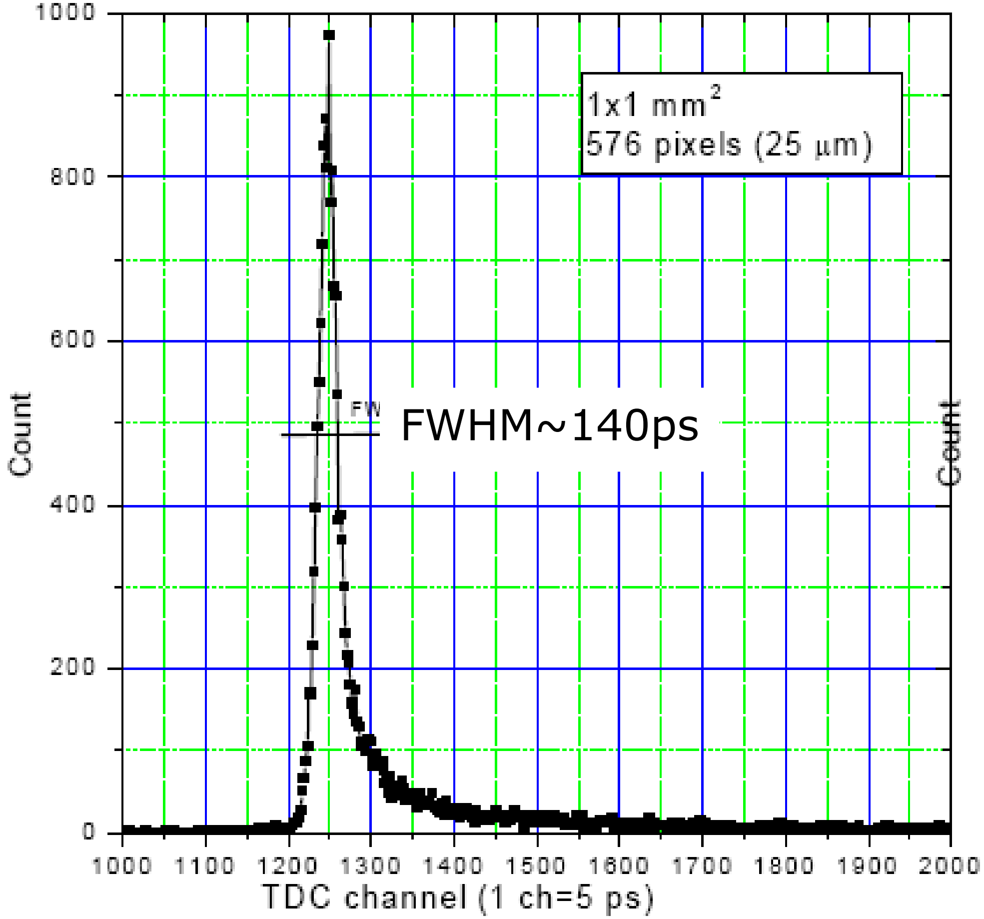

SiPM – MePhI/Pulsar:
1600 cells
(100x100μm^2)
Area = 5x5 mm^2

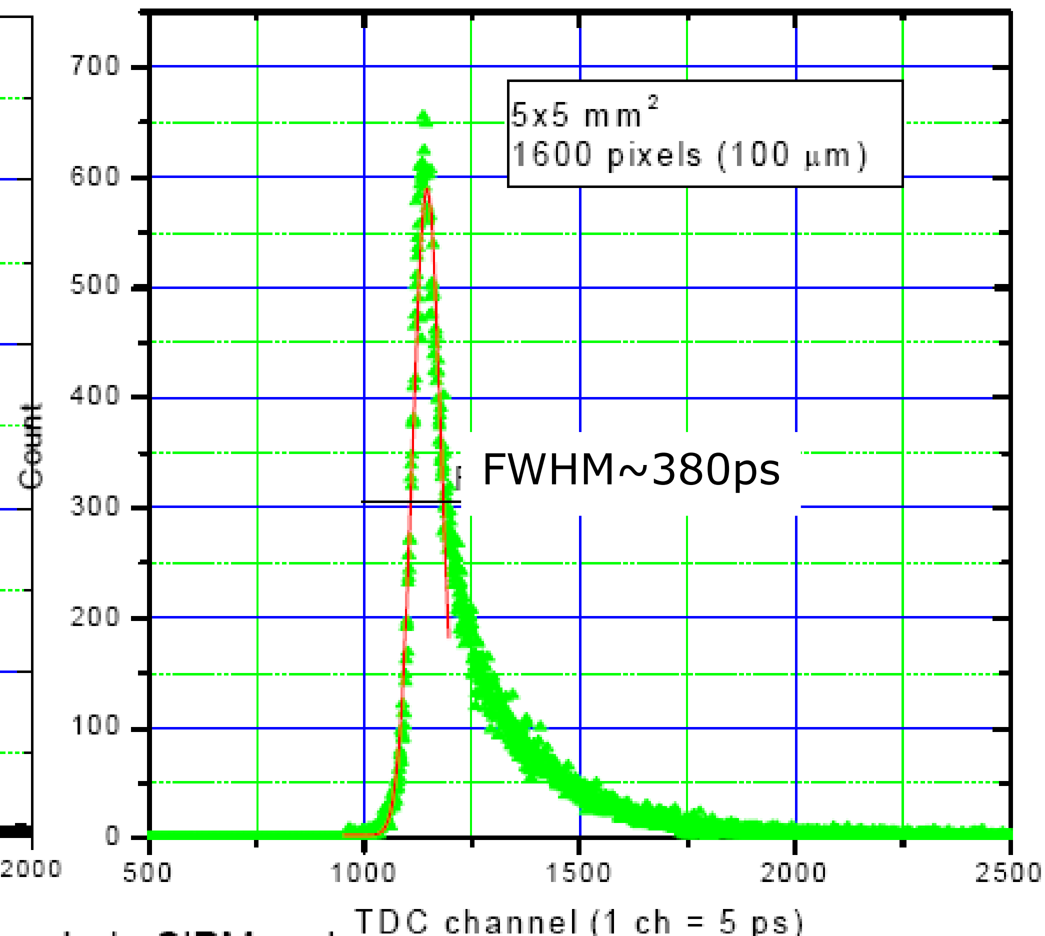

B.Dolgoshein,SiPM review

SiPM signal: effect of C_{tot} and Z_{load}

SiPM – MePhI/Pulsar:
1600 cells (100x100μm²)
Area = 5x5 mm²
C_{tot}~ 160pF

B.Dolgoshein and E.Popova
LIGHT07

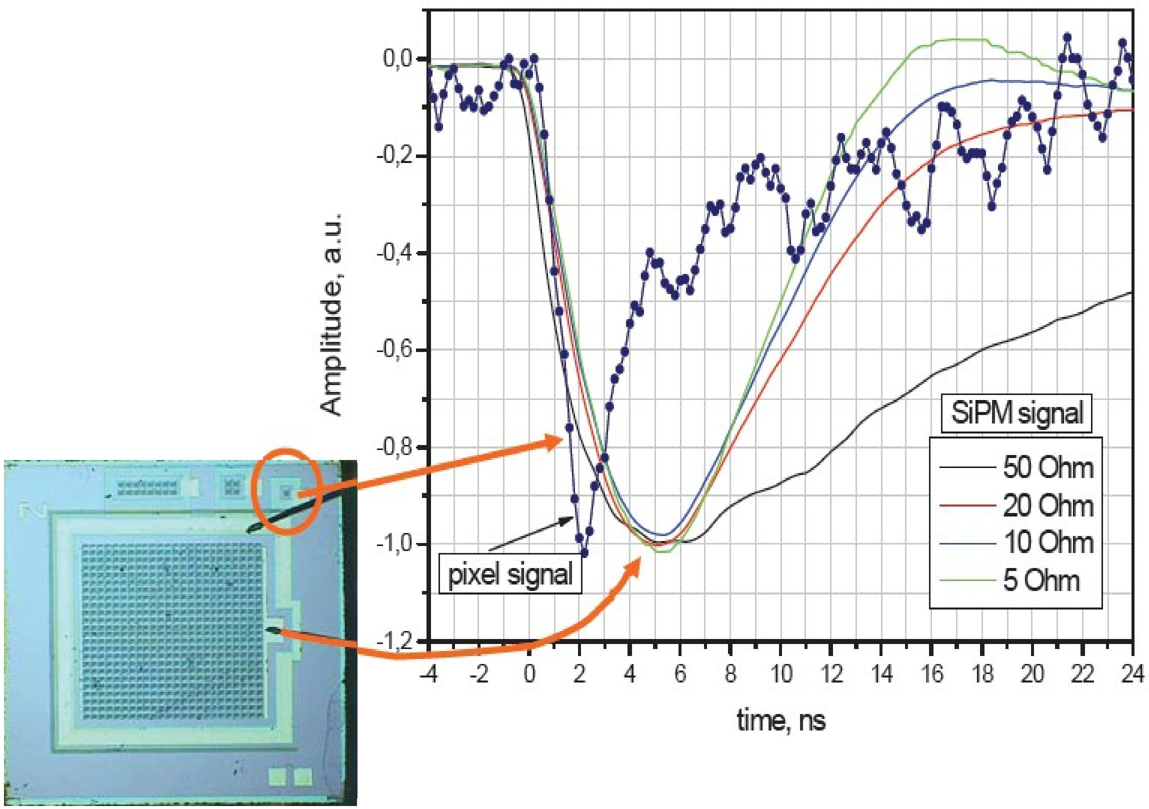

Zin~50Ω
FWHM ~ 15ns

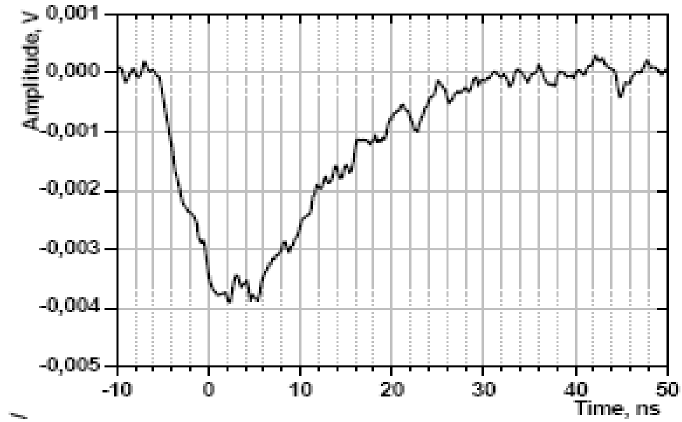

Zin~7Ω + shaper
FWHM ~ 2.5ns

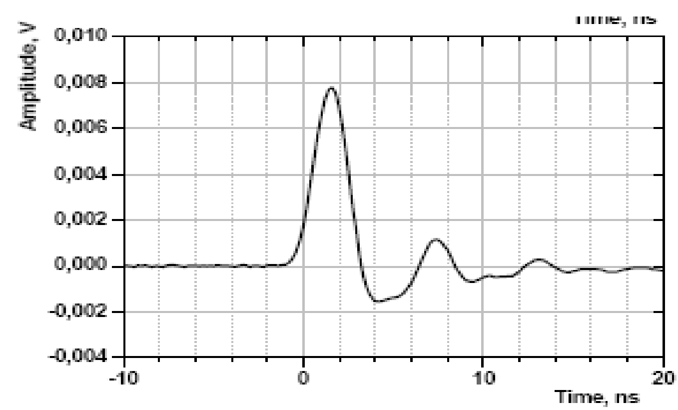

Trans-impedance amplifier

→ peak height ratio $\frac{V_{fast}^{max}}{V_{slow}^{max}} \sim \frac{C_q^2 R_q}{C_d C_{tot} R_{load}}$

Optimizing signal shape for timing (SPTR)

→ peak height ratio $\dfrac{V^{max}_{fast}}{V^{max}_{slow}} \sim \dfrac{C_q^2 R_q}{C_d C_{tot} R_{load}}$

Enhancing C_q does improve timing performances

Hamamatsu test structures

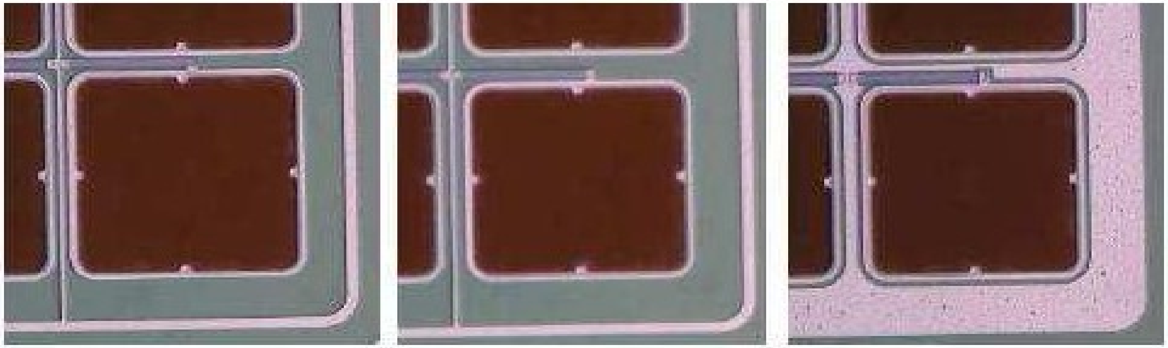

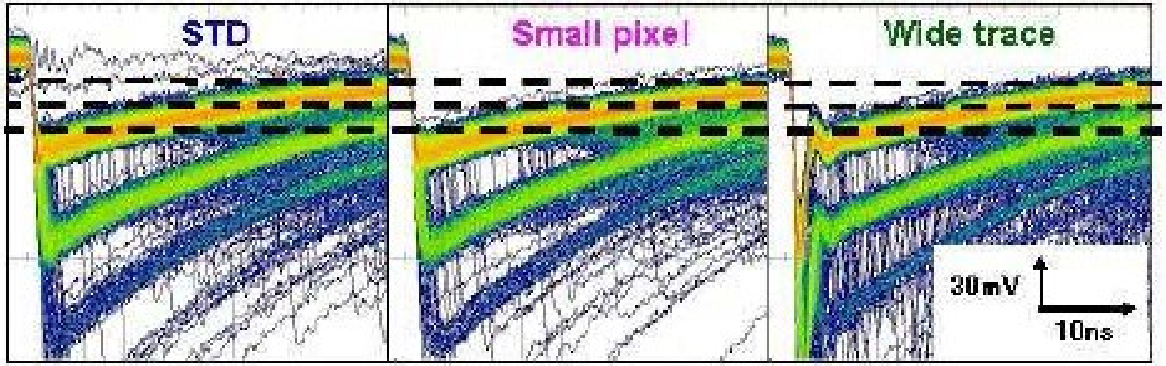

Yamamura et.al. at PD09

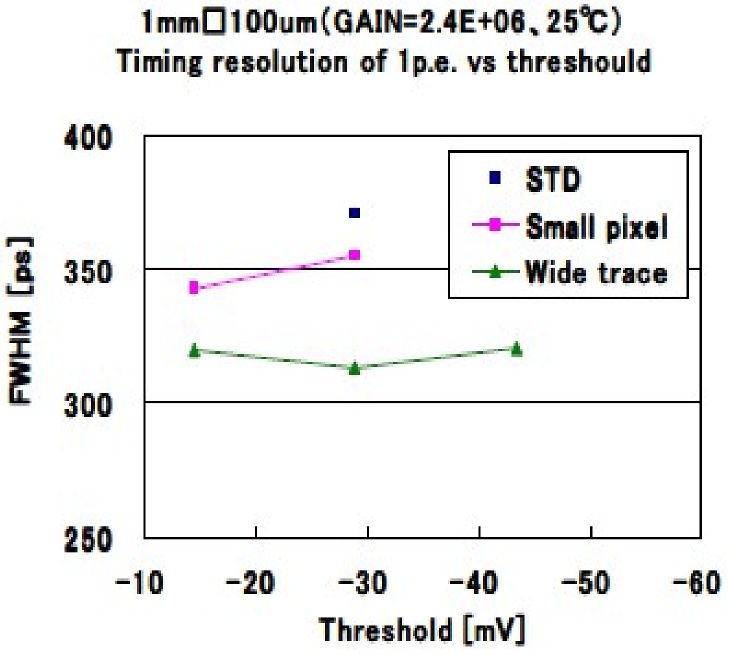

Analogous method for timing optimization proposed in C.Lee et al NIM A 650 (2010) 125 "Effect on MIM structured parallel quenching capacitor of SiPMs"

Note:
The steep falling front of the fast peak could be exploited too for optimum timing

$$\sigma^2_{time} = \frac{\sigma^2_{amplitude}}{N_{samples} \int dt [f'(t)]^2}$$

Optimizing signal shape for timing

… and what about using just AC coupling ...

SiPM std architecture

SensL new SiPM architecture for fast timing

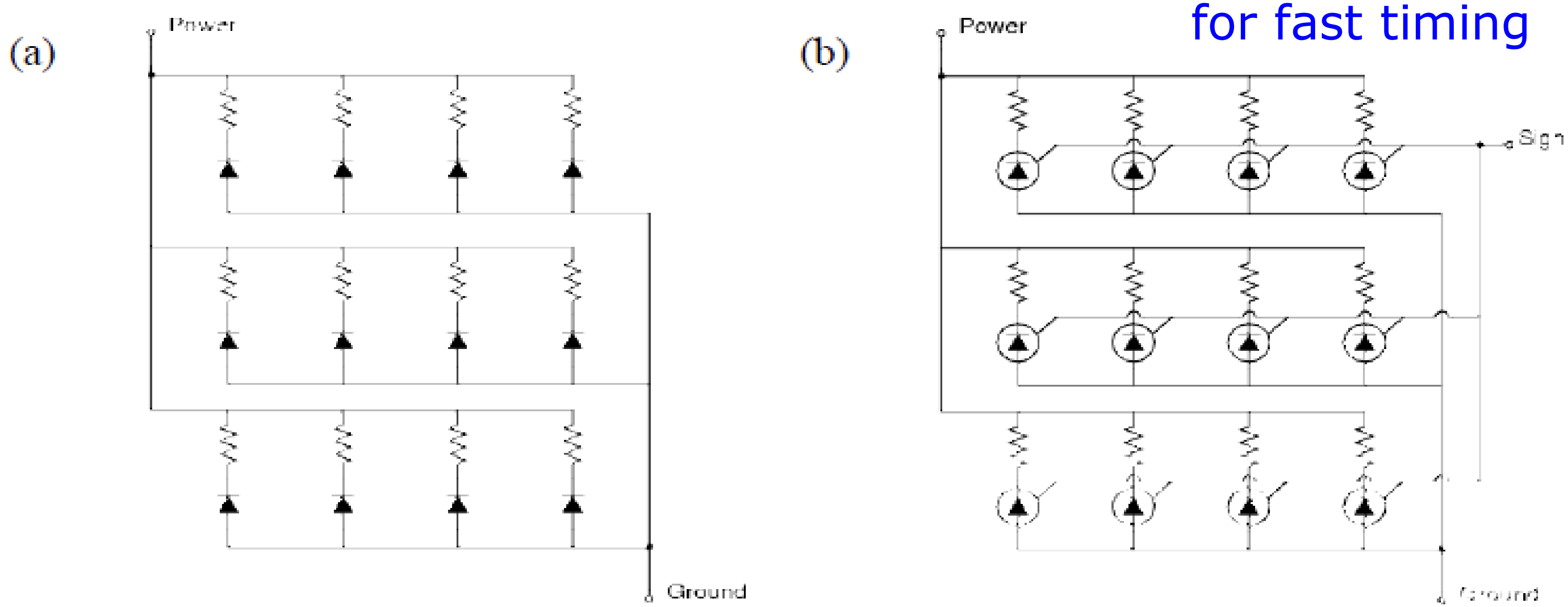

Figure 1: (a) traditional SPM architecture; (b) SPM architecture with inclusion of fast signal terminal.

The traditional SPM consists of a parallel array of avalanche photodiodes each in series with a quench resistor, as shown in Figure 1(a). In this configuration both bias and readout must occur on the same electrode. The introduction of a derivatively coupled electrode to each APD-resistor pair creates single-purpose signal line which delivers steeper rise-time pulses than the traditional SPM discharge which is inherently limited by the large output capacitance of each APD [3].

O'Neill et al " SensL New Fast Timing Silicon Photomultiplier " PhotoDet 2012 - proceedings

Timing fluctuations

- **SiPM are intrinsically very fast**

Two timing components (related to avalanche developement)
1) prompt → gaussian time jitter well below **100ps** (depending on ΔV, and λ)
2) delayed → non-gaussian tails up to **few ns** (depending on λ)

- **Models and Simulations**

- **Measurements**

- **Optimization of devices for timing**

  → use of fast signal shape component
  → use waveform, it's better than CFD and … don't use ToT

- **Timing with scintillators**

Signal shape for timing - many photons

Single ph.e. signal slow falling-time component $\tau_{fall} = R_q\ (C_d + C_d)$

strongly affects multi-photon signal rise time

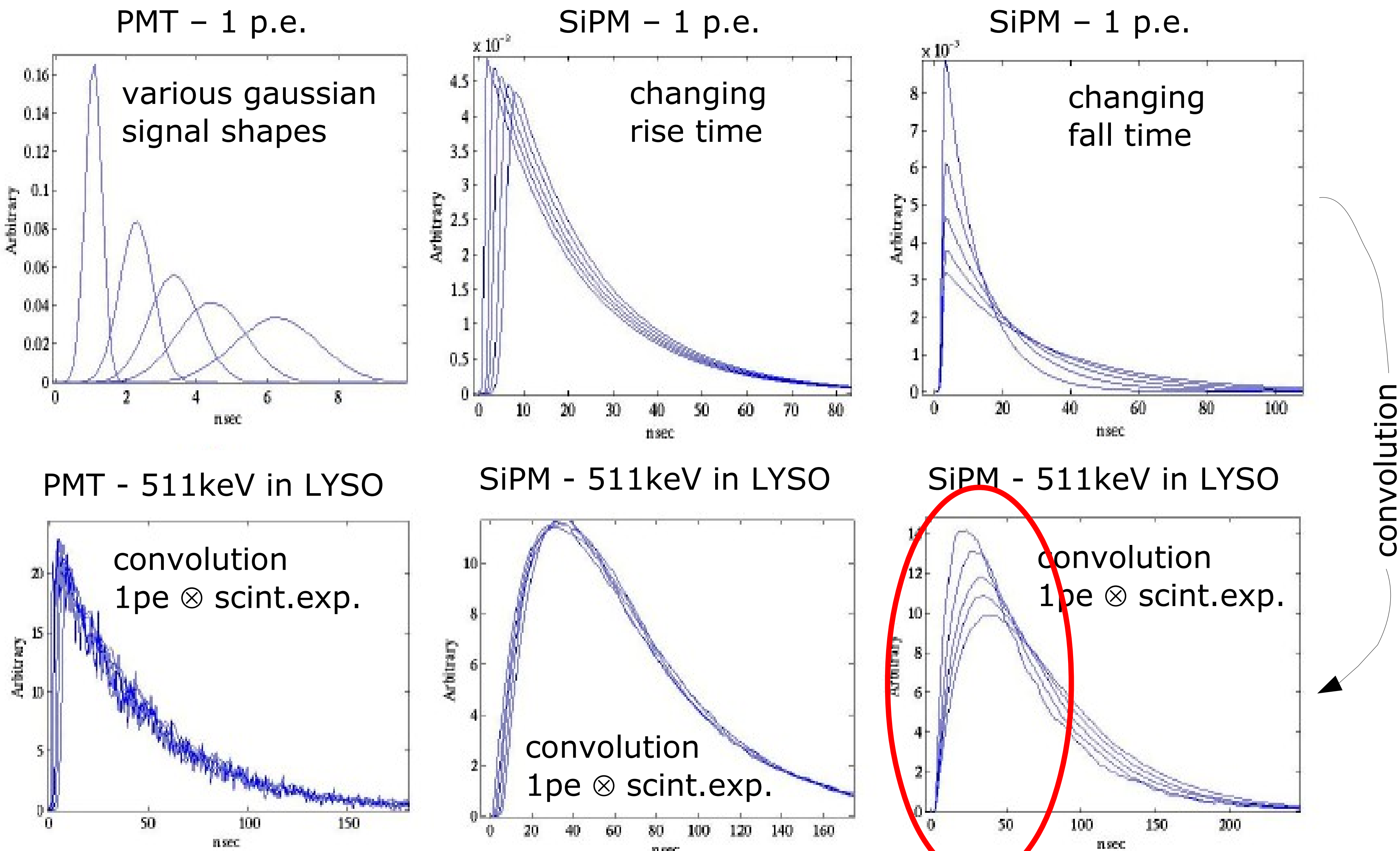

C.L.Kim Procs of Sci. 2009 010 (PD09)

Optimizing shape for timing - many photons

→ peak height ratio $\dfrac{V_{fast}^{max}}{V_{slow}^{max}} \sim \dfrac{C_q^2 R_q}{C_d C_{tot} R_{load}}$

Enhancing C_q and R_q does improve timing performances

FBK devices type:

- Active area: 4x4mm^2;
- Cell size: 67x67μm^2;
- Fill factor: 60%;
- C_Q+C_D: about 180fF;
- R_Q: 1.1M;
- Dark noise rate:
  ~100MHz at DV> 4V

C.Piemonte et al IEEE TNS (2011)

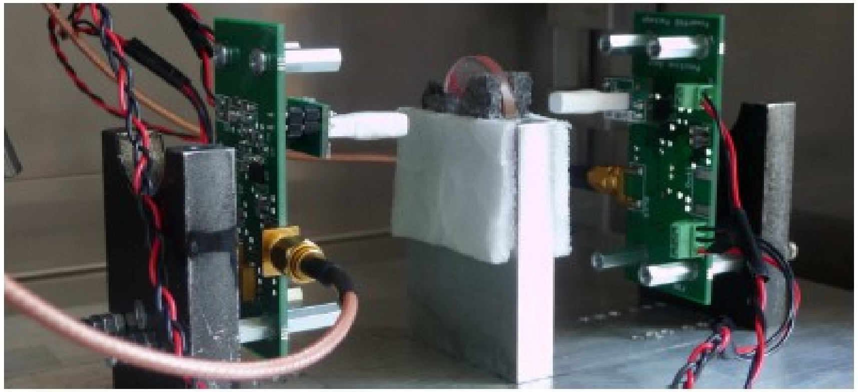

Fig. 2. Test set-up consists of two similar gamma ray detectors (LYSO crystal + SiPM) in coincidence. A ^{22}Na source (disc in the middle) was used to generate two opposite 511keV photons in coincidence.

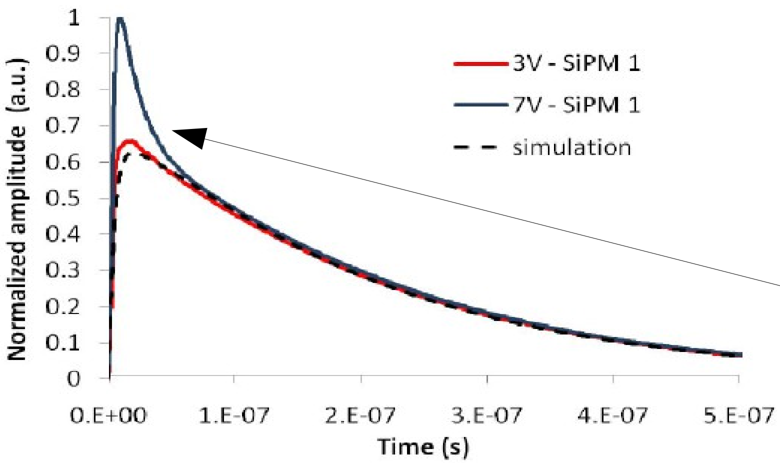

- Signal rise-time < 5ns
- CRT ~320ps (*) FWHM triggering at 5% height

Both are much better than for different structures with high C_{tot} and/or lower Cq, Rq (rise time up to several x 10ns, CRT > 400ps)

??? peak shape is not scaling with ΔV (non linearity in the Corsi et al electrical model)
Can be corrected → energy resol. ~11%

(*) ~40% from light propagation in crystals

Radiation damage

Radiation damage: two types

- Bulk damage due to Non Ionizing Energy Loss (NIEL) ← neutrons, protons
- Surface damage due to Ionizing Energy Loss (IEL) ← γ rays
  (accumulation of charge in the oxide (SiO2) and the Si/SiO2 interface)

Assumption: damage scales linearly with the amount of Non Ionizing Energy Loss (NIEL hypothesis)

G.Lindstrom et al. NIM A426(1999)1-15

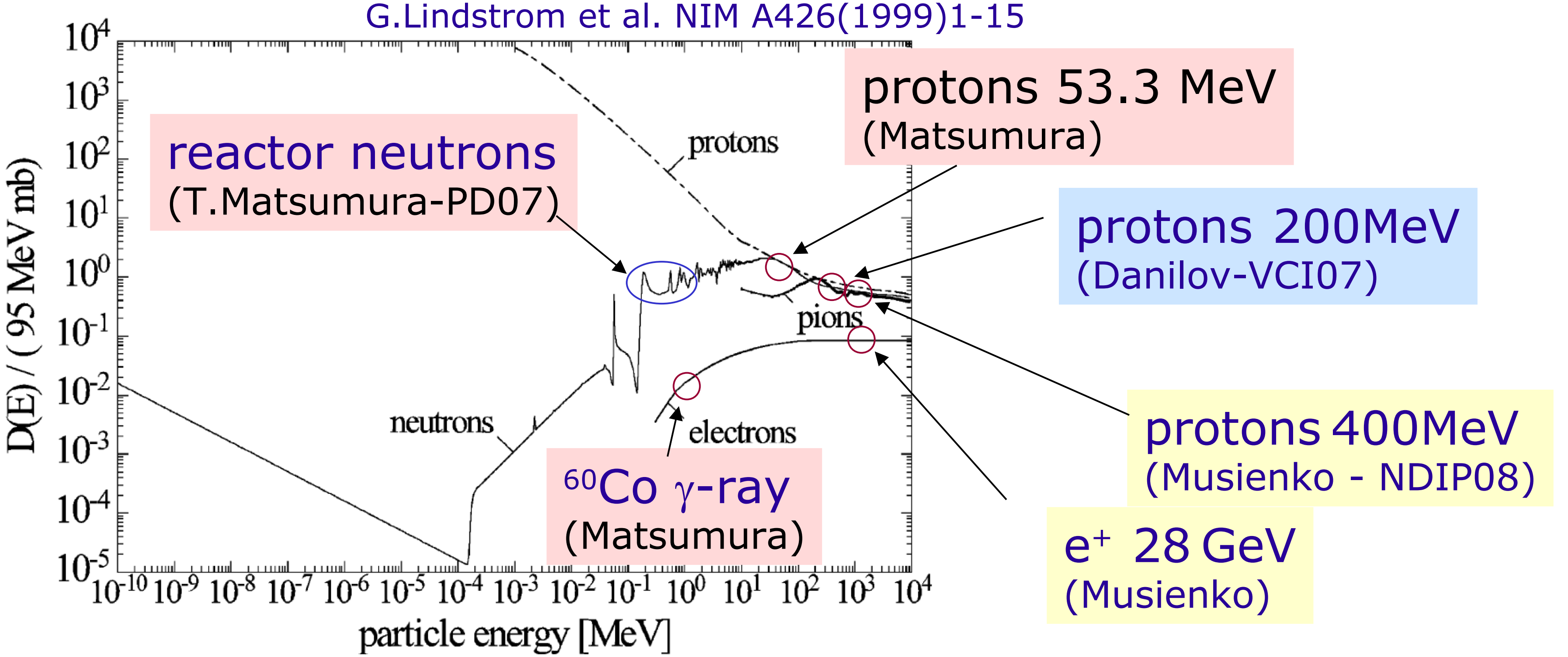

Examples of radiation tolerances for HEP and space physics

ATLAS inner detector ... 3×10^{14} hadrons/cm^2/10 year

~ 10^4 hadrons/mm^2/s

General satellites ... ~ 10 Gy/year

Expectations:

protons / γ-ray ~ 100

protons / neutrons ~ 2~10

Radiation damage: effects on SiPM

1) Increase of dark count rate due to introduction of generation centers

Increase (ΔR_{DC}) of the dark rate:
$\Delta R_{DC} \sim P_{01}\ \alpha\ \Phi_{eq}\ Vol_{eff}\ /q_e$
where $\alpha \sim 3 \times 10^{-17}$ A/cm is a typical value of the radiation damage parameter for low E hadrons and $Vol_{eff} \sim Area_{SiPM} \times \varepsilon_{geom} \times W_{epi}$

NOTE:
The effect is the same as in normal junctions:
- independent of the substrate type
- dependent on particle type and energy (NIEL)
- proportional to fluence

2) Increase of after-pulse rate due to introduction of trapping centers
→ loss of single cell resolution → no photon counting capability

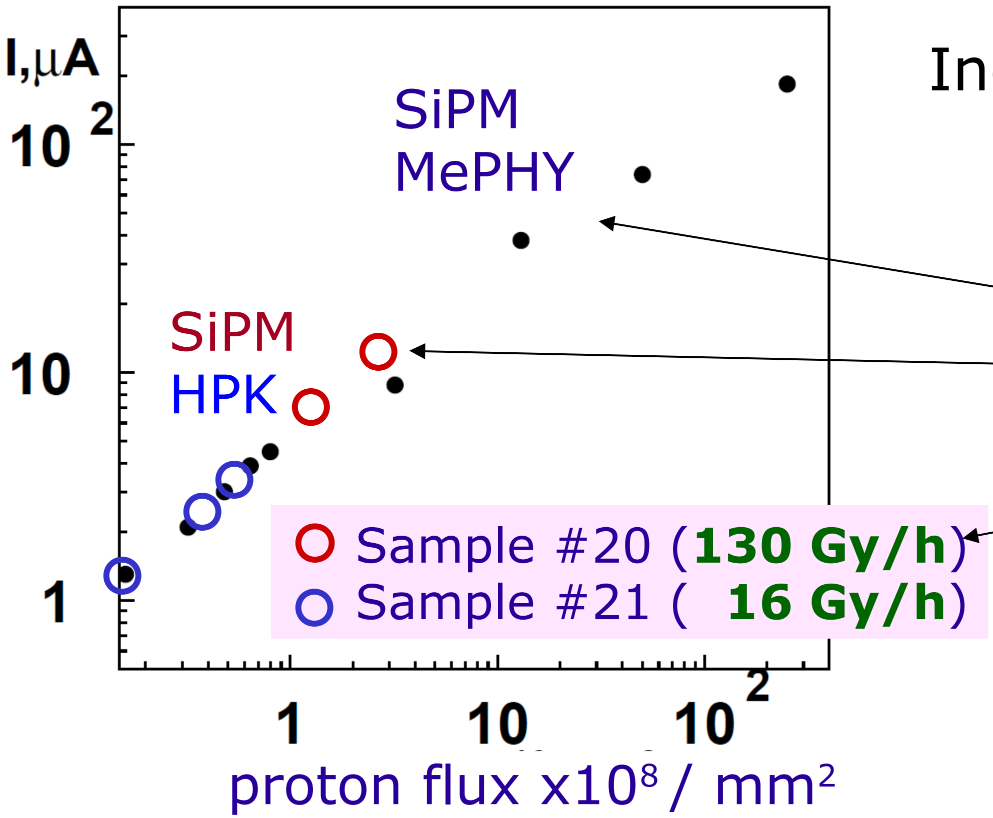

Indications from measurements:

1) no dependence on the device
similar effects found for SiPM from MePHY (Danilov) and HPK (Matsumura) (normaliz. to active volume)

2) no dependence on dose-rate
HPK (Matsumura)

3) n similar damage than p

4) p x10^1-10^2 more damage than γ

Damage comparison

Damage effect ...
almost the same for protons and neutrons

HPK devices
T.Matsumura – PD07

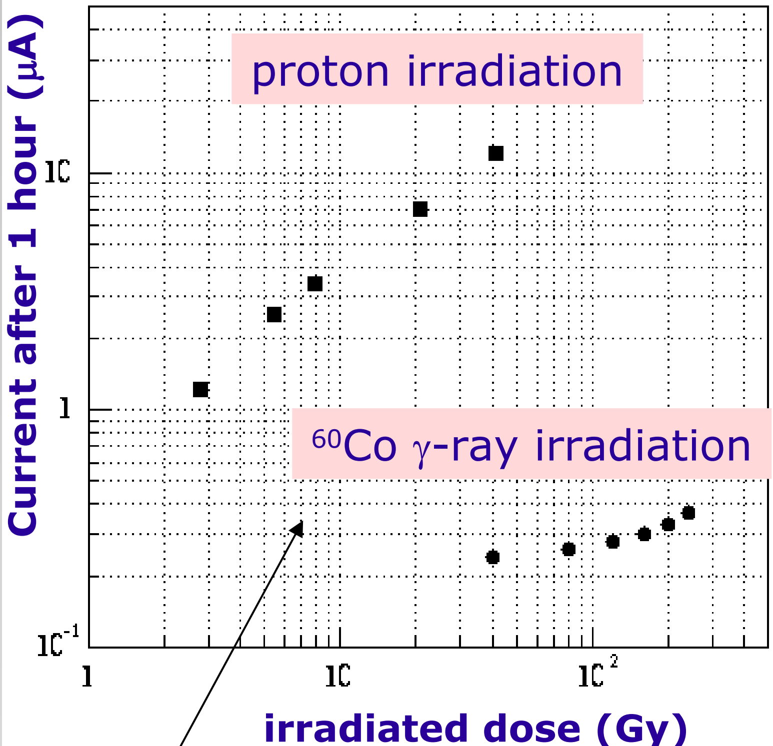

Damage effect ...
1~2 orders larger with protons than γ-ray irradiation

2.3×10^5 p/mm²/s (130 Gy/h)
I_{leak} @ (V_{op}, 1.4×10^8 p/mm²) = 6.7 μA

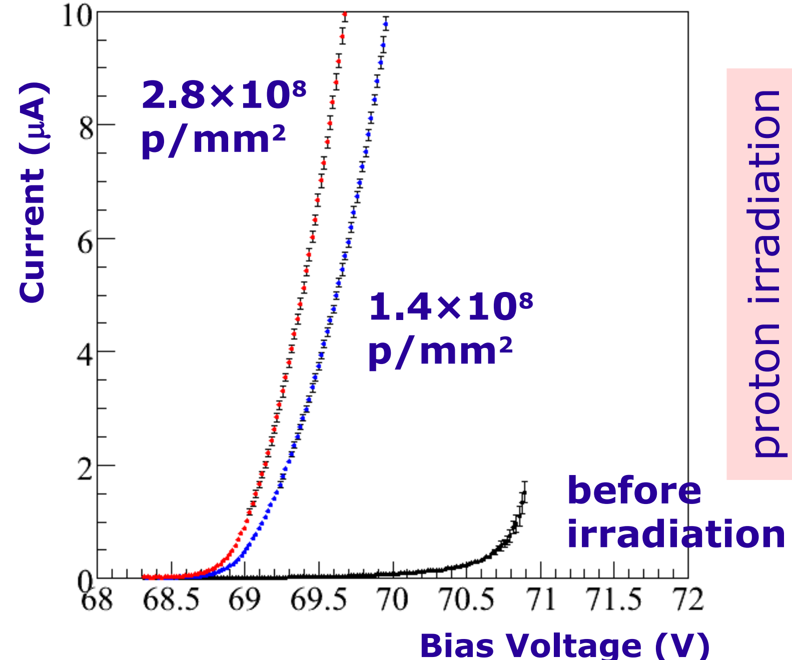

4.2×10^5 n/mm²/s
I_{leak} @ (V_{op}, 1.0×10^8 n/mm²) = 8.5 μA

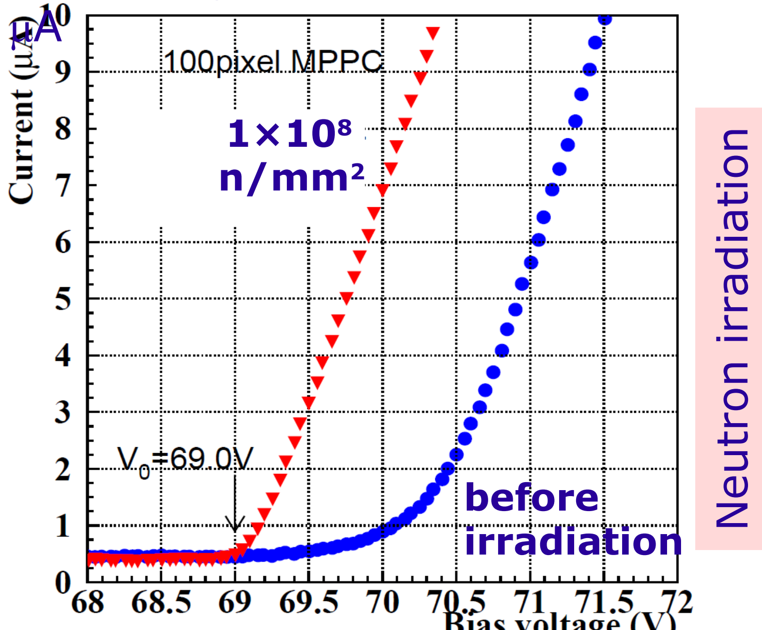

T.Matsumura – PD07

G.Collazuol - Siena - IDPASC 2013

Radiation damage: neutrons (0.1 -1 MeV)

8.3×10^{4} n/mm² | 3.3×10^{5} n/mm² | 1.0×10^{8} n/mm²

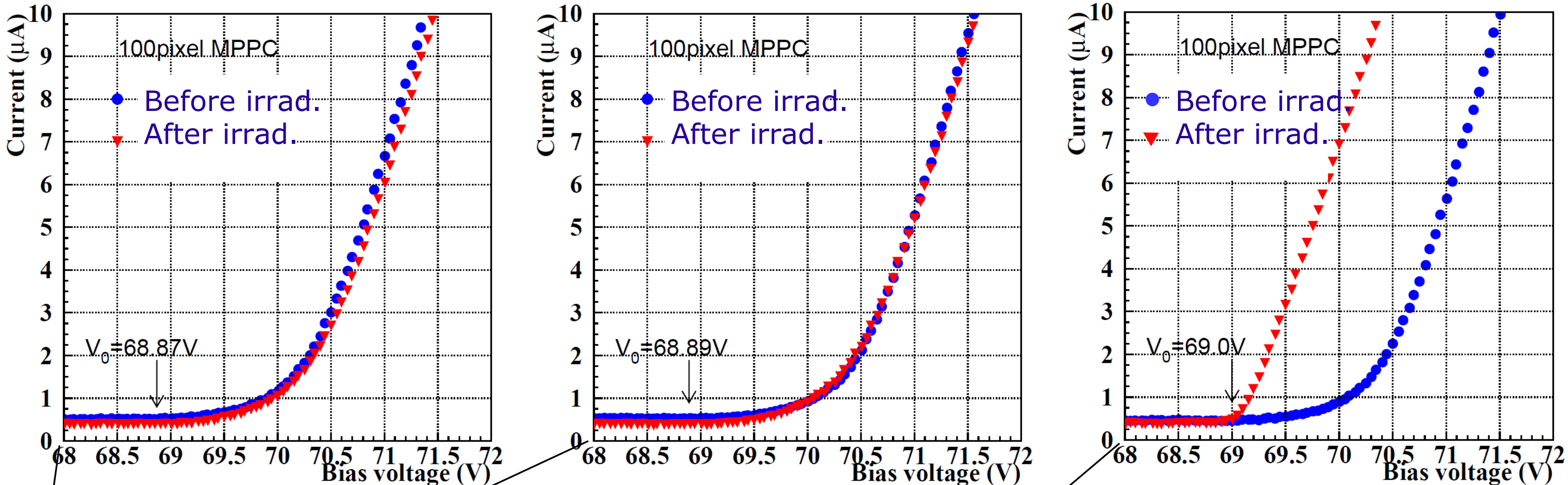

T.Matsumura – PD07

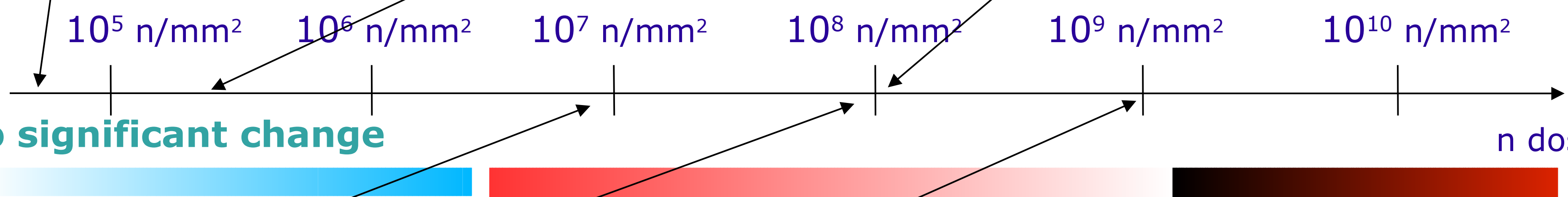

No significant change

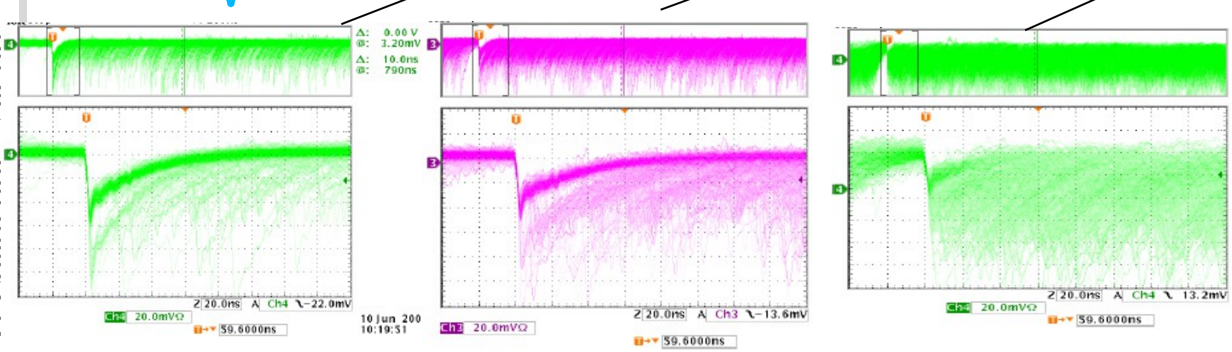

I-V drastically change.
Signal pulse is still there,
but continuous pulse height.
(No photon-counting capability)

No signal

Nakamura at NDIP08

Radiation damage: neutrons 1 MeV E_{eq}

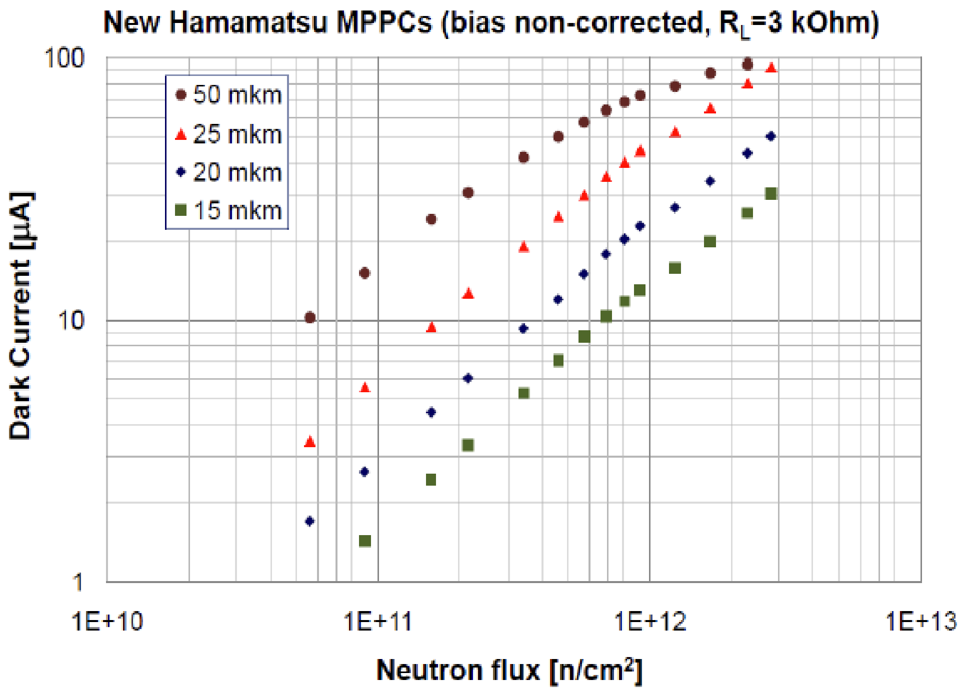

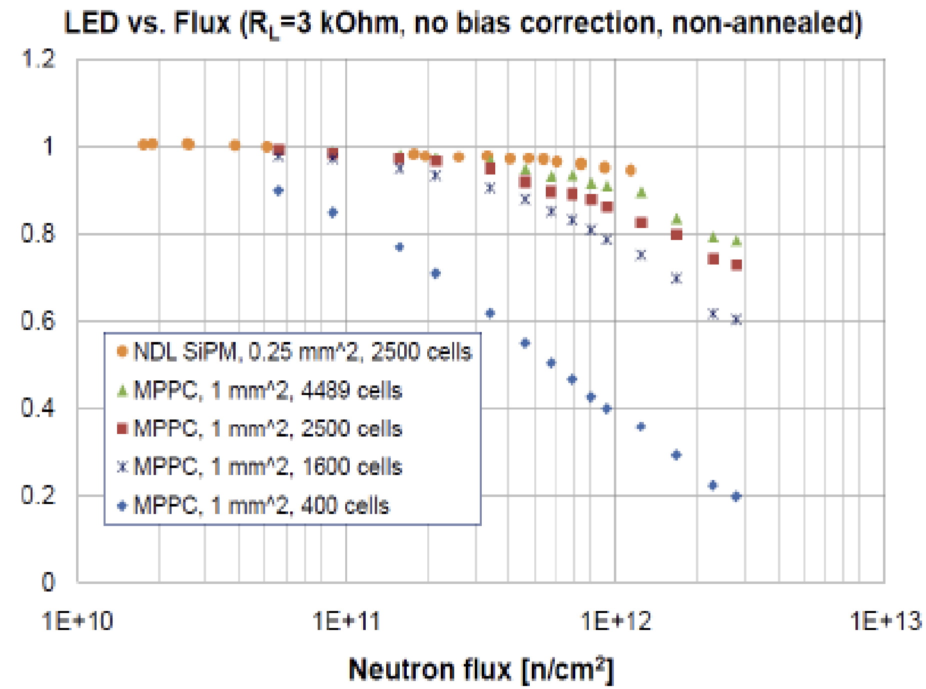

- No change of V_{bd} (within 50mV accuracy)
- No change of R_q (within 5% accuracy)
- I_{dark} and DCR significantly increase

SiPMs with high cell density and fast recovery time can operate up to $3*10^{12}$ n/cm^2 ($\delta G < 25\%$)

Y.Musienko at SiPM workshop CERN 2011

Effects reduced by
→ **small cells** → smaller charge flow (smaller gain → charge)
→ thin epi-layer

Electronics

Front-end electronics: general comments

- **Strong push for high speed front-end > GHz**
  - Essential for timing measurements
  - Several configurations to get GBW > 10 GHz
  - Optimum use of SiGe bipolar transiistors

- **Voltage sensitive front-end**
  - Easiest : 50Ω termination, many commercial amplifiers (MiniCircuits …)
  - Beware of power dissipation
  - Easy multi-gain (time and charge)

- **Current sensitive front-end**
  - Potentially lower noise, lower input impedance
  - Largest GBW product

- **In all cases, importance of reducing stray inductance**

Front-end electronics: different approaches

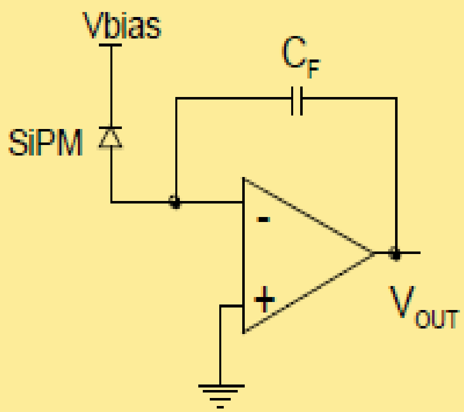

Charge sensitive amplifier

The charge Q delivered by the detector is collected on C_F

If the maximum ΔV_{OUT} is 3V and Q is 50pC (about 300 SiPM microcells), C_F must be 16.7pF

⬇

Perspective limitations in dynamic range and die area with low voltage, deep submicron technologies

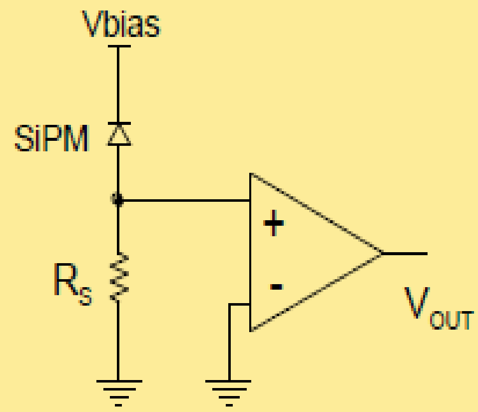

Voltage amplifier

A I-V conversion is realized by means of R_S

The value of R_S affects the signal waveform

V_{OUT} must be integrated to extract the charge information: thus a further V-I conversion is needed

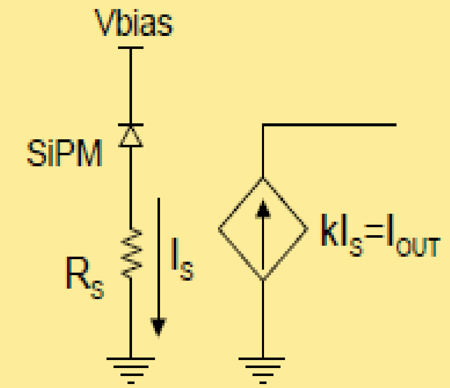

Current buffer

R_S is the (small) input impedance of the current buffer

The output current can be easily replicated (by means of current mirrors) and further processed (e.g. integrated)

The circuit is inherently fast

The current mode of operation enhances the dynamic range, since it does not suffer from voltage limitations due to deep submicron implementation

ASICs for SiPM signal readout (QDC/TDC)

W.Kucewicz "Review of ASIC developments for SiPM signal readout" - talk at CERN 11-2-2011

Chip Name	Measured quantity	Application	Input configuration	Technology
FLC_SiPM	Pulse charge	ILC Analog HCAL	Current input	CMOS 0,8 µm
MAROC	Pulse charge, trigger	ATLAS luminometer	Current input	SiGe 0,35 µm
SPIROC	Pulse charge, trigger, time	ILC HCAL	Current input	SiGe 0,35 µm
NINO	Trigger, pulse width	ALICE TOF	Differential input	CMOS 0,25 µm
PETA	Pulse charge, trigger,time	PET	Differential input	CMOS 0,18 µm
BASIC	Pulse height, trigger	PET	Current input	CMOS 0,35 µm
SPIDER (VATA64-HDR16)	Pulse height, trigger, time	SPIDER RICH	Current input	
RAPSODI	Pulse height, trigger	SNOOPER	Current input	CMOS 0,35 µm

ASICs for SiPM signal readout (QDC/TDC)

W.Kucewicz - CERN 11-2-2011

Chip Name	# of channels	Digital output	Power supply	Area [sqr mm]	Dynamic range	Input resistance	Timing jitter	Year
FLC_SiPM	18	n	5V (0,2W)	10			-	2004
MAROC2	64	y	5 V	16	80 pC	50 Ω		2006
SPIROC	36	y	5 V	32				2007
NINO	8	n	(0,24W)	8	2000 pe	20 Ω	260 ps	2004
PETA	40	y	(1,2W)	25	8 bit		50 ps	2008
BASIC	32	y	3,3 V	7	70 pC	17 Ω	~120 ps	2009
SPIDER (VATA64-HDR16)	64	n		15	12 pC			2009
RAPSODI	2	y	3,3 V (0,2W)	9	100 pC	20 Ω	-	2008

- Only a few of the suitable for low light intensity

SPIDER

Chip VATA64-HDR16 was developed for SiPM applied in Ring Imaging Cherenkov Detector of SPIDER (Space Particle IDentifiER) Experiment

M.G. Bagliesi et al. “A custom front-end ASIC for the readout and timing of 64 SiPM” Nuclear Physics B (Proc. Suppl.) 215 (2011) 344

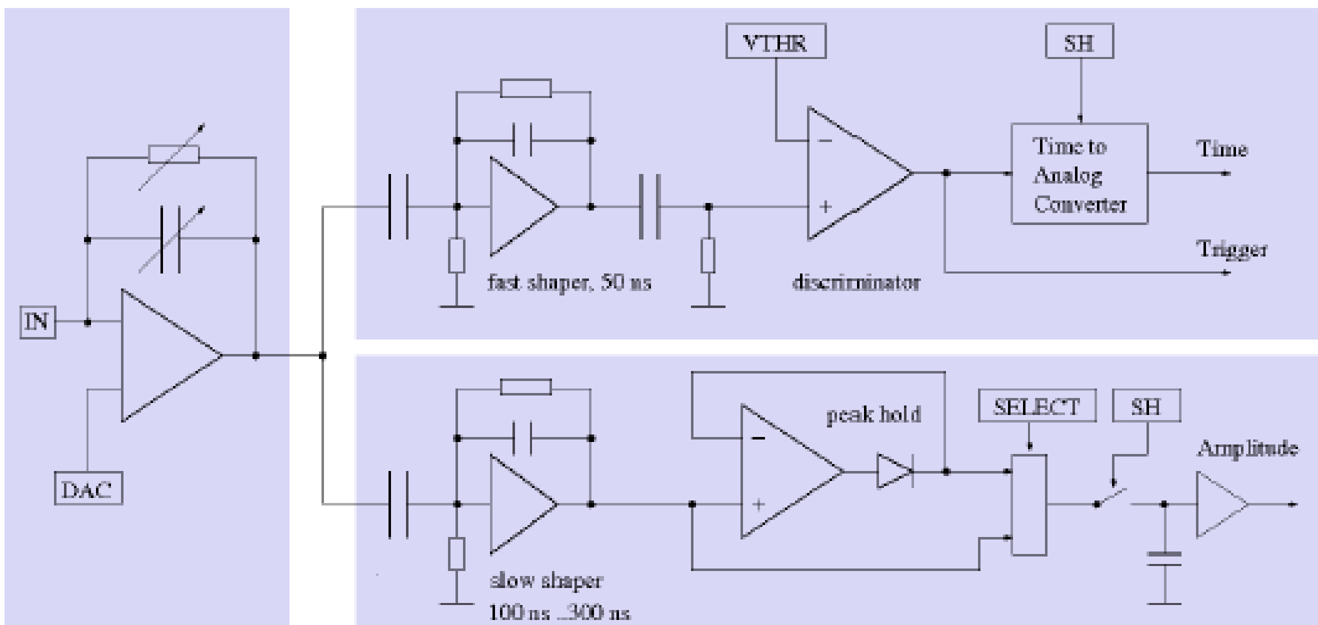

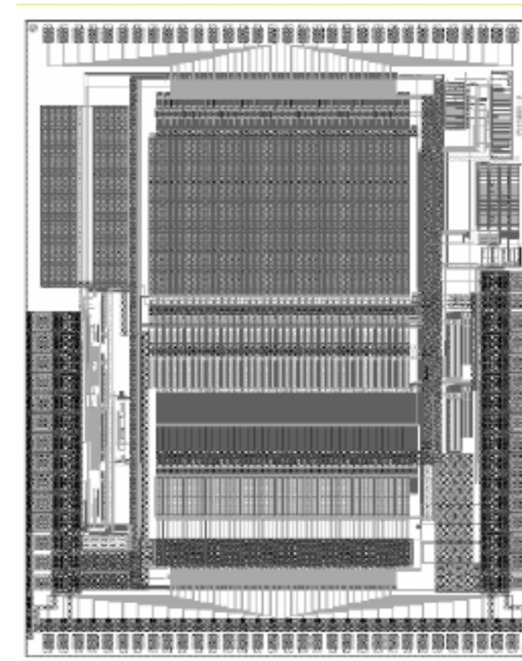

Signal from preamplifier is split in two branches with fast and slow shaper
Branch with fast shaper measures time and other one measures charge

- The DAC on the input of preamplifier allows to moderate the bias voltage
- Signal from preamplifier is shaped by fast (50ns) and slow (100-200ns) shapers.
- Discriminator compared the signal from the output of fast shaper and generate the trigger pulse, which start time counter with 40ps resolution
- Signal from slow shaper is sent to peak&hold detector which measure the pulse height

BASIC

BASIC is a 32 channel SiPM readout chip for simultaneous time and energy measurement, made in 0,35 µm CMOS AMS technology (2009).
F.Corsi et al "BASIC: a Front-end ASIC for SiPM Detectors" 2009 IEEE NSS Conf Rec

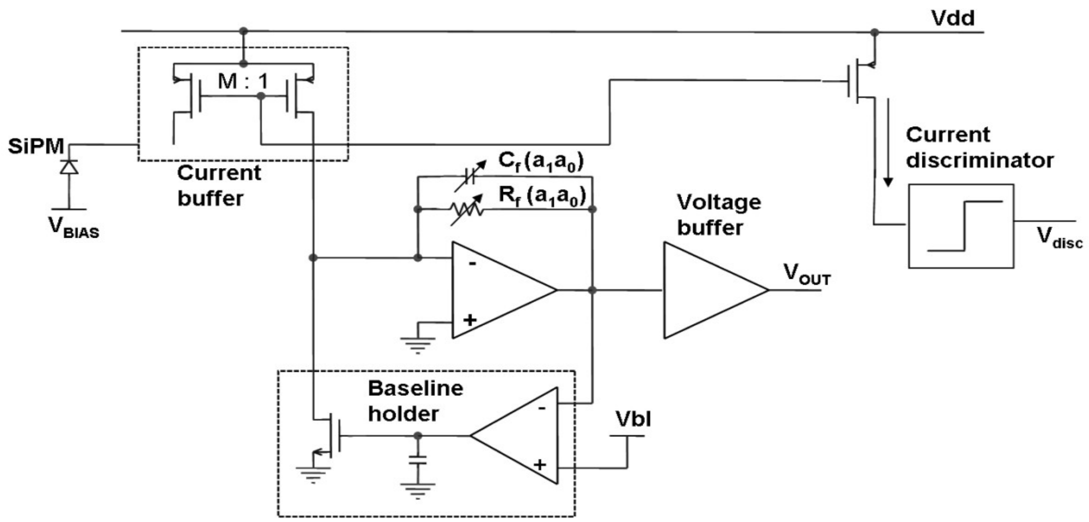

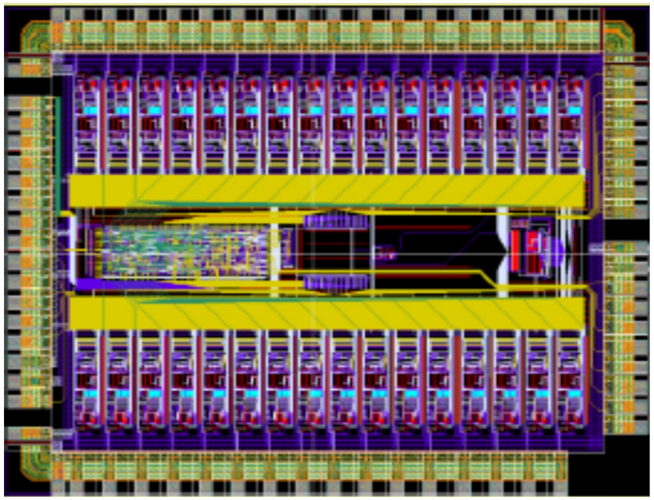

Each front-end channel consists of a current buffer as input, reading on a very low impedance input node the current signal delivered by the detector

The input current buffer is a common gate stage. Feedback applied to increase bandwidth and decrease input resistance. Possible fine tuning SiPM bias by varying Vref. The output of current buffer can be easy replicated by multi-branch current mirrors.

The current mirror at the input allows the splitting of the signal in two branches: one is used to send the output current to a current discriminator, which extracts the trigger signal associated to the timing of the event, while the other is sent to an integrator in order to obtain a voltage proportional to the charge

Trend in electronics → fast sampling

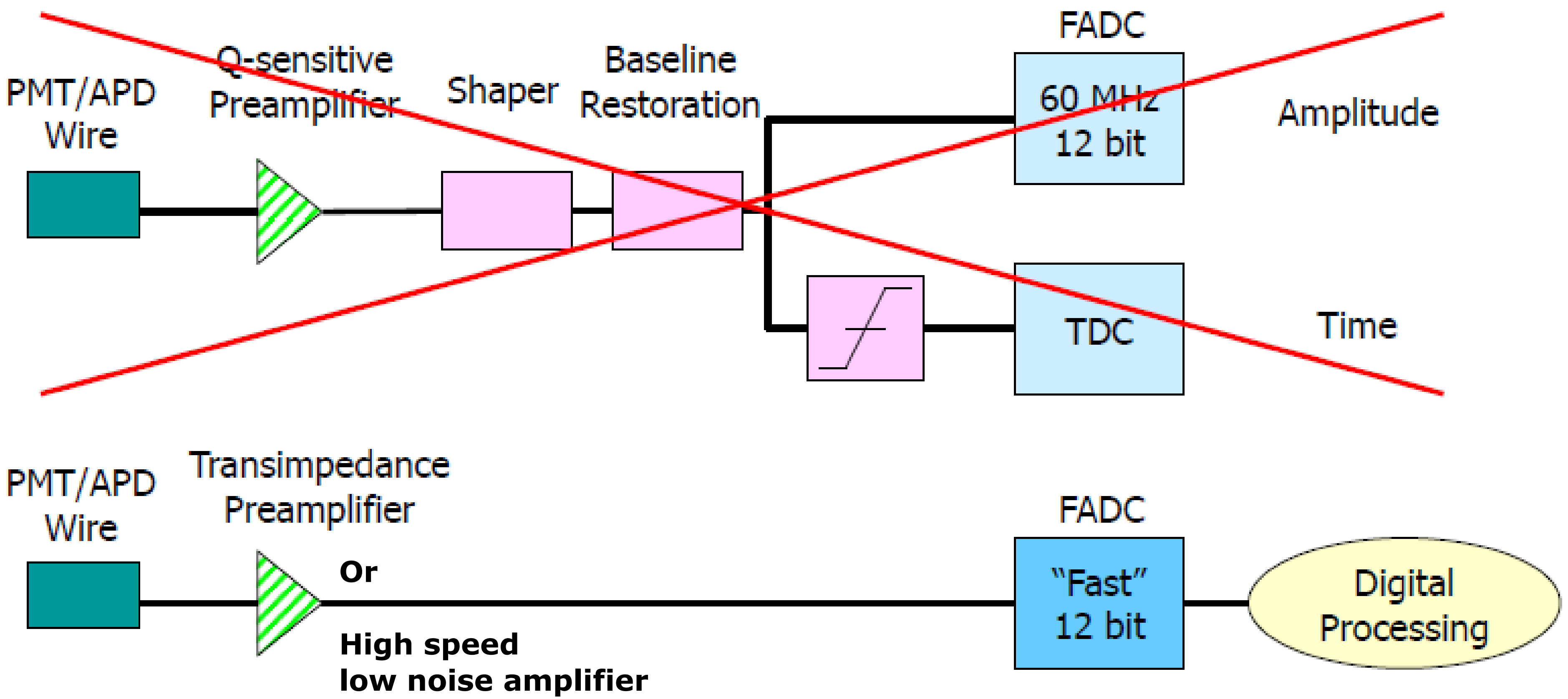

- Shaping stage can only remove information from the signal
- Shaping is unnecessary if FADC is "fast" enough
  = sampling speed 2x maximum frequency (Nyquist-Shannon)
- All operations (CFD, optimal filtering, integration) can be done digitally

J.F.Genat - TWEPP 2010

ASICs for waveform sampling

Best performances for timing with Waveform Sampling
→ allowing proper processing of the peculiar SiPM signal
(handling fast/slow trailing front, after-pulses, cross-talk, ...)

	Hawaii Blab1	Varner Lab1-2	Lab 3	Saclay/Orsay Hamac	Delagnes/ Matacq	Breton Sam	Planned	PSI DRS3	S.Ritt DRS4	This proposal
Sampling	100 MHz-6 GHz		20 MHz-3.7GHz	40 MHz	0.7-2.5 GHz	0.7-2.5 GHz	10 GHz	10 MHz-5 GHz	5 GHz	10-20 GHz
Bandwidth (3db)	300 MHz		900 MHz	50 MHz	200-300 MHz	300 MHz	650 MHz	450 MHz	950MHz	> 1.5 GHz
Channels	1	8	9	8	1	2		12 6 2 1	8 4 2 1	4 16
Triggered mode	Yes		Common stop		Yes			Common stop	Common stop	Channel trigger
Resolution	10 bit			13.3 bit	13.4 bit	11.6 bit		11.6 bit	11.5 bit	8-10-bit
Samples	128 rows of 512	256	256	144	2520	256	2048	1024-12288	1024-8192	256
Clock			33 MHz	40 MHz	100 MHz				fsamp/2048	20-40 MHz
Max latency	560 us	2.2ms	50us							
Input Buffers	Yes			Yes	Yes	Yes	No	No	No	No
Differential inputs	No	No	No	Yes	Yes	Yes		Yes	Yes	Yes
Input impedance	50 Ohms	50 Ohms	50 Ohms Ext	10 MOhm/3pF	50 Ohms				11pF	50 Ohms
Readout clock	500 MHz			5 MHz	5 MHz	16 MHz		33 MHz	33MHz	500 MHz
Locked delays	Ext DAC	Ext DAC	Ext DAC			Yes		Ext PLL	Int PLL	Int PLL
On-chip ADC	12-b +500MHz TDC			No		No		No	No	Yes
R/W simultaneous	Yes			Yes		No		No	Yes	No
Power/ch	15mW/1.6W			36 mW	250-500 mW	150 mW		2-8mW	7.2mW at 2GS/s	
Dynamic range	1mV/1V			0.26mV/2.75V	175 uV-2V	0.65mV-2 V		0.35mV/1.1V	.35mV/1V	1V
Xtalk	Inter-rows 0.1%		10%			0.30%		< 0.5%		
Sampling jitter			4.5ps			25ps			6ps	?
Power supplies	-tbd/+2.5	-tbd/2.5V	-tbd/2.5V	-1.7/3.3V				2.5V	2.5V	1.2V
Process	TSMC .25	TSMC .25	TSMC .25	HP/DMILL .8	AMS .8	AMS .35	AMS .18	UMC .25	UMC .25	IBM .13
Chip area	5.25 mm2	10 mm2	2.5mm2	19.8mm2	30mm2			25mm2		1mm2/ch
Temp coeff	0.2%/°C		0.2%/°C					5e-5/°C	25ppm/°C	
Cost/channel	500$/40 10$/2k								10-15$	

Table by J.F.Genat "A 20 GS/s sampling ASIC in 130nm CMOS technology" - TWEPP 2010

Conclusions – vacuum based PD

PMT: 80 years old... still the most used sensor for low-level light detection

Features
- sensitivity from DUV to NIR
- **high gain**
- **low noise**
  - → single photon sensitivity
  - → large area at low cost
  - → low capacitance
- imaging capabilities (large pixels)
- high frequency response
  - → fast speed
- stability

Issues
- intrinsic **limit QE < 40%**
- broad SER
- high voltage, bulky, fragile
- influenced by B, E fields
- damaged by high-level light
- ageing (eg. He)
- radiopurity

Developement
→ photocathodes: new materials and geometries → high QE
→ ultra-fast, large area, imaging MCP based PMTs
→ hybrids (eg photocathode + SiPM) → narrow SER

Conclusions – solid state PD

PIN photo-diode: used in space since '60s, in HEP experiments since '80s
- **No internal gain**: necessary Q sensitive amplifier (noise, slow)
  → minimum of several 100 photo-electrons (p.e.) detectable
- Nuclear counter-effect

Avalanche photo-diode: massive use in big experiments (CMS at LHC)
- Internal multiplication: S/N improved → still >10 p.e. detectable
- Gain limited by the excess noise due to **avalanche multiplication noise**

GM-APD based PM: technology of **SiPM** is mature
→ candidates for more and more experimental setups
- **Dark noise** still the most limiting factor → **active area**
- **Low T**: SiPM perform ideally in the range 100K < T < 200K
  → quenching R should be tuned shorter recovery (ad hoc)
  → lower gain (small cells) might be desirable for mitigating after-pulses

Development of GM-APD in several directions still missing, e.g.:
- IR/NIR sensitive devices → possibly with different semiconductors
- DUV/VUV sensitive devices → relatively easy with SiPM
- Imaging (small pixels)

...many SSPD devices (CCD, CMOS, ...) not covered in these lectures

Thanks for your attention

Additional material →

The canonical emission equations

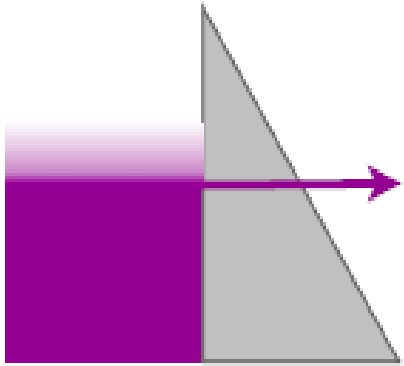

- **Field Emission**
  Fowler Nordheim
  E.L. Murphy, And R.H. Good,
  Physical Review 102, 1464 (1956).

$$J_{FN}(F) = A_{FN}F^2 \exp\left(-\frac{B\Phi^{3/2}}{F}\right)$$

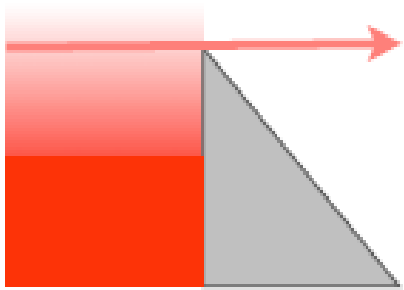

- **Thermal Emission**
  Richardson-Laue-Dushman
  C. Herring, And M. Nichols,
  Reviews Of Modern Physics 21, 185 (1949).

$$J_{RLD}(T) = A_{RLD}T^2 \exp\left(-\frac{\Phi}{k_B T}\right)$$

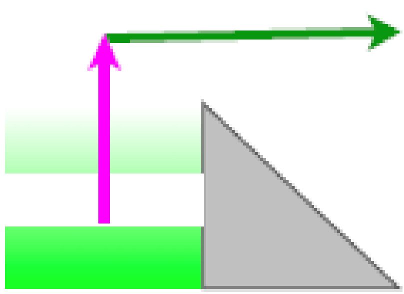

- **Photoemission**
  Fowler-Dubridge
  L.A. DuBridge
  Physical Review 43, 0727 (1933).

$$J_{FD}(F) \propto (\hbar\omega - \Phi)^2$$

K.Jensen – Workshop on Photocathodes – Uni. Chicago 2009

Models of quantum efficiency

- Fowler-Dubridge Model For Metals
  - L.A. DuBridge. "Theory of the Energy Distribution of Photoelectrons." Physical Review 43, 0727 (1933).
  - K.L. Jensen, D.W. Feldman, N.A. Moody, and P.G. O'Shea. "A Photoemission Model for Low Work Function Coated Metal Surfaces and its Experimental Validation." J. Appl. Phys. 99, 124905 (2006).

$$\boxed{QE \propto P_{FD}(\hbar\omega) \propto (\hbar\omega - \phi)^2 + \frac{(\pi k_B T)^2}{6}}$$

T Temperature
Φ Work Function

- (Modified)

$$QE = \frac{q}{\hbar\omega}\underbrace{(1 - R(\omega))}_{\text{absorption}}\underbrace{F_\lambda(\delta,\tau)}_{\text{scattering losses}}\underbrace{P_{FD}(\hbar\omega)}_{\text{transmission}}$$

- Spicer's Model For Semiconductors
  (This Version Looks Different From Spicer, But Is Same)
  - p: quasi-empirical, argued to be 3/2
  - B: (Escape)x(Transport) = B exp(-βx)
  - g: absorption factor
    "over" + "under" barrier terms
  - V_o: Band gap E_g + Electron Affinity E_a

$$\boxed{QE \approx \frac{B}{1 + g\left(E - V_o\right)^{-p}}}$$

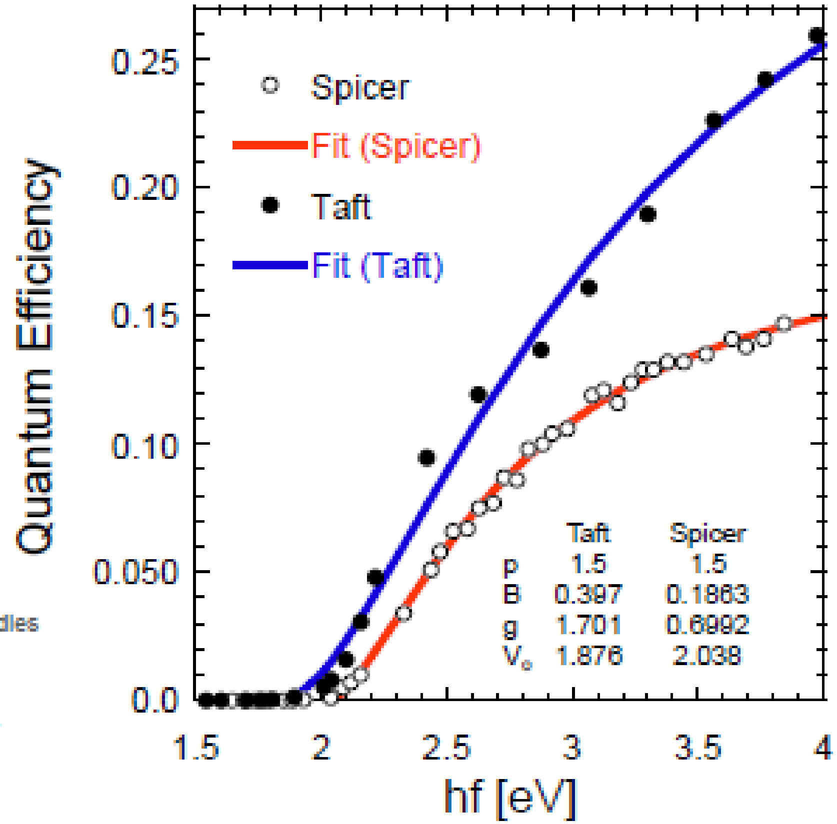

	Taft	Spicer
p	1.5	1.5
B	0.397	0.1863
g	1.701	0.6992
V_o	1.876	2.038

Originals: W.E. Spicer. "Photoemissive, Photoconductive, and Optical Absorption Studies of Alkali-antimony Compounds." Physical Review 112, 114 (1958).

E.A. Taft, and H.R. Philipp. "Structure in the Energy Distribution of Photoelectrons From K_3Sb and Cs_3Sb." Physical Review 115, 1583 (1959).

For Metals: C.N. Berglund, and W.E. Spicer. "I - Photoemission Studies of Copper and Silver: Theory." Physical Review 136, A1030 (1964).

Modern Usage: D.H. Dowell, F.K. King, R.E. Kirby, J.F. Schmerge, J.M. Smedley. "In Situ Cleaning of Metal Cathodes Using a Hydrogen Ion Beam." Physical Review Special Topics Accelerators and Beams 9, 063502 (2006).

K.Jensen – Workshop on Photocathodes – Uni. Chicago 2009

QE Photo-cathodes

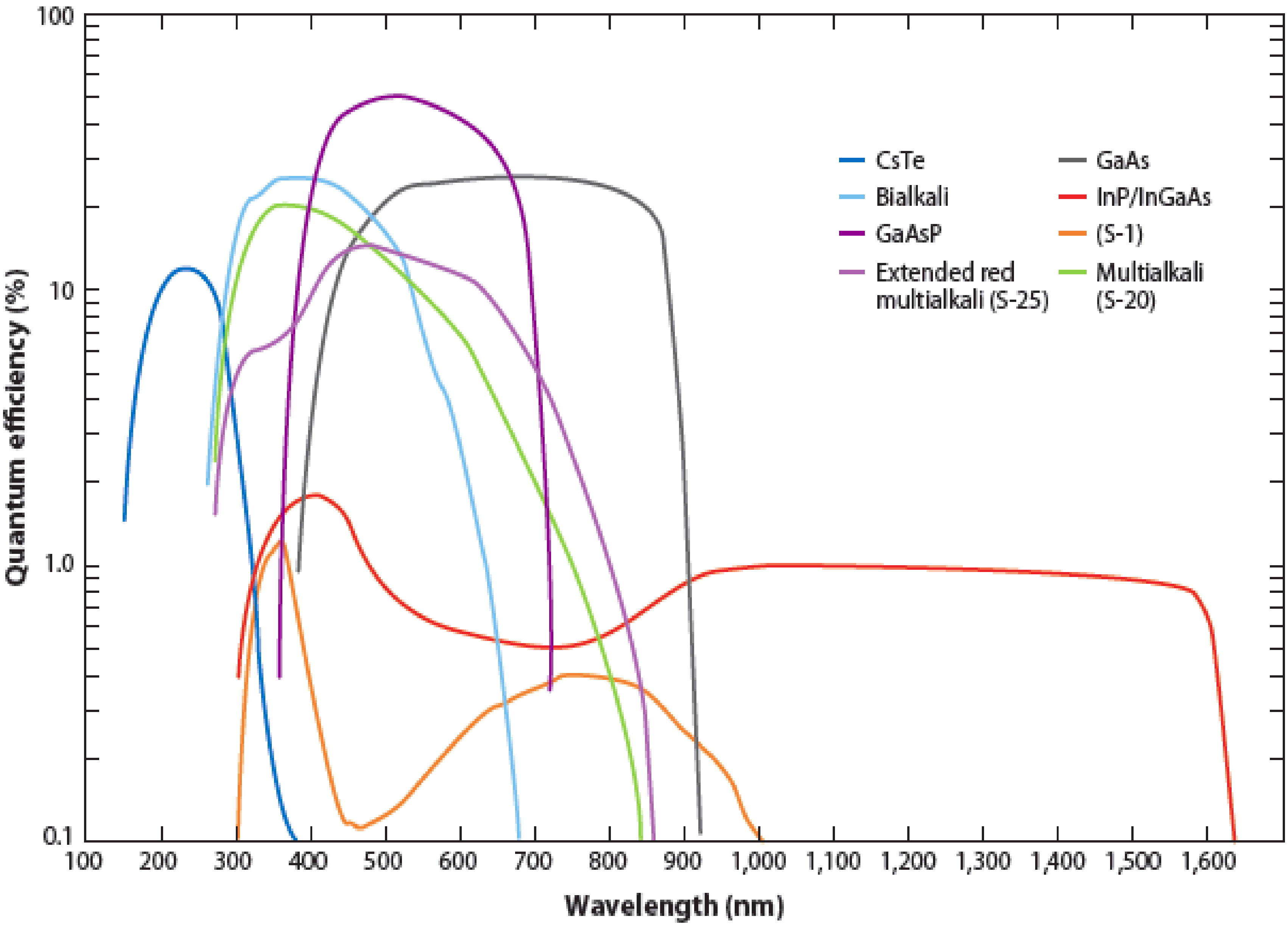

Stability

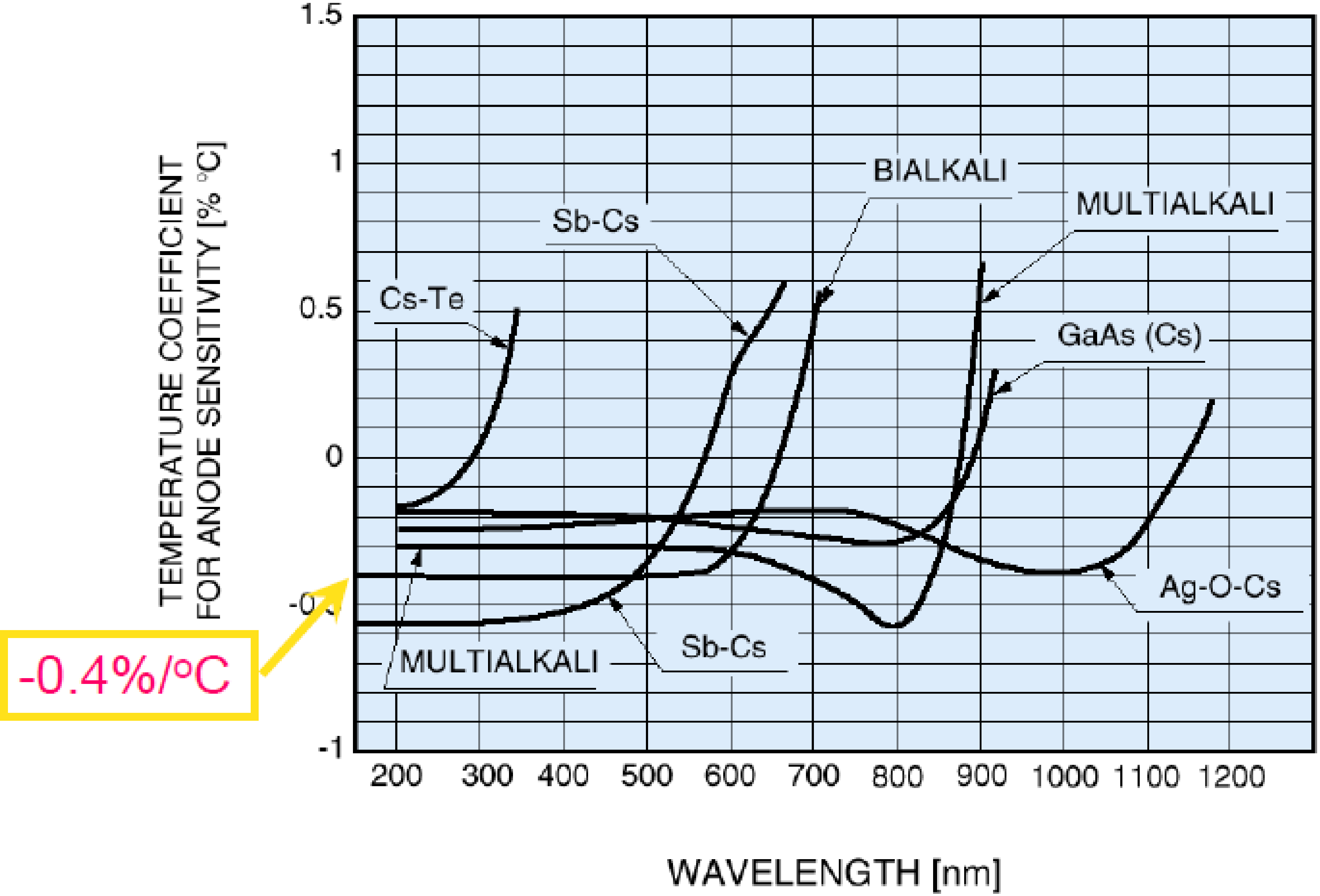

TEMPERATURE COEFFICIENT FOR ANODE SENSITIVITY [% °C]
1.5
1
0.5
0
-1
Cs-Te
Sb-Cs
BIALKALI
MULTIALKALI
GaAs (Cs)
Ag-O-Cs
Sb-Cs
MULTIALKALI
200 300 400 500 600 700 800 900 1000 1100 1200
WAVELENGTH [nm]
-0.4%/°C

Gain fluctuations (single electron spectrum)

Secondary emission process → **large amplitude fluctuations**
→ measure **single electron response**, ie amplitude spectrum (SER)

SER relative variance $$\frac{\sigma_A^2}{A^2} = \frac{g}{g-1}\frac{\sigma_g^2}{g^2} \sim \frac{g}{g-1}\frac{1}{g_1}$$

Main contribution from 1st dynode → improvement at higher $\Delta V_{K\text{-}Dy1}$

Excess Noise Factor = ENC

$$ENC \equiv 1 + \frac{\sigma_M^2}{M^2}$$ ← Multiplication noise

Note:

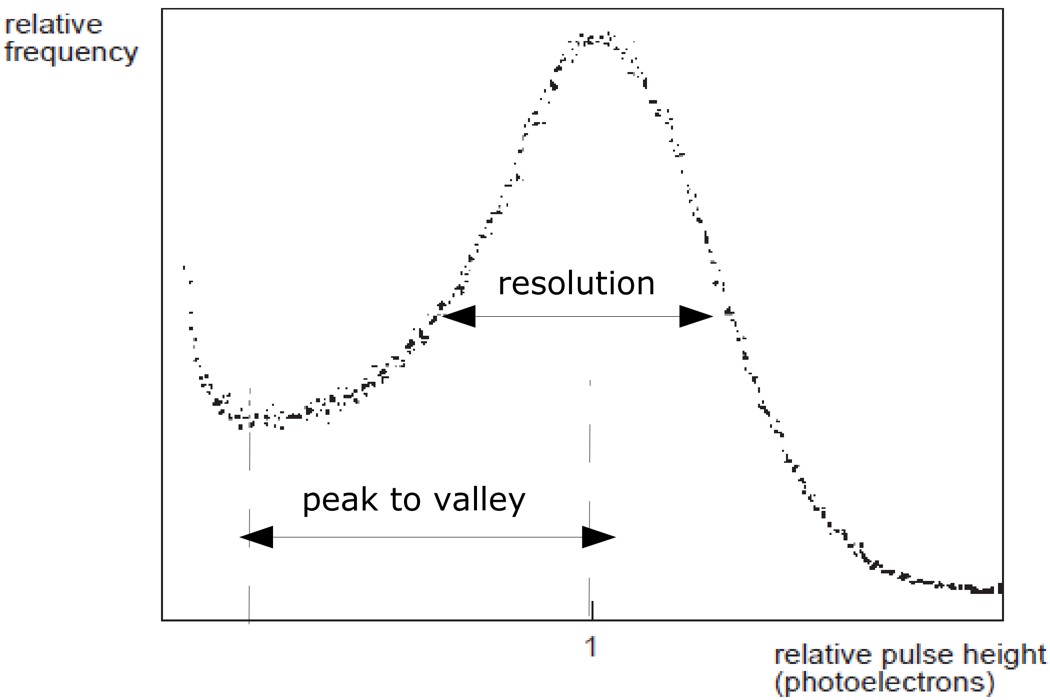

Fig.2.4 Typical single-electron spectrum. Resolution 67% FWHM. Peak-to-valley ratio 2.8:1

Flyckt and Marmorier – "PMT principles and applications"

Operation in B field

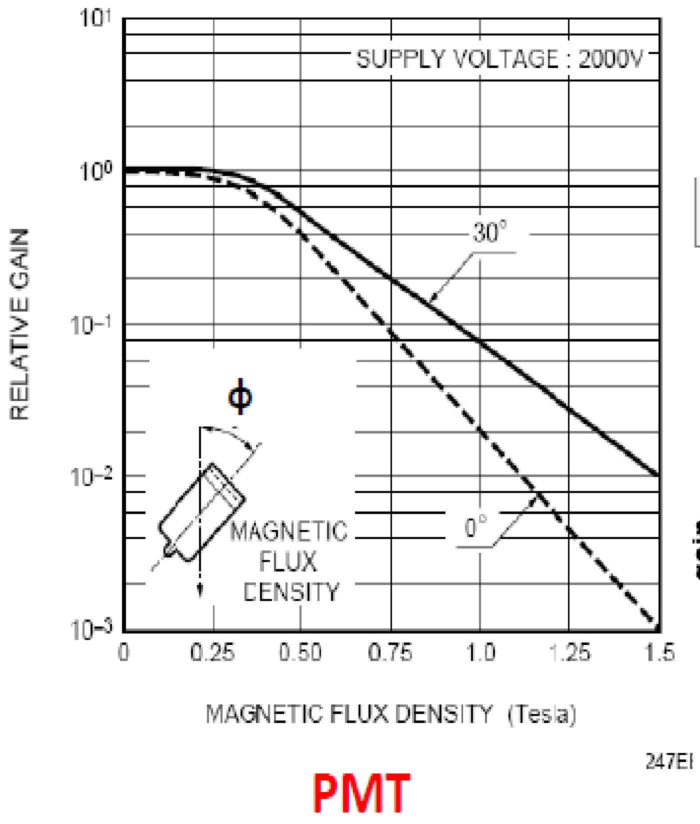

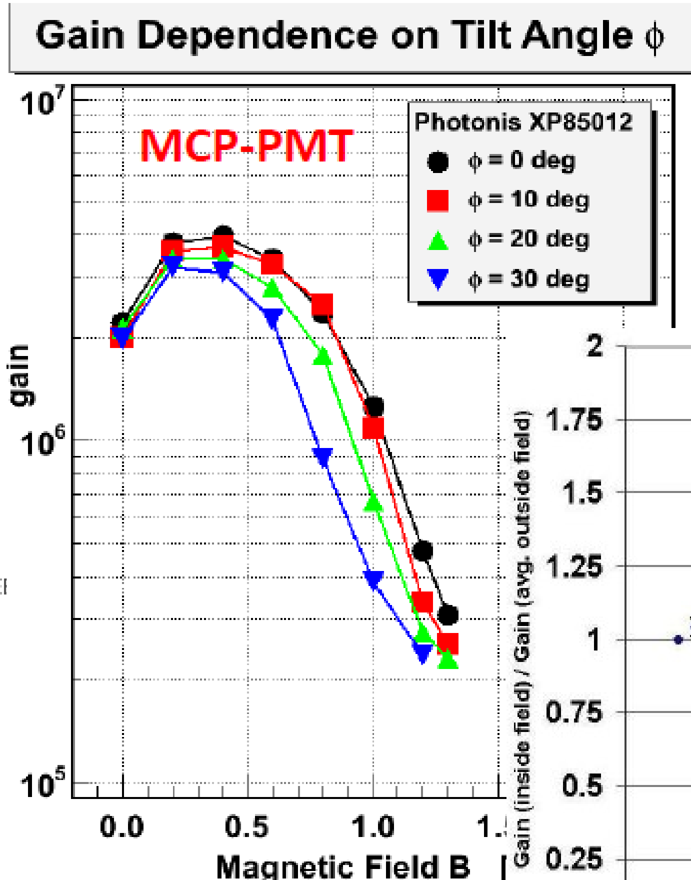

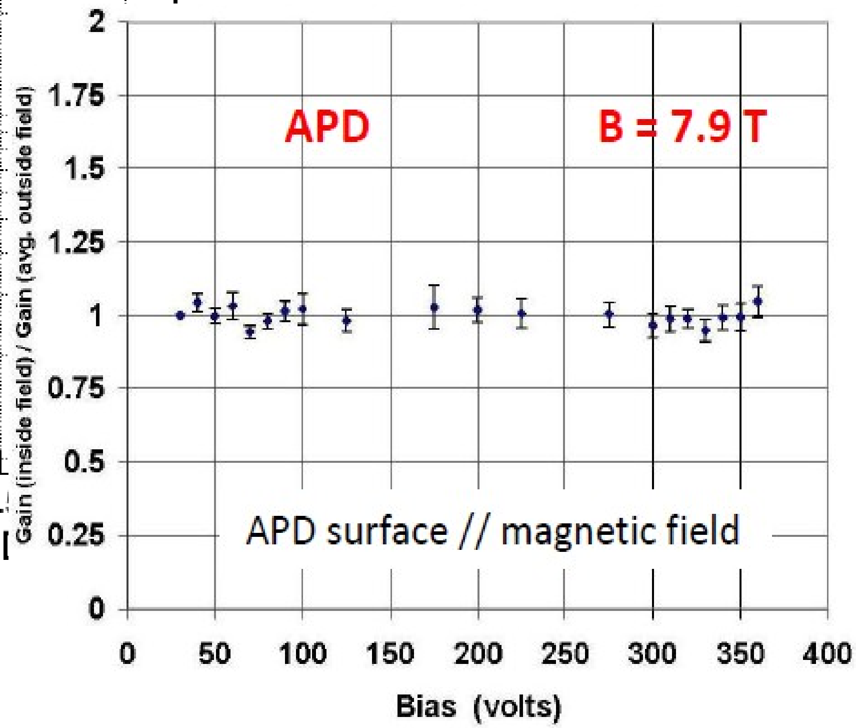

EDIT 2011 School at CERN - photodetectors

Magnetic shielding

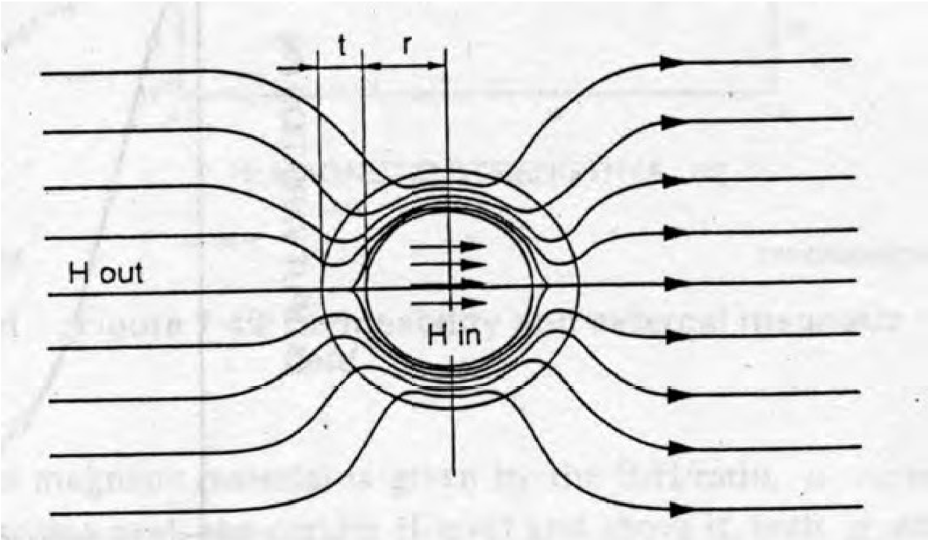

Figure 7-37: Shielding effect of a magnetic shield case

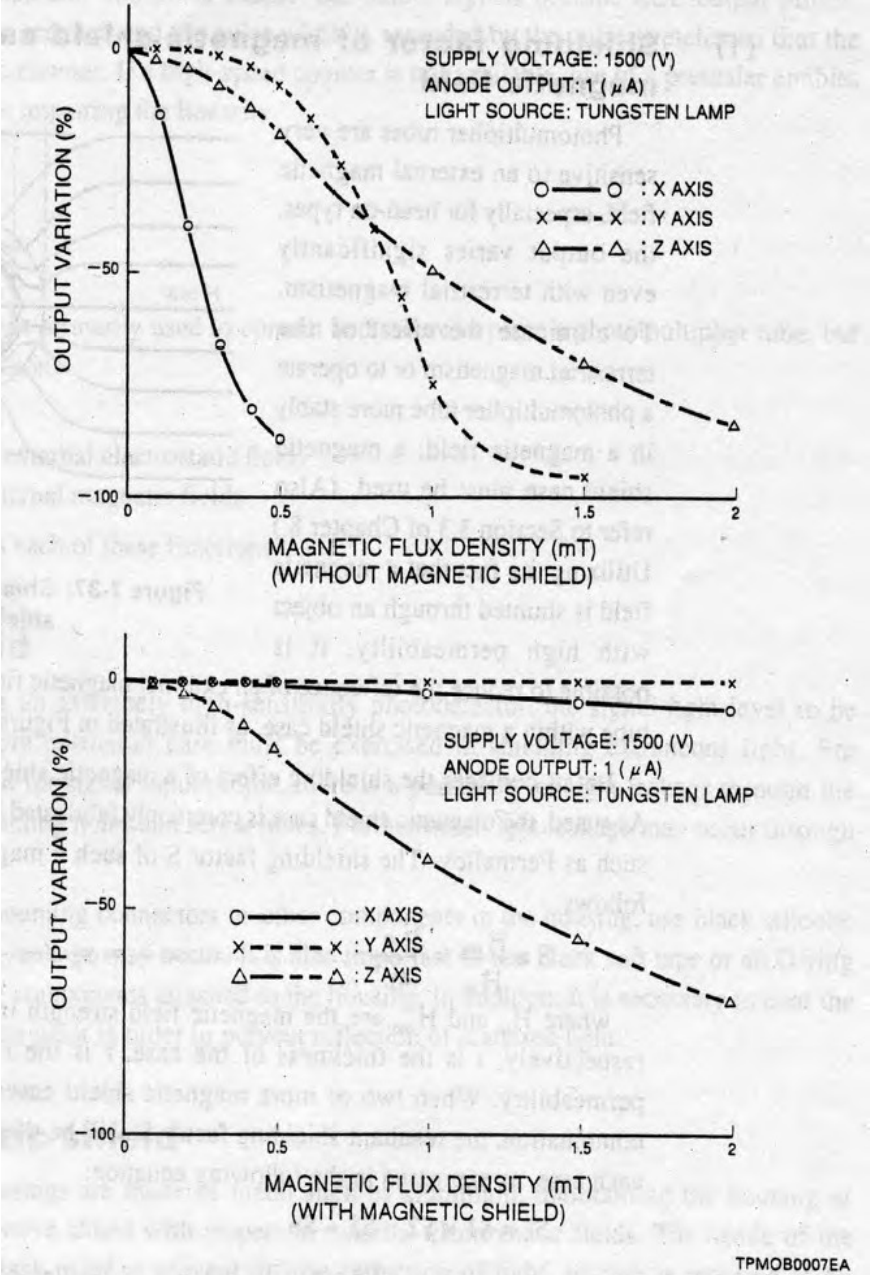

Figure 7-38: Magnetic characteristics of a photomultiplier tube

G.Collazuol - Siena - IDPASC 2013

MCP b-s contribution to timing spectra

Travel time and range of photoelectron

$$t_0 \approx \sqrt{\frac{2m_e l^2}{Ue_0}}$$

$$d_0 \approx 2l\sqrt{\frac{E_0}{Ue_0}}\sin(\alpha)$$

Delay and range of backscattered photoelectrons

$$t_1 \approx 2t_0 \sin(\beta) \qquad d_1 \approx 2l\sin(2\beta)$$

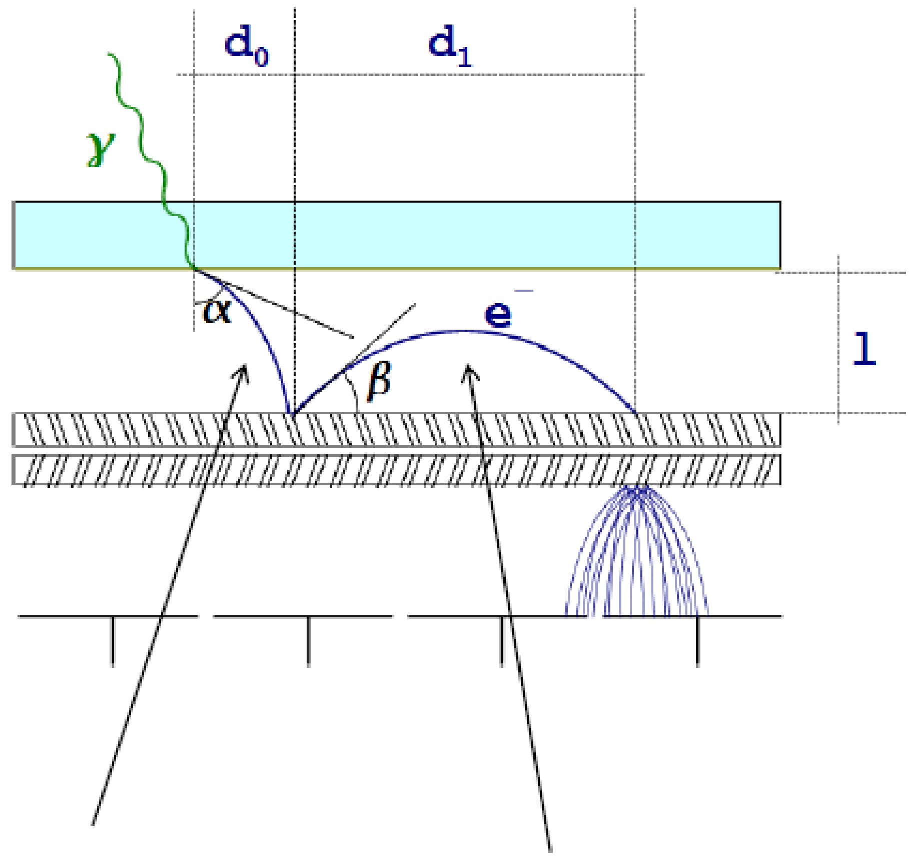

Parameters used:
- U = 200 V
- l = 6 mm
- E_0 = 1 eV
- m_e = 511 keV/c^2
- e_0 = 1.6 10^{-19} As

Photoelectron:
- $d_{0,max}$ ~ 0.8 mm
- t_0 ~ 1.4 ns
- Δt_0 ~ 100 ps

Backscattering:
- $d_{1,max}$ ~ 12 mm
- $t_{1,max}$ ~ 2.8 ns

Hybrid Photo Detectors

1) Photo-emission from photo-cathode
2) Photo-electron acceleration to **$\Delta V \sim$ 10-20kV**
3) charge multiplication in Si by ionization
→ **reduced fluctuations** due to Fano factor (F~0.12 in Si)

$$G = \frac{\Delta V - V_{thr.}}{W_{Si}}$$

$$\sigma_G = \sqrt{F \cdot G}$$

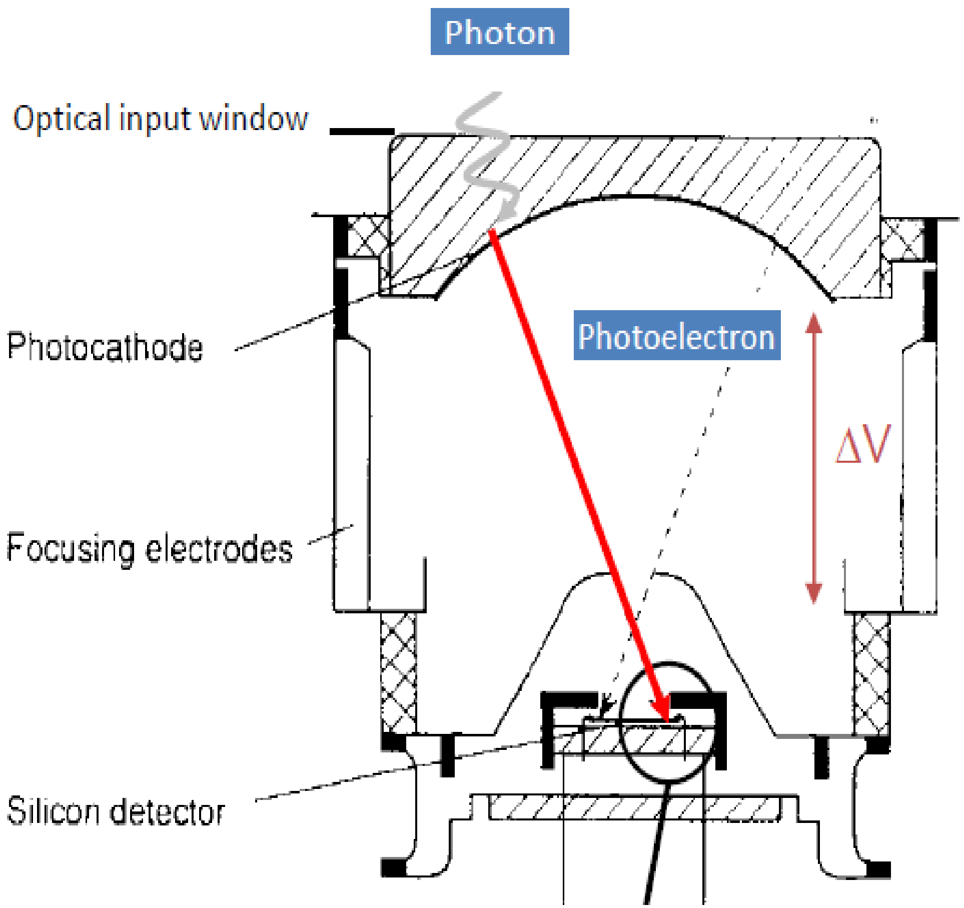

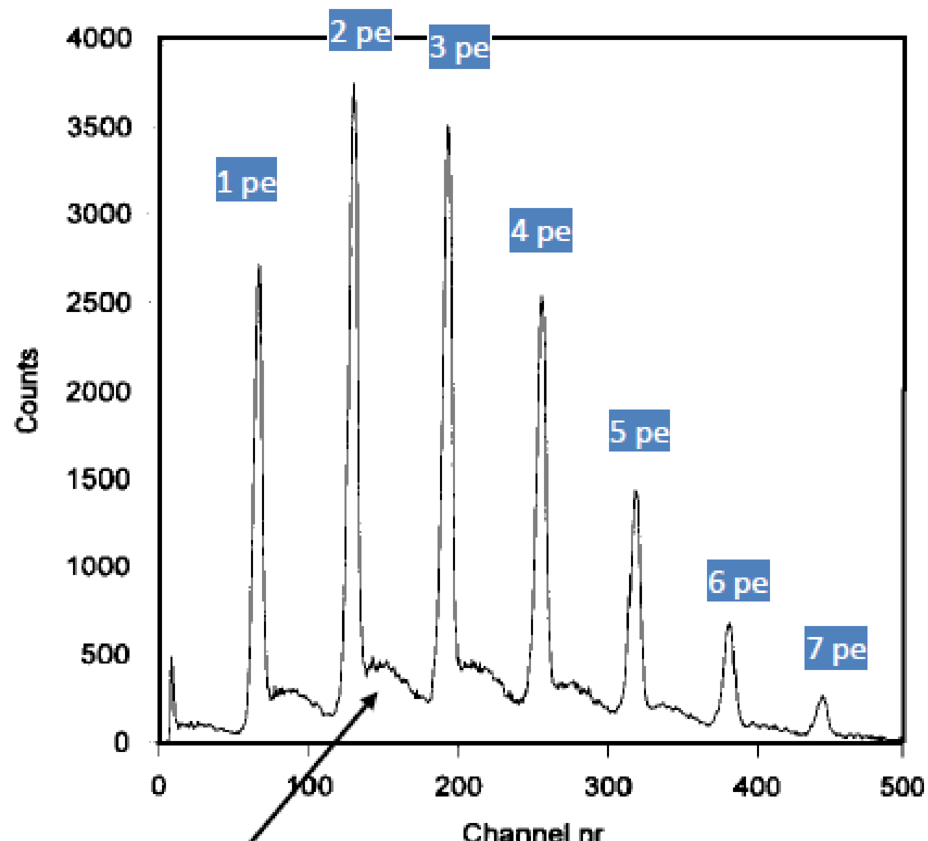

EDIT 2011 School at CERN - photodetectors

background from electron back-scattering at Si surface

G.Collazuol - Siena - IDPASC 2013

Key elements in SiPM cell

Doping and Field profiles

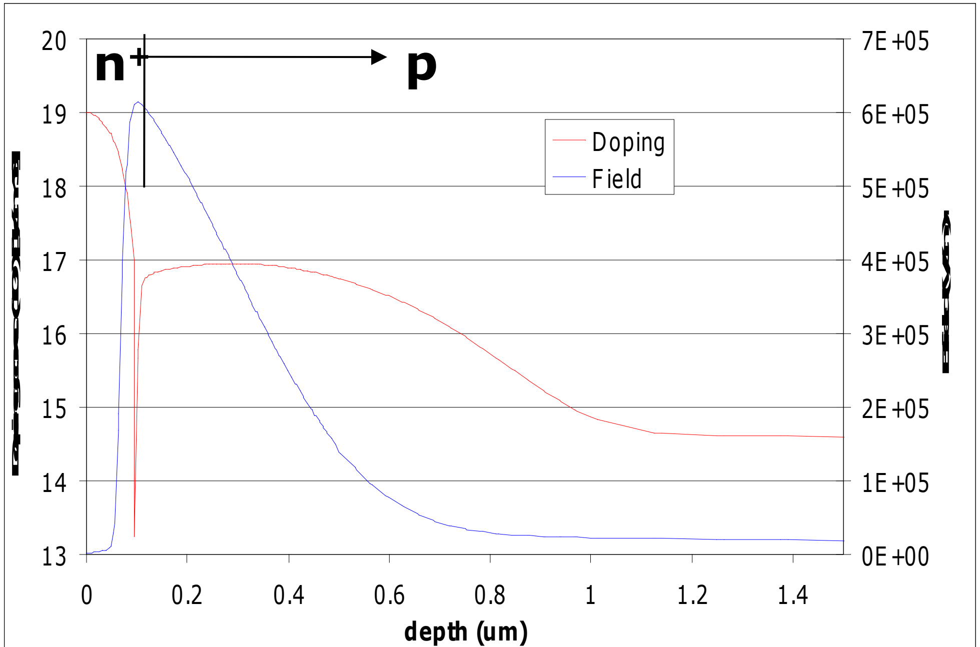

Optical window

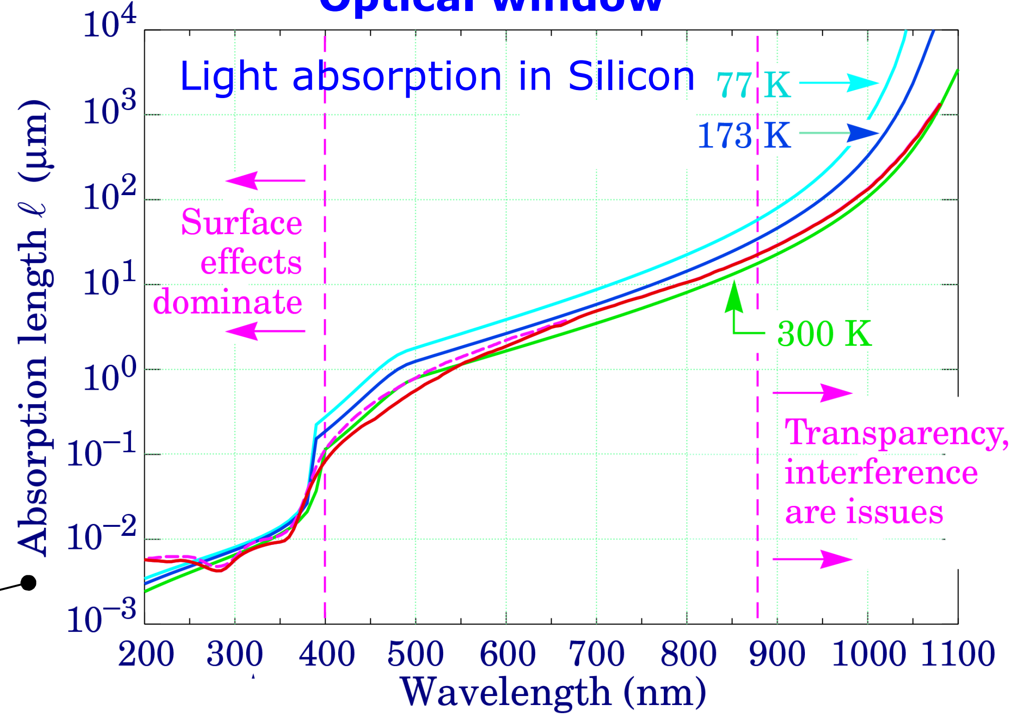

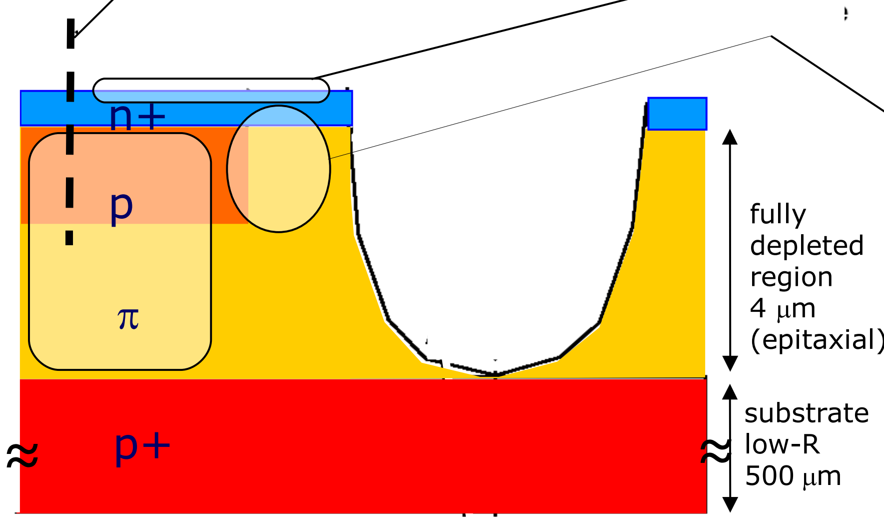

Guard Ring:

→ for avoiding early edge breakdown
→ for isolating cells
→ for tuning E field shape
→ has important impact on fill factor (more than Rq and metal grid)

E_{field} shape → PDE increases with ΔV

Ionization rate in Silicon → P_{01} optimization (n-on-p)

- high over-voltage
- photo-generation in the p-side of the junction

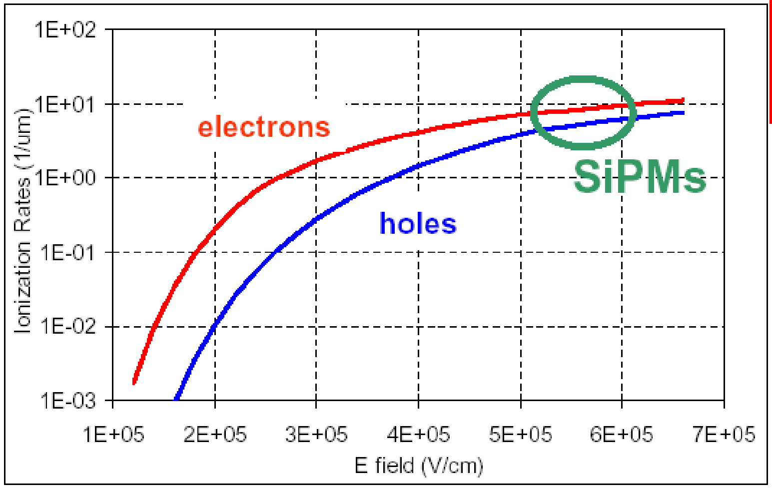

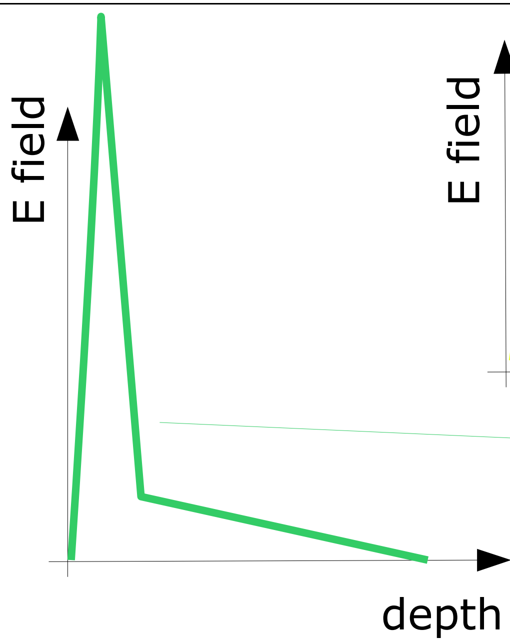

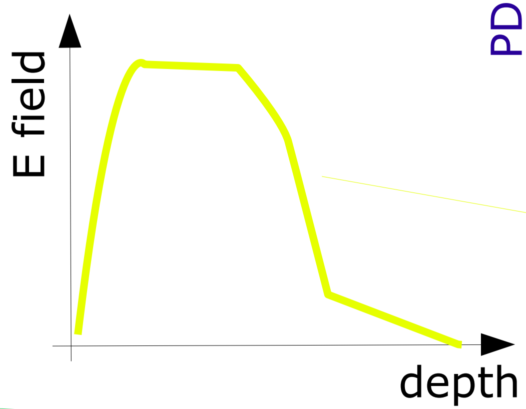

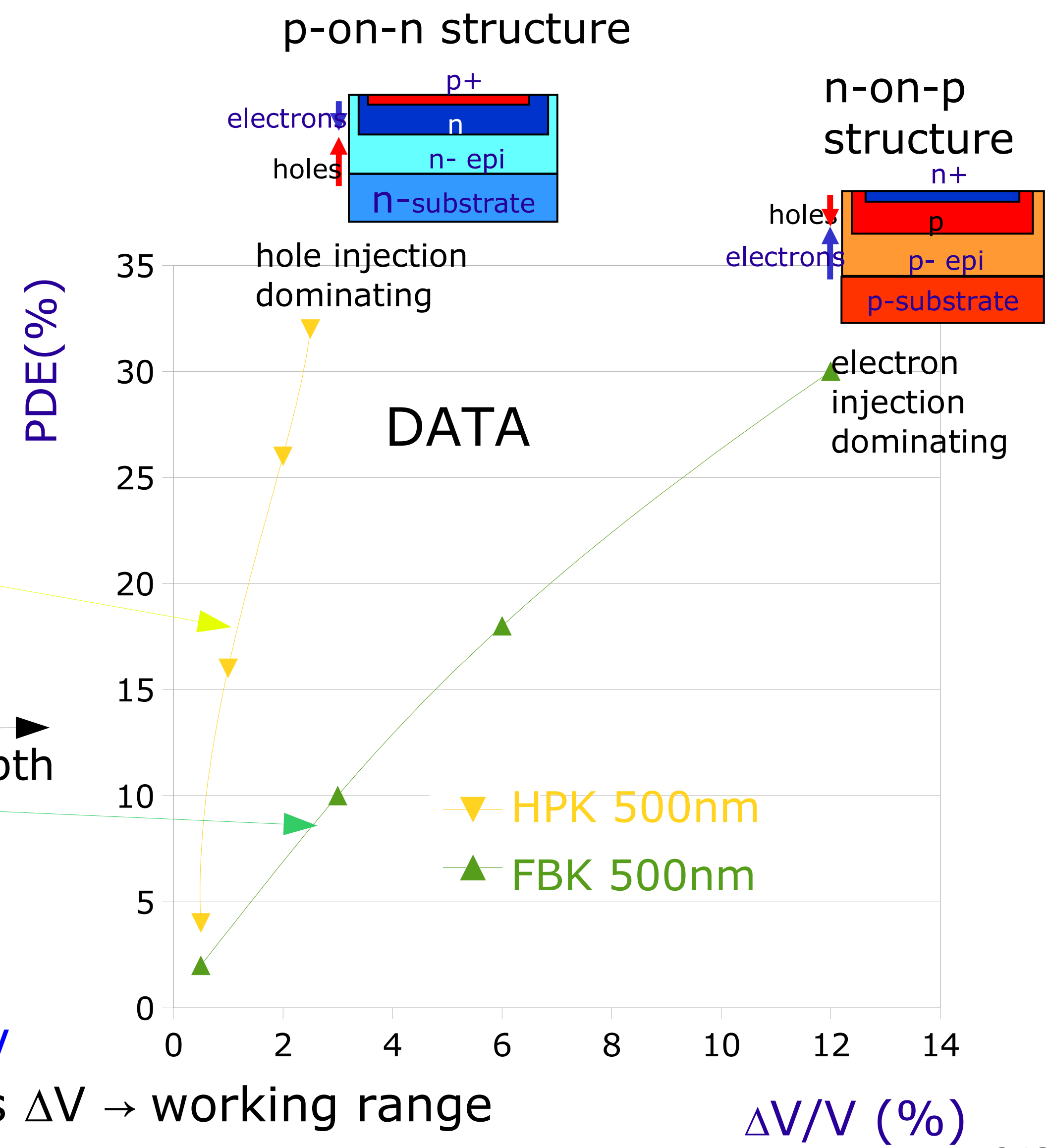

E field profile → the slope of PDE vs ΔV

note: P_{01} fixes also the slope of DCR vs ΔV → working range

SPTR: HPK/CPTA comparison

T.Iijima – PD07

SiPM - HPK (MPPC)

SIPM - CPTA (MRS-APD)

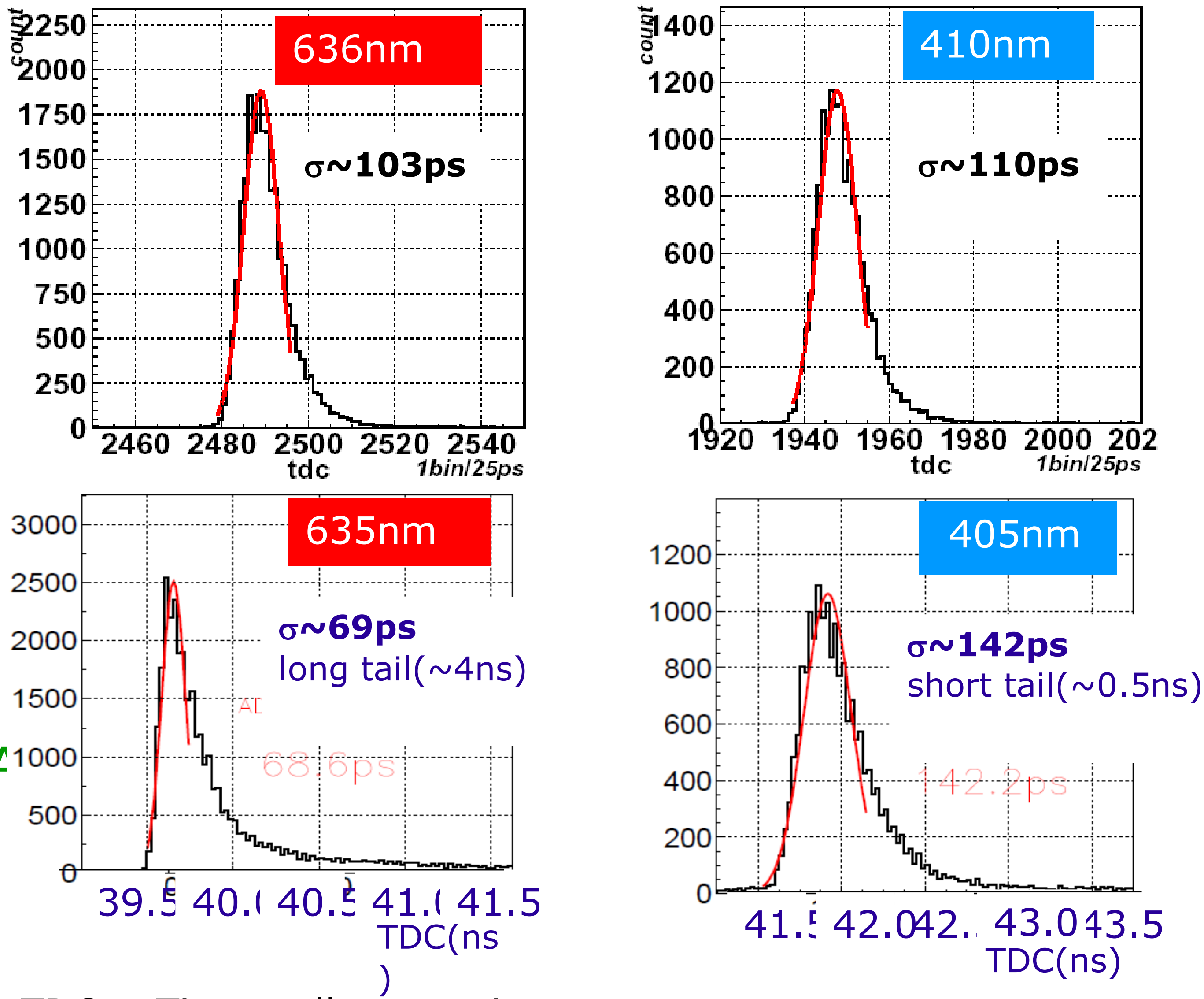

Method: CFD + TDC + Time walk corrections

RPL model vs data: comparison ... not yet

Example of RPL simulation of pure electron injection in Si SPAD

Courtesy of C.H.Tan

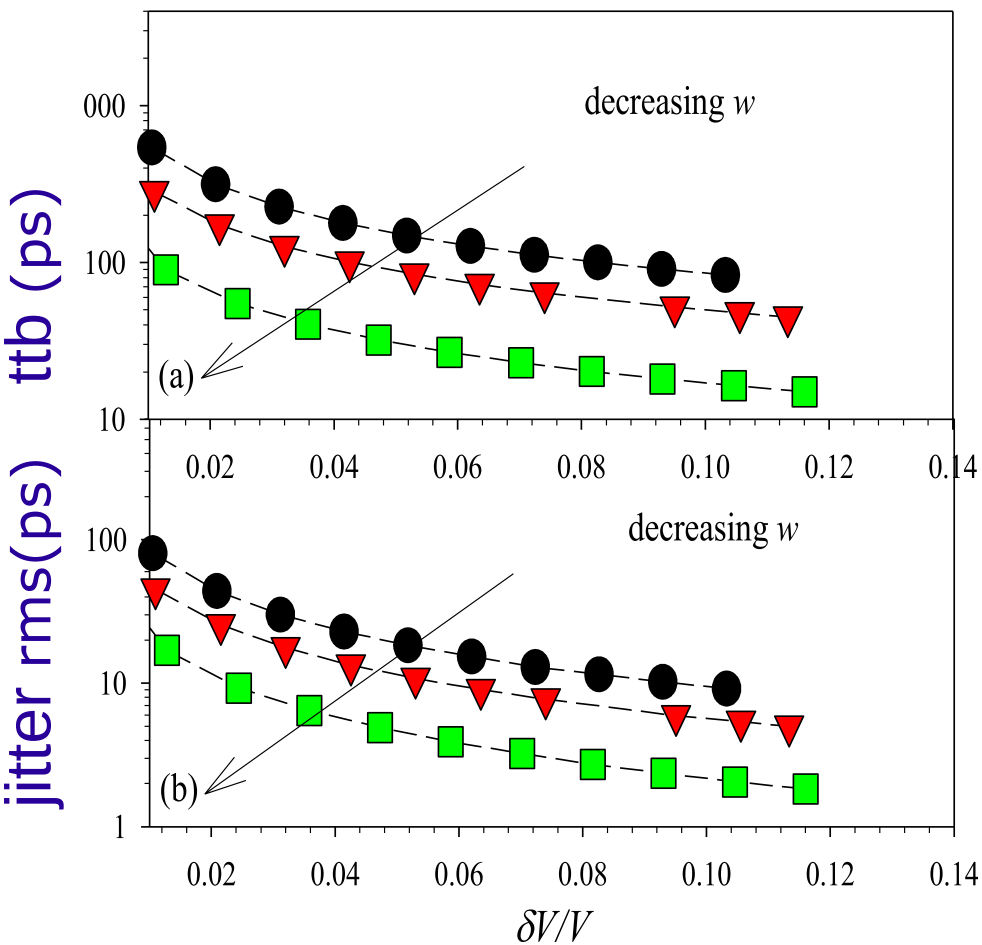

DATA
(DASIPM)

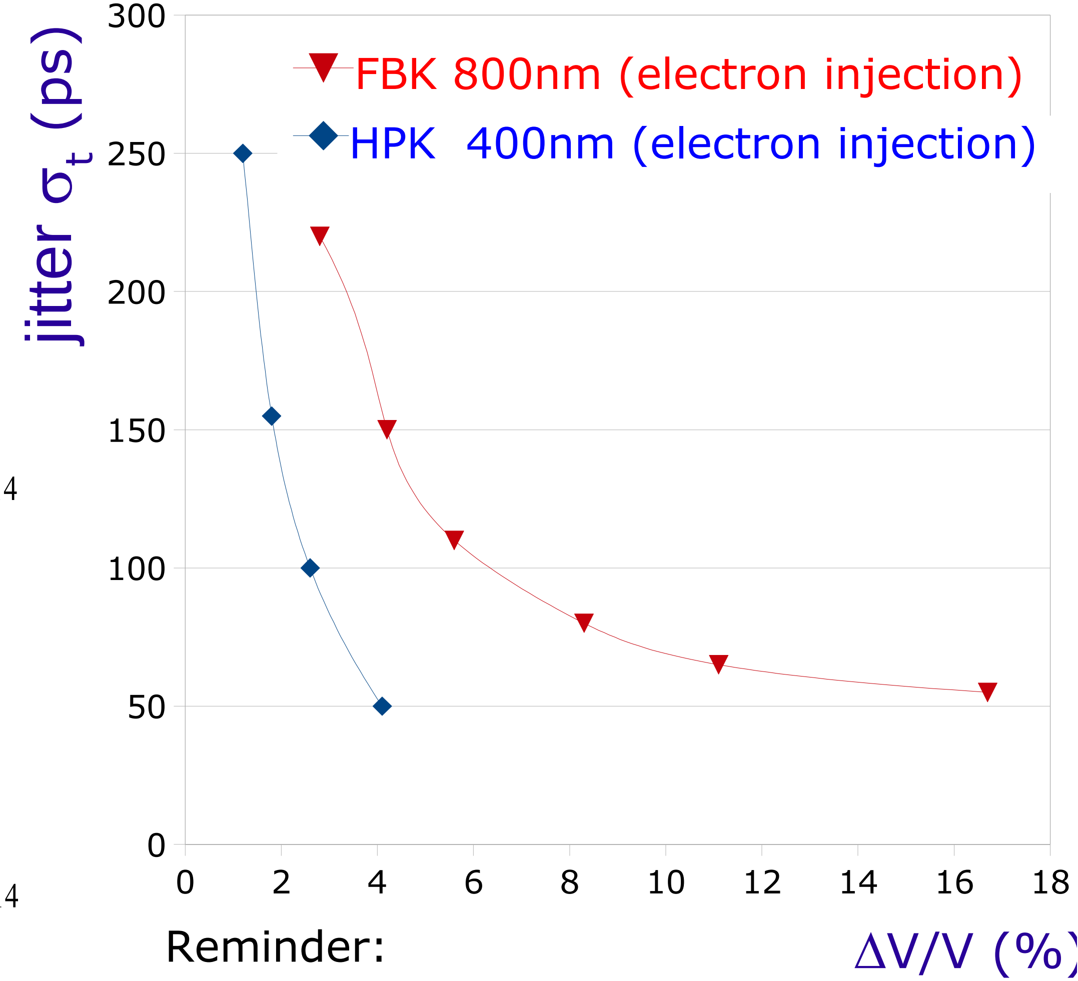

Reminder:
FBK structure is n on p
HPK structure is p on n

SPAD timing at low T

Timing: better at low T

Lower jitter at low T due to higher mobility

(Over-voltage fixed)

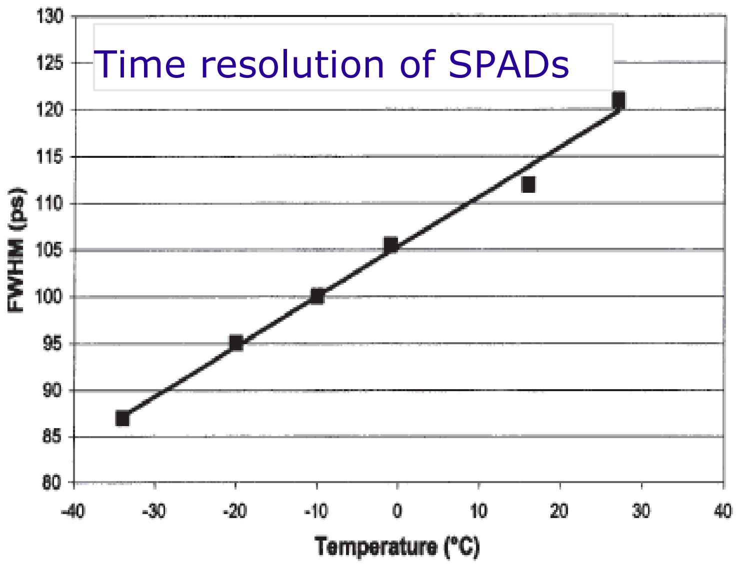

Fig. 11. FWHM of the SPAD response as a function of the temperature for a 20 μm diameter SPAD at 10 V overvoltage.

S.Cova el al, IEEE TED (2003)

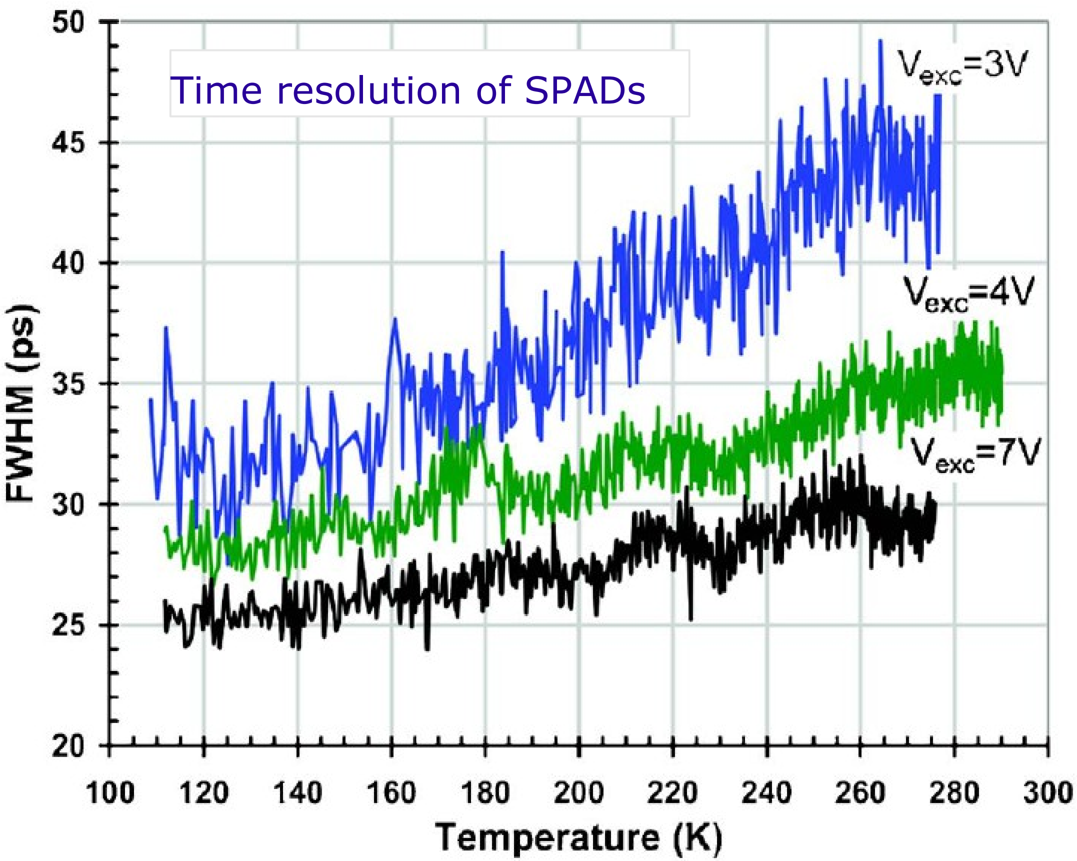

I.Rech el al, Rev.Sci.Instr. 78 (2007)

Quantum Efficiencies (HPK)

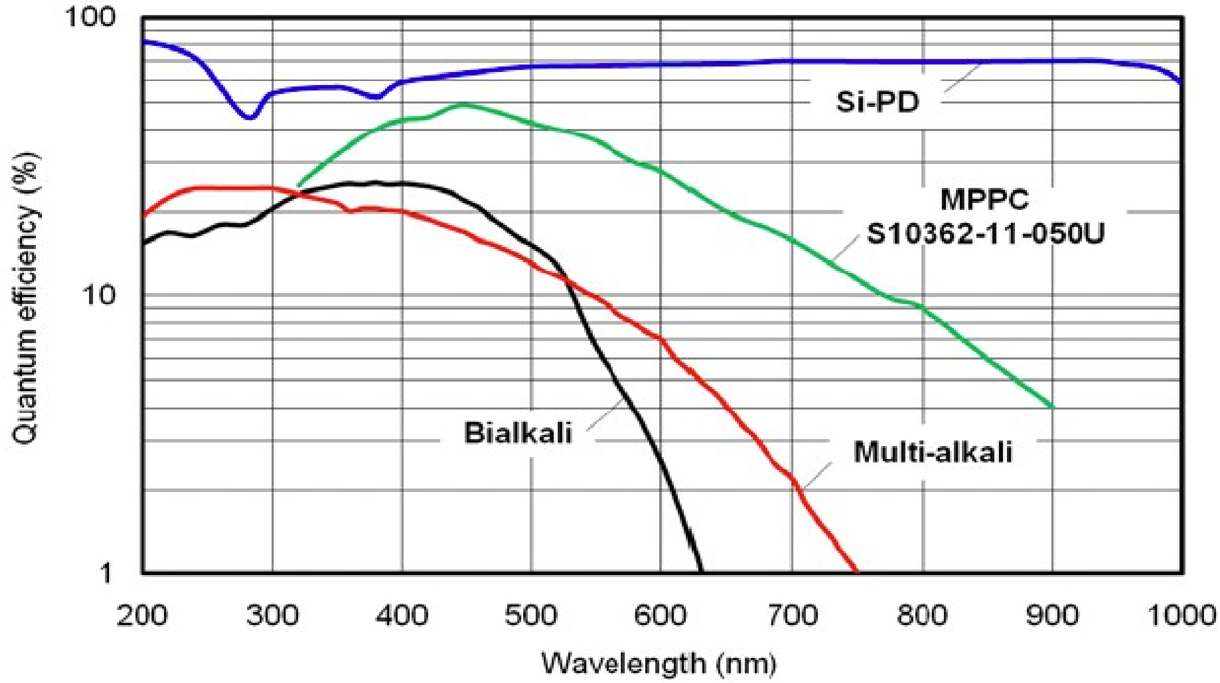

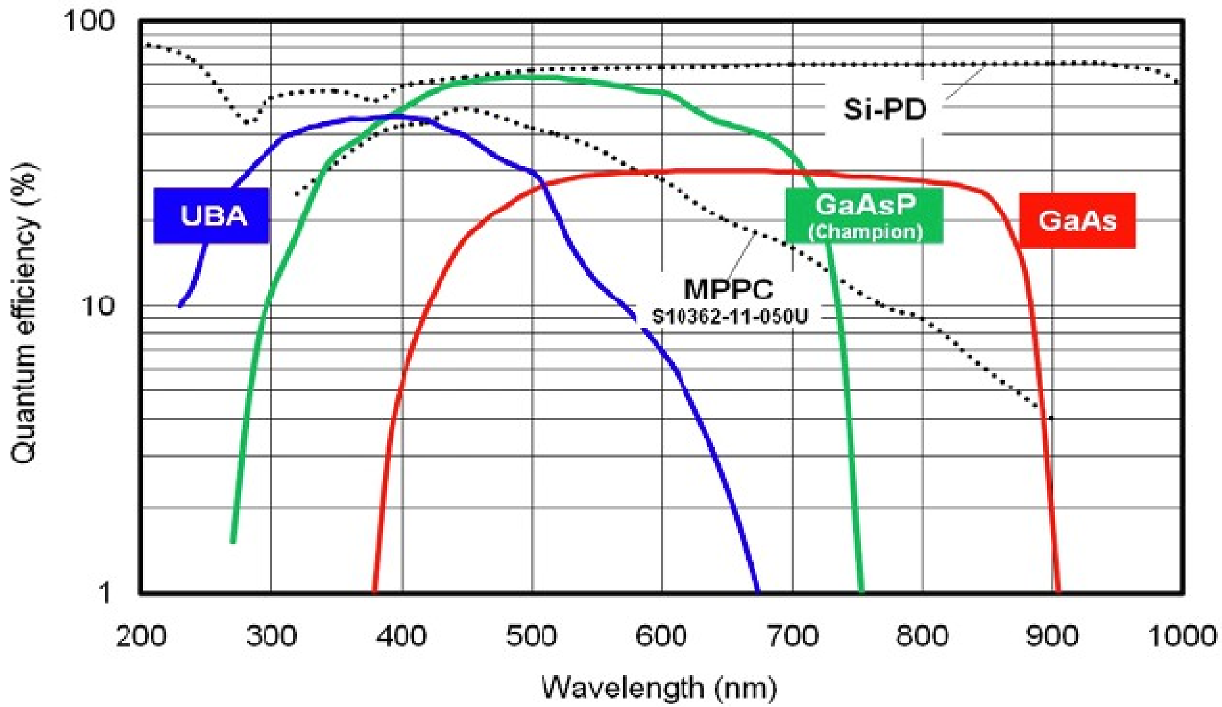

Timing (single photon) vs Area

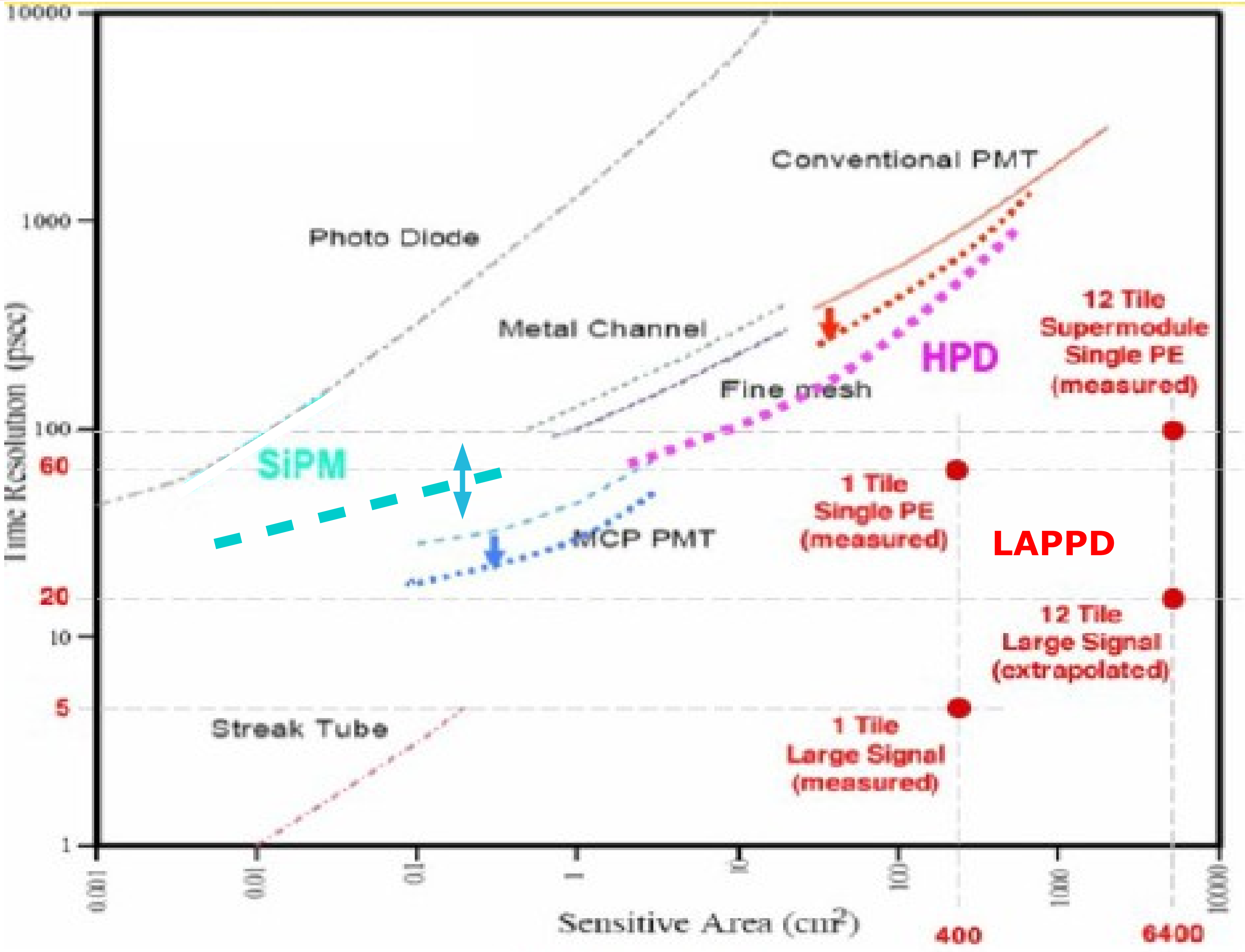

Market price

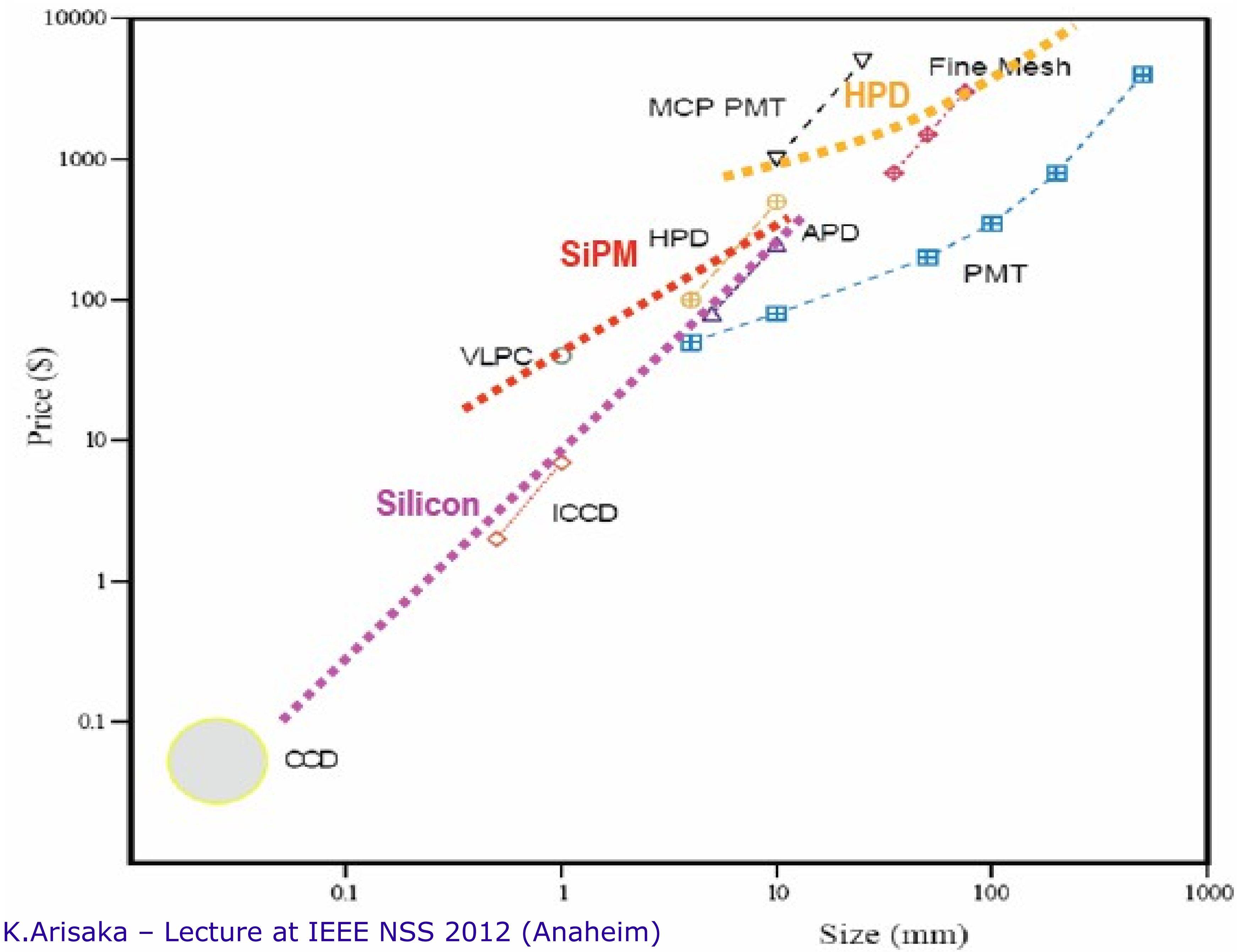

K.Arisaka – Lecture at IEEE NSS 2012 (Anaheim)

Front-End electronics

Charge preamp

Capacitive feedback **Cf**

Vout/Iin = - 1/jωCf

Perfect integrator : vout=Q/Cf∫

Difficult to accomodate large SiPM signals (200 pC)

Lowest noise configuration

Need Rf to empty Cf

Current preamp

Resistive feedback **Rf**

Vout/Iin = - Rf

Keeps signal shape

Need Cf for stability

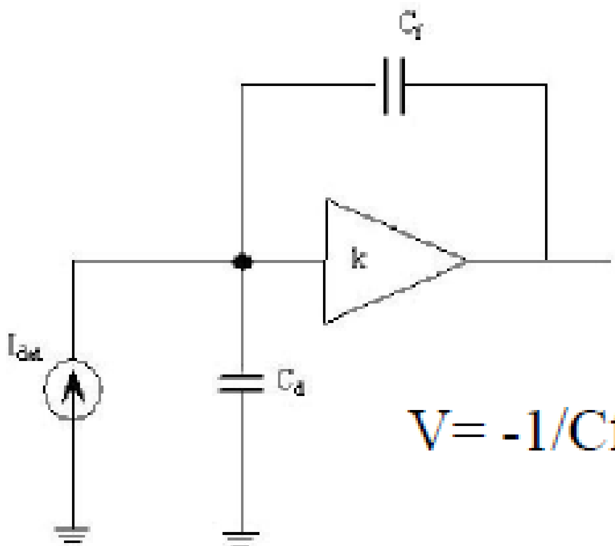

$$V = -1/Cf \int i(t)dt$$

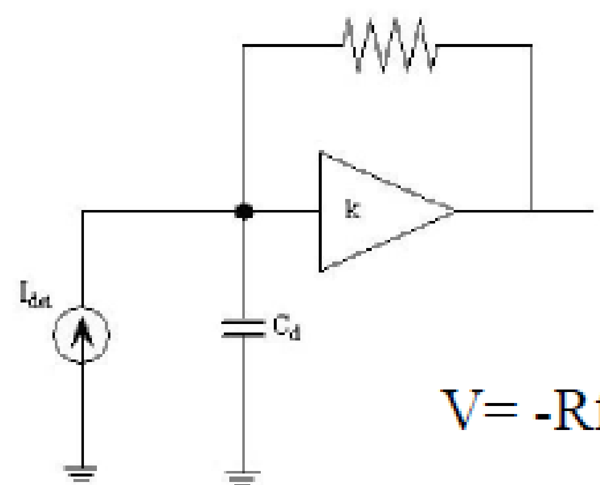

$$V = -Rf\ i(t)$$

C.De La Taille – PhotoDet 2012

Front-End electronics

- **Open loop configurations : current conveyors, RF amplifiers**
- **Usually designed at transistor level MOS or SiGe (ex PETIROC)**

- **Current conveyors**
- Small Zin : current sensitive input
- Large Zout : current driven output
- Unity gain current conveyor
- E.g. : (super) common-base configuration
- Low input impedance : Rin=1/gm
- Transimpedance : Rc
- Bandwitdth : 1/2πRcCu > 1 GHz

- **RF amplifiers**
- Large Zin : voltage sensitive input
- Large Zout : current driven output
- Current conversion with resistor R_S
- E.g. common-emitter configuration
- Transimpedance : -gmRcRs
- Bandwitdth : 1/2πRsCt

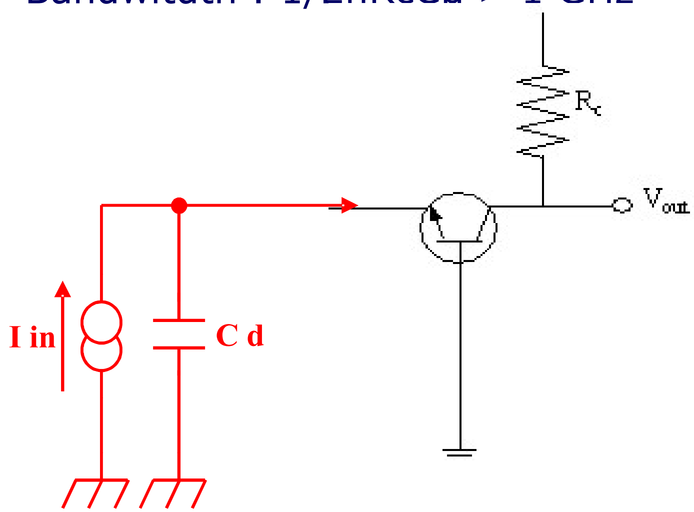

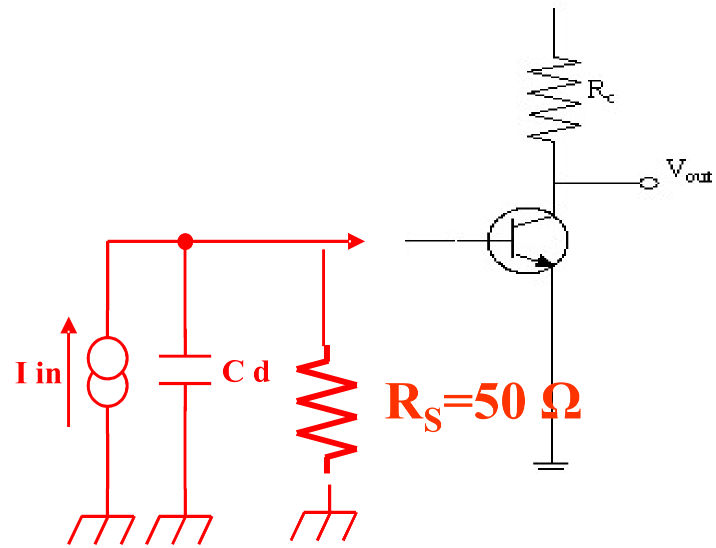

15 jun 2012 CdLT Photodet conference

C.De La Taille – PhotoDet 2012